

UNCLASSIFIED

AD NUMBER

ADB951705

LIMITATION CHANGES

TO:

Approved for public release; distribution is unlimited. Document partially illegible.

FROM:

Distribution authorized to U.S. Gov't. agencies and their contractors;  
Administrative/Operational Use; MAR 1964. Other requests shall be referred to Army Engineer Waterways Experiment Station, Vicksburg, MI.

AUTHORITY

USAE WES notice 22 May 1980

THIS PAGE IS UNCLASSIFIED

THIS REPORT HAS BEEN DELIMITED  
AND CLEARED FOR PUBLIC RELEASE  
UNDER DOD DIRECTIVE 5200.20 AND  
NO RESTRICTIONS ARE IMPOSED UPON  
ITS USE AND DISCLOSURE.

DISTRIBUTION STATEMENT A

APPROVED FOR PUBLIC RELEASE,  
DISTRIBUTION UNLIMITED.

PHOTOGRAPH THIS SHEET

UNANNOUNCED

ADB951705

DTIC ACCESSION NUMBER



LEVEL



INVENTORY

Harvard Univ. Soil Mechanics  
Series No. 71

Control of Leakage in the Triaxial Test "

DOCUMENT IDENTIFICATION

AEWES Contract Rpt. 3-84  
March 1964

Contract Nos. DA22-079-CIVENG-62-3 & DA22-079-CIVENG-63-8



DISTRIBUTION STATEMENT

ACCESSION FOR	
NTIS	GRA&I
DTIC	TAB
UNANNOUNCED	<input checked="" type="checkbox"/>
JUSTIFICATION	
BY	
DISTRIBUTION /	
AVAILABILITY CODES	
DIST	AVAIL AND/OR SPECIAL
2	

DISTRIBUTION STAMP



DATE ACCESSIONED

80 5 30 0 54

DATE RECEIVED IN DTIC

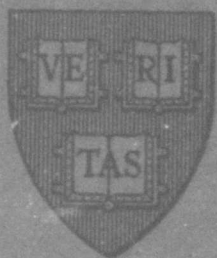
PHOTOGRAPH THIS SHEET AND RETURN TO DTIC-DDA-2

TA7  
W 34c  
no. 3-84  
Cop. 5

63-CE-C  
HARVARD

Property of the United States Government

SOIL MECHANICS SERIES



No. 71

AD B951705

*Report*  
*on*  
*Control of Leakage in the Triaxial Test*

by  
STEVE J. POULOS

A Research Project  
Sponsored By  
THE WATERWAYS EXPERIMENT STATION  
In Cooperation With  
HARVARD UNIVERSITY

Pierce Hall  
Cambridge, Massachusetts  
March 1964

RESEARCH CENTER LIBRARY  
US ARMY ENGINEER WATERWAYS EXPERIMENT STATION  
VICKSBURG, MISSISSIPPI

**Report**

**on**

**CONTROL OF LEAKAGE IN THE TRIAXIAL TEST**

**by**

**Steve J. Poulos**

**A Research Project**

**Sponsored By**

**THE WATERWAYS EXPERIMENT STATION**

**In Cooperation With**

**HARVARD UNIVERSITY**

**Contract Nos. DA22-079-CIVENG-62-3 and DA22-079-CIVENG-63-8**

AEWES Contract Report 3-84

**Pierce Hall**

**Cambridge, Massachusetts**

**March 1964**

TA 7  
W34c  
no. 3-84  
cop. 5

PREFACE

Professor Arthur Casagrande originally suggested to the author that an investigation of the effect of time on the strength of clays at constant water content would be a worthwhile topic for doctoral research. He emphasized that the first phase would have to consist of improving triaxial apparatus and procedures to reduce leakage sufficiently so that long-time tests could be performed at essentially constant water content.

As the author's work on the problem of leakage progressed, it became evident that (1) the design and construction of apparatus for measuring extremely small rates of water flow through membranes, (2) the theoretical and experimental investigation of flow through membranes, and (3) the investigation of the effects of leakage on effective stresses in triaxial specimens, constituted a major undertaking. Therefore the author decided to limit the scope of his doctoral research to the above topics.

As a result of this investigation it is possible to perform triaxial tests with a duration of several months on 100% saturated specimens without excessive errors due to leakage. Further research is needed to solve the problems of (1) air leakage into and out of partially saturated specimens and (2) water leakage into 100% saturated specimens for tests lasting a year or longer. It is hoped that the discussion in Chapter 3 on the theory of flow through membranes will stimulate research into the mechanism of flow through membranes.

The author wishes to express his appreciation to the Corps of Engineers, U. S. Army, who sponsored this investigation.

My deepest appreciation goes to Professor Arthur Casagrande for his continuous encouragement and for his many contributions at every stage of the investigation.

The author is grateful to Dr. Werner Stumm, Associate Professor of Applied Chemistry, who has so willingly answered the author's many questions concerning the theory of flow through membranes.

Special gratitude is extended to Dr. Ronald C. Hirschfeld, Assistant Professor of Soil Mechanics, for his suggestions and continuous support while the study was being carried out.

To Mr. Charles E. Osgood, technical associate in the Harvard Soil Mechanics Laboratory, go many thanks for his suggestions and assistance during testing and in preparation of the figures.

The author is grateful to Mr. Kenneth Hanna and Mr. Fay Welch, machinists in the Pierce Hall machine shop, for their assistance in the design of apparatus and for their careful workmanship.

Thanks are also extended to Miss Rosemary Gibbs and Mrs. Constance Towler for typing the manuscript with care.

Sincerest thanks go to my wife, for typing the rough drafts and portions of the final manuscript and for her continuous encouragement and optimism, as two years turned into four.

TABLE OF CONTENTS

	Page
PREFACE	iii
TABLE OF CONTENTS	iv
LIST OF TABLES	xiii
LIST OF FIGURES	xiv
SYNOPSIS	xxi
<u>CHAPTER 1 INTRODUCTION</u>	1
1-01 GENERAL	1
1-02 DEVELOPMENT OF INTEREST IN LEAKAGE	1
1-03 DEFINITION OF LEAKAGE	2
1-04 PURPOSE	3
1-05 SCOPE	3
1-06 SUMMARY OF PAST LEAKAGE INVESTIGATIONS	4
<u>CHAPTER 2 ANALYSIS OF EFFECTS OF LEAKAGE IN TRIAXIAL TESTS</u>	6
2-01 GENERAL	6
2-02 QUALITATIVE DESCRIPTION OF EFFECTS OF LEAKAGE ON TRIAXIAL SPECIMENS	6
(a) General	6
(b) Water Leakage into 100% Saturated Specimens	7
(c) Distribution of Air in Partially Saturated Specimens	8
(d) Air Leakage into 10% Saturated Specimens	9
(e) Air Leakage into Partially Saturated Specimens	10
(f) Water Leakage into Partially Saturated Specimens	11
2-03 RELATION BETWEEN VOLUME CHANGE AND CHANGE IN EFFECTIVE STRESS	11
2-04 DETERMINATION OF THE SWELLING RATIO	12
(a) General	12
(b) Special Swelling Tests on Canyon Dam Clay	13
(c) Swelling Ratio Obtained from One-Dimensional Consolidation Tests	13
2-05 EFFECT OF WATER LEAKAGE ON 100% SATURATED SPECIMENS	14
2-06 EFFECT OF AIR LEAKAGE ON PARTIALLY SATURATED SPECIMENS	15
(a) Derivation of Equation Relating Change in Effective Stress to Volume of Air Leakage	15
(b) Discussion of Eq. 2-22	17

	Page
2-07 ERRORS INTRODUCED BY SIMPLIFYING ASSUMPTIONS IN THE ANALYSIS OF EFFECTS OF LEAKAGE	17
(a) Qualitative Description of Assumptions	17
(1) Change in pore water pressure is equal but opposite to the change in effective stress in partially saturated specimens	17
(2) Boyle's law is exact	18
(3) Water is incompressible	18
(4) Volume increase of water due to solution of air is zero	18
(5) Henry's law is exact	18
(6) Swelling curve is a straight line	19
(7) Mineral grains are incompressible	19
(8) Membrane does not flex	19
(9) Leakage occurs slowly enough to achieve equilibrium conditions	19
(b) Discussion of Magnitude of Errors	19
2-08 SUMMARY AND CONCLUSIONS	20
<b>CHAPTER 3    <u>THEORY OF STEADY FLOW OF FLUIDS THROUGH MEMBRANES</u></b>	<b>23</b>
3-01 INTRODUCTION	23
(a) Purpose and Scope	23
(b) The Importance of Membrane Science and Technology	23
3-02 THE MEMBRANE-PERMEANT SYSTEM	23
3-03 TYPES OF MEMBRANES	24
(a) General	24
(b) Porous and Non-Porous Membranes; Semi-Permeable Membranes	24
(c) Ordered and Dis-Ordered (Amorphous) Membrane Structure	24
(d) Charged Membranes	25
(e) Stratified Membranes	25
3-04 PERMEANTS AND DRIVING FORCES	25
(a) Permeants	25
(b) Driving Forces	26
3-05 EQUATIONS OF FLOW OF LIQUIDS THROUGH MEMBRANES	27
(a) General	27
(b) Empirical Equations	28
(1) Darcy's Law	28
(2) Fick's Law	28
(3) Starling's Hypothesis	30
(c) Equations of Flow Based on Models of the Membrane-Permeant System	31
(1) Poisseuille's Law	31
(2) Derivation of Fick's Law by Use of Kinetic Model of Diffusing Particles	33
(3) Adsorption-Desorption Equilibria at the Membrane Surfaces	34
(d) The Thermodynamic Approach	36

	Page
3-06 EQUATIONS OF FLOW OF GASES THROUGH MEMBRANES	38
(a) Empirical Equations	38
(1) Darcy's Law	38
(2) Fick's Law	39
(b) Equations Based on Models of the Membrane-Permeant System	40
(1) Poisseuille's Law	40
(2) Knudson Flow	41
(3) Diffusion	42
3-07 SUMMARY AND CONCLUSIONS	44
<u>CHAPTER 4</u> <u>EXPERIMENTAL INVESTIGATION OF LEAKAGE THROUGH MEMBRANES DUE TO</u> <u>                  HYDRAULIC PRESSURE GRADIENTS</u>	47
4-01 INTRODUCTION	47
4-02 APPARATUS	47
(a) General Description	47
(b) Permeability Cell	47
(c) Burettes to Measure Volume Changes	48
(d) System for Applying Pressure	49
(e) Constant Temperature Bath	49
4-03 PROCEDURE FOR WATER PERMEABILITY (W) TESTS	50
(a) General Description	50
(b) Preparation of Membranes	50
(c) Placement of Membrane in Permeability Cell	50
(d) Starting the Test	51
(e) Readings during Test	51
(f) Dismantling the Test	51
4-04 PRESENTATION AND ANALYSIS OF DATA	51
(a) General	51
(b) Analysis of Data for Test W1	52
(c) Analyses for Group I Tests	53
(d) Analyses for Group II Tests	53
4-05 DISCUSSION OF RESULTS	54
(a) Effect of Hydraulic Pressure Difference on Rate of Flow	54
(b) Effect of Oil Soaking on Rate of Flow	54
(c) The Permeability of Natural Rubber to Water	55
4-06 SUMMARY	55
(a) Apparatus and Procedure	55
(b) Rate of Flow of Water Through Natural Rubber	56
<u>CHAPTER 5</u> <u>EXPERIMENTAL INVESTIGATION OF LEAKAGE THROUGH MEMBRANES DUE TO</u> <u>                  MOLE FRACTION (OSMOTIC PRESSURE) GRADIENTS</u>	57
5-01 INTRODUCTION	57
5-02 APPARATUS	57
(a) General	57
(b) The Cell Used for X Tests	57
(c) The Mercury Seal	58

	Page	
5-03	PROCEDURE FOR X TESTS	58
	(a) General	58
	(b) Preparation of Membranes	58
	(c) Placement of Membrane in Cell	58
	(d) Filling the Salt Chamber with Salt Solution	59
	(e) Dismantling the Apparatus After Test	59
5-04	PRESENTATION AND INTERPRETATION OF DATA	60
5-05	DISCUSSION OF FACTORS AFFECTING RATE OF FLOW OF WATER DURING X TESTS	61
	(a) Effect of Mole Fraction Difference	61
	(b) Effect of Membrane Thickness	61
	(c) Effect of Silicone Oil Soaking	61
5-06	COMPARISON OF THE RESULTS OF X TESTS WITH THE RESULTS OF W TESTS	61
	(a) Comparison of K Measured in W and X Tests	61
	(b) Comparison of Rate of Flow Caused by Mole Fraction and Hydraulic Pressure Differences	62
5-07	DISCUSSION OF SUITABILITY OF NATURAL RUBBER MEMBRANES FOR USE IN TRIAXIAL TESTING	62
<u>CHAPTER 6</u>	<u>EXPERIMENTAL INVESTIGATION OF LEAKAGE THROUGH MEMBRANES DUE TO VAPOR PRESSURE GRADIENTS</u>	 64
6-01	GENERAL	64
6-02	THEORY FOR VAPOR PERMEABILITY (V) TESTS	64
6-03	APPARATUS FOR VAPOR PERMEABILITY (V) TESTS	65
6-04	PROCEDURE FOR VAPOR PERMEABILITY (V) TESTS	65
	(a) General Description	65
	(b) Preparation of Membranes	65
	(c) Placement of Membrane in Permeability Cell	65
	(d) Starting the Test	65
	(e) Readings during Test	65
6-05	PRESENTATION AND ANALYSIS OF DATA FOR V TESTS	66
	(a) Presentation of Data	66
	(b) Analysis of Test V1	66
6-06	DISCUSSION OF V TESTS ON NATURAL RUBBER MEMBRANES	67
	(a) Permeability of Untreated Natural Rubber	67
	(b) Effect of Treatment of Membrane on Permeability Constant	67
	(c) Comparison of Permeability Constants Measured in V and W Tests	67
6-07	DISCUSSION OF V TESTS ON SYNTHETIC RUBBER AND PLASTIC MEMBRANES	68
6-08	EVAPORATION OF WATER THROUGH NATURAL RUBBER DURING UNCONFINED TESTS	68
6-09	SUMMARY OF VAPOR PERMEABILITY (V) TESTS	69

	Page
<b>CHAPTER 7</b>	
<b><u>EXPERIMENTAL INVESTIGATION OF LEAKAGE PAST BINDINGS IN TRIAXIAL TESTS</u></b>	70
7-01 INTRODUCTION	70
7-02 APPARATUS	70
(a) General	70
(b) The Pedestals Used for Binding Leakage Tests	70
7-03 PROCEDURE	71
(a) Preparation of Membranes	71
(b) Set-up of Membrane and Bindings on Pedestal	71
(c) Assembly of Cell and Performance of Tests	72
(d) Dismantling the Apparatus after Test	72
7-04 PRESENTATION AND INTERPRETATION OF DATA	72
7-05 DISCUSSION OF RESULTS	73
(a) General	73
(b) Binding Leakage in Group I Tests	74
(c) Effect of Use of Two Membranes on the Binding Leakage (Group II)	74
(d) Effect of Roughness of the Pedestal on the Binding Leakage (Groups III, IV, V)	74
(e) Effect of Greasing the Pedestal on the Binding Leakage (Groups VI, VII)	74
(f) Effect of Soaking Membrane in Silicone Oil on Binding Leakage (Groups IV, VIII, IX)	75
(g) Leakage of Neoprene Rubber Strip Bindings (Groups V, X, XI)	75
7-06 SUMMARY	76
<b>CHAPTER 8</b>	
<b><u>EXPERIMENTAL INVESTIGATION OF LEAKAGE FROM VALVES, FITTINGS AND SARAN TUBING</u></b>	78
8-01 INTRODUCTION	78
8-02 APPARATUS AND PROCEDURE	78
(a) Leakage Tests on Valves and Fittings	78
(b) Tests on Saran Tubing	78
8-03 PRESENTATION AND INTERPRETATION OF RESULTS	79
(a) Results of Valve Leakage Tests	79
(b) Results of Fitting Leakage Tests and Tests on Saran Tubing	79
(c) Temperature Correction of Volume Flow versus Time	80
(d) Accuracy of the Rate of Leakage Data	80
8-04 DISCUSSION OF RESULTS	81
(a) General	81
(b) Valve Leakage Tests	81
(c) Fitting Leakage Tests	82
(d) Tests on Saran Tubing	82
(e) Volume Changes of Valves and Fittings Caused by Application of Pressure	83
8-05 SUMMARY	83

	Page
<b>CHAPTER 9    <u>ANALYSIS OF RESULTS</u></b>	<b>85</b>
9-01    PURPOSE	85
9-02    SUITABILITY OF CONVENTIONAL TRIAXIAL APPARATUS FOR CONTROL OF WATER LEAKAGE	85
(a)    Water Leakage into 100% Saturated Specimens	85
(b)    Water Leakage into Partially Saturated Specimens	86
9-03    SUITABILITY OF CONVENTIONAL TRIAXIAL APPARATUS FOR CONTROL OF AIR LEAKAGE	86
(a)    General	86
(b)    Air Leakage Into or Out of Partially Saturated Specimens	86
9-04    GENERAL DISCUSSION OF PROCEDURES FOR CONTROLLING ERRORS CAUSED BY AIR AND WATER LEAKAGE	88
(a)    Purpose	88
(b)    Derivation of Equation Relating the Decrease in Effective Stress to Parameters Controlling Volume of Leakage	88
(1)    Equation for the Case of Water Leakage	88
(2)    Equation for the Case of Air Leakage	89
(c)    Effect of Increasing Specimen Size on Errors Caused by Leakage	90
(d)    Discussion of Factors Affecting the EK-Coefficient	90
(1)    Methods for Reducing Membrane Permeability	90
(2)    Methods for Reducing the Modulus of Elasticity	92
9-05    SELECTION OF MEMBRANE WITH LOW EK-COEFFICIENT	93
(a)    Purpose	93
(b)    Measurement of Moduli of Elasticity of Membranes	93
(c)    Discussion of Measured EK-Coefficients	93
(d)    Discussion of the Advantages of Using Butyl Rubber Membranes	94
9-06    DISCUSSION OF PROCEDURES FOR REDUCING VAPOR AND PARTIAL PRESSURE DIFFERENCES ACROSS MEMBRANES	95
(a)    Procedure for Reducing Vapor Pressure Difference of Water	95
(b)    Procedure for Reducing Partial Pressure Difference of Air	96
<b>CHAPTER 10    <u>RECOMMENDATIONS FOR CONTROL OF LEAKAGE</u></b>	<b>97</b>
10-01    RECOMMENDATIONS FOR CONTROL OF WATER LEAKAGE	97
(a)    General	97
(b)    Recommended Procedure for 12-Hour Q and R Tests on 100% Saturated Specimens	97
(c)    Recommended Procedure for 100-Day Q and R Tests on 100% Saturated Specimens	97
(d)    Miscellaneous Comments on the Control of Water Leakage	99
10-02    RECOMMENDATIONS FOR CONTROL OF AIR LEAKAGE	99
(a)    Control of Air Leakage into 100% Saturated Specimens	99
(b)    Control of Air Leakage Into or Out of Partially Saturated Specimens	99

	Page
<u>CHAPTER 11</u> <u>SUGGESTIONS FOR FURTHER RESEARCH</u>	101
11-01    SWELLING TESTS	101
11-02    SEARCH FOR CHAMBER LIQUIDS MORE SUITABLE THAN WATER	101
11-03    EFFECTS OF LEAKAGE ON PARTIALLY SATURATED SPECIMENS	102
11-04    EXPERIMENTS TO STUDY THE THEORY OF FLOW THROUGH MEMBRANES	102
11-05    ADDITIVES FOR CHAMBER WATER	103
11-06    SEARCH FOR LESS PERVIOUS MEMBRANES	103
11-07    BINDING LEAKAGE TESTS	103
11-08    TESTS ON VALVES AND FITTINGS	104
<u>CHAPTER 12</u> <u>SUMMARY</u>	105
12-01    INTRODUCTION	105
12-02    THEORY OF FLOW THROUGH RUBBER AND PLASTIC MEMBRANES	105
12-03    SUITABILITY OF CONVENTIONAL TRIAXIAL APPARATUS FOR CONTROL OF WATER LEAKAGE INTO 100% SATURATED SPECIMENS	107
12-04    SUITABILITY OF CONVENTIONAL TRIAXIAL APPARATUS FOR CONTROL OF AIR LEAKAGE INTO OR OUT OF PARTIALLY SATURATED SPECIMENS	108
12-05    PROCEDURES FOR CONTROL OF LEAKAGE IN TRIAXIAL Q AND R TESTS	109
(a)    Control of Air Leakage into 100% Saturated Specimens	109
(b)    Control of Water Leakage into Partially Saturated Specimens	109
(c)    Control of Water Leakage into 100% Saturated Specimens	109
(d)    Control of Air Leakage into or out of Partially Saturated Specimens	110
12-06    SUGGESTIONS FOR FUTURE RESEARCH	110
NOTATIONS AND DEFINITIONS	112
LIST OF REFERENCES	117
TABLES FOR MAIN TEXT	124-133
FIGURES FOR MAIN TEXT	134-145
<u>APPENDIX A</u> <u>REVIEW OF PAST LEAKAGE INVESTIGATIONS</u>	147
A-01    INTRODUCTION	147
A-02    EARLY WORK ON LEAKAGE	147
A-03    HAUSSLER AND WARLAM (1944)	148
A-04    CASAGRANDE AND SHANNON (1948)	148
(a)    General	148
(b)    Permeability of Rubber to Air	148
(c)    Permeability of Rubber to Liquids	149
(d)    Diffusion of Air through Water and Rubber	149
(e)    Permeability of Rubber to Water Vapor	149

A-05	CASAGRANDE AND WILSON (1949)	150
	(a) General	150
	(b) Flow of Water and Castor Oil through Rubber	150
	(c) Permeability of Rubber to Water Vapor	151
	(d) Diffusion of Air through Water and Rubber	151
	(e) Conclusions	152
A-06	CASAGRANDE AND WILSON (1951)	152
	(a) Diffusion of Air through Water and Rubber	152
	(b) Migration of Dissolved Molecules and Ions through Rubber	152
A-07	MORELAND (1957)	153
	(a) General	153
	(b) Flow of Water through Rubber due to a Concentration Gradient	153
	(c) Flow of Ions through Rubber due to a Concentration Gradient	154
	(d) Evaporation from Menisci	155
A-08	N. WILSON (1958)	155
	(a) Permeability of Rubber to Liquid Water	155
	(b) Flow of Water Vapor through Saran and Polyethylene	155
A-09	HIRSCHFELD (1960)	156
	(a) General	156
	(b) Permeability of Rubber to Liquid Water	156
A-10	SEED, MITCHELL AND CHAN (1960)	156
A-11	WISEMAN (1961)	157
A-12	FOST (1962)	158
A-13	WISSA (1962)	158
 <u>APPENDIX B THE FLOW OF AIR THROUGH WATER AND/OR RUBBER</u>		 160
B-01	PURPOSE	160
B-02	EQUATION OF STEADY FLOW OF AIR THROUGH WATER OR RUBBER	160
B-03	FLOW OF AIR THROUGH A COLUMN OF WATER	161
B-04	FLOW OF AIR BETWEEN TWO BUBBLES OF DIFFERENT SIZE IN A WATER MEDIUM	161
B-05	FLOW OF AIR THROUGH A LAYERED SYSTEM OF WATER AND RUBBER	162
B-06	DIFFUSION OF AIR BETWEEN SPECIMEN AND CHAMBER WATER	163
B-07	APPROXIMATE SOLUTION FOR DIFFUSION OF AIR OUT OF SPECIMEN	165
 <u>APPENDIX C SUPPLEMENTARY DERIVATIONS FOR CHAPTER 2</u>		 166
C-01	DERIVATION OF APPROXIMATION FOR HENRY'S LAW	166
C-02	EFFECT OF COMPRESSIBILITY OF WATER ON VOLUME INCREASE CAUSED BY WATER LEAKAGE INTO A 100% SATURATED SPECIMEN	167
C-03	EFFECT OF COMPRESSIBILITY OF MINERAL GRAINS ON VOLUME INCREASE CAUSED BY WATER LEAKAGE INTO 100% SATURATED SPECIMEN	168
C-04	VOLUME CHANGE CAUSED BY DEFLECTION OF MEMBRANE DUE TO CHANGES IN EFFECTIVE STRESS	168

	Page
<b>APPENDIX D</b> <b><u>MEASUREMENT OF SWELLING RATIO FOR CANYON DAM CLAY</u></b>	170
D-01    GENERAL	170
D-02    DESCRIPTION OF CANYON DAM CLAY	170
D-03    APPARATUS FOR SWELLING TESTS	171
(a)    General	171
(b)    The Triaxial Cell	172
(c)    System for Applying Chamber Pressure	173
(d)    System for Applying and Measuring Pore Pressures	173
D-04    PREPARATION OF SOIL AND COMPACTION OF SPECIMENS	174
D-05    SWELLING TEST PROCEDURE	175
(a)    Set-up of Specimen in Triaxial Cell	175
(b)    Consolidation of Specimen	176
(c)    Application of Deviator Load	176
(d)    Application of Pore Pressure Increments to Cause Swelling	176
(e)    Dismantling the Specimen	177
D-06    QUALITATIVE DISCUSSION OF METHOD FOR DETERMINING THE SWELLING CURVE THAT GOVERNS EFFECTS OF LEAKAGE	177
(a)    Discussion of Swelling Curve that Develops when Leakage occurs during an R Test	177
(b)    Procedures for Determining the Swelling Curve that Governs the Effects of Leakage (S-Curve)	177
D-07    METHOD OF INTERPRETATION OF DATA	179
(a)    General	179
(b)    Swelling Curve for Test SW22	180
D-08    DISCUSSION OF RESULTS	181
(a)    Presentation of Results	181
(b)    Variation of the Swelling Curve with the Effective Minor Principal Stress	182
(c)    Variation of the Swelling Curve with the Effective Principal Stress Ratio	183
D-09    DISCUSSION OF ERRORS	184
(a)    Temperature Fluctuations	184
(b)    Shape of Extrapolated Curve of Secondary Consolidation	185
(c)    Other Errors	185
(d)    Summary of Errors	186
D-10    SUMMARY AND CONCLUSIONS	186
<b>APPENDIX E</b> <b><u>DATA FOR WATER AND VAPOR PERMEABILITY TESTS ON MEMBRANES</u></b>	188
<b>APPENDIX F</b> <b><u>DATA FOR OSMOSIS TESTS ON NATURAL RUBBER MEMBRANES</u></b>	188
<b>APPENDIX G</b> <b><u>DATA FOR BINDING LEAKAGE TESTS</u></b>	189
<b>APPENDIX H</b> <b><u>DATA FOR TESTS ON VALVES, FITTINGS AND SARAN TUBING</u></b>	189
TABLES FOR APPENDICES	190-192
FIGURES FOR APPENDICES	193-230

LIST OF TABLES

- 2-1 Initial; Swelling Ratio of Various Soils.
- 2-2 Leakage Required to Cause 2% Decrease in Effective Stress.
- 2-3 Errors Introduced by Simplifying Assumptions.
- 3-1 Some Uses of Membranes.
- 3-2 Variables that Might Affect the Rate of Flow of Fluids through Membranes.
- 4-1 Summary of W Tests on Natural Rubber Membranes.
- 5-1 Summary of X Tests on Natural Rubber Membranes.
- 5-2 Comparison of K Values from W Tests with K Values from X Tests.
- 5-3 Comparison of Rate of Water Flow Caused by Mole Fraction Differences with that Caused by Hydraulic Pressure Differences.
- 6-1 Membranes Tested.
- 6-2 Summary of V Tests on Natural Rubber.
- 6-3 Summary of V Tests on Synthetic Rubbers and Plastics.
- 7-1 Summary of Data for Binding Leakage Tests.
- 7-2 Results of Binding Leakage Tests.
- 8-1 List of Valves Tested.
- 8-2 List of Fittings Tested.
- 8-3 Summary of Valve Leakage Tests.
- 8-4 Summary of Fitting Leakage Tests and Tests on Saran Tubing.
- 8-5 Correlation of Contact Diameter of O-Ring with Rate of Valve Leakage.
- 9-1 Maximum Acceptable Rates of Water Leakage into 100% Saturated Specimens for Decrease in Effective Stress not Exceeding 2%.
- 9-2 Rate of Water Leakage into 100% Saturated Specimen Mounted in Harvard Triaxial Cell.
- 9-3 Maximum Acceptable Air Leakage ( $J_a$ ) into Partially Saturated Specimens for Decrease in Effective Stress Not Exceeding 2%.
- 9-4 Maximum Acceptable Air Leakage ( $J_a$ ) Out of Partially Saturated Specimens for Increase in Effective Stress not Exceeding 2%.
- 9-5 Rubber and Plastic Membranes in Order of Their EK-Coefficient.
- A-1 Permeability of Natural Rubber to Air.
- A-2 Permeability of Natural Rubber to Water Vapor.
- A-3 Tests on Treated and/or Protected Membranes, Casagrande and Wilson (1949).
- A-4 Tests to Measure the Rate of Flow of Air through Water and Rubber, Casagrande and Wilson (1951).
- A-5 Flow of Ions and/or Molecules through Natural Rubber, Casagrande and Wilson (1951).
- D-1 Essential Data on Swelling Tests.
- D-2 Calculation of the Corrected Volume Change for the Data of Swelling Test SW22.
- D-3 Summary of Swelling Data.
- D-4 Initial and Final Conditions of Swelling Test Specimens.

LIST OF FIGURES

- 2-1 Schematic Representation of Air Spaces that Might Form in a Specimen that was 100% Saturated.
- 2-2 Idealized Compression and Swelling Curves of a Soil.
- 2-3 Percent Change in Total Volume versus Initial Swelling Ratio.
- 2-4 Volume of Leakage versus Percent Change in Effective Stress for 100% Saturated Specimens.
- 2-5 Notation Used for Deriving Equations in Paragraph 2-06.
- 3-1 Membrane-Permeant System.
- 3-2 Rate of Flow of Water through Wall of Capillary from a Frog's Mesentery.
- 3-3 Flow of Particles Down a Concentration Gradient.
- 3-4 Mole Fraction Gradient in Membrane During Steady Flow.
- 4-1 Apparatus for Measuring Membrane Permeability.
- 4-2 Photograph of Apparatus for Measuring Membrane Permeability.
- 4-3 Membrane Permeability Cell.
- 4-4 Photograph of Permeability Cell.
- 4-5 Details of Burette and Connecting Tubing.
- 4-6 Photograph of Water Bath.
- 4-7 W Tests on Natural Rubber, Rate of Flow versus Hydraulic Pressure Difference.
- 5-1 Apparatus to Measure Flow Caused by Mole Fraction Gradients.
- 5-2 Cell Used to Measure Flow Caused by Mole Fraction Gradients.
- 5-3 Photograph of Cell Used to Measure Flow Caused by Mole Fraction Gradients.
- 5-4 Tests X1(a) through X1(d), Rate of Flow of Water versus Mole Fraction Difference.
- 5-5 X Tests, Rate of Flow per Unit Mole Fraction Difference versus Reciprocal of Membrane Thickness.
- 6-1 V Tests on Natural Rubber, Permeability Constant versus Thickness.
- 7-1 Apparatus for Binding Leakage Tests.
- 7-2 Photograph of Binding Leakage Cell and Pedestal Containing Ceramic Disc.
- 7-3 Stainless Steel Pedestal with Porous Carbon Disc.
- 7-4 Stainless Steel Pedestal with Porous Ceramic Disc.
- 7-5 Detail of Locations where Leakage Occurs when Using O-Ring Bindings.
- 8-1 Photograph of Valves Tested.
- 8-2 Photograph of Valves Tested (Disassembled).
- 8-3 Photograph of Fittings Tested.
- 8-4 Photograph of Fittings Tested (Disassembled).
- 8-5 Apparatus for Measuring Leakage of Valves and Fittings.
- 8-6 Apparatus for Measuring Volume Change and Leakage through Walls of Saran Tubing.
- 8-7 Comparison of Rates of Leakage of Water from Ten Valves.
- 9-1 Illustration of Effect of Adding Solute to Chamber Water.
- 9-2 Mole Fraction of Sodium Chloride Required to Prevent Flow due to Hydraulic Pressure and/or Mole Fraction Differences.
- 9-3 Mole Fraction of Sucrose Required to Prevent Flow due to Hydraulic Pressure and/or Mole Fraction Differences.

Figures in Appendices

- A-1 Membrane Permeability Cell, Casagrande and Shannon (1948).
- A-2 Flow of Air through Membrane on Dummy Specimen, Casagrande and Wilson (1951).
- A-3 Effect of Adding Castor Oil-Filled Saran Tubing on Rate of Flow of Air through Membrane on Dummy Specimen, Casagrande and Wilson (1951).
- A-4 Membrane Permeability Cell Used by Wiseman (1954).
- A-5 Water Flow through Natural Rubber due to Mole Fraction Gradient, Moreland (1957).
- A-6 Water Flow through Natural Rubber due to Mole Fraction Gradient, Moreland (1957).
- A-7 Membrane Permeability Cell, N. Wilson (1958).
- A-8 Membrane Permeability Cell, Hirschfeld (1960).
- A-9 Membrane Permeability Cell, Wissa (1962).
- B-1 Partial Pressure and Concentration Gradients of Air in Water-Rubber Layered System.
- B-2 Assumed Boundary Conditions for Radial Diffusion of Air from a Cylindrical Specimen into Chamber Water.
- C-1 Model for Calculating Volume Change due to Membrane Deflection.
- D-1 Grain Size Curves, Canyon Dam Clay.
- D-2 Photograph of Triaxial Cell for Swelling Tests.
- D-3 Triaxial Cell for Swelling Tests.
- D-4 Calibration of Triaxial Cell for Swelling Tests.
- D-5 Schematic Diagram of Apparatus for Swelling Tests.
- D-6 Effect of Leakage and Secondary Consolidation on Effective Stresses during Triaxial Tests.
- D-7 Hypothetical Swelling Curves.
- D-8 Time Curves Obtained when the Effective Stress on a Soil Specimen is Decreased.
- D-9 Test SW22, Time Curves for Swelling.
- D-10 Test SW22, Time Curves for Consolidation to  $\bar{\sigma}_3 = 14.18 \text{ kg/cm}^2$ .
- D-11 Test SW22, Burette Reading versus Log Time for Last Increment of Deviator Load.
- D-12 Test SW22, Swelling Curve.
- D-13 Test No. SW1, Time Curves.
- D-14 Test No. SW2, Time Curves.
- D-15 Test No. SW3, Time Curves.
- D-16 Test No. SW4, Time Curves.
- D-17 Test No. SW5, Time Curves.
- D-18 Test No. SW6, Time Curves.
- D-19 Test No. SW7, Time Curves.
- D-20 Test No. SW8, Time Curves.
- D-21 Test No. SW9, Time Curves.
- D-22 Test No. SW10, Time Curves.
- D-23 Test No. SW11, Time Curves.
- D-24 Test No. SW12, Time Curves.

- D-25 Test No. SW13, Time Curves.  
D-26 Test No. SW14, Time Curves.  
D-27 Test No. SW15, Time Curves.  
D-28 Test No. SW16, Time Curves  
D-29 Test No. SW17, Time Curves.  
D-30 Test No. SW18, Time Curves.  
D-31 Test No. SW19, Time Curves.  
D-32 Test No. SW20, Time Curves.  
D-33 Test No. SW21, Time Curves.  
D-34 Test No. SW22, Time Curves.  
D-35 Test No. SW23, Time Curves.  
D-36 Test No. SW24, Time Curves.  
D-37 Swelling Curves for Tests in which  $\bar{\sigma}_3 = 2 \text{ kg/cm}^2$ , Canyon Dam Clay.  
D-38 Swelling Curves for Tests in which  $\bar{\sigma}_3 = 6 \text{ kg/cm}^2$ , Canyon Dam Clay.  
D-39 Swelling Curves for Tests in which  $\bar{\sigma}_3 = 14 \text{ kg/cm}^2$ , Canyon Dam Clay.  
D-40 Summary of Swelling Curves, Canyon Dam Clay.  
D-41 Semi-Logarithmic Plot of Compression and Swelling Curves for Canyon Dam Clay.  
D-42 Average Initial Swelling Ratio versus Effective Principal Stress Ratio for Canyon Dam Clay.
- E-1 Test W1, Change in Burette Reading vs Time, Natural Rubber, Water Soaked.  
E-2 Test W2, Change in Burette Reading vs Time, Natural Rubber, Water Soaked.  
E-3 Test W3, Change in Burette Reading vs Time, Natural Rubber, Water Soaked.  
E-4 Test W4, Change in Burette Reading vs Time, Natural Rubber, Oil Soaked.  
E-5 Test W5, Change in Burette Reading vs Time, Natural Rubber, Oil Soaked.  
E-6 Test W6, Change in Burette Reading vs Time, Natural Rubber, Water Soaked.  
E-7 Test W7(a), Change in Burette Reading vs Time, Natural Rubber, Water Soaked.  
E-8 Test W7(b), Change in Burette Reading vs Time, Natural Rubber, Water Soaked.  
E-9 Test W7(c), Change in Burette Reading vs Time, Natural Rubber, Water Soaked.  
E-10 Test W7(d), Change in Burette Reading vs Time, Natural Rubber, Water Soaked.  
E-11 Test W8, Change in Burette Reading vs Time, Natural Rubber, Water Soaked.  
E-12 Test V1, Volume Flow vs Time, Natural Rubber, Schmid, No Treatment.  
E-13 Test V2, Volume Flow vs Time, Natural Rubber, Schmid, No Treatment.  
E-14 Test V3, Volume Flow vs Time, Natural Rubber, Schmid, No Treatment.  
E-15 Test V4, Volume Flow vs Time, Natural Rubber, Schmid, No Treatment.  
E-16 Test V5, Volume Flow vs Time, Natural Rubber, Schmid, No Treatment.  
E-17 Test V6, Volume Flow vs Time, Natural Rubber, Schmid, Water Soaked.  
E-18 Test V7, Volume Flow vs Time, Natural Rubber, Schmid, Water Soaked.  
E-19 Test V8, Volume Flow vs Time, Natural Rubber, Schmid, Silicone Oil Soaked.  
E-20 Test V9, Volume Flow vs Time, Natural Rubber, Schmid, Silicone Oil Soaked.

- E-21 Test V10, Volume Flow vs Time, Natural Rubber, Schmid, Vacuum Pump Oil Soaked.
- E-22 Test V11, Volume Flow vs Time, Natural Rubber, Schmid, Vacuum Pump Oil Soaked.
- E-23 Test V12, Volume Flow vs Time, Natural Rubber, Schmid, Vacuum Pump Oil Soaked.
- E-24 Test V13, Volume Flow vs Time, Natural Rubber, Test Lab, No Treatment.
- E-25 Test V14, Volume Flow vs Time, Natural Rubber, Test Lab, No Treatment.
- E-26 Test V15, Volume Flow vs Time, Natural Rubber, Mahady, No Treatment.
- E-27 Test V16, Volume Flow vs Time, Natural Rubber, Mahady, No Treatment.
- E-28 Test V17, Volume Flow vs Time, Natural Rubber, Soil Test, No Treatment.
- E-29 Test V18, Volume Flow vs Time, Natural Rubber, Soil Test, No Treatment.
- E-30 Test V19, Volume Flow vs Time, Butyl Rubber (a).
- E-31 Test V20, Volume Flow vs Time, Butyl Rubber (a).
- E-32 Test V21, Volume Flow vs Time, Butyl Rubber (b).
- E-33 Test V22, Volume Flow vs Time, Butyl Rubber (b).
- E-34 Test V23, Volume Flow vs Time, Butyl Rubber (c).
- E-35 Test V24, Volume Flow vs Time, Butyl Rubber (b).
- E-36 Test V25, Volume Flow vs Time, Fluorel.
- E-37 Test V26, Volume Flow vs Time, Kel-F.
- E-38 Test V27, Volume Flow vs Time, Kel-F.
- E-39 Test V28, Volume Flow vs Time, Koroseal.
- E-40 Test V29, Volume Flow vs Time, Kynar.
- E-41 Test V30, Volume Flow vs Time, Kynar.
- E-42 Test V31, Volume Flow vs Time, Neoprene Rubber.
- E-43 Test V32, Volume Flow vs Time, Neoprene Rubber.
- E-44 Test V33, Volume Flow vs Time, Polyethylene (a).
- E-45 Test V34, Volume Flow vs Time, Polyethylene (a).
- E-46 Test V35, Volume Flow vs Time, Polyethylene (b).
- E-47 Test V36, Volume Flow vs Time, Polyethylene (b).
- E-48 Test V37, Volume Flow vs Time, Polyethylene (c).
- E-49 Test V38, Volume Flow vs Time, Polyethylene (c).
- E-50 Test V39, Volume Flow vs Time, Polyethylene (d).
- E-51 Test V40, Volume Flow vs Time, Polyethylene (d).
- E-52 Test V41, Volume Flow vs Time, Polypropylene.
- E-53 Test V42, Volume Flow vs Time, Polypropylene.
- E-54 Test V43, Volume Flow vs Time, Polypropylene.
- E-55 Test V44, Volume Flow vs Time, Polypropylene.
- E-56 Test V45, Volume Flow vs Time, Teflon.
- E-57 Test V46, Volume Flow vs Time, Teflon.
- E-58 Test V47, Volume Flow vs Time, Teflon.
- E-59 Test V48, Volume Flow vs Time, Teflon.

- E-60 Test V49, Volume Flow vs Time, Teflon.
- E-61 Test V50, Volume Flow vs Time, Texin.
- E-62 Test V51, Volume Flow vs Time, Texin.
- F-1 Test X1(a), Volume Flow vs Time,  $\Delta X = 0.0068$ .
- F-2 Test X1(b), Volume Flow vs Time,  $\Delta X = 0.0175$ .
- F-3 Test X1(c), Volume Flow vs Time,  $\Delta X = 0.0719$ .
- F-4 Test X1(d), Volume Flow vs Time,  $\Delta X = 0.0068$ .
- F-5 Test X2, Volume Flow vs Time,  $\Delta X = 0.0168$ .
- F-6 Test X3, Volume Flow vs Time,  $\Delta X = 0.0567$ .
- F-7 Test X4, Volume Flow vs Time,  $\Delta X = 0.0711$ .
- F-8 Test X5, Volume Flow vs Time,  $\Delta X = 0.0719$ .
- F-9 Test X6, Volume Flow vs Time,  $\Delta X = 0.0698$ .
- F-10 Test X7, Volume Flow vs Time,  $\Delta X = 0.0715$ .
- G-1 Test B1, Volume Flow vs Time, Group I.
- G-2 Test B2, Volume Flow vs Time, Group I.
- G-3 Test B3, Volume Flow vs Time, Group I.
- G-4 Test B4, Volume Flow vs Time, Group I.
- G-5 Test B5, Volume Flow vs Time, Group I.
- G-6 Test B6, Volume Flow vs Time, Group II.
- G-7 Test B7, Volume Flow vs Time, Group II.
- G-8 Test B8, Volume Flow vs Time, Group III.
- G-9 Test B9, Volume Flow vs Time, Group III.
- G-10 Test B10, Volume Flow vs Time, Group III.
- G-10(a) Test B10 (continued), Volume Flow vs Time, Group III.
- G-11 Test B11, Volume Flow vs Time, Group IV.
- G-12 Test B12, Volume Flow vs Time, Group IV.
- G-13 Test B13, Volume Flow vs Time, Group IV.
- G-14 Test B14, Volume Flow vs Time, Group V.
- G-15 Test B15, Volume Flow vs Time, Group VI.
- G-16 Test B16, Volume Flow vs Time, Group VI.
- G-17 Test B17, Volume Flow vs Time, Group VI.
- G-18 Test B18, Volume Flow vs Time, Group VII.
- G-19 Test B19, Volume Flow vs Time, Group VIII.
- G-20 Test B20(a), Volume Flow vs Time, Group IX.
- G-21 Test B20(b), Volume Flow vs Time, Group IX.
- G-22 Test B21, Volume Flow vs Time, Group IX.
- G-23 Test B22, Volume Flow vs Time, Group IX.
- G-24 Test B23, Volume Flow vs Time, Group X.
- G-25 Test B24, Volume Flow vs Time, Group XI.

- G-26 Test B25, Volume Flow vs Time, Group XI.
- H-1 Test No. 1(a), Volume Flow vs Time, Hoke Valve Seat.
- H-2 Test No. 1(b), Volume Flow vs Time, Hoke Valve Seat.
- H-3 Test No. 1(c), Volume Flow vs Time, Hoke Valve Seat and Bonnet.
- H-4 Test No. 2(a), Volume Flow vs Time, Hoke Valve Seat.
- H-5 Test No. 2(b), Volume Flow vs Time, Hoke Valve Seat.
- H-6 Test No. 2(c), Volume Flow vs Time, Hoke Valve Seat and Bonnet.
- H-7 Test No. 3, Volume Flow vs Time, Whitey Valve Seat and Bonnet.
- H-8 Test No. 4(a), Volume Flow vs Time, Klinger Valve.
- H-9 Test No. 4(b), Volume Flow vs Time, Klinger Valve.
- H-10 Test No. 5, Volume Flow vs Time, Klinger Valve.
- H-11 Test No. 6, Volume Flow vs Time, Klinger Valve.
- H-12 Test No. 7(a), Volume Flow vs Time, Push-Pull Valve, Harvard.
- H-13 Test No. 7(b), Volume Flow vs Time, Push-Pull Valve, Harvard.
- H-14 Test No. 8, Volume Flow vs Time, Push-Pull Valve, N. G. I.
- H-15 Test No. 9, Volume Flow vs Time, Hydromatics Valve.
- H-16 Test No. 10(a), Volume Flow vs Time, Circle Seal Valve Seat.
- H-17 Test No. 10(b), Volume Flow vs Time, Circle Seal Valve Seat.
- H-18 Test No. 10(c), Volume Flow vs Time, Circle Seal Valve Bonnet.
- H-19 Test No. 10(d), Volume Flow vs Time, Circle Seal Valve Bonnet.
- H-20 Test No. 11(a), Volume Flow vs Time, Schrader Valve.
- H-21 Test No. 11(b), Volume Flow vs Time, Schrader Valve.
- H-22 Test No. 12, Volume Flow vs Time, Snap-Tite Valve Nipple.
- H-23 Test No. 13, Volume Flow vs Time, Snap-Tite Plain Coupler.
- H-24 Test No. 14(a), Volume Flow vs Time, O-Ring Connection for Permeability Cell of Old Design.
- H-25 Test No. 14(b), Volume Flow vs Time, O-Ring Connection for Permeability Cell of Old Design.
- H-26 Test No. 15, Volume Flow vs Time, O-Ring Connection for Permeability Cell of New Design.
- H-27 Test No. 16(a), Volume Flow vs Time, O-Ring Connection for Permeability Cell of New Design.
- H-28 Test No. 16(b), Volume Flow vs Time, O-Ring Connection for Permeability Cell of New Design.
- H-29 Test No. 17(a), Volume Flow vs Time, O-Ring Connection for Binding Leakage Pedestal.
- H-30 Test No. 17(b), Volume Flow vs Time, O-Ring Connection for Binding Leakage Pedestal.
- H-31 Test No. 18, Volume Flow vs Time, O-Ring Connection of Saran Tubing to Lucite.
- H-32 Test No. 19, Volume Flow vs Time, O-Ring Connection of Saran Tubing to Stainless Steel.

- H-33 Test No. 20(a), Volume Flow vs Time, Flex Fitting on 1/8 in. O.D. Saran Tubing.
- H-34 Test No. 20(b), Volume Flow vs Time, Flex Fitting on 1/8 in. O.D. Saran Tubing.
- H-35(a) Test No. 21, Decrease of Water Volume in Burette vs Temperature, Swagelok Union.
- H-35(b) Test No. 21, Leakage of Swagelok Union.
- H-36 Test No. 22, Volume Flow vs Time, Two Epoxy Seals Between Stainless Steel and Glass Tubing.
- H-37 Test No. 23(a), Volume Change vs Hydraulic Pressure Difference, 1/8 in. O.D. Saran Tubing.
- H-38 Test No. 23(b), Volume Change vs Time Due to Change in Hydraulic Pressure Difference, 1/8 in. O.D. Saran Tubing.
- H-39(a) Test No. 23(b), Volume Change vs Log Time for  $\Delta p$  Increase from 0 to 14.0 kg/cm<sup>2</sup>, 1/8 in. O.D. Saran Tubing.
- H-39(b) Test No. 23(b), Volume Change vs Log Time for  $\Delta p$  Decrease from 14.0 to 7.0 kg/cm<sup>2</sup>, 1/8 in. O.D. Saran Tubing.
- H-39(c) Test No. 23(b), Volume Change vs Log Time for  $\Delta p$  Decrease from 7.0 to 0.0 kg/cm<sup>2</sup>, 1/8 in. O.D. Saran Tubing.
- H-40 Test No. 23(c), Evaporation Through Wall of 594 cm of 1/8 in. O.D. Saran Tubing.

## SYNOPSIS

Background and Purpose - Triaxial tests are performed in the laboratory to measure the shear strength of soil specimens. One important question that has arisen in the field of soil mechanics is: "Does the shear strength of a soil specimen change when the duration of loading of a triaxial test carried out at constant water and air content is increased from a few hours to several months?" So far this question has not been answered because of the serious experimental difficulties that arise when the duration of loading is very long. One particularly vexing difficulty is leakage of water and/or air into or out of a specimen through the membrane(s), bindings, fittings, valves, and tubing that are presently used in triaxial testing. Such leakage causes a change in effective stress which, in turn, causes a change in strength that would not otherwise occur. The purpose of this investigation was to determine how much leakage occurs, to determine whether this leakage is significant in triaxial tests that are carried out at constant water and air content, and, if so, to recommend test procedures that will permit one to perform a satisfactory test with a duration of about 100 days.

Volume of Leakage that May Be Significant - The following two cases of leakage were found to be most important (2-02): (1) Leakage of water into 100% saturated specimens and (2) leakage of air into or out of partially saturated specimens. A semi-empirical analysis was carried out to determine the volume of leakage that would cause a 2% decrease in effective stress for each case. The analysis showed that for tests on 1.4 in. diameter by 3.5 in. high specimens of soils that have a very flat swelling curve, a volume of 2 mm<sup>3</sup> of water leakage into a 100% saturated specimen (9-02) or 40 mm<sup>3</sup> of air leakage into a partially saturated specimen (9-03) could cause a 2% decrease in effective stress.

Rate of Water Leakage into 100% Saturated Specimens - Measurements were made of the rate of flow of liquid water through natural rubber membranes, which are usually used in triaxial testing, due to hydraulic pressure (Chapter 4) and osmotic pressure (Chapter 5) gradients. (Note: The permeability constant was the same regardless of which of these gradients was applied across the membrane, Chapter 5). Also, measurements were made of the rate of water leakage past the bindings of the membranes to the cap and base (Chapter 7), and from valves, fittings, and Saran tubing (Chapter 8), all of which are currently used for triaxial testing in many laboratories. A comparison of the measured rates of water leakage with the volume of leakage required to cause a 2% decrease in effective stress in 100% saturated soils, showed that for 1.4 in. diameter by 3.5 in. high specimens of soils with flat swelling curves the maximum permissible test duration is about twelve hours and, for an 'average' soil (e.g. Boston Blue clay), the maximum permissible test duration is about seven days (9-02).

Procedures for Reducing Water Leakage - For 100-day triaxial tests at constant water content, the following procedures are satisfactory, even under very critical conditions (10-01): (1) Add a solute to the chamber water. This causes a reduction in vapor pressure of the chamber water so that the average vapor pressure difference across the membrane is reduced and, therefore, the average rate of water flow is reduced. (2) Use butyl rubber membranes instead of natural rubber, because the former are about ten times better for preventing leakage than natural rubber. Attempts are presently being made to manufacture butyl membranes suitable for triaxial testing. (3) Use a specimen with as large a volume as possible. When the diameter and height of a specimen are doubled, the membrane thickness should also be doubled. If this is done, the restraint applied to the specimen by the membrane will not be changed but the change in effective stress in a given time due to water leakage will be reduced by a factor of four.

Rate of Air Leakage into or out of Partially Saturated Specimens - Using data that were reported elsewhere in the literature on the permeability of natural rubber and of water to air, rough approximations were made of the rates of air leakage (Appendix B). The tentative conclusion was reached that under the most critical conditions air leakage

will cause a 2% change in effective stress in only fifteen minutes(!) whereas in the least critical case that might be of interest, air leakage would cause a 2% change in effective stress in four days (9-03).

Procedures for Reducing Air Leakage - The following tentative procedures are proposed (10-02): (1) For the chamber fluid, use a liquid in which the solubility of air is practically negligible. Water may be used under certain conditions and mercury appears to be a promising alternative, although it introduces difficulties in the laboratory. (2) Saturate the chamber liquid with air at the average pore air pressure that is expected to develop in the specimen during a triaxial test. If this is done, air will flow in during part of the test and out during part of the test, so that little net flow will have occurred at the end of the test. (3) Use a specimen with as large a volume as possible. Doubling the volume will halve the changes in effective stress in a given time. Changing the membrane thickness does not appreciably alter the rate of air leakage. Adherence to these procedures will permit one to perform a 4-day triaxial test under the most critical conditions and a 100-day triaxial test under the least stringent conditions.

Miscellaneous Comments on Triaxial Test Procedures - Two membranes should always be used in case one is punctured. O-Ring bindings are quite suitable so long as the cap and base of the specimen are polished and greased before adding the membrane(s) and O-Rings. Most valves and fittings in general use in the drainage system of triaxial cells are satisfactory (with one important exception, 8-05) but the number of valves and fittings used should be held to an absolute minimum. The temperature of a 100% saturated specimen should be controlled to  $\pm 0.2^{\circ}\text{C}$  so that excessive changes in effective stress will not occur. For partially saturated specimens this restriction may be relaxed to  $\pm 1^{\circ}\text{C}$ . See 10-01.

Future Research - (1) Determine accurately the swelling characteristics of many 100% saturated and partially saturated soils under stress conditions identical to those existing during an R test. (2) Search for a chamber fluid more suitable than water or mercury for testing partially saturated specimens. (3) Study of the changes that occur in partially saturated specimens when air and/or water leakage occurs. See Chapter 11.

## CHAPTER 1

### INTRODUCTION

#### 1-01 GENERAL

The triaxial test is one of several types of laboratory tests used in soil mechanics to measure the shear strength of soils. Many experimental errors arise in triaxial testing which prevent the investigator from obtaining reliable results. Leakage of water or air or both from the triaxial chamber through the membrane is a particularly serious and vexing problem; one which so far has made it impossible to obtain reliable information on the loss of strength due to pore-pressure build-up when a mass of clay is subjected to shear stresses at constant water and air content over a period of several months.

Leakage affects the results of the common triaxial tests as follows:

Q TESTS\* - Leakage into a Q specimen causes a volume increase, which is accompanied by a decrease in effective stress and an increase in pore pressure. Therefore, the maximum load that can be applied to the specimen will be smaller than it would be if no leakage had occurred, i.e. the strength of the soil is decreased.

S TESTS - Leakage into an S specimen causes the level in the drainage burette to rise. Thus, if the drainage burette readings are used for volume change measurements, the measured volume decrease will be greater than the actual volume decrease of the specimen. The area of the specimen calculated from the measured volume change will be smaller than actual. Therefore, the stresses obtained by dividing the applied load by this calculated area will be larger than the real stresses in the specimen.

R TESTS - During the consolidation phase of R tests, the effect of leakage is the same as for S tests. During the axial loading phase of R tests the effect of leakage is the same as for Q tests.

The errors caused by leakage during S tests and during the consolidation phase of R tests are much smaller than the errors that develop during Q tests and during the axial loading phase of R tests. Furthermore, if the quantity of leakage is known, the errors due to leakage during S tests and during the consolidation phase of R tests are easily calculated. Therefore, these latter cases will not be considered further in this investigation.

#### 1-02 DEVELOPMENT OF INTEREST IN LEAKAGE

Interest in leakage developed within the field of soil mechanics for two principal reasons:

- (1) In about 1939, researchers became concerned with the effect of leakage on volume change measurements during (a) S tests lasting up to one month and (b) the consolidation phase of R tests (perhaps lasting up to one week).
- (2) In about 1947, researchers became concerned with the effect of leakage on the shear strength of soils as measured in long-time unconfined tests and in long-time triaxial Q and R tests. Times-of-loading up to one year were being considered.

The present investigation was stimulated by concern with the effect of leakage on the shear strength of soils as measured in long-time Q and R tests. The reasons for this concern are explained in the following paragraphs.

It is well known that the application of shear stresses to a soft normally consolidated soil at constant water content will cause the pore pressure in the soil to

---

\* The notations are explained in the section at the end of the text entitled NOTATIONS AND DEFINITIONS.

increase so that the strength of the soil will decrease (36)\*. The condition of no change in water content can occur in the field during construction if the mass of soil affected by the applied shear stresses has a great extent and has a low permeability. To obtain a value for the shear strength that can be used for design in such cases, it is important to measure the strength with no change in water content permitted. Triaxial Q or R tests are performed in the laboratory for this purpose.

One essential difference between the field conditions and the conditions of triaxial Q or R tests is that the rate-of-loading in the field may be many times slower than that used in the laboratory. For example, a highway fill might be completed in two weeks, or a dam might require a year or more for completion. On the other hand, soils tested in triaxial Q or R tests are generally failed in eight hours or less. Thus the field rate-of-loading may be fifty to several hundred times slower than the laboratory rate-of-loading. In order to determine whether this difference between the two rates-of-loading causes a significant difference in shear strength, one must perform triaxial Q or R tests with varying rates-of-loading. The fastest rate would be that normally used in the laboratory, i.e. failure achieved in about one to eight hours, and the slowest would be the same as occurs in the particular field problem of interest.

Triaxial Q and R tests performed with very slow rates-of-loading are more strongly affected by leakage than the faster tests. If the rate of leakage into a triaxial specimen is constant, then the total volume of leakage increases as the rate-of-loading is decreased. Since a larger volume of leakage causes a correspondingly larger decrease in strength, the measured strength of the soil will decrease continuously as the rate-of-loading is decreased. Therefore, before proceeding with research on the effects of very slow rates-of-loading, one must reduce leakage to a tolerable amount and find a method for calculating the decrease in effective stress (or increase in pore pressure) so that one can judge the quality of the triaxial test data.

### 1-03 DEFINITION OF LEAKAGE

Leakage in the triaxial test is defined herein as the flow of fluid into or out of the soil specimen, drainage lines or pore pressure measuring system through parts of the apparatus which should ideally be perfectly impervious. Leakage can occur through:

- (1) The membrane which confines the soil specimen.
- (2) Bindings of the membrane to the cap and pedestal.
- (3) Packings of fittings and valves.
- (4) Walls of tubing, especially plastic tubing, used in the drainage lines and pore pressure measuring system.

Only that leakage which passes directly through membranes and through properly constructed packings\*\* will be considered in this investigation. It will be shown in Chapter 2 that a rate of leakage on the order of 0.1 mm/day ( $10^{-4}$  cm<sup>3</sup>/day) into specimens with a total volume of about 90 cm<sup>3</sup> may cause appreciable changes in effective stress in triaxial Q or R tests lasting about 100 days.

The causes of leakage that are of interest in this investigation are (1) leakage due to a hydraulic pressure difference, (2) leakage due to a vapor pressure difference, and (3) leakage due to an osmotic pressure difference across a barrier. The flow caused by hydraulic or vapor pressure differences will be called permeation and the flow caused by an osmotic pressure difference will be called osmosis. Osmosis or osmotic pressure differences are caused by differences in the mole fraction of ions or molecules across a barrier. (The mole fraction of a given constituent in a solution is defined as the ratio of the number of moles of the constituent to the total number of moles in a given volume of solution.)

---

\* Numbers in parentheses refer to the corresponding numbers in the LIST OF REFERENCES at the end of the text.

\*\* Leakage through pinholes in a membrane, or through improperly packed valves is far greater than is tolerable and must be eliminated in every case.

The following items may cause volume changes of a triaxial specimen in addition to those caused by leakage and will cause errors in the results of triaxial tests if not taken into account:

- (1) Instantaneous volume changes due to pressure changes in the tubing, valves and fittings of the drainage system and/or pore pressure measuring system.
- (2) Creep of the tubing, valves and fittings.
- (3) Deformation of the membrane into the very small voids between soil grains or between the soil and the cap and base, due to changes in pore pressure and/or chamber pressure.
- (4) Compression and/or solution of air bubbles trapped in the drainage system.
- (5) Exchange of water and air between a partially saturated clay specimen and the coarse porous discs in the cap and base of the triaxial cell.

In general, only leakage is studied herein and the above items are not considered, even though in some cases the errors caused by any one of the items may be larger than those caused by leakage. However, limited data on the magnitude of items (1) and (2) are presented in Chapter 8 and item (3) is considered briefly in Appendix C.

#### 1-04 PURPOSE

The purpose of this investigation is to (1) present a rational method for calculating the changes in effective stress caused by leakage during Q tests and during the axial loading phase of R tests, (2) measure the volume of leakage that occurs when using conventional triaxial apparatus and (3) recommend procedures and apparatus for reducing leakage to a minimum.

#### 1-05 SCOPE

The scope of this investigation is as follows:

- (1) The results of past investigations of leakage in the field of soil mechanics are reviewed.
- (2) The effects of leakage on triaxial tests are evaluated by:
  - (a) Calculating the leakage required to cause a given change in effective stress during Q and R tests by using published consolidation test data.
  - (b) Measuring the leakage required to cause a given change in effective stress during triaxial R tests on 100% saturated Canyon Dam clay by means of special swelling tests.
- (3) The theory of steady flow of fluids through membranes, as determined from a search of the available literature on the subject, is presented. Applicable literature in the fields of chemistry, biology, medicine, physics and engineering was covered. The application of statistical mechanics to derive equations relating driving gradients to rates of flow, based on kinetic models of membranes, gases and/or liquids were not considered.
- (4) The necessary apparatus was constructed and measurements were made of the rate of flow of water through:
  - (a) Rubber and plastic membranes due to hydraulic, vapor and/or osmotic pressure differences across the membrane.
  - (b) O-Ring and rubber strip bindings of the membrane to the cap and pedestal due to hydraulic pressure differences across the binding.
  - (c) Packings of valves and fittings with water under pressure on the inside and room air on the outside of the valve or fitting.
  - (d) The walls of Saran\* tubing (1) with water both inside and outside of the tubing and (2) with water inside and room air outside of the tubing.
- (5) The quantity of leakage measured in (4) above is substituted into the equations developed in (2) to estimate the changes in effective stress that might be caused by leakage when using conventional triaxial apparatus.

---

\* Trade name used by Dow Chemical Co. for products made from polyvinylidene chloride resin.

- (6) Apparatus and testing procedures for reducing the leakage into or out of triaxial specimens are presented and discussed.

#### 1-06 SUMMARY OF PAST LEAKAGE INVESTIGATIONS

A detailed review of past leakage investigations is given in Appendix A. The following is a brief summary of that review.

The first reference to membrane leakage that is known to the author is in a letter by Henry Grace (50), written in 1939 to a manufacturer of membranes, expressing interest in a membrane that would pass water at a rate of less than  $0.50 \text{ mm}^3/\text{cm}^2/\text{day}$  under a hydraulic pressure difference of  $3.5 \text{ kg}/\text{cm}^2$ . (This is equivalent to a coefficient of permeability of  $0.8$  to  $2.5 \times 10^{-14} \text{ cm}/\text{sec}$  for membranes ranging in thickness from  $0.005 \text{ cm}$  to  $0.015 \text{ cm}$ .)

Investigations by Casagrande and his co-workers for the first Cooperative Triaxial Research Program (21, 22) yielded the following qualitative information: (1) Gas bubbles are sometimes observed in the drainage burettes during S tests. (2) Rubber membranes are not sufficiently impervious to water for S tests lasting 20 to 30 days. (3) Glycerine is unsuitable as a chamber fluid because water flows by osmosis out of the specimen into the glycerine.

In 1948 researchers wanted to measure the long-time strength of soils in unconfined compression tests. Therefore, measurements were made of the rate of evaporation from a soil specimen through a natural rubber membrane into room air (33).

In 1958, after a thorough study of the constant volume strength of clays, Hirschfeld (57) suggested that a comprehensive investigation of membrane leakage be made, to insure that pore pressure buildup in long-time constant volume (Q and R) tests would not be influenced by leakage. He then proceeded with an investigation of leakage through membranes (58), which was the starting point of the present study.

The results of investigations made between 1948 and 1960 on each of the following questions are summarized in succeeding paragraphs:

- (1) What causes gas bubbles to form in the burettes during S tests?
- (2) What is the rate of flow of water vapor through rubber membranes?
- (3) What is the rate of flow of water through rubber due to a hydraulic pressure gradient?
- (4) What is the rate of flow of water through rubber membranes due to an osmotic pressure (or mole fraction) gradient?

While attempting to measure the permeability of rubber to water, Casagrande and Wilson (34) found in 1949 that gas would appear on the low-pressure side of the membrane. Therefore they inserted a long, water-filled Saran tube of small diameter between the membrane and the point of application of the high-pressure air to the water over the membrane (35). This expedient was found to prevent the appearance of gas, so it was concluded that the gas observed on the low-pressure side had diffused through the membrane from the high-pressure side. Subsequent work by Wiseman (108), as analyzed in Appendix A and supported by calculations in Appendix B, indicates that the use of a two-meter length of one-sixteenth inch inside diameter Saran tubing, filled with water, will effectively stop the diffusion of air from the high to the low-pressure side.

The rate of evaporation of water through natural rubber was measured during two investigations (33, 34). In the first investigation (33) it was found by Casagrande and Shannon that the natural rubber membranes tested were effective for preventing evaporation for "short periods of time." In the second (34) it was found by Casagrande and Wilson that a single natural rubber membrane (about  $0.012 \text{ cm}$  thick) was not effective for preventing evaporation from a soil specimen into room air for tests lasting up to two weeks. (The results of the present investigation indicate that one  $0.012 \text{ cm}$  thick natural rubber membrane would be satisfactory for preventing excessive evaporation during unconfined tests on 100% saturated specimens of Boston Blue clay with a volume of  $90 \text{ cm}^3$ , so long as the duration of loading is less than one hour.)

Between 1947 and 1960 six attempts were made to measure the rate of flow of water through natural rubber membranes due to hydraulic pressure gradients (33, 34, 35, 107, 58, 108). None of these attempts was successful because one or more of the following deficiencies existed in the apparatus and procedure used: (1) Temperature control was not used. (2) The burettes used for measuring volume changes were not of sufficiently small diameter. (3) Evaporation from the burettes was not prevented. (4) The apparatus was made of lucite, which absorbs excessive quantities of water. (5) No attempt was made to prevent diffusion of air from the high to the low-pressure side. (6) The volume of the apparatus could change with time due to creep, so that the volume flow measurements could be appreciably in error. (7) The tests were not continued for a sufficiently long period to define a straight-line relation between volume flow and time. (8) The thicknesses of the membranes tested were not reported.

Attempts were made to measure the rate of osmosis of water through natural rubber in 1957 (75) and through silicone rubber in 1961 (48). The tests were performed by measuring the rate of flow of pure water through the membrane into a 0.5 molar solution of sodium chloride (i.e. about the same as the concentration of salts in sea water). The measured rate of flow was about  $0.4 \text{ mm}^3/\text{cm}^2/\text{day}$  in both cases. The quality of these data cannot be evaluated since the thicknesses of the membranes tested were not reported. However, the data did indicate that further research was necessary on the rate of flow caused by osmotic pressure gradients.

In summary, the results of past leakage investigations were useful in that the major factors causing leakage were isolated and the main causes of error in permeability tests on membranes were pointed out. However, there was a conspicuous absence of (1) ideas or quantitative data on how much effect a given quantity of leakage will have on the results of triaxial tests, (2) reliable data on the permeability of rubber to water, and (3) data on leakage through fittings on the triaxial cell and through bindings of the membrane to the cap and base.

## CHAPTER 2

### ANALYSIS OF EFFECTS OF LEAKAGE IN TRIAXIAL TESTS

#### 2-01 GENERAL

The principal purposes of this chapter are (1) to derive an equation relating the volume of water\* leakage to the change in effective stress in a 100% saturated Q or R specimen and (2) using this equation, to determine the magnitude of leakage that is important in triaxial Q and R tests. Water leakage into partially saturated specimens is indicated to be less critical than water leakage into 100% saturated specimens.

The changes in effective stress that might be caused by air leakage into 100% saturated or partially saturated specimens are discussed, and an approximate equation relating the volume of air leakage to the change in effective stress in partially saturated specimens is derived.

The volume of leakage that actually occurs during a triaxial test is not discussed in this chapter, but is discussed in Chapter 9, after data on leakage through membranes, bindings, fittings, and valves have been presented.

The changes in effective stress due to leakage will be expressed in terms of the ratio of the change in effective stress  $\Delta\bar{\sigma}$  to the effective stress  $\bar{\sigma}$  that existed in the soil prior to the start of leakage. This ratio usually will be expressed in percent, i.e.  $100 \times \Delta\bar{\sigma}/\bar{\sigma}$ , and it will be called the "percent change (increase or decrease) in effective stress."

The decrease in effective stress caused by leakage into a Q or R specimen is numerically greater than the increase in effective stress caused by an equal volume of leakage out of a specimen. Therefore, in most cases it will be necessary to study only the case of leakage into the specimen, in which case the percent change in effective stress will be a negative quantity.

The derivation of equations relating the volume of leakage to the change in effective stress will proceed as follows:

- (1) A qualitative description will be presented of the effects of water and/or air leakage into 100% saturated and partially saturated soil specimens (2-02).
- (2) An equation will be presented relating the volume increase of a soil specimen to the simultaneous decrease in hydrostatic effective stress (2-03).
- (3) Equations will be derived relating the volume of leakage to the volume change of a specimen (2-05, 2-06).
- (4) The equations from (3) will be substituted into the equation from (2) to obtain the desired relationships.

A discussion of the simplifying assumptions used in the derivation of the equations in this chapter is given in 2-07. A summary of these equations and their limitations is given in 2-08.

#### 2-02 QUALITATIVE DESCRIPTION OF EFFECTS OF LEAKAGE ON TRIAXIAL SPECIMENS

##### (a) General

This discussion will provide the necessary background for deriving equations relating the change in total volume of a specimen to the volume of leakage of water and/or air. The following two laws will be used:

---

\* The term "water" is used herein to refer to pure liquid water which contains neither dissolved nor undissolved air.

Boyle's law relates the volume change of an ideal gas to the pressure of the gas at constant temperature. It will be assumed that air behaves as an ideal gas and that the soil specimen remains at constant temperature while leakage occurs. Hence

$$u_a \cdot V_a = \text{constant} \quad (2-1)$$

where  $u_a$  = pore air pressure (absolute).  
 $V_a$  = volume of air in the soil specimen.

Henry's law states that at equilibrium, the pressure in a gas over a dilute solution of the gas in a liquid is directly proportional to the mole fraction of the gas in solution. (The mole fraction is the ratio of the number of moles of one component in a solution to the total number of moles of all components in the solution.) Hilf (56) has used the following approximation to Henry's law (see Appendix C for derivation), which is convenient for use herein:

$$V_{ad} = s V_w \quad (2-2)$$

where  $V_{ad}$  = volume of dissolved air, measured at the pressure,  $u_a$ , of the undissolved air in the soil voids.  
 $s$  = solubility of air in water (a dimensionless ratio which is a function of temperature).  
 $V_w$  = volume of water in which the air volume  $V_{ad}$  is dissolved.

It will be assumed in all cases that changes in a specimen take place slowly enough so that equilibrium is reached between the dissolved and undissolved air, in which case the volume of air dissolved in a given volume of water can be calculated from Eq. 2-2. The solubility  $s$  of air in water varies with pressure and temperature. The variation with pressure is small and is discussed in 2-07. The variation with temperature is summarized in the following tabulation:

T(°C)	20	22	24	26	28	30
s*(-)	0.0201	0.0194	0.0189	0.0184	0.0179	0.0173

(b) Water Leakage into 100% Saturated Specimens

Assume that a soil specimen which is enclosed in a rubber membrane is consolidated in a triaxial chamber, using water as the chamber fluid, to an effective stress  $\bar{\sigma}_3$  and that a pore water pressure  $u_w$  is applied to increase the degree of saturation to 100%. Assume further that all drainage valves are closed after consolidation is complete, that the rate of secondary consolidation is zero, that the temperature is maintained constant, and that water leaks into the specimen while the axial load and the chamber pressure are both maintained constant. Under these conditions water leakage into the specimen will cause the total volume and the pore water pressure to increase and the effective stress to decrease. Strictly speaking, the net increase in total volume is equal to (1) the volume of water leakage minus (2) the volume change of the pore water, minus (3) the volume change of the mineral grains, plus (4) the volume change within the membrane because of the outward deflection of the membrane, due to the increased pore water pressure. It is shown in Appendix C that for fine-grained soils the quantities (2), (3) and (4) are generally negligible relative to the volume of water leakage. Therefore, for subsequent discussions and derivations the increase in total volume of a 100% saturated soil due to water leakage will be assumed to be equal to the volume of water leakage.

---

\* The values of  $s$  give the volume of air (freed of CO<sub>2</sub> and NH<sub>3</sub> and measured at atmospheric pressure and the temperature T) dissolved in a unit volume of water when the pressure in the atmosphere over the water, i.e. air pressure plus water vapor pressure, is 760 mm Hg. Values were calculated from data presented in ref. 59.

(c) Distribution of Air in Partially Saturated Specimens

Prior to studying the effect of leakage of air and/or water into 100% saturated or partially saturated specimens, one must consider the following possible forms in which the air might be distributed within the voids of a partially saturated soil specimen:

- (1) Bubbles that are smaller than or equal in size to the largest sphere that can be inscribed in a void.
- (2) Air spaces that are bounded by soil grains and by air-water menisci between soil grains. Such air spaces may fill one void or they may extend over several voids and contain trapped water within.
- (3) Connected air spaces, i.e. air spaces that are connected with each other throughout the specimen.
- (4) Combinations of the above.

Assume first that the soil air exists in the form of bubbles. They could be formed in soil specimens in at least the following two ways: (1) If back pressure is used to increase the degree of saturation of a specimen to 100% and then the back pressure is released, air will come out of solution. This air may appear in the form of many bubbles of varying size, depending on the local concentration of air in the pore water. (2) During sampling of a soil that exists well below the water table, the pore water pressure is decreased. Thus air or other gases that may be present will come out of solution and may form bubbles as above in (1). In both examples the quantity of gas released from solution may be great enough to form air spaces rather than to persist as spherical bubbles.

If a soil specimen contained a great many minute bubbles, would such a distribution be stable? Assuming that all water in the specimen is interconnected and that the pore water pressure is constant throughout the specimen, then the air pressure inside each bubble  $u_{ab}$  must be inversely proportional to the bubble diameter  $d_b$ , i.e.  $u_{ab} = 3/d_b$ , where  $d_b$  is in microns and  $u_{ab}$  is in  $\text{kg/cm}^2$  (see 20, p. 49). Thus the partial pressure difference between all bubbles of different size will cause diffusion of air through the water from the smaller bubbles to the larger bubbles. Diffusion would continue until either (1) all bubbles have reached the same size, or (2) until the larger bubbles expand and form air spaces. At equilibrium, the pressure in all such air spaces must be equal, so that the radius of curvature of all menisci also must be equal. The possibility that the air would achieve state (1) above is extremely unlikely since such a condition could only develop if all bubbles achieve the same diameter simultaneously. Thus, it appears likely that the air in a partially saturated soil exists in the form of many connected or unconnected air spaces.

It is now of interest to determine the time required to achieve the equilibrium state if a soil specimen initially contains a great number of minute bubbles. Since, at present, only fine-grained soils are of major interest in long-time triaxial testing, consider a soil such as Canyon Dam clay (see Appendix D for a description of this soil) which consists of about 20% by weight of sizes smaller than two microns. Assume that two bubbles exist with diameters of one micron and one-half micron and that they are one centimeter apart. In Appendix B-04 it is shown that it would take about seven minutes for practically all air from the smaller bubble to be transferred to the larger bubble. If the smaller of these two bubbles had a diameter of 0.75 microns, it would take about thirty minutes to transfer practically all air from one to the other bubble. The spacing of bubbles in an actual soil must be much less than one centimeter. For example, at a degree of saturation of 99%, assuming that each bubble fills 50% of the void it occupies, an average of one out of fifty voids must contain a bubble. Thus each pair of bubbles would be separated by about four ( $\sqrt[3]{50}$ ) voids containing no bubbles. Based on these considerations, it seems likely that air bubbles will not exist as stable entities in

fine-grained partially saturated specimens over periods greater than a few hours. Therefore, in subsequent discussions of air leakage, it will be assumed that the air in a specimen exists in the form of unconnected or connected air spaces. This view is consistent with that previously presented by Hilf (56).

(d) Air Leakage into 100% Saturated Specimens

In Appendix A-11, very good evidence is presented to show that air leakage into 100% saturated specimens can be reduced to negligible values. Thus it is not important to provide equations with which one may calculate the decrease in effective stress caused by air leakage for this case. The following theoretical discussion is presented only to emphasize that air leakage should be prevented, and to give plausible reasons for this requirement. The discussion is confined to the case of a fine-grained soil such as Boston Blue clay or Canyon Dam clay.

Consider a 100% saturated soil specimen that is consolidated in a triaxial chamber in the same manner as described previously in (b). Assume that the drainage valves are closed at the completion of consolidation, that there is no secondary consolidation, that the temperature is maintained constant, that the axial load and chamber pressure are maintained constant, and that no water leakage occurs. Assume further that the pore water is saturated with air at the pore water pressure  $u_w$ , i.e.  $u_a = u_w$ , and that the chamber water is saturated with air at a pressure  $u_{ac}$  which is equal to the chamber pressure  $\sigma_c$ . Thus,  $u_a < u_{ac}$  so that air will flow from the chamber water through the membrane into the pore water. In time, the pore water near the membrane will become saturated with air at a pressure greater than the pore water pressure, i.e.  $u_a > u_w$ , but  $u_a$  must still be smaller than  $u_{ac}$ .

The question now arises: "Will air come out of solution in the specimen?" It can be shown that if Boyle's and Henry's laws are valid in the fine pores of the soil, then bubbles of somewhat larger diameter than  $3/(u_a - u_w)$  microns (where  $u_a$  and  $u_w$  are given in  $\text{kg/cm}^2$ ) are stable if they come out of solution\*. The conditions required to cause such bubbles to come out of solution, e.g. sufficiently large voids, points of nucleation for the bubbles, vibration of the specimen, etc., are not known. However, for the purpose of making a conservative estimate of the effects of air leakage, it will be assumed that such bubbles do form. Two preliminary tests to be described below indicate that, for a compacted soil, this assumption is valid.

Assuming a bubble has formed, the pressure in the bubble will be less than pressure at which the chamber water is saturated with air,  $u_{ac}$ . Therefore more air will diffuse into the bubble and it will increase in diameter until it starts to be deformed by the narrow openings between soil grains. Menisci would then form between soil grains and the radius of curvature of the menisci would decrease until it became equal to  $3/(u_{ac} - u_w)$  microns, at which time the pressure in the bubble would be equal to  $u_{ac}$ . Since the pressure in the bubble and the pressure at which the chamber water is saturated with air would be equal, the flow of air from the chamber into this bubble would cease. At this stage the air might be distributed in a specimen as shown in Fig. 2-1.

The above process of bubble formation and expansion to fill a void and form an air space would be repeated in interior pores and the degree of saturation of the specimen gradually would decrease. As each bubble is formed and increased in size, water would be forced out of the void containing the bubble into adjacent voids, so that the soil grains would move apart, i.e. the water content of the adjacent zones of the specimen would increase. Assuming a unique relationship between water content and effective stress, the effective stress in the specimen would decrease.

---

\* It is assumed that a bubble can exist only if the pressure, at which the pore water surrounding the bubble is saturated with air, is equal to or greater than the pressure in the bubble. Also, it is likely that the voids in the specimen must be at least large enough to contain such bubbles. If not, bubbles probably would not form.

On the basis of the above argument, it is tentatively concluded that air leakage from the chamber into a 100% saturated triaxial specimen should be prevented. It is evident that the assumptions made in the argument must be checked experimentally. The main assumptions are: (1) Henry's law is valid in the fine pores of a soil specimen, (2) Boyle's law is valid in the fine pores of a soil specimen, (3) if the pore water becomes supersaturated with air (as determined from Henry's law) bubbles will come out of solution in the voids.

In an attempt to obtain direct evidence on the effect of air leakage into 100% saturated specimens, Mr. Charles Osgood performed the following tests: Two pairs of identical specimens of compacted Canyon Dam clay were consolidated in a triaxial chamber for two days under a chamber pressure of 14 kg/cm<sup>2</sup> and a back pressure on the pore water of 6 kg/cm<sup>2</sup>, which was sufficient to cause 100% saturation. Water was used as the chamber fluid during the consolidation phase. After two days of consolidation, the chamber water was carefully replaced by air in two of the tests. The dial reading, drainage burette reading, back pressure and chamber pressure did not change during this replacement. For the first pair, the drainage valves were closed after replacement was complete and, for the second pair, they were closed before starting replacement. The chamber pressure then was maintained constant for two more days, after which the axial load was increased to failure. For the first pair of tests, the strength of the specimen in the test with air as the chamber fluid was 20% less and for the second pair it was 35% less than in the test with water as the chamber fluid. These tests confirm the conclusion that the effective stress in a 100% saturated compacted specimen is decreased by leakage of air into the specimen\*. The author believes that air actually came out of solution within the specimen to cause this effective stress decrease.

The replacement of water by air in the second pair of the above tests was accomplished in about fifteen minutes. After fifteen minutes more had elapsed, the vertical dial readings began to show an increase in length of the specimen. This gives some indication of the time required for the air to permeate the membrane and come out of solution inside the membrane. Data presented by Metschl (71) roughly confirm the possibility that about ten minutes would be required for air to come out of solution, even if the water is first supersaturated with air at pressures six times greater than the pore water pressure.

Additional evidence that air comes out of solution in a specimen after it passes through the membrane is offered by the observation of many investigators (21, 35, 90) that air bubbles form in the drainage burette of a triaxial specimen when water is used as a chamber fluid with air above the water in the triaxial chamber. In ref. 90 it is stated specifically that the dummy specimen used had been saturated prior to determining the rate of air flow, and yet air did come out of solution. It seems likely that even if the drainage valves had been closed in this case, air would have come out of solution (although its volume would have been smaller because the pore pressure would have increased) and the effective stress on the specimen would have decreased. In all of these cases, the volume of air passing the membrane apparently was not detectable for at least two days, probably because of the resistance to diffusion of air offered by the chamber water.

#### (e) Air Leakage into Partially Saturated Specimens

Consider a partially saturated soil specimen that is consolidated in a triaxial chamber under a chamber pressure  $\sigma_c$  using water as the chamber fluid. It is assumed that: (1) the chamber water is saturated with air at the chamber pressure, i.e.  $u_{ac} = \sigma_c$ , (2) the pore water of the specimen is connected throughout and has a pressure  $u_w$ , (3) the undissolved air exists as connected or unconnected air spaces, at a pressure  $u_a$ , which is larger than  $u_w$  and smaller than  $u_{ac}$ , and (4) the test is performed slowly enough so that the pore air pressure, the pore water pressure and hence, the

---

\* These tests also indicate that the rate of decrease in effective stress due to air leakage, when air is used as a chamber fluid, is far greater than the rate of decrease in effective stress when water is used as the chamber fluid.

radius of curvature of the air-water menisci, are constant throughout the specimen. These menisci must support the pressure difference ( $u_a - u_w$ ). Under these conditions, the pore water must be saturated with air at the pressure  $u_a$  in the gas phase, as required by Eq. 2-2.

Air will now flow into the specimen through the membranes under the influence of the pressure difference ( $u_{ac} - u_a$ ). One can visualize two extreme conditions that might develop as the air enters the specimen. (1) The menisci may increase in curvature without moving in the voids. (2) The menisci may not change in curvature but they simply may move through the voids and permit the volume occupied by the undissolved air to increase.

For condition (1) the pore water pressure would not change significantly because the volume increase of the specimen required to permit the increased curvature of all menisci is probably very small. Thus only the pore air pressure would increase. For specimens with a degree of saturation of about 85% or higher, the increase in pore air pressure would be much larger numerically than the decrease in effective stress in the specimen. On the other hand, for condition (2), the increases in pore air pressure and pore water pressure would be equal to each other, so that the decrease in effective stress must be numerically equal to the increase in pore air pressure. In reality air leakage probably causes a decrease in effective stress which lies between the decrease that would be calculated for conditions (1) and (2). Since at the present stage of knowledge it is not possible to calculate the changes that actually occur, and since condition (2) gives a conservative (i.e. high) estimate of the decrease in effective stress, only condition (2) will be considered. The equation relating the volume of air leakage to the decrease in effective stress is derived in 2-06.

#### (f) Water Leakage into Partially Saturated Specimens

Considering the same specimen as described in paragraph (e), again two extreme conditions can be visualized. (1) The menisci may decrease in curvature, so that the volume of undissolved air does not change significantly, but the volume of the specimen would increase by an amount equal to the volume of water leakage. (2) The menisci may not change in curvature, but they may simply move through the voids and permit the volume occupied by the undissolved air to decrease.

The decrease in effective stress caused by a given volume of water leakage for condition (1) is somewhat less than would occur due to leakage into a 100% saturated specimen, because the pore water pressure would increase with no substantial increase in pore air pressure.

For condition (2), the increases in pore air and pore water pressure must equal each other, so that the concomitant decrease in effective stress would be numerically equal to the increase in pore water pressure. The decrease in effective stress caused by a given volume of water leakage would be much greater for condition (1) than for condition (2), and the actual case probably lies between these two extremes. Since it is not possible at present to calculate the actual change in effective stress, the conservative assumption will be made that water leakage into 100% saturated specimens causes the same decrease in effective stress as an equal volume of water leakage into partially saturated specimens, in which case the equation to be derived in 2-05 would be applicable.

### 2-03 RELATION BETWEEN VOLUME CHANGE AND CHANGE IN EFFECTIVE STRESS

Consider a soil specimen that is fully consolidated in a triaxial chamber to an hydrostatic effective stress  $\bar{\sigma}_3$  and a void ratio  $e$  as shown in Fig. 2-2. All drainage valves are now closed. When water and/or air enter the specimen in this condition, its volume will normally increase\* along the swelling curve as shown. One will seldom be concerned with volumes of leakage that are sufficient to cause a decrease in effective

---

\* One exception occurs when air enters a specimen that is 100% saturated with de-aired water.

stress,  $\Delta\bar{\sigma}_3$ , greater than about 5% of  $\bar{\sigma}_3$ . Thus only the initial portion of the swelling curve will be of interest in all subsequent discussions of the effects of leakage. Assuming the initial portion of the swelling curve to be a straight line, its slope  $b_0$  is given by

$$b_0 = - \frac{\Delta e}{\Delta\bar{\sigma}_3} \quad (2-3)$$

The change in total volume of a specimen is related to the change in void ratio by the equation

$$\frac{\Delta V}{V} = \frac{\Delta e}{1+e} \quad (2-4)$$

Substituting Eq. 2-4 into Eq. 2-3 gives

$$\frac{\Delta V}{V} = - \frac{b_0}{1+e} \Delta\bar{\sigma}_3 = - \frac{b_0 \bar{\sigma}_3}{(1+e)} \frac{\Delta\bar{\sigma}_3}{\bar{\sigma}_3} \quad (2-5)$$

Where the quantity  $\Delta V/V$  expressed in percent is the percent volume change and the quantity  $\Delta\bar{\sigma}_3/\bar{\sigma}_3$  expressed in percent is the percent change in effective stress.

For convenience, the quantity  $(b_0\bar{\sigma}_3/(1+e))$  will be designated by the letter  $S$  and will be called the "initial swelling ratio." Thus Eq. 2-5 becomes

$$\frac{\Delta V}{V} = -S \frac{\Delta\bar{\sigma}_3}{\bar{\sigma}_3} \quad (2-6)$$

The initial swelling ratio is a dimensionless parameter that may be assumed constant as a first approximation\*. It is equal to the absolute value of the slope of the swelling curve if the curve is plotted in terms of the dimensionless variables  $\Delta V/V$  versus  $\Delta\bar{\sigma}_3/\bar{\sigma}_3$ . It should be noted that a small volume increase will cause a large decrease in effective stress in soils with low swelling ratios.

Eq. 2-6 was derived for the case of leakage into a specimen. If there is leakage out of a specimen, then the swelling ratio must be replaced by the compression ratio,  $C$ , which is a dimensionless parameter equal to the absolute value of the slope of the compression curve plotted in terms of  $\Delta V/V$  versus  $\Delta\bar{\sigma}_3/\bar{\sigma}_3$ .

## 2-04 DETERMINATION OF THE SWELLING RATIO

### (a) General

For the derivation of Eq. 2-6 it was assumed that swelling is accomplished in a triaxial cell by starting from a hydrostatic effective stress and then reducing this stress to cause swelling. However, during axial loading in a triaxial Q or R test, the axial stress is larger than the lateral stress. Thus the swelling ratio applicable for Q and R specimens could be different from the swelling ratio measured by starting from a hydrostatic effective stress. In order to measure the swelling ratio that can be used for calculating the effects of leakage on Q and R specimens, it is necessary to perform the following special swelling tests, which duplicate as nearly as possible the stresses on a specimen during a Q or R test: (1) Consolidate a specimen in a triaxial chamber as for an R test; (2) apply an axial load equal to say 50% of the failure load and measure the pore pressure that develops; (3) wait until the pore pressure comes to equilibrium under the axial load; (4) increase the pore pressure in several small steps and measure the volume of swelling that occurs during each step; (5) plot the swelling curve in

\* The only data known to the author with which one can judge the constancy of the initial swelling ratio with changes in  $\bar{\sigma}_3$  were obtained during this investigation and are presented in Appendix D. The data show a 50% increase of  $S$  for Canyon Dam clay for a seven-fold increase of  $\bar{\sigma}_3$ .

terms of  $\Delta V/V$  versus  $\Delta \bar{\sigma}_3/\bar{\sigma}_3$  and measure its slope. Steps (1) - (5) may be repeated, applying several different consolidation pressures and several different percentages of the failure load prior to the start of swelling, to determine the effects of these two variables on the swelling ratio.

(b) Special Swelling Tests on Canyon Dam Clay

A series of twenty-four of the above described special swelling tests was performed on compacted Canyon Dam clay and the results are reported in Appendix D. Canyon Dam clay was used in these tests because this clay has a very low swelling ratio. By determining the volume of leakage that is acceptable during long-time Q and R tests on Canyon Dam clay (see 2-05), one obtains a lower limit for the volume of leakage that is significant during triaxial tests for most soils.

The initial swelling ratio for Canyon Dam clay was found to range between 0.0010, at an effective consolidation pressure of 2.0 kg/cm<sup>2</sup>, and 0.0015, at an effective consolidation pressure of 14.0 kg/cm<sup>2</sup>. These values are listed in Table 2-1. Also, the results showed that the swelling ratio for Canyon Dam clay is independent of the axial load on the specimen\*. This means that the swelling ratio measured by starting from a hydrostatic effective stress is approximately the same as the swelling ratio measured by starting with an axial load on the specimen. Therefore, in the following discussions, the notation S will be used to designate the initial swelling ratio that is obtained by reducing the effective stress equally in all directions, regardless of the ratio of the axial to lateral effective stress on the specimen at the start of swelling.

Although considerable care was used in carrying out these special swelling tests, the data still showed erratic variations that caused the swelling ratio to be accurate only to within plus or minus 25%. This error was due largely to the effect of relatively small (less than 0.5°C) temperature variations in the laboratory during the period of swelling.

(c) Swelling Ratio Obtained from One-Dimensional Consolidation Tests

The above swelling ratios for Canyon Dam clay are the only values known to the author that are sufficiently accurate to calculate, even approximately, the effects of leakage on triaxial Q and R specimens. However, it is possible to obtain a rough estimate of S from the rebound curves of the many one-dimensional consolidation tests that are available in soil mechanics literature. Such swelling ratios are based on the equation

$$\frac{\Delta V}{V} = - S_c \frac{\Delta \bar{\sigma}_1}{\bar{\sigma}_1} \quad (2-7)$$

where  $S_c$  = swelling ratio obtained from the initial slope of the rebound curve of a one-dimensional consolidation test.  
 $\bar{\sigma}_1$  = effective major principal stress on specimen at the start of swelling in a one-dimensional test.

The value of  $S_c$ , which is the absolute value of the initial slope of the rebound curve plotted in terms of  $\Delta V/V$  versus  $\Delta \bar{\sigma}_1/\bar{\sigma}_1$ , may also be calculated from the equation

$$S_c = \frac{C_{so}}{(1+e) \ln 10} \quad (2-8)$$

---

\* The lack of any dependence of the swelling ratio on the axial load probably is explained by the low sensitivity of this clay to shear strains. The swelling ratio for normally consolidated, undisturbed clays may show a marked dependence on the axial load.

where the initial swelling index  $C_{s0}$  is equal to the change in void ratio, on a semi-logarithmic plot of the swelling curve, that is obtained by extrapolating the initial slope of the curve over an entire log cycle decrease in effective stress.

The initial swelling ratio  $S_c$  should be lower than  $S$  since swelling occurs in only one direction in the one-dimensional test. On the other hand, the first data point on a swelling curve from a one-dimensional consolidation test usually is obtained by reducing the load on the specimen to one-half or one-quarter of its initial value. Therefore the initial slope of the swelling curve is poorly defined at best and probably leads to an over-estimate of the initial swelling ratio. Thus the differences between the results of special swelling tests and conventional one-dimensional consolidation tests tend to balance each other.

It is believed that in most cases, the initial swelling ratio  $S_c$  will be greater than the initial swelling ratio  $S$ , but that it will at least be within a factor of five greater or smaller than  $S$ . Values of  $S_c$  were obtained by the author from published swelling curves for many soils and these are listed in Table 2-1. They will be used in 2-05 as rough approximations for  $S$  when estimating the effects of leakage on soils for which accurate swelling data are not presently available.

#### 2-05 EFFECT OF WATER LEAKAGE ON 100% SATURATED SPECIMENS

The decrease in effective stress due to the volume of water leakage  $J_w$  may be calculated from Eq. 2-6 as follows:

$$\frac{\Delta V}{V} = \frac{J_w}{V} = -s \frac{\Delta \bar{\sigma}_3}{\bar{\sigma}_3} \quad (2-9)$$

According to Terzaghi's principle of effective stress for 100% saturated specimens, the change in pore water pressure  $\Delta u_w$  is equal but opposite in sign to the change in effective stress  $\Delta \bar{\sigma}_3$ . Therefore

$$\frac{\Delta V}{V} = \frac{J_w}{V} = s \frac{\Delta u_w}{\bar{\sigma}_3} \quad (2-10)$$

The ratio  $\Delta u_w / \bar{\sigma}_3$ , expressed in percent, will be referred to as the "percent change (increase or decrease) in pore pressure." If leakage causes an increase in pore pressure, which is equivalent to a decrease in effective stress, the strength of the specimen will be reduced.

Eq. 2-9 may be evaluated using Fig. 2-3. If one knows the volume increase caused by leakage into a soil specimen and the swelling ratio for that soil, the resulting decrease in effective stress may be determined. Conversely, by specifying the upper limit of the ratio  $\Delta \bar{\sigma}_3 / \bar{\sigma}_3$ , one can determine from Fig. 2-3 the maximum acceptable volume increase of a specimen due to leakage.

Fig. 2-4 is presented to illustrate for several clays the volume of leakage that may be objectionable when performing triaxial tests on 1.4 in. diameter by 3.5 in. high soil specimens that are 100% saturated. The lines shown in the figure are straight simply because it was assumed that the swelling curves of all soils are straight lines over the range of effective stress of interest herein (i.e. up to  $\Delta \bar{\sigma}_3 / \bar{\sigma}_3 = 10\%$ ). It should be recalled that the soils represented by the swelling ratios in the figure may actually have swelling ratios that are as much as plus 500% or minus 80% different from the values shown (except for the case of Canyon Dam clay, for which  $S$  is within plus or minus 25%). However, if a soil is found to have the swelling ratio shown, the volume of leakage for a given percent change in effective stress may be obtained from the figure.

In judging the suitability of various triaxial test procedures, it will be assumed herein that the maximum decrease in effective stress must be limited to 2%. To limit the percent decrease in effective stress to less than 2% in a specimen with a total volume of 90 cm<sup>3</sup>, one cannot accept more than about 50 mm<sup>3</sup> (0.05 cm<sup>3</sup>) of leakage, even for a highly swelling material such as Bearpaw Clay-Shale. However, for a soil with a low

swelling ratio, such as Canyon Dam clay, the maximum acceptable leakage for 2% decrease in effective stress is only  $2 \text{ mm}^3$ . For tests of long duration, the acceptable rate of leakage is very small, as can be seen from Table 2-2. The maximum acceptable rate of leakage for 100-day tests with 2% error is only  $0.02 \text{ mm}^3/\text{day}$  for materials with a low swelling ratio such as Canyon Dam clay.

## 2-06 EFFECT OF AIR LEAKAGE ON PARTIALLY SATURATED SPECIMENS

### (a) Derivation of Equation Relating Change in Effective Stress to Volume of Air Leakage

An equation is derived relating the volume of leakage of air into a partially saturated triaxial specimen to the resulting decrease in effective stress. The steps in the derivation are outlined in 2-01 and the qualitative discussion of the effect of air leakage is given in 2-02(e). For convenience, the notation used in the derivation is assembled in Fig. 2-5.

The change in total volume,  $\Delta V$ , of a partially saturated specimen due to air leakage is equal to the change in volume of undissolved air  $\Delta V_{au}$ . The increase in volume of undissolved air is the difference between the final and initial volumes of undissolved air

$$\Delta V = \Delta V_{au} = V'_{au} - V_{au} \quad (2-11)$$

where  $V'_{au}$  = volume of undissolved air in the specimen after leakage has occurred, measured at the final pore air pressure.

$V_{au}$  = volume of undissolved air before leakage, measured at the initial pore air pressure.

A positive sign is used to denote volume increase and leakage into the specimen. The initial volume of free air,  $V_{au}$ , may be calculated from the total volume,  $V$ , the porosity,  $n$ , and the degree of saturation,  $G_w$ , of the specimen. The volume  $V'_{au}$  is determined by first calculating the total volume of air present in the final state,  $V'_{at}$ , and then subtracting the volume of air which is dissolved in the pore water in the final state,  $V'_{ad}$ . Thus:

$$V'_{au} = V'_{at} - V'_{ad} \quad (2-12)$$

The total volume of air present in the final state,  $V'_{at}$ , is the sum of:

- (1) The volume of undissolved air in the initial state,  $V_{au}$ , but compressed according to Boyle's law to the final pore pressure  $u'_a$ .
- (2) The volume of dissolved air in the initial state,  $V_{ad}$ , but compressed according to Boyle's law to the volume it would occupy at the pressure  $u'_a$ .
- (3) The leakage of air,  $J_a$ , but compressed according to Boyle's law to the volume it would occupy at the pressure  $u'_a$ .

In equation form the total volume of air in the final state is

$$V'_{at} = (V_{au} + V_{ad}) \frac{u_a}{u'_a} + J_a \frac{p_g}{u'_a} \quad (2-13)$$

Substituting Eq. 2-13 into Eq. 2-12, the final volume of undissolved air becomes

$$V'_{au} = (V_{au} + V_{ad}) \frac{u_a}{u'_a} + J_a \frac{p_g}{u'_a} - V'_{ad} \quad (2-14)$$

Substituting Eqs. 2-14 into Eq. 2-11, the change in total volume becomes

$$\Delta V = J_a \frac{p_s}{u'_a} + (V_{au} + V_{ad}) \frac{u_a}{u'_a} - V'_{ad} - V_{au} \quad (2-15)$$

Each component in Eq. 2-15 will now be computed:

(1) Initial Volume of Undissolved Air,  $V_{au}$  - The initial volume of undissolved air is the difference between the volume of voids and the volume of water

$$V_{au} = V_v - V_w = n V (1 - G_w) \quad (2-16)$$

(2) Initial Volume of Dissolved Air,  $V_{ad}$  - Using Eq. 2-2, and the known volume of water in the voids, one obtains

$$V_{ad} = s V_w = s n V G_w \quad (V_{ad} \text{ is measured at } u_a) \quad (2-17)$$

(3) Final Volume of Dissolved Air,  $V'_{ad}$  - Eq. 2-2 is applied as in (2), but in this case the air volume is measured at the pressure  $u'_a$ .

$$V'_{ad} = s V_w = s n V G_w \quad (V'_{ad} \text{ is measured at } u'_a) \quad (2-18)$$

Substituting Eqs. 2-16, 2-17 and 2-18 into Eq. 2-15, and rearranging, one obtains

$$\frac{\Delta V}{V} = \frac{J_a p_s}{u'_a V} - n (1 - G_w + s G_w) \left(1 - \frac{u_a}{u'_a}\right) \quad (2-19)^*$$

Letting  $u'_a = u_a + \Delta u_a$ , letting  $f = (1 - G_w + s G_w)$  and substituting for  $\Delta V/V$  from Eq. 2-6, Eq. 2-19 becomes

$$-s \frac{\Delta \bar{\sigma}_3}{\bar{\sigma}_3} = \frac{J_a p_s}{V (u_a + \Delta u_a)} - n f \frac{u_a}{u_a + \Delta u_a} \quad (2-20)$$

Solving for the air leakage, one obtains

$$\frac{J_a p_s}{V} = s \left(-\frac{\Delta \bar{\sigma}_3}{\bar{\sigma}_3}\right) (u_a + \Delta u_a) + n f \Delta u_a \quad (2-21)$$

To obtain the decrease in effective stress as an explicit function of the volume of air leakage into the specimen, one must introduce a relation between  $\Delta \bar{\sigma}_3$  and  $\Delta u_a$ . As was pointed out in 2-02(e), one obtains a conservative estimate of the decrease in effective stress by assuming that  $\Delta \bar{\sigma}_3 = -\Delta u_a$ . Making this substitution in Eq. 2-21, one finds

$$\frac{J_a p_s}{V} = s \left(-\frac{\Delta \bar{\sigma}_3}{\bar{\sigma}_3}\right) (u_a - \Delta \bar{\sigma}_3) + n f (-\Delta \bar{\sigma}_3) \quad (2-22)$$

or, solving for  $(-\Delta \bar{\sigma}_3 / \bar{\sigma}_3)$ ,

\* Eq. 2-19 is similar to an equation derived previously by Bishop and Henkel (12) to determine the effect of trapping air beneath a membrane while setting up a triaxial specimen.

$$-\frac{\Delta\bar{\sigma}_3}{\bar{\sigma}_3} = \frac{-Su_a - n f \bar{\sigma}_3 + \sqrt{(Su_a + n f \bar{\sigma}_3)^2 + \frac{4S\bar{\sigma}_3 p_s J_a}{V}}}{2S\bar{\sigma}_3} \quad (2-23)$$

It should be noted that the volume  $J_a$  is measured at atmospheric pressure and that the product  $J_a p_s$  is proportional to the number of moles of air leakage. The volume occupied by  $J_a$  in the specimen is a function of the final pore air pressure  $u_a$  and the volume of water  $V_w$  in the specimen.

The errors introduced by the simplifying assumptions needed to derive Eq. 2-22 and 2-23 are discussed in 2-07.

(b) Discussion of Eq. 2-22

When the percent decrease in effective stress is held constant, Eq. 2-22 shows that the acceptable volume of air leakage  $J_a$  increases for:

- (1) Increasing swelling ratio,  $S$ .
- (2) Increasing effective stress,  $\bar{\sigma}_3$ .
- (3) Increasing pore air pressure,  $u_a$ .
- (4) Decreasing degree of saturation,  $G_w$ , i.e. increasing  $f (= 1 - G_w + s G_w)$ .

Assuming that the maximum decrease in effective stress in a 1.4 in. diameter by 3.5 in. high specimen should not exceed 2%, then the maximum acceptable volumes of leakage in two examples are as follows:

Boston Blue Clay	S = 0.015	n = 0.43
	$\bar{\sigma}_3 = 6.0 \text{ kg/cm}^2$	$\Delta\bar{\sigma}_3 = -0.12 \text{ kg/cm}^2$
	$u_a = 2.0 \text{ kg/cm}^2$ (gage)	$G_w = 95\%$ ( $f = 0.069$ )
	$J_a = 0.39 \text{ cm}^3$ (measured at atmospheric pressure)	

Canyon Dam Clay	S = 0.001	n = 0.37
	$\bar{\sigma}_3 = 1.0 \text{ kg/cm}^2$	$\Delta\bar{\sigma}_3 = -0.02$
	$u_a = 1.0 \text{ kg/cm}^2$ (gage)	$G_w = 99\%$ ( $f = 0.030$ )
	$J_a = 0.023 \text{ cm}^3$ (measured at atmospheric pressure)	

Thus, for an example that might be considered typical (Boston Blue clay), the air leakage must not exceed about  $0.4 \text{ cm}^3$ , but in a very critical case (Canyon Dam clay), the leakage must not exceed  $0.02 \text{ cm}^3$ . It should be recalled that the volumes of leakage calculated above are conservative.

2-07 ERRORS INTRODUCED BY SIMPLIFYING ASSUMPTIONS IN THE ANALYSIS OF EFFECTS OF LEAKAGE

(a) Qualitative Description of Assumptions

- (1) Change in pore water pressure is equal but opposite to the change in effective stress in partially saturated specimens

It was pointed out in 2-02(e) that air leakage into a partially saturated specimen causes a decrease in effective stress that is smaller in magnitude, rather than equal, to the increase in pore air pressure, and that the assumption  $\Delta\bar{\sigma}_3 = -\Delta u_a$  leads to a conservative estimate of the decrease in effective stress caused by air leakage.

One means for evaluating this error is through the equation tentatively proposed by Bishop, et. al. (11) for defining the effective stress in a partially saturated specimen. This equation can be put in the form

$$\bar{\sigma}_3 = \sigma_c - u_a + \chi u_c \quad (2-24)$$

where  $u_c = u_a - u_w$  = pressure difference across the air-water menisci in the specimen.

$\chi$  = a positive empirical constant that ranges between 1.0 for 100% saturated specimens and 0.0 for dry specimens.

Using Eq. 2-24 one can show that

$$\Delta \bar{\sigma}_3 = -\Delta u_a + \chi' \Delta u_c + u_c \Delta \chi \quad (2-25)$$

where the term  $(\chi' \Delta u_c + u_c \Delta \chi)$  is a measure of the deviation from the assumption that  $\Delta \bar{\sigma}_3 = -\Delta u_a$ . Since  $|\Delta u_a| > |\Delta \bar{\sigma}_3|$ , for the case of air leakage into a partially saturated specimen (see 2-02(e)), it is apparent that the term  $(\chi' \Delta u_c + u_c \Delta \chi)$  must be positive. An attempt was made to evaluate this term on the basis of the rather limited data available in the literature (56, 11, 65, 60) on the magnitude and rate of change of  $\chi$  and  $u_c$ . The results are briefly presented in (b) below.

(2) Boyle's law is exact

The use of Boyle's law for air implies the assumption that air behaves as an ideal gas. However, when air is compressed at room temperature from one to ten atmospheres, the final volume calculated from Boyle's law will be higher than the actual volume by 0.30%. Conversely, if the air is compressed to one-tenth its initial volume, the pressure computed from Boyle's law will be too high by 0.30%. These deviations from ideality cause the calculated final volume of the specimen to be slightly too high, so that the calculated value of  $\Delta \bar{\sigma}_3 / \bar{\sigma}_3$  is slightly conservative.

(3) Water is incompressible

An increase in pore water pressure causes a decrease in volume of the water initially present in a specimen. Thus the increase in total volume of a specimen caused by leakage is somewhat less than would be calculated by assuming water is incompressible. This assumption leads to a conservative (high) estimate of the decrease in effective stress due to a given volume of leakage.

(4) Volume increase of water due to solution of air is zero

A slight decrease in specific gravity of water occurs when air is dissolved in it (41). If the dissolved air occupied zero volume, the specific gravity of water saturated with air would be greater than that of de-aired water. Therefore, the dissolved air must increase the total volume of pore water. Neglect of this small volume causes the calculated decrease in effective stress to be unconservative, i.e. too low.

(5) Henry's law is exact

There are four sources of error involved in the use of Henry's law and the approximation to Henry's law, Eq. 2-2. These are: (a) The decrease of the solubility,  $\underline{g}$ , of air in water as the pressure in the air is increased, (b) the use of Boyle's law to derive Eq. 2-2 (see Appendix C-01 for derivation), (c) when deriving Eq. 2-2, the weight of air dissolved in water is neglected relative to the weight of the water in which it is dissolved, and (d) the possible difference between the solubility of air in "free" water as compared to its solubility in the water that exists in the small-diameter pores of a fine-grained soil.

There are no data known to the author that give the solubility of air in water that is held in fine pores, so the effect of item (d) cannot now be evaluated. Of the remaining three items, only item (a) introduces any significant error. Since  $\underline{g}$  is slightly decreased when the pore pressure is increased (112), there is less air in solution than calculated by assuming  $\underline{g}$  is a constant. Thus the actual volume of the specimen must be greater than calculated, and the actual effective stress decrease also must be greater than calculated. Therefore, the assumption that  $\underline{g}$  is constant is unconservative.

(6) Swelling curve is a straight line

It is assumed that there is a linear relationship between  $\Delta V/V$  and  $\Delta \bar{\sigma}_3/\bar{\sigma}_3$  over a small ( 10%) range of  $\Delta \bar{\sigma}_3/\bar{\sigma}_3$  for decreasing values of effective stress. Swelling tests were performed on one soil during this investigation and it was found that the initial portion of the swelling curve has a definite curvature. If one uses the slope at the origin of the swelling curve to calculate the effects of leakage, the estimated decrease in effective stress due to a given volume of leakage will be too large (i.e. conservative). If one uses an average slope over some small range of effective stress decrease, then the estimated decrease in effective stress may be either slightly too large or too small, depending on the volume of leakage that occurs during any given triaxial test.

(7) Mineral grains are incompressible

A pore pressure increase causes a decrease in volume of the individual mineral grains in a specimen. Therefore, the total volume of the specimen is decreased. (It is interesting to note however that the void ratio is increased!) Whether or not changes in volume of the mineral grains cause changes in effective stress depends on the definition used for effective stress. If one is concerned with the shear strength of a soil, effective stress can be defined simply as "the stress that controls the shear strength of a specimen." On the basis of this definition, a volume decrease of the mineral grains due to increased pore pressure may cause an increased effective stress because each mineral grain, and therefore, the entire specimen, becomes slightly stronger. Thus the actual decrease in effective stress due to leakage would be smaller than the decrease calculated by assuming that the mineral grains are incompressible.

(8) Membrane does not flex

It is assumed that the confining membrane does not bulge locally between mineral grains when the pore pressure in the specimen increases. Such local outward flexing would absorb some of the leakage without causing changes in effective stress. This assumption leads to a conservative (high) estimate of the decrease in effective stress caused by a given volume of leakage.

(9) Leakage occurs slowly enough to achieve equilibrium conditions

It is assumed that leakage occurs so slowly that there are no pore pressure gradients set up in the specimen due to leakage. If pore pressure gradients do exist, then the interior of the specimen does not increase in volume so much as the sides of the specimen nearest the sources of leakage. Thus the decreases in effective stress near the sides is greater than in the interior of the specimen. The equations presented in this chapter give the average decrease in effective stress in the specimen. This average is not affected by pore pressure gradients caused by leakage, so long as the swelling curve is a straight line over the stress range of interest.

It is also assumed that leakage occurs slowly enough so that the air and water in a specimen are in equilibrium with each other at all times. If air or water leakage occurs so rapidly that the air does not have time to dissolve, the volume of the specimen will be larger than would be calculated using the assumption that the equilibrium condition is achieved. Thus the actual decrease in effective stress will be greater than the calculated decrease.

(b) Discussion of Magnitude of Errors

A detailed analysis was made to estimate the magnitude of error introduced in the calculated value of  $\Delta \bar{\sigma}_3/\bar{\sigma}_3$  by each of the assumptions listed in (a) above, with the exception of item (9). This analysis is not presented herein, but a summary of the results is given below and in Table 2-3. The error in the calculated value of  $\Delta \bar{\sigma}_3/\bar{\sigma}_3$  is defined by

$$\text{Error} = \frac{\left(\frac{\Delta\bar{\sigma}_3}{\bar{\sigma}_3}\right) - \left(\frac{\Delta\bar{\sigma}_3}{\bar{\sigma}_3}\right)'}{\left(\frac{\Delta\bar{\sigma}_3}{\bar{\sigma}_3}\right)'} \quad (2-26)$$

where

$\left(\frac{\Delta\bar{\sigma}_3}{\bar{\sigma}_3}\right)$  - calculated from Eq. 2-9 (for water leakage into 100% saturated specimens) or from Eq. 2-23 (for air leakage into partially saturated specimens).

$\left(\frac{\Delta\bar{\sigma}_3}{\bar{\sigma}_3}\right)'$  - corrected value of  $\Delta\bar{\sigma}_3/\bar{\sigma}_3$ .

A positive error means that the calculated value of  $\Delta\bar{\sigma}_3/\bar{\sigma}_3$  is conservative.

The maximum error occurs under different conditions for each assumption. For example, the assumption that Henry's law is exact is most critical for soils that are nearly 100% saturated, and the assumption that Boyle's law is exact causes the greatest error for soils with a low degree of saturation. Therefore the parameters required to calculate the error were varied for each assumption such that the greatest probable error would be obtained in each case. The resulting errors are shown under the heading "Extreme Example" in Table 2-3. The errors that arise for what might be considered a "Typical Example" also are shown in the table.

Based on the assumption that the swelling ratio is known in any given case, the following conclusions may be drawn concerning the magnitude of error in the calculated value of  $\Delta\bar{\sigma}_3/\bar{\sigma}_3$ :

For 100% Saturated Specimens-The error is not likely to exceed +25%, and this large error develops only for soils with a very low swelling ratio, i.e. like compacted Canyon Dam clay.

For Partially Saturated Specimens-

- (1) The error is largest for soils with low swelling ratios.
- (2) When the overall error is large (>10%) the calculated value of  $\Delta\bar{\sigma}_3/\bar{\sigma}_3$  is generally conservative (i.e. too high). When the error is relatively small (< 5%) the calculated value of  $\Delta\bar{\sigma}_3/\bar{\sigma}_3$  may be somewhat high or low.
- (3) The largest error is introduced by the assumption that  $\Delta u_a = \Delta u_w = -\Delta\bar{\sigma}_3$ . The magnitude of this error is not known accurately because the data presently available to evaluate it are limited and questionable.
- (4) The overall error probably will be less than about +15% so long as (a) the degree of saturation is greater than 95%, (b) the swelling ratio is greater than 0.004, and the initial effective stress is smaller than 20 kg/cm<sup>2</sup>.
- (5) The error probably will not be larger than +100% so long as the initial degree of saturation is greater than 90% and the swelling ratio is greater than 0.0015.

## 2-08 SUMMARY AND CONCLUSIONS

The following cases of leakage into triaxial Q and R specimens are of interest:

- I. 100% saturated specimens - (a) Water leakage  
(b) Air leakage
- II. Partially saturates specimens - (a) Water leakage  
(b) Air leakage

Air leakage into 100% saturated specimens, I(b), can be prevented and water leakage into partially saturated specimens, II(a), probably causes either the same or a much smaller decrease in effective stress than water leakage into 100% saturated specimens. Therefore, equations were derived herein for calculating the effects of leakage for cases I(a) and II(b) only.

Assuming that the swelling curve of a soil is a straight line for small decreases in effective stress, the following equation relates the decrease in effective stress to the volume of water leakage into 100% saturated specimens:

$$\frac{\Delta \bar{\sigma}_3}{\bar{\sigma}_3} = -\frac{1}{S} \frac{J_w}{V} \quad (2-9)$$

where  $\frac{\Delta \bar{\sigma}_3}{\bar{\sigma}_3}$  = change in effective stress, usually expressed in percent  
 $S$  = initial swelling ratio  
 $\frac{J_w}{V}$  = volume of water leakage, usually expressed as a percent of the total volume,  $V$ , of the specimen.

The initial swelling ratio has been determined accurately for one soil which is believed to have a very low swelling ratio relative to most soils that might be of interest in long-time triaxial tests. If the decrease in effective stress is not to exceed 2%, the maximum acceptable volume of leakage into a 1.4 in. diameter by 3.5 in. high, 100% saturated specimen of this soil ( $S = 0.001$ ) is only about 2 mm<sup>3</sup>. It is apparent that rates of leakage (and, of course, volume changes) that have heretofore been considered insignificant in triaxial testing, may cause large changes in effective stress during a triaxial Q or R test.

Assuming that the initial swelling ratio is known, the errors introduced by the simplifying assumptions required to derive Eq. 2-9 will cause the calculated decrease in effective stress to be no more than 25% greater than the actual decrease in effective stress. This large error, which is due to the compressibility of water, will develop only in soils with very low swelling ratio.

Based on a theoretical consideration of the equilibrium between air and water in a partially saturated specimen, the author concluded that the undissolved air exists in the form of spaces (rather than bubbles) that are bounded by soil grains and air-water menisci. This conclusion was reached previously by Hilf(56). To calculate the decrease in effective stress caused by air leakage into partially saturated specimens, the conservative assumption was made that the change in pore air pressure and the change in effective stress are equal to each other but opposite in sign, which is equivalent to the assumption that the radius of curvature of the menisci does not change during air leakage. The following equation was derived:

$$\frac{J_a p_g}{V} = S - \left( \frac{\Delta \bar{\sigma}_3}{\bar{\sigma}_3} \right) (u_a - \Delta \bar{\sigma}_3) + nf (-\Delta \bar{\sigma}_3) \quad (2-22)$$

where  $J_a$  = volume of air leakage, measured at atmospheric pressure,  $p_g$  (cm<sup>3</sup>).  
 $u_a$  = pore air pressure (gm/cm<sup>2</sup>).  
 $n$  = porosity of specimen  
 $f$  =  $(1 - G_w + s G_w)$ , where  $g$  is the solubility of air in water and  $G_w$  is the degree of saturation of specimen.

For a critical case of air leakage into a partially saturated specimen, i.e. low swelling ratio, low effective stress, low pore air pressure and high degree of saturation, the maximum acceptable volume of air leakage into a 1.4 in. diameter by 3.5 in. high specimen is found to be about 20 mm<sup>3</sup>, if the decrease in effective stress is not to exceed 2%.

An analysis of the errors introduced by the simplifying assumptions required to derive Eq. 2-22 showed that, so long as the swelling ratio is known and is greater than 0.0015, the calculated decrease in effective stress will not be greater than twice the actual decrease in effective stress, for specimens with a degree of saturation greater than 90%.

The severest limitations to the present usefulness, in the practice of triaxial testing, of Eqs. 2-9 and 2-22 are (1) lack of accurate determinations of the swelling ratio, (2) lack of understanding of the movement of menisci when water or air enter a partially saturated specimen and (3) lack of a proven effective stress equation for partially saturated soils (if such an equation exists).

CHAPTER 3THEORY OF STEADY FLOW OF  
FLUIDS THROUGH MEMBRANES3-01 INTRODUCTION(a) Purpose and Scope

The purpose of this chapter is (1) to introduce the subject and terminology of the field of membrane permeability, (2) to present the equations which have been proposed in the literature to describe the flow of liquids or gases through membranes, and (3) to determine which of these equations might apply to the flow of water through rubber and/or plastic membranes due to a hydraulic pressure gradient, a vapor pressure gradient and a mole fraction gradient across the membrane.

Literature in the fields of chemistry, biology, engineering, physics and medicine was reviewed for information on the flow of fluids through membranes.

(b) The Importance of Membrane Science and Technology

Table 3-1 is a partial list of the uses of natural and artificial membranes. Researchers in many fields are actively engaged in attempting to alter the properties of membranes to suit their various requirements. An understanding of the theory of flow through membranes is essential to this task. The following quotation from an article by Sherwood (92) concerning the desalinization of water emphasizes this need:

"Not enough is known about the mechanism of the membrane process to permit the selection and manufacture of useful osmotic membranes. If such could be developed the process (of water desalinization)\* might be quite efficient . . . . But useful membranes will probably not be developed by trial and error; the basic physics of the process needs to be understood."

3-02 THE MEMBRANE-PERMEANT SYSTEM

Fig. 3-1 shows the membrane-permeant system which will be used as a basis for discussion. The membrane being studied is clamped between chambers A and B. Chambers A and B may contain a pure liquid or gas, a solution of ions or molecules in a liquid, or a mixture of gases. A total pressure difference may be applied across the membrane by increasing the pressure in Chamber B.

The applied driving force (see 3-04) causes flow of the permeant or permeants through the membrane. The rate of flow is measured in volume of permeant per unit time or in moles (gram-molecular weights) of permeant per unit time. The rate of flow is a function of the properties of the membrane, the properties of the permeant and the magnitude of the driving force. A list of specific variables that can affect the rate of flow through membranes is given in Table 3-2.

No membrane is completely impervious. Membranes made of rubber, plastic, wax or a combination of these materials are all pervious to an extent which is measurable at ordinary temperatures (25°C). Even glass and metals become measurably pervious at elevated temperatures (400°C and higher) (8, p. 117). Recent attempts to achieve vacua as low as  $10^{-16}$  mm Hg have shown that glass is pervious to helium to an extent which is now measurable at ordinary temperatures (98).

---

\* Statement in parentheses added by present author.

3-03 TYPES OF MEMBRANES(a) General

Transport processes through membranes are generally classed as either "passive" or "active." Passive transport (81, p. 386) refers to the flow of particles through membranes under the influence of known energy gradients (osmotic pressure, hydraulic pressure, etc.) that are applied to the membrane-permeant system. In such passive transport, processes occurring in the membrane contribute no energy to the flow. On the other hand, active transport is flow through a membrane under the influence of energy derived from chemical reactions that occur within or near the surfaces of the membrane (97, 87, 101). Thus active transport may cause ions or molecules to flow in a direction opposite to the flow direction that would be expected if only the known osmotic pressure or hydraulic pressure gradients were considered. For example, it is suspected that a reaction occurs in the membrane that surrounds the nucleus of the human red blood cell which causes sodium ions to flow in a direction opposite to the osmotic pressure gradient (101).

In subsequent discussions of flow through membranes, only passive transport will be considered. It will be assumed in all cases that no reactions are occurring within the membrane and that the membrane remains unaltered (both physically and chemically) throughout the duration of the flow process.

(b) Porous and Non-Porous Membranes; Semi Permeable Membranes

A pore is defined as any opening in a membrane which is continuous, at least for a limited time, through the entire thickness of the membrane. According to this definition, all membranes must contain some pores so that they all should be classified as the porous type. On the other hand, when considering a specific membrane and a specific permeant, one may ask the question: "Is this membrane porous to this permeant?" Clearly, if the pores have a diameter ten times larger than the diameter of the permeating particle, the membrane must be classed as porous to that permeant. Also, if the pores are much smaller than the permeating particle, the membrane must be classed as non-porous to that specific permeant. If one chooses to use the terms porous and non-porous to describe general classes of membranes, one must be careful to specify both the membrane and the permeant that are being considered.

In the study of osmotic pressure, membranes are used that are porous to water but non-porous to colloidal particles suspended in the water. Membranes permeable to one component of a permeant but impermeable to other components of the permeant are called semi-permeable (74). When using the term semi-permeable, one must specify the membrane-permeant system being considered, since the term semi-permeable does not define a membrane with a specific pore diameter.

Cellulosic membranes (86) are examples of membranes that are porous to water because the pore diameters of such membranes are twenty or more times larger than the diameter of water molecules. Natural rubber membranes have been classified as non-porous membranes (40) even though the spaces between molecules in these membranes may be two or three times larger than water molecules (7).

Although the terms porous and non-porous are used quite frequently in the literature, it appears to the author that the distinction serves no useful purposes and is often ambiguous. As an alternative to the use of these terms, the author suggests that, where necessary, reference be made to the size of the pores relative to the size of the permeating particle.

(c) Ordered and Dis-Ordered (Amorphous) Membrane Structure

Membranes with an ordered structure may be crystalline - such as aluminum foil, Saran (polyvinylidene chloride) (49), Mylar (polyethylene terephthalate) (73) - or they may be non-crystalline but possess a repeating pattern of molecules - such as shown by Teorell (101, facing p. 10). A permeant may pass between the molecules of these ordered membranes or the permeant may pass through cracks between crystals (1). The spaces between crystals may be as small as those between molecules.

Natural rubber, butyl rubber and quickly quenched polyethylene terephthalate (73) are examples of materials which form dis-ordered (or amorphous) membranes. Such materials are generally composed of long-chain molecules arranged in a completely irregular (random) packing. The flow of a permeant through amorphous membranes occurs through openings between the molecules. These openings may be permanent or they may be always changing in size and location due to the continuous movement of the molecules under the influence of their thermal energy.

It should be noted that a membrane may be made up of a combination of large pores, crystals and amorphous zones. For example, polyethylene may contain both amorphous and crystalline zones, the crystalline portions being less pervious to gases than the amorphous portion (72).

(d) Charged Membranes

The matrix of a membrane may carry a surface charge that is balanced by a preponderance of oppositely charged ions in the immediately adjacent liquid or gaseous atmosphere. The matrix of a natural rubber membrane apparently has a negative surface charge (94). Membranes that have a surface charge restrict the flow of ions due to electrostatic repulsive forces between similarly charged ions. This is probably one of the mechanisms by which ion-selective membranes operate (5, p. 528; 93). Even though a membrane carries no surface charge, an ion that passes through such a membrane must pass through electric fields of varying sign and varying magnitude (1). Thus, on a molecular scale the membrane may behave, with respect to a permeating ion, as a locally charged membrane.

No attempt has been made herein to study the effects of membrane charge on the rate of flow of ions or molecules through the membranes.

(e) Stratified Membranes

Stratified membranes are composed of two or more layers of materials with differing physical and chemical properties. For example, Teorell (101, p. 11) describes the myelin sheath of cat nerve fiber which is probably composed of five strata. Ponder (84, p. 949) points out that the main resistance to flow through the membrane surrounding the human red blood cell may be developed in the first 1/100th of its thickness. Membranes are now being manufactured, that are composed of two different plastics, such as polyethylene coated nylon fabric, polyethylene coated aluminum foil and sandwiched saran and polyethylene. Stratified membrane structure may result in membranes that are unsymmetrical with respect to several properties such as the sign of the surface charge and the electrical conductivity (101, p. 16).

Stratified membranes are not considered further in this investigation.

3-04 PERMEANTS AND DRIVING FORCES

(a) Permeants

Permeants may be in the form of:

- Gas - Pure gas.
- Mixture of gases.
- Plasma.
- Liquid - Pure liquid (polar or non-polar).
- Solution of ions or molecules in a liquid.
- Mixture or solution of two or more liquids.
- Liquid suspension of colloids.

A permeant may consist of (1) ions or atoms, (2) polar or non-polar molecules, (3) colloids, or (4) combinations of these items. The total flow of a permeant through a membrane is equal to the sum of the flows of each of its components. For example, assume that a solution of X moles sodium chloride in Y moles water is placed in both chamber A and chamber B in Fig. 3-1 and that a hydraulic pressure is applied to chamber B. The

total flow will be made up of a flow of sodium ions, chloride ions and water molecules from chamber B to chamber A. The rate of flow of each component (in moles/sec) will depend on the permeability of the membrane to each component and on the magnitude of the driving force which acts on each component. The concentration of the solution will change as flow occurs because of the difference between the permeability of the membrane to water molecules and its permeability to sodium or chloride ions. This difference in permeabilities may be small or large, depending on the nature of the membrane.

The following membrane-permeant system will be of interest herein:

Pure Water - Natural Rubber Membrane - Solution of Sodium Chloride in Water

For this system, the rate of ion flow into the pure water is probably about 1/1500th the rate of water flow into the solution (see Appendix A-07). Thus, the ion flow can be neglected in this case.

(b) Driving Forces

The following are the driving forces that can cause flow through a membrane:

- (1) Total (or Hydraulic) } pressure gradient
- Partial (or Vapor) }
- (2) Mole fraction gradient
- (3) Electrical potential gradient
- (4) Temperature gradient
- (5) Others (possibly magnetic field gradient)

The term gradient refers to the change in pressure, mole fraction, etc., per unit path length in the direction of flow. This is not to be confused with the difference in pressure, mole fraction, etc., across a membrane. Formally, the difference in pressure across a membrane is given by

$$\Delta p = p_A - p_B = \int_0^L \left( \frac{\partial p}{\partial x} \right) dx \quad (3-1)$$

where

$\Delta p$  = pressure difference.

$\left. \begin{matrix} p_A \\ p_B \end{matrix} \right\}$  = pressures in chamber A and B as in Fig. 3-1.

$\frac{\partial p}{\partial x}$  = pressure gradient at point x.

L = thickness of membrane.

x = length coordinate in direction of flow.

The differences and the gradients of temperature, mole fraction and electrical potential may be related by equations analagous to Eq. 3-1.

The total driving force causing flow of each component of a permeant through a membrane is equal to the sum of the effects of all of the above gradients. In the present study only pressure and mole fraction gradients will be considered. All other possible gradients will be assumed negligible.

The "total pressure" is that pressure which is registered on a gage (e.g. a Bourdon gage) plus atmospheric pressure. For liquid systems, the total pressure is referred to herein as the "hydraulic" pressure.

The "partial pressure" of one gas in a mixture of gases is defined as that portion of the total pressure which is contributed by the gas of interest. Dalton's law of partial pressures (61), states that the partial pressure is equal to the total pressure that the gas would exert if all other gases in the mixture were absent, the temperature

and volume of the gas being held constant. Dalton's law is strictly valid only for ideal gases. For a pure gas, the partial pressure is identical with the total pressure.

The terms "partial pressure" and "vapor pressure" are often used interchangeably when considering the flow of water vapor (or other vapors) through membranes. Vapor pressure is identical to partial pressure except that the term vapor pressure is reserved only for those elements or compounds that are liquid or easily condensable at ordinary temperature and pressure. For example, one speaks of the vapor pressure of water, alcohol or bromine but one speaks of the partial pressure of oxygen, helium, nitrogen, etc. The "equilibrium vapor pressure" is equal to the vapor pressure when the vapor and the liquid phases are in equilibrium with each other. Depending on the conditions existing in a given system, the vapor pressure of a liquid may vary between zero and the equilibrium vapor pressure. The equilibrium vapor pressure may be increased by increasing the total pressure or by increasing the temperature of the liquid.

As an example, consider pure water and water vapor at 30°C and atmospheric pressure. The equilibrium vapor pressure under these conditions is 31.82 mm Hg. If one removes the atmosphere and applies one atmosphere of pressure to the water through a piston, the vapor pressure of the water will remain at 31.82 mm Hg. On the other hand, if the liquid is removed and only the water vapor remains, mixed with air, the vapor pressure may vary between zero and 31.82 mm Hg. Thus, the equilibrium vapor pressure of a liquid has a specific value at a given temperature, total pressure and composition. However the vapor pressure may take on any value depending on the conditions imposed.

The term mole fraction has been defined in 2-02. The flow caused by a mole fraction gradient is generally called "diffusion" or "osmosis." The term diffusion also is used to describe a mechanism of passage of particles of matter through a membrane. It is distinguished, for example, from laminar flow. However, the flow caused by a mole fraction gradient is not necessarily diffusive. It may be laminar flow or some other type of flow as yet unknown. "Osmosis" is a better term for referring to flow caused by a mole fraction gradient since no mechanism is implied in its use.

As an example of osmosis caused by a mole fraction gradient, consider a system with pure water in chamber A in Fig. 3-1 and a sodium chloride solution in chamber B. Water will flow from chamber A to chamber B simply because the mole fraction of water is lower in chamber B than in chamber A. Also, sodium and chloride ions flow from chamber B to chamber A. This flow is due to a mole fraction gradient of the salt ions and, strictly speaking, must also be called osmotic flow. If the membrane is impervious to the sodium and chloride ions and pervious to water molecules, it is called an ideal "semi-permeable" membrane as defined in 3-03(b). If one closes the valve on chamber B, the flow of water will cause the pressure to build up in chamber B until the flow is stopped because of the back pressure. The equilibrium pressure attained is called the osmotic pressure of the solution in chamber B. It is often convenient to use the osmotic pressure as the independent variable causing flow rather than the mole fraction gradient. However, it must be borne in mind that the osmotic pressure is only a measure of the effect of a mole fraction gradient, and it is measurable only when the semi-permeable membrane used is ideal, i.e. it passes no salt ions whatsoever.

### 3-05 EQUATIONS OF FLOW OF LIQUIDS THROUGH MEMBRANES

#### (a) General

Equations relating the rate of flow of a permeant through a membrane to the driving force causing flow and the characteristics of the membrane-permeant system may be obtained (1) empirically, (2) by the use of conceptual models of the membrane-permeant system and (3) by the application of irreversible thermodynamics to the flow process. The equations that have been used in the literature to describe flow through membranes under the influence of hydraulic pressure differences, vapor pressure differences and/or mole fraction differences across the membrane are presented. Relationships that exist among the various equations will be elucidated.

(b) Empirical Equations(1) Darcy's law

Darcy's law in its original form (37, App. D) is

$$q = kA \frac{\Delta h}{L} \quad (3-2)$$

where

- $q$  = rate of flow ( $\text{cm}^3/\text{sec}$ ).
- $k$  = coefficient of permeability ( $\text{cm}/\text{sec}$ ).
- $A$  = total area of membrane ( $\text{cm}^2$ ).
- $\Delta h$  = total hydraulic head causing flow (cm of permeant).  
 $\Delta h = \Delta p / \gamma$  where  $\Delta p$  = hydraulic pressure difference ( $\text{gm}/\text{cm}^3$ )  
and  $\gamma$  = unit weight of permeant ( $\text{gm}/\text{cm}^3$ ).
- $L$  = thickness of permeated medium (cm).
- $\frac{\Delta h}{L}$  =  $i$  = hydraulic gradient (dimensionless).

In subsequent discussions it will be convenient to use Darcy's law in the following form

$$q = K' A \frac{\Delta p}{L} \quad (3-3)$$

where the permeability constant  $K'$  is equal to  $k/\gamma$ .

Darcy formulated his equation on the basis of experiments on the flow of water through sand caused by a hydraulic gradient across the sand layer. Thus Darcy was first to show that the flow rate of water through a porous medium is directly proportional to the hydraulic gradient. Darcy's law has subsequently been found to be valid for a wide variety of sands and clays (76, ch. 3; 53, ch. 3; 79).

Bigelow (9) has shown that the rate of flow of water through collodion membranes is proportional to the hydraulic pressure difference. Bjerrum and Manegold (13) and Manegold and Hofman (69) have shown that the rate of flow through collodion membranes is inversely proportional to the thickness of the membranes. Thus it appears that Darcy's law applies to collodion membranes.

Recently Renkin (86) has shown that the rate of flow of water through three types of cellulosic membranes is proportional to the hydraulic pressure difference. He gives no data on the effect of thickness of cellulose membranes. Data presented in Chapter 4 show that the rate of flow of water through natural rubber membranes is approximately proportional to the hydraulic pressure difference. No satisfactory data were obtained on the effect of thickness on the rate of flow of liquid water through natural rubber membranes.

Whether or not Darcy's law is strictly applicable to the flow of water through the rubber and plastic membranes of interest herein, it is nevertheless useful to compute the permeability constant  $K'$  from flow data for different membranes. These values may then be compared, at least roughly, to determine which membrane is best for preventing leakage into triaxial specimens.

(2) Fick's law

Fick's first law (77, p. 95) states that if the concentration of particles dissolved in a solution varies from point to point, the particles will flow from the region of higher concentration to the region of lower concentration according to

$$\frac{dm}{dt} = DS \frac{\Delta c}{L} \quad (3-4)$$

where

$\frac{dm}{dt}$  = rate of flow (moles/sec).  
 $D$  = diffusion coefficient ( $\text{cm}^2/\text{sec}$ ).  
 $A$  = area of flow ( $\text{cm}^2$ ).  
 $\Delta c$  = difference in concentration at the two locations in the flow medium ( $\text{moles}/\text{cm}^3$ ).  
 $L$  = distance between the two locations of differing concentration (cm).

When applying Fick's law to the flow of a liquid through a membrane, one can think of a system with pure water in chamber A in Fig. 3-1 and a solution in chamber B. Fick's law applies to the flow of each component of the solution, i.e. both the solvent molecules and solute ions.

For the case of flow through a membrane, the parameters on the right hand side of Eq. 3-4 may be viewed in two ways: (1) If the area  $A$  in Eq. 3-4 is equal to the total area of the membrane and  $L$  is the thickness of the membrane, then  $D$  is the diffusion coefficient in the membrane. This diffusion coefficient is a function of the geometry and porosity of the membrane and of the characteristics of the permeant. (2) The "free" diffusion coefficient of a permeant is the diffusion coefficient that would be measured if no membrane were present. Its value is not a function of the membrane tested. If the "free" diffusion coefficient is inserted in Eq. 3-4, then the ratio  $A/L$  would represent the effective area to length ratio of the pores of the membrane (86) which is quite different from the  $A/L$  ratio defined in (1) above.

In either view of Fick's law, the concentration difference must be that which exists within the membrane, but it is generally desirable instead to put it into a form which contains the concentrations of the adjacent solutions. For this purpose one must know the solubility of the permeant in the membrane. A solubility coefficient is measured by placing a solution of desired concentration in contact with a membrane for a sufficient length of time to achieve equilibrium. The membrane is then removed and the quantity of solute dissolved in the membrane is measured. The ratio of the concentration of solvent in the membrane to that in the solution is the solubility coefficient. The solute may dissolve in the membrane by simple solution (2), i.e. by dispersion of molecules of solute between molecules of the membrane, or by absorption or condensation on the surfaces of the morphological elements of the membrane (18).

The solubility of a permeant in a membrane may follow a law such as

$$c_m = s_c c_s \quad (3-5)$$

where

$c_m$  = concentration of permeant in membrane ( $\text{moles}/\text{cm}^3$  of membrane).  
 $s_c$  = solubility coefficient of permeant in the membrane (dimensionless).  
 $c_s$  = concentration of permeant in solution adjacent to membrane ( $\text{moles}/\text{cm}^3$  of solution).

Substitution of Eq. 3-5 into 3-4 gives

$$\frac{dm}{dt} = Ds A \frac{\Delta c_s}{L} \quad (3-6)$$

Alternatively, the solubility of a permeant in the membrane may be expressed in terms of the vapor pressure of the permeant in the chamber adjacent to the membrane by

$$c_m = s_p p_v \quad (3-7)$$

where

$s_p$  = solubility of permeant in membrane ( $\text{moles}/\text{gm cm}$ )  
 $p_v$  = vapor pressure of permeant in chamber adjacent to membrane ( $\text{gm}/\text{cm}^2$ ).

The vapor pressure is thermodynamically related to the concentration (or mole fraction) of the permeant. This relationship is given in 3-05 (d).

Substitution of Eq. 3-7 into Eq. 3-4 gives

$$\frac{dm}{dt} = D s_p A \frac{(\Delta p_v)_c}{L} \quad (3-8)$$

where the subscript  $c$  denotes that the vapor pressure gradient is caused by a concentration gradient. Both forms of Fick's law, Eq. 3-6 and 3-8, show a direct proportionality between the flow rate and the driving gradient so long as the product  $Ds_p$  (or  $Ds_c$ ) remains constant.

According to Bigelow (9), Fick himself applied his law to the flow of liquids through membranes as early as 1855, although no proof of its validity was given. The data presented in Chapter 6 herein show a direct proportionality between rate of flow of water and the concentration difference across natural rubber membranes. Data obtained by physiologists to prove "Starling's hypothesis" (see next paragraph) can be used to show that the rate of flow of water through some biological membranes is directly proportional to the concentration difference. However, it appears from the data in Chapter 6 that the rate of flow of water through natural rubber (caused by a concentration difference) is not inversely proportional to the membrane thickness. No other data are known to the author which can be used to relate rate of flow to membrane thickness for tests in which a concentration difference is applied across a membrane, with liquids on both sides of the membrane.

### (3) Starling's Hypothesis

In 1895 Starling (95) presented measurements of rates of flow of water through a frog's peritoneal\* membrane due to a hydraulic pressure difference and due to a concentration difference across the membrane. He concluded (on p. 324) that the rate of flow across this membrane was some function of the difference between the hydraulic pressure and the osmotic pressure, implying that the two are linearly related, but he did not express this view in graphical or equation form.

In 1911 von Antropoff (4) made the assumption that the rate of flow of a liquid through a membrane is directly proportional to the quantity  $(\Delta p - \Delta \Pi)$ , where  $\Delta \Pi$ , being the osmotic pressure difference across the membrane, is given approximately by van't Hoff's equation

$$\Delta \Pi = RT \Delta c \quad (3-9)$$

where  $\Delta c$  is the concentration difference across the membrane of the particles to which the membrane is impermeable. In the year 1927, Northrup (74) expressed the rate of flow through a membrane as follows

$$q = \text{constant} \times A \frac{\Delta p - \Delta \Pi}{L} \quad (3-10)$$

Northrup noted that the magnitude of the constant was dependent on the mechanism by which the permeant passes the membrane.

Later in the year 1927 Landis (67) presented the data shown in Fig. 3-2. This graph shows that the rate of flow through the frog's mesentery\*\* can be expressed by Eq. 3-10. Additional data in support of Eq. 3-10 were given by Pappenheimer and Soto-Rivera (82). Pappenheimer (81) refers to Eq. 3-10 as "Starling's hypothesis," giving credit to Starling for the original idea. No data were given by Starling, Landis, or Pappenheimer and Soto-Rivera to prove that  $q$  is indeed inversely proportional to  $L$ . Apparently, it was simply assumed from knowledge of Darcy's law and Fick's law that the form of Eq. 3-10 is reasonable.

\* The peritoneum is the membrane surrounding the abdominal cavity.

\*\* A fold of the peritoneum that connects the intestine with the posterior abdominal wall.

Eq. 3-10 reduces to Darcy's law, Eq. 3-3, if the osmotic pressure across the membrane is zero, and it is identical in form to Fick's law (after inserting Eq. 3-9 into Eq. 3-6), when the difference in hydraulic pressure across the membrane is zero. Thus Eq. 3-10 is a more general equation than either Fick's law or Darcy's law. Since Starling's hypothesis states that  $q$  is linearly proportional to the difference  $(\Delta p - \Delta \pi)$ ,  $q$  must be linearly proportional to either  $\Delta p$  or  $\Delta \pi$  if one or the other is zero. Thus the data of Starling, Landis and Pappenheimer, et. al., which were referred to above, all prove the validity of Darcy's and Fick's laws for the flow of water through the membranes used in the tests. However, it is emphasized that no proof has been given, except in the case of Darcy's law, that  $q$  is also inversely proportional to  $L$ .

(c) Equations of Flow Based on Models of the Membrane-Permeant System

(1) Poiseuille's Law

The derivation of Poiseuille's law is based on the following models of the permeant and of the membrane:

Permeant - The permeant is assumed to be a continuous fluid which obeys Newton's law of viscosity

$$\tau = \eta \frac{dv}{dx} \quad (3-11)$$

where  $\tau$  is the shear stress in the fluid,  $\eta$  is the viscosity of the fluid and  $dv/dx$  is the velocity gradient in a direction perpendicular to the path of flow.

Membrane - The membrane is represented by a bundle of cylindrical capillary tubes which are oriented perpendicular to the exterior surfaces of the membrane. The flow takes place through the openings in the capillary tubes.

The following assumptions must be made to derive Poiseuille's law:

- (1) The velocity of the permeant is zero at the walls of the capillary tubes.
- (2) The velocity distribution over the cross section of each capillary tube is the same at every cross section along the path of flow. This means that the energy required to accelerate the flow to the velocity in the capillaries, which is small for the systems of interest herein, is not accounted for in the derivation.

Under the above conditions, the flow through one horizontal capillary tube can be shown to be (20):

$$q_c = \frac{\pi r_p^4}{8\eta} \frac{\Delta p}{L_c} = \frac{r_p^2}{8\eta} A_p \frac{\Delta p}{L_c} \quad (3-12)$$

where

- $q_c$  = flow rate through one capillary hole ( $\text{cm}^3/\text{sec}$ ).
- $r_p$  = radius of hole in capillary (cm).
- $\eta$  = viscosity of permeant ( $\text{gm sec}/\text{cm}^2$ ).
- $A_p$  = cross sectional area of hole in capillary ( $\text{cm}^2$ ).
- $L_c$  = length of capillary tube (cm).

The total flow through the model membrane is equal to the sum of the flows in all capillaries which make up the model. The number of capillaries  $N_c$  may be expressed as

$$N_c = \frac{nA}{A_p} \quad (3-13)$$

where  $n$  is the porosity and  $A$  is the total area of the membrane. Thus the total flow through the membrane is given by

$$q = N_c q_c = \frac{nA}{A_p} \frac{r_p^2}{8\eta} A_p \frac{\Delta p}{L_c}$$

or

$$q = \frac{nr_p^2}{8\eta} A \frac{\Delta p}{L_c} \quad (3-14)$$

According to Bingham (10), Eq. 3-12 was first derived prior to 1846 by at least three theoreticians. However, in 1846 Poiseuille presented the results of tests on the flow of water through glass capillary tubes from which he concluded that Eq. 3-12 can be considered accurate for all practical purposes. Thus, Eq. 3-12 is called Poiseuille's law.

Subsequent work by Osborne Reynolds (see 20) has shown that Poiseuille's law is valid only for laminar flow. When the flow becomes turbulent Eq. 3-12 does not apply. The flow through rubber and plastic membranes will never have sufficiently high velocity to be in the range of turbulent flow under the conditions of interest herein. Therefore the upper limit of validity of Poiseuille's law need not be considered. The lower limit of the validity of Poiseuille's law will be discussed below.

Actual porous membranes may be different from the capillary model described above because of the following factors (see 20): (1) The pores may vary in size and shape, (2) the pores may not be oriented perpendicular to the surfaces of the membrane and (3) the area of an individual pore may vary along its length. Thus the equation of flow through real porous membranes might be written as

$$q = \text{constant} \times \frac{nr_p^2}{8} A \frac{\Delta p}{L} \quad (3-15)$$

where the constant is inserted to account for the differences between the capillary model and a real membrane. Note that the membrane thickness  $L$  rather than the pore length  $L_c$  is now in the denominator of Eq. 3-15. The difference between  $L$  and  $L_c$  is absorbed in the constant. Factors that might affect the magnitude of the constant in Eq. 3-15 have been discussed by Casagrande (20) and Taylor (99, Ch. 6) for soils, by Bjerrum and Manegold (13) for collodion membranes and by Pappenheimer (81) for physiological membranes.

The validity of Eq. 3-15 can be proven by showing that the rate of flow through a medium is (1) directly proportional to the hydraulic pressure gradient, (2) inversely proportional to viscosity and (3) directly proportional to  $nr_p^2$ . The references quoted, to show the validity of Darcy's law for soils, collodion membranes and for physiological membranes, prove that the flow rate is directly proportional to hydraulic gradient for these materials. Proof that the rate of flow is inversely proportional to viscosity is shown by Muskat (76) for flow of water through sands, by Bigelow (9) for flow of water through collodion and gold beater's skin\* and by Duclaux and Errera (43) for flow of several liquids (including water) through cellulose and cellulose acetate membranes.

Proof that  $q \propto nr_p^2$  has not been given, to the knowledge of the author, except for the case of a bundle of parallel capillaries. For clean filter sands, Hazen (see 63) has shown that the rate of flow of water is directly proportional to the square of the diameter of the grains. If one assumes that the porosity of such sands is independent of grain size, and that the "average" pore radius is directly proportional to the grain diameter, then Hazen's work is proof that  $q \propto nr_p^2$  for sands. Rather than attempting to prove that  $q \propto nr_p^2$  for membranes, several authors (52, 14, 81) have assumed it to be true and have calculated "effective pore radii" from rate of flow measurements.

---

\* Membrane from the large intestine of the ox.

In any case, Eq. 3-15 only approximates the equation of flow through membranes because the assumptions used in its derivation are not strictly applicable. First, the permeant has a finite velocity near the walls of the capillary. This velocity may be very important in determining the rate of flow through pores of molecular dimensions (say 5 to 200 Angstroms diameter). Second, the area available to flow of molecules is restricted to an area less than the total cross sectional area of the pores when the size of the permeating molecules is of the same order as the pore size (82). Third, a small correction must be applied because the permeant must be accelerated from a very low velocity just outside the capillaries to a relatively high velocity inside the capillaries. Attempts have been reported by Barrer (8) and Pappenheimer (81) to apply corrections to Eq. 3-15 to take the above three items into account. These references should be consulted for further details.

As the size of the pores in a membrane relative to the size of the permeant molecules decreases, the rate of flow becomes more dependent on the physical and chemical interactions between the membrane molecules and the permeant molecules. When the permeant molecules are about the same size as the pores in a membrane, one can no longer think in terms of a capillary model of the membrane. Rather, one must consider the processes by which individual molecules can permeate the membrane. Some such processes are described below and in 3-06.

## (2) Derivation of Fick's Law by Use of Kinetic Model of Diffusing Particles

The following derivation is presented to show why flow occurs in the direction of the concentration gradient when particles of matter are distributed non-uniformly in a medium. The derivation is taken from Mysels (77) although the concepts are those of Einstein (45).

Consider a system in which particles are suspended in a medium as shown in Fig. 3-3. The concentration gradient, indicated by the heavy line and by the dots, is linear through the medium. The particles may represent ions, atoms, molecules or colloids. The medium may be either a membrane, a liquid or a gas. All energy gradients except the concentration gradient are assumed to be zero.

According to the kinetic theory, the particles have an average thermal energy of  $kT$ , where  $k$  is Boltzmann's constant and  $T$  is the absolute temperature. The suspended particles move about in the medium under the influence of their thermal energy and follow a completely random path due to continual random collisions with molecules of the medium or with other particles. Because of the random nature of this motion, and because in general one deals with extremely large numbers of suspended particles, half of the particles in any level in Fig. 3-3 will move upward and half will move downward as shown in the right side of the figure. It is assumed here that no concentration gradient exists in the other two dimensions, so that no net flow will occur in those dimensions.

The number of particles that move up across plane  $a$ ,  $N_{up}$ , in time interval  $t$  is

$$N_{up} = 1/2 A (N+2\Delta N) d \quad (3-16)$$

where

$A$	=	total area over which flow takes place ( $\text{cm}^2$ ).
$N+2\Delta N$	=	number of suspended particles per unit volume in the level just below plane $a$ (dimensionless).
$d$	=	average distance travelled by a particle in time $t$ in the direction of the concentration gradient.

Similarly the number of particles which move downward across plane  $a$  in time  $t$  is

$$N_{down} = 1/2 A (N+\Delta N) d \quad (3-17)$$

---

\* The time interval  $t$  must be great relative to the duration of each step in the random path of the particle.

The net number of particles moving up across plane  $a$  in time  $t$  is obtained by subtracting Eq. 3-17 from Eq. 3-16

$$N_{\text{up}} - N_{\text{down}} = 1/2 d A \Delta N \quad (3-18)$$

Dividing Eq. 3-18 by Avogadro's number and by the time  $t$  one obtains the rate of flow upward across plane  $a$

$$\frac{dm}{dt} = 1/2 \frac{d}{t} A \Delta c \quad (3-19)$$

where  $dm/dt$  is the rate of flow in moles per second and  $c$  is the change in concentration in moles per unit volume over the distance  $d$ .

If one analyzes statistically the motion of a particle that moves along a random path, one can show that, if the number of steps is large, the distance (measured in a straight line from the point of origin to the final point) travelled by a particle is proportional to the square root of time. In equation form one has

$$d \propto \sqrt{t} \quad (3-20)$$

or

$$\frac{d^2}{t} = \text{constant} \quad (3-21)$$

Since it was previously assumed that the particles do move along random paths, Eq. 3-21 can be substituted into Eq. 3-19 to obtain

$$\frac{dm}{dt} = \text{constant} A \frac{\Delta c}{L} \quad (3-22)$$

which is identical with Fick's law, Eq. 3-4.

Thus Fick's law simply expresses the net rate of flow of particles through a medium when (1) a concentration gradient of suspended particles exists in the medium, (2) the motion of the particles is random, and (3) there is a large number of particles present per unit volume of the medium. No specific model was used to describe the interaction between the suspended particles and the molecules of the medium. It is this interaction which determines the magnitude of the constant in Eq. 3-22. Two possible models for diffusion of gases through membranes are given in 3-06. These models are also conceptually applicable to the flow of liquids through membranes.

### (3) Absorption-Desorption Equilibria at the Membrane Surfaces

In 1949 Laidler and Shuler (64) proposed a model to describe partially the flow of liquids and dissolved particles through membranes under the influence of a mole fraction gradient. They considered the flow to be the result of an equilibrium among the following distinct processes occurring at each exterior surface of the membrane:

- (a) Absorption of permeant molecules on the surface of the membrane.
- (b) Desorption of permeant molecules from the surface of the membrane.
- (c) Diffusion of absorbed permeant molecules away from the near surface toward the opposite surface of the membrane.

The following assumptions were made with regard to the rate of occurrence of each of the above processes:

- (a) The rate of absorption of molecules on the surface of a membrane is proportional to the concentration of molecules in the adjacent solution and to the number of sites available for the absorption of molecules. The proportionality constant will be designated  $B_a$ .
- (b) The rate of desorption is proportional to the number of sites of adsorption that are filled. This proportionality constant will be designated  $B_d$ .

(c) The rate of diffusion into the membrane away from the surface follows the law

$$\frac{dm}{dt} = D A c_t \frac{X'_A - X'_B}{L} \quad (3-23)$$

where

- $D$  = diffusion constant in the membrane ( $\text{cm}^2/\text{sec}$ ).
- $c_t$  = the total concentration of all solvent and solute molecules in the membrane ( $\text{mole}/\text{cm}^3$  of membrane).
- $X'_A$  = the mole fraction of solute in the solution that is inside the membrane on the high concentration side.
- $X'_B$  = the mole fraction of solute in the solution that is inside the membrane on the low concentration side.

Fig. 3-4 shows the system to which Eq. 3-23 applies.

The desired relation is obtained by setting up an equation for the mass balance at each surface of the membrane which expresses the condition that the number of molecules adsorbed must equal the sum of (1) the number of molecules desorbed and (2) the number of molecules which diffuse away from the surface. These two mass balance equations are equated (since the inflow at one surface must equal the outflow at the other surface) and solved to obtain

$$\frac{dm}{dt} = D \frac{B_a}{B_d} A c_t \frac{X_A - X_B}{L} \quad (3-24)$$

where  $X_A$  and  $X_B$  are the mole fractions of the permeant in the two solutions adjacent to

Eq. 3-24 is valid only when  $B_d \gg B_a$  and  $B_d \gg D$ . These inequalities mean simply that the rate of diffusion through the membrane is the slowest step of the flow process.\* Thus Eq. 3-24 shows that only when the rate of diffusion controls the flow process is the rate of flow directly proportional to the quantity  $(X_A - X_B)$ . This conclusion applies only for this particular model of the equilibria at the surfaces of the membrane.

For a dilute solution (i.e. a solution with a unit weight approximately equal to that of the solvent) Eq. 3-24 can be reduced to:

$$\frac{dm}{dt} = D \frac{B_a}{B_d} A \frac{\Delta c_s}{L} \quad (3-25)$$

Comparing Eq. 3-25 with Eq. 3-6 one can see that the ratio  $B_a/B_d$  is essentially a solubility coefficient which relates the concentration of the permeant in the membrane to the concentration in the adjacent solution.

If one accepts the initial assumptions made by Laidler and Shuler, then one may draw the following conclusions from their analysis:

- (1) Fick's law in the form of Eq. 3-6 applies to the flow through membranes only if the solutions on each side are dilute.
- (2) A linear proportionality between rate of flow and the mole fraction difference  $(X_A - X_B)$  exists only if the rate of diffusion through the membrane is the rate controlling step of the flow process.
- (3) The distribution of the permeant between the solutions in and adjacent to the membrane is governed by the ratio  $B_a/B_d$  if diffusion is the rate controlling step.

---

\*It is entirely possible that these inequalities do not hold in any specific case (see 66) but this possibility will not be considered herein.

(d) The Thermodynamic Approach

In the following it will be shown by thermodynamic considerations how Darcy's and Fick's laws are related to Starling's hypothesis.

Darcy's law, Eq. 3-3 may be used to describe the results of a test in which liquid is forced through a membrane due to a hydraulic pressure difference across the membrane. If the liquid is pure, the hydraulic pressure difference is related to the vapor pressure difference by the equation (74)

$$\Delta p_v = \frac{\bar{v}_\rho}{\bar{v}_v} \Delta p \quad (3-26)$$

where  $\Delta p_v$  = vapor pressure difference ( $\text{gm}/\text{cm}^2$ ).  
 $\Delta p$  = hydraulic pressure difference ( $\text{gm}/\text{cm}^2$ ).  
 $\bar{v}_\rho^*$  = Molar volume of liquid = volume per mole of liquid ( $\text{cm}^3/\text{mole}$ ).  
 $\bar{v}_v$  = molar volume of vapor in equilibrium with liquid ( $\text{cm}^3/\text{mole}$ ).

Assuming that the vapor phase behaves as an ideal gas, one can relate the vapor pressure and the molar volume of the vapor by means of the ideal gas law

$$p_v \bar{v}_v = R T \quad (3-27)$$

where  $p_v = \bar{p}_{v0} + \Delta p_v$   
 $\bar{p}_{v0}$  = equilibrium vapor pressure of the liquid at atmospheric pressure at the temperature of the test.

If the permeant is water, the quantity  $\Delta p_v$  is less than 1% of  $\bar{p}_{v0}$  at a hydraulic pressure of 10  $\text{kg}/\text{cm}^2$  and less than 8% of  $\bar{p}_{v0}$  at 100  $\text{kg}/\text{cm}^2$ . Thus for practical purposes one may neglect  $\Delta p_v$  relative to  $\bar{p}_{v0}$ . Approximating  $p_v$  by  $\bar{p}_{v0}$  and substituting Eq. 3-27 into Eq. 3-26 one finds

$$\Delta p = \frac{RT}{\bar{v}_\rho \bar{p}_{v0}} \Delta p_v \quad (3-28)$$

For water at 30°C, the constant  $(RT/\bar{v}_\rho \bar{p}_{v0})$  is equal to  $3.29 \times 10^4$  (dimensionless). Substituting Eq. 3-28 into Eq. 3-3 one obtains

$$q = K' \frac{RT}{\bar{v}_\rho \bar{p}_{v0}} A \frac{(\Delta p_v)_p}{L} \quad (3-29)$$

or  $q = K A \frac{(\Delta p_v)_p}{L} \quad (3-30)$

where  $K = K' \frac{RT}{\bar{v}_\rho \bar{p}_{v0}} \quad (3-31)$

The subscript p in Eqs. 3-29 and 3-30 denotes that the vapor pressure difference is caused by a hydraulic pressure difference.

---

\* Note that the unit weight of the liquid is related to its molar volume by the equation  $\gamma \bar{v}_\rho = M$ , where  $\gamma$  is the unit weight and M is the molecular weight of the liquid. Molar volumes are used here to conform with notation generally used in texts on thermodynamics. The compressibility of the liquid will be neglected in all cases so that  $\bar{v}_\rho$  can be assumed constant.

A comparison of Eq. 3-30 and Eq. 3-3 shows that it is immaterial, with regard to the form of the equation, whether one considers the vapor pressure or the hydraulic pressure difference as the driving force causing flow. Only the numerical values of the constants in the two equations are changed. In both cases the constants  $K$  and  $K'$  are functions of the properties of the permeant and of the membrane.

To compare Eq. 3-30 and Eq. 3-8, one must convert the dimensions of the rate of flow given by Eq. 3-8 from moles/sec to  $\text{cm}^3/\text{sec}$

$$q = \frac{dm}{dt} \bar{V}_p = D_{sp} \bar{V}_p A \frac{(\Delta p_v) c}{L} \quad (3-32)$$

Comparing Eqs. 3-32 and 3-30 the question arises: "Is there a relationship between the two quantities  $K$  and  $(D_{sp} \bar{V}_p)$ ?" It can be shown that they must be equal to each other. If not a perpetual motion machine could be created. Thus one can write

$$q = K A \frac{\Delta p_v}{L} \quad (3-33)$$

where  $\Delta p_v$  is now a function of both the hydraulic pressure difference and the concentration difference across the membrane.

Eq. 3-33 is an expression for both Darcy's and Fick's laws as they apply to flow through membranes. The relationship between  $\Delta p_v$  and  $\Delta p$  is given in Eq. 3-28. The relationship between the concentration of a solvent (in terms of the mole fraction,  $X$ ) and the vapor pressure of that solvent is given by Raoult's law (74) for ideal solutions

$$P_v = X \bar{p}_{v0} \quad (3-34)$$

and

$$\Delta p_v = \bar{p}_{v0} \Delta X \quad (3-35)$$

Eq. 3-35 can be expressed in terms of the concentration difference  $\Delta c$ , if desired. Substituting Eqs. 3-35 and 3-28 into Eq. 3-33 one obtains

$$q = K A \frac{1}{L} \left[ \frac{\bar{V}_p \bar{p}_{v0}}{RT} \Delta p + \bar{p}_{v0} \Delta X \right] \quad (3-36)$$

Eq. 3-36 expresses the rate of flow of a liquid permeant through a membrane in terms of the hydraulic pressure difference and the mole fraction difference across the membrane. It is emphasized that Eq. 3-36 applies only for the case of ideal liquid solutions on each side of the membrane.

An expression for the osmotic pressure of a solution may be obtained from Eq. 3-36. In a typical osmotic experiment, one places a solution in chamber B of Fig. 3-1 and pure solvent in chamber A. Pressure is then applied to chamber B until the rate of flow through the membrane is zero. When the flow is zero, Eq. 3-36 yields

$$q = 0 = K A \frac{1}{L} \left[ \frac{\bar{V}_p \bar{p}_{v0}}{RT} \Delta p + \bar{p}_{v0} \Delta X \right] \quad (3-37)$$

or

$$(\Delta p)_{q=0} = \Delta \Pi = - \frac{RT}{\bar{V}_p} \Delta X \quad (3-38)$$

Eq. 3-38 gives the osmotic pressure of a solution in terms of the mole fraction difference across the membrane. It must be emphasized that Eq. 3-38 applies only for ideal solutions that are at equilibrium, i.e.  $q = 0$ . If any solvent or solute is passing through the membrane when an osmotic pressure measurement is made, the measured osmotic pressure will be less than that given in Eq. 3-38 (64, 96).

A convenient form of Eq. 3-36 may be obtained by substituting for  $\Delta X$  from Eq. 3-38 and for  $K$  from Eq. 3-31

$$q = K A \frac{\Delta p - \Delta \Pi}{L} \quad (3-39)$$

Eq. 3-39 is identical with Starling's hypothesis, Eq. 3-10.

Eqs. 3-36, 3-38 and 3-39 were derived from a consideration of ideal solutions and ideal gas behavior of the vapors that are in equilibrium with the solutions. The derivations can be made equally well without assumptions of ideal behavior by using thermodynamically exact quantities such as the "chemical potential" and the "activity" (74) with only one essential change in procedure. This change enters at Eq. 3-33. Instead of visualizing  $\Delta p_v$  as the driving force causing flow, thermodynamic arguments (51) show that the chemical potential difference (or electrochemical potential difference if electrical forces are operating) should be considered as the driving force. Exact equations of flow may then be derived by making only one assumption, i.e. that the rate of flow is directly proportional to the chemical potential gradient (51). If this is done, Eqs. 3-36, 3-38 and 3-39 may be obtained from the exact equations by making the same idealizing assumptions that were made herein.

Thermodynamic arguments were used to show the essential relationships among Darcy's law, Fick's law and Starling's hypothesis, which are all empirical laws. It was shown that Starling's hypothesis is a necessary consequence of the second law of thermodynamics if one assumes that Darcy's law and Fick's law are both valid for flow through membranes. One must not interpret these arguments as adding credence to Darcy's law or Fick's law. These were and remain strictly empirical laws that must be validated by experiment.

### 3-06 EQUATIONS OF FLOW OF GASES THROUGH MEMBRANES

#### (a) Empirical Equations

##### (1) Darcy's Law

Darcy's law, originally formulated to describe the flow of water through clean sands, has also been applied to the flow of gases through porous media (76). Darcy's law cannot be applied in the form of Eq. 3-3 directly to the flow of gases since the pressure at which the volume of flow is to be measured is not known. Instead, one assumes that Darcy's law applies over differential distances along the path of flow. Thus

$$q_x = K' A \frac{dp}{dx} \quad (3-40)$$

where  $q_x$  = volume rate of flow measured at that point  $x$  in the flow medium where the total pressure gradient is  $dp/dx$  ( $\text{cm}^3/\text{sec}$ ).

$p$  = total pressure at any point  $x$  in the membrane ( $\text{gm}/\text{cm}^2$ ).

$x$  = length coordinate in direction of flow (cm).

From Boyle's law it follows that

$$q_s p_s = q_x p = \text{constant} \quad (3-41)$$

where  $q_s$  = volume rate of flow measured at standard atmospheric pressure ( $\text{cm}^3/\text{sec}$ ).

$p_s$  = standard atmospheric pressure ( $\text{gm}/\text{cm}^2$ ).

Substituting Eq. 3-41 into Eq. 3-40 and rearranging one arrives at

$$q_s p_s dx = K' A p dp \quad (3-42)$$

Since the quantity  $q_s p_s$  is constant, one may integrate Eq. 3-42 as follows

$$q_s p_s \int_0^L dx = K' A \int_{p_1}^{p_2} p dp \quad (3-43)$$

$$q_s = \frac{K'}{2p_s} A \frac{p_1^2 - p_2^2}{L} \quad (3-44)$$

$p_1$  is equal to the total pressure on the high pressure side of the medium and  $p_2$  is the total pressure on the low pressure side. Thus, the assumption that Darcy's law holds for differential distances in a medium leads to the conclusion that the rate of flow is proportional to the difference between the squares of the up and downstream pressures.

Letting  $\bar{q}$  be the rate of flow measured at the average of the up and downstream pressures,  $(p_1 + p_2/2)$ , one can calculate  $\bar{q}$  from Eq. 3-44 using Boyle's law

$$\bar{q} = q_s \left[ \frac{2p_s}{p_1 + p_2} \right] = K' A \left[ \frac{p_1 - p_2}{L} \right] \quad (3-45)$$

or

$$\bar{q} = K' A \frac{\Delta p}{L} \quad (3-46)$$

Eq. 3-46 is identical in form with Eq. 3-3. Thus, if Darcy's law hold for liquid flow through a membrane, then Eq. 3-46 will hold for gas flow through the same membrane.

When applying Eq. 3-46, a permeant which is a mixture of two or more gases is treated as a single gas. No distinction is made between the rate of flow of each component of the mixture.

Muskat (76) presents data to show that Eq. 3-46 applies to the flow of gases through sands. No data are known to the author to show whether Eq. 3-46 might apply to the flow of gas through collodion, rubber, plastic and similar membranes.

## (2) Fick's law

Fick's first law is the equation most generally used to describe the steady flow of gases through membranes such as rubber, plastic and wax. In order to apply Fick's law to gas flow through membranes, one must relate the concentration in the membrane to the concentration in the chamber adjacent to the membrane, just as in the case of liquid flow through membranes. Assuming that the concentration gradient in the membrane is linear Fick's law is

$$\frac{dm}{dt} = D A \frac{\Delta c_m}{L} \quad (3-47)$$

The data of Wroblewski (110) were probably the first to indicate that the solubility of a gas such as hydrogen in a rubber membrane is linearly related to the pressure in the gas as follows

$$c_m = s_p p_p \quad (3-48)$$

where  $c_m$  = concentration of gas in the membrane (moles/cm<sup>3</sup> of membrane).

$s_p$  = solubility of gas in membrane (moles/gm cm).

$p_p$  = partial pressure of gas outside the membrane (gm/cm<sup>2</sup>).

Wroblewski substituted this linear solubility law into Fick's law to obtain

$$\frac{dm}{dt} = D s_p A \frac{\Delta p_p}{L} \quad (3-49)$$

Thus he indicated that the rate of flow of a gas through a membrane was proportional to both its solubility in the membrane and the coefficient of diffusion in the membrane. Doty, Aiken and Mark (42) have interpreted these two constants as follows

$D$  = a measure of the probability that a gas molecule, having been dissolved in the membrane, will move downstream.

$s_p$  = a measure of the number of molecules available to move downstream.

Data to prove the validity of Eq. 3-49 can be divided into four main groups as follows:

- (1) Flow of gases that are not easily condensed (e.g. oxygen, nitrogen, helium, hydrogen) through plastics.
- (2) Flow of gases that are not easily condensed through rubber.
- (3) Flow of easily condensed gases (e.g. water vapor, hydrogen sulfide) through plastic.
- (4) Flow of easily condensed gases through rubber.

With few exceptions, (e.g. see ref. 42), Eq. 3-49 has been found to hold for the first group by Brubaker and Kammermeyer (16) and by Waack, et. al. (103), for the second group by Daynes (39) and by van Amerongen (2) and for the third group by Doty, Aiken and Mark (42). Van Amerongen has succeeded in showing convincingly that  $q \propto D$  and  $q \propto s_p$  for the first group. In no other case has this been shown explicitly.

Group four, the flow of water vapor through rubber, appears to obey Eq. 3-49 so long as the vapor pressure of water on the high pressure side is low (30%) relative to the equilibrium vapor pressure of the water at the temperature of the test. At vapor pressures approaching the equilibrium vapor pressure of the water, the rate of flow through the membrane is neither proportional to the vapor pressure difference nor inversely proportional to the thickness of the membrane. In both cases the measured flow rates are higher than would be expected. The non-linear relationship with pressure is thought to be caused by the increase of the solubility  $s_p$  with increasing pressure. The non-linear relationship with the reciprocal of thickness<sup>p</sup> is attributed to a surface effect. The surface is thought to contribute a major portion of the resistance to flow so that an increase in membrane thickness will not reduce the flow rate as much as predicted by Eq. 3-49 (see Taylor, Hermann and Kemp, 100).

The most frequent reason proposed in the literature to explain deviations from Eq. 3-49 is the variation in solubility of the permeant with pressure. However, no general rules can be given at present to determine, a priori, whether a given membrane-permeant system will obey Eq. 3-49.

#### (b) Equations Based on Models of the Membrane-Permeant System

##### (1) Poiseuille's Law

The models of the membrane and of the permeant used for the following derivation are the same as those described when discussing the flow of liquids in paragraph 3-05(c). To derive the form of Poiseuille's law that applies to the flow of gases through membranes, one assumes that Poiseuille's law for liquids (Eq. 3-12) holds over differential distances along the path of flow. Thus the flow of gas through one capillary is given by

$$q_c = \frac{r^2}{8\eta} A_p \frac{dp}{dx} \quad (3-50)$$

Following the procedure used for deriving Darcy's law for gas flow, Eq. 3-50 may be integrated over the path of flow to obtain

$$\bar{q} = \frac{r^2}{8\eta} A \frac{\Delta p}{L_c} \quad (3-51)$$

where  $\bar{q}$  is measured at the average total pressure of the permeant in the membrane. Eq. 3-51 applies to the flow of gas through one circular capillary of uniform cross section. The total flow through all capillaries in a membrane is given by the following equation, which is analogous to Eq. 3-14

$$\bar{q} = \frac{nr^2}{8\eta} A \frac{\Delta p}{L_c} \quad (3-52)$$

Poiseuille's law for flow of gases through real porous membranes may then be written in the form

$$\bar{q} = \text{constant} \times \frac{nr^2}{8\eta} A \frac{\Delta p}{L} \quad (3-53)$$

where the constant accounts for the differences between the shape and size distribution of the pores in a real membrane compared with the pores in the capillary model.

It is of interest to compare Eq. 3-53, which was derived from Poiseuille's law, with Eq. 3-49, which was derived from Fick's law. The volume rate of flow  $\bar{q}$  (Eq. 3-53) measured at the average pressure  $\bar{p}$  in the membrane is related to the mole rate of flow  $dm/dt$  (Eq. 3-49) by the equation

$$\bar{q} = \frac{RT}{\bar{p}} \frac{dm}{dt} \quad (3-54)$$

Therefore Eq. 3-53 may be written

$$\frac{dm}{dt} = \text{constant} \times \frac{\bar{p}}{RT} \frac{nr^2}{8\eta} A \frac{\Delta p}{L} \quad (3-55)$$

or, for a given gas-membrane system,

$$\left(\frac{dm}{dt}\right)_p = \text{constant} \times A \times \frac{\Delta p}{L} \bar{p} \quad (3-56)$$

where the subscript  $p$  refers to the mole rate of flow that would occur if the flow were to obey Poiseuille's law. A comparison of Eq. 3-56 with Eq. 3-49 shows that one should be able to distinguish whether gas flow through a membrane obeys Poiseuille's law or Fick's law. This could be accomplished by performing a series of tests using the same total pressure difference across a membrane in all tests but varying the average pressure by changing both the high and low pressures simultaneously. If the mole rate of flow remains unchanged over a wide range of  $\bar{p}$  values, the flow obeys Fick's law, whereas, if the mole rate of flow increases in proportion to  $\bar{p}$ , the flow obeys Poiseuille's law. (Note: It has been assumed that the product  $D s_p$  in Eq. 3-49 remains constant regardless of the absolute value of the pressure on the system. If  $dm/dt$  increases with increasing  $\bar{p}$ , it can be argued that the flow still obeys Fick's law but that the product  $D s_p$  increases with increasing  $\bar{p}$ .)

Muskat (76) has presented evidence to show that the flow of gases through sands obeys Eq. 3-53 in that the rate of flow measured at the average pressure is directly proportional to the pressure difference and inversely proportional to the viscosity of the permeant and membrane thickness. To the author's knowledge, Eq. 3-53 has not been applied to the flow of gases through rubber and/or plastic membranes.

## (2) Knudsen Flow

Eq. 3-53 might apply to the flow of gases through porous media as long as the mean free path\* of the permeating molecules is much smaller than the mean diameter of

\* The mean free path of a molecule is given by the mean velocity of the molecule divided by the number of collisions it makes per second with surrounding molecules. The value of the mean free path may be calculated from the kinetic theory of gases. For example, see Moore (74).

the pores (85, p. 56). When the pore diameters are small compared with the mean free path of the gas molecules, the gas can no longer be considered a continuous fluid and the type of flow passes into what is known as "Knudsen flow" or "molecular streaming". The intermediate range of flow between Poiseuille and Knudsen flow has been treated approximately by Present (85), Loeb (68, p. 290) and Dushman (44, p. 104) and will not be considered herein.

The equation for Knudsen flow is based on the following assumptions:

- (1) The pore length is more than 100 times longer than the pore diameter (68, p. 306).
- (2) The mean free path of the gas molecules is 100 or more times longer than the pore diameter (85, p. 61).
- (3) As the gas molecules pass through the pore, they are reflected from the walls of the pore in random directions, independent of the direction of approach (62, p. 23).
- (4) There are essentially no collisions between gas molecules within the pore. This means that a molecule changes its direction of flow only by collisions with molecules in the wall of the pore (85, p. 56).

For the above conditions, Present (85) has derived the following equation for the flow through one cylindrical pore

$$\frac{dm}{dt} = \frac{4}{3} \sqrt{\frac{2\pi}{MRT}} r_p^3 \frac{\Delta p_p}{L_c} \quad (3-57)$$

where the quantity M is the molecular weight of the permeating gas. For Knudsen flow through real porous membranes, Eq. 3-57 may be written simply as

$$\frac{dm}{dt} = \text{constant} \times \frac{n r_p}{\sqrt{M}} A \frac{\Delta p_p}{L} \quad (3-58)$$

It was stated above that Eqs. 3-57 and 3-58 apply when the mean free path of the permeating molecules is 100 or more times larger than the diameter of the capillary. At room temperature and atmospheric pressure, nitrogen has a mean free path of about 600 Å. Thus, if the pores of a membrane are smaller than 6 Å in diameter (about 5 water molecules in diameter), the flow is in the range of Knudsen flow. However, when pores are as small as 5 Å diameter, the permeant molecule is not freely reflected from one position to the next. Instead the motion is strongly influenced by the potential fields of the membrane molecules which surround the gas molecule. This type of flow is in the range of diffusion flow as described in the following paragraphs. On the other hand, Knudsen flow of nitrogen might occur in a pore with a diameter of 60 Å if the pressure is only 0.1 kg/cm<sup>2</sup>. It appears the Knudsen flow generally will not occur in the systems of interest herein.

### (3) Diffusion

In 3-06(a) it was stated that the equation

$$\frac{dm}{dt} = D s_p A \frac{\Delta p_p}{L} \quad (3-49)$$

which was derived from Fick's law, is consistent with experimental results for the flow of gases that are not easily condensed through rubbers and plastics. It was shown in 3-05(c) that Fick's law is consistent with the kinetic model of diffusion as developed by Einstein. Next it is of interest to discuss the mechanism by which a molecule can diffuse through a membrane, with a view toward understanding the factors which affect the magnitude of the diffusion coefficient. The following discussion is intended only to give a general picture of the process of diffusion.

Diffusion of a gas through a rubber or plastic membrane under the influence of a pressure gradient is visualized as follows (8, p. 422, 7, 42):

- (1) At random, a gas molecule obtains sufficient energy, from its collisions with other molecules, to enter the membrane.
- (2) The adsorbed gas molecule then vibrates (due to its thermal energy) about an equilibrium position within the membrane and continually collides with other gas molecules and with membrane molecules. At random the adsorbed molecule again obtains sufficient energy to move away from its equilibrium position.
- (3) The molecule may now move either upstream or downstream to another equilibrium position. Since there is a greater probability of finding an open space downstream (because of the concentration gradient of molecules within the membrane), it is more likely that the molecule will move downstream than upstream. Thus the flow proceeds in a downstream direction.

Based on the above view of the diffusion process, the following equation has been derived by Wheeler (see B, p. 422):

$$\Gamma = \frac{1}{6} \frac{\nu}{(N_e - 1)!} \left( \frac{\mathcal{E}}{RT} \right)^{N_e - 1} \lambda^2 e^{-\frac{\mathcal{E}}{RT}} \quad (3-59)$$

where:  $\nu$  = vibrational frequency of the gas molecules in the membrane (1/seconds).  
 $N_e$  = number of ways in which the energy  $\mathcal{E}$  may be stored, (e.g. as rotational energy and vibrational energy of both the gas molecules and the membrane molecules) (dimensionless)  
 $\lambda$  = mean free path of the gas molecules within the membrane (cm).  
 $\mathcal{E}$  = the "activation" energy. The energy required to cause a gas molecule to jump from one equilibrium position to the next.

Eq. 3-59 is included here only to illustrate the kind of information that is required to understand how and why the coefficient of diffusion varies. The effect of temperature on the coefficient of diffusion is discussed below. The remaining parameters in Eq. 3-59 will not be considered further.

Eq. 3-59 shows that the diffusion coefficient, and therefore the rate of flow of a gas through a membrane, is dependent on the absolute temperature. Several investigators have found that the rate of flow of gases through membranes varies with temperature as follows:

$$q = \text{constant} \times e^{-\frac{\mathcal{E}}{RT}} \quad (3-60)$$

Some of the data that have been reported include that of Barrer (7) for the system hydrogen-rubber; Doty, Aiken and Mark (42) for the system water vapor-pliofilm; Brubaker and Kammermeyer (15) for the systems oxygen-polyethylene, oxygen-polystyrene and oxygen-vinyl; Heilmann, et. al. (55) for the system hydrogen sulfide-pliofilm; and Taylor, et. al. (100) for the system water vapor-natural rubber. The magnitude of the activation energy is not predictable and must be measured for each membrane-permeant system. The data of Brubaker and Kammermeyer show that  $\mathcal{E}$  may have negative values. For the systems studied by Barrer and by Doty, et. al. the rate of flow doubled when the temperature of test was increased from 20°C to 30°C. The data of Taylor, et. al. showed a 15% increase in rate of flow of water vapor through rubber when the temperature was increased from 20°C to 30°C.

This increase in flow rate with temperature is opposite to what one would expect if the flow obeyed the modified form of Poiseuille's law, Eq. 3-53, because the viscosity of a gas increases with increasing temperature. Thus it is evident that the flow in the membrane-permeant systems referenced above is not laminar flow through capillary holes. Such a conclusion is to be anticipated since the openings between molecules in rubber and plastic membranes are of molecular dimensions.

### 3-07 SUMMARY AND CONCLUSIONS

The following summary of Chapter 3 pertains to the flow of liquids and gases through rubber or plastic membranes due to a hydraulic pressure difference, a vapor pressure difference and/or a mole fraction (osmotic pressure) difference applied across the membrane. Only passive transport processes are considered, i.e. those processes that do not use energy from reactions occurring within the membrane.

The matrix of rubber or plastic membranes generally carries a negative surface charge. Rubber membranes are amorphous in the unstretched state. Plastic membranes may be amorphous or crystalline. The membranes of interest herein have a homogeneous structure. It is assumed in all cases that the resistance to flow through these membranes is related to the thickness of the membrane and is not developed in any one specific zone (such as at the surfaces).

The following three equations have been proposed in the literature to relate the rate of flow through a membrane to the gradient causing flow:

(1) Liquid permeants driven by hydraulic pressure gradients:

$$q = KA \frac{(\Delta p_v)_p}{L} \quad (3-30)$$

where

- $q$  = volume rate of flow (cm<sup>3</sup>/sec)
- $K$  = permeability constant (cm<sup>4</sup>/gm sec)
- $A$  = total area of flow (cm<sup>2</sup>)
- $L$  = thickness of membrane (cm)
- $(\Delta p_v)_p$  = vapor pressure difference (gm/cm<sup>2</sup>) caused by hydraulic pressure difference  $\Delta p$ .

Eq. 3-30 is based on the assumption that Darcy's law is valid and on the assumption that the following thermodynamic relationship between  $(\Delta p_v)_p$  and  $\Delta p$  is exact:

$$(\Delta p_v)_p = \frac{\bar{v}_p \bar{p}_{vo}}{RT} \Delta p \quad (3-28)$$

where

- $\bar{v}_p$  = partial molar volume of liquid permeant (cm<sup>3</sup>/mole)
- $\bar{p}_{vo}$  = equilibrium vapor pressure of permeant measured at a pressure of one atmosphere (gm/cm<sup>2</sup>)
- $R$  = gas constant (gm cm<sup>3</sup>/mole °K)
- $T$  = absolute temperature (°K)

(2) Liquid permeants driven by mole fraction (i.e. osmotic pressure) gradients:

$$\frac{dm}{dt} = D s_p A \frac{(\Delta p_v)_c}{L} \quad (3-8)$$

where  $\frac{dm}{dt}$  = mole rate of flow (mole/sec)

$D$  = diffusion coefficient in membrane (cm<sup>2</sup>/sec)

$s_p$  = solubility coefficient of permeant in membrane (moles/gm cm)

$(\Delta p_v)_c$  = vapor pressure difference (gm/cm<sup>2</sup>) caused by the mole fraction difference  $\Delta X$  where  $(\Delta p_v)_c = \bar{p}_{v0} \Delta X$ , for ideal solutions.

(3) Gaseous permeants driven by partial pressure gradients:

$$\frac{dm}{dt} = D s_p A \frac{\Delta p_p}{L} \quad (3-49)$$

where  $\Delta p_p$  is the partial pressure difference across the membrane.

Eqs. 3-8 and 3-49 are based on the assumptions that (1) Fick's law is valid for flow within the membrane and that (2) the concentration of the permeant in the membrane is directly proportional to the partial pressure (or vapor pressure) of the permeant in the chamber adjacent to the membrane.

Eqs. 3-28, 3-8 and 3-49 all have the form:

$$\frac{dm}{dt} = \text{constant} \times A \times \frac{\Delta p_p}{L} \quad (3-61)$$

(Note: For liquid permeants,  $\Delta p_p = \Delta p_v$  and  $dm/dt = q/\bar{V}_p$ ) Thus, regardless of the state of the permeant, Eq. 3-61 indicates that the flow rate is proportional to the partial (or vapor) pressure gradient. However, proof that Eq. 3-61 is valid for any particular membrane-permeant system must be obtained by experiment.

Experimental evidence on the rate of flow of water through rubber membranes and through some physiological membranes shows that the rate of flow of water is directly proportional to the vapor pressure difference regardless of whether it is caused by a hydraulic pressure or mole fraction difference. No satisfactory data are known to the author to prove the inverse relationship between rate of flow of water and the thickness of the membrane. The indications are (from data in Chapter 6) that this relationship is not valid in general.

Experimental data show that the rate of flow of gases that are not easily condensed (e.g. hydrogen, oxygen, nitrogen) through membranes, is directly proportional to the partial pressure difference across the membrane. Also, data are available to show that the rate of flow of gases that are easily condensed (e.g. water vapor) through some plastic membranes (polyethylene, pliofilm) is proportional to the vapor pressure difference.

The rate of flow of water vapor through rubber is not, in general, directly proportional to the vapor pressure difference and not inversely proportional to the thickness of the membrane. These deviations are thought to be caused by (1) a non-linear relationship between the concentration of water in the membrane and the vapor pressure and/or (2) a stratification of the membrane structure which causes the surface to have higher resistance to flow than the interior of the membrane. No general rules can be given at the present time to determine, a priori, whether a given membrane-permeant system will obey Eq. 3-61.

It has been generally assumed that if Darcy's law is found to be valid for a given membrane-permeant system, the flow is laminar, and that if Fick's law is valid, the flow occurs by diffusion. However, it is seen above that both of these laws lead to Eq. 3-61, the only difference between the two approaches being in the interpretation of the constants  $K$  and  $D s_p$ . Therefore, experiments that show a direct proportionality between

flow rate and hydraulic pressure difference or between flow rate and vapor pressure difference for a membrane-permeant system can not be used to ascertain the mechanism of flow. The mechanism of flow can only be determined by experiments that reveal the nature of the constants  $K$  and  $D s_p$ , where these constants are defined by equations such as Eq. 3-15 or Eq. 3-59.

## CHAPTER 4

### EXPERIMENTAL INVESTIGATION OF LEAKAGE THROUGH MEMBRANES DUE TO HYDRAULIC PRESSURE GRADIENTS

#### 4-01 INTRODUCTION

The purpose of this chapter is to present the results of measurements of flow rate of liquid water through natural rubber membranes. The tests, designated "W" or "water permeability" tests, were performed with water on both sides of the membrane. A difference in hydraulic pressure was applied to cause flow. These W tests are intended to simulate the conditions imposed on membranes used in triaxial testing. The only difference between the conditions during W tests and those during triaxial tests is the membrane support, which is made of porous stainless steel in W tests and is soil in triaxial tests.

The membranes were manufactured by the Julius Schmid Company (under the trade name "Ramses"), by dipping cylindrical forms into natural rubber cement. After drying, the membranes were powdered and stripped from the forms. No further details of the manufacturing process are available. The thickness of the membranes tested was  $0.006 \pm 0.001$  cm. These membranes are presently used in triaxial testing at Harvard University.

#### 4-02 APPARATUS

##### (a) General Description

The purpose of the apparatus is to provide a means to measure accurately the rate of flow of water through various membranes due to hydraulic pressure gradients. The apparatus was designed to measure a rate of flow as low as  $0.0025 \text{ mm}^3/\text{cm}^2/\text{day}$ . This is equivalent to  $0.1 \text{ mm}^3/\text{day}$  in an apparatus of the size used.

The apparatus consists of (1) permeability cell, (2) burettes to measure volume changes, (3) system for applying pressure through a mercury seal, and (4) constant temperature bath. A schematic diagram of the apparatus is shown in Fig. 4-1 and a photograph is in Fig. 4-2. The components are described in paragraphs (b)-(e) below. The procedure used in performing the tests is described in 4-03.

##### (b) Permeability Cell

One permeability cell was first designed and used to perform several W tests. Based on experience with this first apparatus, the design was modified and two new apparatus were built which performed more satisfactorily. Only the second design is described below. The essential differences between the two are described in 4-04(b).

Fig. 4-3 and Fig. 4-4 show a cross sectional view and a photograph of the permeability cell. The following design features are important:

- (1) Measurements of inflow, outflow and leakage past the O-Ring sealing the perimeter of the membrane can be made.
- (2) There is a minimum number of locations where leakage can occur.
- (3) The void volume in the cell is small and the thicknesses of the top and bottom plates are large. Thus volume changes due to temperature changes and/or pressure changes are minimized.

The inflow, outflow and peripheral leakage were measured in burettes connected to the cell through the shop-made O-Ring fittings shown in Fig. 4-3 and 4-5. These fittings are designed so that (a) the O-Ring is highly stressed when the fitting is tightened (i.e. the O-Ring groove depth is only 70% of the height of the O-Ring), (b) the O-Ring fills 96% of the volume of the O-Ring groove when the fitting is tightened, and (c) the sealing surfaces are polished. Each fitting was tested individually for leaks. In all cases the leakage from the fitting into room air was less than  $0.005 \text{ mm}^3/\text{day}$  when a gage pressure of  $10 \text{ kg/cm}^2$  was applied to water inside the fitting. The leakage through two

such fittings could amount to  $0.01 \text{ mm}^3/\text{day}$ , or 10% of the smallest rate of flow through the membranes as measured in the W tests.

The cell was constructed of type 304 stainless steel. No corrosion of the inside of this cell was detected over a period of 18 months of constant use.\* Stainless steel is difficult to machine (relative to brass), but it has the advantages that it corrodes only slightly, it has high strength and it exhibits low creep under stress. The increase in volume of the assembled cell (inside of the inner O-Ring) due to the application of pressure amounted to  $1.9 \text{ mm}^3$  per  $\text{kg}/\text{cm}^2$ . This volume change occurred suddenly (elastically) and caused no experimental difficulties.

The O-Ring grooves in the top plate were designed so that the O-Ring would fill 96% of the volume of the groove when the cell is assembled. Thus when the top and bottom plates are tightened together, the groove is almost entirely filled with rubber and little if any further movement of the rubber in the O-Ring can occur when pressure is applied to the cell.

The total void volume of the cell above the membrane when the cell is assembled is  $4 \text{ cm}^3$ . As the temperature of the cell increases, both the voids and the water within these voids increase in volume. Since water has a much higher coefficient of thermal expansion than stainless steel, there is a net outflow of water when the temperature increases. With the membrane in place, the water is forced out through the inflow fitting and into the HP burette (see Fig. 4-1 and 4-3). A temperature increase of the cell of only  $1^\circ\text{C}$  causes a movement of  $0.7 \text{ cm}$  in a  $1/2 \text{ mm}$  bore capillary. A constant temperature bath is therefore essential for obtaining satisfactory test data.

The porous disc that supports the membrane is made of sintered, type 316 stainless steel. It was manufactured by the Mott Metallurgical Corporation and is designated as Mott Series A-2 porous stainless steel. The porous stainless steel was preferable to a paper or plastic filter because the latter materials are likely to creep a noticeable amount under stress. The disc was hand-lapped to the desired thickness so that when it was placed in the cell the top surface of the bottom plate of the cell would be smooth, which would prevent puncturing of a membrane when pressure was applied. The handlapping caused the pores of the disc to be plugged with metal filings. Therefore, the disc was pickled in a solution of  $65 \text{ gm}$  ferric chloride,  $195 \text{ cm}^3$  of 35% hydrochloric acid and  $5 \text{ cm}^3$  of nitric acid. One or two minutes of pickling at  $65^\circ\text{C}$  was sufficient to dissolve the metal filings and re-open the pores. After pickling the porous disc was rinsed thoroughly in glass-distilled water and passivated\*\* to restore its corrosion resistance. The passivation was accomplished by soaking the porous disc in a 35% solution of nitric acid for 45 minutes at  $65^\circ\text{C}$ .

The permeability of the porous disc after the above treatment was about  $7 \times 10^{-4} \text{ cm}^2/\text{sec}$ , or 10 billion times greater than the permeability of the membranes tested. However, there was some question as to whether the area of flow through the membrane was restricted because it was supported at some points by the solid stainless steel in the porous disc. Therefore two tests were performed using (1) a porous ceramic disc beneath the membrane (permeability  $10^{-6} \text{ cm}^2/\text{sec}$ ) and (2) a layer of filter paper (permeability  $10^{-4} \text{ cm}^2/\text{sec}$ ) beneath the membrane. In two tests, which were identical except for the porous support, the measured rate of flow through a natural rubber membrane was the same. It was concluded that the type of porous disc beneath the membrane probably did not appreciably affect the measurements.

#### (c) Burettes to Measure Volume Changes

The burettes consisted of precision-bore glass capillary tubes obtained from the Fischer-Porter Corp. The burettes used had a total length of about  $75 \text{ cm}$  and an internal diameter of  $0.1 \text{ cm}$  or  $0.05 \text{ cm}$ . Each one was calibrated with mercury to determine the volume per centimeter with an accuracy of  $\pm 0.1\%$ .

\* The exterior of the cell did pit slightly because the conditions in the water bath were favorable to corrosion.

\*\* Passivation causes the formation of surface oxides which are the source of corrosion resistance in stainless steel.

The top of each burette was connected to a No. 19 gage (0.042" O.D., 0.027" I.D.), type 304 stainless steel hyperdermic needle tube about 2 ft long. The connection was an epoxy seal with details as shown in Fig. 4-5. The opposite end of the stainless steel tubing was soft-soldered or glued with epoxy into the O-Ring fitting which, in turn, was attached to the permeability cell during a test.

The bottom end of each burette was attached to a 2 meter length of 1/8 in. O.D. Saran tubing (through which pressure was applied) by means of a type 316 stainless steel "Swagelok" reducer. Nylon ferrules were used in the reducer on the side attached to the glass capillary. A five inch long piece of glass tubing with an outside diameter of 0.250 in.  $\pm$  .005 in. had to be added to the bottom end of the capillary tubes so that the reducer could be attached.

The assembled burettes were tested at a pressure of 22 kg/cm<sup>2</sup> to be sure that the fittings would not blow off in use. The burettes were then attached to wooden meter sticks as can be seen in Fig. 4-2. During W tests, three burettes were used. These were connected to the high pressure side of the membrane, the low pressure side of the membrane and to the chamber in which leakage past the perimeter of the membrane was collected (see Fig. 4-1). These three burettes will be called simply HP, LP and L burettes in the following discussions.

During a test, mercury filled the Saran tubing and the lower portion of each burette. The remaining top portion of each burette, the hyperdermic needle tubing and the permeability cell all were filled with distilled water. Volume change measurements were made by reading the water-mercury meniscus level in the burettes to the nearest 0.1 mm with the aid of a 5-power magnifying glass. Since the burettes were mounted in a vertical position, there was no trouble experienced in maintaining a sharp meniscus. An attempt was made initially to use the burettes inclined at 10° above the horizontal but it was found that the meniscus would not remain intact over long periods.

The only sources of leakage that could affect the measured volume flow into and out of the cell are the connections in the lines between the membrane and the meniscus level in each burette. Thus only the epoxy seal to the burette, the soldered or epoxied joint at the cell, and the O-Ring fitting are potential sources of leaks.

#### (d) System for Applying Pressure

Compressed air was used to apply pressure to the surface of the mercury in the lucite reservoirs in the manner shown in Fig. 4-1. The pressure was read to the nearest 0.01 kg/cm<sup>2</sup> on the gage attached to each ballast tank.

The mercury filled Saran tube served as a seal to prevent air from diffusing into the water which permeated the membrane and to prevent evaporation from the water meniscus in the volume change burettes. The performance of the mercury seal was checked periodically by raising the pressure on the LP burette by a given amount and measuring the volume change of the system. If this volume change increased with time, air was presumably coming out of solution on the downstream side of the membrane. Nearly all tests were checked in this manner to be sure that no measurable air diffusion was occurring during the tests.

During W tests the air-mercury menisci in the HP and LP reservoirs were maintained at the same level as the water-mercury menisci in the corresponding burettes. The mercury level in the L reservoir was maintained 20 cm higher than the water-mercury meniscus level in the L burette and no additional air pressure was applied. The 20 cm of mercury head was applied to be sure a positive pressure existed in the chamber between the two O-Rings in the permeability cell.

#### (e) Constant Temperature Bath

A water bath was used to maintain the permeability cells at constant temperature during each test. The bath (see photograph in Fig. 4-6) was capable of maintaining constant temperature to within  $\pm$  0.02°C. All tests were performed at 30°C. The bath consisted of:

- (1) A 50 gallon glass aquarium.
- (2) A 600 watt copper heating element bent in the form of a U-tube.
- (3) A stirring motor with a 4" diameter propeller rotating at about 1000 RPM.
- (4) A "Red-Top" thermoregulator with a mercury relay to actuate the heater at the desired temperature.

The water bath was insulated to prevent excess heat losses. During operation of the bath the heater was on about 20 seconds during each 3 minute time interval.

The regulation obtained using this bath was well within tolerable limits. However, the regulation could have been made more precise if the rate of temperature rise during the heating cycle were more nearly equal to the rate of temperature decrease during the cooling cycle. This could have been accomplished by either reducing the wattage of the heater (by a factor of three or four), or by removing the insulation, or both.

#### 4-03 PROCEDURE FOR WATER PERMEABILITY (W) TESTS

##### (a) General Description

W tests are performed by placing a membrane in the permeability cell with liquid water on both sides of the membrane. A difference in pressure is then applied across the membrane to start flow. The volume flow of water through the membrane is measured as a function of time.

Owing to the experimental difficulty of measuring the very low permeability of natural rubber to liquid water, W tests must be carried out for 10 days or more to measure the permeability to within  $\pm 10\%$  accuracy.

##### (b) Preparation of Membranes

The membranes were cut into discs with a diameter of 8 cm, so that they were only slightly larger in diameter than the O-Ring which seals the periphery of the membrane in the permeability cell.

The membranes used for tests W4 and W5 were soaked in Dow-Corning silicone oil (viscosity = 500 cm<sup>2</sup>/sec) and the membranes for the six other W tests were soaked in distilled water. The membranes were placed in a container which was evacuated by means of an aspirator to an absolute pressure of about 2 cm Hg. After 24 hours the oil or water was allowed to rise into the container slowly while the vacuum still was maintained. The membranes were kept submerged in the liquid under vacuum for at least 24 hours prior to test. When a test was to be started, one membrane (whether water- or oil-soaked) was removed from the vacuum container and submerged in a bath of distilled water until ready for use. The vacuum was then reapplied to the remaining membranes. The W tests were generally begun within twenty minutes after removing the membrane from the evacuated container.

##### (c) Placement of Membrane in the Permeability Cell

The porous disc of the permeability cell was saturated by placing it in a jar, evacuating the jar with an aspirator and then allowing distilled water to rise slowly in the jar to submerge the disc. The saturated disc and the top and bottom plates of the cell were then submerged in a bath of distilled water at atmospheric pressure. All visible bubbles were carefully removed from all surfaces of the cell so that no air would be trapped inside the cell when the test was begun. It was not necessary to use deaired water for saturating the porous disc and the cell because the tests were performed with high pressures on both sides of the membrane. Any remaining minute air bubbles were dissolved when these high pressures were applied.

With all parts still submerged, the bottom plate of the permeability cell was lightly greased (with silicone stopcock grease) in the area around the periphery of the porous disc where the membrane would be sealed. The porous disc was then inserted in

its recess in the bottom plate and the membrane was placed over the porous disc. The grease caused the membrane to adhere to the bottom plate so that all wrinkles could be easily removed from the membrane. Each O-Ring in the top plate of the cell was also greased to help reduce the peripheral leakage. The top plate was carefully lowered over the guide pins in the bottom plate. The pins assured accurate alignment of the two plates and prevented any relative lateral motion which might cause wrinkles in the membrane. The two plates were bolted together by applying a moment of 12 ft-lb with a torque wrench. Complete saturation of all parts of the cell was assured by assembling it underwater in the above manner.

(d) Starting the Test

The stainless steel tubes leading from the burettes to the permeability cell were saturated with distilled water and the water-mercury menisci in the burettes were brought to the desired level. The HP burette (Fig. 4-1) was then attached to the HP connection of the permeability cell with care so that no air would be trapped in the O-Ring connection. The cell was submerged in the water bath and the high pressure was applied and allowed to remain in place for about 15 minutes before any further operations were performed. This allowed time for the temperature of the cell to rise to the temperature of the water bath and insured that the water-mercury meniscus would stabilize at a suitable level. Next, the LP and the L burettes (Fig. 4-1) were connected to the corresponding fittings on the cell. A back pressure of 6 kg/cm<sup>2</sup> was applied to the LP burette and a pressure of 20 cm Hg was applied to the L burette. The largest hydraulic pressure difference applied across the membrane was 11.5 kg/cm<sup>2</sup> (Test W7d) and the lowest was 1.86 kg/cm<sup>2</sup> (Test W5).

(e) Readings during Test

Each day readings were recorded of the date, time, room temperature, bath temperature, pressure on each burette and scale reading of the water-mercury meniscus in each burette. In some cases the pressure on the LP burette was momentarily increased to determine whether any air was diffusing from the high pressure side to the low pressure side, coming out of solution and giving a false indication of water flow. The readings were continued until the volume flow into the L burette was linear with time for more than 50% of the duration of the test. Such W tests lasted between 8 and 65 days, depending on the quality of the data, the thickness of the membrane, and the pressure difference applied across the membrane.

(f) Dismantling the Test

Upon completion of a test the pressures were released, the valves beneath the mercury reservoirs were closed (to prevent further movement of the menisci), and the O-Ring fittings were disconnected from the permeability cell. The membrane was then removed from the cell and its thickness measured using a microscope with a magnification of 100X or 400X. The membrane was cut into three pieces with a new razor blade and they were turned with one square-cut edge towards the objective lens of the microscope to make the measurement. Using this procedure it was possible to read the thickness to within plus or minus one micron at 100X and to plus or minus one-half micron at 400X. For natural rubber membranes, these tolerances amount to  $\pm 2\%$  of membrane thickness at 100X and  $\pm 1\%$  of the membrane thickness at 400X. The membranes themselves varied in thickness by about  $\pm 4\%$ . Nine measurements were made of the thickness of each membrane. These measurements were averaged to obtain the thickness used in calculations of permeability.

4-04 PRESENTATION AND ANALYSIS OF DATA FOR W TESTS

(a) General

The results of measurements of the flow of water through natural rubber membranes due to a hydraulic pressure gradient are presented and analyzed herein. Data are given on (1) the effect of the magnitude of the hydraulic pressure difference and (2) the effect of soaking the membranes in silicone oil on the measured rate of flow of water. The permeability of natural rubber to liquid water is calculated from the data. Table 4-1

is a summary of the W tests. The data for all W tests are presented in Fig. E-1 through E-11 in Appendix E.

The data for test W1 are analyzed below in detail. Analyses of all other tests are given in summary form only.

(b) Analysis of Data for Test W1

The curves of total inflow and total outflow versus time for test W1 are shown in the lower half of Fig. E-1 in Appendix E. The total inflow is represented by the change in reading of the HP burette. The total outflow is represented by the sum of the changes in readings of the LP and the L burettes. A positive inflow means the meniscus in the HP burette was moving toward the cell. A positive outflow means the menisci in the LP and L burettes were moving away from the cell. If the slopes of the curves of total inflow and of total outflow were parallel, one could safely assume that there were no significant leaks or errors in the data. In such a case the change in reading of the LP burette, plotted at the top of Fig. E-1, would represent the rate of flow of water through the membrane. In the absence of parallelism, one can state that the LP flow may have passed through the membrane but possible reasons why the curves of total inflow and total outflow are not parallel must be considered.

Leakage from any of the fittings or across the outer O-Ring of the permeability cell will cause the measured inflow to be greater than the measured outflow. However, in Fig. E-1 the total inflow is less than the total outflow. This means that the volume of water in the cell is apparently increasing. The following are two possible explanations for this phenomenon:

- (1) CREEP - The top half of the permeability cell is separated from the bottom half by the thickness of the rubber membrane. As the rubber membrane yields under the load of the inner O-Ring in the cell, the top plate of the cell moves toward the bottom plate. Water is then forced into the HP and L burettes, giving the appearance that the volume of water in the cell is increasing.
- (2) GAS - Corrosion inside the permeability cell or in the connections may cause gas to evolve. Also, air may permeate through the membrane from the high pressure side and come out of solution in the porous disc. In either case, the data would indicate that the volume of water in the cell is increasing.

To determine whether creep or gas was causing the discrepancy between total inflow and total outflow, measurement of gas volume in the L and LP burettes were made. These measurements showed that there was no change in gas volume in the L or LP burette with time. Thus creep remains as the only probable explanation.

Assume that the difference between the slopes of the two curves at the bottom of Fig. E-1 is entirely due to creep. From Table 4-1, this difference in slope is found to be  $1.07 \text{ mm}^3/\text{day}$ . Since the area inside the outer O-Ring of the permeability cell is  $79.7 \text{ cm}^2$ , a uniform movement of the top plate toward the bottom plate at a rate of  $0.000014 \text{ cm/day}$  (or about 6 millionths of an inch per day) would explain the discrepancy between the two slopes. Measurements on the first permeability cell constructed (with which test W1 was performed) indicate that the thickness of the membrane under the inner O-Ring is about 60% of its unstressed thickness, i.e. about  $0.004 \text{ cm}$ . Relative movement between the two plates at a rate of  $0.000014 \text{ cm/day}$  (0.25% of the thickness per day) is therefore entirely within reason.

The discovery that creep apparently was excessive in the first permeability cell led to the design of the cell which was described in 4-02(b). The basic differences between the two designs are: (1) The top and bottom plates were 75% thicker in the new cell. (2) The bolt diameter was increased from  $1/4 \text{ in.}$  to  $1/2 \text{ in.}$  and the torque used to tighten the two halves of the cell together was increased from 8 to 12 ft-lb. (3) A shallow recess was provided for the membrane in the new cell (see detail in Fig. 4-3). According to the data which will be presented in (d) below, these changes apparently eliminated creep.

The volume flow measurements in the LP burette are the best measure of the flow which passed through the membrane for the following reasons:

- (1) Creep does not affect the readings in the LP burette.
- (2) The possibility that leakage will occur across the inner O-Ring of the cell from the LP chamber to the L chamber is small because the surface of the bottom plate was polished and then greased before placing the membrane. The binding leakage data presented in Chapter 7 indicate that the leakage across this O-Ring should be less than  $0.1 \text{ mm}^3/\text{day}$ .
- (3) The volume of fluid on the low pressure side of the membrane is small. This means that minor pressure and temperature fluctuations will have a small effect on the readings in the LP burette.
- (4) The data for the W tests, in Appendix E, show that the volume flow into the LP burette increases linearly with time for at least the last 50% of the test in every case. This is not the case for the curves of total inflow.

For the above reasons, the flow measured in the LP burette was taken as the flow through the membrane in all cases. If any leakage occurs from the chamber on the downstream side of the membrane, the use of the LP flow leads to an estimate of the flow through the membrane which is too low. For leakage at a rate of  $0.1 \text{ mm}^3/\text{day}$ , the volume flow measured in the LP burette may be too low by 45% for test W8, and by 20% or less for the remainder of the W tests. However, for tests in which the total inflow was equal to the total outflow, the probable error is much lower than the above values.

The analyses of test W2 through W8 are given below in summary form. The tests are divided into two groups. Tests in the first group, W2 through W5, were performed in the first permeability cell which apparently exhibited excessive creep. Tests in the second group, W6 through W8, were performed in the second cell, i.e. the one described in 4-02(b).

(c) Analyses for Group I Tests

TEST W2 - In Fig. E-2 the final slope of the curve of total inflow is less than that for the total outflow by about 30%. The difference is probably due to creep. However, no gas volume measurements were made in the L and LP burettes, so the possibility that gas was being evolved cannot be excluded. The slopes of the curves in Fig. E-2 changed during the course of the test. No satisfactory explanation was found for this change in slope.

TEST W3 - In Fig. E-3, the final slopes of the curves of total inflow and total outflow are equal. This is an excellent test.

TEST W4 - In Fig. E-4, the final slope of total inflow is approximately zero and is less (algebraically) than the final slope of total outflow. This means creep may have occurred. However, no gas volume measurements were made. The linearity of the plot of flow into the LP burette, for more than 80% of the duration of the test, is a good indication that the LP flow is a reliable measurement of the flow through the membrane.

TEST W5 - In Fig. E-5, the final slopes of the plots of total inflow and total outflow are essentially the same. Note that the leakage across the inner O-Ring in the permeability cell was  $1.32 \text{ mm}^3/\text{day}$  (see Table 4-1). This is the highest leakage recorded in any of the W tests and is probably due to the fact that no back pressure was applied in this test. Thus the inner O-Ring was not stretched by a large seating pressure. It is also possible that dirt was caught under the O-Ring, causing an imperfect seal.

(d) Analyses for Group II Tests

TEST W6 - In Fig. E-6, the slope of the plot of total inflow is less than that for total outflow. Measurements were made of the gas volumes in the L and LP burettes. No gas was found in the LP burette. The plot of gas flow versus time for the L burette is shown dotted in Fig. E-6. The slope of this dotted line is essentially

equal to the difference between the slopes of the total inflow and total outflow curves. Thus the difference is explained by gas formation and not by creep. The reason for gas formation in this test is not known.

TESTS W7a, b, c and d - These tests were all performed on the same membrane without disturbing the membrane between tests except to change the applied pressures. In Figs. E-7, E-8, E-9 and E-10, the slopes of the total inflow curves are within 2% of the slopes of the total outflow curves. From Table 4-1 it can be seen that the leakage across the inner O-Ring was negligible.

TEST W8 - In Fig. E-11 it is seen that the total inflow slope is greater than the total outflow slope. This indicates that leakage was occurring during the test. Gas volume measurements were made in the L and LP burettes but the rate of gas flow was found to be zero in both cases. In Fig. E-11 (and in Table 4-1) it is seen that the total inflow slope is equal to the slope of the curve of flow into the LP burette. Also, the flow into the L burette is negative. These two facts show that leakage must have occurred past the outer O-Ring. In the course of the test, the pressure on the L burette was increased to help seal the outer O-Ring, but this attempt was not successful.

#### 4-05 DISCUSSION OF RESULTS

##### (a) Effect of Hydraulic Pressure Difference on Rate of Flow

Darcy's law can be written in the form:

$$\frac{q \times L}{A} = \text{constant} \times \Delta p \quad (4-1)$$

Thus, if flow through the natural rubber membranes obeys Darcy's law, a plot of  $q \times L/A$  versus  $\Delta p$  should yield a straight line through the origin. Fig. 4-7 is such a plot for all W tests. The line shown connects the points for tests W7a, W7b, W7c and W7d all of which were performed on the same membrane. This line deviates from a straight line through the origin by less than 5%. This deviation is not considered significant in view of the possibility that each of the measured rates of flow through the membrane may be slightly in error due to leakage from the fittings on the LP side of the membrane (see 4-04). Thus, the line shown in Fig. 4-7 is sufficient proof that, for practical purposes, the rate of flow of liquid water through natural rubber is directly proportional to the applied hydraulic pressure difference for the range of  $\Delta p$  between 2 and 11.5 kg/cm<sup>2</sup> which was used in this investigation. Although these data show that the rate of flow of water through natural rubber is directly proportional to the hydraulic pressure difference, this fact does not imply that the flow obeys Poisseuille's law (see 3-07).

The remaining points plotted in Fig. 4-7 (excepting the two triangles) fall into a band with a width of about  $\pm 35\%$  about the line shown for tests W7. This spread of the data is due to (1) errors in the membrane thickness measurements, (2) variations in the thickness at different locations on a membrane, (3) errors in the measurement of the flow through the membrane, (4) variations in the permeability of the membranes and (5) differences among the three permeability cells used for the tests.

The thickness of each membrane tested is shown adjacent to each point in Fig. 4-7. It may be seen that the points do not fall in any consistent pattern with respect to thickness. Apparently, the errors in the data obscured the effect of thickness on permeability, if such an effect exists.

##### (b) Effect of Oil Soaking on Rate of Flow

The two points shown as triangles in Fig. 4-7 represent tests performed on membranes soaked in silicone oil. These points lie above the points for water soaked membranes at the same hydraulic pressure difference ( $\Delta p = 2.0$  kg/cm<sup>2</sup>). This result may be coincidental, but one can safely conclude that silicone-oil soaking has no significant beneficial effect.

(c) The Permeability of Natural Rubber to Water

Using Darcy's law,  $q = kiA$  (Eq. 3-2), one can calculate the coefficient of permeability,  $k$ , from the data for tests W7 in Fig. 4-7. The result is that  $k = 4.8 \times 10^{-16}$  cm/sec. The probable error in this coefficient of permeability is  $\pm 35\%$ . This  $k$ -value was obtained for the following conditions:

- |                 |                |                      |  |
|-----------------|----------------|----------------------|--|
| 1. Membrane:    | Natural rubber | 5. Hydraulic pres-   |  |
| 2. Thickness:   | 0.006 cm       | sure difference:     | 2 to 11.5 kg/cm <sup>2</sup>           |
| 3. Permeant:    | Liquid water   | 6. Membrane support: | Mott Series A2, porous stainless steel |
| 4. Temperature: | 30°C           |                      |  |

It is reasonable to expect that the  $k$ -value is applicable for a much wider range of conditions. The coefficients of permeability for all W tests are shown in Table 4-1.

In 3-05(d) it was shown that Darcy's law may be expressed in terms of the vapor pressure difference  $\Delta p_v$  that is caused by applying a hydraulic pressure difference  $\Delta p$  across a membrane:

$$q = KA \frac{\Delta p_v}{L} \quad (3-33)$$

where the permeability constant  $K$  is given by:

$$K = \frac{k}{\gamma_w} \frac{RT}{\bar{V}_w \bar{p}_{vo}}$$

and

$$\frac{RT}{\bar{V}_w \bar{p}_{vo}} = 3.29 \times 10^4 \text{ at } 30^\circ\text{C}$$

From Eq. 4-2, using  $k = 4.8 \times 10^{-16}$  cm/sec, one finds that for water flowing through natural rubber at 30°C,  $K = 1.6 \times 10^{-11}$  cm<sup>4</sup>/gm sec. The permeability constant for each W test is shown in Table 4-1. These  $K$ -values will be useful for comparison with results to be presented in Chapters 5 and 6.

4-06 SUMMARY(a) Apparatus and Procedure

An apparatus was designed and used to measure the permeability to liquid water of natural rubber membranes 0.006 cm thick. This apparatus has the following features which are essential to obtaining reasonably accurate results:

- (1) Both the inflow to and outflow from the permeability cell are measured. A balance of the inflow and outflow over a sufficiently long period of time strongly indicates that leakage and/or other possible errors have not affected the data.
- (2) Volume measurements are made in burettes with an inside diameter of 0.05 cm.
- (3) Evaporation is prevented by the menisci in the burettes in which volume measurements are made.
- (4) Diffusion of air from the source of high pressure into the low pressure side of the membrane is prevented.
- (5) Leakage can occur through only nine connections. Six of these are epoxy seals or soldered joints and three are specially designed O-Ring connections.
- (6) A water bath is used to maintain the permeability cell and contents at a constant temperature to within  $\pm 0.02^\circ\text{C}$ .

(b) Rate of Flow of Water Through Natural Rubber

In a series of tests in which a hydraulic pressure difference was applied across natural rubber membranes it was found that for practical purposes the rate of flow of water is directly proportional to the hydraulic pressure difference.

The coefficient of permeability of natural rubber membranes with a thickness of about 0.006 cm was found to be  $(5 \pm 2) \times 10^{-16}$  cm/sec. This value applies when (1) the temperature of test is  $30^{\circ}\text{C}$ . (2) the hydraulic pressure difference is between 2 and 11.5 kg/cm<sup>2</sup>, and (3) the support beneath the membrane is made of porous stainless steel of the type used in the permeability cell.

Membranes soaked in silicone oil prior to test were found to have equal or higher permeabilities than those soaked in water.

CHAPTER 5EXPERIMENTAL INVESTIGATION OF LEAKAGE THROUGH MEMBRANES  
DUE TO MOLE FRACTION (OSMOTIC PRESSURE) GRADIENTS5-01 INTRODUCTION

Ten tests were performed by placing a membrane between two chambers, one containing pure water and the other containing a water solution of sodium chloride. The rate of flow (osmosis) of water into the chamber containing the solution was then measured. Since the rate of flow of salt ions from the solution into the pure water is only about 1/1500th of the rate of flow of water into the solution (see Appendix A-07(c)), the ion flow was neglected. For convenience these osmosis tests will be designated "X" tests, since the mole fraction difference  $\Delta X$  of the water across the membrane causes the flow of water.

All X tests were performed on natural rubber membranes manufactured by the Julius Schmid Company with a thickness of  $0.006 \pm .001$  cm. The X tests were performed for the following purposes:

- (1) To measure the rate of flow of water through natural rubber membranes under the influence of a mole fraction gradient. Such measurements can be used to compute approximately the rate of flow of water into triaxial specimens that contain salt solutions in their pores.
- (2) To determine whether the rate of flow of water through natural rubber due to a mole fraction gradient can be reduced by soaking the membrane in silicone oil prior to test.
- (3) To determine whether the results of X tests are comparable to the results of the W tests presented in Chapter 4.

5-02 APPARATUS(a) General

A diagram of the apparatus used for the X tests is shown in Fig. 5-1. The apparatus consists of (1) a cell in which the membrane is placed, (2) burettes connected to the cell to measure the inflow and outflow from the cell, (3) a mercury seal, and (4) a water bath to maintain the cell and contents at constant temperature.

The burettes for measuring volume change and the water bath were the same as used for the W tests. These are both described in 4-03. The cell and the mercury seal used for the X tests are described below.

(b) The Cell Used for X Tests

A schematic cross section of the cell is shown in Fig. 5-2 and a photograph of the parts of the cell is shown in Fig. 5-3.

The cell is made in two halves. One half contains a salt chamber that is large enough so that the quantity of water flowing into the chamber during a test will not dilute the salt solution appreciably. The volume of the salt chamber is  $44.0 \text{ cm}^3$ . The largest volume of water that flowed into the salt chamber during any test was  $0.12 \text{ cm}^3$ . Thus the concentration of the solution did not change by more than 0.3% during any one X test.

The second half of the cell contains a porous disc made from a machinable ceramic, AlSiMag 614, manufactured by the Minnesota Mining and Manufacturing Company. The porous disc performs two functions: first, it supports the membrane, and second, it is a reservoir for the water that flows through the membrane into the salt chamber. The volume of water in this reservoir is small (only  $2 \text{ cm}^3$ ) but, since practically no salt ions

flow through the natural rubber into the pores of the ceramic disc, the water in the disc remains essentially pure throughout the duration of an X test.

The burettes used for measuring volume changes are connected to the two halves of the cell through O-Ring fittings of the type used for the permeability cell described in Chapter 4. An additional fitting is provided in the half of the cell containing the salt chamber so that the liquid in the salt chamber can be changed without dismantling the cell. No provision was made to measure the leakage that might occur across the O-Ring that seals the periphery of the membrane. It was expected that the rate of flow of water through the membrane due to the applied mole fraction gradients would be about 100 times greater than the leakage across the O-Ring.

(c) The Mercury Seal

Mercury was used to fill the lower portion of the burettes, the 1/8 in. O.D. Saran tubing and the lucite reservoirs shown in Fig. 5-1. The mercury prevented evaporation of water from the burettes and provided a means for applying a small hydraulic pressure difference across the membrane to hold the membrane firmly against the porous disc in the cell. This hydraulic pressure difference caused a flow through the membrane in a direction opposite to the flow caused by the mole fraction differences that were applied. The data for the X tests were corrected to take this small flow into account. The method of correction is described in 5-04.

5-03 PROCEDURE FOR X TESTS

(a) General

The essential steps were as follows:

- (1) The membrane was prepared.
- (2) The membrane was placed in the cell with pure water in both chambers. A small hydraulic pressure difference was applied and readings of the menisci were taken daily until the rate of movement of the menisci was less than 5% of the rate of movement expected when the salt was added.
- (3) The water in the salt chamber was replaced by a salt solution and readings were continued until the plotted data were considered satisfactory.
- (4) The test was dismantled.

Each of these steps is described below.

(b) Preparation of Membranes

Natural rubber membranes manufactured by the Julius Schmid Company were used for all X tests. The membranes were cut into discs with a diameter of 5.7 cm, which is just equal to the outside diameter of the O-Ring that seals the periphery of the membrane. The membranes for tests X6 and X7 were soaked in Dow Corning silicone oil (with a viscosity of 500 cm<sup>2</sup>/sec) in the manner described for the W tests in 4-03(b). The membranes for the remainder of the X tests were soaked in distilled water in the manner described in 4-03(b).

(c) Placement of Membrane in Cell

The cell was submerged in a distilled water bath and saturated by drawing water through all openings. Bubbles adhering to the metal were carefully removed. The porous ceramic disc was saturated by boiling it in distilled water for a minimum of 30 minutes and then allowing it to cool slowly prior to use.

The following steps were performed with the cell submerged. The face of the cell around the periphery of the recess for the porous disc was greased with silicone stopcock grease. The porous disc was then set in place and the membrane was laid over the porous disc. Extreme care was taken to prevent wrinkles in the membrane and to remove all bubbles from the surfaces of the cell. With the membrane in place, the two halves of the

cell were aligned using the guide pins (see Fig. 5-3) and were bolted together. The bolts were tightened with a torque wrench to a torque of 8 ft-lb.

Distilled water was now on both sides of the membrane. Prepared in this manner, the cell was placed in the constant temperature bath. The menisci in both burettes were adjusted to the desired levels and the O-Ring fittings connected to the burettes were attached to the cell. The air-mercury interface in the lucite reservoir that was connected to the water side burette was maintained at about 10 cm above the level of the water-mercury interface in the water side burette. The air-mercury interface in the salt-side reservoir was elevated sufficiently to obtain a hydraulic pressure difference across the membrane of about  $0.7 \text{ kg/cm}^2$ . This reservoir was adjusted periodically to maintain a constant hydraulic pressure difference.

The levels of the menisci in the two burettes were then read daily until the rate of movement of the meniscus levels was less than 5% of the rate of movement expected after filling the salt chamber with a salt solution.

#### (d) Filling the Salt Chamber with Salt Solution

To fill the salt chamber with a solution of sodium chloride, the valves under the mercury reservoirs were first closed. Then the salt side burette was disconnected from the cell. A salt solution with the desired mole fraction of salt was pumped into the salt chamber through the lower fitting on the cell (see Fig. 5-2) while the water in the salt chamber was allowed to escape from the upper fitting. About  $200 \text{ cm}^3$  of salt solution were pumped upward through the salt chamber and an additional  $200 \text{ cm}^3$  of salt solution were pumped downward through the salt chamber. The concentration of the salt solution used to fill the salt chamber ranged between 0.4 and 4.0 moles per liter, which means that the mole fraction of the salt ranged between 0.007 and 0.07. (For comparison, the concentration of salts in sea water is about 0.5 moles per liter.) The mole fraction of the salt in the salt chamber was measured at the completion of each test and was found to be about 5% less than the mole fraction of the salt in the solution pumped through the cell. The measured mole fraction of the salt was used in all calculations.

After the water was replaced by a salt solution, the salt side burette was attached to the cell and the valves under the mercury reservoirs were opened to start the test. Readings of the date, time, room temperature, water bath temperature and the meniscus levels in the two burettes were taken as often as necessary to follow the progress of the test. For the tests with the highest mole fraction of salt readings were taken twice daily. For tests with the lowest mole fraction of salt, readings were taken daily or every two days.

Readings were continued until the rate of inflow from the water side burette was in reasonable agreement with the rate of outflow into the salt side burette. In all cases, the difference between the inflow and outflow rates was less than 20% of the inflow rate. In six out of ten tests, the difference between the inflow and outflow rates was less than 3% of the inflow rate.

#### (e) Dismantling the Apparatus After Test

When a test was completed, both burettes were disconnected from the cell and the open fittings in the cell were plugged quickly to prevent any exchange of liquids between the water bath and the salt chamber in the cell. The cell was then removed from the water bath, and wiped dry on the outside. The salt solution was carefully emptied into a clean vial and covered. The membrane was removed from the cell and the thickness of the membrane was measured as described in 4-03(f).

The specific gravity of the salt solution removed from the cell was measured in pycnometers with volumes of  $10 \text{ cm}^3$  and  $25 \text{ cm}^3$ . One determination was made in each pycnometer to check the results. The mole fraction of the salt in the solution was then obtained from tables relating percent by weight of sodium chloride in an aqueous solution to specific gravity of the solution (59). The mole fraction could be calculated from the percent sodium chloride so that a relation between mole fraction and specific gravity

was obtained. The mole fraction determined in this manner is accurate to within  $\pm 0.00018$ . This variation is  $\pm 2.5\%$  of the lowest mole fraction used. In eight out of ten tests, this variation was less than  $\pm 1\%$  of the mole fraction of the salt solution used.

The final concentration of the liquid on the water side of the membrane was not measured. However, a separate test was performed to determine the rate of ion flow through a natural rubber membrane. The results of this test agreed with Moreland's results (see Appendix A-07) and indicated that sodium and chloride ions flow through natural rubber two thousand times more slowly than do the water molecules. This ion flow is negligible for the present purposes.

#### 5-04 PRESENTATION AND INTERPRETATION OF DATA

The curves of volume flow versus time for the inflow from the water side burette and for the outflow into the salt side burette are shown for each X test in Figs. F-1 to F-10, Appendix F.

The measured rates of inflow and outflow (i.e. the slopes of both the inflow and outflow curves) are shown for each test in Table 5-1. The rate of inflow is equal to or greater than the rate of outflow in all cases. The following effects can cause a difference between the two:

CREEP - The half of the cell which contains the salt chamber might move toward the membrane and cause water to flow out of the cell. This effect would cause the measured rate of inflow to be less than the measured rate of outflow.

LEAKAGE - (a) Leakage of water out, from the water side of the membrane, would cause the measured rate of inflow to be greater than the measured rate of outflow.

(b) Leakage of water into the salt chamber from the water bath, due to the mole fraction difference across the submerged fittings on the cell, would cause the measured rate of inflow to be less than the measured rate of outflow.

Of the above two effects - creep and leakage - only leakage of water out of the water side of the membrane can explain the observation that the rate of inflow was greater than or equal to the rate of outflow. Therefore it is concluded that if the rates of inflow and outflow are different, the best estimate of the rate of flow through the membrane is given by the measured rate of outflow from the salt side, and this outflow rate will be used for subsequent discussions of the data.

A small correction must be applied to the measured rate of outflow to account for the hydraulic pressure difference of  $0.7 \text{ kg/cm}^2$  which was applied across the membranes during X tests. From the W tests (Chapter 4) the coefficient of permeability of the natural rubber is about  $5 \times 10^{-16} \text{ cm/sec}$ . The rate of flow of water through a membrane with a thickness of  $0.006 \text{ cm}$  and an area of  $20 \text{ cm}^2$  is:

$$q = k i A = 5 \times 10^{-16} \times \frac{700}{0.006} \times 20$$

$$q = 1.17 \times 10^{-9} \text{ cm}^3/\text{sec} = 0.1 \text{ mm}^3/\text{day}$$

Since this rate of  $0.1 \text{ mm}^3/\text{day}$  is small compared with the rates of outflow measured in the X tests, it is not necessary to further refine the correction by taking into account the actual thickness of each membrane used in the X tests. A correction of  $0.1 \text{ mm}^3/\text{day}$  was added to the rates of outflow measured in the X tests since the hydraulic pressure caused flow in a direction opposite to that caused by the mole fraction difference. The resulting corrected rates of outflow are shown in Table 5-1.

## 5-05 DISCUSSION OF FACTORS AFFECTING RATE OF FLOW OF WATER DURING X TESTS

### (a) Effect of Mole Fraction Difference

A plot of the corrected rate of outflow from the salt side of the membrane versus the mole fraction of sodium chloride in the salt chamber is shown in Fig. 5-4 for tests X1(a) through X1(d). These four tests were performed in succession on the same membrane without dismantling the cell between tests. The results fall practically on a straight line through the origin, with a maximum deviation of less than 1% from a straight line through the origin. Thus the rate of flow of water through a natural rubber membrane is directly proportional to the mole fraction difference across the membrane for the range of mole fractions tested, i.e.  $q \propto \Delta X$ .

### (b) Effect of Membrane Thickness

If the rate of flow of water through a membrane obeys Fick's law as modified by Laidler and Shuler (see Chapter 3), then the rate of flow should be proportional to the mole fraction gradient across the membrane. That is:

$$q \propto \frac{\Delta X}{L}$$

combining this with  $q \propto \Delta X$ , as concluded in subparagraph (a), it follows that a plot of  $q/\Delta X$  versus  $1/L$  should be a straight line through the origin. Such a plot is shown in Fig. 5-5 for the results of all X tests.

The number of data points in Fig. 5-5 is not sufficient to define accurately the relationship between  $q/\Delta X$  and  $1/L$ . However, the data do indicate strongly that the rate of flow of water through natural rubber due to a mole fraction difference is not inversely proportional to the membrane thickness. In fact, the best representation of the data appears to be a curve as shown in Fig. 5-5. When extrapolated, this curve should pass through the origin, since the rate of flow must be zero through a membrane of infinite thickness.

### (c) Effect of Silicone-Oil-Soaking

Two points are shown in Fig. 5-5 representing X tests on membranes soaked in silicone oil. One point falls on the curve and the other point is located approximately 20% below the curve. These two tests indicate that the rate of flow due to a mole fraction difference is either not changed or slightly reduced by soaking the membrane in silicone oil. The results of W tests and V\* tests on membranes soaked in silicone oil indicated that the rate of flow was either equal to or slightly greater than for tests on water soaked membranes. Since the membranes used for all tests were of the same type (natural rubber made by Schmid), it is reasonable to conclude that silicone oil soaking has no effect on the rate of flow of water through natural rubber in X, W or V tests.

## 5-06 COMPARISON OF THE RESULTS OF X TESTS WITH THE RESULTS OF W TESTS

### (a) Comparison of K Measured in W and X Tests

In Chapter 3 it was concluded that the rate of flow through a membrane can be expressed by the equation:

$$q = K A \left( \frac{\Delta p_v}{L} \right) \quad (3-33)$$

The vapor pressure difference  $\Delta p_v$  in the above equation may be caused by a mole fraction difference (as in X tests), or by a hydraulic pressure difference (as in W tests), or both. This means that K should have the same value whether it is calculated from the results of X tests or from the results of W tests.

---

\* Results of V tests are reported in Chapter 6.

The permeabilities  $K$  were calculated for the W tests and are given in Table 4-1. To calculate  $K$  from the data of an X test one must know the magnitude of the vapor pressure difference which is caused when a given mole fraction difference is applied across a membrane. For the X tests, the vapor pressure difference across the membrane is simply equal to the difference between the equilibrium vapor pressure of the pure water and the equilibrium vapor pressure of the water in the solution. The equilibrium vapor pressure of pure water at 30°C is 43.1 gm/cm<sup>2</sup>. The equilibrium vapor pressure of water in solution with sodium chloride may be found in the International Critical Tables (106). The vapor pressure difference across the membrane was determined for each X test and is given in Table 5-1. Knowing these vapor pressure differences,  $K$  can be calculated for the X tests using Eq. 3-33. The value of  $K$  for each X test is also given in Table 5-1.

Table 5-2 gives a comparison between the values of  $K$  computed from W tests and X tests. The tests are listed in order of decreasing membrane thickness. It is seen that the ratio of  $K$  from W tests to  $K$  from X tests varies between 0.74 and 1.37, with an average of 1.0. A different membrane was used for each of the tests listed in Table 5-2 except tests W7 and X5. The same membrane was used for these two tests and it is seen that the values of  $K$  are identical.

The above comparison of the results of X tests with the results of W tests is a satisfactory proof that the value of  $K$  is independent of the type of test. Thus, in future testing of membranes it is only necessary to perform X tests to measure  $K$ . The rate of flow through the same membrane due to a hydraulic pressure difference may then be calculated using the value of  $K$  measured in the X tests. X tests are considerably simpler and faster than W tests, and so they offer the more expedient method for measuring  $K$ .

(b) Comparison of Rate of Flow Caused by Mole Fraction and Hydraulic Pressure Differences

During a triaxial R test on a specimen of soil which contains pore water with a high salt concentration, water flows from the triaxial chamber into the specimen due to both the mole fraction difference and the difference in hydraulic pressure across the membrane. The rate of flow into the specimen due to each driving force may be compared on the basis of tests W7 and X5, both of which were performed on the same membrane.

Table 5-3 shows this comparison for a soil with sea water in its pores and for a soil with water from the Great Salt Lake in its pores. It is seen that the rate of flow into a triaxial specimen with salt water in its pores is much greater than the rate of flow that would be caused by hydraulic pressure differences alone. Thus, if one wishes to perform a 100-day Q or R test on a soil with high pore salt concentration, one is obliged to take adequate measures to prevent the flow caused by the mole fraction difference. One possible method for preventing this flow is to use chamber water which contains salt at the same mole fraction as the salt in the pores of the specimen. This method has not yet been attempted in the laboratory, to the knowledge of the author. If attempted, care must be taken to measure accurately the mole fraction of the salt in the pores of the soil. For example, suppose one is to perform a 100-day Q or R test on a 100% saturated specimen of Canyon Dam clay with a diameter of 1.4 in. and a height of 3.5 in. If the mole fraction of the salt in the chamber water is lower than that in the pore fluid by as little as 0.0003 (i.e. 0.02 moles per liter), then the effective stress in the specimen will decrease by about 15% during the test due only to this small mole fraction gradient, if two natural rubber membranes with a total thickness of 0.012 cm are used.

5-07 DISCUSSION OF SUITABILITY OF NATURAL RUBBER MEMBRANES FOR USE IN TRIAXIAL TESTING

From Table 5-3 it is seen that a hydraulic pressure difference of 1 kg/cm<sup>2</sup> across a 0.006 cm thick natural rubber membrane will cause a flow of 0.007 mm<sup>3</sup>/day/cm<sup>2</sup>. Thus, the rate of flow into a 1.4 inch diameter by 3.5 inch high triaxial specimen would be about 0.7 mm<sup>3</sup>/day. Assuming two membranes are used, the rate of flow would be only 0.35 mm<sup>3</sup>/day. From Table 2-2 it can be seen that this rate of flow would cause the percent reduction in effective stress during a 100-day Q or R test on a 100% saturated

specimen to be 5% or less for Boston Blue clay, Mexico City clay and for the Hard clays. However, a flow rate of  $0.35 \text{ mm}^3/\text{day}$  is far too great to permit satisfactory performance of a 100-day test on Canyon Dam clay. Furthermore, if the hydraulic pressure difference across the membranes is increased to  $10 \text{ kg/cm}^2$  (increasing the flow rate to  $3.5 \text{ mm}^3/\text{day}$ ) excessive errors would develop even in soils with a very high swelling ratio. If a mole fraction gradient also exists across the membranes, it is practically hopeless to attempt a 100-day triaxial test using natural rubber membranes.

From the above discussion it is evident that it would be very desirable to find a membrane that has a coefficient of permeability about two orders of magnitude smaller than that of natural rubber. If such a membrane were used in triaxial testing, errors due to membrane leakage could be reduced to a tolerable minimum. However, the permeability of a membrane is not the sole criterion governing its selection for use in triaxial testing. In addition, a membrane should impose very little lateral restraint on a specimen since large restraint would increase the strength (104). The results of an investigation into the permeability of several synthetic rubber and plastic membranes is presented in Chapter 6. A method for selecting the most suitable membrane, based on the combined requirement of low permeability and low restraint, is presented in Chapter 9.

## CHAPTER 6

EXPERIMENTAL INVESTIGATION OF LEAKAGE THROUGH MEMBRANES  
DUE TO VAPOR PRESSURE GRADIENTS

6-01 GENERAL

The data presented in Chapters 4 and 5 show that natural rubber membranes are not generally satisfactory for use in triaxial testing because they permit excessive leakage. In an effort to select a membrane that is much less permeable than natural rubber, tests were performed to determine the permeability of several synthetic rubber and plastic membranes.

The W tests reported in Chapter 4 had a duration ranging between 7 and 66 days. W tests performed on membranes that are less pervious than natural rubber would be even more time consuming. Therefore a change in test procedure was introduced which reduced the duration of each test by a factor of about 100. This change consisted of applying a vacuum (rather than water under pressure) of less than 0.3 mmHg on the downstream side of the membrane. Water vapor rather than liquid water passes through the membrane in such a test, as will be explained in 6-02. As a result, the data from these tests can also be used to estimate the rate of evaporation from a membrane used in an unconfined test. These new tests will be called "V" or "vapor permeability" tests.

V tests were performed on the rubber and plastic membranes listed in Table 6-1. The thicknesses of these membranes ranged from 0.0012 cm for the thinnest plastic to 0.055 cm for the thickest rubber.

6-02 THEORY FOR VAPOR PERMEABILITY (V) TESTS

From Eq. 3-30 (or Eq. 3-61) it should be expected that the rate of flow of water through a membrane would be directly proportional to the vapor pressure difference, so that if the vapor pressure difference is increased, the rate of flow is correspondingly increased. The vapor pressure difference applied in the W tests is caused by the hydraulic pressure difference. For example, if in a W test the hydraulic pressure difference  $\Delta p$  is 6 kg/cm<sup>2</sup>, then using Eq. 3-28 the vapor pressure difference,  $\Delta p_v$ , is found to be 0.18 gm/cm<sup>2</sup>. One way to increase the vapor pressure difference would be to increase the hydraulic pressure difference. However, large increases in hydraulic pressure difference would give only small increases in vapor pressure difference and would add the complication that apparatus would have to be designed to withstand high pressures. A far more effective means for increasing the vapor pressure difference is simply to apply a vacuum on the downstream side of the membrane while still maintaining a hydraulic pressure on the upstream side. In such a case the vapor pressure difference would be approximately equal to the equilibrium vapor pressure of the permeant at the temperature of the test. For water at a temperature of 30°C, the equilibrium vapor pressure is 43.1 gm/cm<sup>2</sup>, which is about 250 times greater than the vapor pressure difference for the W test cited above. Thus, the test duration required to achieve results of equal accuracy to those obtained in W tests would be correspondingly reduced.

The following discussion shows that in V tests one is really measuring the rate of flow of water vapor through the membrane.

The assumption that a direct proportionality exists between the rate of flow and the vapor pressure gradient across a membrane also implies that the vapor pressure gradient is constant through the membrane. When the vapor pressure in the membrane drops below the equilibrium vapor pressure of the permeant at the temperature of the test, the permeant is vaporized. If one assumes that a gage pressure of 5 kg/cm<sup>2</sup> is applied to water on the upstream side, then the vapor pressure on the upstream side (which is the sum of the equilibrium vapor pressure and the vapor pressure increase caused by the gage pressure), will be 43.25 gm/cm<sup>2</sup> for water at 30°C. Thus, when there is a full vacuum (i.e. zero vapor pressure) on the downstream side, the vapor pressure in the membrane

drops below the equilibrium vapor pressure in the first 0.3% of the membrane thickness. For practical purposes, the water is in the vapor phase through the entire thickness of the membrane.

#### 6-03 APPARATUS FOR VAPOR PERMEABILITY (V) TESTS

The apparatus used for the V tests was the same as that used for W tests, except that the LP burette was omitted (see Fig. 4-1). The LP fitting on the permeability cell was connected directly to a vacuum pump through a two meter length of 5/16 in. outside diameter Saran tubing. The vacuum pump was capable of creating a vacuum of  $10^{-6}$  mm Hg but, with the system used, a vacuum of 0.005 mm Hg was the best attainable. The vacuum readings were made on a glass McLeod gage which had two ranges - one from 15 to 0.001 mm Hg and the other from 0.22 to 0.0001 mm Hg.

#### 6-04 PROCEDURE FOR VAPOR PERMEABILITY (V) TESTS

##### (a) General Description

V tests were performed by placing a membrane in a permeability cell with water at a gage pressure of 5 kg/cm<sup>2</sup> on one side and a vacuum of less than 0.3 mm Hg on the other. All tests were performed at a temperature of 30°C. The details of the test procedure are given in the following paragraphs.

##### (b) Preparation of Membranes

Each membrane was first cut into a disc with a diameter of 8 cm. The membranes for tests V1 through V5 and tests V13 through V50 were not given any further treatment. They were simply tested in the as-received, air-dry condition. The membranes for tests V6 and V7 were soaked in distilled water and the membranes for tests V8 and V9 were soaked in silicone oil in the manner described for the W tests. Membranes for tests V10, V11 and V12 were soaked in Cenco Hyvac (93050, No. 3, Standard) vacuum pump oil (a mineral oil) by submerging the membranes in the oil at atmospheric pressure for over a month.

##### (c) Placement of Membrane in Permeability Cell

The top plate of the permeability cell was submerged in a distilled water bath and all bubbles were removed. The bottom plate and the porous disc were dried in an oven at 60°C. The bottom plate was then greased as for the W tests and the porous disc was inserted in its recess. After removing from the membrane all excess water or oil, if any, the membrane was placed over the porous disc on the bottom plate and all wrinkles were removed. A vacuum was then applied with an aspirator to the bottom of the membrane through the LP connection on the cell to pull the membrane tightly against the porous disc. The bottom plate, with the membrane in place and the vacuum still on, was submerged in the distilled water bath with the top plate. The top plate was then placed over the guide pins and bolted in place as for the W tests. Before removing the vacuum line, the cell was removed from the water. In this manner no water was allowed to enter the low pressure side of the membrane prior to test.

##### (d) Starting the Test

The assembled permeability cell was brought to the water bath and the line from the vacuum pump was attached to the LP connection. The HP and L burettes were saturated, the water-mercury menisci were brought to the proper level and the two burettes were connected to the permeability cell. A gage pressure of 5 kg/cm<sup>2</sup> was applied to the HP burette and a pressure of 20 cm Hg was applied to the L burette. The cell was then submerged in the water bath. Readings were begun after the cell had been in the bath for about 30 minutes.

##### (e) Readings during Test

V tests lasted a total of one-third day to thirty days, depending on the membrane being tested. The readings were taken at a frequency governed by the flow rate. For tests on natural rubber membranes, readings were taken hourly. For tests on butyl

rubber and some plastic membranes, readings were taken daily. At each reading, the date, time, pressure on the HP and the L burettes, vacuum on the LP burette, room temperature, bath temperature and the scale readings in the HP and L burettes were recorded. The readings were continued until the volume flow measured in the HP burette was linear with time for more than 50% of the duration of the test. The apparatus was then dismantled and the thickness of the membrane was measured as described for the W tests in 4-03(f).

#### 6-05 PRESENTATION AND ANALYSIS OF DATA FOR V TESTS

##### (a) Presentation of Data

Tests on Natural Rubber Membranes - Eighteen V tests (V1 through V18) were performed on natural rubber membranes produced by four manufacturers. The thicknesses of the membranes ranged from 0.005 cm to 0.035 cm. Membranes were tested with (a) no treatment prior to test, (b) after soaking in distilled water, (c) after soaking in silicone oil and (d) after soaking in vacuum pump oil. (See 6-04(b) for types of oils.)

The plots of volume flow into the HP and L burettes versus time for tests V1 through V18 are presented in Figs. E-12 through E-29 in Appendix E. Table 6-2 contains a summary of the results of these tests.

Tests on Synthetic Rubber and Plastic Membranes - Thirty-three V tests (V19 through V51) were performed on ten types of membranes with thicknesses ranging between 0.0012 and 0.055 cm. All of these membranes were tested with no treatment prior to test.

The plots of volume flow into the HP and L burettes versus time for tests V19 through V51 are presented in Figs. E-30 through E-62. Table 6-3 contains a summary of the results of these tests.

##### (b) Analysis of Test V1

The results of test V1 are analyzed below as an example to show how the quantities in Tables 6-2 and 6-3 were derived from the test data.

Fig. E-12 shows the data for test V1. The rate of flow measured in the HP burette was 262 mm<sup>3</sup>/day. At the same time water flowed into the L burette at a rate of 16 mm<sup>3</sup>/day. The flow into the L burette may have been caused by creep or by leakage across the inner O-Ring of the permeability cell from the HP chamber (see 4-04(b)). A rate of flow of 16 mm<sup>3</sup>/day is equivalent to a movement of less than 0.0001 cm of the top plate of the cell relative to the bottom plate over the duration of the test. On the other hand the leakage across the O-Ring was probably less than 1% of 16 mm<sup>3</sup>/day. It is concluded that the flow into the L burette was chiefly due to creep of the membrane and that it is therefore necessary to apply a correction to the rate of flow measured in the HP burette. Rough calculations based on the dimensions of the permeability cell and data from the W tests indicate that the rate of flow into the HP burette due to creep is about equal to the simultaneous flow into the L burette due to creep. Assuming that the estimated flow into the HP burette due to creep is equal to the L flow, the corrected rate of flow through the membrane in test V1 is:

$$q = 262 + 16 = 278 \text{ mm}^3/\text{day}$$

The measured rates of flow into the L burette were less than 10% of the HP flows in all cases. Thus, the corrected HP flow must be in error by much less than 10%, depending on the error in the estimated creep flow.

The values of the permeability constant K in Tables 6-2 and 6-3 were computed from Eq. 3-33. For example, the permeability for test V1 is computed as follows:

$$q = KA \frac{\Delta p_v}{L} \quad (3-33)$$

where  $q = 278 \text{ mm}^3/\text{day}$ ;  $A = 38.2 \text{ cm}^2$ ;  $\Delta p_v = 42.9 \text{ gm/cm}^2$ ; and  $L = 0.0062 \text{ cm}$ . The result is that  $K = 1.22 \times 10^{-11} \text{ cm}^4/\text{gm sec}$ . The permeability constant was calculated using Eq. 3-33 for comparative purposes only. This must not be construed as an indication that the rate of flow of water vapor through rubbers and plastics in V tests is directly proportional to  $\Delta p_v$  or inversely proportional to  $L$ .

#### 6-06 DISCUSSION OF V TESTS ON NATURAL RUBBER MEMBRANES

##### (a) Permeability of Untreated Natural Rubber

The permeabilities calculated for tests on untreated natural rubber membranes are plotted against the thicknesses of the membranes in Fig. 6-1. These points are shown as open circles. The permeability appears to increase slightly with increasing thickness but there are not sufficient data to make this a firm conclusion. For practical purposes, the permeability of natural rubber to water vapor is  $K = 1.2(\pm 0.3) \times 10^{-11} \text{ cm}^4/\text{gm sec}$  over the entire range of thickness tested. The scatter of  $\pm 25\%$  may be due to the variation in manufacturing technique, minor differences in the raw material, errors in the flow measurements and errors in the thickness measurements.

Test V4 was performed using two thicknesses of Schmid membranes with no pre-treatment and test V5 was performed using four thicknesses of Schmid membranes with no pre-treatment. Only the total thickness is given in Table 6-2. The permeability constants for these two tests are plotted as open triangles in Fig. 6-1. The points fall in the middle of the range of permeabilities for tests on single thicknesses of Schmid membranes. Thus, increasing the number of layers does nothing more than add thickness to the barrier, the permeability constant being independent of the number of layers used.

##### (b) Effect of Treatment of Membrane on Permeability Constant

In Fig. 6-1 the permeability constants of the treated natural rubber membranes relative to the permeability of the untreated natural rubber membranes are seen to be as follows:

Water soaked - Permeability constant might be decreased by 10% to 50% below that of untreated membranes.

Silicone-oil soaked - Permeability constant is the same as for untreated membranes.

Vacuum-pump-oil soaked - Permeability constant is about 40% less than for untreated membranes.

A comparison of the results on water soaked membranes with those on silicone-oil soaked membranes gives confirmation of the conclusion reached from the W test results, namely that the permeability constant for silicone-oil soaked membranes is probably equal to or greater than the permeability constant for water soaked membranes. None of the treatments used above reduced the permeability constant sufficiently to be of practical value.

##### (c) Comparison of Permeability Constants Measured in V and W Tests

Tests W6 and V6 were performed on the same membrane. Tests W7 and V7 were also performed on the same membrane. A comparison of the permeability constants for these tests (from Tables 4-1 and 6-2) follows:

Test No.	Permeability Constant $K$ ( $\text{cm}^4/\text{gm sec}$ )		Ratio $K_W/K_V$
	W Test	V Test	
6	$0.93 \times 10^{-11}$	$0.56 \times 10^{-11}$	1.7
7	$1.57 \times 10^{-11}$	$0.85 \times 10^{-11}$	1.8

The permeability constant measured in W tests is 75% greater than that measured in V tests.

The essential difference between W and V tests is that the average vapor pressure in the membrane during a test is higher in the W tests. Thus the above data can be explained if one assumes that the permeability constant increases with increasing average

vapor pressure. This possibility has been discussed briefly by Taylor, Hermann and Kemp (100), who also presented data to show that the permeability constant of a "soft vulcanized rubber" membrane increases with increasing average vapor pressure.

#### 6-07 DISCUSSION OF V TESTS ON SYNTHETIC RUBBER AND PLASTIC MEMBRANES

From Table 6-3 one can see that butyl rubber, Kel-F, two of the polyethylenes, polypropylene and Teflon all have permeability constants that are ten or more times smaller than that of natural rubber, which has a permeability constant of  $1.2 \times 10^{-11} \text{ cm}^4/\text{gm sec}$ . However, as was pointed out in 5-07, a membrane used for triaxial testing must have a low permeability constant and simultaneously must apply a small restraint to a triaxial specimen. A method for obtaining the best combination of low permeability constant and low restraint is given in Chapter 9.

#### 6-08 EVAPORATION OF WATER THROUGH NATURAL RUBBER DURING UNCONFINED TESTS

Assume that a 1.4 in. diameter by 3.5 in. high soil specimen is to be tested in unconfined compression and is protected by one 0.006 cm thick untreated Schmid membrane. From Eq. 3-33 it is known that the rate of evaporation of water vapor is proportional to the vapor pressure difference of water across the membrane.

The vapor pressure of the water outside the membrane is determined by the room temperature and the relative humidity. The vapor pressure of the water inside the membrane is dependent on the temperature of the pore water and the salt content of the pore water.\* The largest vapor pressure difference occurs at high temperature, low relative humidity and with no salt in the pore water. The lowest vapor pressure difference occurs under converse conditions. The rate of evaporation for the following two extreme conditions will be calculated:

Case I - Temperature	20°C
Relative humidity	90%
Salt content	0.55 moles NaCl/liter of solution

$$\Delta p_v = 1.9 \text{ gm/cm}^2$$

Case II - Temperature	25°C
Relative humidity	20%
Salt content	zero

$$\Delta p_v = 25.6 \text{ gm/cm}^2$$

The rate of flow is given by Eq. 3-33

$$q = K A \frac{\Delta p_v}{L} \quad (3-33)$$

where  $K = 1.2 \times 10^{-11} \text{ cm}^4/\text{gm sec}$ ;  $A = 100 \text{ cm}^2$ ;  $\Delta p_v = 1.9 \text{ gm/cm}^2$  or  $25.6 \text{ gm/cm}^2$ ; and  $L = 0.006 \text{ cm}$ . The calculated rates of evaporation through one membrane are:

---

\* The small effect of the degree of saturation on the vapor pressure of water inside the membrane is neglected. It amounts to a maximum of  $0.2 \text{ gm/cm}^2$  for soils with  $G_w = 85\%$ .

Case I  $q = 33 \text{ mm}^3$  (liquid water)/day

Case II  $q = 440 \text{ mm}^3$  (liquid water)/day

Thus the rate of evaporation from an unconfined specimen protected by one (or even two) 0.006 cm thick membranes is of the same order as the rates of leakage into a triaxial specimen that are caused by mole fraction gradients (cf. Table 5-3).

#### 6-09 SUMMARY OF VAPOR PERMEABILITY (V) TESTS

The apparatus used for the W tests (Chapter 4) was used to measure the permeability to water vapor of several natural rubber, synthetic rubber and plastic membranes. The permeability constant K defined by the equation

$$q = K A \frac{\Delta p_v}{L} \quad (3-33)$$

was calculated from the data.

The permeability constant for natural rubber membranes was found to be  $1.2 \pm 0.3 \times 10^{-11} \text{ cm}^4/\text{gm sec}$ . Soaking the natural rubber membranes in water prior to test caused reduction in K by 10% to 50% below that for untreated membranes. Soaking in silicone oil did not appear to alter K. Soaking in vacuum pump oil reduced K by about 40%. These reductions in the permeability constant by soaking are not sufficient to be of practical value.

Tests performed on two layers and on four layers of 0.006 cm thick natural rubber caused no change in K.

The permeability constant of natural rubber measured in a W test was found to be 75% higher than that measured in a V test on the same membrane. This difference may be due to the higher average vapor pressure in the membrane during W tests.

The permeability constants of butyl rubber, Kel-F, Teflon, polypropylene and one type of polyethylene were found to be more than ten times smaller than that of natural rubber.

CHAPTER 7EXPERIMENTAL INVESTIGATION OF LEAKAGE PAST BINDINGS IN TRIAXIAL TESTS7-01 INTRODUCTION

The purpose of this chapter is to present the results of twenty-five tests performed to measure the rate of flow of water past the O-Rings or rubber strips that are used to bind the membrane to the cap and base of a triaxial specimen. The leakage caused by a hydraulic pressure difference across the membrane was measured. Such tests will be called "binding leakage" or "B" tests.

All B tests were performed on 1.4 in. diameter caps and bases using natural rubber membranes made by the Julius Schmid Company. The effect of the following variables on the rate of binding leakage was studied:

- (1) The magnitude of the hydraulic pressure difference.
- (2) The number of membranes.
- (3) Roughness of the cap and base.
- (4) Greasing the cap and base prior to applying the membrane and bindings.
- (5) Soaking the membrane in silicone oil prior to applying the bindings.

7-02 APPARATUS(a) General

A diagram of the apparatus used for binding leakage tests is shown in Fig. 7-1. The apparatus consists of (1) a binding leakage cell, (2) a pedestal on which the bindings are placed, (3) a burette for measuring the volume of water which flows from the binding leakage cell into the pedestal, (4) a means for applying pressure to the binding leakage cell and back pressure to the interior of the pedestal, and (5) a constant temperature bath.

A photograph of the binding leakage cell and the pedestal is shown in Fig. 7-2. The binding leakage cell consists of a 2 in. inside diameter chamber and two plates to seal the ends of the chamber. The pedestal is screwed into one of the plates during a test and the other plate contains a fitting through which pressure is applied to the water in the cell. The pedestal is an essential feature of the apparatus and is described in detail in (b) below.

The burettes used for measuring the volume flow were similar to that shown in Fig. 4-5 with the exceptions that (1) the bore of the burettes used in the binding leakage tests was either 0.02 cm or 0.10 cm, depending on the rate of leakage anticipated, and (2) the O-Ring fitting that connected the burette to the pedestal had a slightly different design from that used in the W tests. A photograph of this O-Ring fitting is given in Fig. 8-3 (item 13).

Pressure was applied to the binding leakage cell by means of compressed air through the mercury seal as shown in Fig. 7-1. A lower pressure, called the back pressure, was applied to the water in the interior of the pedestal through the mercury seal and the volume change burette, which are also shown in Fig. 7-1. The details of the systems used for applying pressure are essentially as described for the W tests in 4-02.

The constant temperature bath used for the binding leakage tests was also essentially the same as that described for the W tests in 4-02.

(b) The Pedestals used for Binding Leakage Tests

Pedestals of two different designs were used in the binding leakage tests. A cross section of the first pedestal used is shown in Fig. 7-3. It contains a porous disc made from a No. 60 grit porous carbon plate manufactured by the National Carbon Company. The porous carbon has a minimum grain size of 0.012 mm. The surface roughness of the porous carbon is approximately equivalent to fine sand or coarse silt. Two pedestals

of this type were made. The exterior metal surfaces of one pedestal were polished with No. 600A emery paper using kerosene as a lubricant. The exterior metal surfaces of the second pedestal were deliberately roughened by placing the pedestal in a lathe and machining a spiral groove into the surface. The groove was made using a cut depth of 0.010 in. and a lathe feed of 0.0064 inches per revolution. The depth of the resulting groove was about 0.07 mm and the distance between adjacent grooves was about 0.15 mm.

A cross section of the pedestal of the second design is shown in Fig. 7-4 and in the photograph in Fig. 7-2. It is designed to prevent relative movement between the top and bottom halves of the pedestal due to creep of the porous disc which may occur when cell pressure is applied. It contains a porous ceramic disc of the same type as described for the cell used for X tests (see 5-02). The surface of the porous ceramic is considerably smoother than the surface of the porous carbon. The grain size of the material used to make the porous ceramic disc was one-tenth or less of the minimum grain size in the porous carbon discs. The metal surfaces of this second type pedestal were polished using 600A emery paper with kerosene as a lubricant.

Both types of pedestals were designed so that the thickness of the porous disc was as thin as it could be made in a lathe. In this manner, the rate of leakage directly through the portion of the membrane lying over the porous disc was minimized. However, even with this precaution, the rate of leakage through this portion of the membrane was always at least equal to the leakage of well-made bindings; when high pressure differences were applied it was found to be as much as seven times greater than the binding leakage.

### 7-03 PROCEDURE

#### (a) Preparation of Membranes

The membranes tested were natural rubber manufactured by the Julius Schmid Company. They are cylindrical and have an unstretched diameter of 1.35 in. For this investigation they were cut into short cylinders with a length of one inch and soaked in water or in silicone oil as described for the W tests in 4-03.

#### (b) Set-up of Membrane and Bindings on Pedestal

The pedestals of the first design (containing porous carbon discs) were saturated by placing them in a chamber, evacuating the chamber, and allowing distilled water to enter the pedestal slowly from the bottom. The pedestals of the second design (containing porous ceramic discs) were saturated by removing the disc from the pedestals and boiling them for 30 minutes in distilled water. The two halves of these pedestals were saturated by submerging them in distilled water and drawing water through all openings. The prepared membrane was then placed on the saturated and greased pedestal while the pedestal and membrane both were submerged.

For tests B15, B16, B17 and B18 the surfaces of the pedestal on which the bindings would bear were greased with silicone stopcock grease. In all other tests the surface of the pedestal was not treated in any way.

Each O-Ring was stretched on a brass stretcher ring which was only 0.03 in. larger in inside diameter than the pedestal. The O-Rings were snapped into place on the pedestal as close as possible to the porous disc. The two O-Rings were then pushed apart slightly from each other, to eliminate wrinkles in the membrane. O-Rings are cast in a split mold that leaves a protruding ridge about 0.010 cm high around the inside and outside girth of the ring. Care was taken so that this ridge did not spiral around the specimen and form a continuous path through which water could flow from the cell into the porous disc.

The O-Rings used were made of Buna-N rubber with a Shore A hardness of 70, an outside diameter of 1.262 in. and an inside diameter of 0.984 in. in the unstretched condition. When stretched to fit the 1.4 inch diameter pedestals, the O-Rings were stressed to about 25 kg/cm<sup>2</sup>. This means the contact force between the O-Rings and the pedestal was about 0.85 kg/cm. The area of contact was about 0.05 to 0.1 cm wide, so that the contact pressure was probably between 8 and 17 kg/cm<sup>2</sup>.

Strip bindings made of neoprene rubber were used for tests B14, B23, B24 and B25. Each rubber strip was 1/4 in. wide, 1/32 in. thick and one foot long. Neoprene rubber was recommended for use as bindings by a rubber distributor because neoprene is supposed to have a higher "durability" in the stressed condition than other rubbers. The rubber strips were wrapped around the membrane and pedestal six or seven times and finally secured beneath previous winds. The two strips were placed as close as possible to the porous disc in the pedestal.

(c) Assembly of Cell and Performance of Tests

The binding leakage cell was assembled with the pedestal inside and with all parts still submerged. The assembled cell was placed in a water bath maintained at a constant temperature of 30°C, the connection to the system for applying cell pressure was made up and the cell pressure was applied. A period of 15 min was allowed to elapse so that the temperature of the cell would rise to the bath temperature. Then the volume change burette was connected to the pedestal and a back pressure of 6 kg/cm<sup>2</sup> was applied. The maximum hydraulic pressure difference applied across the membrane in any test was 18 kg/cm<sup>2</sup> and the minimum was 2 kg/cm<sup>2</sup>.

The test was now in operation. Readings of the meniscus level in the burette, room temperature, water bath temperature, cell pressure and back pressure were taken each day, or as required to follow the progress of the test. Readings were continued until the plot of volume change versus time was approximately a straight line.

It should be noted that there was only one burette used to measure volume change, and this burette was on the outflow side of the membrane. No inflow measurements were made. It was therefore necessary to test each fitting on the outflow side of the membrane to ensure that there were no leaks of objectionable magnitude. The results of these tests are reported in Chapter 8. According to the results the total rate of leakage of all fittings on the outflow side of the membrane was probably less than 0.02 mm<sup>3</sup>/day. This rate of leakage is about 20% of the rate of binding leakage measured for well-made bindings.

(d) Dismantling the Apparatus after Test

- (1) The back pressure was decreased slowly to zero.
- (2) The connection between the burette and the pedestal was removed.
- (3) The cell pressure was removed and the cell pressure line was disconnected from the binding leakage cell.
- (4) The cell was removed from the constant temperature bath, submerged in another bath of distilled water and dismantled.
- (5) The distance between the two O-Rings, or between the two rubber strips nearest to each other on opposite sides of the porous disc, was measured.
- (6) The membrane was removed from the pedestal and its thickness measured in the manner described in 4-03.

7-04 PRESENTATION AND INTERPRETATION OF DATA

The plots of volume flow versus time for tests B1 through B25 are given in Figs G-1 through G-26 in Appendix G. Table 7-1 is a summary of data and calculations for all binding leakage tests.

Fig. G-1 is a plot of volume flow versus time for test B1. Initially there was an abrupt outflow of 0.5 mm<sup>3</sup> from the pedestal into the burette. This outflow probably was caused by the deformation of the membrane into the small crevices between the porous disc and the steel of the pedestal. Then a gradual flow from the burette into the pedestal of 0.5 mm<sup>3</sup> occurred over a period of eight days. This flow may have been caused by either (1) the solution of many microscopic bubbles of air which could have remained in the pedestal and tubing, even after careful saturation of the system with water, or (2) leakage past the O-Ring, or (3) creep of the O-Ring in the fitting connecting the pedestal to

the volume change burette. Water then began flowing out of the pedestal at a rate of  $(0.105 \pm 0.005) \text{ mm}^3/\text{day}$  and continued for a period of 24 days, at which time the test was stopped. The final slope of the plot is tabulated as the "measured rate of flow" ( $q_M$ ) in Table 7-1. The minor variations from a smooth curve during the test are due to variations in room temperature and to minor fluctuations in the magnitude of the pressure difference across the membrane.

The shapes of the early portions of the curves of volume flow versus time shown in Appendix G were not all the same as for test B1. However, the factors that probably affected the early shape of the curve for test B1 probably also affected the other curves to a greater or lesser extent than for test B1.

As illustrated in Fig. 7-5, the measured rate of flow from the binding leakage cell into the pedestal consists of three parts:

- $q_1$  - flow through that area  $A_1$  of the membrane which bears on the porous disc.
- $q_2$  - flow through that area  $A_2$  of the membrane between the bindings but not bearing on the porous disc.
- $q_3$  - flow past the bindings along the interface between the pedestal and the membrane.

The total rate of flow  $q_M$ , which is equal to the flow measured during a B test, is

$$q_M = q_1 + q_2 + q_3 = q_1 + q_B \quad (7-1)$$

where the "binding leakage",  $q_B$ , is defined as the sum of the quantities  $q_2$  and  $q_3$ . There are two reasons for introducing the sum  $q_B$ : (1) The magnitude of  $q_2$  can be determined only approximately, and this involves an assumption concerning the variation of pressure in the water in the interface between the membrane and the metal surface of the pedestal. (2) The hydraulic pressure difference across the membrane causes the membrane to seal against the pedestal. This seal is an essential part of the overall resistance offered by the binding to the flow of water. Therefore, the leakage  $q_2$  should be considered as part of the total binding leakage.

The magnitude of  $q_M$  is measured. The magnitude of  $q_1$  can be calculated from Darcy's law using the known coefficient of permeability, area and thickness of the membrane. For test B1,  $q_1$  is  $0.036 \text{ mm}^3/\text{day}$ , as shown in Table 7-1. The binding leakage, as defined above, can then be computed from Eq. 7-1:

$$q_B = q_M - q_1 = 0.105 - 0.036 = 0.069 \text{ mm}^3/\text{day}$$

The values of  $q_B$  for all B tests performed are listed in Table 7-1. Each value is rounded off to the nearest  $0.01 \text{ mm}^3/\text{day}$ .

The computed value of  $q_1$  is only approximate because the permeability used to obtain  $q_1$  may be in error by  $\pm 35\%$  (Chapter 4). The resulting error in  $q_B$ , in terms of both its absolute magnitude and percent of  $q_B$ , is listed for each B test in Table 7-1. For those tests in which the flow through the membrane was large compared to the binding leakage, the possible error in the binding leakage is large. In some cases, e.g. tests B5(a), B5(d) and B16, the tabulated binding leakage can only be considered as having the correct order of magnitude. On the other hand, for tests such as B1, B2 and B20, the binding leakage is accurate to well within  $\pm 35\%$ .

## 7-05 DISCUSSION OF RESULTS

### (a) General

To assist in analyzing all variables, and as a basis of comparison, a B test performed under the following conditions will be considered as the "standard" type of test:

- (1) One membrane on pedestal.
- (2) One O-Ring on each side of porous disc.
- (3) No grease on pedestal.
- (4) Membrane soaked in water prior to test.
- (5) Pedestal has polished surfaces.
- (6) Pedestal contains a smooth porous ceramic disc.

All tests listed in Group I, Table 7-1, are such standard tests. The values of binding leakage from Table 7-1 are given in Table 7-2 in a form which is convenient for the following discussion.

(b) Binding Leakage in Group I Tests

Table 7-2 shows the binding leakage that occurred in the Group I tests at three hydraulic pressure differences. The binding leakage varies between 0.03 and 0.13 mm<sup>3</sup>/day, and has an average value of about 0.08 mm<sup>3</sup>. The values show no significant trend with increasing pressure.

Tests B5(a) through B5(d) were all performed on the same membrane by simply changing the pressure difference between tests. The binding leakages measured in these four tests also show no significant variation with pressure difference.

The binding leakage for test B5(d) was less than the binding leakage for test B5(a). Both tests were performed using the same pressure difference across the membrane. However, test B5(d) was started forty-five days after test B5(a) had been completed. Thus the binding had time to creep and gradually to form a better seal during the interval between the two tests.

The absence of any significant variation of the binding leakage with hydraulic pressure difference might be explained in the following two ways: (1) As the pressure difference is increased, the membrane is held more tightly against the pedestal. Thus the quantity  $q_3$  (Fig. 7-5) must be reduced. On the other hand, the quantity  $q_2$  is increased because of the increased pressure difference. The decrease in  $q_3$  and the increase in  $q_2$  might tend to maintain a constant magnitude of the binding leakage. (2) Assume that  $q_3$  (Fig. 7-5) is zero and that the binding leakage is entirely  $q_2$  flow, which passes directly through the membrane and then flows along the interface between the membrane and the pedestal. In such a case, increased hydraulic pressure difference would increase the tendency for flow through the membrane but would simultaneously increase the resistance to flow along the interface. Thus the net change in binding leakage might be zero.

(c) Effect of Use of Two Membranes on the Binding Leakage (Group II)

The Group II tests in Table 7-2 show that when two membranes were used with one O-Ring on each side of the porous disc, the binding leakage was approximately twice that measured in the Group I tests. This increase may be due to the possibility that two membranes are more easily wrinkled when the O-Ring is snapped over the membranes. However, one might expect that such wrinkles would cause the binding leakage to be erratic whereas, for the two Group II tests, the binding leakage was practically the same. Further tests using two membranes are required to determine the cause of the increased binding leakage in the Group II tests.

(d) Effect of the Roughness of the Pedestal on the Binding Leakage (Groups III, IV, V)

The tests in Groups III, IV, and V were all performed on a rough pedestal. The values of the binding leakage for these tests vary erratically between -0.02 mm<sup>3</sup>/day and 35 mm<sup>3</sup>/day. None of the B tests except those performed using a rough pedestal exhibited such erratic behavior. These data show conclusively that a rough pedestal is likely to permit excessive binding leakage.

(e) Effect of Greasing the Pedestal on the Binding Leakage (Groups VI, VII)

The tests in Groups VI and VII were performed by applying grease to the pedestal before setting the membrane in place. The binding leakages for these tests range

from 0.02 to 0.16 mm<sup>3</sup>/day and have an average value of 0.09 mm<sup>3</sup>/day. Thus the use of grease on the pedestal did not reduce the binding leakage significantly below that for the Group I tests.

The above tests were performed using a well polished pedestal. If a rough pedestal had been used, the application of grease to the pedestal may have reduced the leakage. The author believes that it is good practice in triaxial testing to grease the pedestal prior to applying the membrane(s), to help seal any minute scratches in the surface of the pedestal. Although this will not significantly decrease the leakage of a well made binding, it may be effective when dirt or scratches might otherwise render a binding ineffective.

(f) Effect of Soaking Membrane in Silicone Oil on Binding Leakage  
(Groups IV, VIII, IX)

The test shown in Group VIII was performed using an oil soaked membrane with a polished pedestal. The binding leakage was 0.15 mm<sup>3</sup>/day which is approximately double the leakage measured in the Group I tests. The tests in Group IX were performed using an oil soaked membrane on a polished pedestal which contained a porous carbon disc. The binding leakage for these tests ranged between 0.5 and 0.9 mm<sup>3</sup>/day. This five-to-nine-fold increase in leakage is tentatively explained as follows: When soaked in silicone oil, the natural rubber membranes appear to become more pliable and softer than when soaked in water. The porous carbon disc is many times rougher than the porous ceramic disc. When pressure is applied and the oil soaked membrane is forced against the rough disc, the membrane stretches over each surface grain of the disc and permits a higher rate of leakage than would a tougher, water soaked membrane (cf. Group VII test using water soaked membrane).

Thus the increase of the "binding leakage" tabulated for tests on oil soaked membranes may not be due to binding leakage at all. Instead the greater flow probably is due to the increased permeability of the membrane over that area of the membrane which is supported by the porous disc. Thus, silicone oil soaked natural rubber membranes probably should not be used in triaxial testing.

The tests in Group IV were also performed using oil soaked membranes. In these tests the pedestal was rough and the porous disc was rough. The binding leakage ranged erratically from 0.07 to 8.8 mm<sup>3</sup>/day so that no conclusions can be drawn on the effect of soaking the membranes in silicone oil.

(g) Leakage of Neoprene Rubber Strip Bindings (Groups V, X, XI)

The Group X test was performed in the same manner as the standard Group I tests except that the bindings were neoprene rubber strips. The leakage in this one test is seen to be 0.3 mm<sup>3</sup>/day. Thus the neoprene strip bindings permitted approximately three times greater leakage than the O-Ring bindings.

Group XI tests were performed in the same manner as the Group I tests except that the bindings were neoprene rubber strips and the membranes were soaked in silicone oil. The average binding leakage in these two tests was 0.1 mm<sup>3</sup>/day, which is about equal to the leakage of the Group I tests.

Group V test was performed using a rough pedestal. The binding leakage was 2.4 mm<sup>3</sup>/day for four days, then the leakage abruptly jumped to about 35 mm<sup>3</sup>/day. When the cell was dismantled, it was found that one of the strips had severed and had distorted the membrane when the strip unwound from the pedestal. Thus it appears that this strip binding on a rough pedestal while intact leaked at a rate of 2.4 mm<sup>3</sup>/day.

Of the four tests with neoprene rubber strip bindings there was only one test (B25) in which the neoprene strip bindings did not sever during the test. The failure of the rubber strip bindings probably is induced by the high stresses that were applied to the strips in order to wind them tightly around the pedestal. O-Ring bindings are stretched to a strain of about 40%, whereas the rubber strips were stretched to 100% or more strain.

Of course, it may be possible to make an effective seal using rubber strips without winding them so tightly on the pedestal.

#### 7-06 SUMMARY

Twenty-five binding leakage tests were performed with pedestals of the type shown in Figs. 7-3 and 7-4 using natural rubber membranes with O-Ring or neoprene rubber strip bindings. The binding leakage measured in these tests is the sum of (1) the rate of flow through the two areas of the membrane that are between the bindings but that do not bear on the porous disc in the pedestal and (2) the rate of flow past the two bindings along the interfaces between the pedestal and the membrane.

The results of the binding leakage tests are summarized below:

(1) The leakage of bindings set up in the following manner was found to average  $0.1 \text{ mm}^3/\text{day}$ , with no consistent variation with pressure:

- Pedestal - smooth, stainless steel, 1.4 in. diameter, no grease on pedestal
- Membrane - one, natural rubber, soaked in water prior to test, approximately 0.006 cm thick.
- Binding - one Buna-N rubber O-Ring on each side of porous disc in pedestal. Inside diameter of O-Ring (unstretched) was 70% of pedestal diameter.

(2) With two membranes the binding leakage was about twice as great as with one membrane. It should not be implied from this result that one natural rubber membrane should be used in triaxial testing rather than two. The rate of leakage through a natural rubber membrane on a 1.4 in. diameter by 3.5 in. high triaxial specimen is about 15 times greater than the binding leakage when the pressure difference is  $2 \text{ kg/cm}^2$ . Thus it is more important to reduce the membrane leakage by a factor of two than to concern oneself with the change in binding leakage caused by using two membranes. On the other hand, if butyl rubber membranes, which have about one-thirtieth the permeability of natural rubber, are used in place of natural rubber, the binding leakage may well be greater than the membrane leakage. Additional binding leakage tests will be required to determine the relative importance of binding leakage and membrane leakage when butyl rubber membranes are used.

(3) The leakage past O-Ring or rubber strip bindings, mounted on a pedestal which was deliberately roughened, varied erratically between very small values and  $35 \text{ mm}^3/\text{day}$ .

(4) Greasing the pedestal before adding the O-Ring binding did not significantly reduce the leakage of a well made binding. However, it is recommended that the pedestal be greased, in practice, so that the grease will fill any minute scratches on the pedestal which might otherwise prevent an effective seal.

(5) The use of a membrane soaked in silicone oil caused an apparent increase in binding leakage by a factor of 5 to 9. It was suggested that this increase was really due to a greater rate of flow through the membrane which resulted when the soft, silicone oil soaked membrane was pressed tightly against the rough surface of the porous disc.

(6) Neoprene rubber strip bindings were found to be unsatisfactory because (a) they did not reduce the binding leakage, (b) the strips severed during the test (in one case four days after the start of the test), and (c) the strip bindings were much more difficult to apply than O-Ring bindings.

No tests were performed during this investigation to determine the binding leakage which occurs when a mole fraction difference is applied across the bindings. On the basis of the description of the effect of pressure variation on the rate of binding leakage as given in 7-05(b), one can analyze the effect of a mole fraction difference as follows: salt in water causes a reduction of the vapor pressure of the water, so that if salt water were inside the pedestal, water would flow into the pedestal. The mole fraction difference does not cause any physical force holding the membrane against the

pedestal as would a hydraulic pressure difference. Therefore, as the mole fraction difference is increased, one should expect both  $q_2$  and  $q_3$  in Fig. 7-5 to increase. Consequently, the rate of binding leakage must increase approximately in proportion to the mole fraction difference so long as the hydraulic pressure difference is held constant. If the hydraulic pressure difference is increased, the rate of binding leakage due to a given mole fraction difference should decrease, because the membrane is held more tightly against the pedestal. Additional binding leakage tests are required to determine whether this description is a valid one.

CHAPTER 8EXPERIMENTAL INVESTIGATION OF  
LEAKAGE FROM VALVES, FITTINGS AND SARAN TUBING8-01 INTRODUCTION

The valves, fittings and tubing listed in Tables 8-1 and 8-2 were tested. The valves are shown disassembled in Fig. 8-2 and assembled in Fig. 8-1; and the fittings are shown disassembled in Fig. 8-4 and assembled in Fig. 8-3. A photograph of the Saran tubing tested is shown in Fig. 8-3. The numbers beside the items in Figs. 8-1 through 8-4 correspond to the numbers in Tables 8-1 and 8-2.

The valves and fittings were tested by applying a hydraulic pressure of  $10 \text{ kg/cm}^2$  to distilled water inside the valve or fitting through a burette that was connected to the item tested. The volume of leakage which passed through the packing of the valve or fitting was measured in the burette. Tests performed in this manner simulate the conditions on valves and/or fittings located outside of a triaxial chamber during a triaxial test. Fittings inside the triaxial chamber leak much less than those outside because the vapor pressure gradient causing flow is much smaller when liquid water is on both sides.

Saran tubing was tested by applying water pressure inside the tubing and measuring the resulting volume flow under two conditions: (1) with water at atmospheric pressure on the outside of the tubing and (2) with room air on the outside of the tubing.

8-02 APPARATUS AND PROCEDURE(a) Leakage Tests on Valves and Fittings

The apparatus for these tests consisted of (1) means for applying pressure to the water inside the item tested, (2) a mercury seal to prevent evaporation from the water meniscus in the volume change measuring burette, (3) a burette for measuring volume flow, and (4) a leak-tight connection between the valve or fitting tested and the burette. This apparatus is shown schematically in Fig. 8-5.

A valve or fitting leakage test was set up by first attaching the valve or fitting to the stainless steel tubing by means of two epoxy seals, two soldered joints or one of each. All parts of the valve or fitting, the stainless steel tubing and the burette were carefully saturated with distilled water and the water-mercury meniscus was set at the desired level in the burette (Fig. 8-5). The fitting was assembled while still submerged.

Air pressure was applied to the mercury meniscus in the lucite reservoir in increments of about  $2 \text{ kg/cm}^2$  up to a pressure of  $10 \text{ kg/cm}^2$ . The level of the water-mercury meniscus in the burette was read after the application of each pressure increment. From these data, a curve of volume change versus pressure could be plotted.

After the pressure of  $10 \text{ kg/cm}^2$  was applied, a meniscus reading was taken each day, or as required to follow the progress of the test. Readings of pressure, room temperature and relative humidity were taken each time the meniscus was read. The meniscus readings were corrected for temperature variations in the laboratory for those tests in which the effect of temperature on the meniscus movement was significant.

(b) Tests on Saran Tubing

The leakage of Saran tubing was measured by setting up a six meter length of the tubing as shown schematically in Fig. 8-6. The mercury seals at each end of the tubing prevented evaporation of water from the water meniscus in the tubing. The tubing itself was used as the burette to measure volume changes. The sections of the tubing used to measure volume changes were calibrated and found to contain  $(25.20 \pm 0.05) \text{ mm}^3/\text{cm}$ .

For these tests no fittings are located between the two water-mercury menisci. Thus the only possible causes of movement of the menisci are: (1) leakage through the

walls of the saran tubing, (2) elastic and inelastic volume changes of the Saran tubing caused by the applied pressure, and (3) temperature and pressure fluctuations.

As long as the temperature and pressure fluctuate such that the average values remain constant, no net change in volume will result. Therefore, only leakage and volume changes caused by the applied pressure can cause a monotonic change of the meniscus level in the tubing.

Test Nos. 23(a), (b) and (c) were all performed on the same piece of Saran tubing. The immediate volume change caused by application of hydraulic pressure was measured in test No. 23(a). The Saran tubing was submerged in a water bath and maintained at  $30 \pm 0.02^\circ\text{C}$ . Pressure was applied in increments of  $1 \text{ kg/cm}^2$  each minute, starting at a hydraulic pressure of  $1 \text{ kg/cm}^2$  and stopping at a hydraulic pressure of  $15 \text{ kg/cm}^2$ , so that the hydraulic pressure difference was increased from 0 to  $14 \text{ kg/cm}^2$ . The volume change corresponding to each pressure increment was measured.

In test No. 23(b), the creep of the Saran tubing due to hydraulic pressure differences was measured while the tubing was submerged in the water bath. The hydraulic pressure difference of  $15 \text{ kg/cm}^2$ , which was on the tubing at the completion of Test No. 23(a), was maintained for a period of 56 days, after which the hydraulic pressure was reduced to  $8 \text{ kg/cm}^2$ . After 56 additional days, the hydraulic pressure was reduced to  $1 \text{ kg/cm}^2$  and maintained for 69 days. Readings of room temperature, water bath temperature, pressure and the menisci levels were taken as often as necessary to define the volume change with time.

Test No. 23(c) was performed to measure the rate of evaporation through the walls of the tubing. The Saran tubing which had been used for test Nos. 23(a) and (b) was removed from the water bath, its exterior was carefully dried and a hydraulic pressure of only 4 cm of mercury was applied to the water in the tubing. The water from inside the Saran tubing could then evaporate through the walls of the tubing into the room air. Readings of the levels of the menisci, of room temperature and relative humidity were usually taken every two days.

## 8-03 PRESENTATION AND INTERPRETATION OF RESULTS

### (a) Results of Valve Leakage Tests

The plots of volume flow versus time for all valve leakage tests are given in Figs. H-1 through H-23 of Appendix H. A summary of the valve leakage tests is given in Table 8-3. The valves tested were divided into the following three groups:

Stem Type Valves - contain a stem that moves in and out when the valve is closed and opened, causing fluid to be forced out or sucked into the valve.

Piston Type Valves - are opened and closed by rotating or sliding a piston. Such a valve is open when a hole in the piston is aligned with holes in the body of the valve. A very small volume of fluid is forced into or out of the valve when it is opened or closed.

Snap Valves - are designed so that special fittings can be inserted in the valve which will open the valve. When such a special fitting is removed, the valve snaps into the closed position to prevent escape of fluid.

### (b) Results of Fitting Leakage Tests and Tests on Saran Tubing

The plots of volume flow versus time for all fitting leakage tests are given in Figs. H-24 through H-36 in Appendix H. A summary of the results of the fitting leakage tests is given in Table 8-4. Fig. H-37 contains the plot of volume change versus hydraulic pressure for test No. 23(a). Figs. H-38 and H-39 contain plots of volume change versus time for each hydraulic pressure difference which was maintained on the Saran tubing during test No. 23(b). Fig. H-40 contains the plot of volume flow of liquid water (through the wall of the Saran tubing) versus time for test No. 23(c). The results of test No. 23 are summarized in Table 8-4.

The fittings listed in Table 8-4 are divided into two groups: (1) fittings that are sealed with an O-Ring, and (2) fittings that are sealed by means other than O-Rings. The types of seal in the fittings are described in Table 8-2 and are shown in the photograph of Fig. 8-4.

(c) Temperature Correction of Volume Flow versus Time

For tests in which the rate of leakage was greater than about  $0.01 \text{ mm}^3/\text{day}$ , the plots of volume flow versus time were approximately straight lines for more than 50% of the duration of the tests (e.g. see Figs. H-19 and H-27). However, those plots of volume flow versus time for tests in which the rate of leakage was less than about  $0.01 \text{ mm}^3/\text{day}$  were generally erratic (e.g. see Figs. H-2, H-4 and H-24). The causes of this erratic behavior might be: (1) temperature variations, (2) pressure variations, (3) "sticking" of the meniscus in the burette, perhaps due to the presence of small dirt particles, which caused the shape of the meniscus to vary, and/or (4) other unknown causes.

The data for tests that yielded a rate of leakage of less than about  $0.01 \text{ mm}^3/\text{day}$  were corrected for temperature variations using one of the following approximate procedures.

Procedure (1) - The average temperature of the test was determined and was rounded off to the nearest half degree centigrade. Pairs of consecutive data points were isolated such that one point was taken when the temperature was above the average temperature and the other point taken at a temperature below the average temperature. A corrected point was obtained by interpolating between this pair of points to obtain a point at the average temperature. The data for tests 1(b), 2(a), 2(b), 7(a), 7(b), 10(a), 10(b), 11(b), 14(a), 14(b), 15, 16(b), 17(a), 17(b), 20(a) and 10(b) were corrected using Procedure 1.

Procedure (2) - First, the plot of volume flow versus time was made without correction. Then a curve was drawn through the data points such that those points which, by coincidence, had been taken at equal temperatures would lie approximately on the line. Using this line as a base, the volume change produced in the burette per unit temperature change could be calculated by assuming that all deviations from the line were caused by temperature changes. Each data point taken at some temperature other than the temperature for which the base line was drawn could then be corrected to the temperature of the base line. A good average line could then be drawn through the corrected data points. The data for tests Nos. 3, 9 and 22 were corrected in this manner.

All plots of volume flow versus time that were corrected for temperature variations were still quite erratic. Therefore the maximum probable rate of leakage was estimated from each of the corrected plots and is given in Tables 8-3 and 8-4.

(d) Accuracy of the Rate of Leakage Data

In the apparatus used to measure the leakage of valves and fittings there are two connections where leakage might occur that will affect the test data. These connections are (1) the one epoxy seal between the glass burette and the stainless steel tubing, and (2) the epoxy seals and/or soldered joints between the stainless steel tubing and the valve or fitting being tested. The leakage of item (1) was determined in test No. 22. As shown in table 8-4, the leakage was found to be  $0.0032 \text{ mm}^3/\text{day}$  for two such epoxy seals. Assuming that the leakage of item (2) above is about the same as item (1), then the total leakage from these two fittings might be about  $0.003 \text{ mm}^3/\text{day}$ .

The following conclusions are indicated:

- (1) Rates of leakage smaller than  $0.01 \text{ mm}^3/\text{day}$  are difficult to measure because of temperature fluctuations in the laboratory and other possible errors.
- (2) Rates of leakage smaller than  $0.003 \text{ mm}^3/\text{day}$  may be due to leakage from connections other than the valve or fitting being tested.

Thus the rates of leakage listed in Tables 8-3 and 8-4 may be too large by about  $0.003 \text{ mm}^3/\text{day}$ .

## 8-04 DISCUSSION OF RESULTS

### (a) General

It was shown in Chapter 2 that a total leakage of 0.1 mm<sup>3</sup>/day into a 1.4 in. diameter by 3.5 in. high triaxial specimen is a practical maximum for the rate of leakage that is acceptable during 100-day Q or R tests on a 100% saturated specimen. Since leakage can also occur through membranes, it is evident that the acceptable rate of leakage from the valves, fittings and tubing in the drainage system of a triaxial specimen must be held to rates much lower than 0.1 mm<sup>3</sup>/day. As a guide in judging the quality of a valve or fitting the following criteria will be used:

- (1) For 100-day Q or R tests on 1.4 in. by 3.5 in., 100% saturated specimens, the maximum acceptable rate of leakage from a valve, fitting or the tubing in the drainage system shall be less than 0.01 mm<sup>3</sup>/day.
- (2) For 1-day Q or R tests on 1.4 in. by 3.5 in., 100% saturated specimens, the maximum acceptable rate of leakage from a valve, fitting or the tubing in the drainage system shall be less than 1.0 mm<sup>3</sup>/day.

The above criteria apply only to those valves and fittings that are part of the drainage system of the triaxial specimen. Furthermore, it is assumed that no more than five valves and fittings will be used in the drainage system. In any case, the number of valves and fittings in the drainage system must be kept to an absolute minimum. A well designed triaxial apparatus for long-time tests need only contain one fitting and one valve in the drainage system.

### (b) Valve Leakage Tests

Fig. 8-7 is a plot showing the rates of leakage of the valves in each of the three groups. It is evident from the figure that the stem type valves, as a group, leak the least. The piston type valves leak at a rate somewhat greater than the leakage of the stem type valves but less than the leakage of the snap valves.

Only the stem type valves appear to be suitable for use during 100-day tests, although the Hydromatics valve and the seat side of the Circle Seal valve may also be usable. The snap valves are unsuitable for use during 100-day tests.

For triaxial tests that last only one day or less, all of the valves tested, except the Klinger valves, are suitable. The Klinger valve is suitable for one-day tests only if the packing is carefully saturated with water, greased and tightly compressed by the bonnet nut (see Fig. H-10).

The rates of leakage of all valves that are sealed by O-Rings are compared in Table 8-5. The valves are divided into two groups. Group I contains those valves that seal on the perimeters of the O-Ring(s). Group II contains those valves that seal on the faces of the O-Ring(s). The perimeter and face of an O-Ring are defined in the sketch at the bottom of Table 8-5. The total contact diameter given in Table 8-5 is the sum of the diameters of all contacts that form the seals between the O-Rings and the metal of the valve.

The leakage of the Group I valves is greater than that of the Group II valves by a factor of about five, except that the Snap-tite valve appears to leak excessively. (This valve is manufactured in such a manner that the pressure inside the valve is not fully effective in causing the O-Ring to seal. This is not true of any of the other valves listed in Table 8-5. Probably, the lower sealing pressure on the O-Ring in the Snap-tite valve accounts for its high rate of leakage.) The fact that two out of three of the Group II valves leaked at a lower rate than the Group I valves indicates that, to reduce leakage, valves should be designed so that the face of the O-Ring makes contact with the metal parts to form the seal.

It is also seen in the table that for each group of valves, the rate of leakage is smaller for smaller valves of total contact diameter. Thus, it is best to use a small diameter O-Ring to minimize leakage.

(c) Fitting Leakage Tests

The rates of leakage shown for the fittings in Table 8-4 lead to the following conclusions:

- (1) The rates of leakage of the O-Ring fittings used in the membrane permeability cells were less than  $0.002 \text{ mm}^3/\text{day}$ , except for the fitting used for test No. 16(a). This fitting was found to contain metal chips beneath the O-Ring. After cleaning, the leakage of this fitting was practically zero (Test 16(b)).
- (2) The rates of leakage of the fittings used in the binding leakage cells were less than  $0.01 \text{ mm}^3/\text{day}$ .
- (3) The rates of leakage of fittings sealed by the perimeters of an O-Ring (test Nos. 18 and 19) were five or ten times larger than the rates of leakage for fittings sealed by the face of an O-Ring (test Nos. 14 through 17).
- (4) Flex fittings leaked at a rate of about  $0.01$  to  $0.02 \text{ mm}^3/\text{day}$ .

Test No. 21 on the Swagelok union was continued for only about six days. The following analysis shows why the results of this test cannot be used to determine accurately the leakage of this union. In Fig. H-35(a), the decrease of water volume in the burette is plotted against room temperature. The points fall close to a straight line, indicating that the measured volume changes were due mainly to room temperature fluctuations. The deviations of the points in Fig. H-35(a) from the "best-fit" straight line were plotted in Fig. H-35(b) against elapsed time after the start of test. There is considerable scatter of the points but the line that best fits the points does have a positive slope, indicating that the valve was leaking at about  $0.018 \text{ mm}^3/\text{day}$ . However, the data in Figs. H-35(a) and H-35(b) were also analyzed by neglecting point No. 1 in these figures. When this was done, the best-fit line, analogous to the line shown in Fig. H-35(b), indicated that the leakage was only  $0.007 \text{ mm}^3/\text{day}$ . This test should have been continued for a sufficiently long duration such that the effect of the first points on the calculated leakage would be negligible.

(d) Tests on Saran Tubing

The immediate volume changes of  $1/8$  in. O.D. Saran tubing due to application of pressure were measured in test No. 23(a). The results, plotted in Fig. H-37, show that the measured increase in volume of Saran tubing was  $0.0206 \text{ mm}^3/\text{cm}$  per  $\text{kg}/\text{cm}^2$  of hydraulic pressure difference. This rate of volume increase remained practically constant over the entire range of pressure applied in the test. Approximately 6% of the measured volume change can be attributed to the compression of the water inside the tubing. Therefore the volume of the Saran tubing alone increased at a rate of  $0.0193 \text{ mm}^3/\text{cm}$  per  $\text{kg}/\text{cm}^2$ .

The volume change versus time for test No. 23(b) is plotted on an arithmetic scale in Fig. H-38. The curve shows that the volume change measured after 10 minutes, caused by an increase or a decrease in hydraulic pressure difference, is about 60% of the total volume change that occurs over a period of about 50 days. Thus, from the data in Fig. H-37 and H-38 one can derive the following volume changes (immediate plus creep) of Saran tubing due to the application of pressure:

Volume change after 10 min	$0.020 \text{ mm}^3/\text{cm}/(\text{kg}/\text{cm}^2)$
Volume change after 50 days	$0.032 \text{ mm}^3/\text{cm}/(\text{kg}/\text{cm}^2)$

Volume changes for shorter or longer periods than 50 days can be estimated from the semi-logarithmic plots of the data for test No. 23(b) in Figs. H-39(a), (b) and (c). The points are seen to lie close to a straight line for about 60 days regardless of whether the pressure difference was increased or decreased.

The rate of evaporation of water from Saran tubing was measured in test No. 23(c). The curve of volume flow versus time for this test is shown in Fig. H-40. Initially the curve shows an apparent negative leakage, which was probably caused by the change in stress on the tubing when it was removed from the water bath at the completion of test No. 23(b). Evaporation of water through the walls of the tubing caused the curve to

assume a positive slope approximately 15 days after the start of the test. This positive slope decreased continuously throughout the remainder of the test. The average rate of leakage (i.e. the average slope of the curve for the last half of the test) was about  $0.0007 \text{ mm}^3/\text{day}$  per cm length of the Saran tubing.

The permeability K (see Chapter 4) of the Saran tubing was computed from the results of test No. 24 as shown in Fig. H-40. The result is that  $K = 0.005 \times 10^{-11} \text{ cm}^4/\text{gm sec}$ . This result is in reasonable agreement with data presented by Doty, Aiken and Mark (42). Comparing the above result for Saran with the permeabilities shown in Table 6-3, one can see that the permeability of Saran is about 4 times greater than the permeability of Kel-F, but about half as great as the permeability of Teflon.

#### (e) Volume Changes of Valves and Fittings Caused by Application of Pressure

The total volume change of a valve or fitting including connecting tubing, due to the application of a hydraulic pressure difference equal to  $10 \text{ kg/cm}^2$ , was measured and is recorded in Tables 8-3 and 8-4. The final slopes of the curves of volume change versus pressure are also shown in the two tables. The total volume change and the slopes of the curves of volume change versus pressure varied quite erratically. This erratic behavior might be due to: (1) the compression of small quantities of air in the system, and/or (2) variations in the rate at which pressure was applied. No attempt was made to refine volume change measurements. However, the data are presented here to show the order of magnitude of volume change which can be anticipated even if a valve or fitting is carefully saturated with water prior to test.

#### 8-05 SUMMARY

Valves and fittings in the drainage system connected to the pore water of a tri-axial specimen preferably should not leak at a rate in excess of  $0.01 \text{ mm}^3/\text{day}$  during tests performed under the following conditions:

Size of soil specimen -	1.4 in. diameter; 3.5 in. high
Degree of saturation of specimen -	100%
Duration of axial loading for a Q or R test -	100 days
Total number of valves and fittings in drainage system -	Less than five

For most soils the value of  $0.01 \text{ mm}^3/\text{day}$  is a low (i.e. conservative) estimate of the rate of leakage that might be important for Q or R tests performed under the above conditions. Based on this criterion, the following conclusions may be drawn from the results of the valve, fitting and tubing leakage tests, relative to their suitability for use in the drainage system of a triaxial cell:

- (1) Klinger valves are generally unsuitable because the rate of leakage is large and erratic.\*
- (2) Stem type valves are generally suitable from the standpoint of leakage. (Note: such valves cause a volume change in the system which must be carefully accounted for when they are opened or closed.)
- (3) The piston type valves are not generally suitable, with the exception of the Hydromatics valve. This valve leaks at a rate of  $0.02 \text{ mm}^3/\text{day}$ , which might be tolerated if only one valve is used in the drainage system. (Note: The piston valves have the advantage that very small volume changes occur in the system when the valve is opened or closed.)

---

\* Klinger valves may be modified by using a Teflon rather than asbestos packing. No data have been obtained to determine whether the use of a Teflon packing reduces the leakage of Klinger valves.

- (4) The snap type valves are not suitable.
- (5) All of the fittings tested are suitable. However, it is emphasized that no attempt was made to evaluate in detail the various commercial fittings presently available.
- (6) The rate of evaporation of water through the wall of a 25 cm long piece of Saran tubing is  $0.02 \text{ mm}^3/\text{day}$ , or equivalent to the rate of leakage of one Flex fitting. In addition, the volume of Saran tubing increases slowly with time after pressure is applied. Saran tubing should therefore be replaced by metal tubing for 100-day triaxial tests.

Every attempt should be made to reduce to an absolute minimum the number of valves and fittings and the length of tubing in the drainage system of a triaxial cell.

When using O-Rings as a seal in a fitting or valve, it is advisable to use as small an O-Ring as possible and to form the seal against the faces rather than the inside or outside perimeter of the O-Ring.

## CHAPTER 9

### ANALYSIS OF RESULTS

#### 9-01 PURPOSE

The maximum acceptable rates of leakage in triaxial Q and R tests are compared with the rates of leakage that actually occur when using conventional triaxial apparatus. It is shown that several details of the conventional apparatus and procedures are not suitable for performing 100-day triaxial tests. The conditions under which they are suitable are discussed.

General methods for reducing leakage of water and air are discussed. The suitability of several specific procedures, suggested by the author and other investigators, are analyzed. Based on this analysis, possible procedures to be used for reducing water and air leakage are discussed. Recommended procedures are given in Chapter 10.

#### 9-02 SUITABILITY OF CONVENTIONAL TRIAXIAL APPARATUS FOR CONTROL OF WATER LEAKAGE

##### (a) Water Leakage into 100% Saturated Specimens

The maximum acceptable rates of water leakage into 100% saturated specimens of three soils, for tests of three different durations, are shown in Table 9-1. It was assumed for the purpose of comparison that the maximum acceptable decrease in effective stress due to leakage into a Q or R triaxial specimen is 2% of the initial effective stress on the specimen. The quantities in Table 9-1 were calculated by using Eq. 2-12 and the swelling ratios shown in the table. Most soils probably have swelling ratios that fall within the range used in Table 9-1. Highly organic soils and peats may have higher swelling ratios, and cemented sands or cemented clays may have lower swelling ratios.

The actual rates of leakage that occur when using natural rubber membranes, O-Ring bindings and the Harvard triaxial cell are given in Table 9-2 for several pertinent examples. The rates of leakage shown apply only when the roughness of the soil tested is equivalent to the roughness of the porous disc used in the permeability cell (see Chapter 4). Cracks between the top and bottom of the specimen and the pedestals, or sand grains beneath the membrane are sites where thin spots can develop in the membrane when the chamber pressure is applied. Thus, in practice, the leakage may be greater than the rates shown in Table 9-2.

A comparison of the quantities listed in row (7) of Table 9-2 with the quantities in columns (6) to (8) of Table 9-1 shows that, for a decrease in effective stress not exceeding 2%, the maximum duration of a Q or R test on a 100% saturated specimen is as follows:

- (1) When there is no salt in the pore water, and when the average effective minor principal stress over the duration of the axial loading is less than  $15 \text{ kg/cm}^2$ :
  - (a) Eight-hour tests can be performed on practically any soil (e.g.  $S \geq 0.001$ ).
  - (b) Seven-day tests can be performed on Boston Blue clay ( $S = 0.015$ ).
  - (c) Fourteen-day tests can be performed on Mexico City clay ( $S = 0.03$ ).
- (2) When the mole fraction of the salt in the pore water is approximately equal to that of sea water:
  - (a) Tests lasting up to four hours can be performed on soils with a very low swelling ratio (e.g.  $S = 0.001$ ).
  - (b) Tests lasting up to about five days can be performed on soils with a high swelling ratio (e.g.  $S = 0.03$ ).

It is concluded that leakage which occurs when natural rubber membranes are used is excessive for 100-day Q and R tests and that it is necessary to find means for reducing the leakage to a tolerable minimum in such long-time tests. Reduction of the quantity of leakage by about two orders of magnitude would be desirable.

A volume decrease of the Saran tubing in the drainage system has the same effect as leakage into the specimen since, as its volume decreases, the water must be forced into the specimen. The average rates of volume change of Saran tubing due to creep under pressure are shown at the lower right in Table 9-2. The tubing outside the triaxial chamber gradually increases in volume whereas the tubing inside the chamber gradually decreases in volume. A comparison of the average rates of volume change of Saran tubing with the maximum acceptable rates of water leakage in Table 9-1 shows: (1) For a test on Canyon Dam clay at an effective stress of  $10 \text{ kg/cm}^2$ , the rate of volume change due only to creep of the Saran tubing is 50% more than the maximum acceptable leakage for a 10-day test. Thus, even if the leakage through the membrane were zero, the decrease in effective stress would be excessive if Saran tubing were used in the drainage system. (2) For a test on Boston Blue clay, at an effective stress of  $10 \text{ kg/cm}^2$ , the rate of volume change of the Saran tubing is less than 15% of the maximum acceptable leakage for a 100-day test. (3) For tests at low effective stress, the net increase in volume of the Saran tubing permits a small increase in the maximum acceptable rate of leakage.

It is concluded that for most triaxial tests the volume changes due to creep of Saran tubing in the drainage system are small, but that for long duration tests on soils with a low swelling ratio ( $S = 0.001$ ), Saran tubing must not be used.

#### (b) Water Leakage into Partially Saturated Specimens

In Chapter 2 it was shown that the changes in effective stress caused by water leakage into partially saturated specimens may be just as great as for 100% saturated specimens, or the changes may be considerably smaller, depending on whether or not the air-water menisci change shape when leakage occurs. Therefore, if changes in testing procedure are introduced which will reduce water leakage into 100% saturated specimens to a tolerable minimum, these changes will also be satisfactory for testing partially saturated specimens.

### 9-03 SUITABILITY OF CONVENTIONAL TRIAXIAL APPARATUS FOR CONTROL OF AIR LEAKAGE

#### (a) General

The major pursuit during this investigation was to attempt to control water leakage. However, in the course of the study, it became evident that air leakage into or out of partially saturated specimens may be even more critical than water leakage. Although no measurements of air flow were made, calculations of rates of air flow were made using data reported elsewhere in the literature. These calculations are presented in Appendix B. All subsequent conclusions concerning the effects of air leakage during triaxial tests on partially saturated specimens should be considered tentative and subject to experimental verification.

It is shown in Appendix B that air leakage into a 100% saturated triaxial specimen can be practically eliminated by (1) using water as the chamber fluid and (2) inserting a two meter length of  $1/16$  in. inside diameter tubing, filled with water, between the chamber water and the point of air pressure application. Thus air leakage into 100% saturated triaxial specimens is not discussed further. The control of air leakage into or out of partially saturated specimens is discussed below.

#### (b) Air Leakage Into or Out Of Partially Saturated Specimens

The maximum acceptable rate of air leakage into a partially saturated specimen can be computed using Eq. 2-22 which is based on the assumption that, when air leakage occurs, the change in pore water pressure is equal to the change in pore air pressure. This assumption yields a conservative, i.e. low, estimate of the maximum acceptable leakage. The most critical case of air leakage arises when (1) the swelling ratio of the soil is low, (2) the initial degree of saturation is high, and (3) the initial effective stress is low. The initial pore air pressure only slightly affects the maximum acceptable air leakage. Table 9-3 shows computed values of maximum acceptable rates of air leakage into a specimen, assuming the maximum acceptable decrease in effective stress is 2%, for a range of conditions extending from the most critical to the least critical case that is of interest. A volume of air leakage of  $0.03 \text{ cm}^3$ , for the most critical case, and about  $2.5 \text{ cm}^3$ , for the least critical case, will cause a 2% decrease in effective stress.

The maximum acceptable air leakage out of a partially saturated specimen was also computed for a range of conditions and the results are shown in Table 9-4. The computations were made using Eq. 2-22 except that the swelling ratio  $S$  was replaced by the "compression ratio",  $C$ , which is the slope of a plot of  $\Delta V/V$  versus  $\Delta \bar{\sigma}_3/\bar{\sigma}_3$  for increasing values of effective stress. The estimates were made for high and very low values of the compression ratio. For the most critical case a volume of air leakage of about  $0.04 \text{ cm}^3$  is acceptable whereas for the least critical case a volume of leakage of about  $5.5 \text{ cm}^3$  is acceptable.

In general, whether air flows into or out of a partially saturated specimen, a volume of air leakage of about  $0.05 \text{ cm}^3$  will cause 2% change in effective stress in the most critical case. For the least critical case a volume of air leakage of about 2 to  $5 \text{ cm}^3$  can be tolerated. Of course, for any given soil, the compression ratio might be 5 to 10 times greater than the swelling ratio. Thus, a given volume of inflow will cause a much larger percent change in effective stress than an equal volume of outflow. Because of errors arising from the assumptions used to derive Eq. 2-22, the flow rates quoted above may be too low by as much as a factor of two. (See 2-07 for the discussion of errors.)

The actual rate at which air can flow into or out of a triaxial specimen can be computed using the procedure presented in B-05 of Appendix B. The results show that when the pore air pressure is one  $\text{kg/cm}^2$  greater than the pressure at which the chamber water is saturated with air, about one  $\text{cm}^3$  of air (measured at atmospheric pressure) can flow out of a 1.4 in. diameter by 3.5 in. high triaxial specimen in three hours, and about three  $\text{cm}^3$  can flow out in twenty-four hours. When the air pressure difference across the membrane is opposite in sign, approximately equal flow will occur into the specimen. A study of the simplifying assumptions involved in these calculations indicates that the calculated rates of flow may be up to two times smaller than the rates of flow that actually occur.

A comparison between the acceptable rates of air leakage shown in Table 9-3, and the rates that may actually occur due to a partial pressure difference of one  $\text{kg/cm}^2$  when using water as the chamber fluid gives the following results:

- (1) For the least critical case, the longest permissible duration of a Q or R test on a partially saturated specimen, without exceeding a 2% decrease in effective stress is about four days. This case arises when the swelling ratio is high ( $S = 0.03$ ), the initial effective stress is high ( $\bar{\sigma}_3 = 20 \text{ kg/cm}^2$ ), the initial degree of saturation is low ( $G_w = 90\%$ ).
- (2) For the most critical case, the longest permissible duration of a Q or R test, without exceeding a 2% decrease in effective stress, is about 15 minutes. This case arises when the swelling ratio is low ( $S = 0.001$ ), initial effective stress is low ( $\bar{\sigma}_3 = 1.0 \text{ kg/cm}^2$ ), and the initial degree of saturation is high ( $G_w = 99\%$ ).

From the above conclusions it is evident that long-time Q and R tests on partially saturated specimens cannot be performed unless special precautions are taken to reduce air leakage. To perform 100-day Q and R tests without developing excessive decrease in effective stress, it is necessary to reduce air leakage by a factor of about 25 in the least critical case, and by a factor of about 10,000 in the most critical case. For 100-day tests on a soil with an average swelling ratio, such as Boston Blue clay, with a degree of saturation of about 95% and an effective stress of  $6 \text{ kg/cm}^2$ , the air leakage must be reduced by a factor of about 200. These estimated test durations may be in error by plus 100% or minus 50%, due to errors in the calculations that are introduced by simplifying assumptions.

9-04 GENERAL DISCUSSION OF PROCEDURES FOR CONTROLLING ERRORS CAUSED BY AIR AND WATER LEAKAGE

(a) Purpose

An equation is derived in paragraph (b) to relate the percent decrease in effective stress caused by water leakage into a 100% saturated specimen to the parameters that govern the volume of leakage. Based on this equation, possible procedures for controlling leakage are presented and discussed in paragraphs (c) and (d). A similar discussion is presented for the case of air leakage.

(b) Derivation of Equation Relating the Decrease in Effective Stress to Parameters Controlling Volume of Leakage

(1) Equation for the Case of Water Leakage

From Table 9-2 one can see that the water leakage through natural rubber membranes is far greater than the leakage of bindings, fittings and valves. Therefore, the volume of water leakage into a specimen is essentially equal to the membrane leakage, which can be computed using Eq. 3-33 as follows:

$$J_w = q \cdot t = K A_s \frac{\Delta p_v}{L} t \quad (9-1)$$

where

- $J_w$  = volume of water leakage (cm<sup>3</sup>)
- $q$  = rate of water leakage (cm<sup>3</sup>/sec)
- $K$  = permeability constant (cm<sup>4</sup>/gm sec)
- $A_s$  = surface area of specimen, which is equal to the area of the membrane through which flow occurs (cm<sup>2</sup>)
- $\Delta p_v$  = vapor pressure difference across membrane (gm/cm<sup>2</sup>)
- $L$  = membrane thickness (cm)
- $t$  = time during which leakage occurs (sec)

The vapor pressure difference is made up of two components: (1) The vapor pressure difference caused by a hydraulic pressure difference as given by Eq. 3-28. (2) The vapor pressure difference caused by a mole fraction difference of water across the membrane as determined from measurements of vapor pressure lowering.

Using Eq. 9-1 one can calculate the volume of leakage. On the other hand, Eq. 2-9 relates the volume of leakage to the percent decrease in effective stress. Solving Eqs. 9-1 and 2-9 for  $\frac{\Delta \bar{\sigma}_3}{\bar{\sigma}_3}$ , one obtains

$$\frac{\Delta \bar{\sigma}_3}{\bar{\sigma}_3} = \frac{K}{S} \frac{A_s}{V} \frac{\Delta p_v}{L} t \quad (9-2)$$

Substituting the surface area of the membrane and the volume of the specimen in terms of the height  $H_s$  and diameter  $D_s$  of the specimen, one obtains

$$\frac{\Delta \bar{\sigma}_3}{\bar{\sigma}_3} = \frac{K}{S} \frac{4}{D_s} \frac{\Delta p_v}{L} t \quad (9-3)$$

Eq. 9-3 shows that the effects of leakage upon the effective stress can be reduced by increasing the thickness  $L$  of the membrane. However, the thickness cannot be increased indiscriminately, since too thick a membrane would impose excessive restraint on a specimen. Bishop and Henkel (12, Appendix 1) have derived an equation relating the membrane

restraint to the properties of the membrane and the size of the triaxial specimen. Their equation, which is based on the assumption that a bulge type failure occurs, can be written in the form

$$\sigma_R = 4\varepsilon(1-\varepsilon) \frac{EL}{D_s} \quad (9-4)$$

where  $\varepsilon$  = strain at which restraint is measured.

$\sigma_R$  = membrane restraint, defined as the additional axial stress that must be applied to fail a triaxial specimen, above that which would be needed if the modulus of elasticity of the membrane were zero.

$E$  = modulus of elasticity of membrane. (Hooke's law is assumed to be valid for the membrane over the range of strains that occur in a triaxial test, i.e. up to about 20% strain.)

For constant membrane restraint at a given strain Eq. 9-4 becomes

$$L = \text{constant} \times \frac{D_s}{E} \quad (9-5)$$

Thus, if the parameters  $D_s$  and  $L$  in Eq. 9-3 are varied in accordance with Eq. 9-5, the membrane restraint will remain constant. Substituting Eq. 9-5 into Eq. 9-3 one obtains

$$\frac{\Delta\bar{\sigma}_3}{\bar{\sigma}_3} = \text{constant} \frac{t}{S} \left[ \frac{EK}{D_s^2} \Delta p_v \right] \quad (9-6)$$

The values of  $S$  and  $t$  are fixed by the choice of the soil and rate of loading, but the quantities in brackets can be varied. To reduce the effects of water leakage one can (1) increase the specimen size, (2) use a membrane such that the product  $E \cdot K$ , which will be called the  $EK$ -coefficient, will be small, and (3) decrease the vapor pressure difference across the membrane. Items (1) and (2) are discussed in paragraphs (c) and (d) below and item (3) is discussed in 9-06.

#### (2) Equation for the Case of Air Leakage

It is shown in Appendix B-07 that the volume of air that diffuses between a partially saturated specimen and the liquid in the chamber is given approximately by the equation

$$\frac{J_a}{V} = \text{constant} \times \frac{K_s}{\sqrt{D}} \frac{\Delta p_p}{D_s} \sqrt{t} \quad (B-11)$$

where  $J_a$  = volume of air leakage measured at atmospheric pressure.

$D$  = coefficient of diffusion of air in chamber liquid.

$K_s$  = permeability constant of air in chamber liquid.

$\Delta p_p$  = initial partial pressure difference in air across membrane.

$D_s$  = diameter of specimen

It should be noted that the permeability of the membrane to air does not enter the above equation. It is shown in B-07 that the quantity  $K_s \sqrt{D}$  for natural rubber is practically equal to that for water. Therefore, with respect to the rate of flow of air to or from a specimen, it makes no difference whether the rubber membrane is in place, or whether an equal thickness of water is substituted for it. Eq. B-11 is based on the assumption that

a concentration gradient of air develops in the chamber liquid as air diffuses into or out of a specimen. If convection currents cause complete mixing of the chamber liquid, or if the chamber fluid is a gas, Eq. B-11 gives too low an estimate of the air flow, and the following equation must be used instead:

$$J_a = q_s \cdot t = K_s A_s \frac{\Delta p_p}{L} t \quad (9-7)$$

where  $q_s$  = rate of air flow, measured at standard atmospheric pressure.

$K_s$  = permeability constant of membrane to air.

$A_s$  = surface area of specimen.

$\Delta p_p$  = partial pressure difference of air across membrane.

Since it is unlikely that complete mixing will occur in the chamber when a liquid is used, the actual volume of air flow probably lies between the volumes given by Eqs. B-11 and 9-7. Therefore a liquid chamber fluid should be used for reducing air leakage. For subsequent discussions, it will be assumed that a liquid is used.

Eq. B-11 shows that the ratio of air leakage to specimen volume,  $J_a/V$ , can be reduced by (1) increasing the size of the specimen, (2) decreasing the ratio  $K_s/\sqrt{D}$  (this means that both the solubility and the coefficient of diffusion of air in the chamber liquid should be reduced), and (3) reducing the partial pressure difference of air across the membrane. From Eq. 2-22 it is evident that the percent change in effective stress due to air leakage is practically linearly related to  $J_a/V$  when  $u_a \Delta \bar{\sigma}_3$ . Items (1) and (2) are discussed in paragraph (c) and (d) below, and Item (3) is discussed in 9-06.

#### (c) Effect of Increasing Specimen Size on Errors Caused by Leakage

Water Leakage - Eq. 9-6 shows that if the specimen size is doubled and if the membrane thickness is also doubled so that the membrane restraint remains constant, then, in any given time interval  $t$ , the percent decrease in effective stress due to water leakage into the larger specimen will be one-fourth that due to water leakage into the smaller specimen. For tests of long duration on soils with a very low swelling ratio, it is helpful to test large specimens to reduce effects of water leakage.

Air Leakage - Eq. B-11 shows that the volume of air leakage is inversely proportional to the diameter of the specimen, and hence the percent change in effective stress will be cut in half when the diameter of the specimen is doubled. Thus increasing the size of a specimen is advantageous for reducing the effects of air leakage, but the advantage is smaller than for the case of water leakage. In this case it is not necessary to increase the membrane thickness if the specimen size is increased, because the thickness of the membrane has little effect on the rate of air flow when a liquid is used as the chamber fluid.

#### (d) Discussion of Factors Affecting the EK-Coefficient

One can alter the EK-coefficient by changing the permeability and/or the modulus of elasticity of a given membrane (by treating the membrane) or by changing the membrane material itself. Various procedures that have been suggested for reducing the permeability and the modulus of elasticity of membranes are discussed in the following paragraphs. A detailed discussion of an effort to find a membrane with a low EK-coefficient is given in 9-05.

##### (1) Methods for Reducing Membrane Permeability

The permeability of a membrane to the chamber fluid can be reduced by soaking the membrane in an appropriate liquid, by coating the membrane with an impervious film, or by using a chamber fluid to which the membrane is relatively impervious.

The data in Chapters 4, 5 and 6 show that soaking a natural rubber membrane in silicone oil causes no observable change in permeability to water. Soaking in vacuum pump oil (a mineral oil) may reduce the permeability of natural rubber to water by as much as 50%. However, this 50% reduction is not significant for the present purposes since natural rubber membranes are ten to one hundred times too permeable for use long-time triaxial tests. (see 9-02(a) ). For this reason and for the reason presented in Appendix A-13, the author believes that soaking a membrane as impervious as natural rubber in a liquid is not likely to result in a significant decrease in permeability.

Spray coatings of plastic, coatings of silicone grease, mixtures of silicone oil or stopcock grease with colloidal clay, and several other combinations have been used in efforts to reduce the rate of flow of water through membranes used in triaxial testing, while at the same time avoiding excessive membrane restraint. There are two reasons for using such coatings: (1) If the coating material is much less pervious than the base membrane, and has a much higher modulus of elasticity, then the base membrane simply acts as a support for the very thin membrane formed by the coating. The possibility of finding suitable materials of this type is discussed in 9-05. (2) If the coating material is a grease, then a very thick coating may be used and the base membrane simply prevents flow of the coating material into the specimen. The coating then acts as the chamber fluid. Coatings that are intermediate between items (1) and (2) generally offer no advantage since the same effect could be obtained simply by using additional membranes. One exception is the possibility of using a relatively thick (say one or two mm) and relatively stiff coating of wax, which was used by Casagrande and Shannon (33) for testing Cucaracha Rock. Such a wax sheath probably would be useful in long-time tests even on soft soils, because the wax would creep slowly under the axial load and would not restrain the specimen excessively. This would merit further investigation, especially for use in long-time tests on partially saturated specimens.

The chamber liquid may be changed to reduce the rate of flow of liquid into the triaxial specimen. This has the same effect as reducing the permeability of the membrane, which in turn decreases the EK-coefficient. The requirements that should be fulfilled by the chamber liquid, in approximate order of importance, are as follows:

- (1) The chamber fluid should be in the liquid state at all temperatures of interest. (Preferably the viscosity should be about equal to that of water, although more viscous oils and greases are probably satisfactory.)
- (2) Not harmful to materials used in triaxial cell (metals, plastics and rubbers) or to the hands.
- (3) Low permeability to the chamber liquid of the membrane used to confine the specimen.
- (4) Solubility of water in the fluid should be extremely low.
- (5) Solubility and coefficient of diffusion of air in the fluid should be extremely low.
- (6) Non-poisonous.
- (7) No offensive odor.
- (8) Low specific gravity. (So that pressure variations over height of specimen will be small.)
- (9) Transparent or translucent.
- (10) Not too expensive.

Of these requirements, the first four are the most important when testing 100% saturated soils and number five becomes important when testing partially saturated soils. While the author has made no attempt to select a chamber liquid other than water for use in triaxial testing, he offers the following qualitative comments concerning the suitability of various liquids.

Castor oil, glycerin, silicone oil, mercury, and transformer oil have been suggested. Glycerin can be excluded immediately since it is infinitely soluble in water. Thus, its use in the chamber will permit osmosis of water from the specimen into the chamber, as pointed out by Casagrande (21). The remaining suggested liquids satisfy requirements one and two in the above list, so long as no brass is used when mercury is the chamber fluid and so long as a membrane of an appropriate synthetic rubber is used when oil is the chamber liquid. There are no data presently available to the author on the permeability of rubbers and plastics to these oils and mercury. However, all these liquids have very low vapor pressures and large molecules relative to water. Therefore it is probable that natural or synthetic rubbers are much less pervious, i.e. by more than one order of magnitude, to the oils and mercury than to water. Thus, these liquids may satisfy the third requirement. It is also likely that the fourth requirement is satisfied by silicone oil, castor oil, transformer oil and mercury, because the solubility of water in these liquids is only about 0.005% by weight at atmospheric pressure (91). To essentially prevent osmosis of water from the specimen when using any one of these liquids, it would only be necessary to saturate the chamber fluid with water prior to the start of a test.

The solubility of air in the oils is from four to ten times greater than the solubility of air in water (91), so that the oils offer no advantage for testing partially saturated specimens. No data are known to the author on the solubility and diffusion coefficients of air in mercury. However, judging from the fact that mercury is used in barometers, where a partial pressure difference of one atmosphere is sustained for years through an 80 cm long column of mercury, it would seem likely that, for the purposes of triaxial testing, the permeability of mercury to air is zero. (If mercury were as pervious to air as water, the barometer level would drop at a rate of about 2 mm/day due to air diffusion!) Thus, of the suggested chamber liquids, mercury is probably the only one that fulfills the important requirements for testing partially saturated soils. Mercury has the minor disadvantages that it is poisonous when inhaled, relatively difficult to handle, opaque, expensive and very heavy. The latter is an important disadvantage when testing very soft soils.

The three oils that have been suggested - castor oil, silicone oil and transformer oil - may serve as excellent chamber fluids for testing 100% saturated specimens, but not for testing partially saturated specimens. At present it appears that mercury offers the best possibility of being suitable for testing partially saturated soils over long periods of time. However, it has been previously noted that a very thick wax sheath could be used as a membrane for long-time tests. It is possible that such a wax sheath could reduce the rate of air flow sufficiently so that practically any chamber liquid could be used. A program of research aimed at determining the suitability of various chamber fluids and/or a wax sheath is proposed in Chapter 11.

## (2) Methods for Reducing the Modulus of Elasticity

The modulus of elasticity of plastic membranes can be decreased by adding "plasticizers" to the mix prior to manufacturing the membranes. In Table 9-5 the EK-coefficients for plasticized (a) and unplasticized (c) polyethylene are given. The use of a plasticizing agent decreased the modulus, but increased the permeability more, resulting in a greater EK-coefficient. It should not be inferred that plasticization will always be undesirable.

The use of unvulcanized rubber has been suggested, since presumably the modulus would be smaller than that for vulcanized rubber. However, at the small strains to which membranes are subjected in triaxial testing, the moduli of both vulcanized and unvulcanized rubber are about equal (17). Furthermore, the permeability of unvulcanized rubber has been found to be somewhat higher than that of vulcanized rubber (89). Therefore, it is likely that the EK-coefficient of unvulcanized rubber will be greater instead of smaller than that for vulcanized rubber.

9-05 SELECTION OF MEMBRANE WITH LOW EK-COEFFICIENT(a) Purpose

An attempt was made to find a membrane with an EK-coefficient which is lower than that for natural rubber by about two orders of magnitude. The procedure and results of permeability measurements have been presented in Chapter 6. The procedure and results of tests to measure the moduli of elasticity are presented in paragraph (b) below. In paragraph (c) a discussion of the results is given and the most suitable membrane is selected.

(b) Measurement of the Moduli of Elasticity of Membranes

The following simple test was used to measure the modulus of elasticity of rubber and plastic membranes:

- (1) A one cm wide by seven cm long strip was cut from the membrane.
- (2) The thickness of the membrane was measured with a micrometer with an accuracy of  $\pm 0.0003$  cm.
- (3) A clamp was added on each end of the membrane leaving exactly five cm of membrane showing between the clamps.
- (4) The membrane was hung from a support frame in a vertical position by fastening one of the clamps to the frame.
- (5) A hanger was suspended from the lower clamp.
- (6) Load was added to the hanger in increments, one minute apart, so that the specimen reached 20% strain one minute after the fourth increment had been applied.
- (7) The modulus of elasticity E was calculated from the formula

$$E = 5 \times \frac{\text{Load at 20\% strain}}{\text{Thickness}}$$

All tests were performed at a room temperature of 24°C and a relative humidity of 65%.

The modulus measured in this manner is felt to be accurate to within  $\pm 10\%$  under the conditions imposed during the test. However, the moduli of the membranes tested depend on the strain, rate of strain, temperature, relative humidity, etc. None of these factors were investigated; they were merely held as constant as possible for all tests. Thus the measured modulus should only be considered as an index of the actual modulus and is to be used only for relative comparisons among the membranes.

The measured moduli are recorded in Table 9-5. Two types of polyethylene were tested. The (a) material is low density polyethylene which had been "plasticized" so that it feels rubbery. The (c) material, which is the type commonly used for household wrapping, bags, etc., had not been plasticized and did not feel rubbery. Thus it appears that a modulus of elasticity in the vicinity of 200 kg/cm<sup>2</sup> is the borderline between a material that feels rubbery and one that does not. Note that natural rubber has the lowest modulus.

(c) Discussion of Measured EK-Coefficients

The EK-coefficients of the membranes tested are shown in Table 9-5. Of these membranes, only Kel-F and butyl rubber have a sufficiently low coefficient to offer a significant improvement over natural rubber.

It is evident that a membrane having a high modulus of elasticity (e.g. Kel-F) must be very thin so that it will not impose excessive restraint on a specimen. However, very thin membranes are difficult to handle in the laboratory. The author believes that the thickness of a membrane to be used in triaxial testing should be no less than about 0.001 cm (0.0004 in.). Using Eq. 9-4, and the thickness of 0.001 cm, one can compute the maximum value of the modulus of elasticity that is permissible if the restraint is to be

no larger than that imposed by two natural rubber membranes with a total thickness of 0.012 cm. The largest permissible modulus of elasticity is about 150 kg/cm<sup>2</sup>. It was noted previously that a modulus of about 200 kg/cm<sup>2</sup> marks the approximate borderline between a material that feels rubbery and one that is not rubbery. Thus, membranes that do not feel rubbery probably are not suitable for use on 1.4 in. diameter triaxial specimens, because they would be either too frail or they would impose too much restraint on the specimens.

The above reasoning excludes the use of Kel-F as a membrane material for triaxial testing. Therefore, of the membranes tested, only butyl rubber, which has an EK-coefficient one tenth as large as that of natural rubber, remains as a suitable membrane, i.e., one which has a low EK-coefficient and which does not have to be too frail for easy handling. It is still possible, of course, to apply Kel-F in a very thin coat over a membrane such as natural rubber. However, such a procedure would offer no advantage over the use of butyl rubber. On the other hand, if a material (as yet undiscovered) were found that has a still lower EK-coefficient than butyl rubber, but has too high a modulus, then it may be advantageous to use such a material as a thin coating over natural rubber. Probably it would be very difficult to eliminate all defects in such thin coatings. In any case permeability tests would be needed to check their efficiency. (It should be recalled that membranes with EK-coefficients larger than that of natural rubber cannot even be used as coatings, because in order to be effective, they would have to be so thick that they would impose excessive restraint.)

Some research has been performed to correlate the chemical properties and molecular structure of membrane materials to their permeability (103). However, at present it is still not possible to predict from such data the permeability of a membrane. One reason is that the manufacturing process itself affects the permeability (and modulus). Further attempts to find a membrane with a lower EK-coefficient than butyl rubber, should probably be focused on synthesizing the desired membrane.

#### (d) Discussion of the Advantages of Using Butyl Rubber Membranes

The volume of leakage expected if butyl membranes are used for a triaxial test is shown in Row (2) of Table 9-2, for several pertinent conditions. The total rate of leakage that may be expected during a test with a butyl membrane is shown in Row 8 of Table 9-2. Row (8) contains the sum of the leakage through one 0.006 cm thick butyl rubber membrane and the binding leakage. It is assumed that leaky fittings and tubing would be omitted from the apparatus for long-time tests, so their contributions need not be considered. A comparison of the rates of leakage in Row (8) with the maximum acceptable leakage in Table 9-1, shows that a 100-day test could be performed on a sample of Boston Blue clay under a confining pressure of 10 kg/cm<sup>2</sup> without excessive errors due to leakage, so long as the specimen contains no salt in the pore water. For tests on Canyon Dam clay, the maximum test duration is about 5 days, even when butyl rubber membranes are used. Thus, the use of butyl rubber membranes in triaxial testing decreases the effects of leakage considerably, but additional changes in apparatus and procedure are needed to perform 100-day tests on 100% saturated specimens of soils with a very low swelling ratio.

A comparison of Rows (2) and (3) in Table 9-2 shows that the leakage through a 0.006 cm thick butyl rubber membrane is likely to be less than the binding leakage. However, it should be recalled that the binding leakage was measured with a natural rubber membrane on the pedestal. If a butyl membrane had been used, the binding leakage probably would have been smaller (see 7-05(b)), and this would make the use of butyl membranes somewhat more advantageous than indicated above.

It should be emphasized that to date, butyl rubber membranes with a thickness of 0.006 cm have not been manufactured in cylindrical form for use in triaxial testing. The thinnest butyl membrane tested during this investigation was 0.020 cm thick and was made by pressing butyl latex between two plates. Preliminary attempts were made by the author to manufacture cylindrical butyl membranes in the laboratory by dipping a glass mandrel coated with silicone grease in a butyl rubber cement supplied by the Carlisle Fire and Rubber Company. These attempts indicate that a uniform butyl rubber membrane can be made

with a thickness of only 0.004 cm. Two manufacturers are presently experimenting with procedures for making suitable butyl membranes. The author believes that there will be no unusual difficulties encountered in their manufacture. However, when they do become available, their permeability should be measured using X tests (Chapter 5) and V tests (Chapter 6), to verify that the new membranes have as low a permeability as those tested during the present investigation.

#### 9-06 DISCUSSION OF PROCEDURES FOR REDUCING VAPOR AND PARTIAL PRESSURE DIFFERENCES ACROSS MEMBRANES

##### (a) Procedure for Reducing Vapor Pressure Difference of Water

It was noted in 9-04 (b) that the vapor pressure difference across a membrane used in a triaxial test is a function of the hydraulic pressure difference and the mole fraction difference at a given temperature. The hydraulic pressure difference cannot be eliminated since it is equal to the effective stress on the specimen. However, one can counterbalance the higher vapor pressure of water in the chamber by adding solute (ions or molecules) to the chamber water. Assuming, for example, that the hydraulic pressure difference across a membrane is  $10 \text{ kg/cm}^2$ , and that there is no salt in the pore water, one finds from Eq. 3-28 that the resulting vapor pressure difference is  $0.307 \text{ gm/cm}^2$  at  $30^\circ\text{C}$ . If sufficient sodium chloride or sucrose is added to the chamber water, such that the vapor pressure of the water in solution is lowered  $0.307 \text{ gm/cm}^2$  below that of pure water, the vapor pressure difference across the membrane will be zero and no flow of water will occur. Vapor pressure data in the International Critical Tables (98) show that a vapor pressure lowering of  $0.307 \text{ gm/cm}^2$  may be achieved at  $30^\circ\text{C}$  by using either (1) sodium chloride at a mole fraction of 0.00406 (0.236 moles/liter) or (2) sucrose at a mole fraction of 0.00675 (0.380 moles/liter). If the pore water contains salt, the concentration of the chamber fluid would have to be increased correspondingly to achieve the condition of zero vapor pressure difference.

In practice, the effective minor principal stress on a normally consolidated specimen usually decreases from a high to a low value in the course of a triaxial Q or R test. Therefore the concentration of solute in the pore water should be chosen to balance the vapor pressure difference caused by the "time average" effective minor principal stress on the specimen during the test, where the time average is the area beneath the plot of effective stress versus time, divided by the duration of test. The effect of such a procedure is illustrated in Fig. 9-1. Suppose that axial load is applied very slowly to an R specimen so that the effective minor principal stress decreases linearly with time from  $12 \text{ kg/cm}^2$  at the start of loading to  $2 \text{ kg/cm}^2$  at failure. If no solute is added to the chamber water, the vapor pressure difference causing water leakage is given by the dashed line in Fig. 9-1 (a). The resulting volume of water leakage and decrease in effective stress are shown by the dashed curves in Figs. 9-1 (b) and (c). If solute is added to the chamber water, the vapor pressure difference causing water leakage is given by the solid line in Fig. 9-1 (a). During the first half of the test, water flows into the specimen, and during the second half, water flows out of the specimen, as shown by the solid curve in (b). Thus, as shown by the solid curve in (c), the decrease in effective stress reaches its maximum absolute value, point B, half way through the test and approaches zero at failure, point C. The maximum decrease in effective stress that occurs when solute is added to the chamber water, point B, is less than one-fourth the decrease that would occur if solute were not used (point C). Furthermore, this maximum occurs early in the test, rather than at failure, and the error is a minimum when the strength of the specimen is measured.

The charts in Figs. 9-2 and 9-3 have been prepared on the basis of data on vapor pressure lowering given in the International Critical Tables. These charts may be employed to select the concentration of sodium chloride or sucrose to be used in the chamber water to balance the effect of a hydraulic pressure difference or of salt in the pore water. In preparing the charts it was assumed that the solute in the pore water is sodium chloride. If the vapor pressure lowering is different for the solute actually present from that of sodium chloride at equal mole fraction, then the mole fraction

determined from the charts must be altered accordingly. For example, assume that the solute in the pore water were sucrose with a mole fraction of 0.002. From Fig. 9-3, on the ordinate at zero pressure, it is seen that a mole fraction of 0.0012 of sodium chloride is equivalent to sucrose with a mole fraction 0.002, i.e. if a semi-permeable membrane separates a solution of sucrose ( $X = 0.002$ ) from a solution of sodium chloride ( $X = 0.0012$ ), there would be no flow of water. Thus, if sodium chloride is used in the chamber fluid, its mole fraction must be 0.0012 plus whatever mole fraction is needed to balance the hydraulic pressure difference.

Successful use of the charts in Figs. 9-2 and 9-3 is contingent on the careful application of the procedures recommended in Chapter 10.

(b) Procedure for Reducing Partial Pressure Difference of Air

The partial pressure difference of air across a membrane can be eliminated by saturating the chamber liquid with air at a pressure equal to the pore air pressure. Since the pore air pressure varies during a test, the pressure at which the chamber liquid should be saturated is the "time average" pore air pressure, as for the case of water leakage. This procedure introduces some error because air can flow whenever the pore air pressure and the partial pressure in the chamber liquid are not equal, but the net air flow should be zero if the time average pore air pressure is properly chosen. The largest error develops at the time when the partial pressures are balanced (i.e. pore air pressure equal to pressure at which chamber liquid is saturated), because at this point the maximum volume of inflow has occurred.

The maximum permissible duration of the axial loading phase of a Q or R test on a 1.4 in. diameter by 3.5 in. high specimen will now be estimated, assuming the above procedure is used. The greatest possibility for error arises when a large change in pore air pressure occurs during the test. In such a case there will be large gradients causing air to flow when the pore air pressure is well below or well above the pressure at which the chamber water is saturated with air. The greatest changes in pore air pressure during axial loading occur when the initial effective stress on the specimen is high ( $10 \text{ kg/cm}^2$ ), the initial degree of saturation is about 95% and the initial pore air pressure is low ( $1 \text{ kg/cm}^2$ ). Even under these critical conditions, the change in pore air pressure will seldom be greater than about  $4 \text{ kg/cm}^2$  in tests performed with an initial effective stress of  $10 \text{ kg/cm}^2$  or less. Assume, for this critical case, that the pore air pressure increases linearly with time, so that the time average pore air pressure is  $2.0 \text{ kg/cm}^2$ . If the chamber liquid is saturated at  $2.0 \text{ kg/cm}^2$ , the maximum partial pressure difference will be  $2.0 \text{ kg/cm}^2$  at the start of the test, and it will decrease to zero half way through the test. During the first half of the test the average partial pressure difference would be  $1.0 \text{ kg/cm}^2$ . Therefore, according to calculations shown in Appendix B, about  $1.0 \text{ cm}^3$  of air would enter the specimen in three hours. The maximum acceptable leakage for 2% decrease in effective stress may be interpolated from Table 9-3, where, for  $S = 0.001$ ,  $G_w = 95\%$  and  $\bar{\sigma}_3 = 8.0 \text{ kg/cm}^2$ , it is found to be about  $0.8 \text{ cm}^3$ . But  $0.8 \text{ cm}^3$  of air would enter the specimen in about 2 hours, so that for a decrease in effective stress of 2%, the first half of the test should have a maximum duration of about 2 hours. Therefore the duration of axial loading when testing a partially saturated soil using water as the chamber liquid, can be 4 hours, even for a very critical case of air leakage, without developing excessive error. The calculations on which this estimate is based are rough at best but it is estimated that for the above example, the maximum permissible duration of the test is actually between 2 and 8 hours. An examination of the least critical case of any importance (i.e. soil with high swelling ratio,  $S = 0.03$ , tested at high initial degree of saturation,  $G_w = 98\%$ , and high initial effective stress,  $\bar{\sigma}_3 = 10 \text{ kg/cm}^2$ ), indicates that the maximum permissible test duration may be more than 100 days without developing more than 2% decrease in effective stress.

CHAPTER 10

RECOMMENDATIONS FOR CONTROL OF LEAKAGE

10-01 RECOMMENDATIONS FOR CONTROL OF WATER LEAKAGE

(a) General

Specific procedures for control of water leakage into 100% saturated specimens are given in the following paragraphs. The procedures described are also adequate for controlling the effects of water leakage into partially saturated specimens. However, the effects of air leakage into or out of partially saturated specimens are far more critical than the effects of water leakage (see 9-03). Therefore, the investigator testing partially saturated soils should concentrate on reducing air leakage. Some tentative recommendations for reducing air leakage are presented in 10-02.

From Eq. 9-6 it is seen that there are three possible ways to reduce the change in effective stress caused in a given time by water leakage through the membrane(s): (1) reduce the vapor pressure difference in the water across the membrane, (2) reduce the EK-coefficient of the membrane, and (3) increase the size of the specimen. Regardless of the type of membrane used or the size of the specimen, there will be no water leakage if the vapor pressure difference of the water is zero. Therefore, the first step is to use enough salt or other solute in the chamber fluid to balance the vapor pressure difference caused by the hydraulic pressure difference across the membrane. The second step is to use butyl rubber membranes if possible, rather than natural rubber, because the butyl rubber has the lowest EK-coefficient of the membranes tested during this investigation. The third step is to increase the size of the specimen as far as practicable, keeping in mind other factors that control the maximum size.

In addition to reducing leakage through the membrane(s), the leakage of bindings, valves and fittings should be held to a minimum by using the procedures outlined below.

(b) Recommended Procedure for 12-Hour Q and R Tests on 100% Saturated Specimens

The total leakage\* through membranes, valves, fittings, tubing and bindings will not cause an error in effective stress in excess of 2%, if the following conditions are met

- (1) Swelling ratio:  $S \geq 0.001$
- (2) Pore salt concentration: zero
- (3) Specimen size: Equal to or greater than 1.4 in. diameter by 3.5 in. high.
- (4) Membranes: Two natural rubber, each 0.006 cm thick.
- (5) Bindings: O-Rings on polished and greased cap and base.
- (6) Effective minor principal stress:  $\bar{\sigma}_3 \leq 10 \text{ kg/cm}^2$ .

(c) Recommended Procedure for 100-day Q and R Tests on 100% Saturated Specimens

For tests performed with  $\bar{\sigma}_3 \leq 10 \text{ kg/cm}^2$  on soils with  $S \geq 0.001$ , adherence to the procedures described below will not cause a decrease in effective stress larger than 2% and will usually result in a much smaller decrease.

Preliminary Tests - (1) Perform swelling tests of the type described in Chapter 2 (for details see Appendix D) to determine accurately the initial swelling ratio of the soil to be tested. The value of the swelling ratio should be measured under stress conditions identical to those applied during the triaxial tests.

(2) Perform pilot triaxial tests of the type to be used in the main investigation, to determine approximately the time average of the effective minor principal stress which will develop during the axial loading phase of a Q or R test. The "time average" is

---

\* It is assumed that there are no gross leaks, such as punctures in the membrane or poorly made packings or bindings.

equal to the area beneath the curve of effective stress versus time, divided by the duration of axial loading.

(3) Measure to within  $\pm 0.0001$  the mole fraction of sodium chloride in the pore water of the soil tested. (If the pore water contains salts and/or molecules other than sodium chloride, the concentration of sodium chloride required to produce equal vapor pressure lowering should be determined by direct measurement or from data on vapor pressure lowering in the International Critical Tables.) Only the ions in excess of those ions needed to balance the "surface charges" of the clay mineral particles should be considered in determining the mole fraction of salts in the pore water.

Temperature Control - Perform all tests in a temperature controlled room such that the specimen temperature will be constant to within  $\pm 1/4^{\circ}\text{C}$ . This restriction is satisfactory for soils with  $S \geq 0.001$ . A greater tolerance is permissible for soils with a higher swelling ratio. For example, a tolerance of  $\pm 2^{\circ}\text{C}$  might be permissible for normally consolidated Boston Blue clay, from the standpoint of changes in effective stress caused by the temperature fluctuations.

Chamber Water - Based on the mole fraction of sodium chloride in the pore water and the time average of the effective minor principal stress, use Fig. 9-2 or 9-3 to determine the mole fraction of sodium chloride or sucrose to be used in the chamber fluid.

The mole fraction of salt required in the chamber water is not affected by the type of membrane used.

Membranes - Butyl rubber membranes should be used rather than natural rubber membranes. Since butyl rubber has a low EK-coefficient, the effect of any error in the choice of the time average of the effective minor principal stress or of the pore water ion concentration, will be minimized. Two membranes should be used in all cases as a safety precaution in the event that one membrane is punctured.

As noted in 9-05(d), butyl membranes have not been fabricated in cylindrical form with wall thickness as low as 0.003 in., as would be desirable for triaxial testing. After development of such butyl membranes, they should be used consistently in all triaxial tests since the possible errors due to leakage are reduced by a factor of ten below the errors that develop when natural rubber membranes are used.

Cap, Base and Bindings - Use stainless steel or other non-reactive metal for the cap and base. The exterior surfaces of the cap and base must be polished carefully and then handled carefully to prevent scratching the polished surfaces. The surfaces should be greased (silicone stopcock grease is used at Harvard) so that any microscopic striations will be filled. After the membranes are placed, two rubber O-rings should be placed on both the cap and base very close to the specimen so that there will be a minimum area of the membrane exposed between the top and bottom bindings. Care should be taken to prevent spiralling around the cap or base of the molded projection on the O-Ring.

Plastics such as Lucite or Delrin may also be used for caps and bases so long as they are first submerged in water for a sufficiently long period, as determined by water absorption tests, to reduce the rate of absorption to a tolerable magnitude. (One 1.4 in. diameter Lucite base of the type used at Harvard University will absorb water at a rate of 0.1 mm<sup>3</sup>/day through the face in contact with the specimen, even after being soaked in water for a period of 80 days under atmospheric pressure at room temperature. This means that for 100-day tests on 100% saturated specimens of soils with very low swelling ratios, Lucite caps and bases should be soaked for more than 80 days. Probably the volume of water absorbed would increase slightly under pressure, in which case a still longer period of soaking would be required.)

Valves and Fittings - The number of valves and fittings in the drainage system must be reduced to an absolute minimum when long-time Q and R tests are to be performed.

Klinger valves were found to leak excessively when used as manufactured, i.e. with asbestos packing sleeves. They should not be used in the drainage system of a triaxial cell. Whitey valves of the stem type, with Teflon bonnet packings, and Hydromatics valves which have O-Ring packings, were found best suited for use in the drainage system.

Soldered or epoxy-sealed joints are recommended for all permanent seals. O-Ring fittings of the type used for the membrane permeability cell (see Chapter 8) are preferred for joints that must be disconnected. No program of research was carried out to compare in detail the available commercial fittings.

Weighings and Volume Change Measurements - All weighings of the specimen before and after test and all volume change measurements should be made with an accuracy of  $\pm 0.001\%$ . The overall leakage into or out of a specimen during a test should always be checked by comparing the weight of the specimen before test with the weight after test, taking proper account of the flow of water into or out of the specimen through the drainage burette.

(d) Miscellaneous Comments on the Control of Water Leakage

If tests with a duration greater than 100 days are to be performed, or if tests are performed under conditions more stringent than those prescribed in (c), then the following additional steps can be taken to control water leakage. (1) The size of the specimens tested may be increased. The error in effective stress that occurs in a given time is inversely proportional to the square of the specimen diameter, so long as the thickness of the membrane is increased in direct proportion to the specimen diameter. This increase in membrane thickness will not change the membrane restraint. (2) A thicker membrane may be used, so long as the additional membrane restraint is considered tolerable.

10-02 RECOMMENDED PROCEDURES FOR CONTROL OF AIR LEAKAGE

(a) Control of Air Leakage into 100% Saturated Specimens

When air is used to apply pressure to the chamber water, the diffusion of air from the pressure source into the specimen may be stopped, for practical purposes, by inserting a one meter length of water-filled 1/16 in. inside diameter tubing between the pressure source and the chamber water. Use of this procedure will permit air to enter the chamber water at a rate of only 0.06 mm<sup>3</sup>/day, which would have practically no effect on the effective stress in a specimen, even if it were to enter directly into the specimen.

Another procedure for eliminating the problem of air flow into 100% saturated specimens, is to apply the chamber pressure hydraulically, e.g. as recommended by Bishop and Henkel (12).

(b) Control of Air Leakage into or out of Partially Saturated Specimens

The recommendations made below are tentative, since no data on rates of air flow were obtained by the author. The recommendations stem from calculations based on air flow data presented elsewhere in the literature. The calculations are presented in Appendix B.

Use of Water as Chamber Fluid - When water is used as the chamber fluid, air can flow relatively quickly across the confining membrane, to or from the specimen, depending on the partial pressure of air on each side. To reduce the partial pressure difference as much as possible one should:

- (1) Perform pilot tests to determine the time average of the pore air pressure that will develop during the tests for the main investigation.
- (2) Saturate the chamber water with air at the time-average pore air pressure. For Q tests, the air may be mixed with the water before filling the chamber. For R tests, the air may be injected through fittings in the bottom of the triaxial chamber after the consolidation phase of the test is complete.
- (3) Insert a one or two meter length of 1/16 in. inside diameter tubing, filled with chamber water, between the air pressure source and the chamber. This prevents diffusion of air from the pressure source into the chamber water during the test.

It is estimated that use of the above procedure with water as the chamber fluid will permit performance of Q and R tests on 1.4 in. diameter by 3.5 in. high, partially

saturated specimens, without exceeding a 2% change in effective stress, if the maximum test durations are as follows:

For the most critical case ( $S = 0.001$ ,  $G_w = 95\%$ ,  $\bar{\sigma}_3 = 8 \text{ kg/cm}^2$ ) 2 to 8 hours

For the least critical case ( $S = 0.03$ ,  $G_w = 90\%$ ,  $\bar{\sigma}_3 = 20 \text{ kg/cm}^2$ ) > 100 days.

Use of Mercury as Chamber Fluid - It appears that air passes through mercury at least three orders of magnitude more slowly than through water (see 9-04(d)). If this is the case, then mercury might be usable for tests lasting 100 days or longer on practically any soil. Unfortunately, the author has had no experience with the use of mercury and there are no quantitative data available on the diffusion and solubility coefficients of nitrogen and oxygen in mercury, so that one cannot carry out computations to determine its suitability. Mercury has the disadvantages of being poisonous when inhaled, of being heavy, expensive, opaque and relatively difficult to handle. A program of research should be carried out to determine the suitability of mercury and other possible chamber fluids for testing partially saturated specimens.

Temperature Control - The specimen temperature should be maintained constant to within plus or minus  $1^\circ\text{C}$ . Temperature control is not as critical when testing partially saturated specimens as when testing 100% saturated specimens because probably the change in water volume is small relative to the maximum acceptable volume of water leakage. A  $1^\circ\text{C}$  temperature change probably will cause no more than 0.5% change in effective stress in a partially saturated specimen of a soil with a swelling ratio  $S = 0.001$ , even though the degree of saturation is as high as 99%.

Size of Specimen - The effect of air leakage on partially saturated specimens is approximately inversely proportional to the size of the specimen tested. Thus as large a specimen as practicable should be tested.

Thickness of Membrane - It is practically of no value to increase the thickness of natural rubber membranes when attempting to reduce the effects of air leakage because the membranes offer little more resistance to air flow than an equal thickness of chamber water. The use of membranes with low permeability (such as butyl rubber) probably are of little value for reducing air flow because they must be so thin (for low membrane resistance) that a very thin layer of chamber liquid would impede air flow just as much.

CHAPTER 11SUGGESTIONS FOR FURTHER RESEARCH11-01 SWELLING TESTS

Practically no reliable information is available on the initial swelling ratio of clay soils. Therefore, swelling tests of the type described in Appendix D should be performed on 100% saturated and partially saturated soils to measure accurately the swelling ratio for:

- (1) Both undisturbed and remolded recompacted specimens.
- (2) Clays of low, medium, and high sensitivity to disturbance.
- (3) Clays with low, medium, and high swelling ratios.

The effects on the swelling ratio of (1) the magnitude of the effective principal stress ratio during swelling, (2) the rate of decrease of the effective stress, and (3) the duration of the consolidation phase, should be investigated.

The swelling tests on partially saturated specimens would require the measurement of volume changes of the specimen by means of external strain gages, photographic methods or measurements of the chamber fluid volume. The measurement of chamber fluid volume is probably the only technique that is adaptable for measuring volume changes smaller than  $0.010 \text{ cm}^3$ . Specially designed swelling apparatus will be required to obtain the required dependability and accuracy of measurement. Until further information is available on the suitability of various chamber liquids for preventing air leakage, it is suggested that mercury be used in the chamber for these swelling tests. Furthermore, the drainage line through which the pore pressure is measured should contain a mercury seal to prevent loss of air during the test. Alternatively, an electrical pressure transducer could be used to measure the pore pressure. Porous discs that have sufficiently small openings to prevent exchange of air and water between the specimen and the porous disc should be used at the base of the swelling specimens. At the top of the specimen, one should use either a fine porous disc or no porous disc. In all such swelling tests on partially saturated specimens the swelling increments must be applied slowly, so that equilibrium between the pore air and pore water is achieved at all stages of the tests. (This points out one of the errors involved in testing of partially saturated specimens. In the laboratory, equilibrium between the pore air and water does not always exist because the tests are performed too rapidly. In the field, equilibrium probably does exist. The extent of the error is not known.)

11-02 SEARCH FOR CHAMBER LIQUIDS MORE SUITABLE THAN WATER

For testing 100% saturated specimens the two most important requirements of the chamber liquid are (1) low solubility of water in the liquid and (2) low permeability of the membrane used to the liquid. Two additional important requirements for testing partially saturated specimens are (1) low solubility of air and (2) low coefficient of diffusion of air in the proposed chamber liquid.

Silicone oil, castor oil and transformer oil may be more suitable than water for testing 100% saturated specimens. Mercury may be suitable for testing partially saturated specimens. Lists of commercially available oils and other compounds are given in the Handbook of Chemistry and Physics (106). Such lists should be studied by a chemist familiar with the properties of the liquids, together with the requirements for a satisfactory chamber liquid, to determine which of the liquids might have important advantages over water and mercury for triaxial testing. The properties of these liquids should then be measured to determine their suitability as chamber liquids.

### 11-03 EFFECTS OF LEAKAGE ON PARTIALLY SATURATED SPECIMENS

A theoretical and experimental investigation should be made to determine the form of the undissolved air in the pores of partially saturated specimens of various soils and the changes in curvature of the air-water interfaces that occur due to water and/or air leakage. One possible means for obtaining data on such changes is to measure the changes in pore air pressure, e.g. as suggested by Bishop and Henkel (12), that occur when water is forced into a partially saturated specimen. Also, air could be forced into a specimen from the top and the pore water pressure measured at the bottom to obtain information on the changes in curvature caused by air leakage into a specimen. If the air in a partially saturated specimen exists in the form of bubbles, then one can not speak of the pore air pressure, since the pressure will vary with the size of bubble. This possibility must be taken into account when interpreting pore air pressure measurements.

Assuming that air in the form of bubbles is an unstable condition in fine-grained soils, as was concluded in 2-02 and previously by Hilf (56), an experimental study should be made to determine the time required to achieve the equilibrium state, wherein air exists in the form of spaces that are bounded by soil grains and by menisci which span between the grains.

Theoretical considerations of the equilibrium between the air and water in the pores of a soil are dependent on the validity of Henry's law in the very fine pore spaces of a soil. An investigation should be made into the possible variations from Henry's law in fine pores and the effect of such variations on the theoretical discussion presented in Chapter 2 concerning the form of air in partially saturated specimens.

### 11-04 EXPERIMENTS TO STUDY THE THEORY OF FLOW THROUGH MEMBRANES

Accurate experiments should be performed to determine the range of validity of the equation

$$q = K A \frac{\Delta p_v}{L} \quad (3-33)$$

for a wide variety of rubbers and plastics. Specifically, the relation between  $q$  and  $\Delta p_v$  should be investigated for hydraulic pressures up to 50 kg/cm<sup>2</sup>. For such tests it may be necessary to measure the thickness of the membranes while they are under pressure, since the high pressures may decrease their thickness substantially. The relation between  $q$  and  $L$  should be investigated for a range of membrane thicknesses between 0.003 cm and 0.100 cm. Also, the effect of the roughness of the surface supporting the membrane on the measured rate of flow should be investigated. All tests should be performed using liquid permeants on both sides of the membrane. Up to now the great majority of tests have been performed using gaseous permeants, because the rates of flow of gases through membranes are much more easily measured. However, even for the case of gas flow, the equation has not been verified for many membrane-permeant systems.

One possible experimental technique for distinguishing whether Poisseuille's law or Fick's law applies to the flow of gases through a membrane would be as follows: Perform a series of tests in which a pure gas is forced under pressure through a membrane. For each test of the series, alter the average pressure of the gas in the membrane. Calculate the rate constants by assuming that Eq. 3-49 is applicable and by assuming that Eq. 3-56 is applicable to the flow process. If the rate constant in Eq. 3-49 remains substantially constant for all tests in the series, then Fick's law is applicable to the flow process. Similarly, Poisseuille's law applies if the rate constant in Eq. 3-56 remains substantially constant for all tests.

It was shown in Chapters 4, 5, and 6 that the permeability constant for flow of water through natural rubber has the same value when measured with a hydraulic pressure or mole fraction gradient across a membrane when liquid is on both sides, but has a somewhat lower value when measured with liquid on one side and a vacuum on the other. These three types of tests should be used to determine the permeability to water and other liquids of several rubber and plastic membranes. For each series of three tests, the same membrane

should be used and, after the last test is complete, the first test should be repeated to be sure that no changes in the membrane have occurred during the tests. The test with vacuum on one side should be performed first and last since this test has the shortest duration. It is a thermodynamic necessity that the rate constants for the two types of tests with liquid on both sides of the membrane be identical. Having reliable experimental data that the rate constants are identical will be proof for the statement that the mechanism of flow is identical in both types of tests, i.e. if the mechanism of flow is diffusion when a mole fraction difference is applied across a membrane, then it is also diffusion when a hydraulic pressure difference is applied across a membrane, and if the flow is laminar in one case, it is laminar in the other.

#### 11-05 ADDITIVES FOR CHAMBER WATER

It was recommended in Chapter 9 that sodium chloride or sucrose be added to the chamber water to reduce the vapor pressure difference of water across the membrane and thereby reduce the rate of leakage. Additives such as glycerol and potassium dichromate may also be satisfactory. Potassium dichromate has been used by Warlam (105) to prevent corrosion of the steel parts in his triaxial apparatus. Thus it would serve a double purpose if used in the proper concentration in the chamber. However, potassium dichromate may have deleterious effects on natural rubber over long periods (105) and it may irritate the skin.

Each of the above-mentioned additives, and others, should be tested over long periods to determine their effects on (1) natural rubber, (2) butyl rubber, (3) brass, (4) stainless steel, and (5) the human skin. If a compound more suitable than sodium chloride or sucrose is found, then measurements of the vapor pressure lowering of this compound should be made. The results would establish the concentration required to minimize the vapor pressure difference across the membrane during Q and R tests.

#### 11-06 SEARCH FOR LESS PERVIOUS MEMBRANES

A search should be made for membranes that might be less pervious and possess a lower coefficient of elasticity than butyl rubber. The water permeabilities of new membranes can be compared with that of butyl rubber by means of tests with water on one side and a vacuum on the other (Chapter 6). The coefficients of elasticity can be compared by using the simple test described in 9-05.

The possibility of using a relatively thick layer of wax, either by itself or as a coating over a membrane, should be investigated, particularly for testing partially saturated specimens. Waxes with formulations that would exhibit a great deal of creep under load and which have very low permeability are desirable. The creep characteristics of proposed waxes would have to be determined, perhaps by performing long-time triaxial tests on annular cylinders of the waxes. All such tests must be performed in a constant temperature room. The results of these tests would have to be analyzed theoretically to determine the probable effect on a specimen. An alternative approach would be to coat cylinders of gelatin (see Warlam (104)) or other "specimens" of known strength, and determine the increase in strength caused by the wax coating in tests of several different durations. Finally the solubility and coefficient of diffusion of water in the wax, and the permeability of the wax to water and air should be measured.

#### 11-07 BINDING LEAKAGE TESTS

Binding leakage tests should be performed using butyl rubber membranes sealed with O-Rings, and the results should be compared with the results presented in Chapter 7. Then an estimate of the relative values of  $q_2$  and  $q_3$  (Fig. 7-5) could be made.

Binding leakage tests should also be made to determine the effect on binding leakage of (1) a mole fraction gradient across the bindings, (2) using two instead of one membrane beneath the O-Ring binding, (3) using two instead of one O-Ring and (4) greasing a pedestal which is purposely roughened prior to test. The same membrane should be used in as many tests as possible, in order to eliminate errors due to possible differences

among the membranes. Alternatively, a large number of tests could be performed using different membranes so that a statistical analysis of the results could be made.

#### 11-08 TESTS ON VALVES AND FITTINGS

A complete series of leakage measurements should be made on a representative sampling of the many valves and fittings that are commercially available. Tests are required to determine (1) the relation between rate of leakage and applied pressure and (2) the rate of leakage caused by mole fraction differences across the valve packing.

The ideas presented in this investigation could be applied to the design of a valve that would be ideally suited for use in the drainage system of a triaxial cell. For example, a piston valve might be suitable if the following design requirements were met:

- (1) Polish all sealing surfaces of the valve carefully, including the surfaces of the O-Ring groove.
- (2) Design the O-Ring grooves so that the O-Rings fill about 95% of the groove volume and are tightly compressed when inserted in the valve.
- (3) Use O-Rings that do not have a molded projection on their perimeters.
- (4) Use O-Rings that are as small as practicable, so that the length of contact that forms the seal will be as short as possible.

## CHAPTER 12

### SUMMARY

#### 12-01 INTRODUCTION

One of the most urgent problems in soil testing is to develop means for measuring the effect of times-of-loading of several months on the shear strength of a clay that is strained at constant water and air content.

The principal purpose of this investigation was to develop procedures that would permit one to perform triaxial tests of long duration without objectionable changes in pore pressure due to leakage. To achieve this purpose it was necessary to (1) understand the theory of flow of water and air through membranes, (2) measure the rate of leakage that occurs through membranes, bindings, fittings, valves and tubing, (3) determine whether this measured leakage causes excessive errors, and (4) develop procedures which effect satisfactory control of leakage.

The reader should bear in mind that the smallest volume of water leakage that is significant in triaxial testing is about  $2 \text{ mm}^3$ .

#### 12-02 THEORY OF FLOW THROUGH RUBBER AND PLASTIC MEMBRANES

The following is a helpful model of the mechanism of flow of a permeant such as water or air through a membrane: Openings between molecules of the membrane constantly change in shape and size due to motions caused by the thermal energy of these molecules. At random an opening will be large enough to fit a permeant molecule and, if there is a permeant molecule in the vicinity with sufficient energy, it will enter the opening. Thus one step of the flow process is complete. Such a step can take place in any direction in the membrane. However, when an energy gradient is applied, e.g. a total pressure gradient and/or a mole fraction gradient, then more steps will occur in one direction than in the opposite direction and a uni-directional flow will begin. (Total pressure is defined as the sum of the gage pressure on a system plus atmospheric pressure. For liquid systems, the total pressure is referred to as the hydraulic pressure. Mole fraction is defined as the ratio of the number of moles of solute to the sum of the number of moles of solute plus solvent in a solution.)

Equations are given below with which one can compute the leakage into or out of a triaxial specimen through membrane(s) for the following cases:

- CASE I - Flow of water due to a hydraulic pressure difference across the membrane, when the chamber fluid is water.
- CASE II - Flow of water due to a mole fraction difference of water across the membrane, i.e. osmosis of water.
- CASE III - Evaporation of water vapor from a specimen through the membrane into a room atmosphere at less than 100% relative humidity. The flow is caused by the vapor pressure difference in this case. (The partial pressure of a gas is that portion of the total pressure on a mixture of gases that is contributed by the gas in question. For the case of water vapor, the partial pressure is referred to as the vapor pressure.)
- CASE IV - Flow of air due to a total pressure difference, when the chamber fluid is air.
- CASE V - Diffusion of air through water in chamber and through membrane due to a partial pressure difference between the air in the chamber water and the air in the pore water.

For Case I the rate of flow of water,  $q$ , may be computed using Darcy's law,  $q = kiA$ , where  $k$  is the coefficient of permeability of the membrane,  $i$  is the hydraulic gradient, and  $A$  is the area of the membrane through which flow occurs.

For Case I, the rate of steady flow of water through a membrane also can be computed using the equation

$$q = K A \frac{\Delta p_v}{L} \quad (3-33)$$

where  $q$  = rate of flow ( $\text{cm}^3$  of liquid water/sec).

$K$  = permeability constant of membrane to water ( $\text{cm}^4/\text{gm sec}$ ).\*

$A$  = area through which flow takes place ( $\text{cm}^2$ ).

$\Delta p_v$  = vapor pressure difference of water across the membrane ( $\text{gm}/\text{cm}^2$ ).

$L$  = membrane thickness (cm).

The permeability constant to be used in Eq. 3-33 is determined by measuring the rate of flow of liquid water through a membrane due to a hydraulic pressure difference. The vapor pressure difference caused by a hydraulic pressure difference is computed from the thermodynamic relationship

$$\Delta p_v = \frac{\bar{V}_w \bar{p}_{vo}}{R T} \Delta p \quad (3-28)$$

where  $\bar{V}_w$  = volume per mole of water ( $\text{cm}^3/\text{mole}$ ).

$\bar{p}_{vo}$  = equilibrium vapor pressure of water at standard atmospheric pressure at temperature of test ( $\text{gm}/\text{cm}^2$ ).

$R$  = gas constant ( $\text{gm cm}/\text{mole}^\circ\text{K}$ ).

$T$  = absolute temperature of test ( $^\circ\text{K}$ ).

$\Delta p$  = hydraulic pressure difference across membrane ( $\text{gm}/\text{cm}^2$ ).

For water, Eq. 3-28 becomes  $\Delta p_v = 3.07 \times 10^{-5} \Delta p$  at  $30^\circ\text{C}$  and  $\Delta p_v = 1.74 \times 10^{-5} \Delta p$  at  $20^\circ\text{C}$ . Eq. 3-28 is accurate to within 1% for hydraulic pressures up to  $10 \text{ kg}/\text{cm}^2$  and to within 8% for hydraulic pressures up to  $100 \text{ kg}/\text{cm}^2$ .

For Case II, the rate of flow is computed using Eq. 3-33 with the same permeability constant  $K$  as determined for Case I. The vapor pressure difference caused by a mole fraction difference must be determined by actual measurement of the vapor pressure lowering of water due to the presence of a solute. Such measurements are given in the International Critical Tables for many solutes, e.g. sodium chloride.

For Case III, the rate of flow also is computed using Eq. 3-33. When the relative humidity of the room atmosphere is above about 50%, the permeability constant to be used for Case III is about the same as that used for Cases I and II. When the relative humidity is very low, the permeability constant to be used for Case III may be as much as 20% lower than that used for Cases I and II. The vapor pressure difference between the pore water in a specimen and the outside room atmosphere is equal to the product of the equilibrium vapor pressure of water at the temperature of the test and the relative humidity. The effect of any pore water tension on this vapor pressure difference may be neglected.

For Case IV, the rate of steady flow of air through the membrane is computed using the equation

$$q_s = K_s A \frac{\Delta p_p}{L} \quad (B-3)$$

where  $q_s$  = rate of flow ( $\text{cm}^3$  of air measured at standard atmospheric pressure/sec).

$K_s$  = permeability of membrane to air ( $\text{cm}^4/\text{gm sec}$ ).

$\Delta p_p$  = partial pressure difference of air across membrane ( $\text{gm}/\text{cm}^2$ ). Equal to the difference between the chamber pressure and the pore air pressure.

\* The gram is used to mean a gram of force in all cases herein. The units shown were used herein, but any consistent system of units may be used in all equations presented.

It is emphasized that  $q_a$  in Eq. B-3 is the rate of flow of air measured at atmospheric pressure. If the pore air pressure is not atmospheric, the volume occupied by the air after passing through the membrane must be calculated using Boyle's law.

For Case V, the rate of diffusion of dissolved air into or out of a specimen can only be approximated. The problem is roughly equivalent to the diffusion of heat from a solid cylinder into an infinite surrounding medium or vice versa. If it is assumed that there are no convection currents in the chamber water, so that a partial pressure gradient of air can develop in the chamber water, then the volume of air that diffuses into or out of a specimen is given approximately by the equation

$$\frac{J_a}{V} = \frac{8}{\sqrt{\pi}} \frac{K_g}{\sqrt{D}} \frac{\Delta p_p}{D_s} \sqrt{t} \quad (\text{B-11})$$

where  $J_a$  = volume of air flow measured at standard atmospheric pressure ( $\text{cm}^3$ ).  
 $D$  = coefficient of diffusion of air in water ( $\text{cm}^2/\text{sec}$ ).  
 $t$  = elapsed time (sec).  
 $D_s$  = diameter of specimen (cm).

On the other hand, if the chamber water is well stirred, no partial pressure gradient will develop in the chamber water. Instead the partial pressure gradient will develop only in the membrane(s), in which case the rate of air flow is computed using Eq. B-3. The rate of flow of air will always be less for Case V than for Case IV, because of the impedance offered by the chamber water to the diffusion of air. Therefore a liquid chamber fluid should always be used in triaxial testing. The actual rate of flow of air when using water as the chamber fluid probably will be greater than calculated using Eq. B-11, because convection currents will prevent the formation of a steep partial pressure gradient in the chamber water. It is estimated that the actual rate of air flow usually will be no more than twice that given by Eq. B-11.

#### 12-03 SUITABILITY OF CONVENTIONAL TRIAXIAL APPARATUS FOR CONTROL OF WATER LEAKAGE INTO 100% SATURATED SPECIMENS

Water leakage into a 100% saturated specimen causes a decrease in effective stress which may be calculated using the equation

$$\frac{\Delta \bar{\sigma}_3}{\bar{\sigma}_3} = - \frac{1}{S} \frac{J_w}{V} \quad (\text{2-9})$$

where  $\frac{\Delta \bar{\sigma}_3}{\bar{\sigma}_3}$  = change in effective stress; usually expressed in percent. A decrease in effective stress carries a negative sign.  
 $S$  = initial swelling ratio. Equal to the slope of the straight line approximation for the swelling curve over the range  $0\% < \Delta \bar{\sigma}_3 / \bar{\sigma}_3 < 5\%$ .  
 $V$  = total volume of specimen.  
 $J_w$  = volume of water leakage. Equal to the change in total volume  $\Delta V$ .

To derive this equation it was assumed that the swelling curve, plotted in terms of  $\Delta V/V$  versus  $\Delta \bar{\sigma}_3 / \bar{\sigma}_3$ , is a straight line over a range of effective stress decrease of about 5%. This assumption does not introduce significant error. The initial swelling ratio was measured accurately by the author for one compacted soil, Canyon Dam clay. It was found to range between 0.001 and 0.0015 for effective consolidation pressures ranging between 2 and 14  $\text{kg}/\text{cm}^2$ . Also an attempt was made to derive the initial swelling ratio from the swelling curves of conventional one-dimensional consolidation tests that have been presented in the literature. Although such data probably lead to an overestimate of the initial swelling ratio, they do indicate that most clays have initial swelling ratios greater than 0.001.

Assuming that 2% is the maximum decrease in effective stress acceptable in a triaxial Q or R test on a 100% saturated, 1.4 in. diameter by 3.5 in. high specimen, then Eq. 2-9 shows that the maximum acceptable volume of leakage, for a specimen with  $S = 0.001$ , is about  $2 \text{ mm}^3$  ( $0.002 \text{ cm}^3$ ). This is an extremely small volume of leakage, but it is probably close to the lower limit of the leakage that is important in triaxial testing.

Measurements showed that leakage of water through natural rubber membranes usually is far greater than leakage past bindings, fitting, valves and tubing, provided the bindings are properly made up and the valves are properly chosen and in good condition. The permeability constant for several natural rubber membranes was found to be the same regardless of the thickness or method of manufacture. The permeability constant  $K$  (to be used in Eq. 3-33) of natural rubber to water, measured with a hydraulic pressure difference across the membrane, is  $1.6 \times 10^{-11} \text{ cm}^4/\text{gm sec}$ . This value is accurate to within plus or minus 35%. The coefficient of permeability  $k$ , to be used in Darcy's law, is  $5 \times 10^{-16} \text{ cm}^2/\text{sec}$ . These values were determined with a support under the membrane that has a roughness approximately equivalent to a medium silt. If the soil is rougher than this, the permeability constants may be higher by some unknown amount.

Calculation of the volume of leakage that occurs through two, 0.006 cm thick natural rubber membranes on a 1.4 in. diameter by 3.5 in. high specimen, shows that Q and R tests not exceeding a duration of about 12 hours can be performed on a specimen with  $S = 0.001$ , if the hydraulic pressure difference causing flow is less than  $10 \text{ kg}/\text{cm}^2$ . When there is sodium chloride in the pore water at about the same concentration as the salts in sea water, then the maximum duration of test is reduced to only about 4 hours. These estimates of the effects of leakage on Canyon Dam clay probably are accurate at least to within plus or minus 50%.

Based on one-dimensional consolidation test data in the literature the greatest probable value of the swelling ratio for any soil, except peats, is about 0.03. Even when assuming this high  $S$  value, the volume of leakage would be excessive for tests of 100 days duration.

#### 12-04 SUITABILITY OF CONVENTIONAL TRIAXIAL APPARATUS FOR CONTROL OF AIR LEAKAGE INTO OR OUT OF PARTIALLY SATURATED SPECIMENS

Reliable data on the effect of air leakage into or out of partially saturated specimens are lacking. Tentative conclusions were derived theoretically, based on the validity of Boyle's and Henry's laws in the fine pores of a clay, and on other assumptions to be stated below.

The decrease in effective stress caused by air leakage into partially saturated specimens may be calculated using the equation

$$\frac{J_a p_s}{v} = s \left( - \frac{\Delta \bar{\sigma}_3}{\bar{\sigma}_3} \right) (u_a - \Delta \bar{\sigma}_3) + n f ( - \Delta \bar{\sigma}_3) \quad (2-22)$$

where  $J_a$  = volume of air leakage ( $\text{cm}^3$  measured at standard atmospheric pressure,  $p_s$ ).

$u_a$  = initial pore air pressure ( $\text{gm}/\text{cm}^2$ ).

$n$  = initial porosity (dimensionless).

$f = (1 - G_w + sG_w)$ , where  $G_w$  is the initial degree of saturation and  $s$  is the solubility of air in water. This number, when multiplied by the void volume, gives the initial total volume of air (dissolved and undissolved) in the specimen measured at the pressure  $u_a$ .

Eq. 2-22 is based on the assumption that the curvature of the menisci surrounding the air spaces in a partially saturated specimen, does not change when air leakage occurs, which

means that the change in effective stress in a specimen is equal but opposite in sign to the change in pore air pressure. The discussion presented in the paragraphs below is correct only if this assumption is a valid one. It should be emphasized that the assumption is only approximate and that the degree to which it is valid cannot be estimated with any precision at present. A theoretical analysis based on the very limited data available in the literature indicates that the decrease in effective stress calculated using Eq. 2-22 probably is not more than twice as great as the actual decrease in effective stress, for specimens with a degree of saturation greater than 90%.

For a critical example, i.e. Canyon Dam clay with  $S = 0.001$ ,  $\bar{\sigma}_3 = 1 \text{ kg/cm}^2$  and  $G_w = 98\%$ , Eq. 2-22 shows that the maximum acceptable air leakage into a 1.4 in. diameter by 3.5 in. high specimen is about  $0.05 \text{ cm}^3$  for a decrease in effective stress of 2%. Using Eq. B-11 one can compute that a partial pressure difference of  $1.0 \text{ kg/cm}^2$  will cause leakage of about  $1 \text{ cm}^3$  of air into a 1.4 in. diameter by 3.5 in. high, partially saturated specimen in three hours. It follows that an excessive change in effective stress is likely to occur within one hour. If a more typical example is considered, i.e. Boston Blue clay with  $S = 0.013$ ,  $\bar{\sigma}_3 = 6 \text{ kg/cm}^2$  and  $G_w = 98\%$ , one finds that excessive changes in effective stress would occur in about twelve hours. In any case, the maximum acceptable test duration is far less than 100 days, so that triaxial test procedures must be modified to reduce substantially the rate of air leakage during long-time tests on partially saturated specimens.

#### 12-05 PROCEDURES FOR CONTROL OF LEAKAGE IN TRIAXIAL Q AND R TESTS

The reader is referred to Chapter 10 for details of the procedures that are presented below in summary form.

##### (a) Control of Air Leakage into 100% Saturated Specimens

Air leakage into 100% saturated specimens may be essentially prevented by (1) inserting a two-meter length of small diameter tubing, filled with the chamber liquid between the point of air pressure application and the chamber or (2) applying the chamber pressure by means of a hydraulic system.

##### (b) Control of Water Leakage into Partially Saturated Specimens

The maximum acceptable water leakage into partially saturated specimens is probably either equal to or greater than for the case of water leakage into 100% saturated specimens. Therefore the procedures summarized in (c) below are also satisfactory for controlling water leakage into partially saturated specimens.

##### (c) Control of Water Leakage into 100% Saturated Specimens

For 12-hour Q and R tests, the water leakage usually will not cause more than a 2% decrease in effective stress in a 1.4 in. diameter by 3.5 in. high specimen if the following apparatus is used: (1) two, 0.006 cm thick natural rubber membranes, (2) two O-Rings on both the cap and pedestal, (3) cap and pedestal with well polished surfaces that are greased before application of the O-Rings, and (4) valves and fittings that are properly chosen and in good condition.

For 100-day Q and R tests, the water leakage into a 1.4 in. diameter by 3.5 in. high specimen usually will not cause more than a 2% decrease in effective stress if the following apparatus and procedures are used:

Temperature of Specimen - should be maintained constant to within plus or minus one-quarter degree Centigrade.

Bindings of Membranes to Cap and Base - Same comments as for 12-hour tests.

Valves - The number of valves used in the drainage and/or pore pressure measuring systems should be held to an absolute minimum. Preferably only one valve should be used. Any valves used should be checked for leaks periodically. Valves with a stem that forms a metal to metal seal with a seat were found to leak at least one order of magnitude less than valves sealed with O-Rings.

Fittings - The number of fittings used in the drainage and/or pore pressure measuring systems should be held to a minimum. Preferably only one fitting that can be disconnected should be used and it should be checked for leaks periodically. Fittings that can be disconnected should be replaced by soldered joints or epoxy seals wherever possible. No extensive investigation was made of the various commercial fittings available. However it was found that the fittings with O-Ring seals that were used in the membrane permeability cell during this investigation are sufficiently leaktight and are dependable.

Tubing - The length of tubing used in the drainage lines and/or the pore pressure measuring system should be held to an absolute minimum. Metal rather than plastic tubing should be used to minimize both immediate and long-term volume changes due to pressure changes.

Membranes - Two butyl rubber membranes with a thickness of 0.004 cm each should be used. Such membranes have not yet been manufactured. Two firms are presently attempting to make them and the author anticipates no unusual difficulties in the manufacturing process. When the butyl membranes are made, their permeability should be checked to ensure that it is as low as the permeability of the butyl membranes tested during the present investigation.

Chamber Fluid - Water may be used as the chamber fluid so long as a solute, such as sodium chloride or sucrose, is added to reduce the vapor pressure difference across the membrane. The concentration of the solute should be so chosen that the average vapor pressure difference across the membrane for the duration of the test will be as close as possible to zero.

(d) Control of Air Leakage into or out of Partially Saturated Specimens

Temperature of Specimen - should be maintained constant to within plus or minus about one degree Centigrade.

Bindings, fittings, valves and tubing - same comments as for tests on 100% saturated specimens.

Membranes - two, 0.006 cm thick natural rubber membranes are satisfactory although the use of two, 0.004 cm butyl rubber membranes would offer a small advantage when they become available. Changes in the thickness or composition of the membrane has little effect on the rate of air leakage because most of the impedance to air flow probably is developed in the chamber fluid.

Chamber Fluid - Always use a liquid chamber fluid. If water is used it should be saturated with air at the time average of the pore air pressure that is expected to develop during the test. For the most critical case of air leakage into a 1.4 in. diameter by 3.5 in. high specimen, a 2% decrease in effective stress will occur in about two to eight hours when this procedure is used during a Q or R test.

Mercury may be a satisfactory chamber fluid for preventing air leakage into or out of partially saturated specimens. Unfortunately, the author has had no experience with the use of mercury and there are no quantitative data on the solubility and rate of diffusion of air (oxygen and nitrogen) in mercury, with which one could at least compute the rate of air flow to be expected under the conditions for a triaxial test.

12-06 SUGGESTIONS FOR FUTURE RESEARCH

The initial swelling ratio should be determined for many different soils. Both 100% saturated and partially saturated specimens should be tested. The effect on the initial swelling ratio of the effective principal stress ratio and the effective stress at which swelling is begun should be investigated.

Chamber fluids more satisfactory than water for Q and R tests on partially saturated specimens should be sought. In particular, the possibility of using mercury or a thick wax coating should be studied. The use of chamber fluids other than water offers

the best prospects for increasing the maximum permissible Q or R test duration to more than about 100 days for 100% saturated specimens, and for increasing the maximum permissible test duration for partially saturated specimens to greater than a few days.

A theoretical and experimental investigation should be made on the effects of air and/or water leakage on partially saturated specimens. The form in which the air occurs and the changes that take place when leakage occurs should be determined.

NOTATIONS AND DEFINITIONS

- (prime) Added to the symbol for any parameter to denote a changed value of the parameter.
- A Area of flow. Used with subscripts to designate particular areas through which flow occurs ( $\text{cm}^2$ ).
- $a_v$  Coefficient of compressibility of a soil. Equal to the absolute value of the slope of the compression curve, plotted in terms of the void ratio versus effective stress using arithmetic scales ( $\text{cm}^2/\text{gm}$ ).
- B Constant with varying units as defined in text. Used with numerical subscripts to increase the number of available constants.
- B test Test performed to measure the rate of binding leakage caused by the application of a hydraulic pressure difference across the bindings.
- $B_a$  Constant of proportionality relating the rate of adsorption of molecules onto a membrane to (1) the concentration of molecules in the adjacent solution and (2) to the number of available adsorption sites ( $\text{cm}^3/\text{sec}/\text{site}$ ).
- $B_d$  Constant of proportionality relating the rate of desorption to the number of adsorption sites that are filled (moles/second/site).
- $b_o$  Coefficient of swelling of a soil. Equal to the absolute value of the slope of the swelling curve, plotted in terms of void ratio versus effective stress using arithmetic scales ( $\text{cm}^2/\text{gm}$ ).
- C Compression ratio. Equal to the absolute value of the slope of an arithmetic plot of  $\Delta V/V$  versus  $\Delta \bar{\sigma}/\bar{\sigma}$  for increasing  $\bar{\sigma}$  (dimensionless).
- $C_s$  Swelling index. The change in void ratio on a semi-logarithmic plot of a swelling curve for one log cycle change in effective stress (dimensionless).
- c Concentration of a permeant in a medium. Used with subscripts to denote concentrations at particular locations or in particular media, e.g. s = solution, m = membrane (moles/ $\text{cm}^3$  of medium).
- $c_t$  Total concentration of all solvent and solute molecules of a permeating solution in a membrane (moles/ $\text{cm}^3$  of membrane).
- D Coefficient of diffusion ( $\text{cm}^2/\text{sec}$ ).
- $D_S$  Diameter of triaxial specimen (cm).
- d Distance travelled by a diffusing particle in a given time interval (cm).
- E Coefficient of elasticity. Used herein with reference to membranes ( $\text{gm}/\text{cm}^2$ ).
- e Void ratio. Volume of voids per unit volume of soil solids (dimensionless).
- $F_M$  Coefficient of volume compressibility of mineral grains ( $\text{cm}^2/\text{gm}$ ).
- $F_W$  Coefficient of volume compressibility of water ( $\text{cm}^2/\text{gm}$ ).
- f =  $(1-G_w+sG_w)$ . Degree of total air saturation. Equal to the quotient of (1) the sum of the dissolved and undissolved air volumes, measured at the pressure in the undissolved air, and (2) the void volume in a soil specimen (dimensionless).
- $G_w$  Degree of saturation. Usually expressed in percent. The volume of water divided by the volume of voids in a soil specimen (dimensionless).
- H Constant in Henry's law,  $v_a = HX$  ( $\text{kg}/\text{cm}^2$ ).
- $H_S$  Height of triaxial specimen (cm).

- HP burette Burette on high pressure side of membrane permeability cell. Used to measure volume of flow toward membrane from high pressure side.
- h Total hydraulic head causing flow (cm of permeant).
- i Hydraulic gradient (dimensionless).
- $J_a$  Volume of leakage of air into or out of a soil specimen through parts of the triaxial apparatus which should ideally be perfectly impervious. ( $\text{cm}^3$  of gaseous air, measured at atmospheric pressure,  $p_g$ ).
- $J_w$  Volume of leakage of water into or out of a specimen through parts of the triaxial apparatus which should ideally be perfectly impervious ( $\text{cm}^3$  of liquid water).
- K Permeability constant defined by the equation  $q = K(A/L)\Delta p_p$ . Distinguished from  $K'$  because partial pressure difference is used as driving force rather than hydraulic pressure difference ( $\text{cm}^4/\text{gm sec}$ ).
- $K'$  Permeability constant defined by the equation  $q = K'(A/L)\Delta p$ . Distinguished from  $k$ , the Darcy coefficient of permeability because the hydraulic pressure difference, rather than the total head difference, is assumed to be the driving force, i.e. pressure differences caused by elevation differences are assumed negligible ( $\text{cm}^4/\text{gm sec}$ ).
- $K_s$  Permeability constant defined by:  $q_g = K_s(A/L)\Delta p_p$ . The volume rate of flow  $q_g$  is measured in  $\text{cm}^3$  of gaseous permeant (at atmospheric pressure  $p_g$ ) per second ( $\text{cm}^4/\text{gm sec}$ ).
- k Coefficient of permeability defined by Darcy's law,  $q = kiA$ . Note that the total hydraulic head is considered the driving force causing flow in this definition ( $\text{cm}/\text{sec}$ ).
- L Thickness of membrane or other permeated medium. Used with capital subscripts to denote particular media (cm).
- L burette Burette in the membrane permeability apparatus that is used to measure the volume of leakage of water past the O-Ring which seals the periphery of the membrane into the permeability cell.
- $L_c$  Length of a capillary tube through which flow occurs (cm).
- LP burette Burette in the membrane permeability apparatus that is used to measure the volume of outflow of water through the membrane into the low pressure side of the membrane permeability cell.
- M Molecular weight. Used with lower case subscripts (gm).
- m Number of moles. Used with lower case subscripts (dimensionless).
- N Number of particles (dimensionless).
- $N_c$  Number of capillaries (dimensionless).
- $N_e$  Number of ways in which energy can be stored in a molecule (dimensionless).
- n Porosity. The ratio of the void volume to the total volume of a soil (dimensionless).
- p Total pressure (for gaseous systems) or hydraulic pressure (for liquid systems). Equal to the sum of gage pressure plus atmospheric pressure. Used with subscript numerals to indicate high and low pressures and with capital letter subscripts to denote pressure at a given location ( $\text{gm}/\text{cm}^2$ ).
- $p_p$  Partial pressure of one gas in a mixture of gases. When only one gas is present, the partial pressure is equal to the total pressure on the gas ( $\text{gm}/\text{cm}^2$ ).

- $p_s$  Standard atmosphere (= 1033.3 gm/cm<sup>2</sup>)
- $p_v$  Vapor pressure. The partial pressure of an easily condensible gas (such as water vapor) (gm/cm<sup>2</sup>).
- $\bar{p}_v$  Equilibrium vapor pressure. The vapor pressure of the gaseous phase of a liquid which is in equilibrium with the liquid phase at any given pressure, temperature and composition (gm/cm<sup>2</sup>).
- $\bar{p}_{v0}$  Equilibrium vapor pressure measured when the total pressure on the system is one atmosphere (gm/cm<sup>2</sup>).
- Q test A triaxial compression test at constant water content in which the specimen is first subjected to a hydrostatic confining pressure and then the axial stress is increased to failure.
- q Volume rate of flow of liquid. Used with numeral and capital subscripts to denote specific volume rates of flow (cm<sup>3</sup>/sec or mm<sup>3</sup>/day).
- $\bar{q}$  Volume rate of flow of a gas, with the volume of gas measured at the average total pressure in the flow medium (cm<sup>3</sup>/sec).
- $q_B$  Rate of binding leakage (cm<sup>3</sup>/sec or mm<sup>3</sup>/day).
- $q_C$  Volume rate of flow of liquid through one capillary (cm<sup>3</sup>/sec).
- $q_{Cx}$  Volume rate of flow of a gas through one capillary tube at a distance x from one end of the tube. Volume is measured at the total pressure existing at x (cm<sup>3</sup>/sec).
- $q_M$  Measured volume rate of flow of liquid (cm<sup>3</sup>/sec or mm<sup>3</sup>/day).
- $q_g$  Volume rate of flow of a gas, with the volume of gas measured at a pressure of one atmosphere (cm<sup>3</sup>/sec or mm<sup>3</sup>/day).
- $q_x$  Volume rate of flow of a gas at a distance x from the face of a medium, with the volume measured at the total pressure existing at point x (cm<sup>3</sup>/sec).
- R Gas constant (= 84,787 gm cm<sup>3</sup>/mole °C)
- R test A triaxial compression test in which the specimen is first consolidated under an effective hydrostatic consolidation pressure  $\bar{\sigma}_c$  and then, without permitting any further change in water content, the axial load is increased to failure.
- $R_b$  Burette reading (cm).
- r Radius of a pore or opening. Used with lower case subscripts (cm).
- S Initial swelling ratio. Equal to the slope of an arithmetic plot of  $\Delta V/V$  versus  $\Delta \bar{\sigma}/\bar{\sigma}$  for decreasing  $\bar{\sigma}$ . Used with subscripts to denote the type of test used to measure the swelling ratio (dimensionless).
- S test A triaxial compression test in which the specimen is consolidated under a hydrostatic confining pressure, and then is subjected to axial load increase which is applied in small increments, allowing full consolidation under each increment, until failure is reached.
- $S_c$  Initial swelling ratio measured in one-dimensional consolidation test.
- SW test A test performed to measure the initial swelling ratio.
- s Solubility of air in medium (a dimensionless ratio which is a function of temperature and slightly dependent on pressure).
- $s_c$  Solubility of a permeant in a membrane in terms of concentration. Defined by  $c_m = s_c c_g$  (dimensionless).
- $s_p$  Solubility of a permeant in a membrane in terms of vapor pressure. Defined by  $c_m = s_p p_v$  (moles/gm cm).

- T Temperature ( $^{\circ}$ Celsius or  $^{\circ}$ Kelvin).
- t Time (sec, min, hr, day).
- $t_{100}^c$  Time to achieve 100% primary consolidation (min).
- $t_{100}^s$  Time to achieve 100% primary swelling (min).
- $u_a$  Pore air pressure (gm/cm<sup>2</sup>).
- $u_c$  Capillary pressure. Equal to the difference in pressure across the air-water menisci in a partially saturated soil.
- $u_w$  Pore water pressure (gm/cm<sup>2</sup>).
- V Total volume of a soil specimen. Used with lower case subscripts to denote portions of the total volume of a specimen (cm<sup>3</sup>).
- V test Test to measure the rate of flow of water vapor through a membrane by applying a high hydraulic pressure to water on one side and a vacuum on the opposite side.
- $\bar{V}$  Partial molar volume of a constituent of a mixture or solution in liquid or gaseous state (cm<sup>3</sup>/mole). In the pure state the partial molar volume is equal to the molar volume, which is the reciprocal of the density measured in units of moles/cm<sup>3</sup>. Used with subscripts to denote specific partial molar volumes, e.g. w = water,  $\rho$  = liquid, g = gas, v = vapor (cm<sup>3</sup>/mole).
- $V_{ad}$  Volume of air dissolved in the pore water of a soil specimen measured at pore air pressure  $u_a$  (cm<sup>3</sup>).
- $V_{at}$  Total volume of air in a soil specimen. Equal to ( $V_{au} + V_{ad}$ ) (cm<sup>3</sup>).
- $V_{au}$  Volume of undissolved air in a soil specimen measured at pore air pressure  $u_a$  (cm<sup>3</sup>).
- $V_s$  Volume of soil solids in a specimen (cm<sup>3</sup>).
- $V_v$  Volume of voids in a soil specimen. Equal to ( $V_{au} + V_w$ ) (cm<sup>3</sup>).
- $\bar{V}_v$  Partial molar volume of a vapor at equilibrium with adjacent liquid (cm<sup>3</sup>/mole).
- $V_w$  Volume of water in a soil specimen (cm<sup>3</sup>).
- $\bar{V}_w$  Partial molar volume of water (cm<sup>3</sup>/mole).
- W test A test to measure the permeability of a membrane by applying a hydraulic pressure difference with water on both sides of the membrane.
- $W_a$  Weight of air (gm).
- $W_w$  Weight of water (gm).
- X Mole fraction. The ratio of the number of moles of an element, ion or compound in a solution or mixture to the total number of moles of all components. Used with capital subscripts (dimensionless).
- X test Test to measure the rate of flow of water through a rubber membrane due to an osmotic pressure gradient (i.e. mole fraction gradient) across the membrane.
- x Length coordinate (cm).
- $\gamma$  Unit weight (gm/cm<sup>3</sup>).
- $\gamma_w$  Unit weight of water (gm/cm<sup>3</sup>).
- $\Delta$  Always used with another symbol, such as  $\Delta\bar{\sigma}$ , to indicate the difference:  $\bar{\sigma}' - \bar{\sigma}$ , where the primed term is the value of  $\bar{\sigma}$  after a change has occurred.

$\frac{\Delta V}{V}$	Volumetric strain (dimensionless).
$\Delta V_c$	Volume change correction applied to volume changes measured in swelling tests to account for volume change of apparatus (cm <sup>3</sup> ).
$\frac{\Delta \bar{\sigma}}{\bar{\sigma}}$	The change (increase or decrease) in effective stress caused by leakage of air and/or water into or out of a specimen of soil (dimensionless, usually expressed in percent.)
$\frac{\Delta u_w}{\bar{\sigma}}$	The change in pore pressure, usually expressed in percent (dimensionless).
$\epsilon$	Activation energy (gm cm/mole).
$\eta$	Dynamic viscosity (gm sec/cm <sup>2</sup> )
$\lambda$	Mean free path of gas molecules flowing through a membrane (cm)
$\nu$	Vibration frequency of gas molecules in a membrane (sec <sup>-1</sup> ).
$\Pi$	Osmotic pressure (gm/cm <sup>2</sup> ).
$\sigma$	Total stress (kg/cm <sup>2</sup> )
$\bar{\sigma}$	Effective stress (kg/cm <sup>2</sup> ).
$\sigma_c$	Chamber pressure (kg/cm <sup>2</sup> ).
$\bar{\sigma}_c$	Effective consolidation pressure (kg/cm <sup>2</sup> ).
$\sigma_{dmax}$	Maximum deviator stress (= $\bar{\sigma}_1 - \bar{\sigma}_3$ ) (kg/cm <sup>2</sup> ).
$\bar{\sigma}_1$	Effective major principal stress (kg/cm <sup>2</sup> ).
$\frac{\bar{\sigma}_1}{\bar{\sigma}_3}$	Effective principal stress ratio (dimensionless).
$\bar{\sigma}_3$	Effective minor principal stress (kg/cm <sup>2</sup> ).
$\tau$	Shear stress (kg/cm <sup>2</sup> ).
$\chi$	Bishop's "chi" factor defined by the equation: $\bar{\sigma} = \sigma - u_a + \chi u_c$ (dimensionless).

LIST OF REFERENCES

1. ALTY, T. "The Diffusion of Monatomic Gases Through Fused Silica," Philosophical Magazine (London), Seventh Series, vol. 15, 1933, pp. 1035-1048.
2. AMERONGEN, G. J. van. "The Permeability of Different Rubbers to Gases and Its Relation to Diffusivity and Solubility," Journal of Applied Physics, vol. 17, 1946, pp. 972-985.
3. AMERONGEN, G. J. van. "Influence of Structure of Elastomers on their Permeability to Gases," Journal of Polymer Science, vol. 5, 1950, pp. 307-332.
4. ANTROPOFF, A. von. "Die Dynamik osmotischer Zellen. I Vorläufige Mitteilung," Zeitschrift für physikalische Chemie, vol. 76, 1911, pp. 721-731.
5. AUSTIN, A. T., HARTUNG, E. J. and WILLIS, G. M. "Studies in Membrane Permeability, IV. An Improved Apparatus for Determining Diffusion Rates and the Permeability of Copper Ferrocyanide to Eleven Solutes," Transactions Faraday Society, vol. 40, 1944, pp. 520-530.
6. AVERY, S. B. Report to Massachusetts Commissioner of Public Works on Soil Tests for East Boston Express Highway, Federal Aid Project No. UI-241(5). Harvard University, Cambridge, Mass., Sept. 1949. (Unpublished, typewritten.)
7. BARRER, R. M. "Permeation, Diffusion and Solution of Gases in Organic Polymers," Transactions Faraday Society, vol. 35, 1939, pp. 628-643.
8. BARRER, R. M. Diffusion in and through Solids. Cambridge University Press, Cambridge, 1951.
9. BIGELOW, S. L. "The Permeability of Collodion, Gold Beater's Skin, Parchment Paper and Porcelain Membranes," Journal American Chemical Society, vol. 29, 1907, pp. 1675-1692.
10. BINGHAM, E. C. (ed.). "Experimental Investigations upon the Flow of Liquids in Tubes of Very Small Diameter, by J. L. M. Poiseuille," Rheological Memoirs, vol. 1, no. 1, Jan. 1940, pp. 1-97. (Translated from the French by W. H. Herschel.)
11. BISHOP, A. W., ALPAN, I., BLIGHT, G. E. and DONALD, I. B. "Factors Controlling the Strength of Partly Saturated Cohesive Soils," Research Conference on Shear Strength of Cohesive Soils, University of Colorado, Boulder, Colorado, June 1960, pp. 503-532.
12. BISHOP, A. W. and HENKEL, D. J. The Measurement of Soil Properties in the Triaxial Test. Edward Arnold, London, 1962.
13. BJERRUM, N. and MANEGOLD, E. "Ueber Kollodium Membranen," Kolloid-Zeitschrift, vol. 42, 1927, pp. 97-112.
14. BJERRUM, N. and MANEGOLD, E. "Ueber Kollodium Membranen, II. Der Zusammenhang zwischen Membranstruktur und Wasserdurchlässigkeit," Kolloid-Zeitschrift, vol. 43, July 4, 1927, pp. 5-14.
15. BRUBAKER, D. W. and KAMMERMEYER, K. "Separation of Gases by Means of Permeable Membranes, Permeability of Plastic Membranes to Gases," Industrial and Engineering Chemistry-Industrial Edition, vol. 44-1, 1952, pp. 1465-1474.

16. BRUBAKER, D. W. and KAMMERMEYER, K. "Flow of Gases through Plastic Membranes," Industrial and Engineering Chemistry-Industrial Edition, vol. 45, 1953, pp. 1148-1152.
17. CAMPBELL, J. B. "Synthetic Elastomers," Science, vol. 141, no. 3578, July 26, 1963, pp. 329-334.
18. CARMAN, P. C. "Properties of Capillary-Held Liquids," Journal of Physical Chemistry, vol. 57, 1953, pp. 56-64.
19. CARSLAW, H. S. and JAEGER, J. C. Conduction of Heat in Solids. Clarendon Press, Oxford, 1947.
20. CASAGRANDE, A. Notes on Soil Mechanics-First Semester, Harvard University, Cambridge, Mass., Revised Nov. 1939. (Mimeographed.)
21. CASAGRANDE, A. First Progress Report to U.S. Waterways Experiment Station, Vicksburg, Miss. on Cooperative Research on Stress-Deformation and Strength Characteristics of Soils. Harvard University, Cambridge, Mass., June 1940. (Mimeographed.)
22. CASAGRANDE, A. Second Progress Report to U.S. Waterways Experiment Station, Vicksburg, Miss. on Cooperative Research on Stress-Deformation and Strength Characteristics of Soils. Harvard University, Cambridge, Mass., July 1940. (Mimeographed.)
23. CASAGRANDE, A. One-dimensional consolidation test data on Boston Blue Clay from Everett, Mass. Obtained during investigations for the Mystic Power Station of the Edison Electric Co. on Harvard Project No. H75, Cambridge, Mass., 1941. (Unpublished data on file in Harvard Soil Mechanics Laboratory.)
24. CASAGRANDE, A. Third Progress Report to U.S. Waterways Experiment Station, Vicksburg, Mississippi on Cooperative Research on Stress-Deformation and Strength Characteristics of Soils. Harvard University, Cambridge, Mass., May 1941. (Mimeographed.)
25. CASAGRANDE, A. Fifth Progress Report to U.S. Waterways Experiment Station, Vicksburg, Mississippi on Cooperative Research on Stress-Deformation and Strength Characteristics of Soils. Harvard University, Cambridge, Mass., June 1942. (Mimeographed.)
26. CASAGRANDE, A. Seventh Progress Report to U.S. Waterways Experiment Station, Vicksburg, Mississippi on Cooperative Research on Stress-Deformation and Strength Characteristics of Soils. Harvard University, Cambridge, Mass., April 1944. (Mimeographed.)
27. CASAGRANDE, A. Notes on Swelling Characteristics of Clay-Shales. Harvard University, Cambridge, Mass., July 1949. (Mimeographed.)
28. CASAGRANDE, A. "An Unsolved Problem of Embankment Stability on Soft Ground," First Pan-American Conference on Soil Mechanics and Foundation Engineering, Mexico City, Sept. 1959, vol. II, pp. 721-746.
29. CASAGRANDE, A. and CASAGRANDE, L. Report to Metcalf & Eddy, Engineers, on Foundation Investigation for Prudential Center in Boston, Volume I. Harvard University, Cambridge, Mass., March 1958. (Mimeographed.)

30. CASAGRANDE, A., CORSO, J. M. and WILSON, S. D. Report to Waterways Experiment Station on the 1949-1950 Program of Investigation of Effect of Long-Time Loading on the Strength of Clays and Shales at Constant Water Content. Harvard University, Cambridge, Mass., July 1950. (Mimeographed.)
31. CASAGRANDE, A. and HIRSCHFELD, R. C. First Progress Report on Investigation of Stress-Deformation and Strength Characteristics of Compacted Clays. Soil Mechanics Series No. 61, Harvard University, Cambridge, Mass., May 1960.
32. CASAGRANDE, A. and HIRSCHFELD, R. C. Second Progress Report on Investigation of Stress-Deformation and Strength Characteristics of Compacted Clays. Soil Mechanics Series No. 65, Harvard University, Cambridge, Mass., April 1962.
33. CASAGRANDE, A. and SHANNON, W. L. Research on Stress-Deformation and Strength Characteristics of Soils and Soft Rocks Under Transient Loading. Soil Mechanics Series No. 31, Harvard University, Cambridge, Mass. June 1948. (Appendix F.)
34. CASAGRANDE, A. and WILSON, S. D. Investigation of Effect of Long-Time Loading on the Strength of Clays and Shales at Constant Water Content. Harvard University, Cambridge, Mass., July 1949. (Appendix III.)
35. CASAGRANDE, A. and WILSON, S. D. Report to Waterways Experiment Station on Triaxial Research Performed During 1950-1951. Harvard University, Cambridge, Mass., 1951. (Appendix II.)
36. CASAGRANDE, A. and WILSON, S. D. Effects of Stress History on the Strength of Clays. Soil Mechanics Series No. 43, Harvard University, Cambridge, Mass., June 1953.
37. DARCY, H. Les Fontaines Publiques de la Ville de Dijon. Victor Dalmont, Éditeur, Paris, 1856, pp. 570 and 590-594.
38. DAVIS, D. W. "Isostatic Method for Determining the Gas Permeability of Sheet Materials," Paper Trade Journal, vol. 123, no. 9, Aug. 29, 1946, pp. 33-40.
39. DAYNES, H. A. "The Process of Diffusion through a Rubber Membrane," Proceedings of the Royal Society of London, Series A, vol. 97, 1920, pp. 286-307.
40. DENBIGH, K. G. "Thermo-osmosis of Gases through a Membrane," Nature, vol. 163, 1949, p. 60.
41. DORSEY, N. E. Properties of Ordinary Water-Substance. Reinhold, New York, 1940.
42. DOTY, P. M., AIKEN, W. H. and MARK, H. "Water Vapor Permeability of Organic Films," Industrial and Engineering Chemistry - Analytical Edition, vol. 16, 1944, pp. 686-690.
43. DUCLAUX, J. and ERRERA, J. "Der Mechanismus der Ultrafiltration," Kolloid-Zeitschrift, vol. 38, 1926, pp. 54-57.
44. DUSHMAN, S. Scientific Foundations of Vacuum Technique. Wiley, New York, 1962.
45. EINSTEIN, A. Investigations on the theory of the brownian movement. Dover, 1956. (Translated from the German by A. D. Cowper.)

46. ELFORD, W. J. "Principles Governing the Preparation of Membranes having Graded Porosities. The Porosities of 'Gradocol' Membranes as Ultrafilters," Transactions Faraday Society, vol. 33, 1937, pp. 1094-1104.
47. FERRIS, W. R. Report to Stuart B. Avery, Jr. on Laboratory Investigation of Soil Samples from the Site of the Proposed Boston Arts Center. Harvard University, Cambridge, Mass., March 1959. (Typewritten.)
48. POST, R. B. Development of Equipment for Clay Swelling Tests. Thesis for Master of Architectural Engineering, Oklahoma State University, Stillwater, May 1962. (Multilithed.)
49. GOGGIN, W. C. and LOWRY, R. D. "Vinylidene Chloride Polymers," Symposium on Recent Progress in High Polymer Plastics, Paint, Varnish and Plastics Division, American Chemical Society, March 18, 1942, pp. 1-23.
50. GRACE, H. Letter to Goodyear Tire and Rubber Company, July 27, 1939.
51. de GROOT, S. R. and MAZUR, P. Non-Equilibrium Thermo-Dynamics. Interscience, New York, 1962.
52. GUEROUT, A. "Sur les dimensions des intervalles poreux des membranes," Comptes Rendus des Séances de l'Academie des Sciences de l'Institut de France, vol. 75, 1872, pp. 1809-1812.
53. HANSBO, S. "Consolidation of Clay, with Special Reference to Influence of Vertical Sand Drains," Proceedings Swedish Geotechnical Institute, no. 18, 1960, pp. 1-160.
54. HAUSSLER, R. W. and WARLAM, A. A. Appendix III of Seventh Progress Report to U.S. Waterways Experiment Station, Vicksburg, Mississippi on Cooperative Research on Stress-Deformation and Strength Characteristics of Soils. Harvard University, Cambridge, Mass., April 1944. (Mimeographed.)
55. HEILMAN, W., TAMMELA, V., MEYER, J. A., STANNETT, V. and SZWARC, M. "Permeability of Polymer Films to Hydrogen Sulfide Gas," Industrial and Engineering Chemistry-Industrial Edition, vol. 48, 1956, pp. 821-824.
56. HILF, J. W. An Investigation of Pore-Water Pressure in Compacted Cohesive Soils. Technical Memorandum 654, U.S. Bureau of Reclamation, Denver, October, 1956.
57. HIRSCHFELD, R. C. The Constant Volume Strength of Clays. Ph.D. Thesis, Harvard University, Cambridge, Mass., June 1958. (Typewritten.)
58. HIRSCHFELD, R. C. Data on leakage through membranes, Harvard University, Cambridge, Mass., 1960. (Unpublished, on file in Harvard Soil Mechanics Laboratory.)
59. HODGMAN, C. D. (ed.) Handbook of Chemistry and Physics, 43rd Edition. Chemical Rubber, Cleveland, 1962.
60. JENNINGS, J. E. B. and BURLAND, J. B. "Limitations to the Use of Effective Stresses in Partly Saturated Soils," Geotechnique, vol. 12, June 1962, pp. 125-144.
61. KEENAN, J. H. Thermodynamics. Wiley, New York, 1952.
62. KNUDSEN, M. Kinetic Theory of Gases. Methuen, London, 1950.

63. KOENIG, A. C. "Dams on Sand Foundations: Some Principles Involved in their Design, and the Law Governing the Depth of Penetration Required for Sheet-Piling," Transactions ASCE, vol. 73, 1911, pp. 175-189. (See Allen Hazen's discussion on pp. 199-203 and Koenig's closure on pp. 208-224.)
64. LAIDLER, K. J. and SHULER, K. E. "The Kinetics of Membrane Processes, I. The Mechanism and the Kinetic Laws for Diffusion through Membranes," Journal of Chemical Physics, vol. 17, 1949, pp. 851-860.
65. LAMBE, T. W. "Residual Pore Pressures in Compacted Clay," Proceedings Fifth International Conference on Soil Mechanics and Foundation Engineering, Paris, 1961, vol. 1, pp. 207-211.
66. LA MER, V. K. Retardation of Evaporation by Monolayers: Transport Processes. Academic Press, New York, 1962.
67. LANDIS, E. M. "Micro-injection Studies of Capillary Permeability," American Journal of Physiology, vol. 82, Oct. 1, 1927, pp. 217-238.
68. LOEB, L. B. The Kinetic Theory of Gases. McGraw Hill, New York, 1934.
69. MANEGOLD, E. and HOFMANN, R. "Ueber Kolloidium membranen IV," Kolloid-Zeitschrift, vol. 50, 1930, pp. 22-39.
70. MARSAL, R. J. and MAZARI, M. "El Subsuelo de la Ciudad de Mexico," First Pan-American Conference on Soil Mechanics and Foundation Engineering, University of Mexico, Mexico City, September 1959. (See Parte A-Estratigrafia y Propiedades.)
71. METSCHL, J. "The Supersaturation of Gases in Water and Certain Organic Liquids," Journal of Physical Chemistry, vol. 28, 1924, pp. 417-437.
72. MICHAELS, A. S. and BIXLER, H. J. Flow of Gases through Polyethylene. M.I.T. Dept. of Chemical Engineering, Sept. 1960, pp. 1-35. (Multilithed preprint for publication in the Journal of Polymer Science.)
73. MICHAELS, A. S., VIETH, W. R. and BARRIE, J. A. Solution of Gases in Polyethylene Terephthalate. Annual Meeting of American Physical Society, Division of High Polymer Physics, March 27 to 30, 1962, pp. 1-42. (Multilithed preprint.)
74. MOORE, W. J. Physical Chemistry. Prentice-Hall, Englewood Cliffs, New Jersey, 1962.
75. MORELAND, R. E. Osmotic Flow through Natural Latex Membranes. Research Report for Engineering 362, Harvard University, Cambridge, Mass., Spring Term 1957. (Typewritten.)
76. MUSKAT, M. The Flow of Homogeneous Fluids through Porous Media. Edwards, Ann Arbor, 1946.
77. MYSELS, K. J. Introduction to Colloid Chemistry. Interscience, New York, 1959.
78. NORTHRUP, J. H. "The Kinetics of Osmosis," Journal of General Physiology, vol. 10, Apr. 27, 1927, pp. 883-892.
79. OLSEN, H. W. Hydraulic Flow through Saturated Clays. Ph.D. Thesis, M.I.T., Feb. 1961. (Multilithed.)

80. OSWIN, C. R. "The Permeability of Transparent Wrappings," Journal Society of the Chemical Industry (London), April 1943, pp. 45-48.
81. PAPPENHEIMER, J. R. "Passage of Molecules through Capillary Walls," Physiological Reviews, vol. 33, 1953, pp. 387-423.
82. PAPPENHEIMER, J. R. and SOTO-RIVERA, A. "Effective Osmotic Pressure of the Plasma Proteins and other Quantities Associated with Capillary Circulation in the Hindlimbs of Cats and Dogs," American Journal of Physiology, vol. 152, 1948, pp. 471-491.
83. PARCHER, J. V. Letter to S. J. Poulos dated Dec. 5, 1960. (Typewritten.)
84. PONDER, E. "The Physical Structure of the Red Cell Membrane, with Special Reference to its Shape," Transactions Faraday Society, vol. 33, 1937, pp. 947-954.
85. PRESENT, R. D. Kinetic Theory of Gases. McGraw Hill, New York, 1958.
86. RENKIN, E. M. "Filtration, Diffusion and Molecular Sieving through Porous Cellulose Membranes," Journal of General Physiology, vol. 38, 1954, pp. 225-243.
87. ROSENBERG, T. "The Concept and Definition of Active Transport," Symposia of the Society for Experimental Biology, Number VIII, Active Transport and Secretion, Academic Press, New York, 1954, pp. 26-41.
88. RUTLEDGE, P. C. Compression Characteristics of Clays and Application to Settlement Analyses. Sc.D. Thesis, Harvard University, Cambridge, Mass., April 25, 1939. (Typewritten.)
89. SCHUMACHER, E. E. and FERGUSON, L. "Diffusion of Water through Rubber," Industrial and Engineering Chemistry-Industrial Edition, vol. 21, 1929, pp. 158-162.
90. SEED, H. B., MITCHELL, J. K. and CHAN, C. K. "The Strength of Compacted Cohesive Soils," Research Conference on Shear Strength of Cohesive Soils, University of Colorado, Boulder, June 1960, pp. 877-964.
91. SEIDELL, A. Solubilities of Inorganic and Metal Organic Compounds. Van Nostrand, New York, 1940.
92. SHERWOOD, T. K. "Obtaining Water by Desalinization," Technology Review, M.I.T., April 1963, pp. 17-20 and 42.
93. SKIENS, W. E. and MAHON, H. I. Permeation Rate Constants for Water and Salt Flux through Synthetic Membranes. 141st Meeting of American Chemical Society, Division of Colloid and Surface Chemistry, Washington, D.C., March 21-29, 1962, pp. 1-14 (Multilithed preprint.)
94. STAMBERGER, P. The Colloid Chemistry of Rubber. Oxford University Press, London, 1929.
95. STARLING, E. H. "On Absorption of Fluids from the Connective Tissue Spaces," Journal of Physiology, vol. 19, May 5, 1896, pp. 312-326.
96. STAVERMAN, A. J. "The Theory of Measurement of Osmotic Pressure," Recueil travaux chimiques des Pays-Bas, vol. 70, 1951, pp. 344-352.
97. STEIN, W. D. and DANIELLI, J. F. "Structure and Function in Red Cell Permeability," Discussions Faraday Society, vol. 21, 1956, pp. 238-251.

98. STEINHERZ, H. A. and REDHEAD, P. A. "Ultrahigh Vacuum," Scientific American, March 1962, pp. 78-90.
99. TAYLOR, D. W. Fundamentals of Soil Mechanics. Wiley, New York, 1948.
100. TAYLOR, R. L., HERMANN, D. B. and KEMP, A. R. "Diffusion of Water through Insulating Materials," Industrial and Engineering Chemistry-Industrial Edition, vol. 28, 1936, pp. 1255-1263.
101. TEORELL, T. "Transport Phenomena in Membranes (Eighth Spiers Memorial Lecture)," Discussions Faraday Society, vol. 21, 1956, p. 9-26.
102. TERZAGHI, K. and PECK, R. B. Soil Mechanics in Engineering Practice. Wiley, New York, 1948.
103. WAACK, R. A., FRISCH, N. H., STANNETT, V. and SZWARC, M. "Permeability of Polymer Films to Gases and Vapors," Industrial and Engineering Chemistry-Industrial Edition, vol. 47, 1955, pp. 2524-2527.
104. WARLAM, A. A. Stress-Strain and Strength Properties of Soils. Ph.D. Thesis, Harvard University, Cambridge, Mass., May 1, 1946. (Typewritten.)
105. WARLAM, A. A., Private conversation with S. J. Poulos, May 2, 1963.
106. WASHBURN, E. W. (ed.). International Critical Tables of Numerical Data. McGraw Hill, New York, 1926.
107. WILSON, N. Report on Research Carried out by Nyal E. Wilson during the Fall Semester of 1958. Harvard University, Cambridge, Mass., 1958. (Typewritten.)
108. WISEMAN, G. Notes on Leakage through Rubber membranes. Israel Institute of Technology, Haifa, Israel, 1961. (Typewritten manuscript on work carried out at Harvard University in the summer of 1954.)
109. WISSA, A. E. Z. The Effect of Water on the Permeability of Rubber Latex Films to Nitrogen. Term report for course No. 1-43, M.I.T., Cambridge, Mass., 1962. (Typewritten.)
110. WROBLEWSKI, S. von. "Ueber die Natur der Absorption der Gase," G. Wiedemann Annalen der Physik und Chemie, Neue Folge, vol. 8, no. 2, 1879, pp. 29-52.

References for which names of authors are not given

111. "Curing Blankets Hold Moisture," Construction Methods and Equipment, July 1963, p. 145.
112. Tables of Thermal Properties of Gases. Circular 564, U.S. Department of Commerce, Bureau of Standards, Nov. 1, 1955.
113. The Unified Soil Classification System. Technical Memorandum No. 3-357, U.S. Army Corps of Engineers, Waterways Experiment Station, Vicksburg, Miss., March 1953.

TABLE 2-1

INITIAL SWELLING RATIO OF VARIOUS SOILS

Name of Soil and Source of Data	Initial Effective Stress $\sigma_1$ (kg/cm <sup>2</sup> )	Initial Void Ratio $e$ (-)	Estimated Initial Swelling Ratio* $S_c$ (-)	Name of Soil and Source of Data	Initial Effective Stress $\sigma_1$ (kg/cm <sup>2</sup> )	Initial Void Ratio $e$ (-)	Estimated Initial Swelling Ratio* $S_c$ (-)
Caddoa Loess (24)	4	0.609	0.002	Boston Blue Clay (29)	57	0.540	0.017
Canyon Dam Clay (32)	21	0.333	0.007		15	0.634	0.007
	16	0.365	0.006		15	0.676	0.007
	21	0.355	0.006		15	0.765	0.015
	21	0.407	0.003		9.9	0.865	0.010
	16	0.400	0.007**	Organic Clay Panama (88)	17	0.795	0.009
	16	0.405	0.005**	Organic Clay Boston (88)	22	0.732	0.010
	16	0.379	0.005**		4.8	2.59	0.02
	21	0.366	0.003	Organic Clay (88)	1.4	1.051	0.02
	21	0.366	0.002	Organic Silt (6)	17		0.016
	21	0.344	0.002	Highly Organic Peaty Silt (6)	17		0.03
Canyon Dam Clay (Appendix D)	2	0.410	0.0010**	Varved Clay, Springfield (34)	46	0.601	0.019
	6	0.375	0.0012**		46	0.641	0.02
	14	0.348	0.0015**	Mexico City Clay (88)	1.60	10.0	0.02
Hard Clay, Philadelphia (88)	7	0.462	0.007		4.25	5.11	0.03
Clay, Guadalupe, Texas (88)	12	0.648	0.008		4.30	6.32	0.03
Clay, Cairo, Egypt (88)	17	0.694	0.008		4.80	5.34	0.03
Hard Clay, Boston (88)	17	0.551	0.008		8.40	4.63	0.05
Soft Laurentian Clay (26)	38	0.741	0.005		11.0	1.125	0.02
	44	0.775	0.002		13.8	3.32	0.04
	43	0.782	0.009		17.0	2.72	0.03
Chicago Blue Clay (88)	11	0.583	0.010		50.0	1.63	0.016
	15	0.502	0.006	Mexico City Clay (70)	8.0	2.30	0.05
	11	0.515	0.008		8.0	2.60	0.014
	11	0.582	0.009		8.0	1.90	0.04
Detroit Blue Clay (88)	16	0.423	0.010		8.0	2.00	0.05
	18	0.772	0.017		8.0	2.15	0.03
Boston Blue Clay (88)	21	0.771	0.02	Midway Shale, Little Rock (27)	16	0.732	0.03
	21	0.712	0.014		8.0	0.862	0.018
	21	0.628	0.018	Bearpaw Clay-Shale (27)	16	0.592	0.03
	21	0.544	0.017	Peat, Newfoundland (99)	8.0	3.6	0.08
	21	0.418	0.019	Peat, East Boston (47)	4.3	5.6	0.09
	21	0.604	0.02		7.6	5.87	0.04
	21	0.763	0.03		7.6	6.53	0.04
Boston Blue Clay (23)	37	0.467	0.014	Peat, East Boston (6)	17		0.07
	39	0.540	0.003		17		0.10
	44	0.528	0.013		17		0.09
Boston Blue Clay (57)	23	0.896	0.002		17		0.09
	17	0.600	0.008		17		0.07

\* Calculated by the author from swelling curves obtained in consolidation tests reported in the literature cited.

\*\* Data obtained from triaxial swelling tests using a hydrostatic effective stress equal to that tabulated under  $\bar{\sigma}_1$  in the table. All other data are from one-dimensional swelling tests.

TABLE 2-2

LEAKAGE REQUIRED TO CAUSE 2% DECREASE IN EFFECTIVE STRESS

(For 100% saturated specimens with a total volume of 90 cm<sup>3</sup>)

Soil	Swelling Ratio* $S_c$ (-)	Volume of Leakage to Cause 2% Decrease $J_w$ (mm <sup>3</sup> )	Rate of Leakage to Cause 2% Decrease (mm <sup>3</sup> /day)	
			7 day Test	100 day Test
Canyon Dam Clay	0.001	2	0.3	0.02
Hard Clays	0.007	13	2	0.13
Boston Blue Clay Chicago Clay	0.015	27	4	0.27
Bearpaw Clay-Shale Mexico City Clay	0.03	54	7.7	0.54

\* From Table 2-1

TABLE 2-3

ERRORS INTRODUCED BY SIMPLIFYING ASSUMPTIONS

No.	Simplifying assumption*	Values of the parameters required to calculate the error** in $\Delta\bar{\sigma}_3/\bar{\sigma}_3$ for the "Extreme Example"						Magnitude of error	
		S (-)	n (-)	$C_w$ (%)	$\frac{\Delta\bar{\sigma}_3}{\bar{\sigma}_3}$ (%)	$\bar{\sigma}_3$ (kg/cm <sup>2</sup> )	$u_a$	Extreme Example	Typical Example
1	$\Delta u_a = -\Delta\bar{\sigma}_3$	0.0015	0.37	90	-0.1	0.25	1.0	+47	+0.4
2	Boyle's law is exact	0.0015	0.37	90	-0.1	20	-	+15	+0.2
3	Water is incompressible	0.0015	0.37	100	-	20	-	+23	+1.0
4	Volume increase of water due to solution of air is zero	0.0015	0.37	99.9	-	20	-	-10	-0.4
5	Henry's law is exact	0.0015	0.37	99.9	-0.1	20	10	-6	-1.1
6	Swelling curve is a straight line	-	-	-	0 to -10	-	-	***	~±5
7	Mineral grains are incompressible	0.0015	-	-	-	20	-	+3	+0.1
8	Membranes do not flex	-	-	100	-	-	-	****	0+
	Values of parameters for "Typical Example"	0.013	0.43	98	-5	6	6		

\* See 2-07(a) for qualitative description of assumptions.

\*\* Positive error means calculated value of  $\Delta\bar{\sigma}_3/\bar{\sigma}_3$  is conservative, i.e. too high.

\*\*\* Can not be evaluated because accurate swelling data are not available.

\*\*\*\* Generally will be negligible for fine-grained soils (see C-04).

TABLE 3-1

SOME USES OF MEMBRANES

In Animal, Fish and Plant Life

The human lungs, capillary walls, skin, leaves of plants etc. are only a few examples of membranes in living systems each of which performs a special function. Teorell (101) has described the biological membrane as "the fundamental unit of transport in our human body."

For Purification and Filtration

Ion-selective and ion exchange membranes are used for water desalination and purification. Ion-selective membranes have been suggested for separating a mixture of gases into its pure components (15). Chemists, biologists and physiologists use specially prepared membranes which will pass a certain sized colloid or molecule but will retain all larger particles in a mixture or solution (46).

For Prevention of Evaporation

Membranes are used in food packaging to prevent the food from losing its water by evaporation (80). Researchers are attempting to find suitable chemicals which will form thin surface films on reservoirs behind dams. Such films would prevent loss of water by evaporation but would permit oxygen to pass freely so that fish life would not be killed (66). Plastic membranes are used to prevent loss of water by evaporation from concrete while it is setting.

For Waterproofing

Wood, metal and textile surfaces are coated or impregnated with thin plastic membranes for water proofing. Electrical cables are insulated from water by plastic membrane coverings.

Miscellaneous Uses

- Balloons and tires
- Molecular weight determination by osmotic pressure measurement
- Wind breaks in construction
- Water reservoir linings
- Triaxial testing

TABLE 3-2

VARIABLES THAT MIGHT AFFECT THE RATE OF FLOW OF FLUIDS THROUGH MEMBRANES

A. The Properties of the Membrane

1. Size, shape, length, number and distribution of openings in structure or between molecules or groups of molecules.
2. Electrical charge on exterior and interior surfaces.
3. Availability of sites for adsorption of permeant molecules or ions.

NOTE: The age, prior treatment, ambient pressure and temperature of the membrane may all affect its properties.

B. The Properties of the Permeant

1. Ambient pressure, temperature and composition of permeant.
2. Size, weight and shape of permeating particles.
3. Electrical charge of colloidal particles or dissolved ions.
4. Strength of inter- and intra-particle forces.

C. The Magnitude of the Driving Force

1. Ambient temperature and temperature difference across membrane.
2. Pressure difference.
3. Mole fraction difference.
4. Electrical potential difference.
5. Others (magnetic field difference).

TABLE 4-1

SUMMARY OF W TESTS ON NATURAL RUBBER MEMBRANES  
(Manufactured by Julius Schmid Co.)

Test Number	Treatment	Hydraulic Pressure Difference ( $\Delta p$ ) kg/cm <sup>2</sup>	Membrane Thickness (L) (cm)	LP <sup>1</sup> Flow (q) (mm <sup>3</sup> /day)	L <sup>2</sup> Flow (mm <sup>3</sup> /day)	Total Outflow (LP+L) (mm <sup>3</sup> /day)	Total Inflow (HP) (mm <sup>3</sup> /day)	Duration of Test (days)	Permeability constants		Figure Number
									(k) (cm/sec)	(K) (cm <sup>4</sup> /gm sec)	
W1	Water	6.00	.0057	1.84	0.60	2.44	1.38	66	$5.2 \times 10^{-16}$	$1.7 \times 10^{-11}$	E-1
W2	water	6.00	.0071	1.57	1.89	3.46	2.10	47	5.6	1.3	E-2
W3	Water	2.01	.0064	0.69	-0.02	0.67	0.66	31	6.6	2.2	E-3
W4	Oil	2.00	.0064	0.71	1.10	1.81	-0.16	27	6.3	2.3	E-4
W5	oil	1.36	.0061	0.96	1.32	2.28	2.36	23	9.5	3.0	E-5
W6 <sup>3</sup>	Water	6.00	.0073	0.63	0.62	1.30	0.82	59	$2.6 \times 10^{-15}$	$0.9 \times 10^{-11}$	E-6
W7(a) <sup>4</sup>	Water	11.5	.0061	3.15	-0.06	3.09	3.21	7.1	5.0	1.7	E-7
(b)	Water	6.00	.0061	1.52	-0.02	1.50	1.54	10	4.7	1.5	E-8
(c)	Water	2.00	.0061	0.52	-0.02	0.50	0.52	9.0	4.8	1.6	E-9
(d)	Water	11.5	.0061	3.06	0	3.06	3.07	7.9	4.9	1.6	E-10
W6	Water	2.00	.0067	0.24	-0.46	-0.23	0.26	57	2.5	0.5	E-11

<sup>1</sup> Permeated area of membrane = 33.2 cm<sup>2</sup>.

<sup>2</sup> Negative flow means meniscus moving toward permeability cell.

<sup>3</sup> Same membrane as for test W6.

<sup>4</sup> Same membrane as for test W7. Tests W7 (a)-(d) on same membrane.

TABLE 5-1

SUMMARY OF X TESTS ON NATURAL RUBBER MEMBRANES  
(Membranes manufactured by Julius Schmid Co.)

Test Number	Treatment of Membrane	Measured Rates of Flow <sup>2</sup>		Specific Gravity of Salt Solution <sup>1</sup>	Membrane Thickness (L) cm	Corrected Rate of Outflow (q) mm <sup>3</sup> /day	Mole Fraction of NaCl (X) -	Molarity of NaCl moles/l.	Vapor Pressure Difference ( $\Delta p_v$ ) gm/cm <sup>2</sup>	Permeability constant (K) cm <sup>4</sup> /gm sec	Figure Number
		Inflow mm <sup>3</sup> /day	Outflow mm <sup>3</sup> /day								
X1(a)	Water	2.1	2.1	1.0140	0.0070	2.2	0.0068	0.33	0.50	$1.68 \times 10^{-11}$	F-1
X1(b)	Water	5.5	5.5	1.0376	0.0070	5.6	0.0175	0.97	1.36	1.67	F-2
X1(c)	Water	26.7	23.0	1.1433	0.0070	23.1	0.0719	3.95	6.86	1.37	F-3
X1(d)	Water	3.0	2.1	1.0140	0.0070	2.2	0.0068	0.38	0.50	1.68	F-4
X2	Water	5.6	5.6	1.0363	0.0064	5.7	0.0168	0.93	1.32	1.60	F-5
X3	Water	34.0	33.0	1.1191	0.0055	33.1	0.0567	3.13	4.65	2.26	F-6
X4	Water	18.0	17.4	1.1475	0.0074	17.5	0.0711	3.91	6.80	1.06	F-7
X5	Water	32.0	31.0	1.1495	0.0061	31.1	0.0719	3.96	6.90	1.59	F-8
X6	silicone	29.0	24.0	1.1455	0.0058	24.1	0.0698	3.84	6.63	1.21	F-9
X7	oil	30.7	28.3	1.1480	0.0062	28.4	0.0715	3.93	6.85	1.49	F-10

<sup>1</sup> Corrected to 20°C.

<sup>2</sup> All tests performed at 30°C. Permeated area of membrane = 20.0 cm<sup>2</sup>.

<sup>3</sup> Used same membrane as used for tests W7 and V7. (Results of V tests are presented in Chapter 6.)

TABLE 5-2

COMPARISON OF K VALUES FROM W TESTS  
WITH K VALUES FROM X TESTS

Test Number	Membrane Thickness (L) cm	Permeability in W Tests* (K) cm <sup>4</sup> /gm sec	Test Number	Membrane Thickness (L) cm	Permeability in X Tests** (K) cm <sup>4</sup> /gm sec	Ratio	
						K (W Tests)	K (X Tests)
W6	0.0073	$0.9 \times 10^{-11}$	X4	0.0074	$1.1 \times 10^{-11}$	0.82	
W2	0.0071	1.8	X1(a)	0.0070	1.7	1.06	
W3	0.0064	2.2	X2	0.0064	1.6	1.37	
W7	0.0061	1.6	X5	0.0061	1.6	1.00	
W1	0.0057	1.7	X3	0.0055	2.3	0.74	

\* From Table 4-1

AVERAGE RATIO = 1.05

\*\* From Table 5-1

TABLE 5-3

COMPARISON OF RATE OF WATER FLOW  
CAUSED BY MOLE FRACTION DIFFERENCES  
WITH THAT CAUSED BY HYDRAULIC PRESSURE DIFFERENCES

Mole Fraction Difference	Rate of Flow* mm <sup>3</sup> /day/cm <sup>2</sup>	Hydraulic Pressure Difference kg/cm <sup>2</sup>	Rate of Flow** mm <sup>3</sup> /day/cm <sup>2</sup>	Ratio of Mole Fraction Flow to Pressure Flow -
0.009 (Sea Water)	0.19	1	0.0070	27
		10	0.070	2.7
0.06 (Water from Great Salt Lake)	1.30	1	0.0070	185
		10	0.070	18.5

\*Flow of water through one natural rubber membrane with a thickness of 0.0061 cm. Based on results of test X5.

\*\*Flow of water through one natural rubber membrane with a thickness of 0.0061 cm. Based on results of test W7(d).

TABLE 6-1

MEMBRANES TESTED				
Trade Name	Supplier	Chemical Name	Manufacturer's Number or Designation	Manufacturing Process
Natural Rubber	(a) Julius Schmid, Inc. New York, New York	Polyisoprene	Ramses 19	Rubber cement process
	(b) Soil Test, Inc. Chicago, Illinois	Polyisoprene	T632	Dipped on mandrel
	(c) Test Lab, Inc. New York, New York	Polyisoprene	Not known	Not known (probably dipped)
	(d) E. F. Mahady Co. Surgical Supplies Boston, Massachusetts	Polyisoprene	Pale Crepe	Calendered, open steam cured
Polyethylene	(a) Dow Chemical Co. Midland, Michigan	Polyethylene-ethyl acrylate	QX-4333.1	Extruded blown film
	(b) Chippewa Plastics Co. Chippewa Falls, Wisconsin	Polyethylene copolymer	SF-444	Blown film process
	(c) E.I. DuPont de Nemours & Co., Inc. Film Department Wilmington, Delaware	Polyethylene	100 B 301	Extruded (blown film or fiat die)
	(d) Food Film, Inc. Pine Brook, New Jersey	Polyethylene, density = 0.915	Flat, gusseted 2" tubing	
Polypropylene	Enjay Chemical Co. New York, New York	Polypropylene	CD-26 BH4	Extruded and cooled by chill roll technique
Teflon	E.I. DuPont de Nemours & Co., Inc.	Fluorinated ethylene-propylene	50A, 100A	Calendered
Kel F	W. S. Shamban & Co. Culver City, California	Polytetrafluoro-chloroethylene	Califilm	Not known
Kynar	Pennsalt Chemicals Corp. Philadelphia, Pennsylvania	Vinylidene fluoride	None given	Cast
Texin	Mobay Chemical Co. Pittsburgh, Pennsylvania	Polyurethane	192A	Blown film
Fluorel	International Packings Corp.	Fluorocarbon rubber	Sample	Dipped
Butyl rubber	(a) Carlisle Corp. Carlisle Tire & Rubber Division Carlisle, Pennsylvania	Polyisobutylene isoprene	Sure Seal, 20 gauge	Pasticized calendered, open steam cured
	(b) Chase & Sons, Inc. Randolph, Massachusetts	Polyisobutylene isoprene	C-253-V Tape	Calendered, vulcanized
	(c) Quartermaster Research & Engineering Command U. S. Army Natick, Massachusetts	Polyisobutylene isoprene	Sample	Pressed and cured
Neoprene	Dewey and Almy Chemical Div. W. R. Grace & Co. Boston, Massachusetts	Chlorobutadiene	N750, Weather balloon	Dipped
Koroseal	B. F. Goodrich Company Akron, Ohio	Polyvinyl chloride	None given	Plasticized, calendered

TABLE 6-2

SUMMARY OF V TESTS ON NATURAL RUBBER

Test Number	Source of Membrane	Treatment	Vapor Pressure Difference	Membrane Thickness	Corrected Flow*	HP Flow	L Flow	Permeability constant	Figure Number
			( $\Delta p_v$ ) gm/cm <sup>2</sup>	(L) cm	(q) mm <sup>3</sup> /day	mm <sup>3</sup> /day	mm <sup>3</sup> /day	(K) cm <sup>4</sup> /gm sec	
V1	Schmid	None	42.9	0.0062	278	262	16	1.2x10 <sup>-11</sup>	E-12
V2	Schmid	None	43	0.0056	231	231	0.2	0.9	E-13
V3	Schmid	None	43	0.0062	240	240	-0.4	1.0	E-14
V4	Schmid	None	43.2	0.0119	149	149	-	1.2	E-15
V5	Schmid	None	43.2	0.0234	76	76	-	1.2	E-16
V6	Schmid	Water	43	0.0073	101	101	-3.2	0.5	E-17
V7	Schmid	Water	43.0	0.0061	203	203	0	0.9	E-18
V8	Schmid	Silicone	43.0	0.0058	256	256	-1.6	1.0	E-19
V9	Schmid	Oil	43.0	0.0070	228	228	-3.1	1.1	E-20
V10	Schmid	Vacuum	43	0.0080	121	110	11	0.7	E-21
V11	Schmid	Pump	42	0.0081	124	118	6	0.7	E-22
V12	Schmid	Oil	43.0	0.0083	105	95	10	0.5	E-23
V13	Test Lab	None	42.2	0.0330	56	55	1.1	1.3	E-24
V14	Test Lab	None	41	0.0347	51	51	-0.4	1.3	E-25
V15	Mahady	None	43.0	0.0206	82	82	-1.2	1.2	E-26
V16	Mahady	None	42.7	0.0235	72	71	1.0	1.2	E-27
V17	Soil Test	None	43.1	0.0275	74	74	-2.0	1.4	E-28
V18	Soil Test	None	43.1	0.0309	65	65	0.3	1.4	E-29

\*Corrected flow = HP flow plus L flow if L flow is positive,  
= HP flow alone if L flow is negative.

Permeated area of membrane is 38.2 cm<sup>2</sup> in all cases. Tests performed at 30°C.

TABLE 6-3

SUMMARY OF V TESTS ON SYNTHETIC RUBBERS AND PLASTICS

Test Number	Membrane*	Vapor Pressure Difference	Membrane Thickness	Corrected Flow**	HP Flow	L Flow	Permeability constant	Figure Number
		( $\Delta p_v$ ) gm/cm <sup>2</sup>	(L) cm	(q) mm <sup>3</sup> /day	mm <sup>3</sup> /day	mm <sup>3</sup> /day	(K) cm <sup>4</sup> /gm sec	
V19	Butyl rubber (a)	43.0	0.0552	0.5	0.46	0.06	0.019x10 <sup>-11</sup>	E-30
V20	(a)	43.0	0.0546	0.5	0.50	-0.09	0.019	E-31
V21	(b)	43.1	0.0292	1.6	1.60	0	0.033	E-32
V22	(b)	43.2	0.0289	1.4	1.44	0	0.028	E-33
V23	(c)	43.2	0.0212	2.2	2.20	0	0.033	E-34
V24	(b)	43.2	0.0208	2.4	2.37	-0.5	0.034	E-35
V25	Fluorel	42.0	0.0258	14.9	14.9	-0.5	0.30	E-36
V26	Kel-F	43.1	0.0032	0.7	0.67	0	0.0016	E-37
V27	Kel-F	43.1	0.0032	0.7	0.68	0	0.0016	E-38
V28	Koroseal	43.1	0.0100	85.1	85.1	-0.3	0.60	E-39
V29	Kynar	43.1	0.0069	29.0	29.0	-0.7	0.14	E-40
V30	Kynar	43.1	0.0066	28.0	28.0	0	0.13	E-41
V31	Neoprene rubber	43.0	0.0140	260	260	-2.1	2.7	E-42
V32	Neoprene rubber	43.0	0.0135	272	272	0	2.6	E-43
V33	Polyethylene (a)	42.8	0.0038	177	177	-3.4	0.48	E-44
V34	(a)	43.1	0.0029	222	222	-4.4	0.45	E-45
V35	(b)	43.0	0.0030	206	200	6.2	0.44	E-46
V36	(b)	42.8	0.0027	210	200	10.4	0.40	E-47
V37	(c)	43.0	0.0026	42.5	42.5	0	0.078	E-48
V38	(c)	43.0	0.0025	43.8	42.5	1.3	0.077	E-49
V39	(d)	43	0.0012	51.3	51.3	-1.6	0.043	E-50
V40	(d)	41.6	0.0012	52	52	-22	0.045	E-51
V41	Polypropylene	43.1	0.0027	20.7	20.7	-0.2	0.039	E-52
V42	Polypropylene	43.1	0.0024	21.4	20.8	0.6	0.041	E-53
V43	Polypropylene	43.1	0.0024	22.5	22.4	0.1	0.038	E-54
V44	Polypropylene	43.1	0.0024	22.1	22.1	0	0.037	E-55
V45	Teflon	43.1	0.0028	6.4	6.3	0.1	0.013	E-56
V46	Teflon	43.1	0.0028	9.4	9.1	0.3	0.018	E-57
V47	Teflon	43.1	0.0012	16.4	16.4	0	0.014	E-58
V48	Teflon	43.1	0.0012	18.8	18.5	0.3	0.016	E-59
V49	Teflon	42.6	0.0012	15.6	14.4	1.2	0.013	E-60
V50	Texin	43.0	0.0066	905	904	1.4	4.2	E-61
V51	Texin	41.7	0.0060	956	956	0	4.2	E-62

\*See Table 6-1 for sources of membranes.

\*\*Corrected flow = HP flow plus L flow if L flow is positive,  
= HP flow alone if L flow is negative.

Permeated area of membrane is 38.2 cm<sup>2</sup> for all tests. All tests performed at 30°C.

**TABLE 7-1**  
SUMMARY OF DATA FOR BINDING LEAKAGE TESTS

Group Number	Test Number	Hydraulic Pressure Difference ( $\Delta p$ ) kg/cm <sup>2</sup>	Membrane Thickness cm	Membrane Area on Porous Disc (1) $A_1$ cm <sup>2</sup>	Computed Flow through Membrane (2) $q_1$ mm <sup>3</sup> /day	Measured Flow $q_M$ mm <sup>3</sup> /day	Computed Binding Leakage $q_B = q_M - q_1$ mm <sup>3</sup> /day	Possible Error in Computed Binding Leakage		Figure Number
								Absolute Value (3) mm <sup>3</sup> /day	Percent (3) %	
I	B1	2.0	0.0070	3.02	0.036	0.105	0.07	0.013	19	G-1
	B2	2.0	0.0072	3.02	0.034	0.133	0.10	0.012	12	G-2
	B3	6.0	0.0061	3.02	0.123	0.255	0.13	0.043	32	G-3
	B4	6.0	0.0069	3.02	0.109	0.185	0.08	0.038	50	G-4
	B5 (a)	18.0	0.0064	3.02	0.352	0.460	0.11	0.123	113	G-5
	B5 (b)	6.0	0.0064	3.02	0.107	0.140	0.03	0.037	112	G-5
	B5 (c)	2.0	0.0064	3.02	0.039	0.090	0.05	0.014	27	G-5
	B5 (d)	18.0	0.0064	3.02	0.352	0.420	0.07	0.123	180	G-5
II	B6	6.0	0.0131	3.02	0.057	0.252	0.20	0.020	10	G-6
	B7	6.0	0.0123	3.02	0.061	0.254	0.19	0.021	11	G-7
III	B8	6.0	0.0062	4.90	0.197	23.6	23.4	0.069	0.3	G-8
	B9	6.0	0.0069	4.90	0.177	0.271	0.09	0.062	66	G-9
	B10	6.0	0.0064	4.90	0.190	0.170to28.1	-0.02to27.9	0.066	to0.2	G-10 G-10a
IV	B11	2.0	0.0064	4.90	0.064	8.90	8.84	0.022	0.2	G-11
	B12	6.0	0.0081	4.90	0.150	0.222	0.07	0.053	74	G-12
	B13	6.0	0.0071	4.90	0.172	0.922	0.75	0.060	8	G-13
V	B14	6.0	0.0057	4.90	0.214	2.6to35	2.4to35	0.075	3to0.2	G-14
VI	B15	6.0	0.0060	3.02	0.125	0.274	0.15	0.044	29	G-15
	B16	6.0	0.0064	3.02	0.117	0.135	0.02	0.041	228	G-16
	B17	6.0	0.0049	3.02	0.153	0.310	0.16	0.054	34	G-17
VII	B18	6.0	0.0075	4.71	0.156	0.202	0.05	0.055	120	G-18
VIII	B19	2.0	0.0059	3.02	0.042	0.189	0.15	0.015	10	G-19
IX	B20(a)	2.0	0.0070	3.6	0.043	0.555	0.51	0.015	3	G-20
	B20(b)	4.0	0.0070	3.6	0.085	0.985	0.90	0.030	3	G-21
	B21	6.0	0.0060	3.6	0.149	0.766	0.62	0.052	8	G-22
	B22	6.0	0.0072	3.6	0.124	0.610	0.49	0.043	9	G-23
X	B23	6.0	0.0078	3.02	0.096	0.362	0.27	0.033	12	G-24
XI	B24	6.0	0.0060	3.02	0.125	0.226	0.10	0.044	44	G-25
	B25	6.0	0.0060	3.02	0.125	0.238	0.11	0.044	39	G-26

- (1)  $A_1$  values - Carbon, 60 grit, smooth pedestal - 4.71 cm<sup>2</sup> and 3.6 cm<sup>2</sup>  
 Carbon, 60 grit, rough pedestal - 4.90 cm<sup>2</sup>  
 ALSiMg, smooth pedestal - 3.02 cm<sup>2</sup>
- (2) Computed for  $k = 4.8 \times 10^{-16}$  cm/sec for natural rubber membrane.
- (3) Absolute value of error is equal to 0.35 times flow through membrane. Percent error is absolute value of error divided by  $q_B$  and multiplied by 100. For tests in which  $q_1$  was large relative to  $q_B$ , the possible error is large, e.g. tests B5(d) and B16, but for tests such as B1, B2 and B20,  $q_B$  is accurate to within plus or minus 35%.

**TABLE 7-2**  
RESULTS OF BINDING LEAKAGE TESTS

Group Number	Test Number	Test Conditions for Group	Binding Leakage (mm <sup>3</sup> /day) due to a Hydraulic Pressure Difference of:			
			2 kg/cm <sup>2</sup>	4 kg/cm <sup>2</sup>	6 kg/cm <sup>2</sup>	18 kg/cm <sup>2</sup>
I	B1	One membrane, one O-Ring each side, polished pedestal, ungreased pedestal, water soaked membrane, ceramic disc.	0.07			
	B2		0.10			
	B3				0.13	
	B4				0.08	
	B5 (a)					0.11
	B5 (b)				0.03	
	B5 (c)		0.05			
II	B6	Same as Group I except two membranes.			0.20	
	B7				0.19	
III	B8	Same as Group I except rough pedestal and porous carbon disc.			23.4	
	B9				0.09	
	B10				-0.02to27.9	
IV	B11	Same as Group III except silicone oil soaked membrane.	8.84			
	B12				0.07	
	B13				0.75	
V	B14	Same as Group III except neoprene rubber strips.			2.4to35	
VI	B15	Same as Group I except greased pedestal.			0.15	
	B16				0.02	
	B17				0.16	
VII	B18	Same as Group VI except porous carbon disc.			0.05	
VIII	B19	Same as Group I except silicone oil soaked membrane.	0.15			
IX	B20(a)	Same as Group VIII except porous carbon disc.	0.51			
	B20(b)			0.90		
	B21				0.62	
	B22				0.49	
X	B23	Same as Group I except neoprene rubber strips.			0.27	
XI	B24	Same as Group X except silicone oil soaked membrane.			0.10	
	B25				0.11	

TABLE 8-1

LIST OF VALVES TESTED

Item* Number	Name	Manufacturer	Manufacturer's Identifying Number	Body Material	Description	Packing
1	Hoke	Hoke, Inc. One Tenakill Park Cresskill, N.J.	304	Brass	1/8" N.P. male, type 303 stainless steel V stem.	Asbestos (bonnet) Metal to metal (seat)
2	Whitey	Whitey Research Tool Co. 5525 Marshall St. Oakland 8, California	ORM-2	Brass	1/8" N.P. male, type 316 stainless steel stem, micro-regulating.	Teflon (bonnet) Metal to metal (seat)
3	Klinger	Joseph Robb & Co. Ltd. 5575 Cote St. Paul Road Montreal, P.Q., Canada	AB10	Brass		Asbestos
4	Push-Pull	Harvard University Pierce Hall Machine Shop Cambridge 38, Mass.	-	Brass Brass		Three Buna-N O-Rings 0.254" O.D., 0.070" thick
5	Push-Pull	Norwegian Geotechnical Institute Oslo, Norway	-	Brass		Three O-Rings 0.316" O.D., 0.070" thick
6	Hydromatics	Hydromatics, Inc. Livingston, N.J.	715 A1	303 stainless steel	1/8" N.P. female	Two Teflon seats on type 302 stainless steel ball. Buna-N O-Rings; 0.070" thick: 2 at 0.71" O.D. 2 at 0.44" O.D. 1 at 0.38" O.D.
7	Circle Seal	Circle Seal Products Co. Inc. 2181 East Foothill Blvd. Pasadena, California	9559B- 1MM	Brass	1/8" N.P. male	Buna N O-Rings, 0.070" thick: 2 at 0.441" O.D. (bonnet) 1 at 0.285" O.D. (seat)
8	Schrader	A. Schrader's Son 470 Vanderbilt Avenue Brooklyn 38, N.Y.	3060C-12	Cadmium over steel	1/4" N.P. male, swivel type quick-connect	One flat rubber washer 0.56" O.D., 0.10" thick
9	Snap-tite	Snap-tite Union City, Penn.	VHN4-2	Brass	Valve nipple	One O-Ring 0.57" O.D., 0.070" thick
10	Snap-tite	Snap-tite Union City, Penn.	PHC4-2	Brass	Plain coupler	Rubber "U"-Ring packing

\* See Figs. 8-1 and 8-2 for photographs of valves.

TABLE 8-2

LIST OF FITTINGS TESTED

Item Number*	Description of Fitting	Body Material	Packing Material
11	O-Ring connection for membrane permeability cell, old design.	Type 316 stainless steel	One Buna-N O-Ring 0.241" O.D. 0.070" thick
12	O-Ring connection for membrane permeability cell, new design, see Figs. 4-3 and 4-5.	Type 304 stainless steel	One Buna-N O-Ring 0.441" O.D. 0.070" thick
13	O-Ring connection for binding leakage pedestal, see Figs. 7-3 and 7-4.	Type 304 stainless steel	One Buna-N O-Ring 0.316" O.D. 0.070" thick
14	O-Ring fitting to connect 1/8" O.D. Saran tubing to lucite.	Brass to lucite	One Buna-N O-Ring 0.254" O.D. 0.070" thick
15	O-Ring fitting to connect 1/8" O.D. Saran tubing to stainless steel.	Brass to type 304 stainless steel	One Buna-N O-Ring 0.254" O.D. 0.070" thick
16	Flex connection, No. 68-FL. Imperial Brass Manufacturing Co. 6300 West Howard Street Chicago 48, Illinois.	Brass	Cylindrical rubber gasket 3/16" tall 9/32" O.D.
17	Swagelok reducing union, No. 400-6-2-316. Crawford Fitting Company 884 East 140th Street Cleveland 10, Ohio.	Type 316 stainless steel	Two nylon ferrules and two stainless steel ferrules
18	Epoxy resin seal between stainless steel hyperdermic needle tubing and precision bore glass tubing.	-	Hysol Epoxy Patch Kit 1-C (white)
19	Saran tubing, 1/8" O.D. by 1/16" I.D. Dow Chemical Company Midland, Michigan.	-	-

\* See Figs. 8-3 and 8-4 for photographs of fittings.

TABLE 8-3

SUMMARY OF VALVE LEAKAGE TESTS

Test Number	Item Number*	Valve Tested	Rate of Leakage mm <sup>3</sup> /day	Average Relative Humidity %	Duration of Test days	Immediate Volume Changes Due to Applied Pressure		Figure Number
						Total mm <sup>3</sup>	Final Rate mm <sup>3</sup> /kg/cm <sup>2</sup>	
<u>STEM TYPE VALVES</u>								
1(a)	1	Hoke-seat	0.011	60	76	**	**	H-1
1(b)		Hoke-seat(200 closings)	0.002	~59	100	2.8	0.03 to 0.08	H-2
1(c)		Hoke-seat and bonnet	-0.03	43	63	6.1	0.02 to 0.03	H-3
2(a)	1	Hoke-seat	0.004	60	74	0.2	0.01	H-4
2(b)		Hoke-seat(500 closings)	<0.0006	59	100	4.5	0.02 to 0.04	H-5
2(c)		Hoke-seat and bonnet	0.018	42	99	1.4 to 5.6	0.04 to 0.11	H-6
3	2	Whitey-seat and bonnet	0.004	43	123	3.5	0.05 to 0.14	H-7
<u>PISTON TYPE VALVES</u>								
4(a)	3	Klinger(untreated packing)	186	50	0.2	1.8	0.13	H-8
4(b)		Klinger(packing boiled in distilled water and greased)	79	50	0.4	1.1	0.10	H-9
5(a)	3	Klinger(packing boiled in distilled water and greased)	26.7	42	11	3.9	0.13	H-10
5(b)		Same, but bonnet re-tightened	14.3	40	6.2	**	**	H-10
5(c)		Same, but bonnet re-tightened	4.1	38	18	**	**	H-10
5(d)		Same, but bonnet re-tightened	0.52	37	9.0	**	**	H-10
6	3	Klinger(packing boiled in distilled water and greased and bonnet nut screwed down as far as it would go)	0.20	45	123	2.0	0.05	H-11
7(a)	4	Push-pull(Harvard)	0.09	57	110	>1.6	~0.25	H-12
7(b)		Push-pull(Harvard,1000 closings)	0.07	62	42	1.8	0.18	H-13
8	5	Push-pull(N.G.I.)	0.1	44	21	1.4	0.14	H-14
9	6	Hydromatics	0.02	42	62	8.7	0.81	H-15
10(a)	7	Circle Seal-seat	0.005	60	53	46	0.04	H-16
10(b)		Circle Seal-seat	0.001	41	43	0.7	0.29 to 0.48	H-17
10(c)		Circle Seal-bonnet	0.20	41	34	20	0.36	H-18
10(d)		Circle Seal-bonnet	0.30	30	35	4.0	0.19	H-19
<u>SNAP VALVES</u>								
11(a)	8	Schrader( $\Delta p = 10 \text{ kg/cm}^2$ )	0.47	49	37	44	2.34	H-20
11(b)		Schrader( $\Delta p = 0.13 \text{ kg/cm}^2$ )	0.02 to 0.08	41	58	**	**	H-21
12	9	Snap-tite(valve nipple)	0.12	38	35	4.9	0.31	H-22
13	10	Snap-tite(plain coupler)	0.32	38	34	**	~1.6	H-23

\* See Figs. 8-1 and 8-2 for photographs of valves.

\*\* Not measured.

TABLE 8-4

SUMMARY OF FITTING LEAKAGE TESTS

AND TESTS ON SARAN TUBING

Test Number	Item Number*	Fitting Tested	Rate of Leaka mm <sup>3</sup> /day	Average Relative Humidity %	Duration of Test days	Immediate Volume Changes Due to Applied Pressure		Figure Number
						Total mm <sup>3</sup>	Final Rate mm <sup>3</sup> /kg/cm <sup>2</sup>	
<u>FITTINGS SEALED WITH O-RINGS</u>								
14(a)	11	Connection for membrane permeability cell (old design).	0.002	57	81	0.6	~0	H-24
14(b)		Same as 14(a) except greased O-Ring.	~0	**	43	6.2	0.09	H-25
15	12	Connection for membrane permeability cell (new design).	0.002	58	66	0.6	0.03	H-26
16(a)		Same as 15.	0.002	45	109	0.2	0.02 to 0.04	H-27
16(b)		Same as 15.	0	30	35	0.2	0.004	H-28
17(a)	13	Connection for binding leakage pedestal.	<0.01	61	27	**	**	H-29
17(b)		Same as 17(a).	0.006	58	63	14	0.16	H-30
18	14	Saran tubing to lucite.	0.021	52	54	0.9	0.05	H-31
19	15	Saran tubing to stainless steel.	0.080	43	25	1.3	0.12	H-32
<u>MISCELLANEOUS FITTINGS AND TUBING</u>								
20(a)	16	Flex fitting on 1/8" O.D. Saran tube.	0.019	57	81	**	**	H-33
20(b)		Same as 20(a).	0.011	**	64	1.2	0.04	H-34
21	17	Swagelok union on 1/8" O.D. glass.	<0.018	**	5.6	**	**	H-35(a) (b)
22	18	Two epoxy seals between glass and stainless steel tubing.	0.0032	**	45	1.5	0.06	H-36
23(a)	19	Saran tubing (immediate volume change due to application of pressure, 594 cm long).	-	100***	0.014	0.205/cm	0.0193/cm	H-37
23(b)		Saran tubing (Creep under pressure).	-	100***	181	-	-	H-38, J-39
23(c)		Saran tubing (Evaporation through walls).	0.0007/cm	60	194	-	-	H-40

\* See Figs. 8-3 and 8-4 for photographs of fittings.

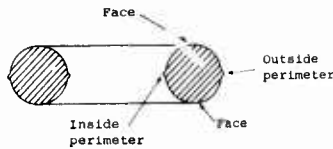
\*\* Not measured.

\*\*\* Submerged in water during test.

**TABLE 8-5**

CORRELATION OF CONTACT DIAMETER OF O-RING WITH RATE OF VALVE LEAKAGE

Valve Tested	Total Contact Diameter in.	Rate of Leakage mm <sup>3</sup> /day
<b>I. SEAL MADE BY PERIMETERS OF O-RING</b>		
Circle Seal (Bonnet)	1.62	0.20-0.30
Push-Pull (N.G.I.)	1.10	0.11
Push-Pull (Harvard)	0.86	0.07-0.09
<b>II. SEAL MADE BY FACES OF O-RING</b>		
Snap-Tite (Valve nipple)	2.38	0.12
Hydromatics	~2.0	0.02
Circle Seal (Seat)	0.43	0.001-0.005



DETAIL OF TYPICAL O-RING (Approximately to scale)

**TABLE 9-1**

MAXIMUM ACCEPTABLE RATES OF WATER LEAKAGE INTO 100% SATURATED SPECIMENS FOR DECREASE IN EFFECTIVE STRESS NOT EXCEEDING 2%

SOIL	INITIAL SWELLING RATIO	RATE OF LEAKAGE WHICH WILL CAUSE 2% DECREASE OF EFFECTIVE STRESS					
		Percent change in Volume per day			Volume rate of leakage (mm <sup>3</sup> /day) for specimen volume of 90 cm <sup>3</sup>		
		Test Duration			Test Duration		
		8 hours	10 days	100 days	8 hours	10 days	100 days
Mexico City Clay	.03*	18x10 <sup>-4</sup>	60x10 <sup>-6</sup>	6x10 <sup>-6</sup>	160	5.4	0.5
Boston Blue Clay	.015*	9x10 <sup>-4</sup>	30x10 <sup>-6</sup>	3x10 <sup>-6</sup>	80	2.7	0.3
Canyon Dam Clay	.001**	0.6x10 <sup>-4</sup>	2x10 <sup>-6</sup>	0.2x10 <sup>-6</sup>	5.4	0.1 <sup>P</sup>	0.02

\* Estimated from one-dimensional consolidation test data. See Table 2-1 for source of data.  
 \*\* Method of measurement given in Appendix D.

**TABLE 9-2**

RATE OF WATER LEAKAGE INTO 100% SATURATED SPECIMEN MOUNTED IN HARVARD TRIAXIAL CELL

Row or Item No.	Time Average of the Effective Minor Principal Stress on Specimen during Axial Loading (1)	1 kg/cm <sup>2</sup>		5 kg/cm <sup>2</sup>		10 kg/cm <sup>2</sup>	
		0	0.009 <sup>(2)</sup>	0	0.009 <sup>(2)</sup>	0	0.009 <sup>(2)</sup>
	Mole Fraction of Sodium Chloride in Pore Water	0	0.009	0	0.009	0	0.009
	<b>Rates of Leakage (mm<sup>3</sup>/day):</b>						
1	Membranes - Natural rubber	0.36	9.26	1.80	10.70	3.60	12.50
2	Butyl rubber	0.024	0.61	0.12	0.71	0.24	0.83
3	Bindings	0.09	0.45	0.09	0.45	0.09	0.45
4	Fittings (3) - Inside of chamber	0	0	0	0	0	0
	Outside of chamber	-0.14	-0.13	-0.14	-0.13	-0.14	-0.13
5	Valves (3) - Outside of chamber	-0.02	-0.02	-0.02	-0.02	-0.02	-0.02
6	Tubing (3) - Inside of chamber	0	0	0	0	0	0
	Outside of chamber	-0.044	-0.042	-0.044	-0.042	-0.045	-0.042
	<b>Total Rates of Leakage (mm<sup>3</sup>/day):</b>						
7	Natural rubber plus all items except No. 2	0.25	9.52	1.69	10.96	3.49	12.76
8	Butyl rubber leakage plus binding leakage	0.11	1.06	0.21	1.16	0.33	1.28

DETAILS OF APPARATUS CONSIDERED FOR TABLE (5)

Specimen size: 1.4 in. dia. by 3.5 in. high, volume = 90 cm<sup>3</sup>, permeated area = 100 cm<sup>2</sup>.  
 Membranes: Two natural rubber (Schmid), each 0.006 cm thick or one butyl rubber, 0.006 cm thick. (6)  
 Bindings: One O-Ring on cap and one on base. Stretched to 40% strain. Shore A hardness 70. Cap and base are polished and greased.  
 Fittings: Seven flex fittings outside triaxial chamber and two inside chamber.  
 Valves: Three Hoke valves which can leak through bonnet packing and two Hoke valves which can leak past seat.  
 Tubing: 1/8 in. outside diameter Saran, 60 cm inside chamber and 55 cm outside chamber.

- Effective minor principal stress on specimen is equal to hydraulic pressure difference across membrane.
- A mole fraction of sodium chloride equal to 0.009 is approximately equal to the concentration of sodium chloride in sea water.
- It is assumed that a back pressure of 6 kg/cm<sup>2</sup> is applied to the pore water to cause 100% saturation. A plus sign means the volume inside the tubing is increasing.
- Average rates shown do not include immediate volume change due to pressure application. Only volume changes subsequent to 10 min. after pressure application are included.
- Details of membranes, bindings valves and fittings are described in Chapters 4, 7 and 8.
- Butyl rubber membranes have not been manufactured to date in a thickness of 0.006 cm for use in triaxial testing. A butyl membrane with a thickness of 0.006 cm will impose about 50% more restraint on a specimen than two 0.006 cm thick natural rubber membranes.

AVERAGE RATE OF VOLUME CHANGE DUE TO CREEP OF SARAN TUBING (3) (4)

Test Duration	mm <sup>3</sup> /day			
	8 hours	10 days	100 days	
Lateral Effective Stress	1	+3.18	+0.26	+0.04
kg/cm <sup>2</sup>	5	+0.33	+0.03	+0.004
	10	-3.24	-0.26	-0.04

TABLE 9-3

MAXIMUM ACCEPTABLE AIR LEAKAGE\* ( $J_a$ )  
 INTO PARTIALLY SATURATED SPECIMENS  
 FOR DECREASE IN EFFECTIVE STRESS NOT EXCEEDING 2%

$J_a$ (cm <sup>3</sup> )		$G_w = 99\%$		$G_w = 90\%$	
		$s = 0.001$	$s = 0.03$	$s = 0.001$	$s = 0.03$
$\bar{\sigma}_3 = 1$ kg/cm <sup>2</sup>	$u_a = 1$ kg/cm <sup>2</sup> (gage)	0.03	0.14	0.11	0.22
	$u_a = 6$ kg/cm <sup>2</sup> (gage)	0.04	0.40	0.12	0.47
$\bar{\sigma}_3 = 20$ kg/cm <sup>2</sup>	$u_a = 1$ kg/cm <sup>2</sup> (gage)	0.52	0.65	2.05	2.18
	$u_a = 6$ kg/cm <sup>2</sup> (gage)	0.53	0.91	2.06	2.44

\* Calculated using Eq. 2-22 (which is based on assumption that  $\Delta u_a = \Delta \bar{\sigma}_3$  when air leakage occurs) with  $\Delta \bar{\sigma}_3 / \bar{\sigma}_3 = 0.02$ ,  $V = 90$  cm<sup>3</sup>, and  $n = 0.5$ . Volume  $J_a$  is measured at atmospheric pressure.

TABLE 9-4

MAXIMUM ACCEPTABLE AIR LEAKAGE\* ( $J_a$ )  
 OUT OF PARTIALLY SATURATED SPECIMENS  
 FOR INCREASE IN EFFECTIVE STRESS NOT EXCEEDING 2%

$J_a$ (cm <sup>3</sup> )		$G_w = 99\%$		$G_w = 90\%$	
		$C = 0.005$	$C = 0.3$	$C = 0.005$	$C = 0.3$
$\bar{\sigma}_3 = 1$ kg/cm <sup>2</sup>	$u_a = 1$ kg/cm <sup>2</sup> (gage)	0.04	1.08	0.12	1.15
	$u_a = 6$ kg/cm <sup>2</sup> (gage)	0.87	3.68	0.16	3.76
$\bar{\sigma}_3 = 20$ kg/cm <sup>2</sup>	$u_a = 1$ kg/cm <sup>2</sup> (gage)	0.54	1.3	2.03	2.90
	$u_a = 6$ kg/cm <sup>2</sup> (gage)	0.58	3.98	2.11	5.50

\* Calculated using Eq. 2-22 (which is based on the assumption that  $\Delta u_a = -\Delta \bar{\sigma}_3$  when air leakage occurs) with  $\Delta \bar{\sigma}_3 / \bar{\sigma}_3 = 0.02$ ,  $V = 90$  cm<sup>3</sup> and  $n = 0.5$ . Volume  $J_a$  is measured at atmospheric pressure.

TABLE 9-5

RUBBER AND PLASTIC MEMBRANES  
 IN ORDER OF THEIR EK-COEFFICIENT

Membrane	Permeability Constant*	Modulus of Elasticity	EK-Coefficient
	(K) cm <sup>6</sup> /gm sec		
Texin	$4.2 \times 10^{-11}$	160	$670 \times 10^{-8}$
Kynar	0.14	1300	170
Polyethylene (a)	0.45	190	85
Neoprene	2.7	24	65
Polypropylene	0.039	1000	39
Polyethylene (c)	0.078	340	26
Natural rubber (c)	1.2**	15	18
Fluorel	0.30	57	17
Natural rubber (a)	1.2**	13	16
Teflon	0.014	660	9.2
Kel-F	0.0016	960	1.5
Butyl rubber (b)	0.033	38	1.3

\*Values of permeability constant taken from Table 6-3.

\*\*Taken from Table 6-2.

FIG. 2-1

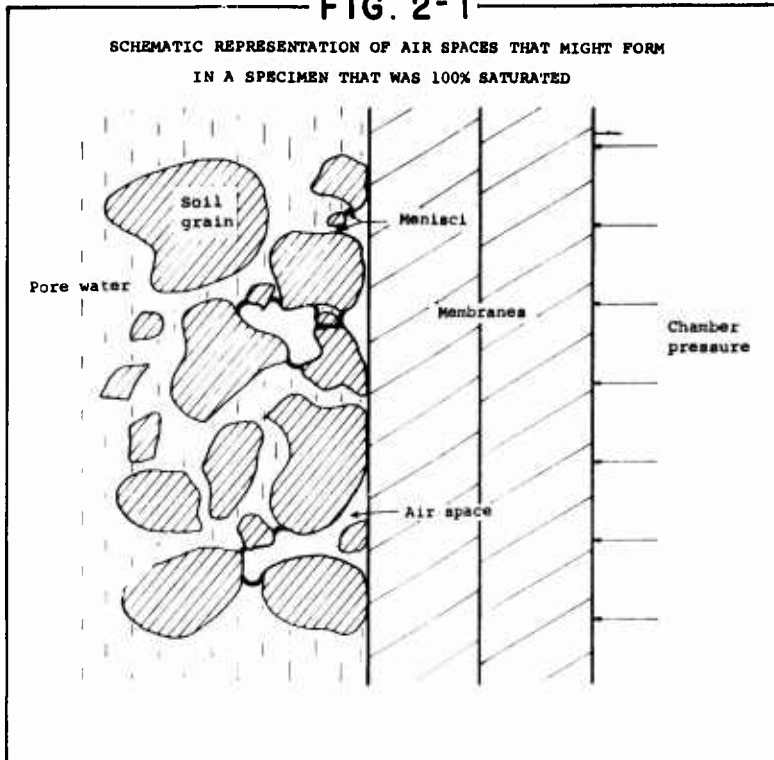


FIG. 2-2

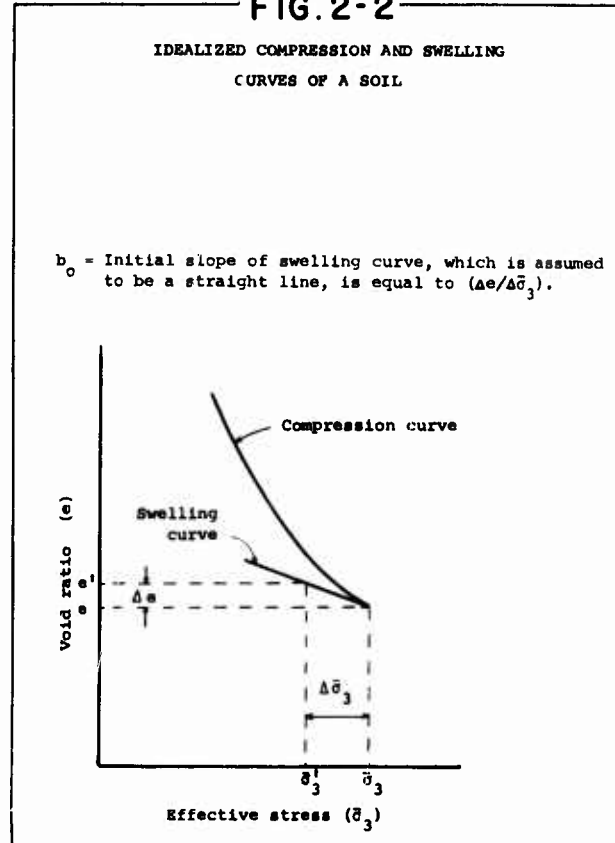


FIG. 2-3

PERCENT CHANGE IN TOTAL VOLUME  
VERSUS INITIAL SWELLING RATIO

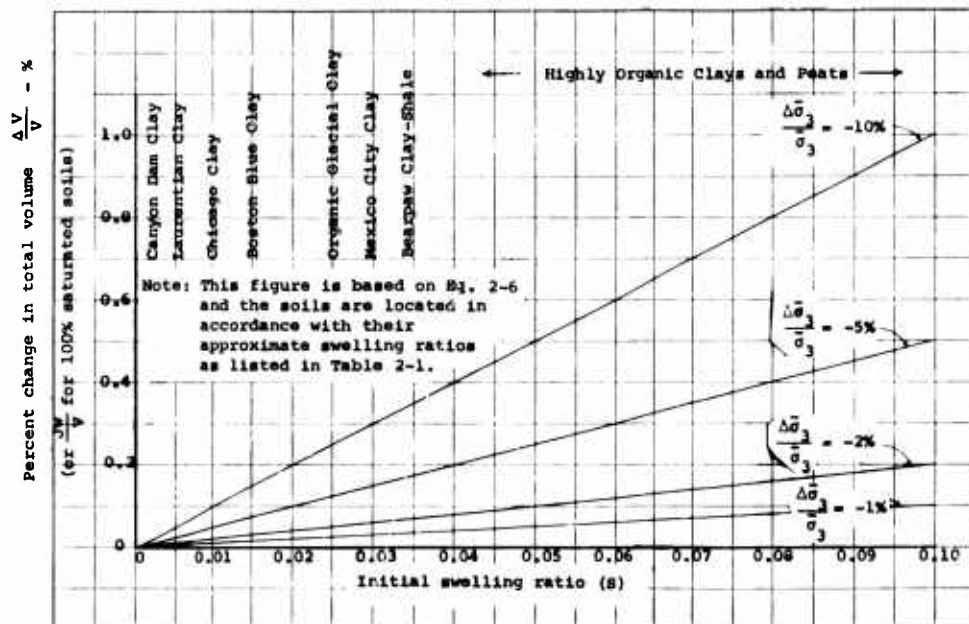


FIG.2-4

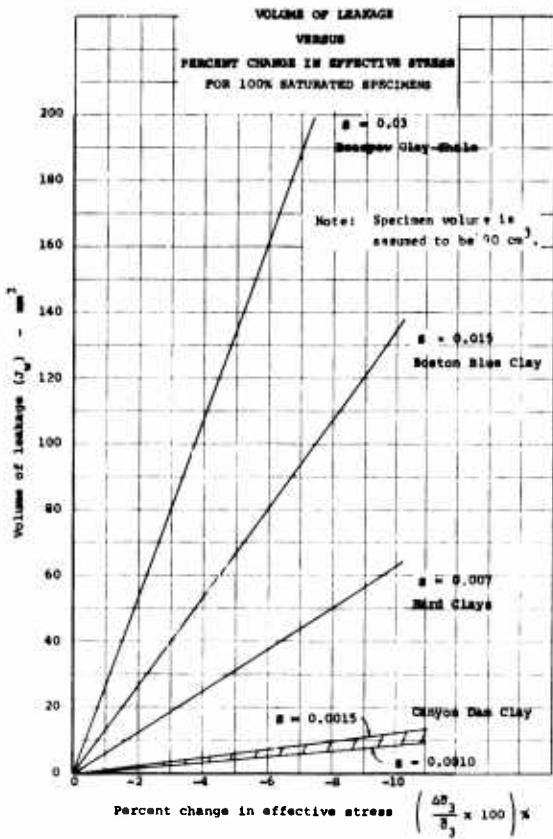


FIG.2-5

NOTATION USED FOR DERIVING EQUATIONS  
IN PARAGRAPH 2-06

**INITIAL STATE:** Given:  $V$  = initial total volume of specimen.  
 $e$  = initial void ratio.  
 $G_w$  = initial degree of saturation.  
 $u_a$  = initial pore air pressure (absolute).

Initial volume of voids  $V_v$

Air	$V_{au}$ = initial volume of undissolved air measured at pore air pressure, $u_a$ .
Water	$V_w$ = initial volume of water. $V_{ad}$ = initial volume of air dissolved in $V_w$ at pressure $u_a$ .
Soil Solids	$V_s$ = initial volume of solids.

$V = V_{au} + V_w + V_s$

**FINAL STATE:** Given:  $u'_a$  = final pore air pressure (absolute).  
 $J_a$  = volume of air leakage measured at standard atmospheric pressure,  $p_a$ .

Final volume of voids  $V'_v$

Air	$V'_{au}$ = final volume of undissolved air measured at pore air pressure, $u'_a$ .
Water	$V'_w$ = final volume of water (= initial volume of water)
Soil Solids	$V'_{ad}$ = volume of air dissolved in $V'_w$ measured at $u'_a$ . $V'_s$ = final volume of solids (= initial volume of solids)

$V' = V'_{au} + V'_w + V'_s$  = final total volume

FIG. 3-1

MEMBRANE-PERMEANT SYSTEM

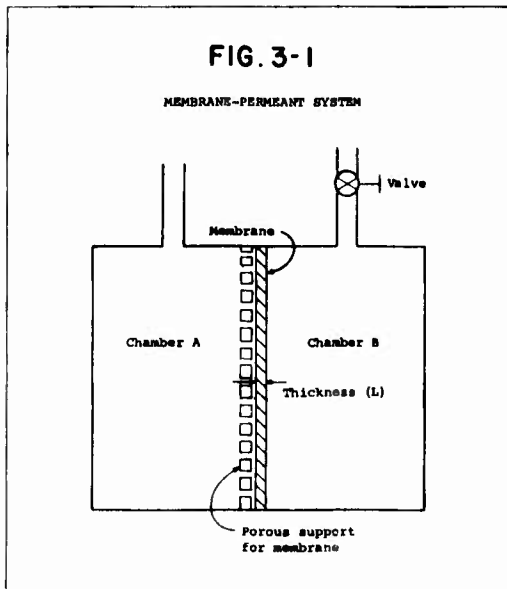
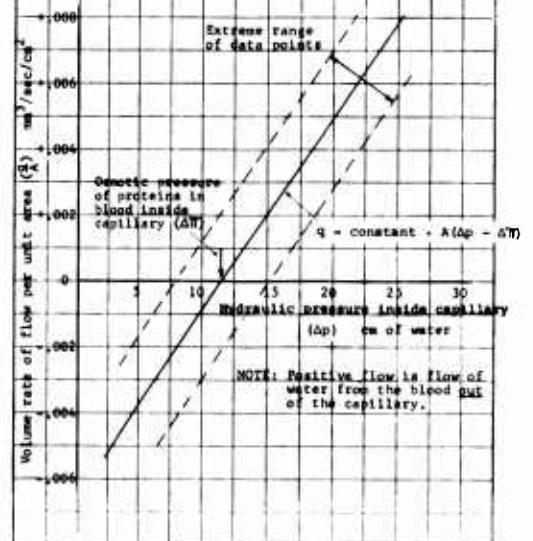
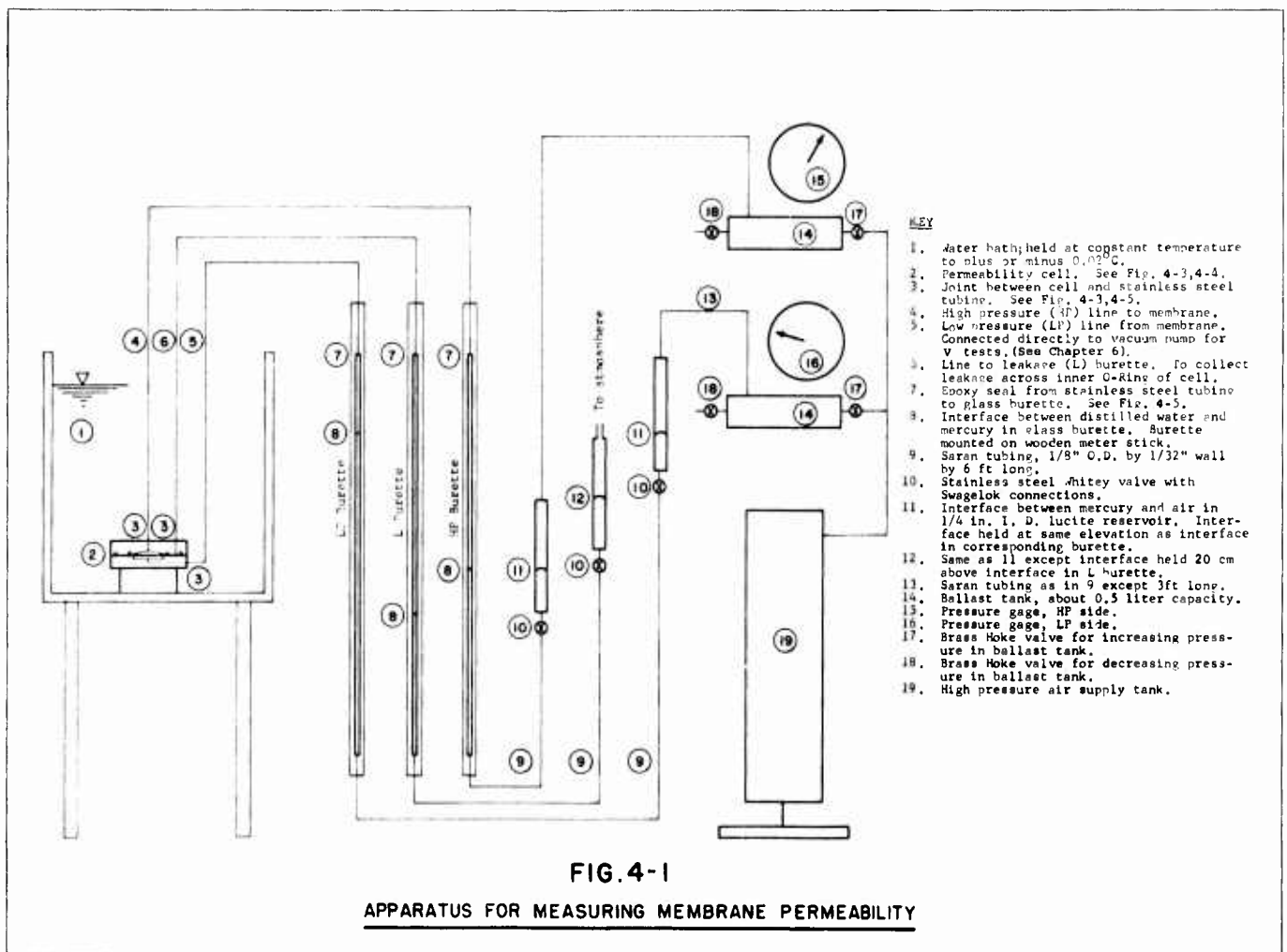
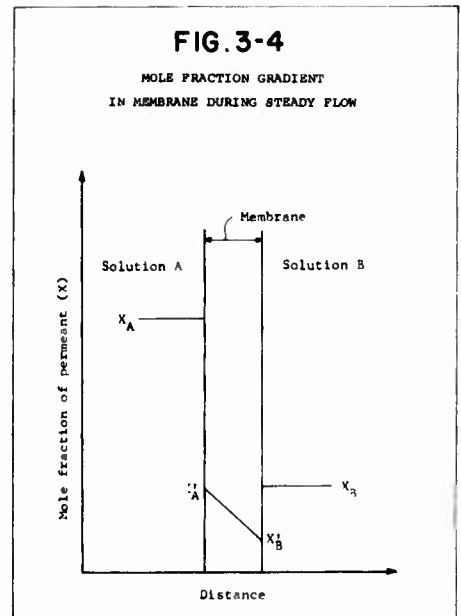
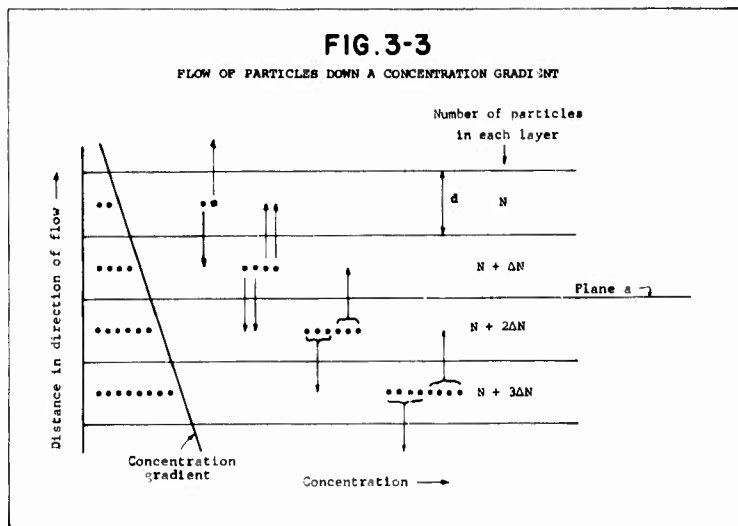


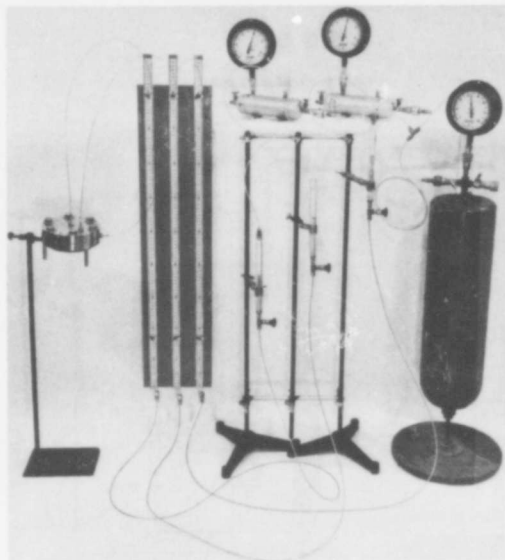
FIG. 3-2

RATE OF FLOW OF WATER  
THROUGH WALL OF CAPILLARY  
FROM A FROG'S MESENTERY  
from LANDIS (67, Fig.10)





**FIG. 4-2**  
PHOTOGRAPH OF APPARATUS  
FOR MEASURING MEMBRANE PERMEABILITY



Note: Meter sticks and attached capillary tubes are in reverse order from that shown in Fig. 4-1.

**FIG. 4-4**

PHOTOGRAPH OF PERMEABILITY CELL

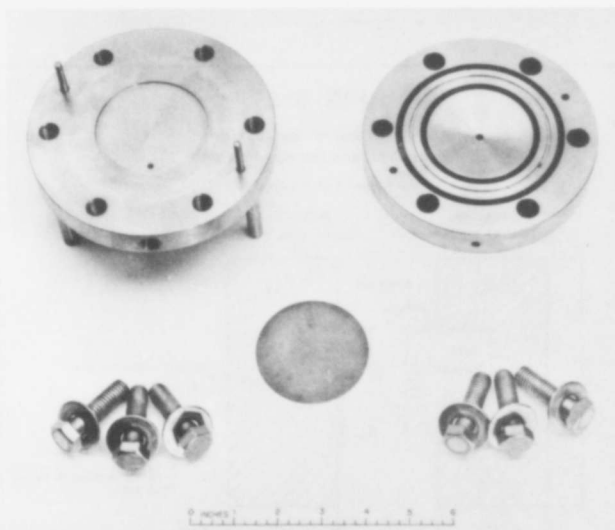


**FIG. 4-3**

MEMBRANE PERMEABILITY CELL  
(Used for V and W tests)

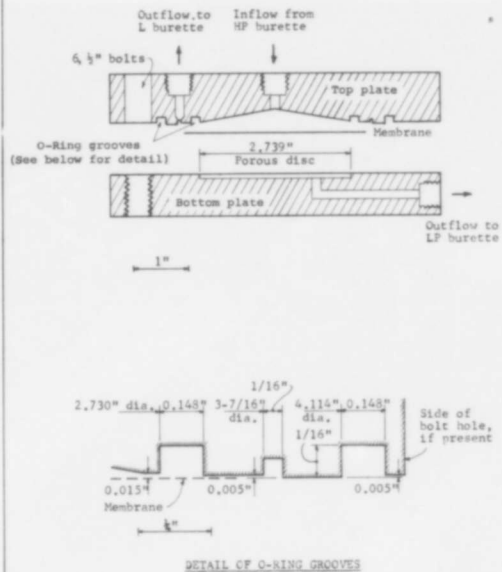


**FIG. 4-5**

DETAILS OF BURETTE  
AND CONNECTING TUBING

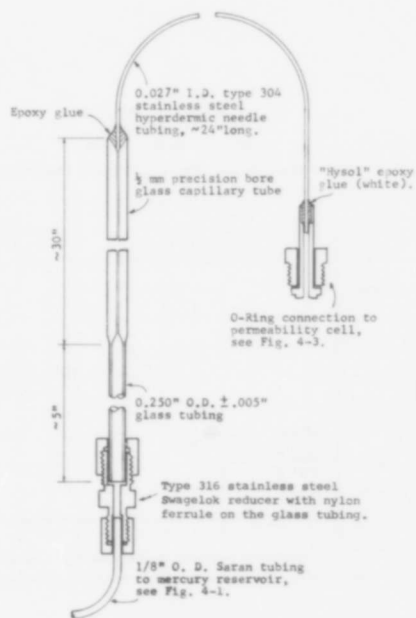
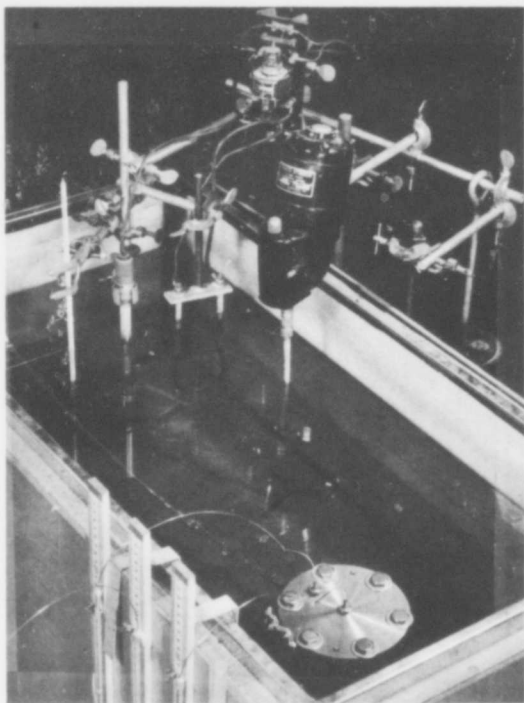


FIG. 4-6



PHOTOGRAPH OF WATER BATH

(V test in progress)

FIG. 5-1

APPARATUS TO MEASURE FLOW  
CAUSED BY MOLE FRACTION GRADIENTS

(Used for X tests)

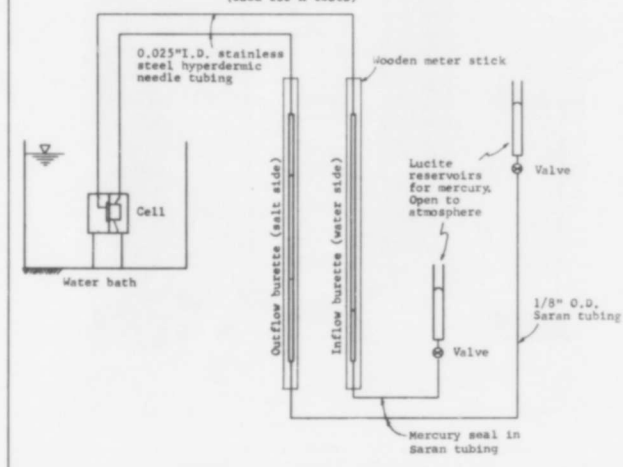


FIG. 4-7

W TESTS ON NATURAL RUBBER

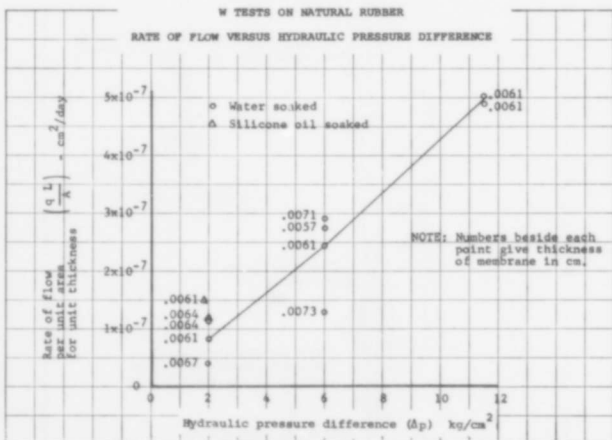
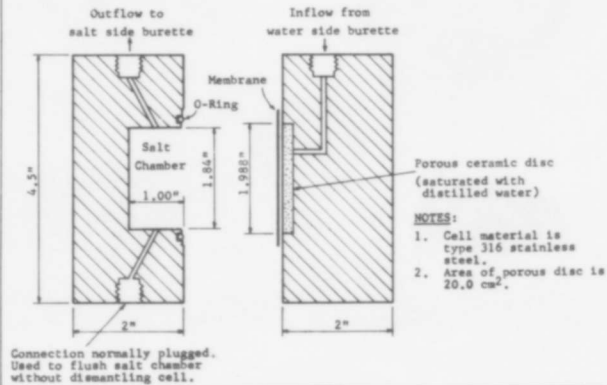


FIG. 5-2

CELL USED TO MEASURE FLOW  
CAUSED BY MOLE FRACTION GRADIENTS

(Used for X tests)



**FIG. 5-3**

PHOTOGRAPH OF CELL USED TO MEASURE FLOW CAUSED BY MOLE FRACTION GRADIENTS (Used for X tests)

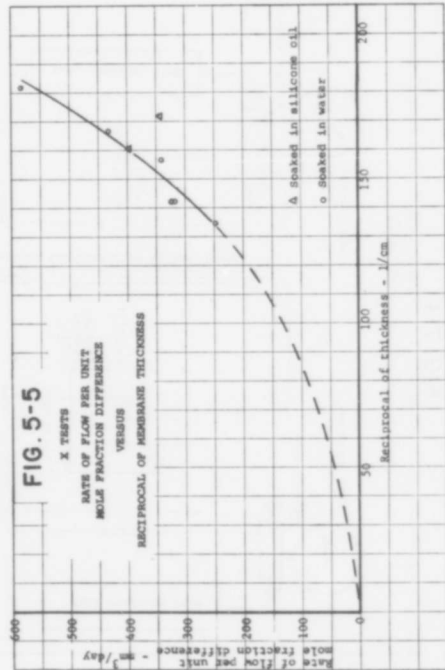
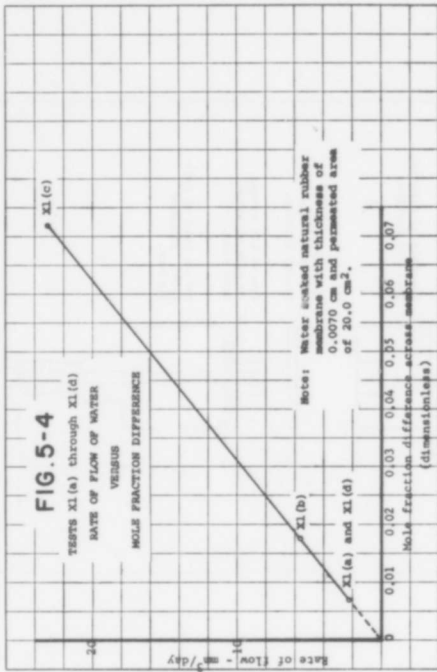
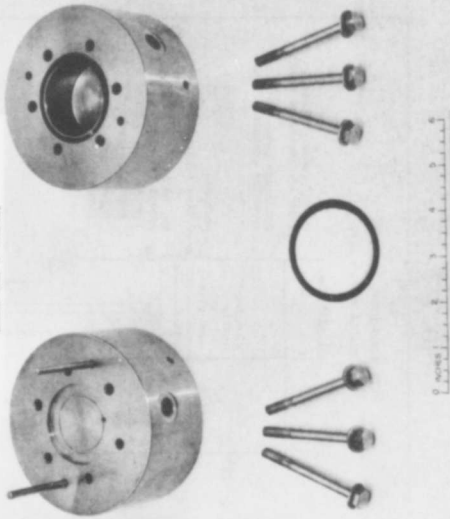


**FIG. 6-1**

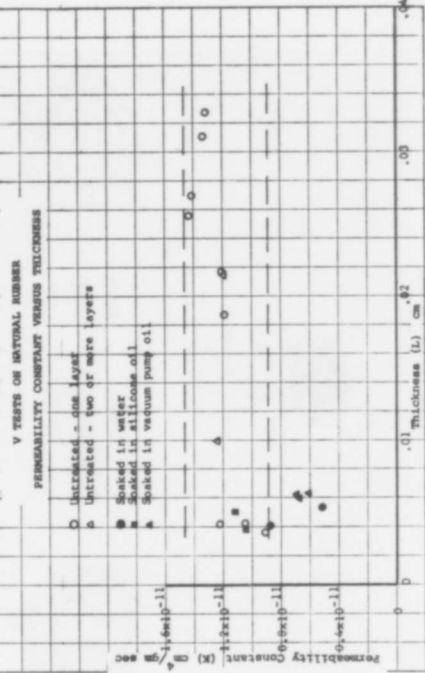


FIG. 7-2

PHOTOGRAPH OF BINDING LEAKAGE CELL AND  
PEDESTAL CONTAINING CERAMIC DISC

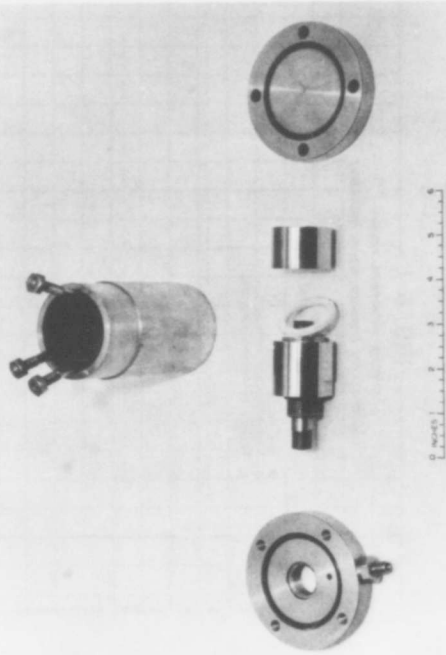


FIG. 7-1

APPARATUS FOR BINDING LEAKAGE TESTS

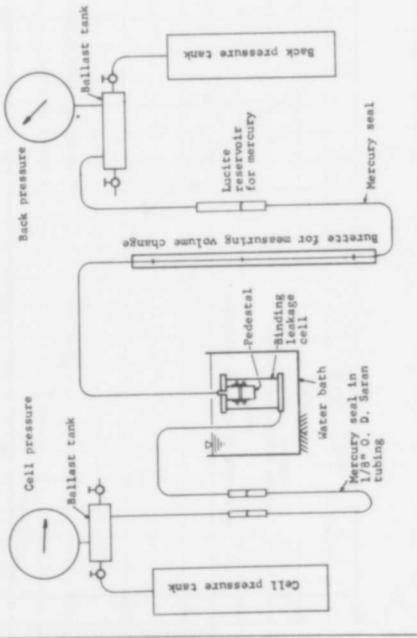


FIG. 7-4

STAINLESS STEEL PEDESTAL  
WITH POROUS CERAMIC DISC

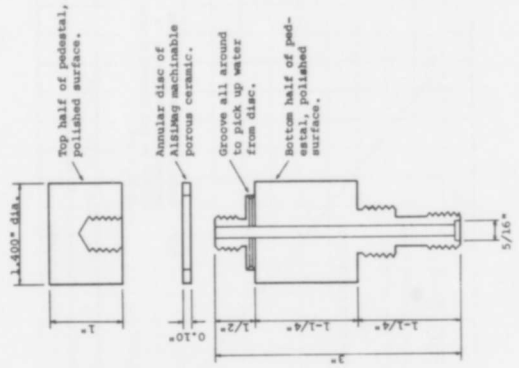
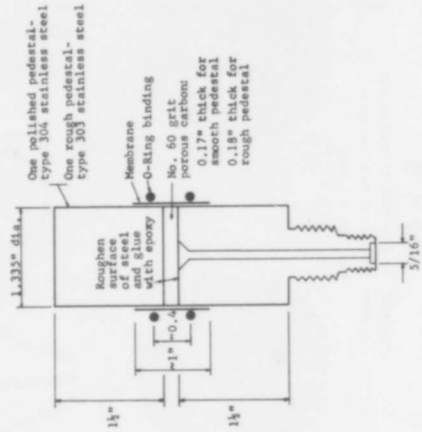


FIG. 7-3

STAINLESS STEEL PEDESTAL  
WITH POROUS CARBON DISC



# FIG. 7-5

DETAIL OF LOCATIONS WHERE LEAKAGE OCCURS  
WHEN USING O-RING BINDINGS

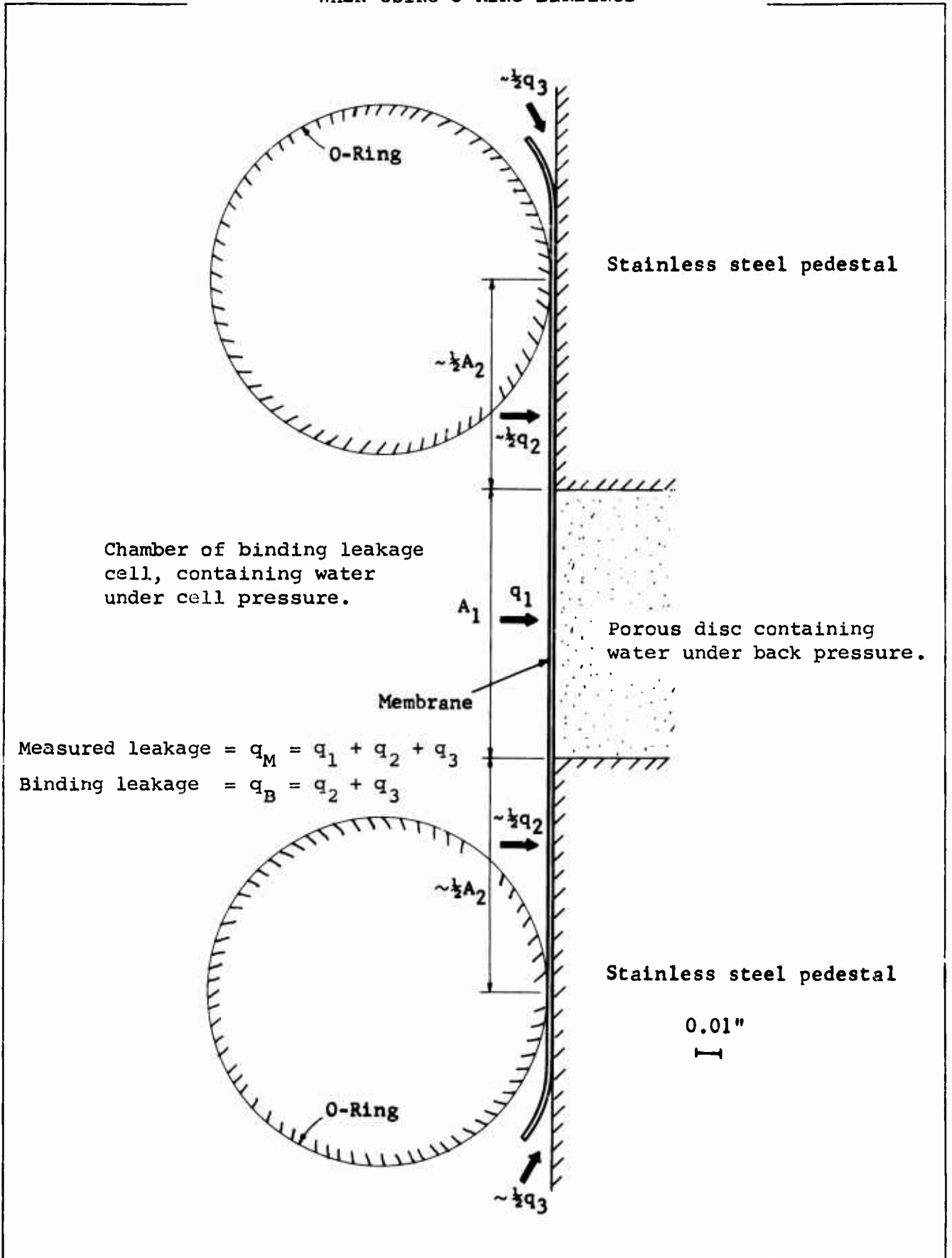
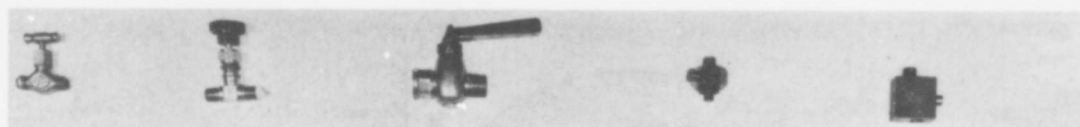


### FIG. 8-1

PHOTOGRAPH OF VALVES TESTED



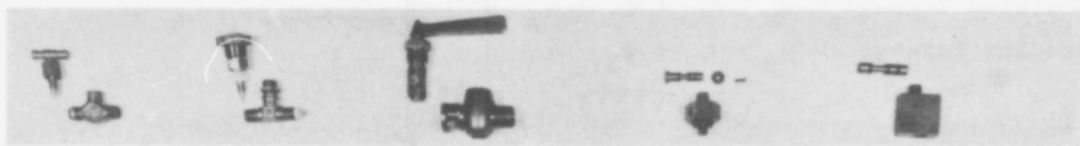
1 HOKE                      2 WHITEY                      3 KLINGER                      4 PUSH-PULL (HARVARD)                      5 PUSH-PULL (N.G.)



6 CIRCLE SEAL                      7 HYDRAMATICS                      8 SCHRADER                      9 SNAP-TITE (VALVE NIPPLE)                      10 SNAP-TITE (PLAIN COUPLER)

### FIG. 8-2

PHOTOGRAPH OF VALVES TESTED  
(Disassembled)



1 HOKE                      2 WHITEY                      3 KLINGER                      4 PUSH-PULL (HARVARD)                      5 PUSH-PULL (N.G.)



6 CIRCLE SEAL                      7 HYDRAMATICS                      8 SCHRADER                      9 SNAP-TITE (VALVE NIPPLE)                      10 SNAP-TITE (PLAIN COUPLER)

## FIG.8-3

PHOTOGRAPH OF FITTINGS TESTED

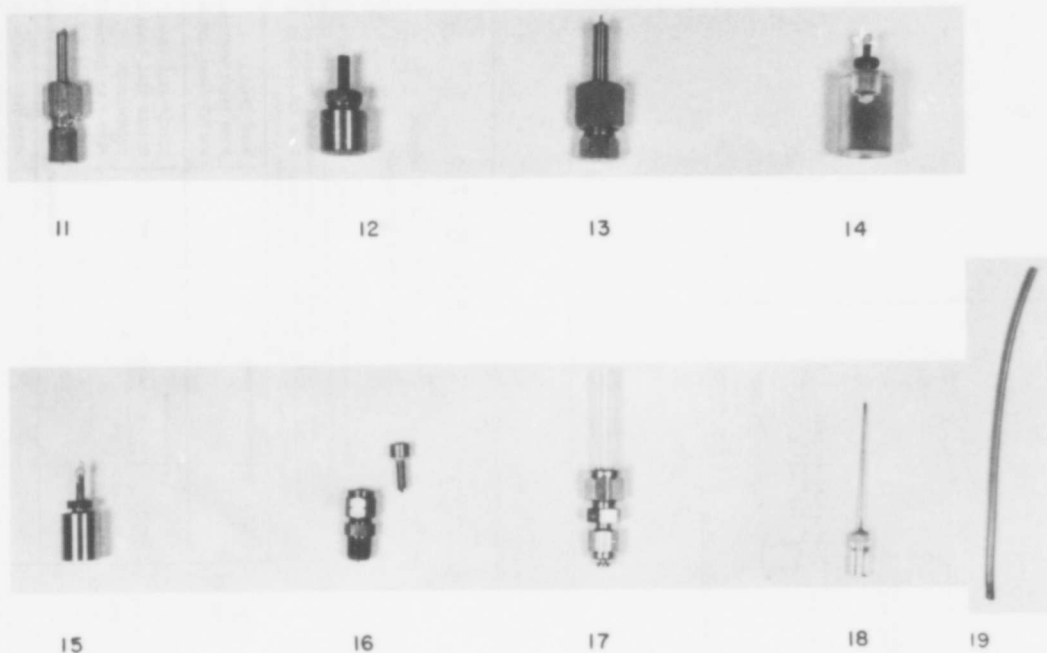


## FIG.8-4

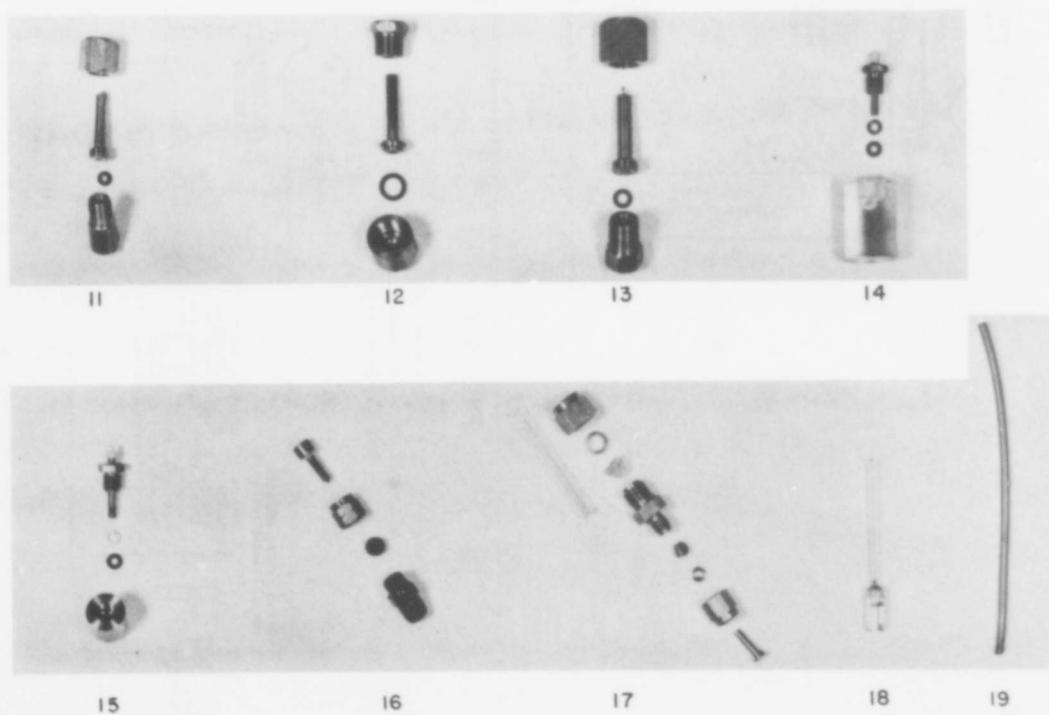
PHOTOGRAPH OF FITTINGS TESTED  
(Disassembled)

FIG. 8-5

APPARATUS FOR MEASURING LEAKAGE OF VALVES AND FITTINGS

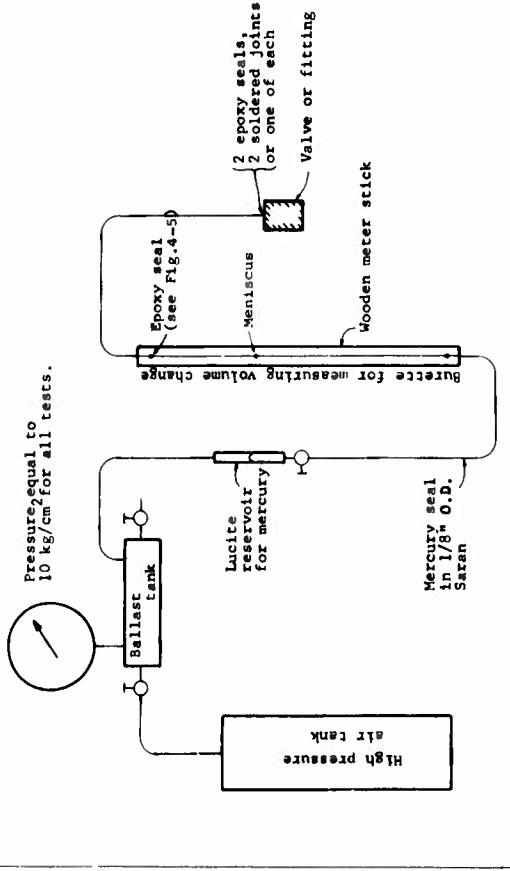


FIG. 8-6

APPARATUS FOR MEASURING VOLUME CHANGE AND LEAKAGE THROUGH WALLS OF SARAN TUBING

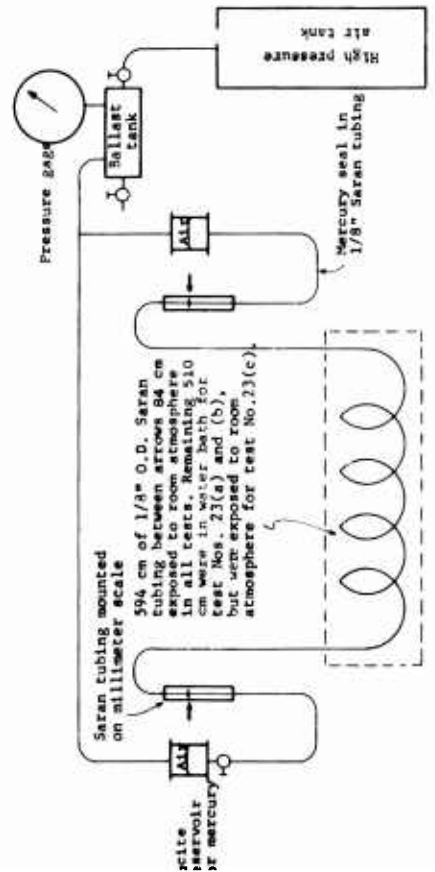


FIG. 8-7

COMPARISON OF RATES OF LEAKAGE OF WATER FROM TEN VALVES

NOTE: All tests performed with water inside, at gage pressure of 10 kg/cm<sup>2</sup>, and room air outside at relative humidity of about 50% and temperature of about 23°C. See Tables 8-3 and 8-4 for more details. Rates of leakage smaller than 0.003 mm<sup>3</sup>/day may be due to leakage from fittings in the line between the maniscus in the burette and the valve tested.

STEM TYPE VALVES	ROKE (seat)	ROKE (seat and bonnet)	WHITEY (seat and bonnet)
PISTON TYPE VALVES	Length of bar indicates range of measured rates of leakage from the valves tested.	CIRCLE SEAL (seat)	CIRCLE SEAL (seat and bonnet)
		HYDROMATICS	PUSH-PULL (Harvard)
		PUSH-PULL (N.C.I.)	KLINGER
		SNAP VALVES	SNAP-TITE (valve nipple)
		SCHRADER	

Rate of Leakage - mm<sup>3</sup>/day of liquid water

FIG. 9-2

MOLE FRACTION OF SODIUM CHLORIDE REQUIRED TO PREVENT FLOW DUE TO HYDRAULIC PRESSURE AND/OR MOLE FRACTION DIFFERENCES

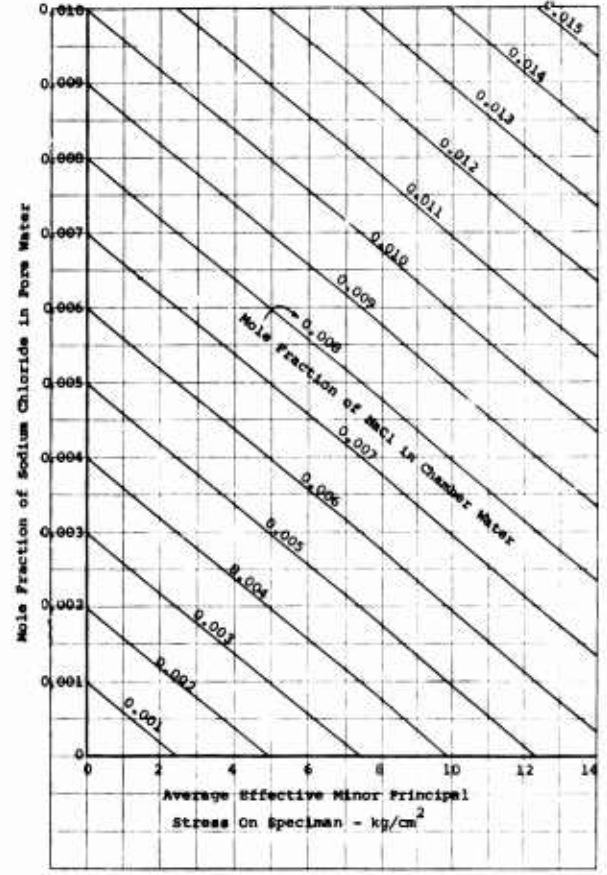


FIG. 9-1

ILLUSTRATION OF EFFECT OF ADDING SOLUTE TO CHAMBER WATER

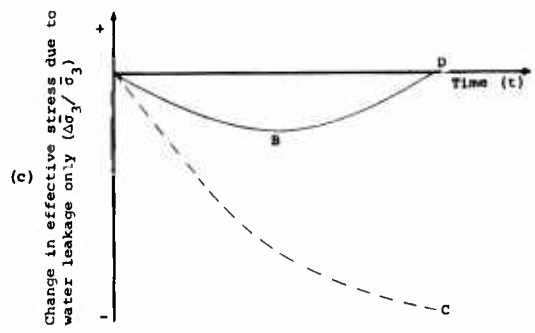
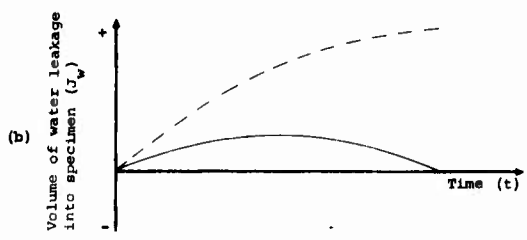
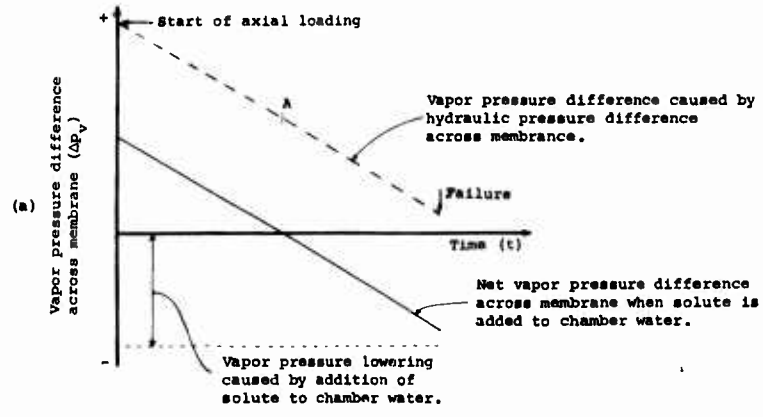
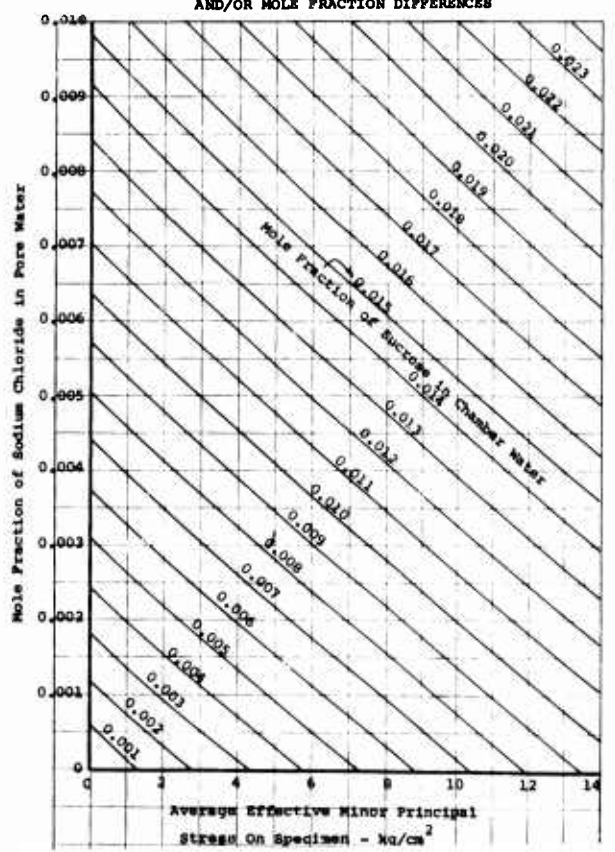


FIG. 9-3

MOLE FRACTION OF SUCROSE REQUIRED TO PREVENT FLOW DUE TO HYDRAULIC PRESSURE AND/OR MOLE FRACTION DIFFERENCES



APPENDIX AREVIEW OF PAST LEAKAGE INVESTIGATIONSA-01 INTRODUCTION

The purpose of this review is to present in chronological order and to evaluate the investigations of leakage which have been made in the field of soil mechanics. The review covers all published and unpublished reports that are available to the author and that contain significant contributions of data, ideas or apparatus development.

A short review of early work on leakage is given in A-02. Then, in paragraphs A-03 through A-13, eleven papers are reviewed in detail. A summary of this appendix is given in 1-06.

Past leakage investigations were directed only towards measuring the rate or total volume of leakage. None of the reports gave any rational method for judging whether a given quantity of leakage is important in triaxial testing. Furthermore, the test procedures used were generally not described in sufficient detail to allow an accurate analysis of their reliability. Therefore, the data from the past investigations will be judged relative to the results of the present investigation. Data published outside the field of soil mechanics are also used for reference if such data are deemed reliable. Judgment of the experimental procedure will generally be qualitative, based on the experience gained in the present study.

A-02 EARLY WORK ON LEAKAGE

In the late 1930's there was apparently a general interest in the effects of leakage on the results of triaxial tests. The first evidence of interest in leakage that is known to the author is a letter written to Mr. Henry Grace, a student at Harvard University in 1939 (50). He was seeking a material which could be used to coat rubber membranes so that they would "not pass more than 0.01 cc of water per sq cm per 20 days when subjected to a pressure difference of 50 lbs per sq in." This rate, equivalent to  $0.5 \text{ mm}^3/\text{cm}^2/\text{day}$ , is 500 times greater than is acceptable in triaxial Q and R tests with a 100-day duration of axial loading.

Some qualitative ideas on the suitability of various chamber fluids for minimizing leakage were formed during the first Cooperative Triaxial Research Program. In the First Progress Report (1940) (21), A. Casagrande pointed out that: (1) glycerine is unsuitable as a chamber fluid for long-time tests because water flows by osmosis from the soil specimen through the rubber membranes into the glycerine, (2) the rubber membranes used are not sufficiently impervious to water in long-time tests and (3) castor oil gives excellent results as a chamber fluid but is difficult to handle during testing.

In the Second Progress Report (1940) (22), Lt. Jagow pointed out that the measured decrease in volume of a specimen, based on observations of pore water flow during triaxial S tests lasting ten to thirty days, was larger than the actual volume decrease because of leakage and the "formation of gas bubbles" in burettes. He also emphasized that castor oil was "entirely satisfactory" as a pressure medium for long-time tests. Since the only long-time tests being conducted at that time were S tests, these investigators were concerned only with the effect of leakage on volume change measurements. It was realized in 1940 that leakage during Q and R tests would also cause errors. However, the duration of axial load application in Q and R tests was then only about one hour, and no appreciable leakage was expected to occur in such a short time.

The first quantitative data on leakage was reported during the Cooperative Triaxial Research Program by Haussler and Warlam in 1944.

A-03 HAUSSLER, R. W. and WARLAM, A. A. (1944) (REF. 54)

During the development of improved triaxial apparatus, tests were performed to determine the rate of evaporation of water through the walls of rubber and Saran tubing. The details of the tests are not given, but the data presented are as follows:

Tubing Material	Tubing Size	Rate of Evaporation (mm <sup>3</sup> /cm/day)
Para rubber	1/2" O.D. by 1/4" I.D.	0.186
White rubber	same	0.170
Saran	1/8" O.D. by 1/16" I.D.	0.022

These rates of evaporation are comparable because the ratios of the outside diameter to the inside diameter are all equal to each other. Thus the rubber tubing is about nine times more pervious to water vapor than Saran. On the basis of these data, the authors recommended the use of Saran tubing for drainage lines in the triaxial apparatus.

Data presented by Doty, Aiken and Mark (42) indicate that the rate of evaporation through natural rubber should be more than twenty times that of an equal thickness of Saran, which confirms roughly the data of Haussler and Warlam.

A-04 CASAGRANDE, A. and SHANNON, W. L. (1948) (REF. 33)(a) General

Tests were performed to measure (1) the permeability of rubber membranes to air, water and castor oil due to a total (or hydraulic) pressure difference, and (2) the rate of evaporation of water vapor through several types of membranes.

(b) Permeability of Rubber to Air

Two types of natural rubber membranes were tested in the apparatus shown in Fig. A-1, using air pressure against the upper surface of the membrane and water on the lower surface. Air which passed through the membrane caused the water level in the burette to rise, so that the air flow could be measured.

The reported rates of flow through two natural rubber membranes were used by the author to calculate the air permeability of the rubber. The results of the tests are shown in Table A-1 together with data reported in references 2, 38, and 109, which were obtained using the apparatus described below.

- (1) van Amerongen (2) - This apparatus is typical of that used by many researchers interested in the gas permeability of membranes. It consists of a steel cell in two parts. The membrane rests on a fine wire gauze in the bottom half. The upper half is a chamber which contains the permeant gas at one kg/cm<sup>2</sup> pressure. A chamber in the lower half is evacuated and then connected to a vacuum gauge. The rate of rise of pressure in the lower chamber is used to determine the volume flow of gas through the membrane.
- (2) Davis (38) - In Davis' apparatus the membrane is clamped between two chambers of equal volume. A "test" gas is continuously passed through the upper chamber at one kg/cm<sup>2</sup> pressure and a "sweep" gas is continuously passed through the lower chamber, also at one kg/cm<sup>2</sup>. Thus there is no total pressure difference across the membrane although the partial pressure difference of the test gas is one kg/cm<sup>2</sup>. The sweep gas picks up the test gas which permeates the membrane, and carries it out of the lower chamber to be analyzed. When using oxygen as the test gas, the sweep gas used was carbon dioxide or nitrogen. The oxygen was removed from the sweep gas and its volume measured.
- (3) Wissa (109) - This apparatus is described in A-13.

In the quoted references three different apparatus were used to determine the air permeability of natural rubber from five different sources, yet the permeabilities in Table A-1 vary within  $\pm 10\%$  of the average value, if the data for the membrane manufactured by Holland-Rantos is excluded. This is a strong indication that one can rely on the results and use them for quantitative calculations of air flow through natural rubber membranes.

(c) Permeability of Rubber to Liquids

Casagrande and Shannon (33) also reported measurements of the rate of flow of castor oil and water through 0.035 cm thick natural rubber membranes using the apparatus in Fig. A-1. Air pressure was applied to the surface of the liquid permeant, which filled the upper half of the cell to a depth of about two centimeters. During these tests gas appeared on the low-pressure side of the membrane at a constant rate, independent of the duration of the test. The volume of gas was measured by applying a partial vacuum to the burette and measuring the change in burette reading. This volume change was used with Boyle's law to compute the initial volume of gas in the system. The change in burette reading was reduced by the change in gas volume in order to obtain the volume of liquid which presumably had been transmitted in a given interval of time. The observed rates of flow through the membranes under a pressure difference of 6 kg/cm<sup>2</sup> were about 0.005 cm<sup>3</sup>/cm<sup>2</sup>/hr for water and 0.001 cm<sup>3</sup>/cm<sup>2</sup>/hr for castor oil. This value for water is about 20,000 times higher than that obtained during the present investigation. Such large differences could be explained only by errors or defective membranes (pin holes). Casagrande and Shannon did point out that variations in the properties of the membranes precluded satisfactory interpretation of their results.

(d) Diffusion of Air through Water and Rubber

Several possible explanations were given by Casagrande and Shannon (33) for the appearance of gas on the low-pressure side of the membranes in the liquid permeability tests discussed in (c) above. One suggestion was that air was carried through the membrane while dissolved in the permeating water. Once it was at low pressure on the downstream side, the water could no longer hold as much dissolved air (Henry's law) and the air came out of solution. For one test it was reported that gas appeared downstream at a rate of 0.002 cm<sup>3</sup> (STP)/cm<sup>2</sup>/hr when a hydraulic pressure difference of 6 kg/cm<sup>2</sup> was applied across the layered system consisting of a 2 cm layer of water and a 0.035 cm thick natural rubber membrane. At the same time water passed through the membrane at a rate of 0.005 cm<sup>3</sup>/cm<sup>2</sup>/hr. If the air passed through the membrane while dissolved in the water, and if the upstream water were saturated with air at 6 kg/cm<sup>2</sup>, then the measured rate of air flow could have been no more than 0.0007 cm<sup>3</sup> (STP)/cm<sup>2</sup>/hr. Thus, some other process must have been occurring in addition to that postulated.

The rate of diffusion of air through the above layered system is calculated in Appendix B using data given in ref. (33) on the permeability of dental dam to air, together with data from other sources (59, 106) on the solubility and diffusion coefficients of air in water. The calculated rate of flow is 0.0037 cm<sup>3</sup> (STP)/cm<sup>2</sup>/hr, which is 75% greater than the measured rate of appearance of gas on the downstream side. Thus all air that appeared downstream could have diffused through the membrane, regardless of whether or not water passed through the membrane simultaneously.

(e) Permeability of Rubber to Water Vapor

Casagrande and Shannon also reported two tests in which the rate of evaporation of water through natural rubber membranes was measured. A soil specimen was enclosed in a membrane and placed in room atmosphere. The measured loss in weight of the soil specimen was assumed to be caused by evaporation of water through the membrane.

The permeability of the rubber membranes was computed by the author from the reported data by assuming an average room temperature of 25°C, an average relative humidity of 50%, and a constant rate of flow. The results are presented in Table A-2 together with similar data from other sources (34, 89, 100 and the present investigation). The apparatus used by Casagrande and Wilson (34) is described in A-05 and that used by the

author is described in Chapters 4 and 6 herein. The apparatus used by Schumacher and Ferguson (89) and by Taylor, Hermann and Kemp (100) are described below.

Schumacher and Ferguson - A membrane was clamped between two metal half-cells and supported on a glass or alundum porous disc. Both chambers were evacuated, then a glass vial containing water was broken inside one chamber. The rate of rise of pressure in the opposite chamber was used to calculate the rate of flow of water vapor.

Taylor, Hermann and Kemp - The apparatus consisted of a shallow metal cup with a wide flange. A metal ring was used to seal the membrane to the flange of the cup. A vial of water inside the cup was broken and the cell was placed within an evacuated bell jar. Sodium pentoxide, a desiccant, was suspended from a sensitive quartz spring inside the bell jar over the membrane. The desiccant absorbed the water as it evaporated through the membrane and caused the spring to extend. The volume flow of water could be calculated from measurements of the extension of the spring.

The agreement among the permeabilities given in Table A-2 is quite good, considering the fact that weighing errors, loss of soil, differences among the membranes and apparatus could each account for the variations in the results.

Measurements of evaporation rates of water through coatings of paraffin, ceresin wax and beeswax were made by Casagrande and Shannon but quantitative data were not presented. They indicate that the waxes were much less permeable than rubber or dipped collodion membranes.

A-05 CASAGRANDE, A. and WILSON, S. D. (1949) (REF. 34)

(a) General

In reference (33) it was concluded that a satisfactory method for preventing evaporation from soil specimens during compression tests which last for weeks had not been found. Therefore new tests were performed to determine the suitability of various protective coatings and chamber fluids for preventing such evaporation. Also, two types of membranes were tested under a hydraulic pressure difference in an effort to determine their permeability to water and castor oil.

(b) Flow of Water and Castor Oil through Rubber

Table A-3 shows the results of tests that were used to evaluate several protective coatings for use in unconfined compression tests. Specimens of Cambridge clay were enclosed in one or two Trojan membranes (0.005 cm thick) which were then bound to a plastic cap and base with a rubber strip. The specimen thus prepared was immersed in water, or castor oil, or was exposed to room atmosphere. No external pressure was applied to the specimens during these tests. The change in weight of the specimens, after being immersed for the periods indicated in the table, was assumed to be entirely due to a gain or loss of water. The tabulated rates of flow were computed by the author from the reported change in water content and duration of test, by assuming that the water flowed through the membrane at a constant rate.

The results of the computations for specimens immersed in water show that water flowed into the specimens at a rate of about 14 mm<sup>3</sup>/day when one membrane was used, and flowed out of the specimens at a rate of about 6 mm<sup>3</sup>/day when two membranes were used. In both cases there should have been a net inflow of water because the pore water was probably in tension, so that there actually was a small vapor pressure difference causing flow into the specimen. The observed losses of water when two membranes were used were probably due to errors in weighing or evaporation of water during handling. Such losses apparently were smaller than the weight of water that flowed into the specimen when only one membrane was used. These data indicate that two membranes will diminish the flow of water into the soil under the conditions of these tests. The effectiveness of the Cello-Seal or Castor Oil cannot be evaluated since no tests were performed using two membranes without grease between them.

The results of tests on specimens immersed in castor oil show that there was a net flow of water out of the specimen of about  $30 \text{ mm}^3/\text{day}$  regardless of the type of protection used. Thus, in this case, two membranes with Cello-Seal between them were no better than one untreated membrane. The fact that water flowed out of the specimen when immersed in castor oil cannot be explained by the author.

The data for immersion of specimens in water or castor oil are not sufficiently accurate to warrant a calculation of the permeability of the membranes to these two liquids. However, there is an indication that castor oil is not as good as water when used as a chamber fluid.

(c) Permeability of Rubber to Water Vapor

The results shown in Table A-3 for specimens that were exposed to room atmosphere, show that the rate of evaporation through the membranes decreased from about  $200 \text{ mm}^3/\text{day}$ , when one membrane was used, to  $80 \text{ mm}^3/\text{day}$ , when two membranes with Cello-Seal between them were used. Thus two membranes appear to be more effective than one for preventing evaporation and the Cello-Seal grease appears to have little effect on the rate of flow.

The rate of evaporation is so great in this case that errors in weighing and losses during handling do not introduce appreciable errors. Therefore a calculation may be made for the permeability of a single membrane to water vapor. For this purpose it is assumed that (1) the relative humidity in the room was 50%, (2) the temperature in the room was  $25^\circ\text{C}$ , and (3) the surface area of the specimen was  $100 \text{ cm}^2$ . The result, shown in Table A-2, is seen to be about one-third as large as the value obtained during the present investigation. In part this may be due to the difference in temperature at which the two tests were performed. An error in the assumed relative humidity, or differences between the membranes, could easily account for the remaining discrepancy between the two measurements.

(d) Diffusion of Air through Water and Rubber

The apparatus shown in Fig. A-1 was used in an attempt to determine the permeability to liquids of (1) two rubber membranes (Trojans, 0.005 cm thick) with a coating of stopcock grease between, and (2) one thick latex rubber membrane fabricated in the laboratory.\* The depth of liquid in the upper chamber was between 0.6 and 1.2 cm. A hydraulic pressure difference of 3.0 to 6.0  $\text{kg}/\text{cm}^2$  was applied in order to simulate the condition of the membrane during a triaxial compression test.

In five tests, using water or castor oil as the permeant, the burette levels rose at a rate which ranged from 0.3 to  $5.0 \text{ cm}^3/\text{day}$ . No attempt was made to determine whether the measured flow was liquid or gas, although in two tests bubbles were seen rising in the burette. On the basis of the discussion in A-04(d), it can be assumed that most, if not all, of the measured outflow was due to diffusion of air through the chamber fluid and the membrane. Since the volume flow of air was not measured separately, the tests furnish no information on the permeability of the membranes to liquids.

Two additional tests were performed with the apparatus in Fig. A-1, using a thick latex rubber membrane fabricated in the laboratory. The top half of the permeability cell and about 150 cm of 3/8 in. O.D. Saran tubing were filled with the permeant (water or castor oil). Air pressure was applied to the permeant inside the Saran tubing. When water was used as the permeant, the burette level rose at a rate of  $0.1 \text{ cm}^3/\text{day}$ . With castor oil as the permeant, the level dropped at a rate of  $1.0 \text{ cm}^3/\text{day}$ . Although these results are far from conclusive, it is evident by comparison with the first five tests above that the simple expedient of inserting a long water-filled tube in the pressure

---

\* The expression "thick latex rubber membrane fabricated in the laboratory" refers to membranes with a thickness of about 0.012 cm fabricated in the Harvard Soil Mechanics Laboratory in accordance with the procedure given in (34).

line reduced the rate of diffusion of air considerably. (Note: An analysis of the effectiveness of a long column of water in preventing the diffusion of air is given in Appendix B.)

(e) Conclusions

The results of these investigations by Casagrande and Wilson lead to the following conclusions:

- (1) Five feet of 3/8 in. outside diameter Saran tubing filled with water probably reduces the rate of diffusion of air from the high to the low pressure side of a membrane during a triaxial test.
- (2) Two membranes are more effective than one in preventing evaporation of water from a soil specimen during an unconfined test. The effectiveness of stop-cock grease in preventing exchange of water between the soil and its surroundings is questionable.
- (3) Specimens that are protected by two rubber membranes and immersed in water lose less water than those immersed in castor oil or those exposed to room atmosphere. Thus castor oil does not appear to be as good as water as a chamber fluid.

A-06 CASAGRANDE, A., and WILSON, S. D. (1951) (REF. 35)

(a) Diffusion of Air through Water and Rubber

The results of the previous investigation (34) indicated that a long water-filled tube of small diameter could be used to slow down the rate of diffusion of air, so tests were made to verify this conclusion.

A 1.4 in. diameter by 3.5 in. high porous carbon specimen was saturated, placed in a triaxial cell and protected by rubber membranes (apparently two Trojan membranes were used). Air pressure was applied to the chamber fluid and a burette was used to measure the outflow from the specimen. The results of three tests are shown in Table A-4.

In test No. 1 the triaxial chamber was filled to just above the top of the membrane with water, and the volume of air which emerged as undissolved air was measured by periodically applying a back pressure of 1.0 kg/cm<sup>2</sup> to the burette. The results are plotted in Fig. A-2 and they show that within the error of the measurements all outflow was due to the passage of air through the chamber fluid and the membranes.

Test No. 2 in Table A-4 and Fig. A-3 shows that the outflow decreased from 1.7 cm<sup>3</sup>/day to 0.01 cm<sup>3</sup>/day or less when a 10 foot length of castor oil-filled Saran tubing was added. On the other hand test No. 3 shows that when the long water-filled tube was removed, the outflow "increased greatly" over its original value of 0.3 cm<sup>3</sup>/day. These tests prove that the introduction of a long, small diameter column of chamber fluid effectively prevents the appearance of undissolved air downstream.

(b) Migration of Dissolved Molecules and Ions through Rubber

The two tests summarized in Table A-5 were performed to determine whether gas molecules dissolved in a liquid solution can pass through a water-membrane system separately from any flow of water even when no pressure difference is involved. However, the rate of water flow through the membrane was not measured in these tests, and so the data cannot be used for the intended purpose. On the other hand, the data are valuable for establishing whether molecules or ions or both can permeate natural rubber membranes. The data will be analyzed below with this purpose in mind.

The apparatus consisted of two half-cells which were separated by a thick latex rubber membrane fabricated in the laboratory. Each half-cell was filled with a specially chosen solution and observations were made to determine whether any of the dissolved substances migrated through the membrane. No hydraulic pressure differences were applied across the membrane.

In test No. 1, the two solutions were KOH and  $\text{FeCl}_3$ . After 12 hours, no precipitate was formed in either chamber, as shown in Table A-5. Precipitate would have formed if the membrane had been pervious to any one of the following pairs of ions simultaneously:

- (1) both  $\text{Fe}^{+++}$  and  $\text{K}^+$ ; (2) both  $\text{OH}^-$  and  $\text{Cl}^-$ ; or (3) both  $\text{OH}^-$  and  $\text{K}^+$ .

These ions are able to pass in pairs because if both ions pass the membrane, electro-neutrality of both solutions would be maintained. Pair (1) shows that the membrane is not pervious to  $\text{Fe}^{+++}$ , because if it were, then the membrane would also have to be pervious to  $\text{K}^+$  since the latter is the smaller ion.\* Pair (2) similarly shows that the membrane is not pervious to  $\text{Cl}^-$ . One is left with  $\text{K}^+$  and  $\text{OH}^-$  to which the membrane might be pervious. But pair (3) shows that the membrane can be pervious to only one of these two ions. Therefore, the membrane is impervious to both  $\text{Fe}^{+++}$  and  $\text{Cl}^-$  and to either  $\text{K}^+$  or  $\text{OH}^-$ .

In test No. 2, the solutions used were  $\text{Ca}(\text{OH})_2$  and water saturated with  $\text{CO}_2$ . Precipitate was formed on the  $\text{Ca}(\text{OH})_2$  side as shown in Table A-5. Any of the following possibilities would explain this result: (1) membrane is pervious to both  $\text{CO}_3^{--}$ \*\* and  $\text{H}^+$ ; (2) membrane is pervious to both  $\text{CO}_3^-$  and  $\text{OH}^-$ ; or (3) membrane is pervious to  $\text{CO}_2$  only. From test No. 1 it is known that the membrane was not pervious to  $\text{Cl}^-$ .  $\text{CO}_3^-$  is larger than  $\text{Cl}^-$  therefore the membrane is also not pervious to  $\text{CO}_3^-$ . This means that items (1) and (2) are eliminated and the only remaining possibility is that the  $\text{CO}_2$  passed in molecular form. On the other hand, precipitate would have formed on the  $\text{CO}_2$  side if the membrane had been pervious to both  $\text{Ca}^{++}$  and  $\text{H}^+$ . If the membrane were pervious to  $\text{Ca}^{++}$ , it must also be pervious to  $\text{H}^+$  because the latter is much smaller. Since precipitate did not form on the  $\text{CO}_2$  side, the membrane must be impervious to  $\text{Ca}^{++}$ .

Test No. 2 showed that  $\text{CO}_2$  could pass through natural rubber, yet ions that are smaller than  $\text{CO}_2$  ( $\text{Ca}^{++}$ ,  $\text{Cl}^-$ ) could not. It is concluded that, within the limits of error of these tests, natural rubber is pervious to neutral particles but impervious to ions. This conclusion is based only on consideration of the sizes of the particles and it is invalidated if specific interactions occur between the membrane and  $\text{Fe}^{+++}$  or between the membrane and  $\text{CO}_3^-$  which would allow passage of these ions.

A-07 MORELAND, R. E. (1957) (REF. 75)

(a) General

While performing a triaxial test program on Great Salt Lake Clay, Parcher (83) noted that considerable leakage into the specimens occurred. He suggested that the leakage was caused by osmosis of chamber water into the pore water of the clay, which had an abnormally high salt concentration. Therefore, measurements of flow of water through natural rubber membranes due to a concentration gradient were made.

(b) Flow of Water Through Rubber due to a Concentration Gradient

A permeability cell similar to the one shown in Fig. A-4 was used. A 3/16 in. outside diameter Saran tube (with approximately 1/8 in. inside diameter) was attached to the up- and down-stream halves of the cell and each was fastened to a meter stick so that volume changes could be measured. A thick natural rubber membrane fabricated in the laboratory was fastened between the two porous stones. One half of the cell was saturated with 0.52 moles/liter of sodium chloride (approximately the concentration of salts in sea water) and the opposite half with distilled water. No hydraulic pressure difference was applied across the membrane. Four tests were performed. Test Nos. 1, 2 and 3 were performed on water soaked membranes and Test No. 4 was performed on a silicone oil soaked membrane. The plot of volume flow versus time for each test was reported.

\* It is assumed that there is no specific reaction between the membrane and  $\text{Fe}^{+++}$  which might allow passage of the latter.

\*\*  $\text{CO}_3^-$  and  $\text{HCO}_3^-$  both exist in equilibrium in the solution, but  $\text{CO}_3^-$  is the smaller ion, hence the most likely to pass the membrane.

In Test No. 1, the inflow did not equal the outflow and the flow direction was opposite to that which is predicted from osmotic theory. Test No. 3 was not continued long enough to obtain a balance of inflow and outflow. The results of these two tests are therefore not of interest.

Test No. 2 gave a linear plot of volume flow versus time for a period of 26 days, as shown in Fig. A-5. The measured flow into the membrane from the water side was  $0.47 \text{ mm}^3/\text{cm}^2/\text{day}$  and the flow out of the membrane on the salt solution side was  $0.30 \text{ mm}^3/\text{cm}^2/\text{day}$ . This difference is partially explained by evaporation of water from the menisci, as shown in paragraph (d) below. These are the only quantitative data available, other than those obtained in the present investigation, on osmotic flow through natural rubber.

The results of Test No. 4, on a silicone-oil-soaked membrane are shown in Fig. A-6, plotted to the same scale as Fig. A-5. There was no detectable change on the water side or the salt side for 11 days. Based on this result, Moreland stated that "silicone oil treatment of a membrane will be a great help in reducing flow through the membrane." The results of the present investigation show that silicone-oil-soaking has no such effect. The difference between Moreland's results and the present result may be explained by either (1) non-uniform thickness or pinholes in the membranes used by Moreland or (2) the insensitivity of Moreland's apparatus for measuring volume changes. From the results of the present investigation, one would predict that Moreland should have measured a total flow of only  $20 \text{ mm}^3$  in 10 days through either a silicone-oil-soaked or an unsoaked membrane of the type he used. This is about the smallest volume measurable in Moreland's apparatus.

Moreland also performed a test in which he filled a thick rubber membrane with 0.52 molar sodium chloride, sealed the top, and immersed it in distilled water for 21 days. He then measured the change in volume, weight and concentration of the solution inside the membrane. If one assumes that ions permeated the membrane at a negligible rate relative to the water, the volume inflow of water that would be required to cause the measured change in concentration can be estimated. The volume calculated in this manner by the author from Moreland's data is about  $4.0 \text{ cm}^3$ . Moreland's measurements of volume change and weight change were  $9 \text{ cm}^3$  and  $7.0 \text{ gm}$  respectively. These data are equivalent to a flow of water into the membrane of  $0.9$  to  $1.8 \text{ mm}^3/\text{cm}^2/\text{day}$ , or two to four times the value Moreland measured in the permeability cell.

(c) Flow of Ions Through Rubber due to a Concentration Gradient

At the conclusion of each test performed in the permeability cell, Moreland measured the salt concentration in the chamber which originally contained pure water. The final salt concentrations are given in the following tabulation:

Test No.	Duration (days)	Salt Concentration (milligram/liter)	Rate of Change (milligram/liter/day)
1	14	48.1	3.4
2	38	98.0	2.6
3	16	36.5	2.3
4	15	8.2	0.55

These data are the only available information on the flow of ions through natural rubber membranes. While water was passing through the membrane towards the salt solution, ions were also passing from the solution into the water. This ion flow causes a small change in volume of the solution into which the flow occurs. It is of interest to compare (1) the volume increase on the water side due to the flow of ions with (2) the volume decrease on the water side caused by the flow of water into the salt solution. From experimental data on the change in specific gravity of a salt solution as salt is added to water, one can determine the resulting volume change. If this is done, it can be shown that the rate of volume increase in  $\text{mm}^3/\text{cm}^2/\text{day}$  is equal to  $94.8 \times 10^{-6}$  times the rate of

change of concentration in mg/l/day for the cell Moreland used. Thus, for Test No. 2, the rate of volume increase amounts to  $0.25 \times 10^{-3} \text{ mm}^3/\text{cm}^2/\text{day}$ . This value is about 1500 times less than the rate of water flow measured by Moreland in Test No. 2.

(d) Evaporation from Menisci

Moreland pointed out that evaporation from the menisci in the Saran tubing which he used for burettes may have introduced an error in his results. He performed two tests in which he measured the rate of evaporation of water from pure water and from salt water with a concentration of 0.5 molar. A partially opened valve was attached to the top of a 3/16 in. outside diameter Saran tube and was filled with liquid so that the set up was the same as for the tests described in (c) above. The measured rate of evaporation\* was about  $1.6 \text{ mm}^3/\text{day}$  in both cases. Since the area of his diffusion apparatus was  $40 \text{ cm}^2$ , the above rate of evaporation is equivalent to a flow rate through the membrane of  $0.04 \text{ mm}^3/\text{cm}^2/\text{day}$ . This rate is 10% of the rate of flow of water measured by Moreland in his Test No. 2, and so evaporation introduces some error if not taken into account.

A-08 WILSON, N.E. (1958) (REF. 107)

(a) Permeability of Rubber to Liquid Water

A lucite apparatus, shown in Fig. A-7, was used to measure the permeability of a thick latex rubber membrane fabricated in the laboratory. An O-Ring seal was used to prevent leakage around the perimeter of the membrane, as had been suggested previously by Moreland (75). In order to prevent air from diffusing through the membrane from the high pressure side, the pressure was applied by a head of mercury, rather than high pressure air. Inflow and outflow measurements were made in 1/8 inch outside diameter Saran tubing connected to the inflow and outflow sides of the membrane and attached to meter sticks. This apparatus was a considerable improvement over that shown in Fig. A-1. However, in the one test that was performed the inflow and outflow measurements did not agree. The following important deficiencies in this "improved" apparatus were observed by Wilson: (1) The Hoke valves used in the system were defective. (2) The brass fittings could not be well sealed into the Lucite. (3) It was thought that the data were obscured by the absorption of water by the Lucite and Saran. (4) Air was easily trapped in the porous stone.

A new apparatus shown in Fig. A-8 was therefore designed by Hirschfeld (58). The new permeability cell was made of brass, and all valves were eliminated. The porous disc was replaced by several layers of filter paper which could be saturated easily. Wilson used this apparatus for one test on a "drug store" type membrane. Volume changes were measured in 1/8 in. outside diameter Saran tubing. The inflow and outflow measurements did not agree, but based on the inflow burette readings, the measured flow was  $0.05 \text{ mm}^3/\text{cm}^2/\text{day}$  under a pressure difference of  $1.2 \text{ kg}/\text{cm}^2$ . The actual flow through the membrane must have been less than this value since the rate quoted includes loss by leakage from the apparatus. Further tests were performed in this apparatus and are reported in Paragraph A-09.

(b) Flow of Water Vapor through Saran and Polyethylene

N. E. Wilson measured the rate of evaporation through the walls of Saran and Polyethylene tubing in order to determine whether such losses would cause a significant error during a membrane permeability test. A six meter length of tubing was filled with water and subjected to an internal pressure of  $0.1 \text{ kg}/\text{cm}^2$ . No other details of the tests were given. The results were as follows:

---

\* The rate of evaporation through the wall of the Saran tubing is negligible relative to the rate of evaporation from the menisci.

Tubing Material	Size	Rate of Evaporation mm <sup>3</sup> /cm/day
Saran	1/8" O.D. 1/16" I.D.	0.0012
Polyethylene	1/4" O.D. ? I.D.	0.005

If the ratio of wall thickness to diameter were the same for both tubes, then polyethylene would be four times more pervious to water vapor than Saran. One test during the present investigation yielded a rate of evaporation of 0.0007 mm<sup>3</sup>/cm/day for 0.140 in. outside diameter by 0.071 in. inside diameter Saran. This is in fair agreement with Wilson's result, but a detailed comparison is not warranted since the details of Wilson's test procedure are not available.

A-09 HIRSCHFELD, R. C. (1960) (REF. 58)

(a) General

Hirschfeld (57, Fig. 27) measured water leakage by comparing the change in weight of a triaxial specimen with the volume change measured in the drainage burette. In 76 triaxial R tests he found that the rate of leakage scattered considerably but in 70% of the tests it was between 0 and 0.3 cm<sup>3</sup>/day with an average for all tests of about 0.15 cm<sup>3</sup>/day. It was not known whether the major portion of this leakage was occurring past the bindings (rubber strips) or directly through the membranes. As a first step in determining the source of the leakage, Hirschfeld constructed the apparatus shown in Fig. A-8 to measure the permeability of membranes to water.

(b) Permeability of Rubber to Liquid Water

Six tests were performed on natural rubber membranes which were about 0.006 cm thick. The inflow and outflow measurements did not agree in any of these tests, but the measured flow, based on the inflow burette readings of the three best tests was 0.05 mm<sup>3</sup>/cm<sup>2</sup>/day under a pressure difference of 1.1 kg/cm<sup>2</sup>. This value agrees with the data of N. E. Wilson above. The following deficiencies of the apparatus can be detected from the plots of volume flow versus time: (1) Evaporation and/or leakage of water from the downstream side was greater than the leakage through the membranes tested. (2) Room temperature variations caused the upstream meniscus to move erratically. (3) All plots of flow versus time were non-linear, indicating that leakage or other errors were obscuring the data.

The results of these tests indicated that temperature control and finer burettes for volume change measurements would be required. The rate at which the upstream burette levels dropped, although partly due to leakage, furnished an upper limit for the permeability of membranes which was used as a guide to develop the apparatus used in the present investigation.

A-10 SEED, H. B., MITCHELL, J. K., AND CHAN, C. K. (1960) (REF. 90)

The flow of air through two rubber membranes (prophylactics) was measured by placing the membranes on a 1.4 in. diameter by 3.5 in. high porous cylinder in a triaxial apparatus. The porous cylinder and drainage lines were saturated with water and a burette was connected and left open to the atmosphere to measure outflow. The chamber was filled three-fourths full of water (about 4 cm above the top of the porous cylinder) and air pressure of 1 kg/cm<sup>2</sup> was applied to the water. The outflow rate steadily increased for three days, after which time it remained constant at 2.2 cm<sup>3</sup>/day for 5 days. It was found that the entire outflow was air, since, when a vacuum was applied to the burette, air was removed and the burette reading returned to its initial value.

An "air-seal" was designed to reduce the high rate of flow of air through the water and membrane into the porous cylinder. The air seal consisted of a 1-1/4 in. diameter by 2-1/2 in. long chamber within which the air and water were separated by a 0.043 cm thick rubber membrane. A test similar to the one described above was then performed, except

that the air seal was used and the chamber pressure was  $5 \text{ kg/cm}^2$ . "No signs of air leakage in 14 days" were noted. A calculation may be made based on the information in Appendix B to determine the effect of this device on the rate of diffusion of air. With the air seal in place, the distance between the top of the porous cylinder and the air is about 20 cm, rather than 4 cm as in the first test. Also, with the air seal in place the air was forced to diffuse through fittings which had a far smaller cross section than the entire triaxial chamber. Taken together, the effect of the decreased area available to flow and the longer path length would decrease the rate of air diffusion by a factor of at least one thousand. This would mean that  $0.03 \text{ cm}^3$  of air would diffuse into the porous stone in 14 days. Even without the rubber air seal, the system would have been practically air tight. If the air seal were made of a highly impervious rubber or plastic (butyl rubber or teflon), then it could be equivalent to a column of water about 25 cm long. However, a short length of small diameter tubing filled with water would serve the purpose equally well.

A-11 WISEMAN, G. (1961) (REF.108)

The work reported in this note was performed at Harvard University during the summer of 1954 at the suggestion of Professor A. Casagrande.

Three tests were performed in the apparatus shown in Fig. A-4 to measure the permeability of natural rubber membranes to water. The membranes were fabricated in the laboratory and were 0.012 cm thick. The following important precautions in the technique of testing were employed:

- (1) The porous stone was saturated prior to test by boiling it in water for two hours. The remainder of the apparatus was soaked for 24 hrs so that it would absorb very little water during the test. The membrane was placed in the apparatus while the apparatus was submerged.
- (2) A 3/16 in. outside diameter Saran tube was attached to the up and downstream halves of the cell and filled with water to a distance of 5 ft from the membrane. Air pressure of  $6 \text{ kg/cm}^2$  was applied to the meniscus in the Saran tube. The low pressure side was left at atmospheric pressure. The tubes were calibrated and mounted on meter sticks so that flow measurements could be made. Thus, both the inflow and outflow rates were measured as a check.
- (3) The entire cell was submerged in a water bath and held at  $25^\circ\text{C}$  during the tests.

In all three tests the downstream burette levels dropped, but the entire decrease occurred in one day and was due to the measured decrease in volume of undissolved air in the system. There was no increase in undissolved air volume on the outflow side of the membrane for 60 days. This is convincing experimental evidence that a long column of water will prevent air from appearing on the outflow side of a membrane. The tubing was 3/16 in. outside diameter and the water column was 5 ft long, as compared with the 1/8 in. outside diameter tubing and 10 ft water column used by Casagrande and Wilson (34). The permeability to air of Wiseman's system was four times greater than that of Casagrande and Wilson, yet no measurable quantity of air permeated the membrane.

The upstream burette levels also dropped, as would be expected. Assuming a linear drop with time, then the rate of flow was  $0.17 \text{ mm}^3/\text{cm}^2/\text{day}$  under a pressure difference of  $6 \text{ kg/cm}^2$ . Under the same conditions, data obtained in the present investigation would have given a flow of  $0.02 \text{ mm}^3/\text{cm}^2/\text{day}$ . The large difference might be explained by leakage from the periphery of the membrane in Wiseman's apparatus.

Wiseman pointed out that it was known (no references were given) that the vapor pressure difference across a membrane controls the rate of flow, all other variables being constant. He used published data on water vapor permeability of rubber and correctly calculated that in 60 days, the duration of his tests, he would expect  $0.01 \text{ cm}^3$  of water to pass the membrane. Thus Wiseman felt that his apparatus was not sufficiently sensitive to measure leakage through the membranes used in triaxial testing.

It is unfortunate that Wiseman did not prepare a report on the results after completion of his investigation in 1954, to stimulate later investigators (75,107,58) to use more refined apparatus for their studies of membrane permeability.

A-12 FOST, R. B. (1962) (REF.48)

Fost performed one test to determine the rate of osmotic flow of water through a silicone rubber membrane due to a concentration gradient. The membrane was made in the laboratory from RTV-60 silicone rubber. It may be inferred that the membrane tested was 0.018 cm thick although its thickness is not given explicitly. A 0.51 molar solution of sodium chloride was placed inside the membrane which was then sealed and immersed in distilled water for 135 days. The net flow of water into the membrane was 13.6 cm<sup>3</sup> through an area of 200 cm<sup>2</sup>, which is equivalent to 0.50 mm<sup>3</sup>/cm<sup>2</sup>/day. This value is in agreement with Moreland's (75) data for natural rubber.

A-13 WISSA, A. E. (1962) (REF.109)

The purpose of this study was to determine the "effect of water on the permeability of rubber latex" to nitrogen.

The apparatus used is shown in Fig. A-9. The top of the cell can be removed while the membrane is still held in place by the central ring. Thus, water could be added after measuring the dry permeability of the membrane, so that the permeability to nitrogen in the presence of water could also be measured. The flow of nitrogen was measured by allowing the nitrogen to pass out of the connection on the cell and into a U-tube. The bottom of the U was filled with water to prevent the escape of nitrogen. A reading was taken by equalizing the water levels in both arms of the U-tube and measuring the length of the column of nitrogen on the cell side.

Wissa reported a value of  $5 \pm 0.5 \times 10^{-11}$  cm<sup>4</sup>/gm sec as the permeability to nitrogen of a dry natural rubber membrane about 0.007 cm thick. Since the permeability of natural rubber to oxygen is about three times higher than to nitrogen, Wissa would have measured a permeability to air of about  $8 \times 10^{-11}$  cm<sup>4</sup>/gm sec. This value is included in Table A-1 and is seen to agree exactly with the data of Casagrande and Shannon (33).

Wissa also found that when a 0.775 cm thick layer of water was placed over the membrane, the rate of flow of nitrogen through the water and rubber was reduced by a factor of thirty below that which occurred through the dry rubber under the same pressure difference. Having this result, Wissa then considered the water and membrane as a layered system in order to estimate the permeability to nitrogen of the membrane in the presence of water. Using essentially the same method of calculation as presented in Appendix B, he found that the permeability of natural rubber with water present, was one hundred times less than the permeability of the dry membrane. However, Wissa pointed out that if he had used a value of  $1 \times 10^{-5}$  cm<sup>2</sup>/sec for the diffusion coefficient of nitrogen in water, instead of  $2 \times 10^{-5}$  cm<sup>2</sup>/sec, the wet and dry permeabilities would have been equal to each other. The reason for this large effect of the value of the coefficient of diffusion is that practically all of the resistance to flow was developed in the water layer rather than in the rubber. Therefore, Wissa's method was not sufficiently accurate to obtain a reliable value of the permeability of natural rubber to nitrogen in the presence of water.

One test was also reported in which considerable turbulence was introduced in the water layer over the rubber membrane. Wissa found that the rate of flow of nitrogen through the membrane in this case was a maximum of half the rate measured for a dry membrane. He concluded that water soaking probably does not reduce the permeability to nitrogen by the factor of one hundred, as he had previously calculated.

The author's reaction to Wissa's proposal that water soaking should reduce the permeability of rubber to water is as follows: A rubber membrane might be visualized as a matrix of impermeable rubber perforated by many minute pores through which flow takes place. If this were a correct model, then the presence of water in these pores would decrease the rate of flow considerably. However, it is shown in Appendix B that air, when measured in units of moles per second, diffuses through water four times faster than

through an equal thickness of rubber. This means that if rubber can be visualized as having "pores", then diffusion of gas through water also might occur through "pores"! It is concluded that rubber should not be thought of as a matrix perforated by small pores. Water molecules probably permeate rubber by passing between rubber molecules which must be forced aside during the flow process. If this is the true physical mechanism of flow, then the presence of a very low concentration of water molecules in the rubber (6% by weight) cannot appreciably affect the permeability of the rubber to gas.

APPENDIX BTHE FLOW OF AIR THROUGH WATER AND/OR RUBBER**B-01** PURPOSE

The following items will be covered in this Appendix:

- (1) The equation governing the steady flow of air through water and/or rubber.
- (2) Calculation of the rate of flow of air through a column of water.
- (3) Calculation of the rate of flow of air through a system consisting of a layer of water and a layer of rubber.
- (4) Calculation of the rate of diffusion of air into or out of a triaxial specimen into the chamber water.

**B-02** EQUATION OF STEADY FLOW OF AIR THROUGH WATER OR RUBBER

Van Amerongen (2) indicated that gas diffuses through either water or rubber in accordance with Fick's first law, Eq. 3-47. Combining Henry's law of solubility with Fick's law, van Amerongen showed that

$$q_s = \frac{sD}{p_s} A \frac{\Delta p}{L} \quad (\text{B-1})$$

where  $q_s$  = rate of flow of air through medium (cm<sup>3</sup>/sec). Volume of air is measured at atmospheric pressure.  
 $p_s$  = standard atmospheric pressure (gm/cm<sup>2</sup>).  
 $s$  = solubility of air in medium as defined by Eq. 2-2 (cm<sup>3</sup> of air per cm<sup>3</sup> of medium).  
 $D$  = coefficient of diffusion in the membrane (cm<sup>2</sup>/sec).  
 $\Delta p$  = partial pressure difference in air across the medium (gm/cm<sup>2</sup>).

One can define the "permeability" of the medium to air as follows

$$K_s = \frac{sD}{p_s} \quad (\text{B-2})$$

so that Eq. B-1 becomes

$$q_s = K_s A \frac{\Delta p}{L} \quad (\text{B-3})$$

Using Eq. B-2 and the known values of  $s$  and  $D$  for air in water or rubber one can compute the permeability of water or rubber to air. The coefficient of diffusion of nitrogen or oxygen in water is about  $2 \times 10^{-5}$  cm<sup>2</sup>/sec at 22°C (106, vol. 5, p. 64). The solubility of air in water is 0.019 at 22°C. Therefore the permeability of water to air is

$$(K_s)_w = \frac{sD}{p_s} = \frac{0.019 \times 2 \times 10^{-5}}{1033} = 3.7 \times 10^{-10} \text{ cm}^4/\text{gm sec}$$

where the subscript  $w$  denotes water. To determine the permeability of natural rubber to air one may use the rate of flow data of Casagrande and Shannon (33) or of Wissa (109)

and calculate the permeability from Eq. B-3. For both sets of data one obtains

$$(K_g)_r = 0.80 \times 10^{-10} \text{ cm}^4/\text{gm sec}$$

Thus the permeability of water to air is 4.6 times greater than the permeability of natural rubber to air.

#### B-03 FLOW OF AIR THROUGH A COLUMN OF WATER

Using the value of permeability of water to air given above, it is a simple matter to calculate the rate of flow of air through water for any given case. In triaxial testing, a long column of water within a 1/16 in. inside diameter Saran tube is used to restrict the flow of air from an air pressure source through the water in the tube and chamber into the triaxial specimen. At Harvard University, the length of the Saran tubing used for this purpose is generally about two meters.

A numerical example for the rate at which air can flow through the water inside a Saran tube follows. Given:

- (1) Length of Saran tube = one meter
- (2) Inside diameter of tube = 0.16 cm
- (3) Pressure of air at one end of tube = 10 kg/cm<sup>2</sup>
- (4) No air present in the water on the end of the tubing that is attached to the triaxial chamber.

For the above conditions, the quantities to be substituted into Eq. B-3 are:

$(K_g)_w = 3.7 \times 10^{-10} \text{ cm}^3(\text{STP}) \text{ cm}/\text{gm sec}$ ;  $A = 0.0201 \text{ cm}^2$ ;  $\Delta p_p = 10,000 \text{ gm}/\text{cm}^2$ ;  $L = 100 \text{ cm}$ . Thus the rate of flow of air is  $q_g = 6.3 \times 10^{-5} \text{ cm}^3(\text{STP})/\text{day}$  or  $0.06 \text{ mm}^3(\text{STP})/\text{day}$ . In 100 days, only  $6 \text{ mm}^3$  of air would enter the chamber even if the chamber initially contained no air. One liter of water can dissolve  $20,000 \text{ mm}^3$  of air under a pressure of only one atmosphere, so that the air that flows through the long column of water in 100 days can easily be dissolved in the chamber water. From Table 9-3 it can be seen that if the  $6 \text{ mm}^3$  of air were to enter directly into the soil specimen, the effective stress would not change appreciably, even for a very critical case.

#### B-04 FLOW OF AIR BETWEEN TWO BUBBLES OF DIFFERENT SIZE IN A WATER MEDIUM

Consider two air bubbles in the water filled voids of a specimen of clay. The bubbles have a diameter of one micron and one-half micron respectively. The air pressure in the bubbles is given by (see 20)

$$u_{ab} = \frac{0.3}{d} \quad (\text{B-4})$$

where  $d$  is the diameter of the bubble in cm and  $u_{ab}$  is the air pressure in the bubble in gm/cm<sup>2</sup>. Due to the difference in air pressure in the two bubbles, air will flow from the smaller to the larger bubble in accordance with Eq. B-3. A rough estimate of the rate of air flow can be obtained by assuming that the flow will occur in a straight line between bubbles in a path with an area equal to the cross sectional area of the smaller bubble. These assumptions will yield a conservative (low) estimate of the rate of air flow. The values to be substituted in Eq. B-3 to calculate the rate of flow are:

$(K_g)_w = 3.7 \times 10^{-10} \text{ cm}^4/\text{gm sec}$ ;  $A = 19.5 \times 10^{-10} \text{ cm}^2$ ;  $L = 1 \text{ cm}$ ;  $\Delta p_p = 3000 \text{ gm}/\text{cm}^2$ . The result is:  $q_g = 1.90 \times 10^{-7} \text{ mm}^3/\text{day}$ , where the air volume is measured at atmospheric pressure.

The initial volume of air in the small bubble is  $V_b = 0.66 \times 10^{-10} \text{ mm}^3$ . The initial air pressure in the small bubble is  $6 \text{ kg}/\text{cm}^2$  above the pressure in the surrounding water. Assuming the water pressure is  $6 \text{ kg}/\text{cm}^2$  (gage), then, using Boyle's law, the initial volume of air in the small bubble measured at atmospheric pressure  $(V_b)_{\text{atm}}$  is

$$(v_b)_{\text{atm}} = v_b \frac{u_a}{P_g} = 0.66 \times 10^{-10} \times \frac{13}{1}$$

$$(v_b)_{\text{atm}} = 0.85 \times 10^{-9} \text{ mm}^3$$

A comparison between the initial air volume in the bubble and the rate of flow under the initial conditions shows that if the initial rate of flow remained constant, the small bubble would disappear in seven minutes! If the small bubble were even smaller than 0.5 microns diameter, the time required to transfer all air in the small bubble to the large bubble would be even shorter. Therefore the estimate of seven minutes is probably somewhat on the high side. However, if the two bubbles were more nearly equal in size, the time required would be longer. For example, if the initial diameter of the small bubble were 0.75 microns, the time required for it to disappear would be about 30 minutes.

#### B-05 FLOW OF AIR THROUGH A LAYERED SYSTEM OF WATER AND RUBBER

Assuming that Fick's law and Henry's law apply to the flow of air through rubber and water, the partial pressure gradient through a layered system of water and natural rubber, Fig. B-1(a), would be as shown in Fig. B-1(b). The partial pressure gradient in the rubber is 4.6 times as steep as the pressure gradient in the water because rubber is 4.6 times less permeable to air than water.

Again assuming that Fick's and Henry's laws apply, the variation in concentration of air in the rubber and water is shown in Fig. B-1(c). The concentration gradients in water and rubber are not in the ratio 1:4.6 because the solubility of air in water is different from that in rubber. Instead, the concentration gradients in water and rubber are in the ratio 1:13.7, which is the inverse ratio of the coefficients of diffusion of the media. The abrupt jump in concentration at the water-rubber interface is also due to the difference between the solubility of air in water and the solubility of air in rubber.

The equivalent permeability of the layered system of water and rubber can be calculated using the same analysis as is used to calculate the equivalent vertical permeability of horizontally stratified deposits of soils (102, p. 49). Thus the equivalent permeability of the water and rubber system is

$$(K_s)_{\text{eq}} = \frac{\frac{L_w}{L_w} + \frac{L_r}{L_r}}{\frac{(K_s)_w}{(K_s)_w} + \frac{(K_s)_r}{(K_s)_r}} \quad (\text{B-5})$$

Example: Compute the rate of flow of air through a layered system consisting of 2 cm of water and one 0.035 cm thick natural rubber membrane, with an area of one cm<sup>2</sup>, due to a pressure difference of 6.0 kg/cm<sup>2</sup>. (These are approximately the test conditions used by Casagrande and Shannon (33) to measure the permeability of natural rubber to liquid water.) The equivalent permeability of the system is

$$(K_s)_{\text{eq}} = \frac{\frac{2}{2.0} + \frac{0.035}{0.035}}{\frac{3.7}{3.7} + \frac{0.035}{0.80}} \times 10^{-10}$$

$$(K_s)_{\text{eq}} = 3.5 \times 10^{-10} \text{ cm}^4/\text{gm sec}$$

From Eq. B-3 the rate of air flow is

$$\begin{aligned}
 q_g &= 3.5 \times 10^{-10} \times \frac{6000}{2.035} \\
 &= 10.3 \times 10^{-7} \text{ cm}^3 \text{ (STP) / sec / cm}^2 \\
 q_g &= 0.0037 \text{ cm}^3 \text{ (STP) / hr / cm}^2
 \end{aligned}$$

#### B-06 DIFFUSION OF AIR BETWEEN SPECIMEN AND CHAMBER WATER

Assume that a partially saturated specimen is consolidated to an effective stress  $\bar{\sigma}_3$  in a triaxial cell, that the pore air pressure is  $u_a$ , that the chamber water at pressure  $\sigma_c$  is saturated with air at a pressure  $u_{ac}$ , that  $u_a > u_{ac}$  and that  $u_a < \sigma_c$ . Thus, air will flow from the specimen into the chamber water and will dissolve therein. The volume of air that will flow out of the specimen in a given time will be calculated by two approaches.

First, it will be assumed that the partial pressure gradient in air occurs only in the membrane. Thus, the confining membrane controls the rate of air flow from the specimen and no partial pressure gradient develops in the pore water or in the chamber water. For this approach, the air flow is governed by Eq. B-3 and the rate of air flow for the following example

Membrane: Natural rubber;  $(K_g)_r = 0.80 \times 10^{-10} \text{ cm}^4 / \text{gm sec}$ ;  $L = 0.012 \text{ cm}$ .

Specimen size: 1.4 in. diameter by 3.5 in. high; surface area =  $100 \text{ cm}^2$ .

Partial pressure difference  $u_a - u_{ac}$ :  $\Delta p_p = 1.0 \text{ kg/cm}^2$

is found to be:  $q_g = 2.40 \text{ cm}^3 / \text{hr}$ , where the volume is measured at atmospheric pressure. If the partial pressure gradient were in the opposite direction, the same rate of flow would occur into the specimen. This approach approximates the rate at which air would flow into a triaxial specimen if air were used as a chamber fluid, or if the chamber fluid were kept well stirred while flow occurs.

For the second approach, it is assumed that the problem may be represented approximately as a case of radial diffusion from a short section of an infinitely long cylinder into a surrounding medium, with the initial boundary conditions as shown in Fig. B-2. To simplify the problem it is assumed that the resistance of the rubber membrane to air flow is the same as an equal thickness of water and that the pressure  $u_a$  remains constant\* and uniform within the specimen. After some time  $t$  the partial pressure gradient might be represented by the lines shown dashed in Fig. B-2. In order that such a gradient be possible, there must be no convection currents in the chamber water, which would tend to make the partial pressure of the air uniform throughout the chamber. With these assumptions, the equations governing flow across the specimen boundary will be the same, regardless of the sense of the pressure gradient.

The radial diffusion problem as stated above is analogous to heat flow from a hot cylindrical opening into an infinite surrounding medium. This problem has been solved by Carslaw and Jaeger (19, p.282) who show the exact solution and approximate solutions for small and large times. Computations were made using the exact solution and it was found that, for cases of interest herein, the exact solution yielded flow rates only 5% greater than did the approximate solution for small times. Converting the notation for analogous quantities, the approximate solution for small times is

\* This assumption is quite reasonable for the small changes in  $u_a$  of interest herein.

$$q_s = \frac{2K_s A \Delta p_p}{D_s} \left[ \frac{1}{\sqrt{\pi T}} + \frac{1}{2} - \frac{1}{4} \sqrt{\frac{T}{\pi}} + \frac{1}{8} T \dots \right] \quad (\text{B-6})$$

which gives the flow rate  $q_s$  across the boundary of the cylinder at a time when the time factor is  $T$ . The time factor is:

$$T = \frac{4 D t}{D_s^2} \quad (\text{B-7})$$

where  $D$  = coefficient of diffusion of air in water  
 $t$  = time after start of diffusion  
 $D_s$  = diameter of specimen

The total volume of air flow  $J_a$  in time  $t$  is given by the integral

$$J_a = \int_0^t q_s dt \quad (\text{B-8})$$

Substituting Eq. B-6 into Eq. B-8 and integrating one obtains

$$J_a = \frac{2K_s A \Delta p_p}{D_s} \left[ 2 \sqrt{\frac{D_s^2}{\pi D}} t^{1/2} + \frac{1}{2} t - \frac{1}{3} \frac{D}{\pi D_s^2} t^{3/2} + \frac{1}{4} \frac{D}{D_s^2} t^2 \dots \right] \quad (\text{B-9})$$

Example: Compute volume of air flow in three hours and in twenty-four hours for an initial partial pressure difference of  $1.0 \text{ kg/cm}^2$ . The given data are:

$$\begin{aligned} (K_s)_w &= 3.7 \times 10^{-10} \text{ cm}^4/\text{gm sec} & D_s &= 3.56 \text{ cm} \\ \Delta p_p &= 1000 \text{ gm/cm}^2 & t_1 &= 10,800 \text{ sec} \\ D &= 2 \times 10^{-5} \text{ cm}^2/\text{sec} & A &= 100 \text{ cm}^2 & t_2 &= 86,400 \text{ sec} \end{aligned}$$

Substitution of these data into Eq. B-9 gives  $J_a = 1.0 \text{ cm}^3$  in 3 hours and  $J_a = 3.3 \text{ cm}^3$  in 24 hours.

The above air flow volumes should be compared with the air flow volumes  $J_a = 7.2 \text{ cm}^3$  in 3 hours and  $J_a = 57.6 \text{ cm}^3$  in 24 hours, obtained using the first approach. The results show that if the chamber water is thoroughly mixed so that the partial pressure gradient can develop only inside the membrane (approach (1)), then the three hour flow is seven times greater, and the twenty-four hour flow is fifteen times greater than for the case of no mixing of the chamber water. Since most soil specimens of interest in triaxial testing contain less than  $10 \text{ cm}^3$  of air (measured at atmospheric pressure), the above flow rates obviously can introduce large errors. The following factors can cause the rates of flow calculated using the second approach to be in error:

Causing the calculated rates of flow to be too high - (1) The pore air must flow from the interior to the sides of the specimen through the water-filled voids (if the air spaces are not inter-connected), so that a gradient will develop within the specimen. (2) The resistance of the membrane to air flow is somewhat higher than the resistance of an equal thickness of water. However, it is shown in B-07 that, for a natural rubber membrane, the difference is negligible.

Causing the calculated rates of flow to be too low - (1) Convection currents can cause mixing in the chamber water to maintain a steep gradient across the membrane. (2) There are no impervious boundaries at the top and bottom of the specimen, so that actually more "area" is available for flow in the chamber than would be available for the infinitely long cylinder considered, i.e. there is actually leakage by the impervious boundaries shown in Fig. B-2.

The author believes that the air volumes calculated using approach (2) are probably too low by not more than a factor of two. Information on the rate of mixing that might occur in the chamber water should be obtained in order to estimate its effect. The remaining assumptions mentioned above are believed to have lower order effects.

#### B-07 APPROXIMATE EQUATION FOR DIFFUSION OF AIR OUT OF SPECIMEN

In the calculations using Eq. B-9 it was found that the first term in the series was the largest single contributor to the calculated flow rate. For the three hour flow, the first term contributed 91% of the total, and for the twenty-four hour flow, the first term contributed 80% of the total. Thus the volume of air flow may be approximated using only the first term of the series in Eq. B-9, which gives

$$J_a = \frac{2K_s A \Delta p_p}{\sqrt{\pi D}} \sqrt{t} \quad (\text{B-10})$$

Dividing by the volume of the specimen, and substituting the equations for the surface area and volume in terms of the diameter and height, one obtains the following approximate equation

$$\frac{J_a}{V} = \frac{8}{\sqrt{\pi}} \frac{K_s}{D} \frac{\Delta p_p}{D_s} \sqrt{t} \quad (\text{B-11})$$

Eqs. B-10 and B-11 show that the volume of leakage is proportional to the ratio  $(K_s/\sqrt{D})$ , which is a constant peculiar to the medium of diffusion. From the data given in B-02 one can calculate this ratio. The results are

$$\begin{aligned} \text{Natural rubber} &- K_s/\sqrt{D} = 6.8 \times 10^{-8} \text{ cm}^3/\text{gm}\sqrt{\text{sec}} \\ \text{Water} &- K_s/\sqrt{D} = 8.2 \times 10^{-8} \text{ cm}^3/\text{gm}\sqrt{\text{sec}} \end{aligned}$$

The close agreement of these two constants shows that for a rough computation of the volume of air flow into or out of a specimen, it is immaterial whether the membrane is present, or whether it is replaced, for the purposes of calculation, by a quiescent film of water of equal thickness. It is not known whether synthetic rubbers have substantially lower values of  $K_s/\sqrt{D}$ .

APPENDIX CSUPPLEMENTARY DERIVATIONS FOR CHAPTER 2C-01 DERIVATION OF APPROXIMATION FOR HENRY'S LAW

The following derivation which is essentially identical to that given by Hilf (56), results in an approximate equation giving the volume of gas (measured at the pressure and temperature in the gas phase) dissolved in a given volume of liquid, when the liquid is saturated with gas.

Henry's law of solution of gases in liquids, which applies only for the case of dilute solutions, is

$$u_g = HX \quad (C-1)$$

where  $u_g$  = pressure in gas phase.

$H$  = Henry's constant for air dissolving in water, which has a value of 68,500 kg/cm<sup>2</sup> at 20°C and increases slowly with increasing temperature.

$X$  = mole fraction of gas in solution.

The mole fraction of gas in solution is given by

$$X = \frac{m_g}{m_g + m_p} \quad (C-2)$$

where  $m_g$  and  $m_p$  are the number of moles of gas and liquid respectively. Since Henry's constant is very large, the mole fraction of air dissolved in water, at pressures ordinarily used in triaxial testing, is very small. (For  $u_g = 20$  kg/cm<sup>2</sup>,  $X = 2.9 \times 10^{-4}$ .) Thus, in Eq. C-2, the quantity  $m_g$  can be neglected relative to  $m_p$  giving

$$X = \frac{m_g}{m_p} \quad (C-3)$$

The ideal gas law gives

$$u_g V_g = m_g RT \quad (C-4)$$

where  $V_g$  is the volume of gas,  $R$  the gas constant and  $T$  the absolute temperature. Substituting for  $m_g$  in Eq. C-3, one obtains

$$X = \frac{u_g V_g}{RT m_p} \quad (C-5)$$

which may in turn be substituted in Eq. C-1, and solved for  $V_g$  to obtain

$$V_g = \frac{RT m_p}{H} = \frac{RT W_p}{H M_p} = \frac{RT \gamma_p}{H M_p} V_p \quad (C-6)$$

where  $W_p$  = weight of liquid in which air volume  $V_g$  is dissolved.

$M_p$  = molecular weight of liquid.

$\gamma_p$  = unit weight of liquid.

For the case of air dissolving in water, Eq. C-6 becomes

$$V_{ad} = \frac{RT \gamma_w}{H M_w} V_w \quad (C-7)$$

and letting

$$s = \frac{RT \gamma_w}{H M_w}, \text{ one obtains}$$

$$V_{ad} = s V_w \quad (2-2)$$

From Eq. C-4 it is evident that the volume  $V_{ad}$  is measured at the pressure in the air,  $u_a$ .

C-02 EFFECT OF COMPRESSIBILITY OF WATER ON VOLUME INCREASE CAUSED BY WATER LEAKAGE INTO A 100% SATURATED SPECIMEN

The compressibility of water is defined by

$$F_w = - \frac{(\Delta V_w / V_w)}{\Delta u_w} \quad (C-8)$$

where  $F_w = 4.55 \times 10^{-5} \text{ cm}^2/\text{kg}$

$\Delta V_w / V_w$  = volumetric strain of water due to the pore pressure increment  $\Delta u_w$ .

The volumetric strain of a soil specimen due to the compressibility of the water in the pores is

$$\frac{\Delta V_w}{V} = \left( \frac{\Delta V}{V} \right)_{\text{comp}} = - \frac{\Delta u_w V_w F_w}{V} \quad (C-9)$$

Since  $V_w = V_v$  in a 100% saturated specimen, Eq. C-9 becomes

$$\left( \frac{\Delta V}{V} \right)_{\text{comp}} = - n \Delta u_w F_w \quad (C-10)$$

where  $n$  is the porosity of the specimen.

Eq. 2-13 relates the volume of leakage  $J_w$  with the change in pore pressure  $\Delta u_w$ ,

$$\frac{J_w}{V} = s \frac{\Delta u_w}{\bar{\sigma}_3} \quad (2-13)$$

Thus, the ratio of the volume change due to compressibility of pore water to the volume of leakage is found by dividing Eq. C-10 by Eq. 2-13, which gives

$$\frac{(\Delta V)_{\text{comp}}}{J_w} = - F_w \frac{n \bar{\sigma}_3}{s} \quad (C-11)$$

Eq. C-11 shows that when a soil with a very low swelling ratio is tested at high effective stress, the volume change due to compressibility of water will be large compared to the volume of water leakage. As an extreme example consider a soil such as Canyon Dam clay with  $s = 0.0015$ ,  $n = 0.375$ ,  $\bar{\sigma}_3 = 20 \text{ kg/cm}^2$ . Eq. C-11 gives

$$- \frac{(\Delta V)_{\text{comp}}}{J_w} = - 0.23 \quad (= - 23\%)$$

which means that when  $10 \text{ mm}^3$  of water leakage occurs, the pore water volume decreases  $2.3 \text{ mm}^3$ , so that the net volume increase of the specimen is only  $7.7 \text{ mm}^3$ . For a soil such as Boston Blue clay, tested at  $\bar{\sigma}_3 = 20 \text{ kg/cm}^2$ , the volume change due to water compressibility is only about 3% of the water leakage. For most triaxial tests, the effect of water compressibility will be small, but in some extreme cases, it becomes important.

**C-03 EFFECT OF COMPRESSIBILITY OF MINERAL GRAINS ON VOLUME INCREASE CAUSED BY WATER LEAKAGE INTO A 100% SATURATED SPECIMEN**

The compressibility of the mineral grains in a soil is defined by the equation

$$F_M = - \frac{(\Delta V_s / V_s)}{\Delta u_w} \quad (C-12)$$

where  $F_M = 2.7 \times 10^{-4}$  /kg for quartz and is probably higher for clay minerals.

$V_s$  = volume of solids in specimen.

$\Delta V_s / V_s$  = change in volume of solids due to change in pore pressure  $\Delta u_w$ .

The ratio  $(\Delta V / V)_{\text{comp}}$  of the change in total volume of a specimen to the initial total volume of the specimen is equal to the ratio  $(\Delta V_s / V_s)$ , because both the individual grains and the total specimen change in volume in proportion to the cube of the change in size of an individual grain. Thus Eq. C-12 gives

$$\left(\frac{\Delta V}{V}\right)_{\text{comp}} = - F_M \Delta u_w \quad (C-13)$$

The ratio of the volume change due to compressibility of the mineral grains to the volume of leakage is found by dividing Eq. C-13 by Eq. 2-13, which gives

$$\frac{(\Delta V)_{\text{comp}}}{J_w} = - F_M \frac{\bar{\sigma}_3}{S} \quad (C-14)$$

The effect of mineral grain compressibility becomes large when the swelling ratio is low and the initial effective stress on the specimen is high. As an extreme example, consider a specimen of Canyon Dam clay,  $s = 0.0015$ , that is tested at  $\bar{\sigma}_3 = 20.0 \text{ kg/cm}^2$ . Eq. C-14 gives

$$\frac{(\Delta V)_{\text{comp}}}{J_w} = - 0.036 \quad ( = - 3.6\%)$$

Thus, even when conditions of test are chosen to make the effect of compressibility as large as possible the effect turns out to be relatively small.

**C-04 VOLUME CHANGE CAUSED BY DEFLECTION OF MEMBRANE DUE TO CHANGES IN EFFECTIVE STRESS**

Consider a cylindrical specimen of soil composed entirely of one size of spherical grains which are packed in the loosest state, as shown in Fig. C-1. The number  $N$  of openings between grains is given in terms of the diameter  $D_s$  and height  $H_s$  of the specimen and the diameter  $d$  of the grains by the equation

$$N = \frac{\pi D_s H_s}{d^2} \quad (C-15)$$

As pressure is applied to the membrane, it deflects into the openings between grains. To be conservative, assume the maximum deflection of the membrane at the center between four soil grains is equal to the deflection at the center of a uniformly loaded, fixed-end beam, which is

$$\delta_{\text{max}} = \frac{w d^4}{96 E I} \quad (C-16)$$

where  $w$  = uniform load per unit length of beam.  
 $d$  = span (= grain diameter).  
 $E$  = modulus of elasticity of beam.  
 $I$  = moment of inertia of beam.

In the present case, the load  $w$  is equal to the change in effective stress (caused by leakage) per unit width  $b$  of membrane, i.e.  $w = b\Delta\bar{\sigma}_3$ . Also, the moment of inertia of the beam, i.e. the membrane, is equal to  $(1/12) b L^3$  where  $L$  is the membrane thickness. Thus, the maximum deflection of the membrane becomes

$$\delta_{\max} = \frac{\Delta\bar{\sigma}_3 d^4}{8 E L^3} \quad (\text{C-17})$$

For the natural rubber membranes used in triaxial testing at Harvard University, Eq. C-17 becomes

$$\delta_{\max} = 5600 \Delta\bar{\sigma}_3 d^4 \quad (\text{C-18})$$

where  $\delta_{\max}$  and  $d$  are in cm and  $\Delta\bar{\sigma}_3$  is in units of  $\text{kg}/\text{cm}^2$ . The total volume change  $\Delta V$  that occurs due to this deflection is approximately equal to the volume of a pyramid, with a height  $\delta_{\max}$  and a base area of  $d^2$ , times the number of openings between grains

$$\Delta V = \frac{1}{3} d^2 \delta_{\max} N \quad (\text{C-19})$$

Substituting Eqs. C-15 and C-18 into Eq. C-19 one obtains

$$\Delta V = 1840 \pi D_s H_s \Delta\bar{\sigma}_3 d^4 \quad (\text{C-20})$$

For a 1.4 in. diameter by 3.5 in. high specimen Eq. C-20 becomes

$$\Delta V = 184000 \Delta\bar{\sigma}_3 d^4 \quad (\text{C-21})$$

where  $\Delta V$  is in  $\text{cm}^3$ ,  $\Delta\bar{\sigma}_3$  is in  $\text{kg}/\text{cm}^2$  and  $d$  is in cm.

For a uniform fine sand, the diameter  $d$  which controls the membrane deflection may be about 0.01 cm. If the effective stress change were  $10 \text{ kg}/\text{cm}^2$ , which is a very large change, the volume change due to membrane deflection between the voids would be only about  $0.012 \text{ cm}^3$ . It is evident that for a clay with  $d \sim 0.001 \text{ cm}$ , the volume change would be negligible.

APPENDIX DMEASUREMENT OF SWELLING RATIO FOR CANYON DAM CLAYD-01 GENERAL

The purpose of this Appendix is to present the results of twenty-four special tri-axial swelling tests to determine the initial swelling ratio,  $S$ , of 100% saturated specimens of Canyon Dam clay. (See D-02 for a description of this soil.) The procedure and apparatus used were designed so that:

- (1) The conditions of stress on the specimen just prior to the start of swelling were practically the same as those which would exist during the axial loading phase of an R test.
- (2) The initial slope of the swelling curve could be determined with reasonable accuracy. The values obtained are felt to be accurate to within plus or minus 30% in all cases and to within plus or minus 5% for the best tests.

The initial swelling ratio measured in the above manner is felt to be a close approximation to that swelling ratio which governs the effect of leakage during triaxial Q or R tests on 100% saturated specimens.

The swelling tests were identical to triaxial R tests except that the application of the deviator load was stopped at between 25% and 75% of the deviator stress that would cause failure. Then, after the pore pressure induced by the deviator load had practically stopped changing, the pore pressure was artificially increased in small steps so that the effective stress was decreased in similar steps. The resulting increase in volume of the specimen was measured for each step and the swelling curve was then plotted. The swelling ratio was calculated from the slope of the swelling curve. Leakage into a triaxial R test specimen would cause almost exactly the same changes in the specimen as occur when using the above procedure for the swelling tests. The only difference is that in a swelling test the increase in pore pressure (or the decrease in effective stress) is the independent variable, whereas during an R test with leakage, the volume of leakage is the independent variable.

Only the initial portion of the swelling curve was determined, i.e. the portion within a range of effective stress from 80% to 100% of the effective minor principal stress,  $\bar{\sigma}_3$ , which existed in the specimens at the start of swelling. Using the notation of Chapter 2 the range studied was

$$0 < \left| \frac{\Delta \bar{\sigma}_3}{\bar{\sigma}_3} \right| < 20\%$$

Most of the effort was concentrated on determining the swelling curve for  $|\Delta \bar{\sigma}_3 / \bar{\sigma}_3| < 10\%$ .

The effects of

$\bar{\sigma}_3$  - the effective minor principal stress at the start of swelling and

$\frac{\bar{\sigma}_1}{\bar{\sigma}_3}$  - the effective principal stress ratio at the start of swelling

on the initial swelling ratio were considered.

The errors that arose when performing the swelling tests are discussed in D-09. A summary of this Appendix is given in D-10.

D-02 DESCRIPTION OF CANYON DAM CLAY

The following description of Canyon Dam clay is quoted from Casagrande and Hirschfeld (31):

## 1. Source of Material

The clay used in this investigation was obtained in a borrow area for the Canyon Dam project in Texas. It was excavated from the B\*-horizon, between depths of 5 and 9 ft. The average in-situ water content was 16%. As excavated, this clay was chunky and friable.

About 1000 lb of this clay were shipped to the Waterways Experiment Station where it was dried to about 5.5% water content, and then mixed without removing any coarse particles. About 500 lb of that mixture were shipped to Harvard University for this investigation.

## 2. Description of Clay and Classification Tests

The color of this material in the dry state is a very light tan, and when mixed with water a darker tan. At the plastic limit this material is quite tough. Its dry strength is high. The results of liquid and plastic limit tests performed at WES and at Harvard are tabulated below:

Tests Performed At	Liquid Limit	Plastic Limit
WES	33	15
Harvard	34	15

These results place the material on the plasticity chart high above the A-line, indicating that the colloidal fraction consists largely of montmorillonite-type clay minerals. The toughness at the plastic limit and the high dry strength agree with these results.

In Figure 1\*\* are plotted grain size curves of this clay which were determined at WES and Harvard. It can be seen that for practical purposes the entire sample passes No. 40 mesh, and that 70 to 80% of the material passes No. 200 mesh. Only about 20% falls into the clay fraction, i.e. is finer than 0.002 mm. The small percentage of particles larger than No. 40 mesh consists in part of shells\*\*\*.

Although on the basis of the grain size curves this material could be described as a clayey silt, its physical characteristics are such that it should be classified as a tough, inorganic clay of low plasticity (CL)\*\*\*\*.

The specific gravity of the solids was found to be 2.71."

The footnotes to the above quotation were added by the author.

## D-03 APPARATUS FOR SWELLING TESTS

### (a) General

The apparatus used for the swelling tests consists of (1) a triaxial cell, (2) the means for applying and measuring chamber pressure and (3) the means for applying and measuring pore pressure.

The apparatus was designed so that volume changes of the specimen as small as 0.2 mm<sup>3</sup> could be detected. Four identical apparatus were constructed and used for the swelling tests. The components of the apparatus are described in (b) through (d) below.

---

\* Reference (31) contained "A-horizon" but this was later corrected in (32) to read "B-horizon."

\*\* See Fig. D-1.

\*\*\* Calcium carbonate concretions were also present in this fraction.

\*\*\*\* Unified Soil Classification System (113).

(b) The Triaxial Cell

The triaxial cell was of the current Harvard type (31). A photograph of the cell, as modified for the swelling tests, is shown in Fig. D-2. The minor changes made by the author in order to permit accurate measurement of very small volume changes are:

- (1) Reduction in the bore of the burette, in which volume changes are measured from 0.6 cm to 0.1 cm.
- (2) Reduction of leakage and volume changes in the drainage system by reducing the number of valves and fittings and shortening the length of tubing.
- (3) Use of a porous ceramic disc which was glued into the pedestal of the triaxial cell. Only the bottom of the specimen was drained.
- (4) Use of finely polished stainless steel caps and pedestals to help prevent leakage past the point where the membranes were bound with one O-Ring to the cap and the pedestal.

While consolidating a specimen the volume changes were measured in a 0.6 cm bore lucite burette as normally used in triaxial tests. However, before swelling was begun, the burette was changed to one with a bore of 0.1 cm. The four 0.1 cm bore burettes were made from one length of precision-bore glass tubing which was calibrated with mercury in three locations<sub>3</sub> (before cutting the tubing) and found to contain a volume of  $7.82 \pm 0.005 \text{ mm}^3/\text{cm}$ . The tubing was cut to four lengths of about 20 cm and each length was fastened to a wooden centimeter scale to make the burettes, as shown in Figs. D-2 and D-3. The addition of about two centimeters of dyed kerosene on the air-water meniscus in the burette helped to reduce evaporation and aided in the formation of a well-rounded meniscus. The level of the bottom of the meniscus was read to 0.01 cm with the<sub>3</sub> aid of a five-power magnifying glass. With this system, volume changes of 0.1 to 0.2 mm<sup>3</sup> could be detected.

Only the left hand side of the valve block, which is shown obliquely in Fig. D-2, was part of the drainage system during a swelling test. The half used is shown in Fig. D-3. By using only the left side of the block and by eliminating the drainage line from the top cap of the specimen, the number of locations where leakage could occur that could affect volume change measurements was reduced from 24 to 12. Also, the Saran tubing leading to the cap of the specimen was eliminated so that the volume changes which could occur in the system due to pressure changes were minimized. Each drainage system was tested for leaks under air pressure of 20 kg/cm<sup>2</sup> for two days. No leaks that could be detected by submerging the pressurized system in water were present.

Leakage past the bindings of the two membranes to the cap and base (see Fig. D-3) was effectively eliminated by applying the results obtained during the present investigation which are reported in Chapter 7. The cap and pedestal were made of stainless steel and polished in a lathe with No. 600A emery paper, using kerosene as a lubricant. These polished surfaces were coated with silicone stopcock grease, to fill any microscopic striations with grease. The membranes were rolled down and pressed firmly against the coating of grease. One O-Ring, which was two-thirds of the diameter of the specimen when unstretched, was stretched onto a slightly oversize brass ring and then slipped over both membranes. (O-Rings are cast in a split mold which leaves a protruding ridge about 0.010 cm high around the inside and outside girth of the ring. Care must be taken so that this ridge does not spiral around the specimen and form a continuous path through which water can flow from the chamber to the specimen.)

After modifying the four triaxial cells as described above, one of the cells was calibrated to determine the volume changes that occur in the drainage system due to pore pressure changes. The cell was set up as shown in Fig. D-3 except that the soil specimen and the vertical filter strips were omitted. It was found that the presence or omission of the horizontal filter disc did not change the calibration appreciably. The chamber pressure and pore pressure, i.e. the pressure within the membranes between the cap and base, were increased in steps to reproduce identically the stress systems that

were applied in the swelling tests. The resulting volume changes were measured in the 0.1 mm burette. At each chamber pressure the volume change due to a pore pressure increment was found to be directly proportional to the effective stress holding the cap and base together. (This means that when the initial pore pressure was high, the drainage system was less compressible, or stiffer.) Thus a unique calibration curve could be obtained for each chamber pressure by plotting the measured volume change versus the ratio of the pore pressure increment to the initial effective stress. This form of the calibration, Fig. D-4, is also convenient for application to the swelling test data.

It should be noted that the swelling portion of each swelling test was begun after the drainage system had been under a high pore pressure (greater than 5.6 kg/cm<sup>2</sup> in every case) for four days. Therefore, the effect of any air bubbles or other "slack" in the system was at a minimum when the swelling increments were applied.

#### (c) System for Applying Chamber Pressure

The chamber pressure was applied and maintained by means of compressed air as shown in Fig. D-5. The compressed air tank, indicated (a) in the figure, was used to apply pressure to the air-water interface located in the reservoir (b). The pressure was transmitted to the chamber through a two meter length of one-eighth inch outside diameter Saran tubing which was filled with water. In this manner, the possibility that air would diffuse from the air tank through the water in the Saran tube, and ultimately into the soil specimen, was for practical purposes eliminated. Calculations in support of this statement are given in Appendix B-03, and test data which confirm these calculations are reviewed in Appendix A-11.

The chamber pressure was read on the gage (c) which was calibrated to within  $\pm 0.01$  kg/cm<sup>2</sup> by means of a Crosby dead weight gage tester or an eight inch Bourdon test gage manufactured by the U. S. Gage Corporation. The chamber pressure varied somewhat during the swelling tests due to leaks and also due to room temperature fluctuations. The variation in chamber pressure over the four to six day<sub>2</sub> duration of a test was less than  $\pm 0.15$  kg/cm<sup>2</sup> in all tests and less than  $\pm 0.05$  kg/cm<sup>2</sup> in 65% of the tests. During each swelling step, the variation in chamber pressure was maintained constant to within  $\pm 0.005$  kg/cm<sup>2</sup>. To accomplish this, one side of the pointer of the gage was located accurately with respect to the markings on the face of the gage. The pointer was maintained (with the aid of a magnifying glass) at the precise location it had occupied at the start of the swelling step by adding or bleeding air from the tank as needed.

#### (d) System for Applying and Measuring Pore Pressures

The system for applying and measuring pore pressures was used to perform three functions:

- (1) During consolidation, back pressures up to 10 kg/cm<sup>2</sup> had to be applied, measured and maintained for two to four days.
- (2) During application of deviator load, induced pore pressures up to 15 kg/cm<sup>2</sup> had to be measured. After the deviator load had been applied, the final pore pressure had to be maintained for two days.
- (3) During swelling, pore pressure increments as small as 0.05 kg/cm<sup>2</sup> had to be applied, accurately measured and maintained for at least four hours.

Back pressures were applied during the consolidation phase of the swelling tests by using a compressed air tank, indicated (d) in Fig. D-5, as a source of high pressure. The one liter ballast tanks (e) and (f), were filled to the desired pressure from the air source. The valve (g) in Fig. D-5 was open during consolidation so that the pressure on gage (h) was equal to the back pressure. The interface between the air and the pore water was located in the drainage burette (k) which is mounted on the triaxial cell. The maximum back pressure variation during consolidation was  $\pm 0.10$  kg/cm<sup>2</sup> in one test and was less than  $\pm 0.025$  kg/cm<sup>2</sup> in 65% of the tests.

When the deviator load was applied, the induced pore pressure was measured by a "null" system. The pressure in ballast tanks (e) and (f), Fig. D-5, was changed as

required to maintain the meniscus in the burette (i) (which had a bore of 0.1 cm) at a constant level. The pore pressure that was measured after completion of axial loading was then maintained constant for two days. The maximum variation in pore pressure during the last day before the start of swelling was  $\pm 0.14 \text{ kg/cm}^2$  for one test and was within  $\pm 0.025 \text{ kg/cm}^2$  for 65% of the tests.

The increments of swelling pressure were measured by means of the mercury U-tube manometer shown in Fig. D-5. To apply a swelling increment valve (g) was first closed. Then, while maintaining the pressure on gage (h) at the exact reading it had when valve (g) was closed, the pressure in ballast tank (f) was increased to the desired pressure. The difference between the initial pore pressure and the pore pressure after the swelling increment had been applied was read on the manometer. The manometer could be read to within  $\pm 0.1 \text{ cm Hg}$  ( $0.0014 \text{ kg/cm}^2$ ). The errors involved in this system for applying pore pressures are discussed in the following paragraphs.

In Fig. D-5 it can be seen that the system to the right of valve (g) is separate from that to the left. Therefore, if either half of the system has a leak, it is reflected by a change in the manometer reading which is five or more times more sensitive than the pressure gage (h). It is improbable that both halves of the system would leak at the same time. Therefore, when a leak occurred it was always assumed that the side indicating a loss of pressure was the only side which had leaked. Air was then added to the side which had lost pressure to return the manometer to its initial reading. Thus, the error in measurement of the increment in pore pressure was probably only slightly greater than the error in the manometer readings, i.e. about  $\pm 0.002 \text{ kg/cm}^2$ .

A decrease in chamber pressure affects a 100% saturated soil specimen in the same manner as an equal increase in pore pressure. Therefore the variations in chamber pressure during swelling, as described in subparagraph (c) above, introduce an error of  $\pm 0.005 \text{ kg/cm}^2$  in the magnitude of the swelling steps. The total effect of errors in pore- and chamber-pressure measurement on the magnitude of a swelling step can be as high as  $\pm 0.007 \text{ kg/cm}^2$ . The percent error in the measurement of the first swelling step in the twenty-four tests, assuming a possible variation of  $\pm 0.007 \text{ kg/cm}^2$  is as follows:

No. of Tests	First Swelling Step ( $\text{kg/cm}^2$ )	Maximum Probable Error (%)
1	0.040	$\pm 18$
12	0.054	$\pm 13$
2	0.070	$\pm 10$
6	0.12	$\pm 6$
3	0.30	$\pm 2$

Thus in all but one test the magnitude of the first (and smallest) swelling increment may be in error, at most, by  $\pm 13\%$ . The average error for the first increment is probably about  $\pm 7\%$ . Although the error in measurement of the first swelling increment is rather large, it should be remembered that the pressure changes occur slowly during a swelling increment. Thus, the measured volume change reflects the effect of the time average of the pore pressure acting on the specimen during the increment. As long as the average pressure is used in calculations, no appreciable error in the swelling curve will occur due to pressure variations.

#### D-04 PREPARATION OF SOIL AND COMPACTION OF SPECIMENS

The Canyon Dam clay was prepared for the swelling tests by first passing the material through a No. 10 sieve (2 mm opening). The soil passing the No. 10 sieve was mixed in two 10 lb batches to a water content of 16%. Each batch was then stored in a screw-top glass jar in a humid room for a period of at least two weeks prior to test. Tests SW9, SW10, SW11 and SW12 were performed on Batch 2 material. The other twenty swelling tests were performed on Batch 1 material.

The specimens were compacted in the humid room in a modified Harvard miniature mold which was made of brass and split into three vertical sections to facilitate removal of the specimens. The mold was lightly oiled with silicone oil and then the compaction was performed using ten 10 lb tamps on each of 30 layers. The tamper was spring-loaded (30) and had a flat-bottomed bakelite tip (to prevent scratching the mold) with a diameter of one-half inch and a thickness of one-eighth inch. Both ends of the compacted specimen were trimmed. Then the clamps holding the split mold together were slightly loosened and the specimen was gently extruded using a piston of the same diameter as the specimen. The length of the specimen was measured in three locations and the diameter was measured in nine locations to the nearest 0.001 inch. The specimens were approximately 1.4 inches in diameter and 3.5 inches long. The specimen was then removed from the humid room without any protection for a period of about thirty seconds so that it could be weighed to  $\pm 0.01$  gm. After weighing, the specimen was immediately returned to the humid room and set up in a triaxial cell as described in D-05.

The initial water contents of the specimens prepared in this manner ranged between 15.68 and 16.00% for Batch 1, and between 16.05 and 16.20% for Batch 2. This water content is about 1% above optimum for the compaction effort used. The initial dry unit weights of the specimens from Batch 1 ranged between 114.4 and 115.8 pcf and those from Batch 2 ranged between 114.4 and 114.9 pcf. Table D-3 contains these data.

#### D-05 SWELLING TEST PROCEDURE

##### (a) Set-Up of Specimen in the Triaxial Cell

Prior to starting compaction of each specimen, the following preparations were made:

- (1) The valve block and porous ceramic disc in the triaxial cell (Fig. D-3) were saturated with distilled water. The saturation was accomplished by detaching the pedestal from the cell and boiling it in distilled water for one hour. After allowing it to cool slowly, the pedestal was submerged in distilled water together with the valve block. The bonnet nut of each valve on the block was removed, saturated and replaced. Then water was drawn through each valve and line in the block. Finally the connection between the Saran tubing and the pedestal was made under water. This procedure was used only once for each cell. The cells were kept saturated by maintaining a head of water on top of the porous disc at all times during storage between tests.
- (2) The grease seal on the top of the triaxial cell (shown in Fig. D-3) was renewed.
- (3) Five filter strips, each 1/8 inch wide by 8.8 cm long, were cut from a disc of Whatman's No. 1 filter paper and were saturated with water. Also, one filter disc 1.4 inches in diameter was cut and saturated.
- (4) Two Ramses No. 19 prophylactic membranes (manufactured by the Julius Schmid Company) were soaked for at least one day in silicone oil. The excess oil was removed from the membranes just before compaction was begun. Ramses membranes are made of natural rubber and have an average thickness of 0.006 cm.
- (5) Air tanks for application of chamber pressure and pore pressure were pumped up to the desired pressures.

After weighing a freshly-compacted specimen, it was set up in the triaxial cell in the humid room. First, the vertical filter strips were pressed lightly with a paper towel to remove excess water and then were placed at approximately equal intervals around the circumference of the specimen. One membrane was applied, the specimen was placed on the stainless steel cap (in the upside-down position) and another membrane was added. The O-Ring was used to bind the membranes to the cap. The pre-cut filter disc was then placed on the wet pedestal of the cell and excess water was removed. The specimen was immediately

placed on top of the filter disc, the membranes were rolled down over the pedestal and an O-Ring was added. Figs. D-2 and D-3 show a specimen set up in this manner.

The steel triaxial chamber was placed around the specimen, the top of the cell was set in place over the tie rods and the wing nuts were tightened to seal the cell. These parts of the apparatus can be seen in Figs. D-2 and D-3. Distilled water which had been partially de-aired under an absolute pressure of two or three centimeters of mercury was used to fill the cell and the two meter long line of Saran tubing shown schematically in Fig. D-5. The chamber pressure was applied as described in D-03.

#### (b) Consolidation of Specimen

Three effective consolidation pressures were used as shown in Table D-1. These were:  $\bar{\sigma}_c = 2, 6$  and  $14 \text{ kg/cm}^2$ . A back pressure,  $u_w$ , of 6, 8 or  $10 \text{ kg/cm}^2$  was used to saturate the specimens. The chamber pressure,  $\sigma_c$  (equal to the sum of the effective consolidation pressure and the back pressure) was applied to the specimen after a period of 55 to 65 min from the start of compaction had elapsed. The chamber pressure was applied for a period of two minutes with the pore water drainage valve (Fig. D-3) closed. Consolidation was begun by opening the drainage valve and recording the dial and burette readings after 30 seconds, 1, 2, 4, 8, 15, 30 min, etc. Primary consolidation was essentially complete in 800 min or less. After twenty-four hours of consolidation, the 0.6 cm diameter burette was changed to one with a bore of 0.1 cm so that the rate of secondary consolidation could be measured accurately. Twenty-four more hours were allowed for consolidation, so that a total of forty-eight hours were allowed for consolidation prior to the application of the deviator load. For tests in which no deviator load was applied (see Table D-1), the specimens were allowed to consolidate for a period of seventy-two hours prior to the start of swelling, except for tests SW17 and SW18 which were consolidated for forty-eight hours.

#### (c) Application of Deviator Load

At the end of the consolidation phase of the test, a deviator load,  $\sigma_d$ , equal to 25%, 50% or 75% of the estimated deviator load at failure was applied. The deviator load at failure,  $\sigma_{dmax}$ , for each effective consolidation pressure was estimated from the data reported by Casagrande and Hirschfeld (32) and is shown in Table D-1. The deviator load was applied in increments of 10% of  $\sigma_{dmax}$  at five minute intervals. In some cases the final load increment was less than 10% of  $\sigma_{dmax}$  and this small increment also was added five minutes after the previous increment of deviator load. The induced pore pressure was measured for each load increment. After application of the final increment of load, the pore pressure was measured continuously for a period of about thirty minutes. Then the pore pressure was maintained at exactly the value it had attained at the elapsed time of about thirty minutes. That is, the specimen was allowed to consolidate under the effective minor and major principal stresses that had developed thirty minutes after the last deviator load increment had been applied. Subsequent changes in the burette readings were recorded for a period of forty-eight hours, so that the rate of volume change would be very small when swelling was begun. Burette readings were taken two times each day during this period. Towards the end of the period more frequent measurements were made so that the rate of volume change at the end of the deviator load phase could be determined accurately.

#### (d) Application of Pore Pressure Increments to Cause Swelling

Swelling was begun at the end of the fourth day after the application of chamber pressure. This was done by increasing the pore pressure by an amount which ranged from about 0.4% to 25% of the effective minor principal stress,  $\bar{\sigma}_3$ , which existed before the start of swelling, i.e.  $\Delta u_w / \bar{\sigma}_3 = -\Delta \bar{\sigma}_3 / \bar{\sigma}_3 = 0.004$  to 0.25. The change in the burette and dial readings which occurred due to the pore pressure increment were recorded for a period of about 200 minutes, after which two or three additional increments were applied as listed in Table D-3.

For tests in which a total of three swelling steps (i.e. three pore pressure increments) were used, the swelling phase of the test was generally completed in twelve hours.

For tests in which four swelling steps were used, the final step was left in place until twenty-four hours after swelling had been begun.

(e) Dismantling the Specimen

After the measurements for the final swelling step had been recorded, the specimen was dismantled as follows: (1) The drainage valve was closed. (2) The pore pressure was released. (3) The chamber pressure was released. (4) The final dial reading was taken. (5) The chamber was drained and the specimen was carefully removed so that no water would come in contact with it and no water would be lost. (6) The entire specimen was weighed. (7) The water content of the specimen was determined.

D-06 QUALITATIVE DISCUSSION OF METHOD FOR DETERMINING THE SWELLING CURVE THAT GOVERNS EFFECTS OF LEAKAGE

(a) Discussion of Swelling Curve that Develops when Leakage Occurs During an R Test

Consider a 100% saturated specimen that is normally consolidated in a triaxial cell to a hydrostatic effective stress (point A in Fig. D-6), using water as the chamber fluid. Assume that the drainage valves are then closed and that no water leakage occurs. Under these conditions, the tendency for volume decrease due to secondary consolidation will cause the pore pressure to increase and the effective stress to decrease along line (a) in Fig. D-6. For the purposes of illustration, the length of line (a) is exaggerated and the scale of the curves in Fig. D-6 is magnified so that only the initial portions of the curves, i.e. those portions that are of interest when discussing the effects of leakage, are shown.

Assume that another identical specimen is consolidated to point A and that the drainage valves again are closed. In this case assume further that no secondary consolidation occurs after the specimen has reached point A but that leakage does occur. This leakage would cause the specimen volume to increase and the effective stress to decrease along a curve such as (S).

Actually, the ideal situations represented by line (a) and curve (S) do not ever develop. Instead, both leakage and secondary consolidation occur simultaneously and a curve such as (b) would represent their combined effects. If one had measured curves (S) and (b) for a particular soil, it would be possible to separate the decrease in effective stress caused by leakage from that caused by secondary consolidation as follows: Assume that in time  $t$  a volume of leakage occurs such that the void ratio change is  $\Delta e_t$ . The effective stress on the specimen would then be given by point B. If no secondary consolidation were to occur simultaneously with leakage, the effective stress on the specimen would be given by point C, so that the decrease in effective stress due to leakage alone is given by the horizontal distance between points C and A. Thus the decrease in effective stress due to secondary consolidation alone is given by the distance BC.

It is evident that the initial portion of curve (S), which does not contain any effects of secondary consolidation, must be determined in order to calculate the changes in effective stress caused by leakage. This curve will be frequently referred to, so it will be called simply the S-curve. If it is assumed that the S-curve is a straight line on an arithmetic plot of void ratio versus effective stress, as was done in Chapter 2, then the change in effective stress caused by a given volume of leakage can be calculated using Eq. 2-9. It should be re-emphasized that the S-curve must be determined when the stresses on the specimen are practically the same as exist in a triaxial specimen into which leakage occurs during axial loading.

(b) Procedures for Determining the Swelling Curve that Governs the Effects of Leakage (S-curve)

Two approaches are available for determining the S-curve of a soil. One approach, and perhaps the most obvious one, is to consolidate a specimen long enough so that the rate of secondary consolidation is negligible compared with the volumes of swelling to be measured. At this stage, the void ratio and effective stress are

represented by point A in Fig. D-7. Then, the effective stress on the specimen is decreased in steps such that the rate of volume increase will be approximately equal to the rate at which leakage might occur during a triaxial Q or R test, so that curve (e) is obtained. If only R tests are of interest, and if the consolidation phase of these R tests is continued until the rate of secondary consolidation is insignificant, then curve (e) is the desired S-curve which governs the effects of leakage. However, during axial loading of any real triaxial specimen there is a significant tendency for secondary consolidation. Thus, when axial loading is begun, the void ratio and effective stress are represented by a point such as A' in Fig. D-7, and the actual S-curve might be as shown emanating from A'. This S-curve would have a different shape from curve (e) because of the different degree of secondary consolidation at the start of swelling. Of course it may be that this difference is small. It was originally intended during this investigation to measure curve (e) and assume that it is a close approximation to the S-curve. However, the forty-eight hour period allowed for secondary consolidation prior to the start of swelling was too short. Therefore the second approach, described below, was used.

The second approach for determining the S-curve consists of first consolidating a specimen to point A' in Fig. D-7 and then decreasing the effective stress in steps. In this case a swelling curve such as (f) in Fig. D-7 would be obtained. Curve (f) drops below point A' because, during the first decrements of load, the secondary consolidation overrides the tendency of the specimen to swell. An estimate must be made of the volume change caused by the secondary consolidation so that the ordinates of curve (f) may be increased accordingly to obtain the S-curve.

To estimate the volume decrease caused by secondary consolidation, consider a specimen that is consolidated to point A' in Fig. D-7. Assume that at time  $t_0$  the rate of volume decrease due to secondary consolidation is  $q$  mm<sup>3</sup>/day. Then, starting at time  $t_0$ , let the effective stress be decreased in four steps, the first step having a magnitude  $\Delta\bar{\sigma}_a$ , the second  $\Delta\bar{\sigma}_b$ , etc. so that the effective stress at the end of primary swelling\* is reduced to  $\bar{\sigma}_b$ , then to  $\bar{\sigma}_c$ , etc. Assuming that primary swelling is complete in  $t_p$  minutes, allow each step to remain on the specimen for  $2 t_p$  minutes. The resulting time curves (i.e. the plots of volume change versus time) would be approximately as shown by solid lines in Figs. D-8(a) through D-8(d).

Consider the time curve for the first decrement of effective stress, Fig. D-8(a). The initial steep rise of the curve is due to primary swelling and a small amount of elastic rebound. At the end of primary swelling, the point representing the void ratio and effective stress on the specimen lies above curve (c) in Fig. D-7 which is the compression curve that would be obtained if the specimen were loaded extremely slowly. Therefore, after time  $t_p$  has elapsed, the volume of the specimen will be decreasing due to secondary consolidation at the rate indicated by the final slope  $q'$  of the time curve and this rate will continue until  $2t_p$ \*\* Thus, the decrease in effective stress by an amount  $\Delta\bar{\sigma}_a$  has caused the rate of volume decrease due to secondary consolidation to drop from  $q$  to  $q'$ . It is now possible to estimate the volume decrease that would have occurred if no swelling had occurred when the effective stress was decreased. This volume decrease is shown by the dotted line in Fig. D-8(a). The initial slope of this line is  $q$ , and, as the effective stress is decreased during primary swelling, this slope gradually decreases to a value  $q'$  at time  $t_p$ , when the effective stress is  $\bar{\sigma}_b$ . It then continues at a slope  $q'$  because the effective stress remains constant. The difference in ordinate between the solid and dotted curves gives the volume increase of the specimen due solely to the decrease in effective stress. It is this difference in ordinate that must be added to the

\* The term "primary swelling" will always be used to mean "essentially 100% of the primary swelling."

\*\* It is assumed that the time period  $2t_p$  is so short that the rate of secondary consolidation would not decrease significantly during the time interval ( $t_p$  to  $2t_p$ ) even when plotted on an arithmetic scale.

corresponding ordinate of curve (f) in Fig. D-7, to obtain one point on the S-curve. For the analysis of the swelling tests reported herein, the dotted line in Fig. D-8(a) was approximated by the two straight line segments shown dashed. The first segment, with slope  $q$ , was continued for half the period of primary swelling. The second, with slope  $q'$ , was continued from the end of the first segment up to time  $2t$ . This procedure is equivalent to assuming that the rate of volume decrease due to secondary consolidation is equal to the average of  $q$  and  $q'$  for the entire period of primary swelling. It usually gives a slight overestimate of the volume decrease caused by secondary consolidation so the ordinates of the S-curve obtained are slightly too high.

The above procedure may be applied with slight modifications to the time curves for the remaining decrements of effective stress. When the effective stress is decreased to  $\bar{\sigma}_b$  by applying the second decrement  $\Delta\bar{\sigma}_b$ , the void ratio at the end of primary swelling would be slightly above curve (c) in Fig. D-7. Therefore the specimen would tend to return to its initial volume as indicated by the time curve in Fig. D-8(b). In this case the initial slope of the extrapolated curve of secondary consolidation (shown dashed) would be  $q'$ , i.e. equal to the final slope from the previous decrement of load. The final slope of the extrapolated curve of secondary consolidation would be equal to the final slope  $q''$  of the time curve.

For the third decrement, the time curve might be as shown in Fig. D-8(c). The final slope is practically zero or slightly positive because the point representing the void ratio and effective stress at the end of primary consolidation lies only very slightly below curve (g) in Fig. D-7, which is the curve that would be reached if secondary swelling had essentially stopped. For this case the initial slope of the extrapolated curve of secondary consolidation (dashed in Fig. D-8(c)) is  $q''$ , and the final slope is approximately zero, because there is no longer any tendency for secondary consolidation at the end of this decrement.

For the final decrement, there is no tendency for secondary consolidation at any time during swelling and no correction is needed. The final slope of this time curve, Fig. D-8(d) is strongly positive because the point representing the void ratio and effective stress on the specimen at the end of primary swelling lies well below curve (g), so that secondary swelling would continue at a significant rate.

For some of the swelling tests to be reported below, the first decrement of effective stress was considerably larger than  $(\Delta\bar{\sigma}_a + \Delta\bar{\sigma}_b)$  shown in Fig. D-7. Therefore the effective stress on the specimen was less than  $\bar{\sigma}_b$  at some time before the end of primary swelling and the final slope of the time curve was positive. In such cases it was not necessary to apply a correction for the volume decrease caused by secondary consolidation during the swelling phase of the tests.

#### D-07 METHOD OF INTERPRETATION OF DATA

##### (a) General

The data for each swelling increment of a swelling test consists of a series of readings of the drainage burette and the elapsed time at which each reading was taken. For example, the time curves for the three swelling increments of test SW22 are shown as solid lines in Fig. D-9. The data for test SW22 will be used in (b) below to illustrate the method used to obtain the swelling curve of Canyon Dam clay from the original data of the swelling tests.

The errors which arise in the interpretation of the data are discussed in D-09 as part of a general discussion of errors in the determination of the swelling ratio.

(b) Swelling Curve for Test SW22

Test SW22 was performed using an effective consolidation pressure of  $14.2 \text{ kg/cm}^2$ . The stresses on the specimen at the start of swelling were:  $\bar{\sigma}_3 = 5.4 \text{ kg/cm}^2$ ;  $(\bar{\sigma}_1/\bar{\sigma}_3) = 2.86$ ;  $(\sigma_d/\sigma_{dmax}) = 0.50$ ;  $u_w = 6.0 \text{ kg/cm}^2$ .

The pore pressure was increased in three steps such that  $\Delta u_w = 0.053, 0.136, \text{ and } 0.271 \text{ kg/cm}^2$ , where  $\Delta u_w$  is always referred to the pore pressure which existed just prior to application of the first pore pressure increment\*. The time curves in Fig. D-9 show that essentially 100% of the primary swelling had occurred in 40 to 100 minutes after the application of each swelling increment because, after this time had elapsed, the rate of swelling was zero or negative in every case. As a check, one can compare this estimate with that which can be predicted from the consolidation data of the test.

The time curve for consolidation for test SW22 is shown in Fig. D-10. The figure shows that essentially 100% primary consolidation occurred in 700 to 800 minutes. From the theory of consolidation one obtains

$$t_{100}^c = \text{constant} \times \left( \frac{de}{d\bar{\sigma}} \right)_c \quad (D-1)$$

where  $t_{100}^c$  = time required to achieve essentially 100% primary consolidation.

$$a_v = \left( - \frac{de}{d\bar{\sigma}} \right)_c = \text{the coefficient of compressibility.}$$

Thus  $t_{100}^c$  is proportional to the slope of the compression curve. Assuming that Eq. D-1 holds for primary swelling, then

$$t_{100}^s = \text{constant} \times \left( \frac{de}{d\bar{\sigma}} \right)_s \quad (D-2)$$

where the s means that the parameters are evaluated for the swelling curve of the soil. Dividing Eq. D-2 by Eq. D-1 and rearranging, one obtains

$$t_{100}^s = t_{100}^c \frac{(de/d\bar{\sigma})_s}{(de/d\bar{\sigma})_c} \quad (D-3)$$

The ratio of the slope of the swelling curve to that of the compression curve was about 1/22 for test SW22. Thus, substituting  $t_{100}^c = 750 \text{ min}$  into Eq. D-3, one obtains  $t_{100}^s = 35 \text{ min}$  for test SW22. This value is slightly below the range of 40 to 100 minutes estimated from the curves of Fig. D-9. It will be assumed that essentially 100% of the primary swelling is complete in 40 min for test SW22.

The initial slope of the extrapolated curve of secondary consolidation for the first pore pressure increment ( $\Delta u_w = 0.054 \text{ kg/cm}^2$ ) is obtained from the final slope of the plot of burette reading versus the logarithm of time for the last increment of deviator load\*\*, shown in Fig. D-11. The semi-logarithmic plot was used because the points generally fall along a satisfactory straight line on this plot for large elapsed times. The slope of an arithmetic plot of burette reading versus time at the time when swelling was begun was calculated from the slope of the semi-logarithmic plot.

\*  $\Delta u_w$  is referred to the start of swelling simply because the manometer used to measure pore pressure changes gave the total change in pore pressure directly, rather than the incremental change in pore pressure.

\*\* The reader is reminded that the pore pressure which developed about 30 min after this last deviator load increment had been applied, was subsequently maintained constant until swelling was begun. Volume changes were recorded during this period.

These slopes are tabulated for all tests in the last column of Table D-4. Note that when no deviator load was applied, the plot of burette change versus time during the consolidation phase of the test was used as the initial slope of the extrapolated curve of secondary consolidation. The final slope of the extrapolated curve of secondary consolidation for  $\Delta u_w = 0.054 \text{ kg/cm}^2$ , shown in Fig. D-9(a), is equal to the final slope of the corresponding time curve.

The initial slope of the extrapolated curve of secondary consolidation for the second pore pressure increment,  $\Delta u_w = 0.136$ , was taken as equal to the final slope of the previous time curve, i.e. the time curve for  $\Delta u_w = 0.54 \text{ kg/cm}^2$  in this case.

Sometimes the final slope of the time curve for the previous increment indicated that no secondary consolidation was occurring at the end of that increment, e.g. see Fig. D-16, in these cases no secondary consolidation would occur in succeeding increments and no correction for secondary consolidation was necessary.

The change in burette reading due solely to the decrease in effective stress during a swelling increment is given by the difference in ordinate between the time curve and the extrapolated curve of secondary consolidation. This measurement was made at a period of 200 minutes after the application of each swelling increment. The period of 200 minutes was chosen because the first tests performed (see Figs. D-19, D-25 and D-26) indicated that practically all swelling was complete in 200 minutes. Subsequent experience indicated that it would have been preferable to use a period of about twenty-four hours. (Extension to a period of twenty-four hours would necessitate use of a constant temperature room, see paragraph D-10.) However, the use of the 200 minute choice gives a conservative value of the swelling ratio. That is, if one uses this swelling ratio for calculating the change in effective stress caused by leakage, the calculated change in effective stress will be higher than the actual change. Table D-2 shows the method used for calculating the volume change from the changes in burette reading shown in Fig. D-9 for each swelling increment.

It is convenient to plot the swelling curve in terms of the percent change in total volume versus the percent decrease in effective stress as shown in Fig. D-12.\* The percent change in total volume is obtained by dividing the corrected volume change calculated in Table D-2 by the total volume of the specimen immediately before swelling is begun. The percent decrease in effective stress given in Table D-2 is obtained by dividing the actual change in effective stress by the effective minor principal stress before the start of swelling.

The swelling ratio may be calculated from Fig. D-12 by applying Eq. 2-13:

$$\frac{\Delta V}{V} = s \frac{\Delta u_w}{\bar{\sigma}_3} \quad (2-13)$$

Thus the swelling ratio is simply the slope of the plot of  $\Delta V/V$  versus  $\Delta u_w/\bar{\sigma}_3$ .

## D-08 DISCUSSION OF RESULTS

### (a) Presentation of Results

Table D-3 contains a summary of the swelling data for the twenty-four swelling tests. Table D-4 contains the data on the initial and final conditions of each specimen. The time curves from which the swelling data in Table D-3 were computed are shown in Figs. D-13 through D-36.

\* The values of  $\Delta u_w/\bar{\sigma}_3$  used herein are small relative to 1.0, so that the logarithm to the base 10 of  $\Delta u_w/\bar{\sigma}_3$  is approximately equal to  $\Delta u_w/2.3 \bar{\sigma}_3$ . Therefore the swelling curve as plotted in Fig. D-12 has very nearly the same shape as the swelling curve which would be obtained if the logarithm of the percent change in effective stress had been plotted on the abscissa.

(b) Variation of the Swelling Curve with the Effective Minor Principal Stress

The points on the swelling curves for all tests in which the effective minor principal stress at the start of swelling was about 2 kg/cm<sup>2</sup> are shown in Fig. D-37. Similarly, the tests with  $\bar{\sigma}_3 = 6$  kg/cm<sup>2</sup> are shown in Fig. D-38 and those with  $\bar{\sigma}_3 = 14$  kg/cm<sup>2</sup> are shown in Fig. D-39. The heavy line shown in each figure is considered to be the best average swelling curve for each value of  $\bar{\sigma}_3$ . These average lines are shown together in Fig. D-40. The average swelling ratio was computed for each curve over three ranges of  $\Delta u_w/\bar{\sigma}_3$ , as shown below:

Range of $\frac{\Delta u_w}{\bar{\sigma}_3}$ (%)	Average Swelling Ratio at $\bar{\sigma}_3 =$		
	2	6 (kg/cm <sup>2</sup> )	14
0 to 2	0.0009	0.0010	0.0011
0 to 5	0.0010	0.0011	0.0015
0 to 10	0.0011	0.0012	0.0017

Thus, the swelling ratio of Canyon Dam clay increases relatively slowly with increasing  $\bar{\sigma}_3$ . The upward curvature of the swelling curves is reflected by the fact that the average swelling ratio increases with increasing ranges of  $\Delta u_w/\bar{\sigma}_3$  in the above table. These swelling ratios may be used in the equations of Chapter 2 to compute the change in effective stress caused by leakage.

The curves in Fig. D-40 cover a very small range of effective stresses. This point is strikingly evident from Fig. D-41 in which the curves are presented in a conventional plot of void ratio versus the logarithm of effective stress. The compression curve for the Canyon Dam clay is also shown. The curvature of the swelling curves is barely noticeable in Fig. D-41.

The possible causes of the variations from the average lines shown in Figs. D-37, D-38 and D-39 are discussed in D-09. It should be recalled that the volume change caused by each pore pressure increment was measured 200 min after the application of the increment. This procedure does not introduce a variation of the swelling curves from the average because the 200 min reading was used consistently in all tests. However, in most cases the volume change due to a pore pressure increment would be increased if more time were allowed for swelling to occur. This can be seen from an inspection of the time curves in Figs. D-13 through D-36. Those time curves which show an upward slope at the end of 200 min would continue to rise, so that the volume increase would be larger for longer times than those used herein. A detailed examination of Figs. D-13 through D-36 and the data in Table D-3 indicates that over the range  $0\% < \Delta u_w/\bar{\sigma}_3 < 2\%$  the swelling curves in Figs. D-38 and D-39 would be no different if more time were allowed for swelling. However, the upward curvature of these two swelling curves would be more pronounced than that shown if a period longer than 200 min were chosen for measuring the volume change. If swelling were allowed to proceed for one day, the ordinates of the swelling curves at  $\Delta u_w/\bar{\sigma}_3 = 10\%$  in Figs. D-38 and D-39 would probably be 50% larger than shown. In the case of Fig. D-37 there are no data in the range  $\Delta u_w/\bar{\sigma}_3 < 2\%$  so which to base an estimate of the effect of a longer duration of swelling. At  $\Delta u_w/\bar{\sigma}_3 = 10\%$ , a one day duration of swelling would probably raise the swelling curve by about 50% as in the previous case.

The following conclusions may be drawn from the discussion in this subparagraph, and they apply only for Canyon Dam clay for the type of swelling tests performed:

- (1) The slope of the swelling curves in Fig. D-40 increases slowly with increasing effective minor principal stress.
- (2) The swelling curves exhibit an upward curvature over the small range of effective stress studied herein. This shape is consistent with the shape of swelling curves obtained previously from conventional one-dimensional

consolidation tests for much larger ranges of effective stress and for many different soils (88).

- (3) The swelling ratios calculated from the curves in Fig. D-40 are considered satisfactory for calculating the change in effective stress caused by leakage for  $|\Delta\bar{\sigma}_3/\bar{\sigma}_3| < 5\%$ . For larger values of  $|\Delta\bar{\sigma}_3/\bar{\sigma}_3|$ , the swelling ratios based on the curves in Fig. D-40 will result in an overestimate of the change in effective stress caused by a given volume of leakage.

(c) Variation of the Swelling Curve with the Effective Principal Stress Ratio

The value of the effective principal stress ratio applied to the specimens for the tests plotted in Fig. D-37 ranges from 1.00 to 4.66. A detailed examination of the data in Fig. D-37 shows that there is no consistent relation between the slope of the swelling curve for each test and the magnitude of  $\bar{\sigma}_1/\bar{\sigma}_3$ .

The effect of  $\bar{\sigma}_1/\bar{\sigma}_3$  on the swelling curve is more clearly seen in Fig. D-42. The average swelling ratios shown on this plot were calculated by using the method of least squares to determine the slope of the best straight line through the points on the swelling curve for each test. (The coordinates of these points are shown in Table D-3. The origin was not considered as a point on the swelling curve when calculating the average swelling ratio.) Since the swelling curves shown in Fig. D-40 curve upward in every case, it is evident that the ordinates in Fig. D-42 will increase as the range of  $\Delta u_w/\bar{\sigma}_3$  applied in a test is increased. The numbers located beside each point in Fig. D-42 show the range of  $\Delta u_w/\bar{\sigma}_3$  (in percent) used in each test.

Fig. D-42 shows that the swelling ratio for Canyon Dam clay is not affected by  $\bar{\sigma}_1/\bar{\sigma}_3$  when tested in the manner described in this chapter. The correlation between the range of  $\Delta u_w/\bar{\sigma}_3$  and the magnitude of the average swelling ratio indicates that the total range of variation of the swelling ratio would be about one-half that shown if the range of  $\Delta u_w/\bar{\sigma}_3$  had been the same for all tests. The remainder of the variation seen in Fig. D-42 is due to (1) the variation of  $\bar{\sigma}_3$  and (2) the errors discussed in D-09.

The above discussion indicates that the swelling ratio is virtually independent of  $\bar{\sigma}_1/\bar{\sigma}_3$  for Canyon Dam clay. Thus, when using Eq. 2-9 to calculate changes in effective stress due to leakage, one may use the same swelling ratio regardless of the shear stress on the specimen. This result is surprising since one might expect that high values of  $\bar{\sigma}_1/\bar{\sigma}_3$  would strain the soil, cause a partial structural breakdown and change the swelling ratio. Seed, Mitchell and Chan (90) have postulated that the kneading type of compaction used herein produces a structure which is insensitive to further change by application of shear stresses. Hence, the Canyon Dam clay specimens were thoroughly remolded before the application of shear stress in the swelling tests so that the swelling ratio would not be expected to vary substantially with  $\bar{\sigma}_1/\bar{\sigma}_3$ . It would be instructive in the future to study the variation of the swelling ratio with  $\bar{\sigma}_1/\bar{\sigma}_3$  for more sensitive soils such as undisturbed Leda clay or possibly Canyon Dam clay which is compacted on the dry side of the optimum water content by a static compaction procedure.

Since the swelling ratio varies with  $\bar{\sigma}_3$  but is independent of  $\bar{\sigma}_1/\bar{\sigma}_3$ , it follows that the swelling ratio should not be dependent on  $\bar{\sigma}_1$ . This is only a consequence of the procedure used to obtain the swelling data. To understand this point it is helpful to consider the total volume increase of a specimen during swelling as being composed of\* (1) the volume increase in the two lateral directions (i.e. in the direction of  $\bar{\sigma}_3$  in the present case) and (2) the volume increase in the axial direction. Assume that a homogeneous and isotropic specimen of soil is set up in a triaxial cell for a swelling test and that  $\bar{\sigma}_1/\bar{\sigma}_3 = 1.0$ . If the pore pressure is now increased, the specimen will swell. The volume increase in the lateral direction will be twice as great as the volume increase in the axial direction because the strains will be equal in both directions. Thus a small

\* The concept of dividing the total volume change into its components in each direction was proposed by Casagrande and Wilson (36).

change in the lateral effective stress will affect the measured volume change two times more than an identical small change in the axial effective stress.

On the other hand, if the axial effective stress were much greater than the lateral effective stress, the soil would be stiffer in the axial direction. Thus the soil would become, in effect, anisotropic. The strain in the axial direction due to a given increment in pore pressure would now be less than the strain in the lateral direction. Therefore the volume increase in the lateral direction will be more than twice that in the axial direction.

The two effects described in the preceding paragraphs are additive and cause the effective minor principal stress to control the total volume changes, and therefore the swelling ratio, in the swelling tests performed herein. It is evident that if the lateral effective stress were greater than the axial effective stress at the start of swelling, the two effects would act in opposite directions. Such a series of swelling tests would most likely show a dependence of the swelling ratio on both  $\bar{\sigma}_1$  and  $\bar{\sigma}_3$  (or  $\bar{\sigma}_3$  and  $\bar{\sigma}_1/\bar{\sigma}_3$ ). Also, if a series of swelling tests were performed with constant lateral effective stress, the measured swelling ratio would be dependent only on the axial effective stress. Thus, the procedure used to obtain the swelling data has a direct influence on whether  $\bar{\sigma}_1$  or  $\bar{\sigma}_3$  or both, will affect the swelling ratio.

#### D-09 DISCUSSION OF ERRORS

##### (a) Temperature Fluctuations

A temperature increase of a specimen causes the water in its pores and in the drainage system of the triaxial cell to increase in volume relative to the soil skeleton and drainage tubing. For the specimens used in the present investigation, an increase in temperature of 1°C will cause the water level in a 0.1 mm bore drainage burette to rise about 0.6 cm. This change in burette reading can be very important during the swelling phase of a test. An increase in temperature also causes the chamber and pore pressures to rise because the pressure in the air storage tanks (Fig. D-5) increases with increasing temperature. This in turn causes the effective stress on the specimen to increase. Calculations show that the change in burette reading caused by the increase in effective stress is negligible relative to that caused by expansion of the water in the system.

The laboratory temperature was recorded at intervals during the swelling phase of tests SW2, 8, 19, and 20, which were performed simultaneously. The largest temperature fluctuation was a rise of 0.6°C over the duration of the third swelling increment. The time curves for the four tests are shown in Figs. D-14, D-20, D-31 and D-32. The swelling curves for the third increment show a tendency for volume decrease toward the end of the increment. If one assumes that the temperature increased in proportion to time after swelling was begun, the correct time curves would be as shown dotted in the figures. The shape of these corrected time curves follows the pattern of the time curves for the previous and succeeding swelling increments.

The volume change calculated from a measured time curve may be in error by  $\pm 2.5 \text{ mm}^3$ , if the effect of an increase or decrease in temperature of the specimen\* of 0.5°C in 200 minutes is not taken into account. For Canyon Dam clay, this would introduce an error as large as  $\pm 50\%$  in the ordinates of the swelling curve! If (1) the final slope of the measured time curve is zero or negative and the temperature increases during a swelling increment, or (2) the final slope of the correct \*\* time curve is zero or negative and the temperature decreases during a swelling increment, then the method given in

---

\* The room temperature would have to change by something more than 0.5°C, perhaps 1.0°C, in order to cause a change in temperature of the specimen of 0.5°C.

\*\* To obtain the correct time curve from the measured time curve, one must know the temperature change which occurred in the specimen during the swelling increment.

D-06(b) for calculating the volume change from the time curves would account for the effects of temperature changes. However, the final slopes of the time curves for the tests represented in Fig. D-37 are positive in nearly all cases, so that the effect of temperature changes on the results is not accounted for in those tests. Thus, specimen temperature variations probably account for the major portion of the variation from the average line in Fig. D-37. The variation from average is smaller in Figs. D-38 and D-39 than in Fig. D-37 because, by chance, a larger percentage of the time curves represented by points in Figs. D-38 and D-39 had a negative final slope.

The above discussion of the effect of temperature changes on the swelling data shows that it is essential to measure the temperature changes of the specimen, or preferably to maintain the specimen at constant temperature, when accurate measurements of volume changes on the order of 2 mm<sup>3</sup> are desired. Also, the discussion shows that the effect of minor ( $\pm 1^\circ\text{C}$ ) temperature changes on the volume change measurements probably accounts for the major portion of the error in the results of the swelling tests presented herein.

(b) Shape of the Extrapolated Curve of Secondary Consolidation

The following items can cause the extrapolated curves of secondary consolidation, shown dotted in Figs. D-8 and D-9, to be in error:

- (1) The time required to complete essentially 100% primary consolidation may be in error.
- (2) The rate of secondary consolidation at the start of swelling may be in error.
- (3) The rate of volume change due to secondary consolidation after the swelling increment has been applied and after primary swelling is essentially complete, may not be equal to that given by the final slope of the time curve.

The total error which might be introduced due to items (1) and (2) in the volume change calculated from the data of a swelling test is believed to be a maximum of  $\pm 10\%$ . In most cases this error probably is much smaller. The error introduced by item (3) is discussed below.

In interpreting the volume change data, it was assumed that the final slope of the extrapolated curve of secondary consolidation is equal to the final slope of the time curve (Fig. D-8). Actually, during the 200 minute period of swelling used herein, the final slope of the time curve may not yet have reached its ultimate value. In such a case the final slope of the curve of secondary consolidation should be more negative than that used herein to interpret the data. This would make the actual volume change that occurred in 200 minutes greater than the volume change used to plot the swelling curves; and the swelling ratios would be correspondingly greater. To evaluate the error one would need a time curve that extends over a period of at least twenty-four hours to determine how its slope changes with time. Three such time curves are shown in Fig. D-26. However, the changes in laboratory temperature over such long periods so obscured the data that it is not possible to compare the slope after 200 minutes with that after, say, 1000 minutes. Thus the data are not satisfactory for evaluating the error.

The overall error caused by poor extrapolation of the curve of secondary consolidation during a swelling increment is believed to be on the order of  $\pm 10\%$  of the estimated volume of swelling. However, additional tests in which (1) the time curves are recorded for a period of about one day and (2) the temperature of the specimen is held accurately constant, are needed to evaluate the error.

(c) Other Errors

The errors introduced in the swelling curves by the items listed below are felt to be small relative to the errors introduced by the items discussed in subparagraphs (a) and (b).

- (1) Pressure variations and inaccurate measurement of pressure during a swelling increment. (See also D-03(d)).

- (2) Inaccurate calibration of the triaxial cell.
- (3) Variations in the as-molded water contents and unit weights of the specimens tested.
- (4) Variations in the duration of the consolidation or deviator load phase of the tests.
- (5) Variation in size of the swelling increments in one test, and from test to test.

(d) Summary of Errors

Temperature variations in the laboratory cause the major error in the swelling curves shown in Figs. D-37, D-38 and D-39. A change in temperature of a swelling test specimen of 0.5°C in 200 minutes may cause the volume change caused by a small increment of pore pressure to be in error by as much as  $\pm 50\%$ . In order to obtain more consistent swelling data in future swelling tests of the type performed herein it will be necessary to maintain the temperature of the specimens accurately constant. A minimum requirement is that the temperature be maintained constant to within  $\pm 1/4^\circ\text{C}$ .

The method used to interpret the volume change data introduces error into the results of the swelling tests because the volume change that occurs due to secondary consolidation during a swelling increment cannot be accurately determined. The error is probably on the order of + 10%. This error probably can be eliminated by increasing the duration of each swelling increment from 200 min (as used herein) to about one day.

Other errors are not considered significant, for the range  $0\% < |\Delta\bar{\sigma}_3/\bar{\sigma}_3| < 5\%$ . However, for  $|\Delta\bar{\sigma}_3/\bar{\sigma}_3| > 5\%$ , the duration of each swelling increment may cause an appreciable increase of the swelling ratio. The effect of increasing the duration of each increment was not investigated.

D-10 SUMMARY AND CONCLUSIONS

The swelling curves (plotted in terms of percent volume increase versus percent decrease in effective stress) for twenty-four identical specimens of Canyon Dam clay were determined. It was found that the swelling curve has an upward curvature on an arithmetic or semi-logarithmic plot for ranges of effective stress from 80 to 100 percent of the effective stress on the specimen at the start of swelling (see Fig. D-40). This is in agreement with the shape of the swelling curves obtained from conventional consolidation tests on many different soils by other investigators.

The swelling ratio for 100% saturated specimens of Canyon Dam clay compacted to a water content of 16% and a dry unit weight of 115 pcf, for the range  $0 < |\Delta\bar{\sigma}_3/\bar{\sigma}_3| < 5\%$ , was found to be:

$\bar{\sigma}_3$ (kg/cm <sup>2</sup> )	s (-)
2	0.0010 $\pm$ 30%
6	0.0011 $\pm$ 5%
14	0.0015 $\pm$ 20%

The swelling ratio was found to be independent of the magnitude of the effective principal stress ratio on the specimen during swelling. Therefore, the above values of the swelling ratio may be used in Eq. 2-9 to calculate the change in effective stress caused by leakage at any stage during a triaxial Q or R test on Canyon Dam clay.

The range of error in the swelling ratios quoted above is almost entirely due to the volume change of the water in the specimen relative to the soil grains when the temperature of the specimen varied during the swelling phase of a test.

The procedures used in the swelling tests should be modified as follows for future tests:

- (1) Maintain the specimen temperature to within  $\pm 1/4^{\circ}\text{C}$  during those portions of the tests when volume changes smaller than  $10\text{ mm}^3$  must be accurately measured. It would be helpful also to determine experimentally the effect of temperature variations on the volume change measurements.
- (2) The duration of each swelling increment should be increased to about twenty-four hours, for the case of 1.4 in. by 3.5 in. specimens of Canyon Dam clay.
- (3) Use swelling increments that are equal in size for all tests. Increase the number of swelling increments used for each test so that the swelling curve will be better defined.
- (4) Perform the tests in such a manner that  $\bar{\sigma}_3$  will be constant for several different values of  $\bar{\sigma}_1/\bar{\sigma}_3$ . In this manner the effect, if any, of  $\bar{\sigma}_1/\bar{\sigma}_3$  on the swelling ratio can be easily discerned.
- (5) Perform tests using the first approach described in D-06(b). The period that must be allowed for secondary consolidation prior to the start of swelling must be determined for each soil tested.
- (6) Make all weighings and volume change measurements accurate to within  $\pm 0.001\%$ .

The apparatus used in the swelling tests was satisfactory. However, the results may be improved if the following details were changed:

- (1) Eliminate all plastic tubing from the drainage system. Eliminate all but one valve and minimize the number of connections in the drainage system.
- (2) Use more sensitive equipment for measuring the chamber and pore pressures during and prior to the application of a swelling increment.

APPENDIX EDATA FOR WATER AND VAPOR PERMEABILITY TESTS ON MEMBRANES

FIGS. E-1 through E-11 - Water permeability (W) tests on natural rubber membranes.

Plots show total inflow, total outflow and outflow from the low pressure (LP) side burette for tests W1 through W8.

FIGS. E-12 through E-29 - Water vapor permeability (V) tests on natural rubber membranes.

The lower plot in each figure is the inflow from the high pressure (HP) side burette for tests V1 through V18.

The upper plot shows the outflow into the leakage (L) burette which collected the leakage across the O-Ring sealing the perimeter of the membrane. Note that the ordinate scale for the upper plot is much larger than the ordinate scale for the lower plot.

FIGS. E-30 through E-62 - Water vapor permeability (V) tests on synthetic rubber and plastic membranes.

The lower plot in each figure is the inflow from the high pressure (HP) side burette for tests V19 through V51.

The upper plot shows the outflow into the leakage (L) burette which collected the leakage across the O-Ring sealing the perimeter of the membrane. Note that the ordinate scale for the upper plot is much larger than the ordinate scale for the lower plot.

APPENDIX FDATA FOR OSMOSIS TESTS ON NATURAL RUBBER MEMBRANES

FIGS. F-1 through F-10 -

Plots show volume flow versus time for both inflow to and outflow from the cell for tests X1 through X7.

APPENDIX GDATA FOR BINDING LEAKAGE TESTSFIGS. G-1 through G-26 -

Plots show volume flow versus time for tests B1 through B25. Short tick marks indicate slope used to calculate the measured flow,  $q_M$ , for each test.

APPENDIX HDATA FOR TESTS ON VALVES, FITTINGS AND SARAN TUBINGFIGS. H-1 through H-23 - Leakage tests on valves.

Plots show volume flow versus time for test Nos. 1 through 13. For several tests, points are shown that have been corrected for effects of room temperature fluctuations. Tick marks show slope chosen to calculate valve leakage.

FIGS. H-24 through H-36 - Leakage tests on fittings.

Plots show volume flow versus time for test Nos. 14 through 22. For several tests, points are shown that have been corrected for effects of room temperature fluctuations. Tick marks, where shown, indicate slope used to calculate fitting leakage.

FIGS. H-37 through H-40 - Tests on Saran tubing.

Fig. H-37 shows immediate volume change caused by application of hydraulic pressure inside tubing with atmospheric pressure outside.

Fig. H-38 shows volume change due to creep of Saran tubing caused by long term application of hydraulic pressure inside tubing with atmospheric pressure outside.

Figs. H-39(a) through H-39(c) show volume change due to creep of Saran tubing, plotted with a logarithmic time scale.

Fig. H-40 shows the volume of liquid water evaporated through the walls of Saran tubing plotted against time.

TABLE A-1

PERMEABILITY OF NATURAL RUBBER TO AIR

Membrane Material	Thickness L (cm)	Temperature T (°C)	Permeability Constant $K_p$ (cm <sup>4</sup> /gm sec)	Reference
Dental dam	0.035	Room	$8.1 \times 10^{-11}$	Casagrande and Shannon (1948) (33)
Holland-Rantos	0.029	Room	$2.9 \times 10^{-11}$	Casagrande and Shannon (1948) (33)
Dental dam	0.022	21	$9.7 \times 10^{-11}$ **	Davis (1946) (38)
Natural rubber	***	25	$9.7 \times 10^{-11}$	van Amerongen (1946) (2)
Natural rubber	***	25	$8.7 \times 10^{-11}$	van Amerongen (1950) (3)
Trojan	0.007	21 ± 0.5	$8.0 \times 10^{-11}$ ***	Wissa (1962) (109)

\* All  $K_p$  values computed by the author using data given in the reference.  
 \*\* Estimated from Davis' data for permeability to oxygen.  
 \*\*\* Thickness not given.  
 \*\*\*\* Estimated from Wissa's data for permeability to nitrogen.

TABLE A-3

TESTS ON TREATED AND/OR PROTECTED MEMBRANES  
 CASAGRANDE AND WILSON (1949) (Ref. 34)

Original Test Number	Test Duration (days)	Estimated Rate of Inflow (mm <sup>3</sup> /day)	Number of Membranes*	Type of Treatment and/or Type of Protection of Membranes
<b>IMMERSED IN WATER</b>				
12	14	+16.1	1	No treatment
14	14	+12.8	1	Saturated with water
18	14	-6.4	2	Cello-seal grease between
21	16	-5.6	2	Cello-seal grease between
23	90	-0.3	2	Saturated with water and
24	14	-6.4	2	cello-seal grease between
26	14	-9.6	2	Castor oil between
27	14	-9.6	2	Castor oil between
29	14	-3.2	2	Saturated with water and
				castor oil between
<b>IMMERSED IN CASTOR OIL</b>				
13	14	-29.0	1	No treatment
15	14	-29.0	1	Saturated with water
19	14	-29.0	2	Cello-seal grease between
22	14	-37.5	2	Cello-seal grease between
25	14	-32	2	Saturated with water and
				cello-seal grease between
28	14	-29	2	Castor oil between
30	14	-29	2	Saturated with water and
				castor oil between
<b>EXPOSED TO ROOM ATMOSPHERE</b>				
6	3	-195	1	Rubbed with stopcock grease
7	13	>-173	1	Treated with "Dri-Film"
9	27	>-100	1	Covered with glycerin and
				ceramic clay powder mixture
10	27	>-167	1	Covered with stopcock grease
				and clay powder mixture
11	27	>-167	1	Covered with castor oil and
				clay powder mixture
20	14	-83	2	Cello-seal greases between

\* Membranes: Natural rubber (Trojans), 0.005 cm thick.  
 Specimens: Cambridge Clay, volume=90cm<sup>3</sup>, water content= 40%, assumed specific gravity of solids=2.78.  
 \*\* Change in water content of 0.1% is equivalent to 45 mm<sup>3</sup> of water flow.

TABLE A-2

PERMEABILITY OF NATURAL RUBBER TO WATER VAPOR

Membrane Material	Thickness L (cm)	Temperature T (°C)	Permeability Constant $K_p$ (cm <sup>4</sup> /gm sec)	Reference
Dental dam	0.035	Room	$4.0 \times 10^{-9}$ *	Casagrande and Shannon (1948) (33)
"Thin" latex	0.005	Room	$3.6 \times 10^{-9}$ *	Casagrande and Shannon (1948) (33)
Trojan	0.005	Room	$3.9 \times 10^{-9}$ *	Casagrande and Wilson (1949) (34)
Dental rubber	0.025	25	$3.2 \times 10^{-9}$ **	Shumacher and Ferguson (1929) (89)
Dental rubber	0.0354	25	$11.5 \times 10^{-9}$ **	Taylor, Hermann and Kemp (1936) (100)
Ramses	0.005	30	$12.4 \times 10^{-9}$	Poulos (Chapter 6)

\* Calculated by the author from the reported data and the assumptions given in the text.  
 \*\* Units converted from those used in the reference to the units used in the table.

TABLE D-1

ESSENTIAL DATA ON SWELLING TESTS

Test No.	$\bar{\sigma}_c$ kg/cm <sup>2</sup>	$\bar{\sigma}_d$ max kg/cm <sup>2</sup>	$\frac{d_d}{d_c}$ max %	$\frac{\Delta V}{V_0}$ %
SW1	2	6.5	0	2,5,10
SW2			0	2,5,10,20
SW3			25	5,10,20
SW4			50	5,15,25
SW5			75	5,10,20
SW6			75	5,15,20
SW7	6	11.0	0	1,2,5
SW8			0	2,5,10,20
SW9			0	2,5,10
SW10			0	2,5,10
SW11			0	2,5,10
SW12			0	2,5,10
SW13			25	1,3,6
SW14			37	2,5,10
SW15			50	3,6,12,24
SW16			75	2,5,10
SW17	14	19.7	0	0,5,1,2
SW18			0	2,5,10,15
SW19			0	2,5,8
SW20			0	2,5,10,15
SW21			25	0,5,1,2
SW22			50	1,2,5,5
SW23			75	1,3,6
SW24			75	3,5,10,16

\* Values shown are approximate. See Table D-3 for exact values.  
 \*\* deviator load at failure estimated from data reported by Casagrande and Hirschfeld (82).

TABLE D-2

CALCULATION OF THE CORRECTED VOLUME CHANGE FOR THE DATA OF SWELLING TEST SW22

(1)	(2)	(3)	(4)	(5)	(6)	(7)
Pore Pressure Increase kg/cm <sup>2</sup>	Percent Decrease in Effective Stress %	Change in Burette Reading dB <sub>2</sub> cm	Cumulative Change in Burette Reading Σ (dB <sub>2</sub> ) cm	Measured Volume Change mm <sup>3</sup>	Correction to Volume Change ΔV <sub>c</sub> mm <sup>3</sup>	Corrected Volume Change ΔV mm <sup>3</sup>
.054	0.98	0.14	0.14	+1.1	-0.1	+1.0
.136	2.50	0.16	0.30	+2.3	-0.3	+2.0
.271	5.00	0.35	0.65	+5.1	-0.7	+4.4

\*A volume increase is positive.

- Manometer readings in centimeters times unit weight of mercury, in kg/cm<sup>3</sup>, at temperature of test.
- Column (1) divided by  $\bar{\sigma}_3$  at the start of swelling (5.43 kg/cm<sup>2</sup>).
- From Fig. D-9.
- From column (3).
- Column (4) times volume of burette per centimeter (7.82 mm<sup>3</sup>/cm).
- From calibration curve of triaxial cell, Fig. D-4.
- Column (5) plus column (6).

TABLE A-4

TESTS TO MEASURE THE RATE OF FLOW OF AIR THROUGH WATER AND RUBBER CASAGRANDE AND WILSON (1951) (ref.35)

Test Number	Chamber Fluid	Total Pressure Difference (kg/cm <sup>2</sup> )	Portions of Apparatus Filled with Chamber Fluid	Outflow
1	Water	4	Chamber*	See Fig. A-2
2(a)	Castor oil	6	Chamber*	See Fig. A-3
2(b)			Chamber plus 10 ft of 1/8" O.D. Saran tubing	See Fig. A-3
3(a)	Water	6	Chamber plus 10 ft of 1/8" O.D. Saran tubing	Air and/or water: 0.3 cm <sup>3</sup> /day
3(b)			Chamber*	Air and/or water: >> 0.3 cm <sup>3</sup> /day after twelve hours

\* Chamber fluid filled to level just above the top of membrane.

TABLE A-5

FLOW OF IONS AND/OR MOLECULES THROUGH NATURAL RUBBER CASAGRANDE AND WILSON (1951) (ref.35)

Test Number	Solutions Used	Method of Detection	Results
1	Strong FeCl <sub>3</sub> solution vs. equally strong KOH solution	Weight of precipitate	FeCl <sub>3</sub> side - no precipitate in 12 hours KOH side - no precipitate in 12 hours
2	Concentrated Ca(OH) <sub>2</sub> solution vs. saturated CO <sub>2</sub> solution	Weight of precipitate	Ca(OH) <sub>2</sub> side - 0.0443 gm CaCO <sub>3</sub> in 12 hours CO <sub>2</sub> side - no precipitate

TABLE D-3

SUMMARY OF SWELLING DATA

Test No.	$\bar{\sigma}_c$	$\frac{\bar{\sigma}_1}{\bar{\sigma}_3}$	$\bar{\epsilon}_3$	$V$	$\frac{\Delta u_w}{\bar{\sigma}_3}$	$\frac{\Delta V}{V}$	Average s $\times 10^3$						
	kg/cm <sup>2</sup>	-	kg/cm <sup>2</sup>	cm <sup>3</sup>	%	% $\times 10^3$							
SW1	2.54	1.00	2.54	84.96	2.12	0.82	5.43	5.30	10.67	11.90			0.0014
SW2	1.91	1.00	1.91	85.22	2.20	3.29	5.24	9.04	10.41	13.85	21.04	35.1	0.0017
SW3	2.00	2.36	1.21	85.11	4.46	3.38	11.22	10.00	22.40	23.4			0.0012
SW4	1.99	4.08	1.47	85.66	3.67	1.52	9.24	9.33	18.42	27.05			0.0017
SW5	2.16	4.11	1.02	85.25	5.30	5.63	13.52	20.6	26.6	51.0			0.0022
SW6	2.00	4.66	1.24	84.94	5.40	3.53	16.40	19.79	22.1	35.2			0.0019
SW7	5.52	1.00	5.52	83.42	1.01	1.08	2.43	2.52	4.91	5.29			0.0012
SW8	5.98	1.00	5.98	83.10	2.02	1.68	5.02	6.38	10.03	13.10	20.30	38.2	0.0021
SW9	5.89	1.00	5.89	82.13	1.88	1.83	5.06	6.09	10.38	14.00			0.0014
SW10	6.02	1.00	6.02	82.37	1.83	1.82	4.95	5.83	10.13	13.11			0.0013
SW11	5.86	1.00	5.86	82.45	1.93	1.58	5.30	6.31	10.80	14.31			0.0014
SW12	5.88	1.00	5.88	82.33	1.85	2.55	5.10	6.44	10.40	14.32			0.0014
SW13	6.05	1.63	4.50	83.33	1.24	0.72	3.02	2.40	6.02	5.77			0.0011
SW14	6.36	2.20	3.09	83.19	1.75	4.69	4.40	9.50	8.76	17.68			0.0019
SW15	5.96	3.45	2.25	83.53	3.02	4.19	6.00	8.02	12.00	19.23	24.15	46.1	0.0020
SW16	6.10	4.02	2.58	83.26	2.15	1.68	5.27	5.28	10.50	12.00			0.0012
SW17	13.9	1.00	13.9	81.61	0.39	0.25	0.97	0.98	1.94	2.94			0.0017
SW18	14.07	1.00	14.07	81.42	2.41	5.04	4.84	9.70	9.74	19.53	13.49	28.15	0.0021
SW19	13.92	1.00	13.92	81.35	2.00	1.72	5.04	6.40	8.34	12.19			0.0017
SW20	14.00	1.00	14.00	81.33	1.99	1.85	5.01	6.52	9.99	13.90	15.00	25.6	0.0018
SW21	14.00	1.48	10.53	81.60	0.51	0.49	1.29	1.10	2.57	3.31			0.0014
SW22	14.18	2.86	5.43	81.62	0.98	1.23	2.50	2.45	5.00	5.52			0.0011
SW23	14.14	3.80	5.17	81.42	2.67	10.70	5.25	17.59	10.47	28.9	15.71	37.4	0.0020
SW24	14.04	4.10	4.60	81.89	1.22	0.85	2.96	3.54	5.90	9.41			0.0019

TABLE D-4

INITIAL AND FINAL CONDITIONS OF SWELLING TEST SPECIMENS

Test No.	As-Molded Condition			Initial Back Pressure kg/cm <sup>2</sup>	Final Water Content %	Time for 100% Primary Consolidation min	Rate of Secondary Consolidation at Start of Swelling* cm/100 min
	Water Content %	Dry Unit Weight lb/ft <sup>3</sup>	Degree of Saturation %				
	SW1	15.72	115.1				
SW2	16.00	115.2	92.9	5.98	15.17	460	0.108
SW3	16.02	115.3	93.1	7.91	15.12	290	-0.362**
SW4	15.79	115.3	91.6	8.01	15.29	220	0.130
SW5	15.80	114.8	90.6	7.77	15.10	230	0.105
SW6	15.75	115.2	91.2	5.92	15.29	350	0.081
SW7	15.77	115.0	90.8	8.07	13.91	390	0.164
SW8	15.89	115.4	92.5	6.00	13.91	500	0.199
SW9	16.05	114.9	92.1	6.05	13.56	620	0.113
SW10	16.05	114.5	91.8	8.00	13.62	400	0.158
SW11	16.12	114.8	92.4	10.07	13.70	500	0.145
SW12	16.20	114.5	92.6	9.03	13.67	800	0.140
SW13	15.63	115.4	91.4	8.04	13.85	470	0.184
SW14	15.68	114.4	88.9	7.54	14.10	250	0.164
SW15	15.85	115.2	92.6	5.98	14.00	370	0.080
SW16	15.92	115.1	92.0	7.85	13.89	450	0.008
SW17	15.89	115.2	92.1	5.92	12.97	470	0.464
SW18	15.68	115.8	92.2	5.95	12.63	650	0.611
SW19	15.92	115.3	92.5	6.03	12.79	780	0.241
SW20	15.76	115.6	92.2	6.02	12.68	900	0.289
SW21	16.00	115.0	92.2	5.92	12.98	720	0.123
SW22	15.90	115.0	91.6	5.99	12.90	800	0.143
SW23	15.70	115.8	92.5	5.94	12.71	680	0.057
SW24	15.98	114.7	91.3	5.64	13.11	720	0.068

\* Equal to rate of change of burette reading due to secondary consolidation (under consolidation pressure or last deviator load increment) at the time when swelling was begun.

\*\* Leak in drainage system.

FIG. A-1

MEMBRANE PERMEABILITY CELL  
CASAGRANDE AND SHANNON (1948) (Ref. 33)

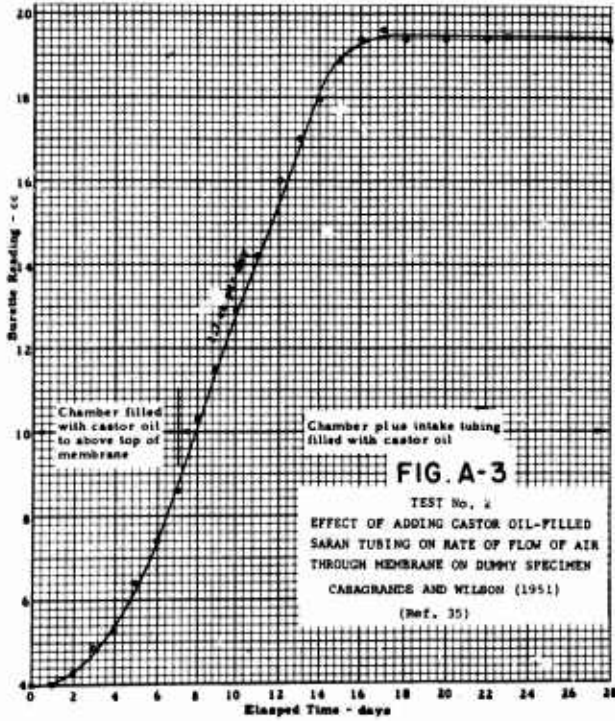
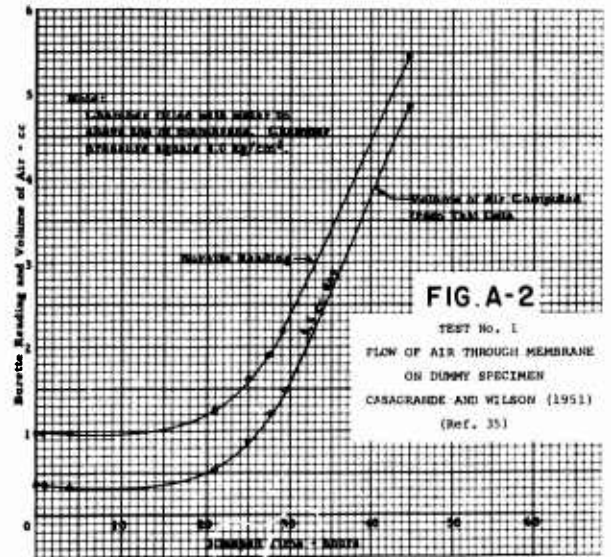
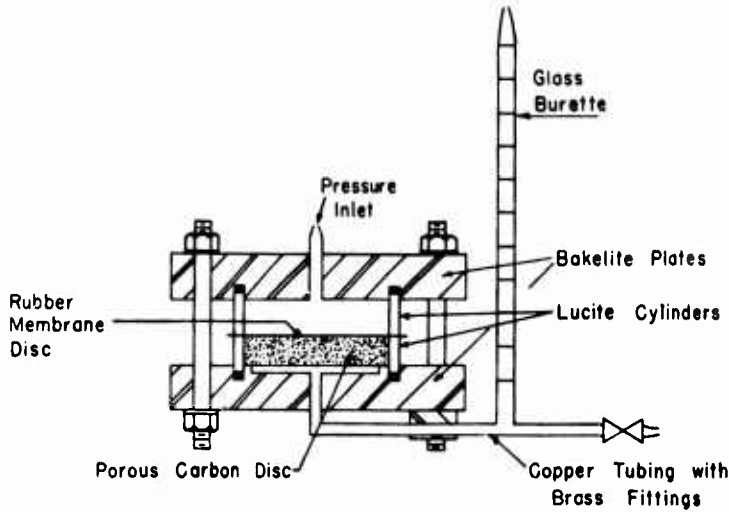
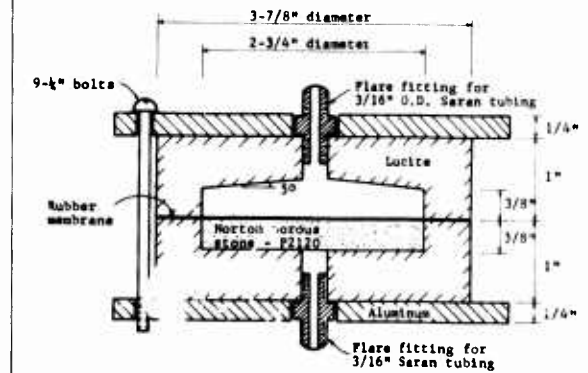


FIG. A-4

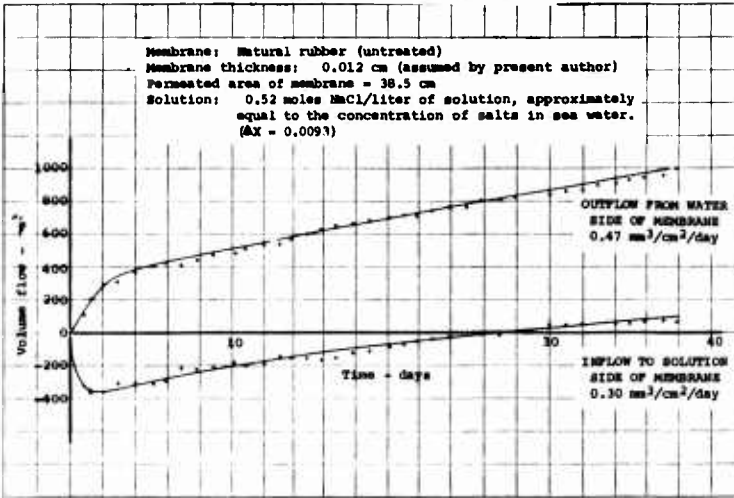
MEMBRANE PERMEABILITY CELL  
USED BY WISEMAN (1954) (Ref. 108)



**FIG. A-5**

WATER FLOW THROUGH NATURAL RUBBER  
DUE TO MOLE FRICTION GRADIENT

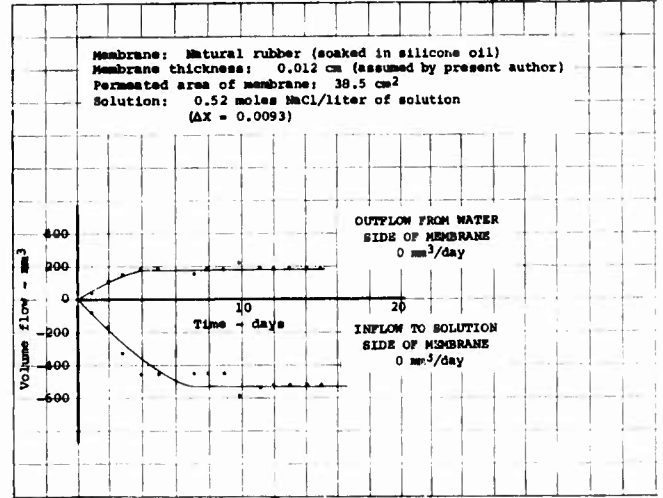
Test No. 2 by Moreland (1957) (Ref. 75)



**FIG. A-6**

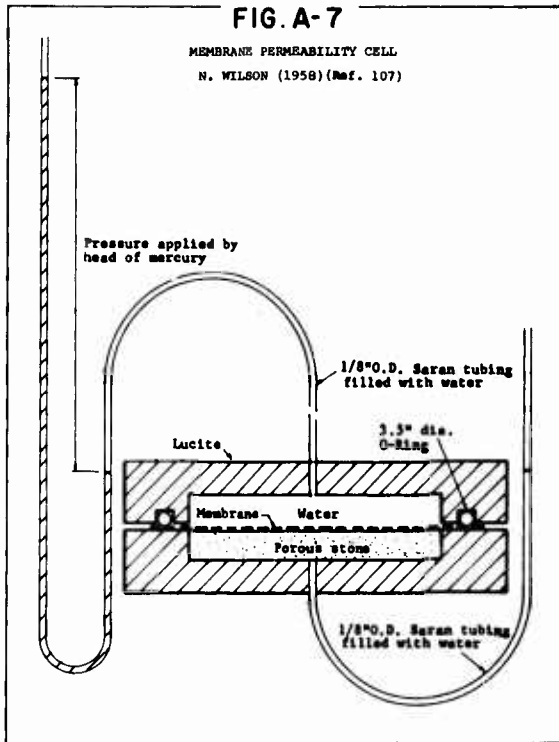
WATER FLOW THROUGH NATURAL RUBBER  
DUE TO MOLE FRACTION GRADIENT

Test No. 4 by Moreland (1957) (Ref. 75)



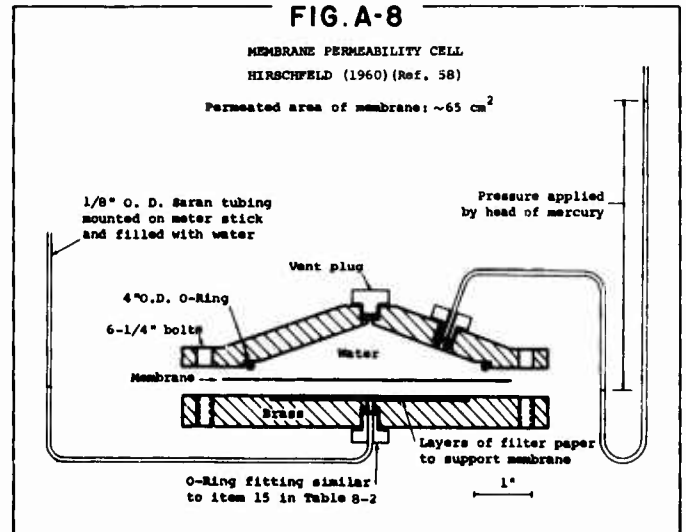
**FIG. A-7**

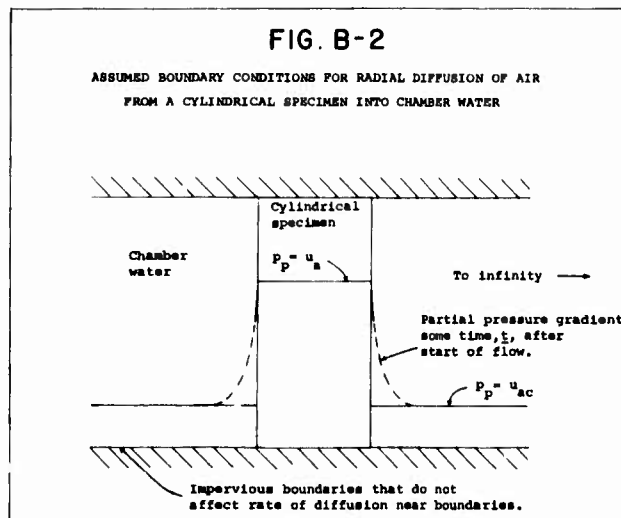
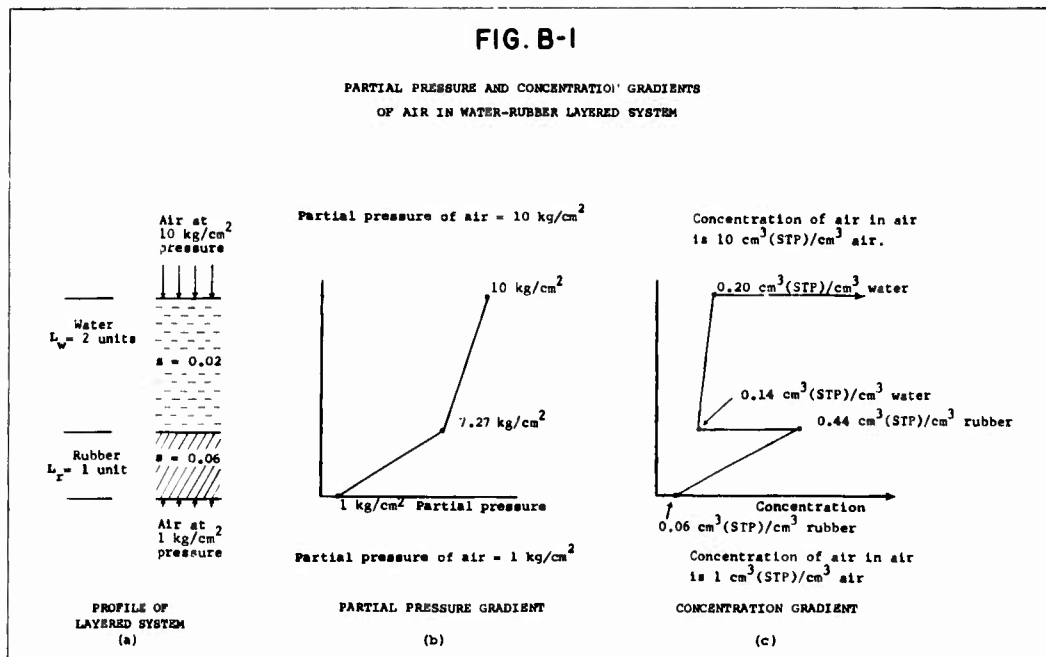
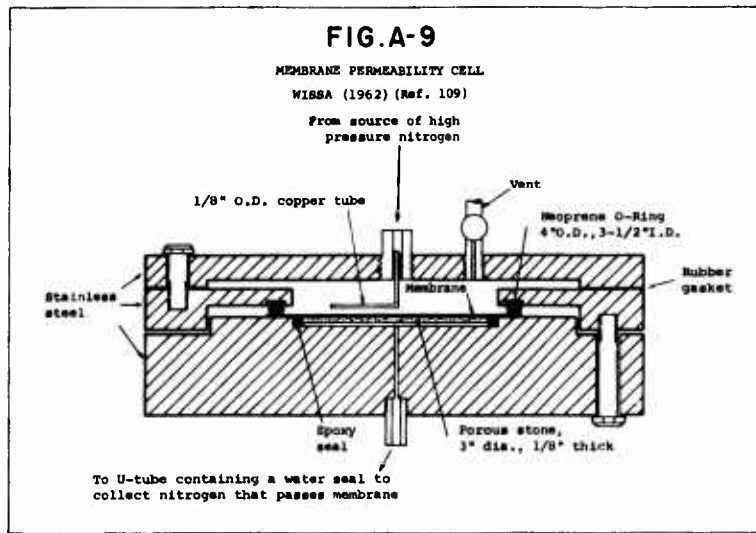
MEMBRANE PERMEABILITY CELL  
N. WILSON (1958) (Ref. 107)



**FIG. A-8**

MEMBRANE PERMEABILITY CELL  
HIRSCHFELD (1960) (Ref. 58)  
Permeated area of membrane: ~65 cm<sup>2</sup>





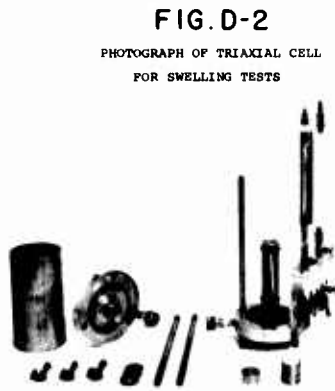
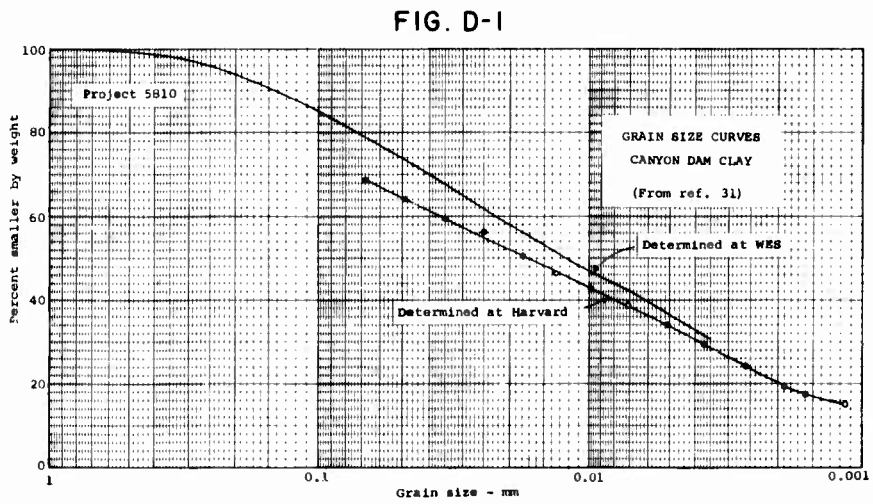
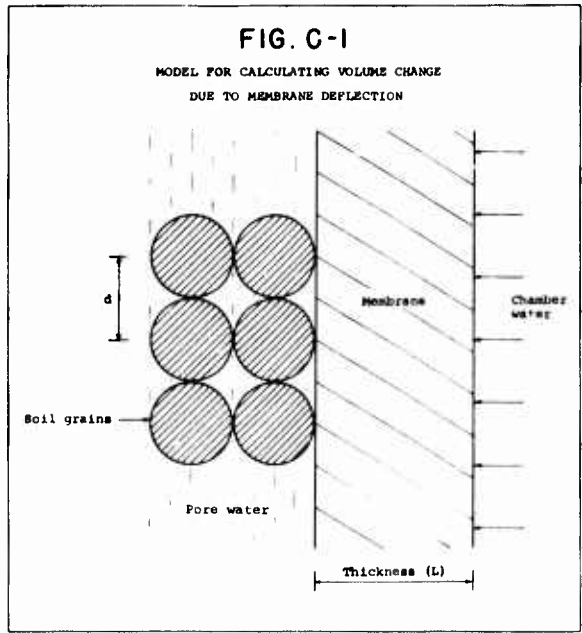


FIG.D-3

TRIAXIAL CELL FOR SWELLING TESTS

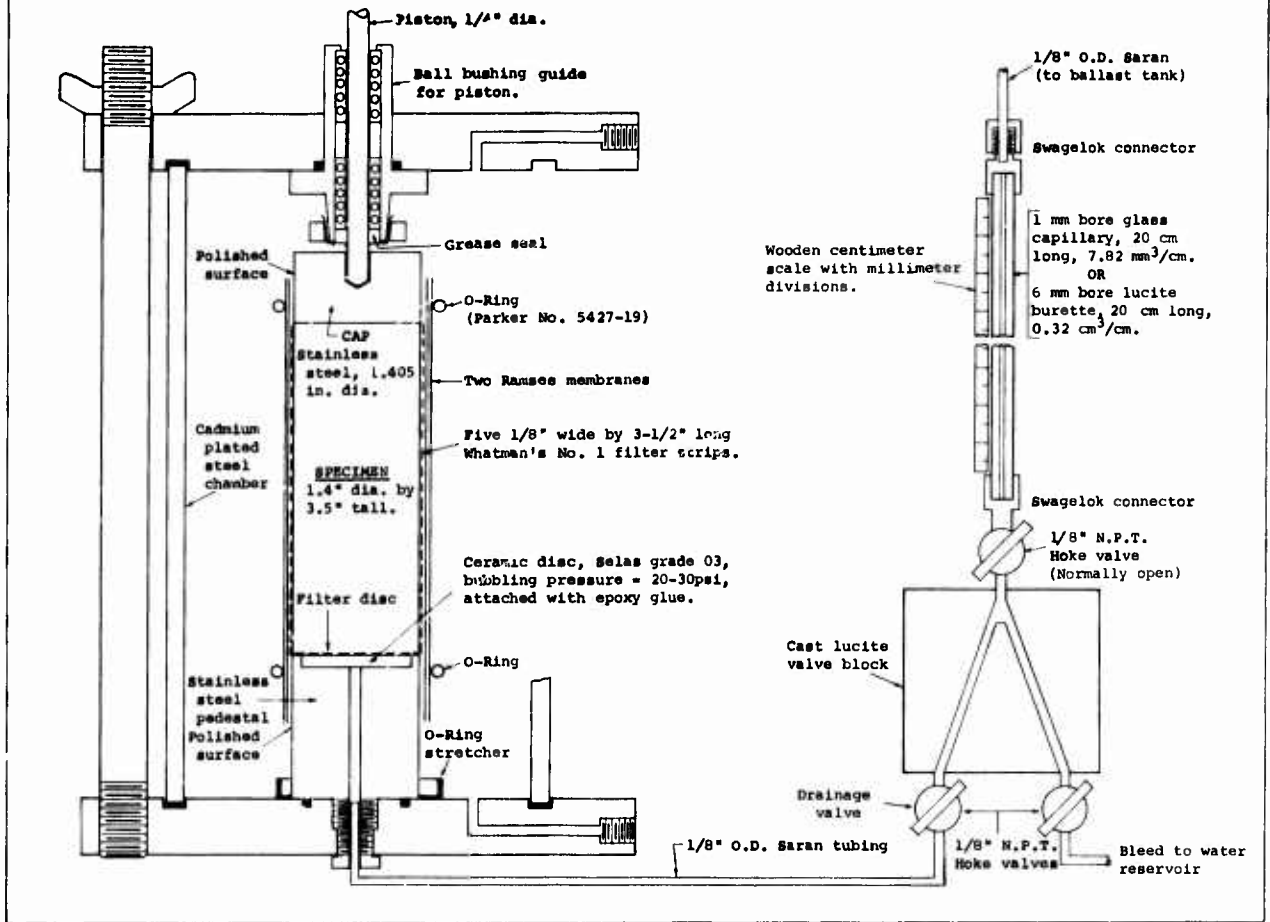


FIG.D-4

CALIBRATION OF TRIAXIAL CELL FOR SWELLING TESTS

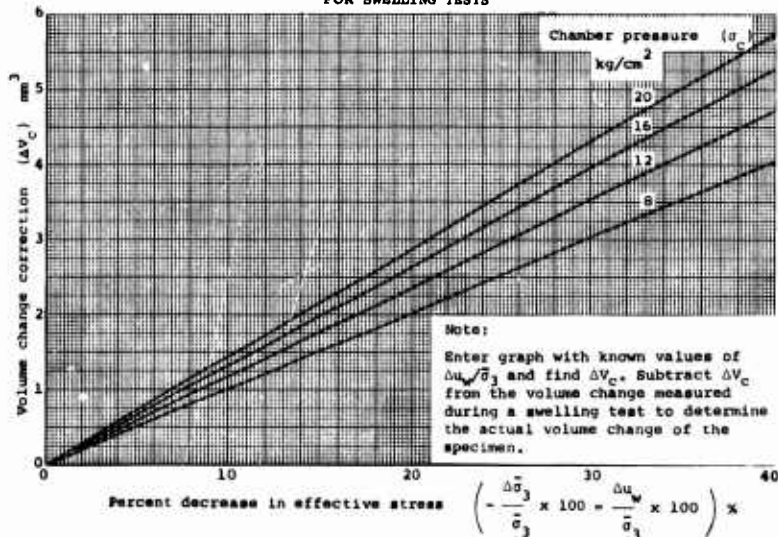


FIG. D-5

SCHMATIC DIAGRAM  
OF APPARATUS FOR SWELLING TESTS

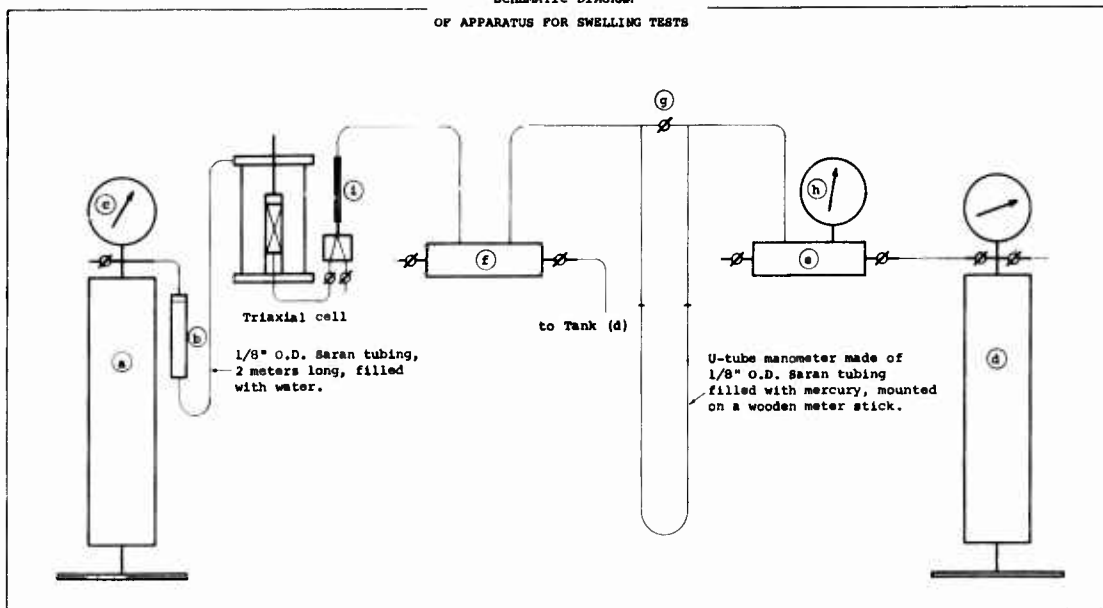


FIG. D-6

EFFECT OF LEAKAGE AND SECONDARY CONSOLIDATION  
ON EFFECTIVE STRESSES DURING TRIAXIAL TESTS

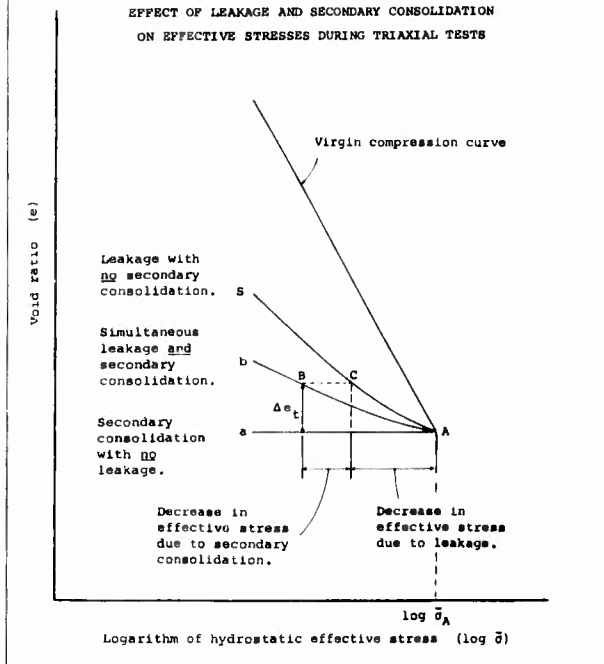


FIG. D-7

HYPOTHETICAL SWELLING CURVES

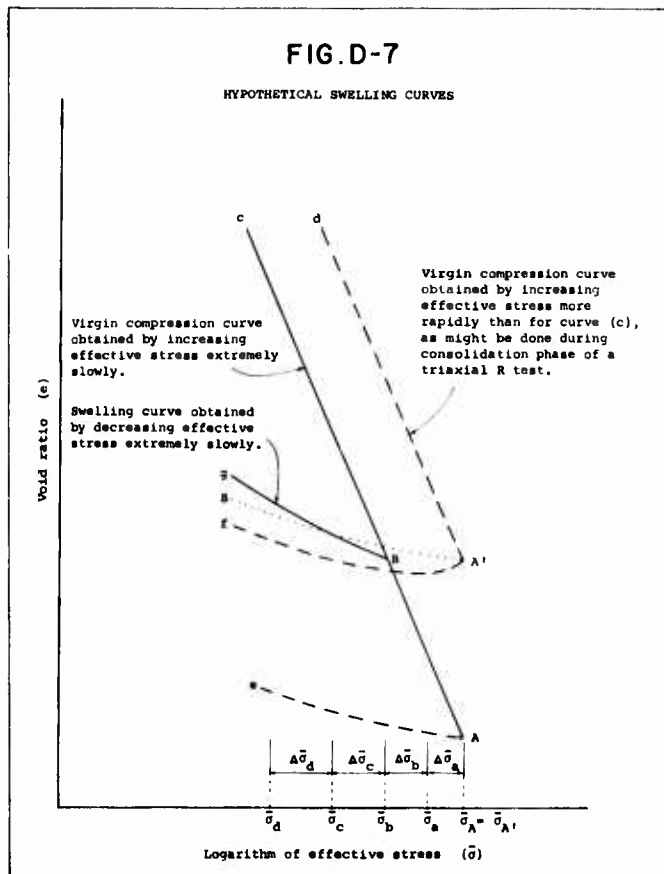


FIG. D-8

TIME CURVES OBTAINED WHEN THE EFFECTIVE STRESS OF A SOIL SPECIMEN IS DECREASED

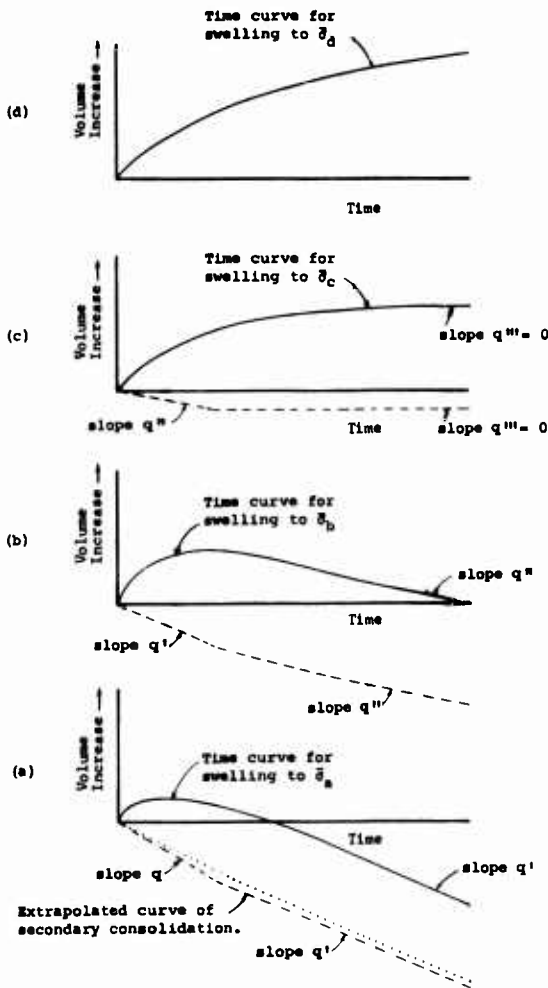


FIG. D-9

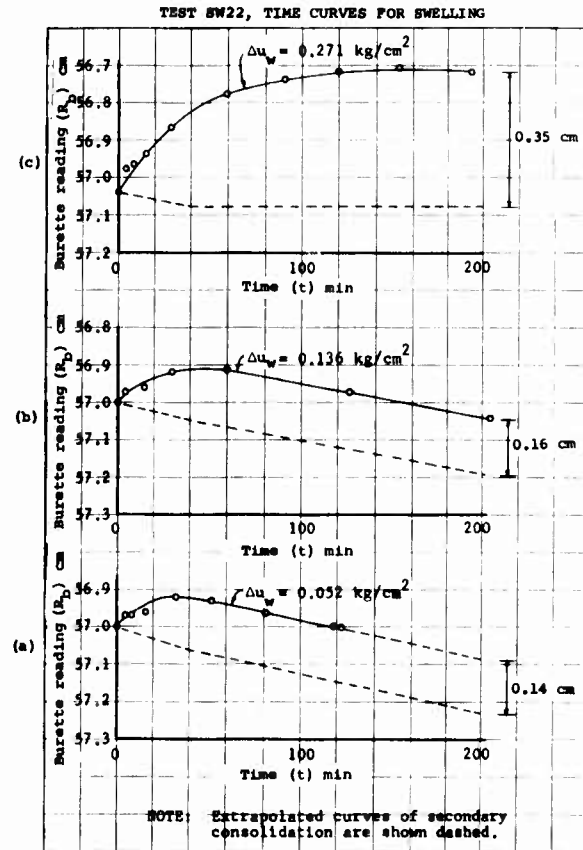


FIG. D-10

TEST SW22, TIME CURVES FOR CONSOLIDATION TO  $\bar{\sigma}_3 = 14.18 \text{ kg/cm}^2$

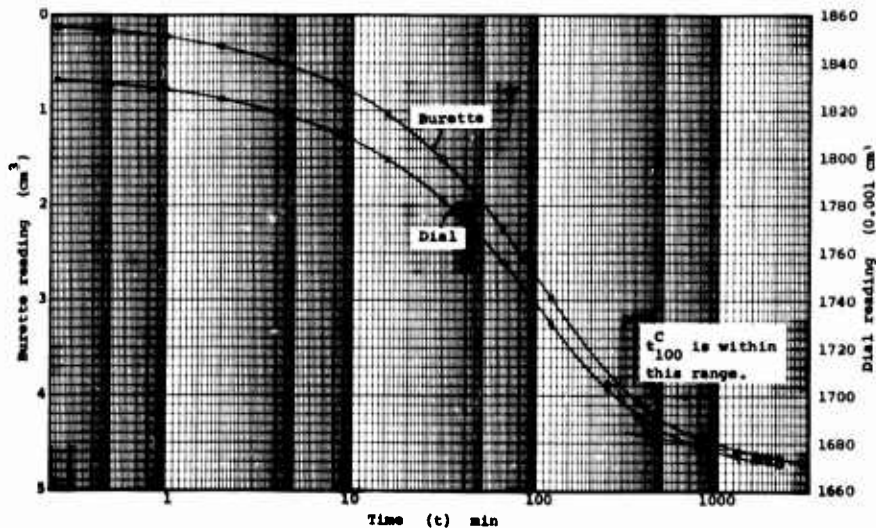


FIG. D-11

TEST SW22  
 BURETTE READING VERSUS LOG TIME  
 FOR LAST INCREMENT OF DEVIATOR LOAD

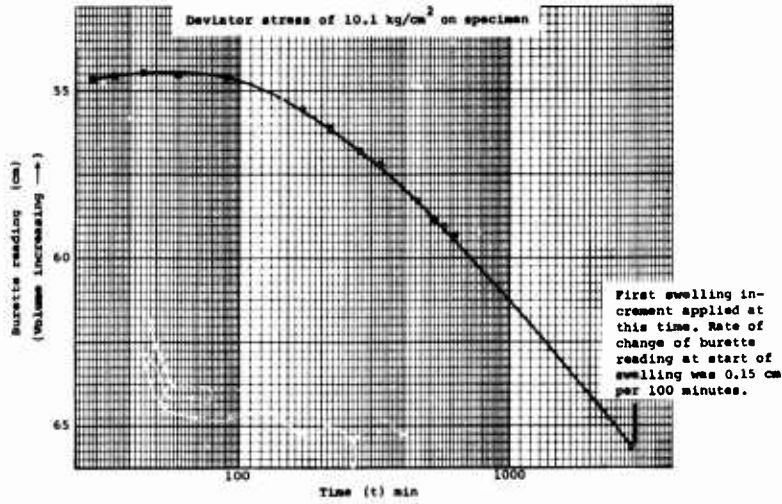


FIG. D-12

TEST SW22  
 SWELLING CURVE

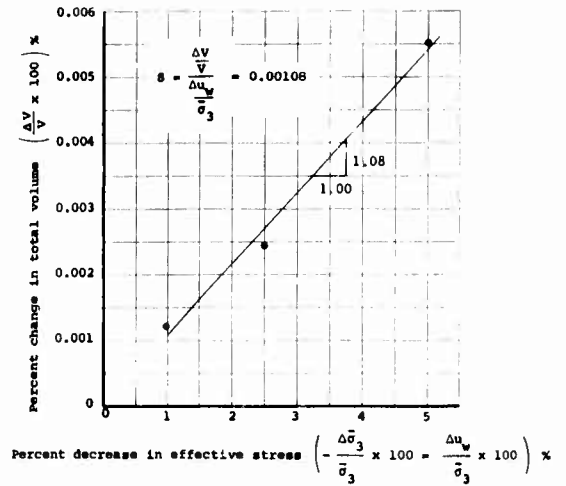


FIG. D-13

Test No. SW1  
 TIME CURVES

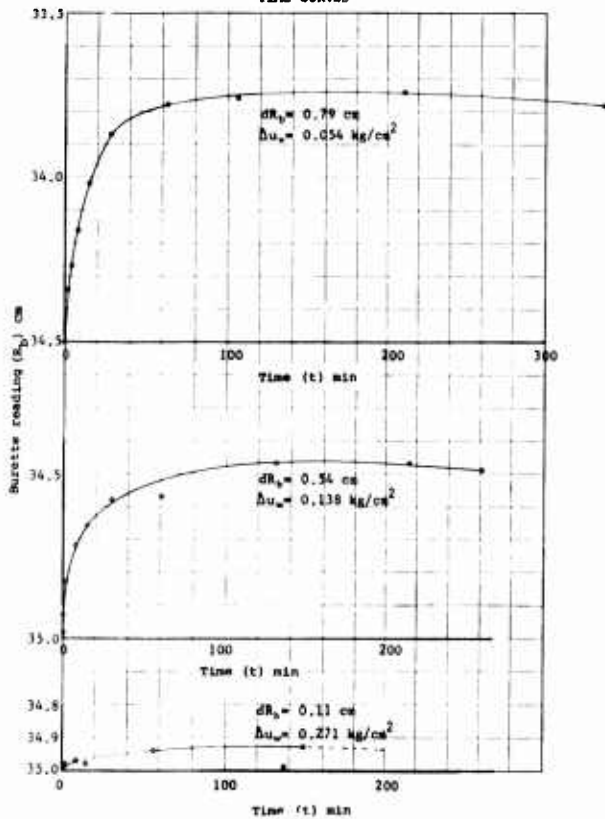
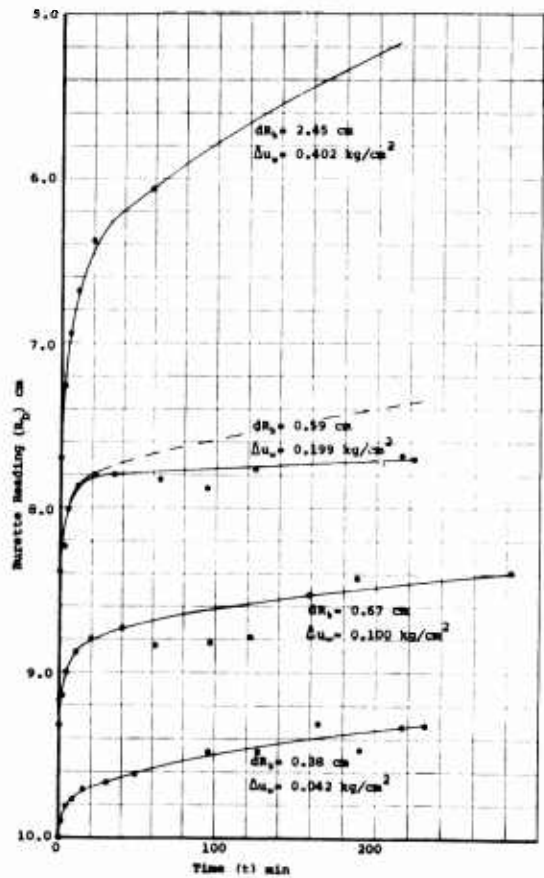


FIG. D-14

Test No. SW2  
 TIME CURVES



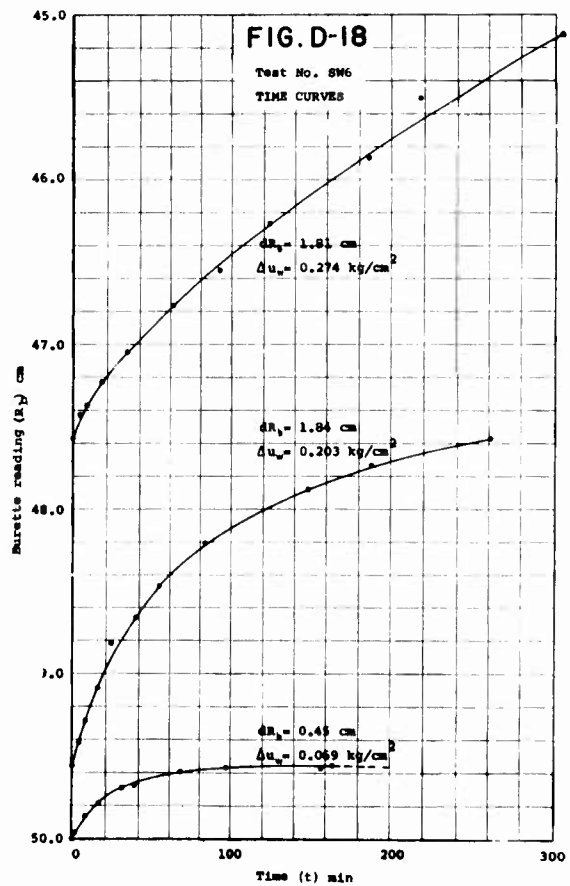
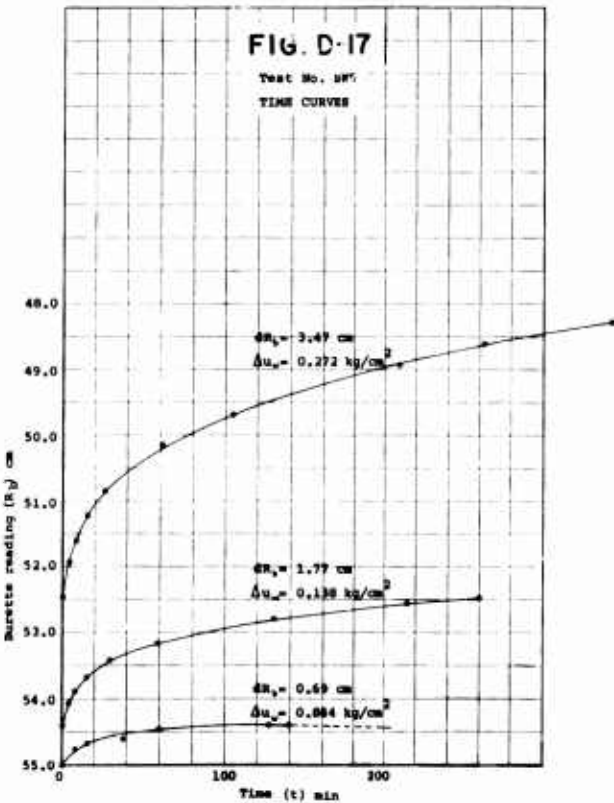
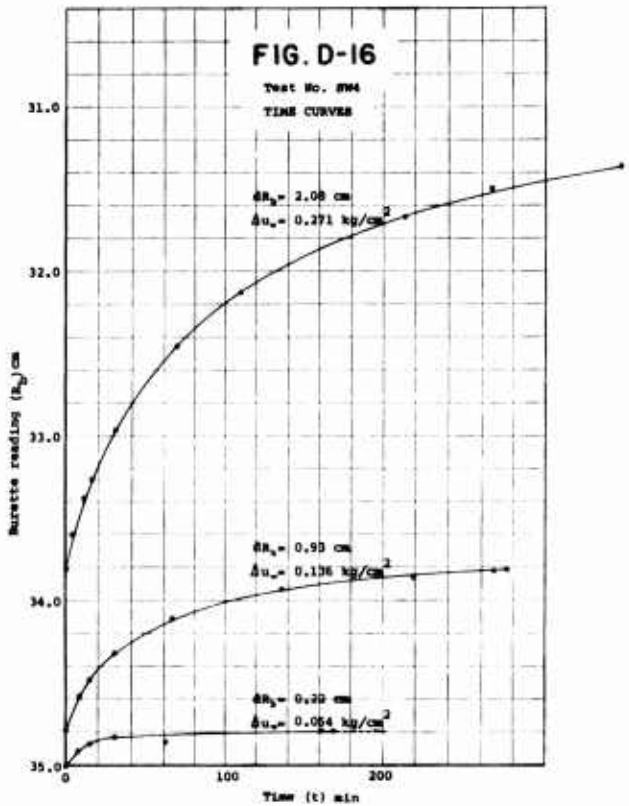
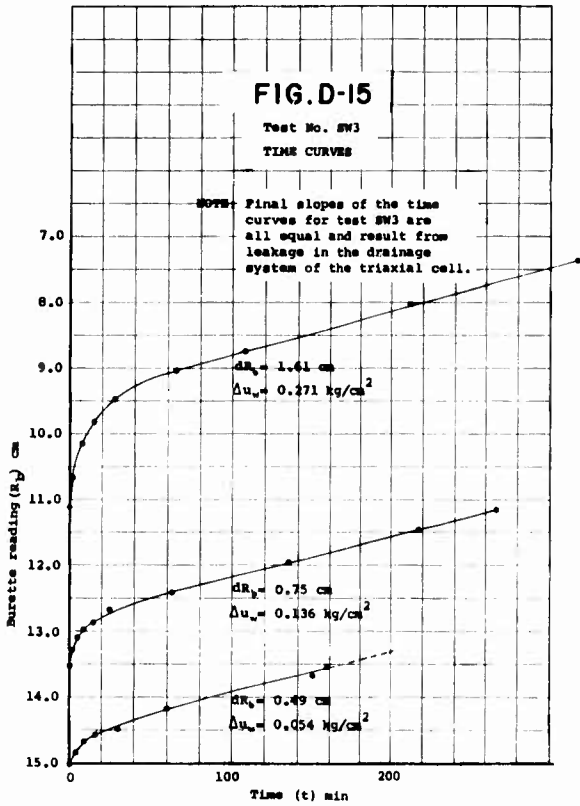


FIG. D-20

Test No. SW8  
TIME CURVES  
to 18.05 cm  
at 780 min.

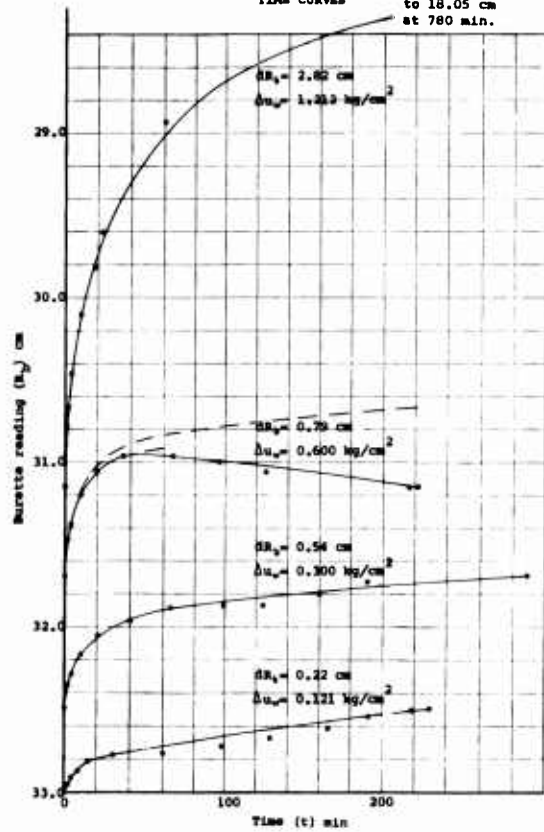
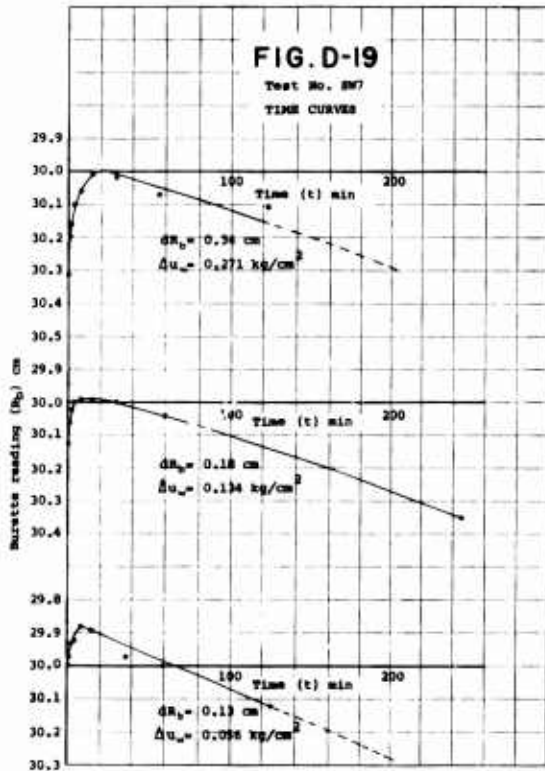


FIG. D-21

Test No. SW9  
TIME CURVES

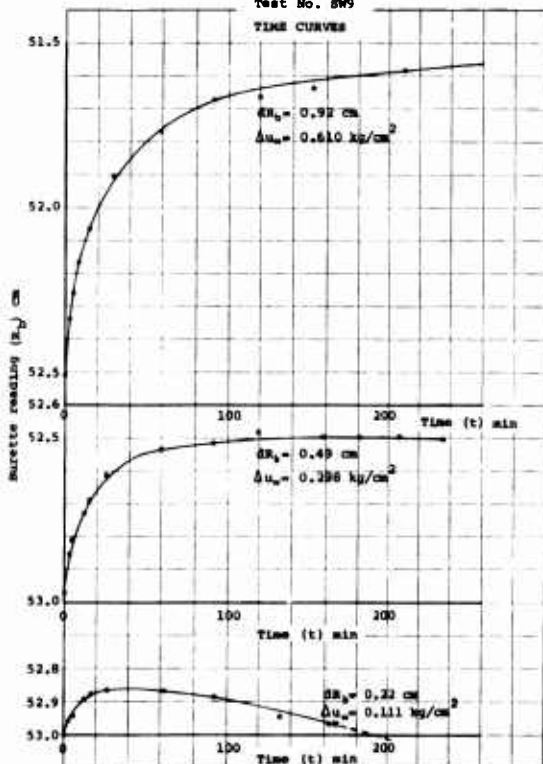
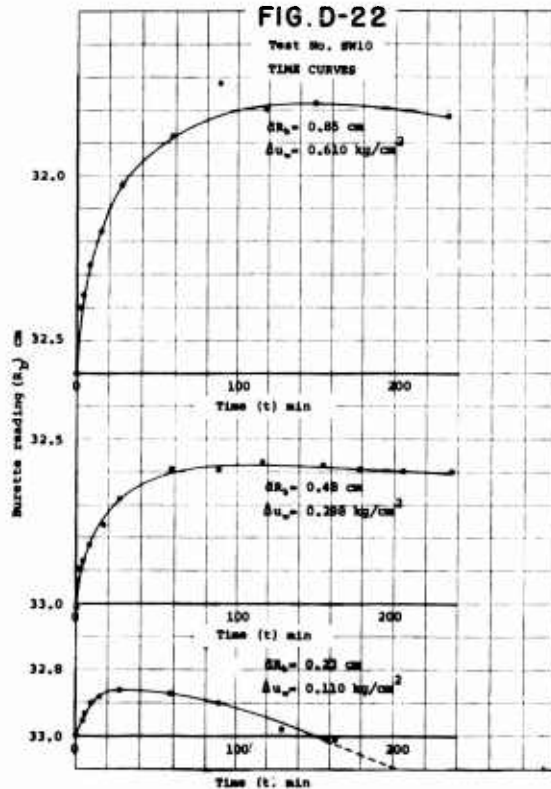
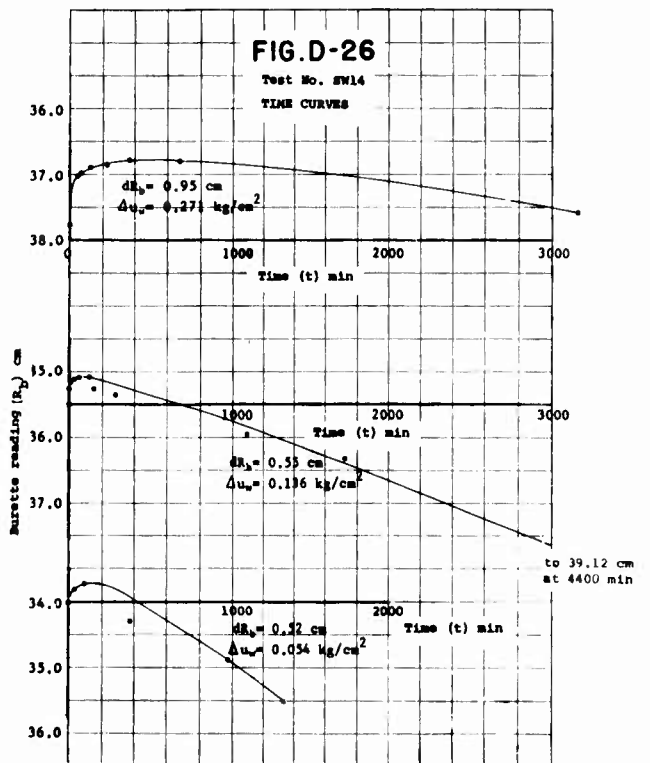
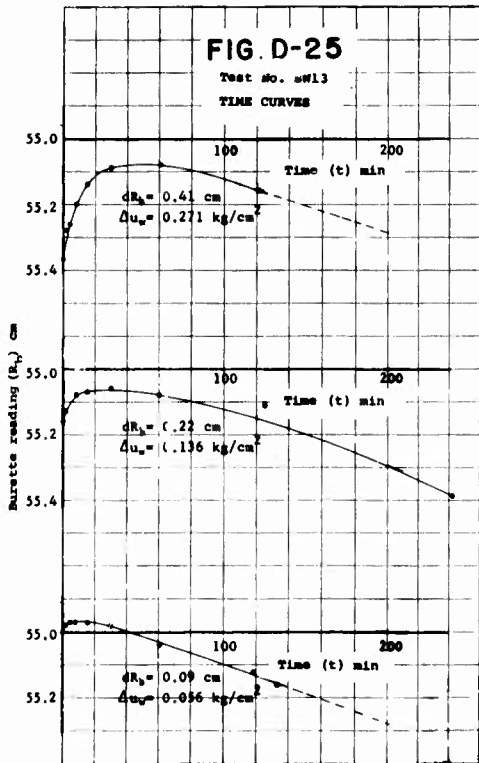
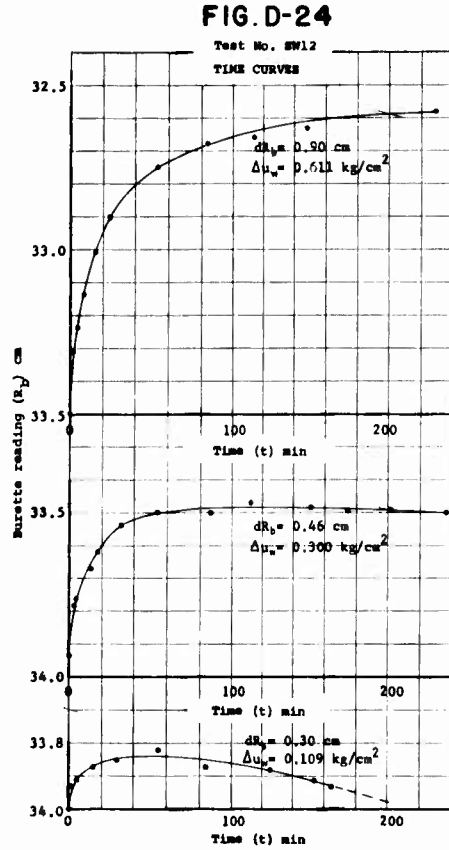
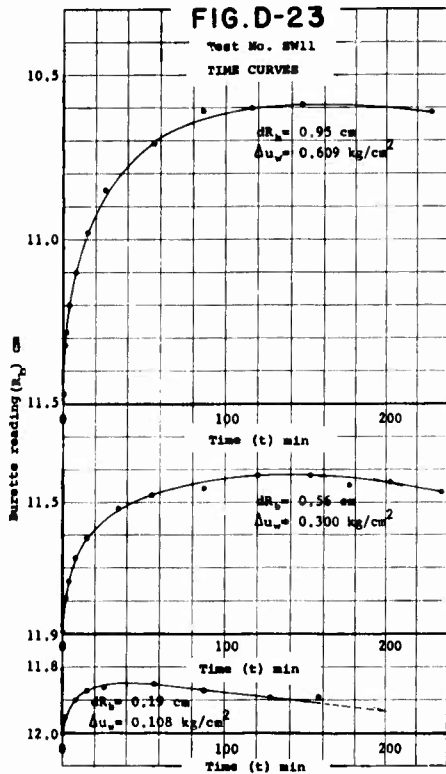
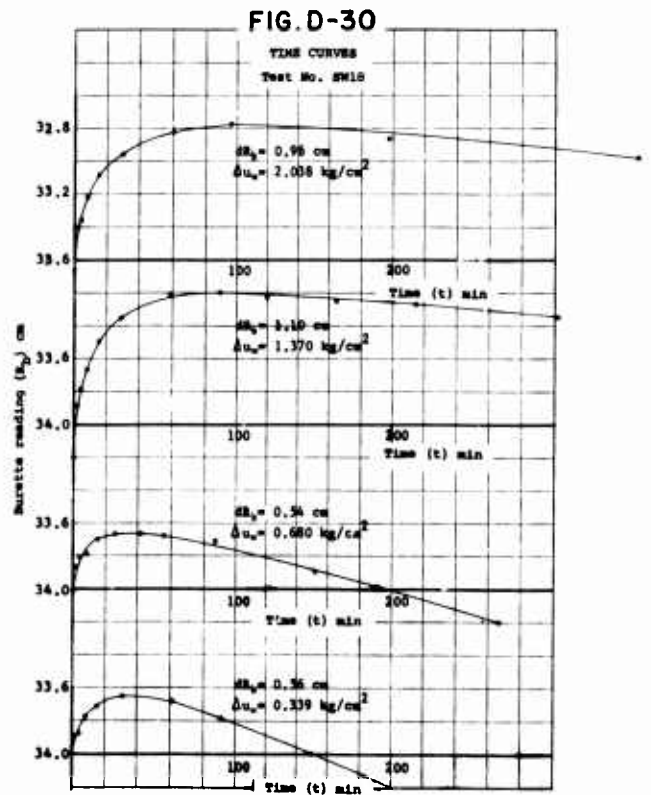
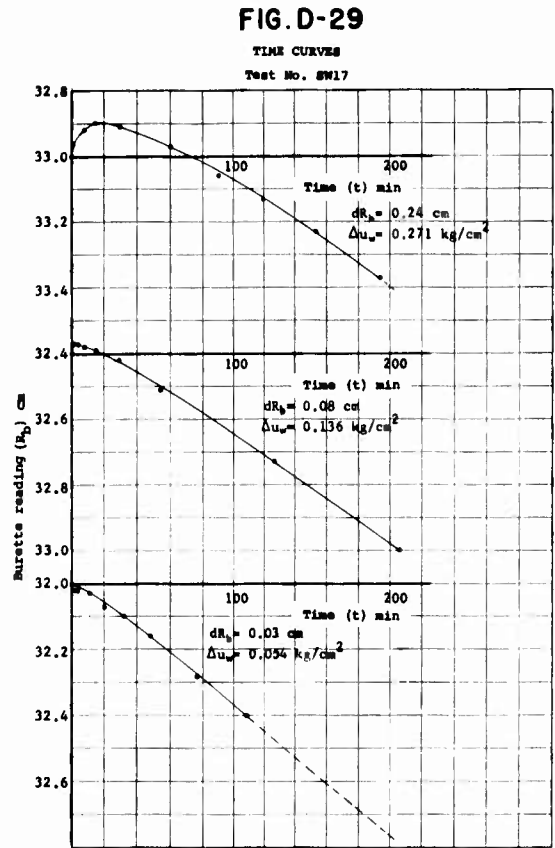
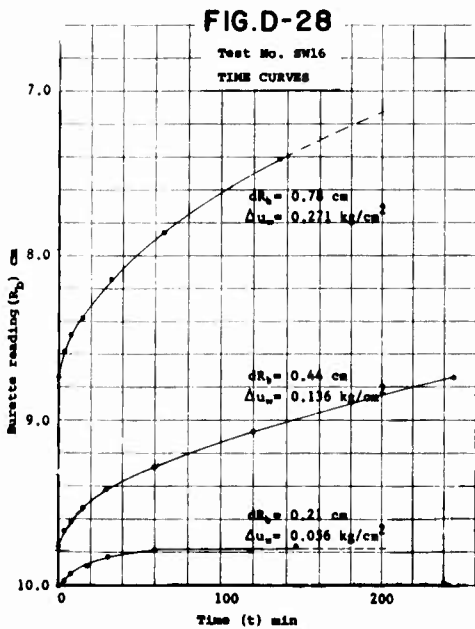
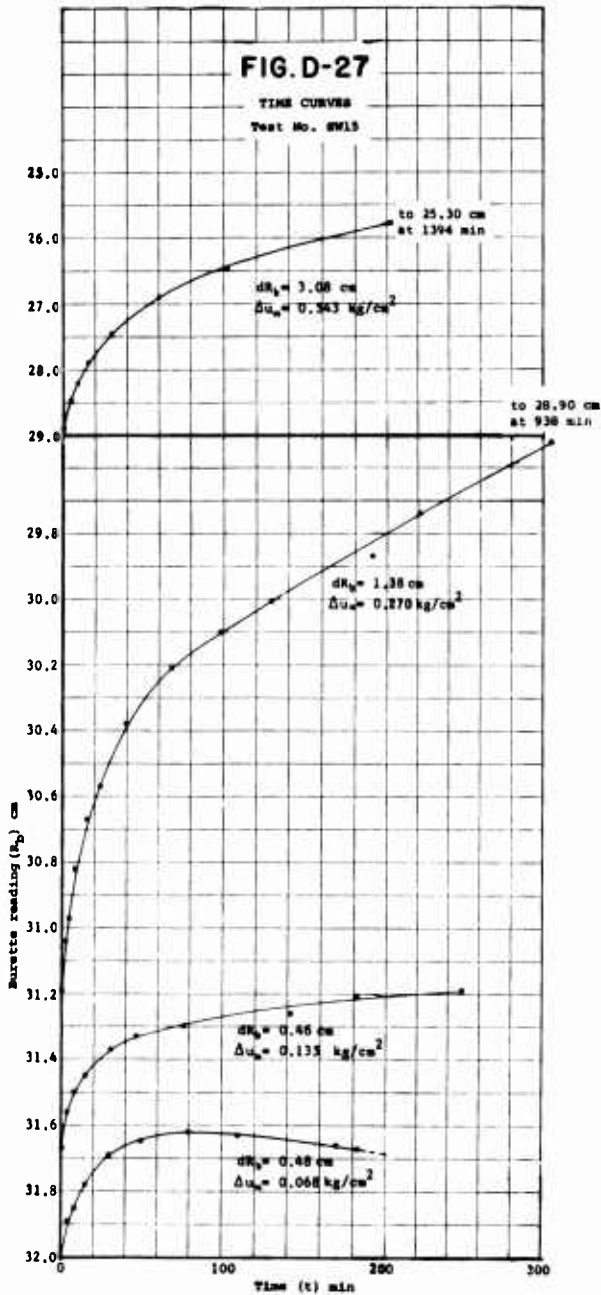


FIG. D-22

Test No. SW10  
TIME CURVES







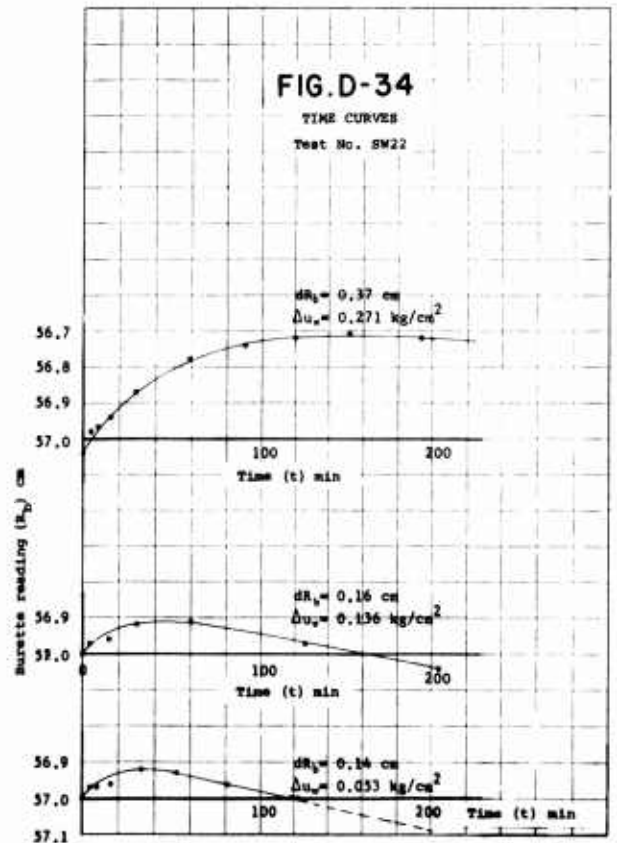
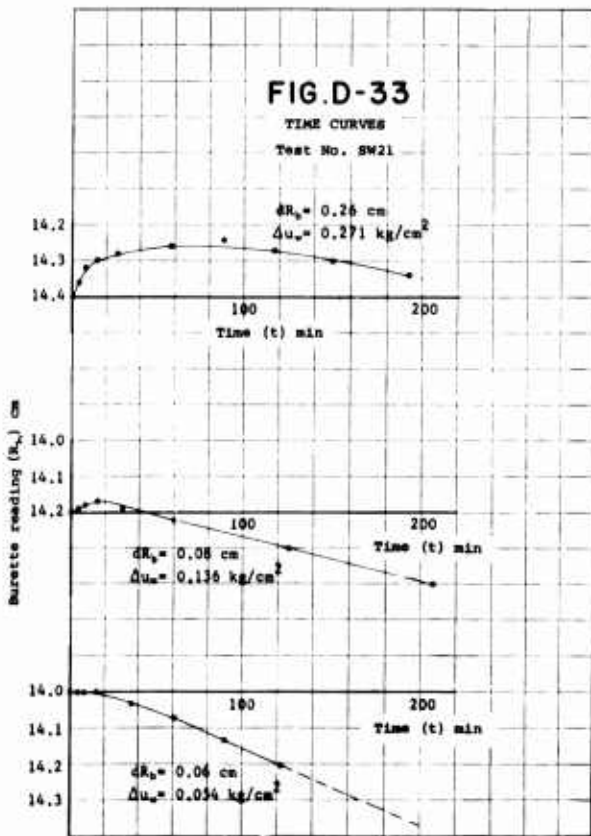
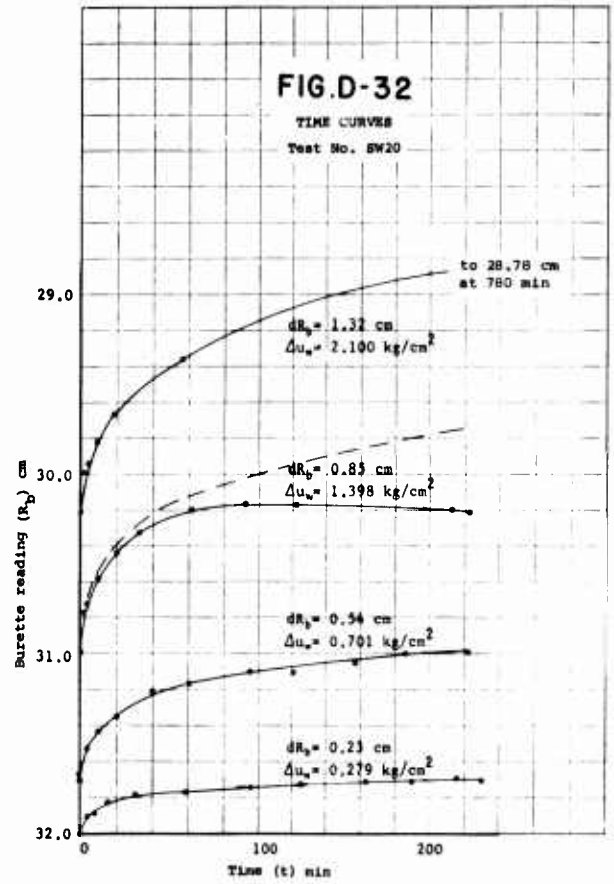
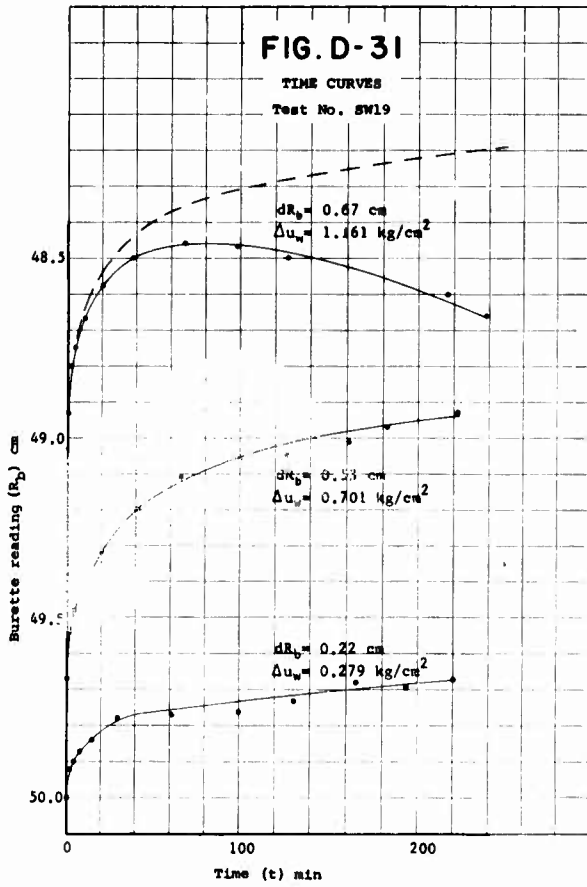


FIG. D-35

TIME CURVES  
Test No. SW23

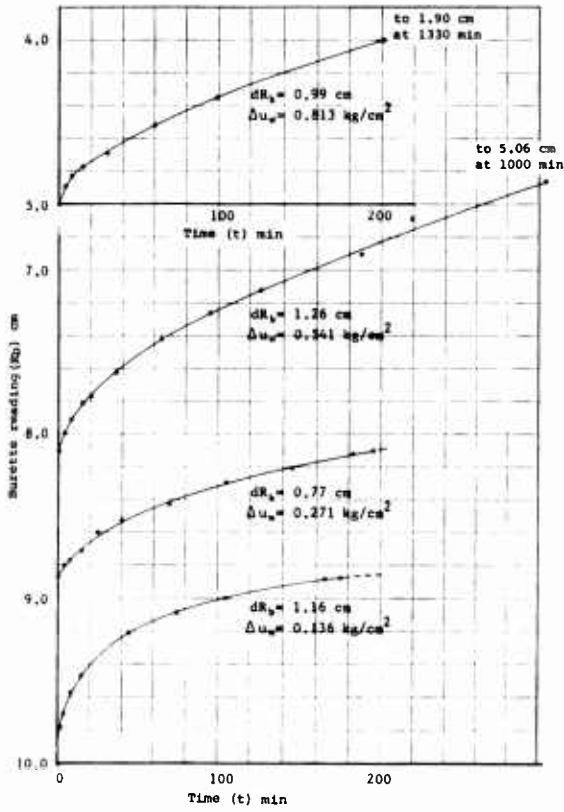


FIG. D-36

TIME CURVES  
Test No. SW24

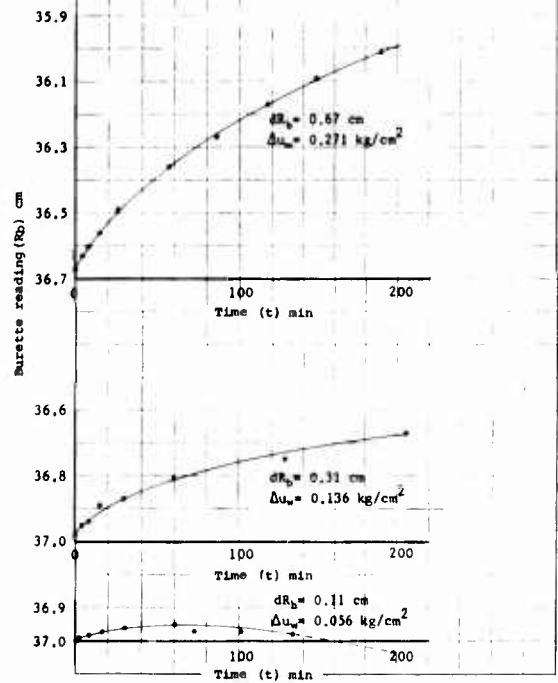


FIG. D-37

SWELLING CURVES FOR TESTS  
IN WHICH  $\bar{\sigma}_3 = 2 \text{ kg/cm}^2$

CANYON DAM CLAY

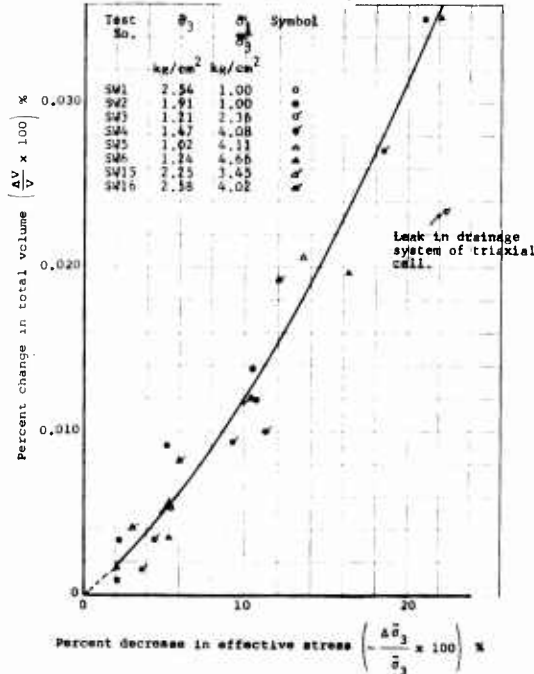


FIG. D-38

SWELLING CURVES FOR TESTS  
IN WHICH  $\bar{\sigma}_3 = 6 \text{ kg/cm}^2$

CANYON DAM CLAY

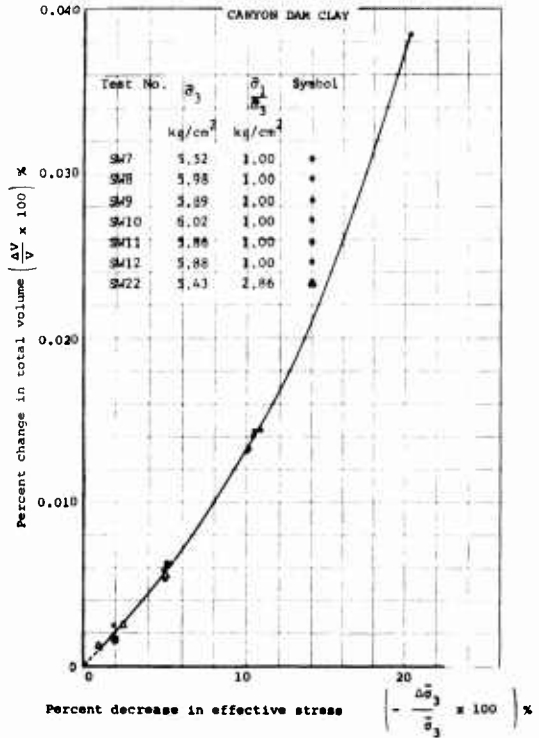


FIG.D-39

SWELLING CURVES FOR TESTS  
IN WHICH  $\bar{\sigma}_3 = 14 \text{ kg/cm}^2$

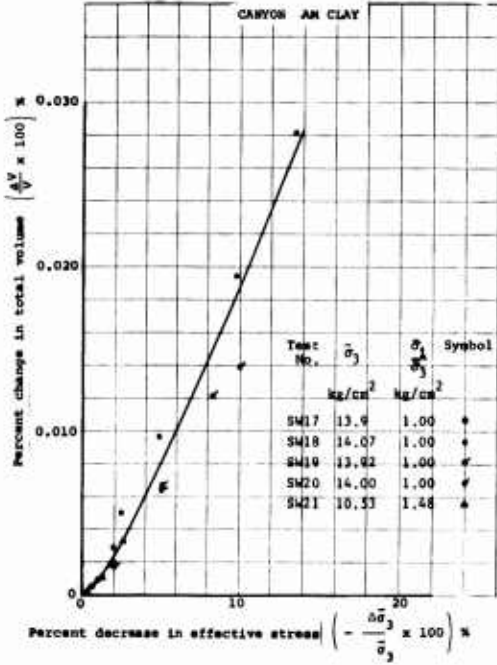


FIG.D-42

AVERAGE INITIAL SWELLING RATIO VERSUS  
EFFECTIVE PRINCIPAL STRESS RATIO  
FOR CANYON DAM CLAY

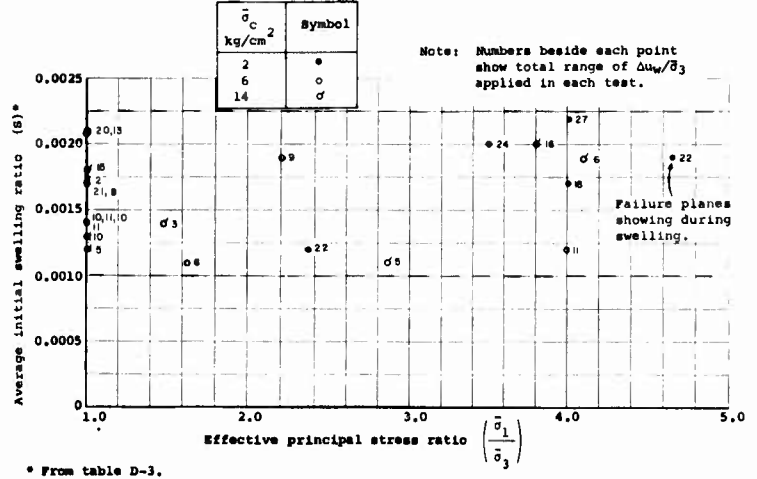


FIG.D-40

SUMMARY OF SWELLING CURVES  
CANYON DAM CLAY

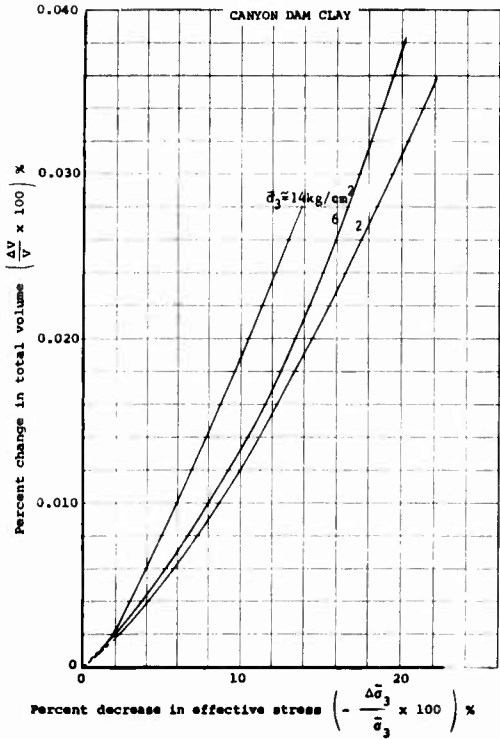


FIG.D-41

SEMI-LOGARITHMIC PLOT OF  
COMPRESSION AND SWELLING CURVES  
FOR CANYON DAM CLAY

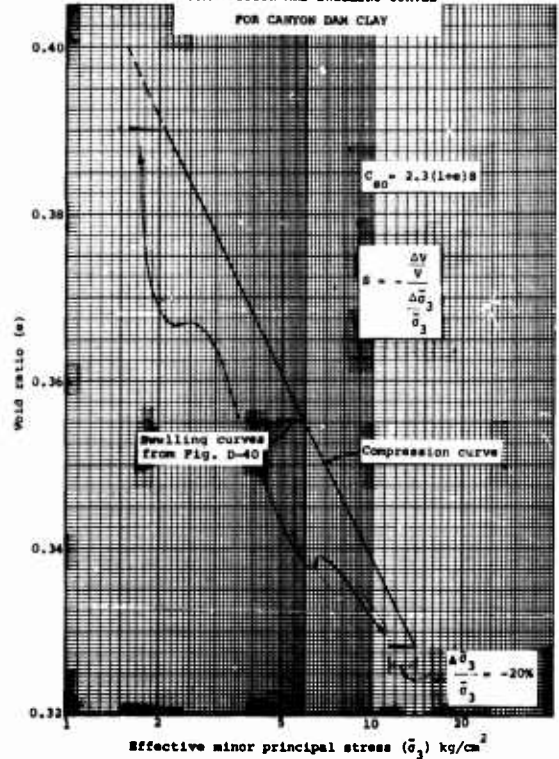


FIG. E-1

TEST W1  
CHANGE IN BURETTE READING VS TIME  
Natural Rubber - Water Soaked  
 $\Delta p = 6.0 \text{ kg/cm}^2$   $L = 0.0057 \text{ cm}$

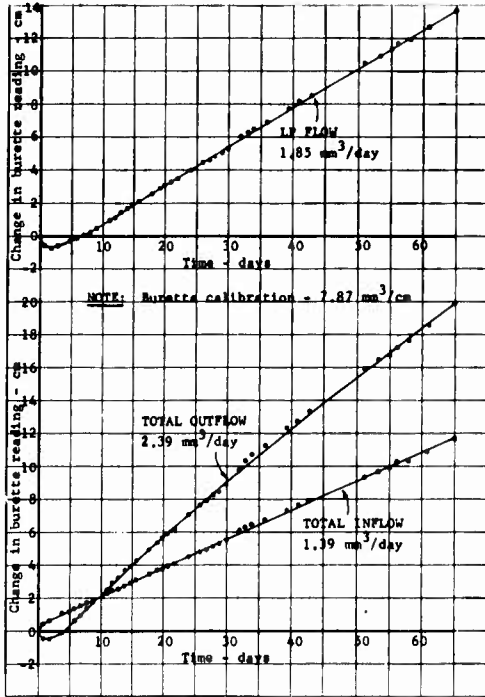


FIG. E-2

TEST W2  
CHANGE IN BURETTE READING VS TIME  
Natural Rubber - Water Soaked  
 $\Delta p = 6.0 \text{ kg/cm}^2$   $L = 0.0071 \text{ cm}$

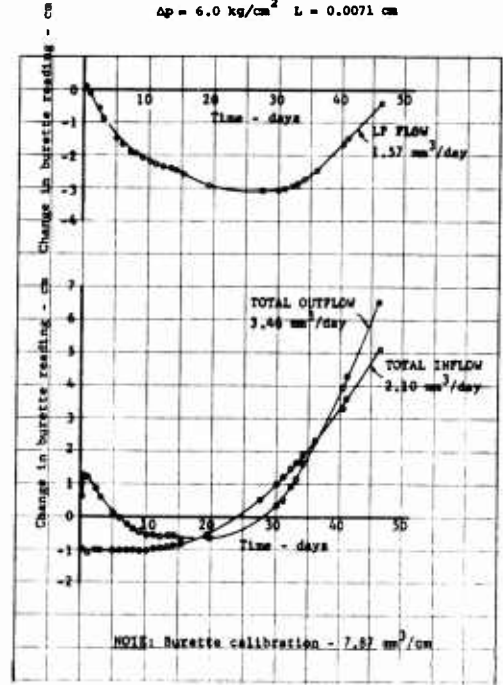


FIG. E-3

TEST W3  
CHANGE IN BURETTE READING VS TIME  
Natural Rubber - Water Soaked  
 $\Delta p = 2.0 \text{ kg/cm}^2$   $L = 0.0064 \text{ cm}$

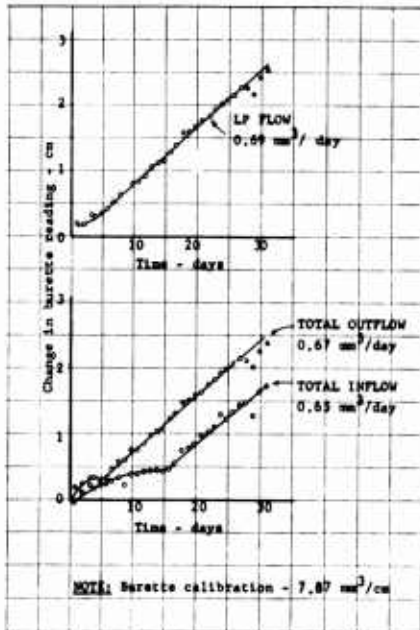


FIG. E-4

TEST W4  
CHANGE IN BURETTE READING VS TIME  
Natural Rubber - Oil Soaked  
 $\Delta p = 2.0 \text{ kg/cm}^2$   $L = 0.0064 \text{ cm}$

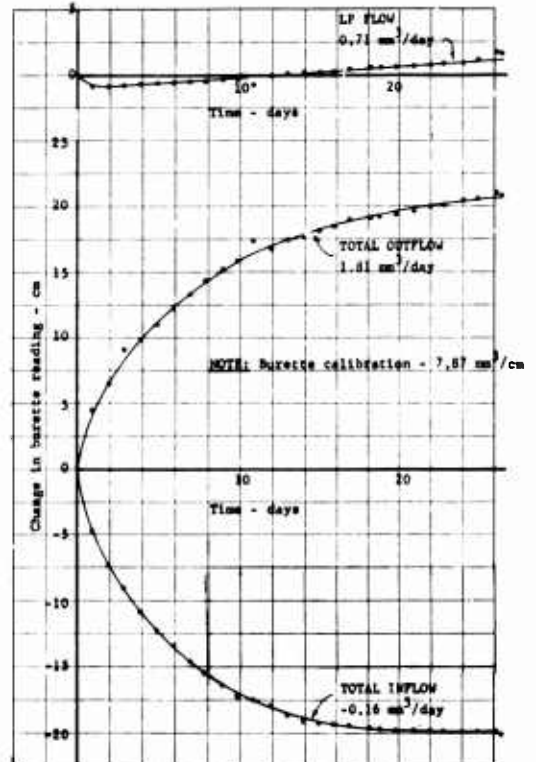


FIG. E-5

TEST W5  
CHANGE IN BURETTE READING VS TIME  
Natural Rubber - Oil Soaked  
 $\Delta p = 1.86 \text{ kg/cm}^2$   $L = 0.0061 \text{ cm}$

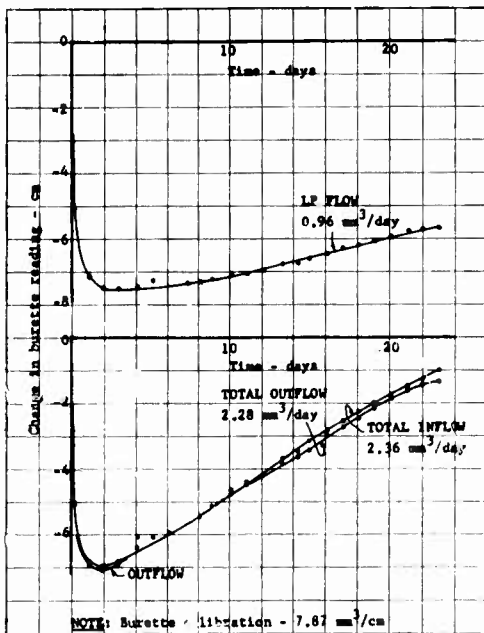


FIG. E-6

TEST W6  
CHANGE IN BURETTE READING VS TIME  
Natural Rubber - Water Soaked  
 $\Delta p = 6.0 \text{ kg/cm}^2$   $L = 0.0073 \text{ cm}$

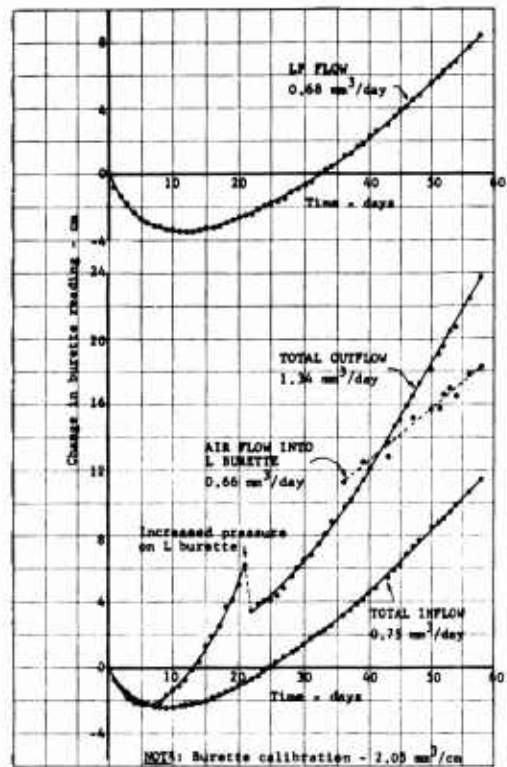


FIG. E-7

TEST W7A  
CHANGE IN BURETTE READING VS TIME  
Natural Rubber - Water Soaked  
 $\Delta p = 11.5 \text{ kg/cm}^2$   $L = 0.0061 \text{ cm}$

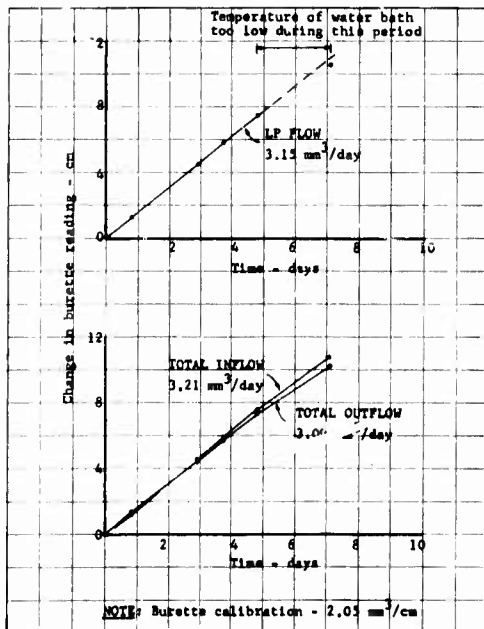


FIG. E-8

TEST W7B  
CHANGE IN BURETTE READING VS TIME  
Natural Rubber - Water Soaked  
 $\Delta p = 6.0 \text{ kg/cm}^2$   $L = 0.0061 \text{ cm}$

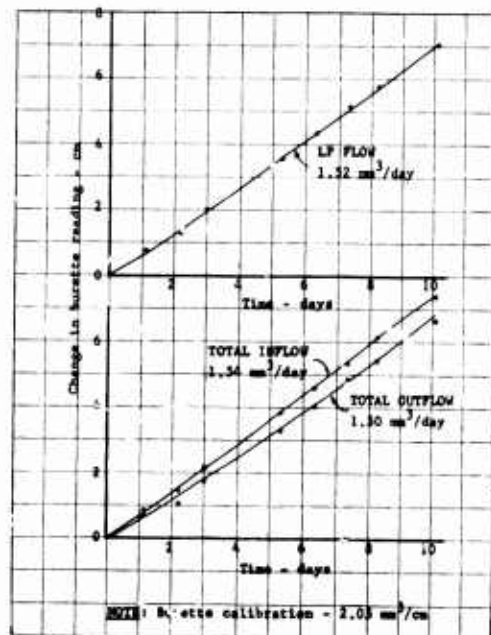


FIG. E-9

TEST W7c  
CHANGE IN BURETTE READINGS VS TIME  
Natural Rubber - Water Soaked  
 $\Delta p = 2.0 \text{ kg/cm}^2$   $L = 0.0061 \text{ cm}$

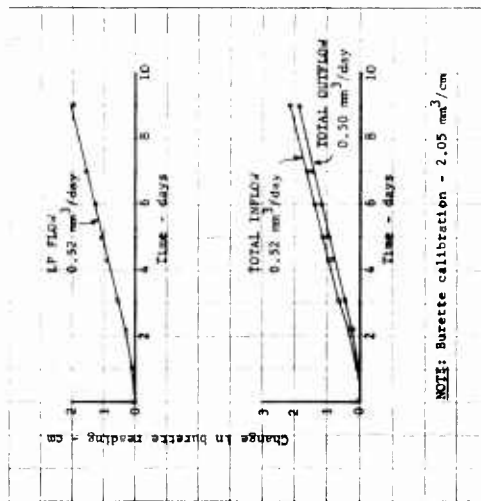


FIG. E-10

TEST W7d  
CHANGE IN BURETTE READINGS VS TIME  
Natural Rubber - Water Soaked  
 $\Delta p = 11.5 \text{ kg/cm}^2$   $L = 0.0061 \text{ cm}$

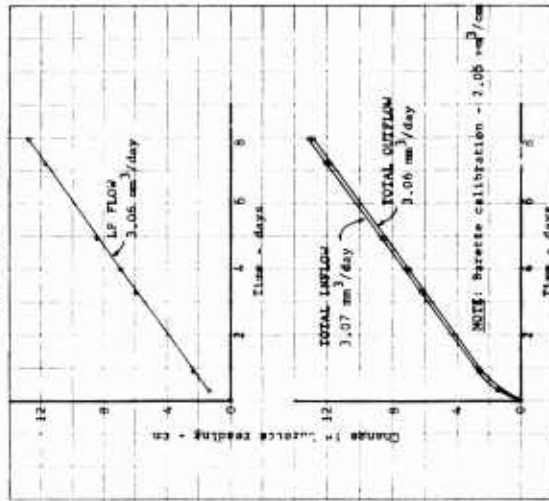


FIG. E-12

TEST VI  
VOLUME FLOW VERSUS TIME  
Natural Rubber - Schmid  
No treatment  $L = 0.0062 \text{ cm}$

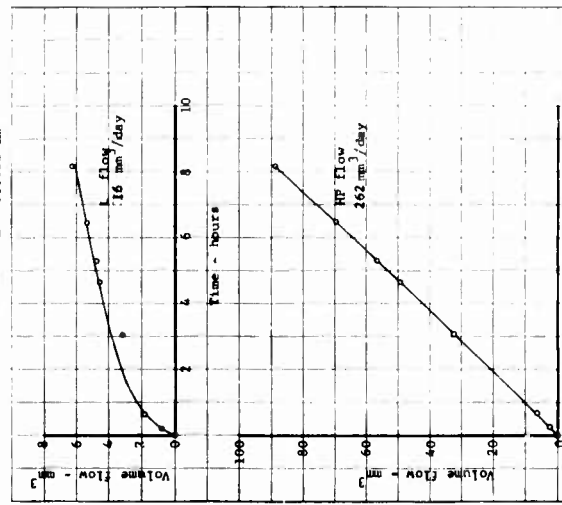


FIG. E-11

TEST W8  
CHANGE IN BURETTE READINGS VS TIME  
Natural Rubber - Water Soaked  
 $\Delta p = 2.0 \text{ kg/cm}^2$   $L = 0.0067 \text{ cm}$

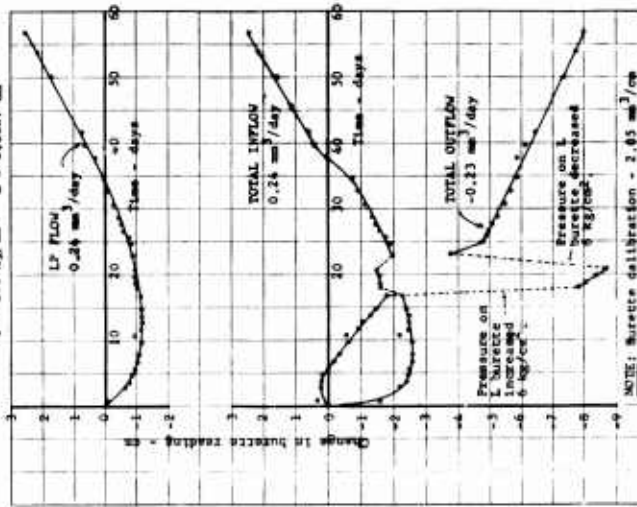


FIG. E-13

TEST V2  
VOLUME FLOW VS TIME  
Natural Rubber - Schmid  
No treatment  $L = 0.0056 \text{ cm}$

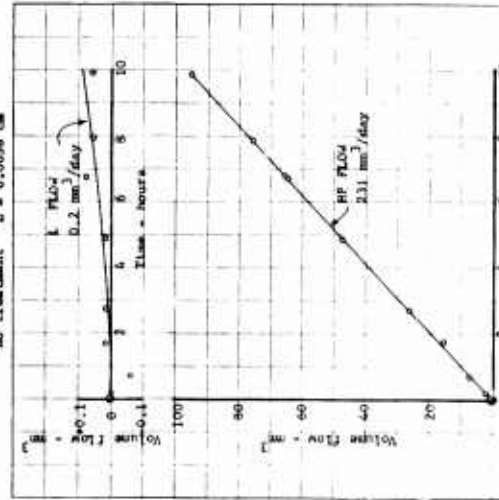


FIG. E-14

TEST V3  
VOLUME FLOW VS TIME  
Natural Rubber - Schmid  
No treatment  $L = 0.0062 \text{ cm}$

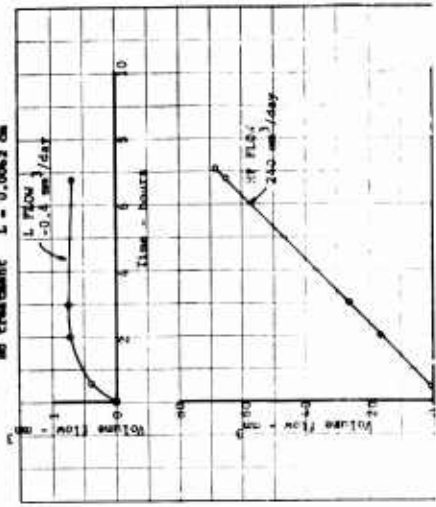


FIG. E-15

TEST VA  
VOLUME FLOW VS TIME  
Natural Rubber - Schmidt  
No treatment L = 0.0119 cm

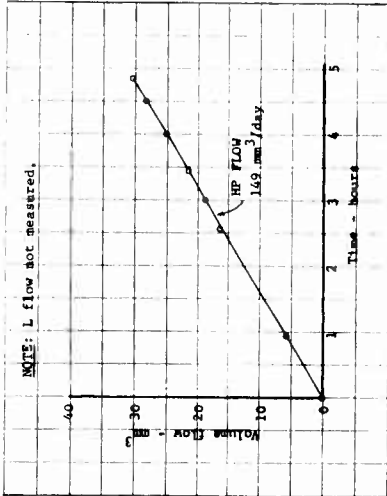


FIG. E-16

TEST VS  
VOLUME FLOW VS TIME  
Natural Rubber - Schmidt  
No treatment L = 0.0234 cm

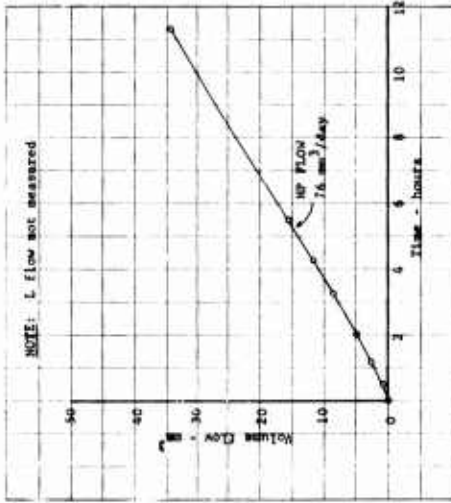


FIG. E-17

TEST VS  
VOLUME FLOW VS TIME  
Natural Rubber - Schmidt  
Water soaked L = 0.0073 cm

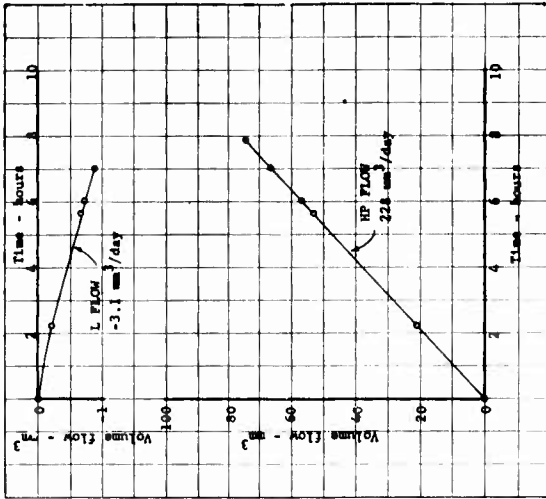


FIG. E-18

TEST V7  
VOLUME FLOW VS TIME  
Natural Rubber - Schmidt  
Water Soaked L = 0.0061 cm

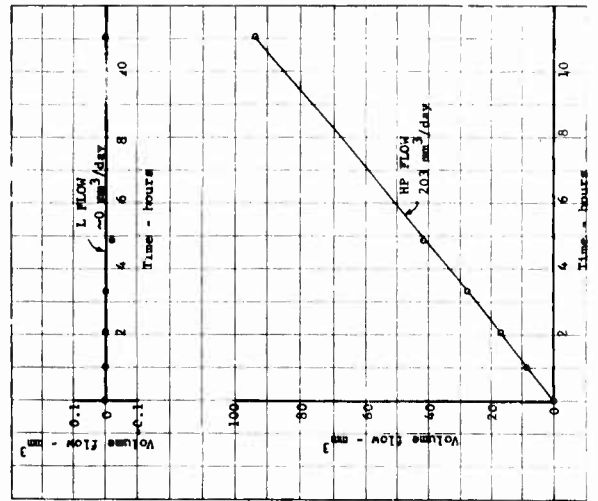


FIG. E-19

TEST VS  
VOLUME FLOW VS TIME  
Natural Rubber - Schmidt  
Silicone oil soaked L = 0.0058 cm

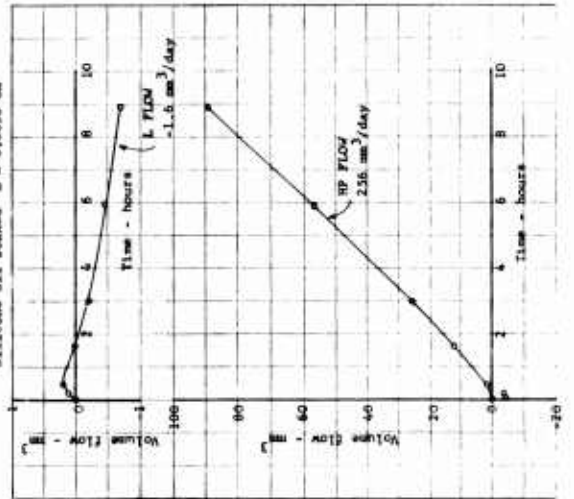
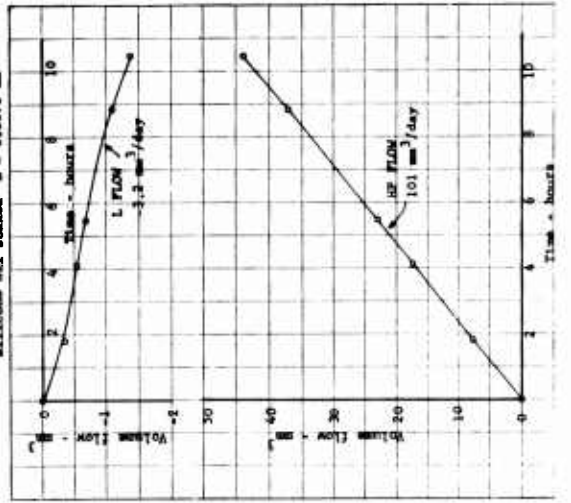


FIG. E-20

TEST V9  
VOLUME FLOW VS TIME  
Natural Rubber - Schmidt  
Silicone oil soaked L = 0.0070 cm



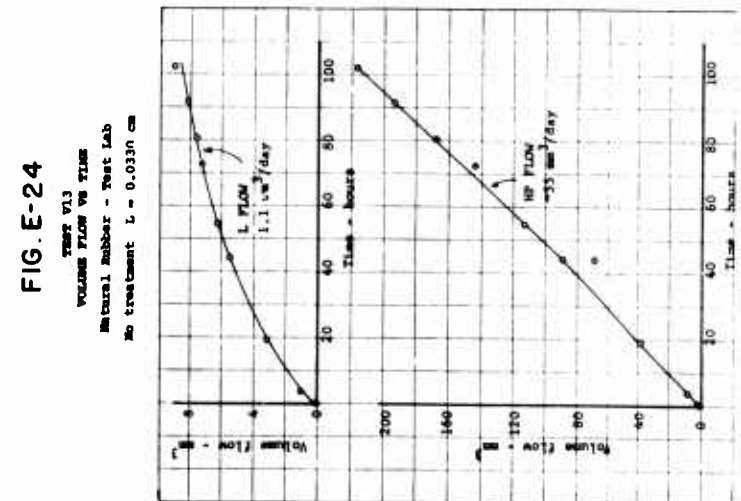
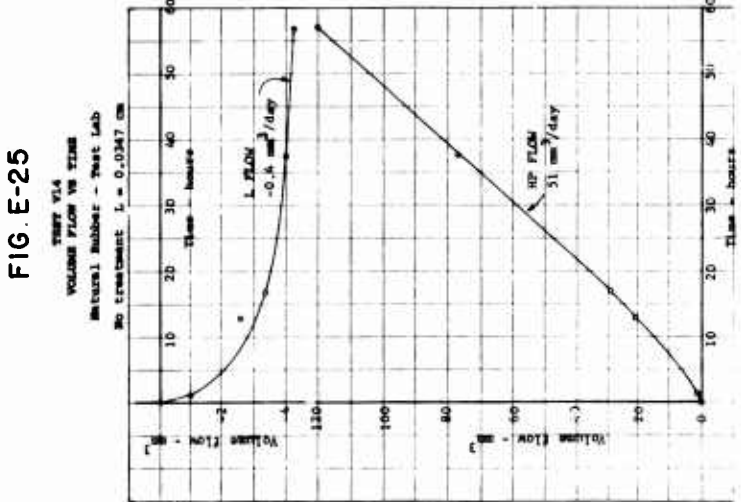
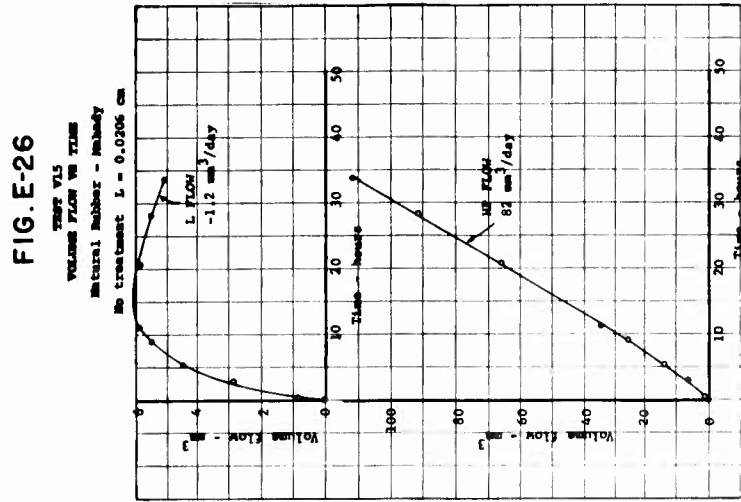
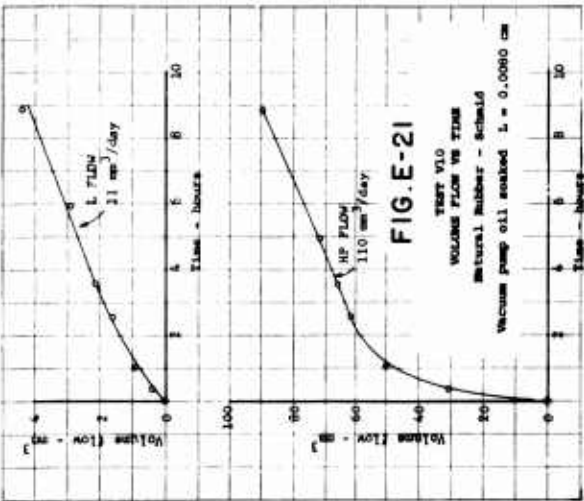
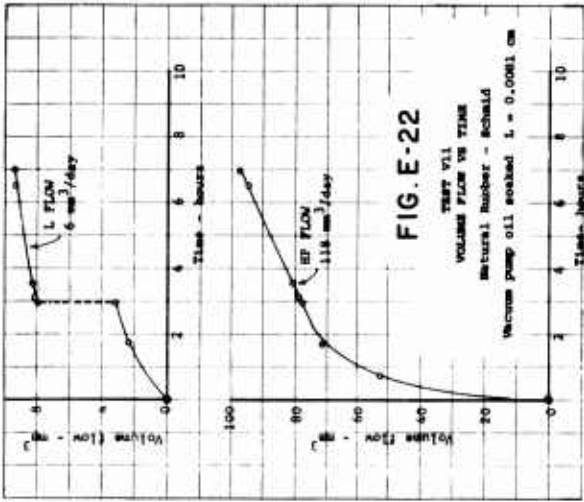
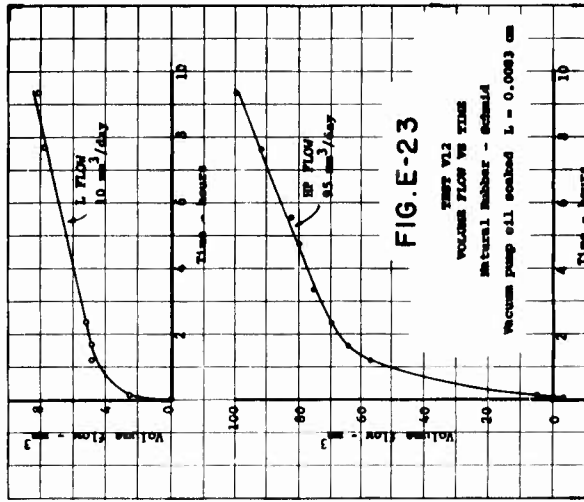


FIG. E-29

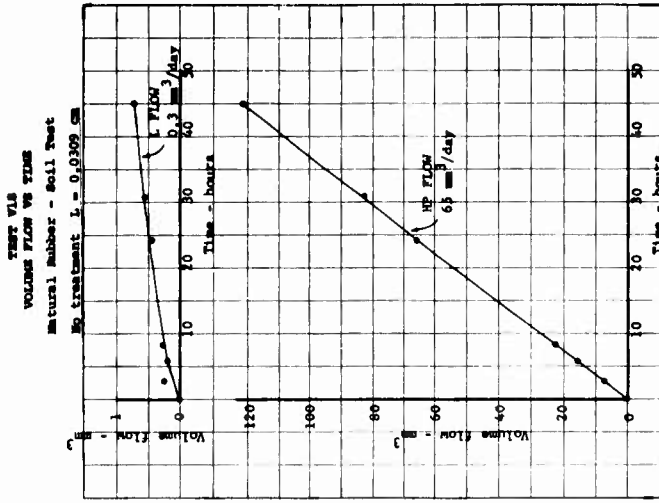


FIG. E-28

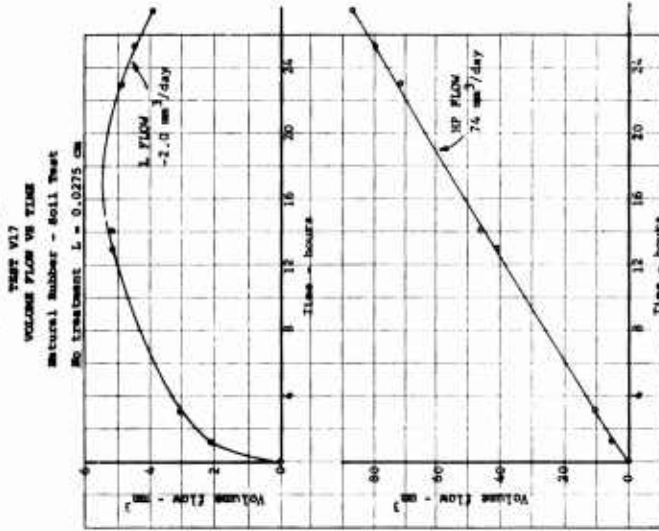


FIG. E-27

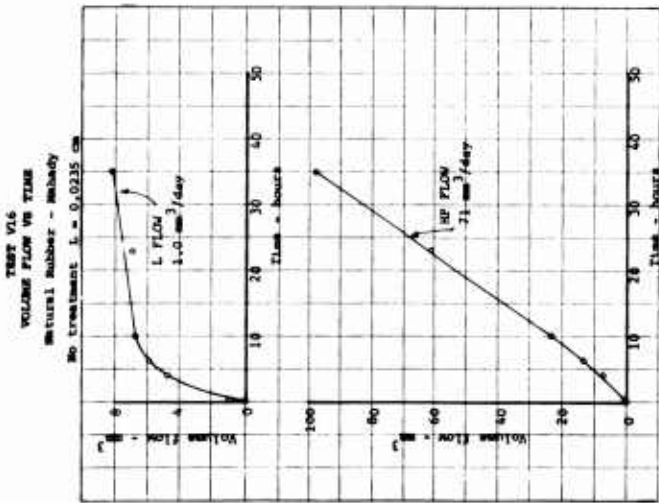


FIG. E-32

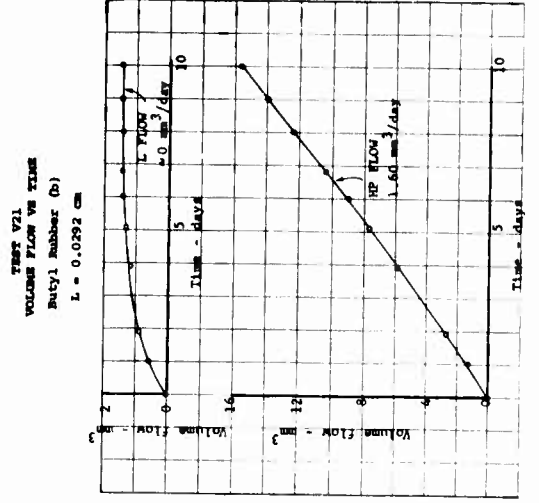


FIG. E-31

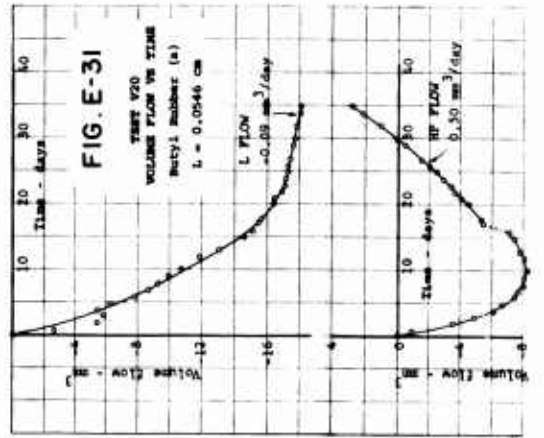


FIG. E-30

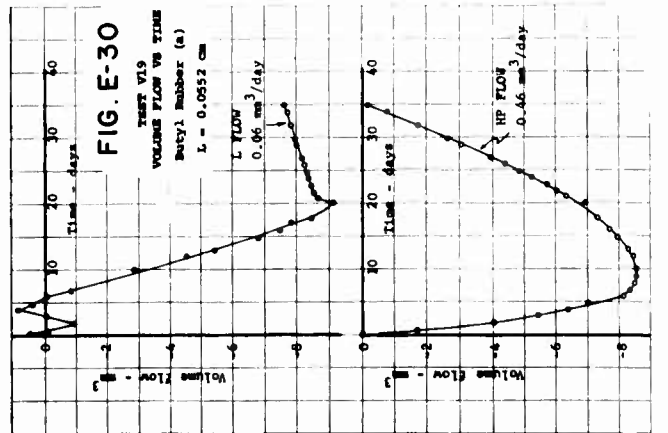


FIG. E-35

TEST V24  
VOLUME FLOW VS TIME  
Butyl Rubber (b)  
L = 0.0208 cm

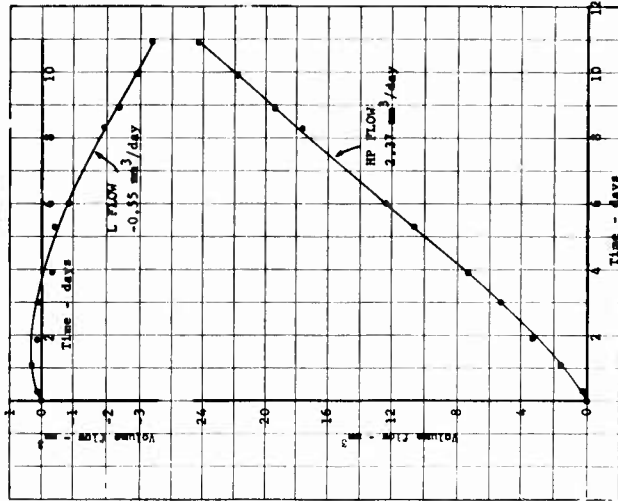


FIG. E-34

TEST V23  
VOLUME FLOW VS TIME  
Butyl Rubber (c)  
L = 0.0212 cm

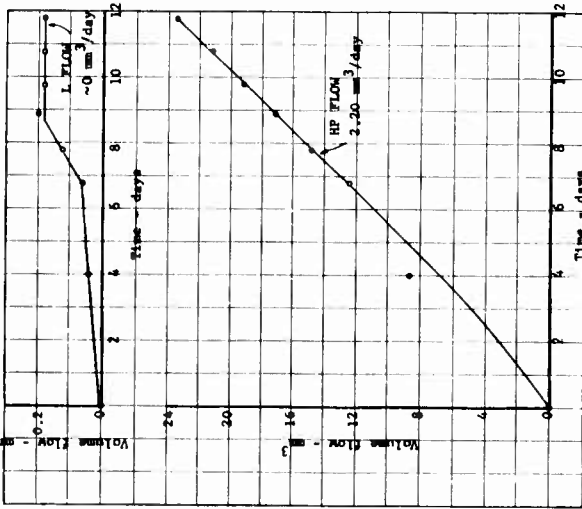


FIG. E-33

TEST V22  
VOLUME FLOW VS TIME  
Butyl Rubber (b)  
L = 0.0289 cm

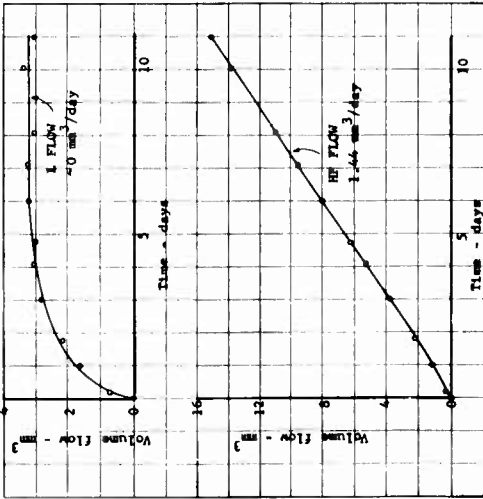


FIG. E-37

TEST V26  
VOLUME FLOW VS TIME  
SAL-P  
L = 0.0032 cm

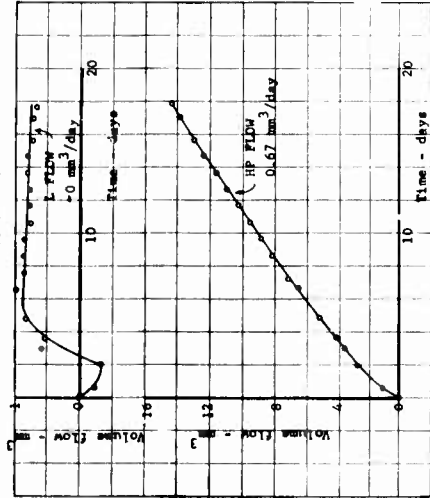


FIG. E-36

TEST V25  
VOLUME FLOW VS TIME  
Fluorel  
L = 0.0258 cm

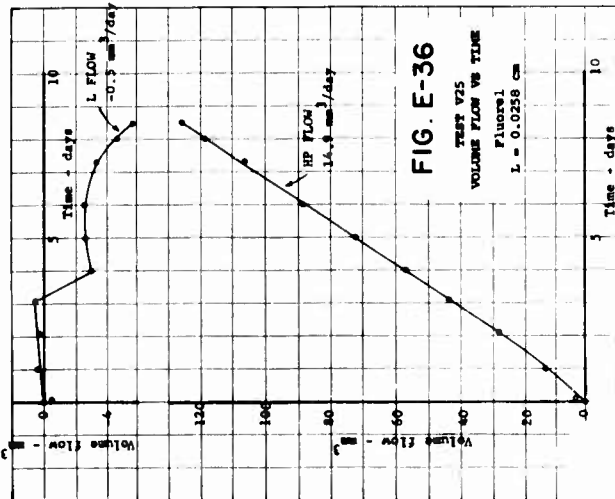
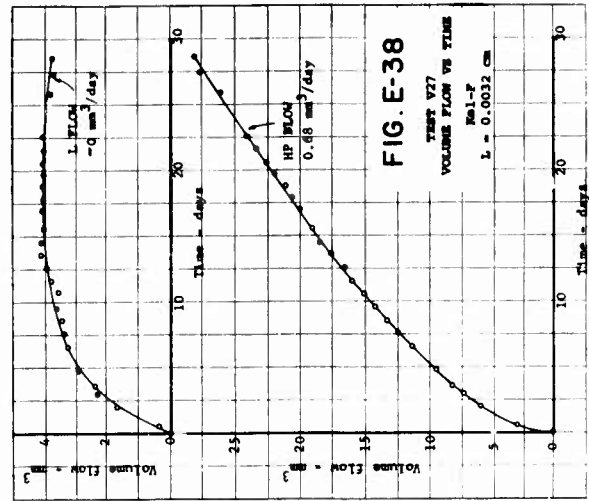


FIG. E-38

TEST V27  
VOLUME FLOW VS TIME  
SAL-P  
L = 0.0032 cm



**FIG. E-39**

TEST V28  
VOLUME FLOW VS TIME  
Korozeel  
L = 0.0100 cm

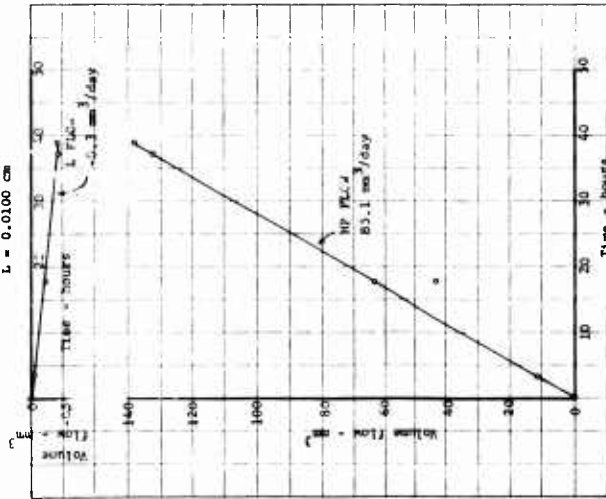


**FIG. E-40**

TEST V29  
VOLUME FLOW VS TIME  
Nynar  
L = 0.0069 cm

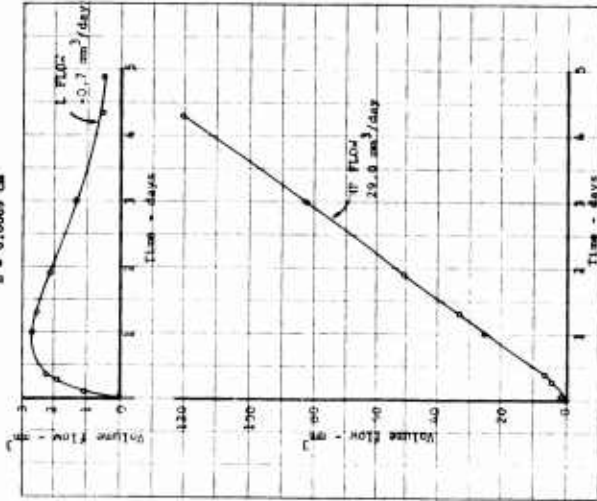


**FIG. E-41**

TEST V30  
VOLUME FLOW VS TIME  
Nynar  
L = 0.0066 cm

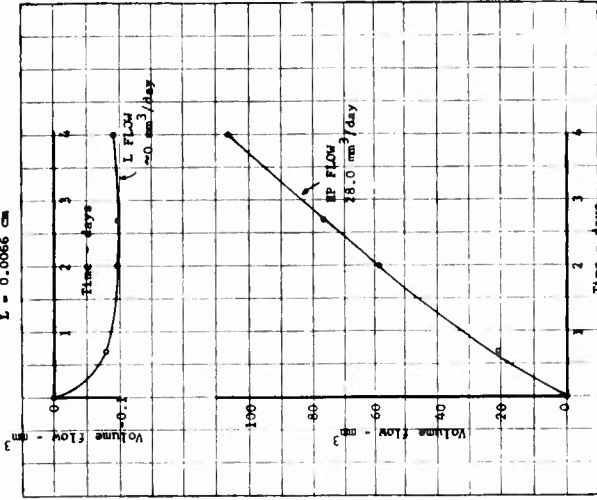


**FIG. E-42**

TEST V31  
VOLUME FLOW VS TIME  
Neoprene Rubber  
L = 0.0140 cm

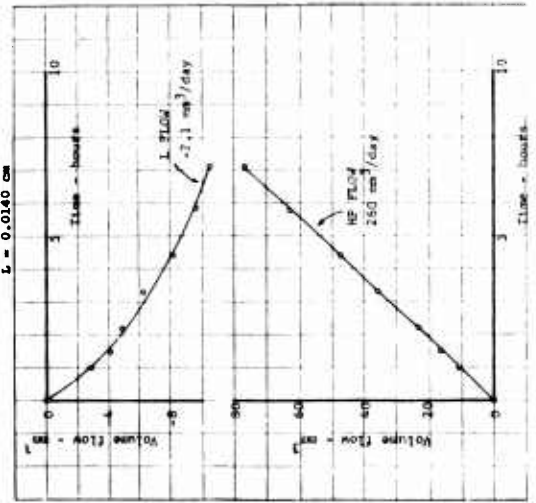


**FIG. E-43**

TEST V32  
VOLUME FLOW VS TIME  
Neoprene Rubber  
L = 0.0135 cm

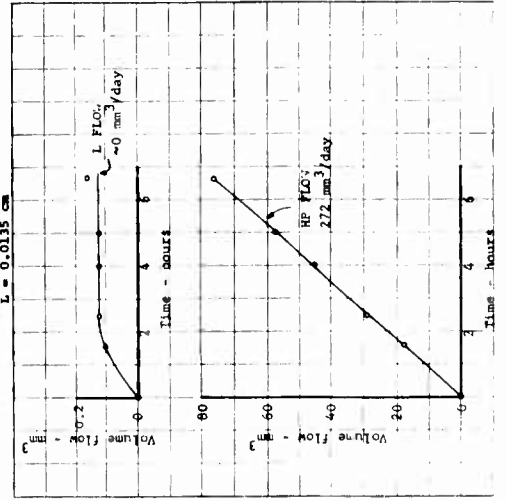


**FIG. E-44**

TEST V33  
VOLUME FLOW VS TIME  
Polychloro (a)  
L = 0.0038 cm

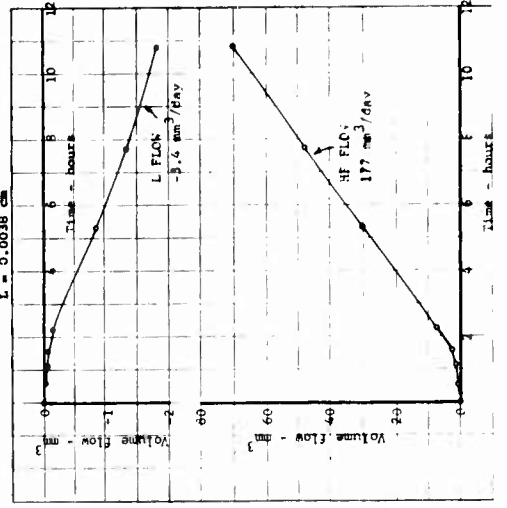


FIG. E-45

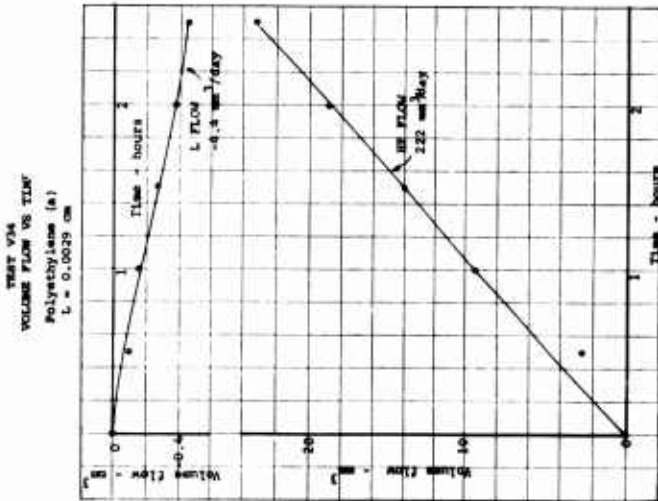


FIG. E-46

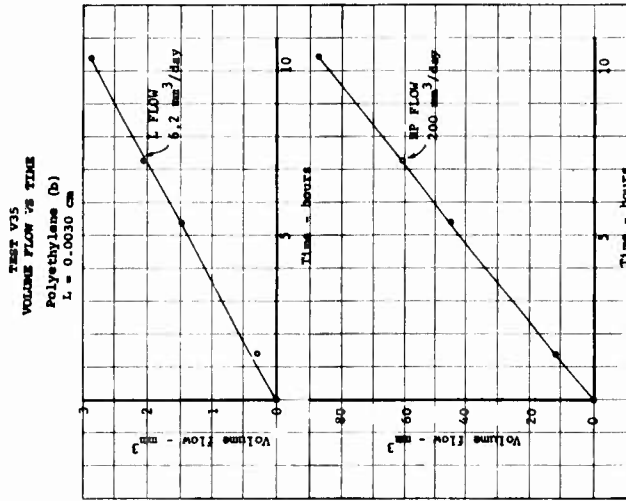


FIG. E-47

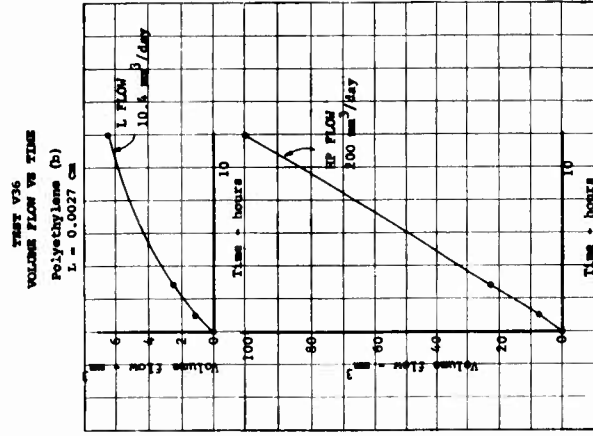


FIG. E-49

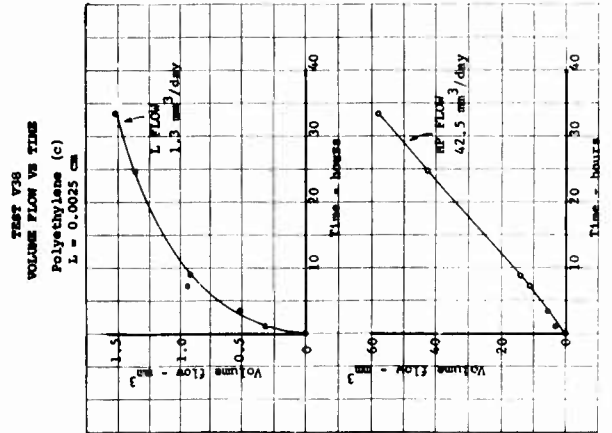


FIG. E-48

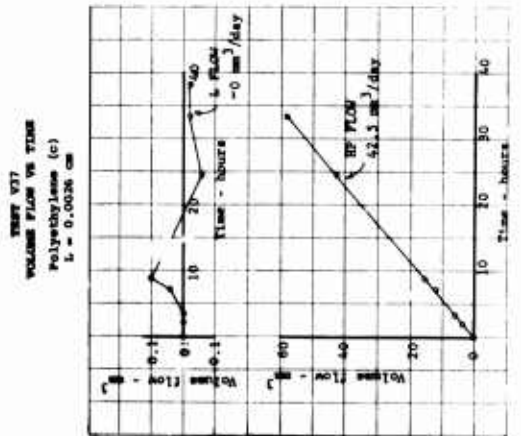


FIG. E-50

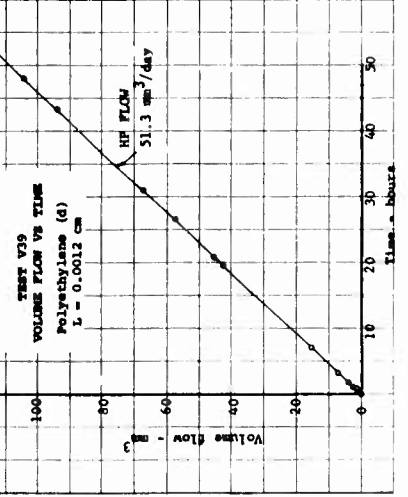


FIG. E-53

TEST W42  
VOLUME FLOW VS TIME  
Polypropylene  
L = 0.0024 cm

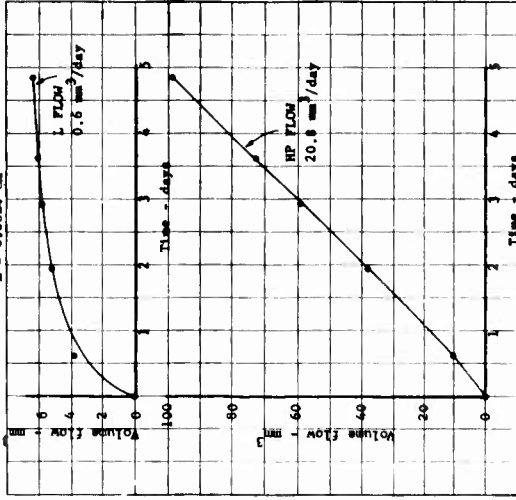


FIG. E-52

TEST W41  
VOLUME FLOW VS TIME  
Polypropylene  
L = 0.0027 cm

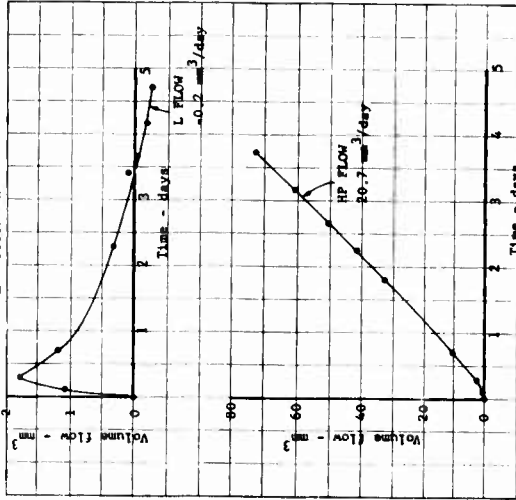


FIG. E-56

TEST W45  
VOLUME FLOW VS TIME  
Teflon  
L = 0.0028 cm

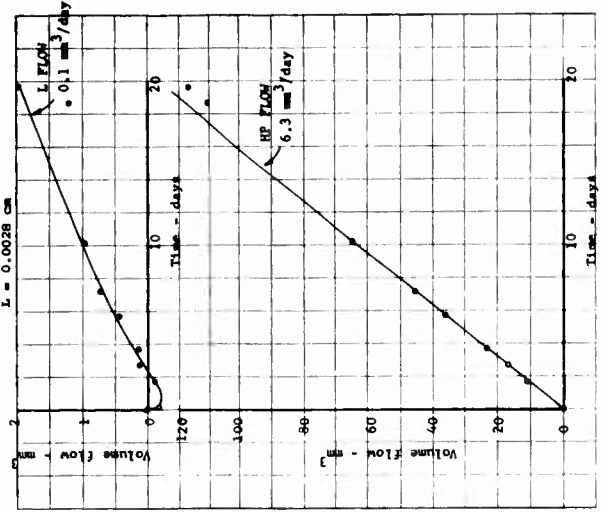


FIG. E-55

TEST W44  
VOLUME FLOW VS TIME  
Polypropylene  
L = 0.0024 cm

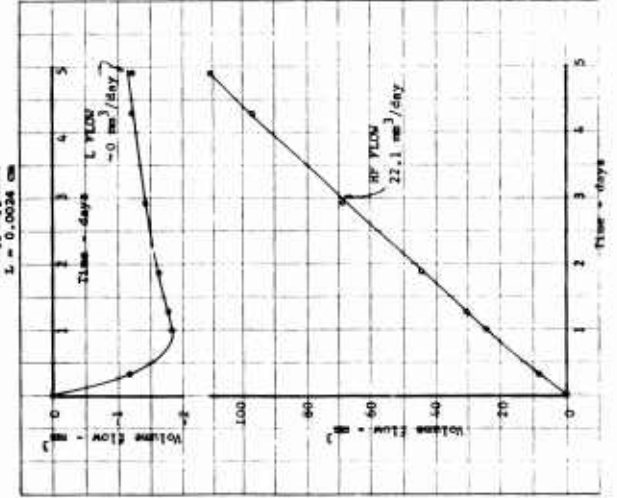


FIG. E-54

TEST W43  
VOLUME FLOW VS TIME  
Polypropylene  
L = 0.0024 cm

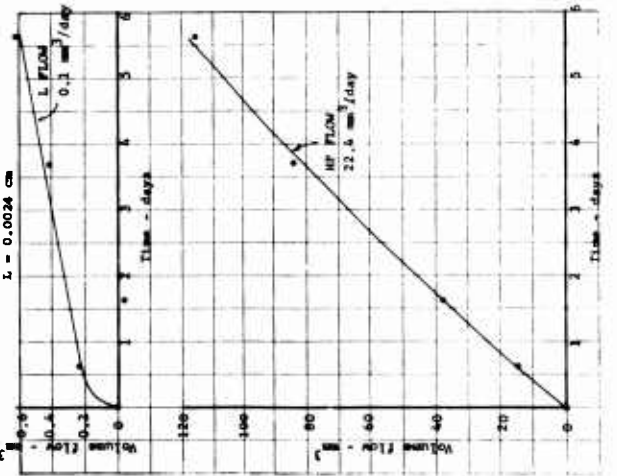


FIG. E-51

TEST W40  
VOLUME FLOW VS TIME  
Polyethylene (8)  
L = 0.0012 cm

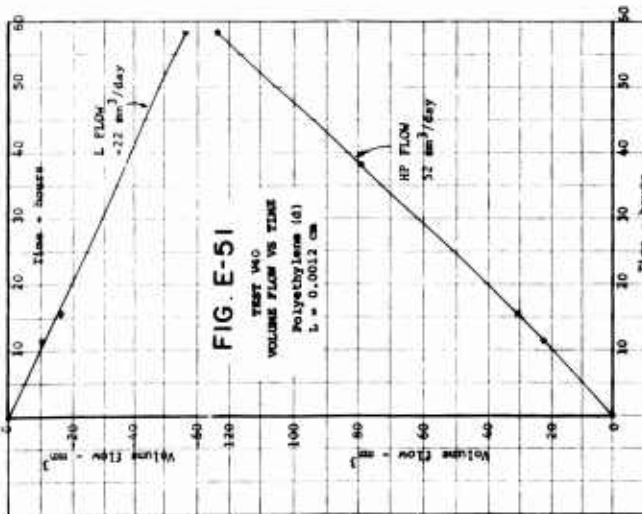


FIG. E-57

TEST V46  
 Teflon  
 L = 0.0028 cm  
 VOLUME FLOW VS TIME

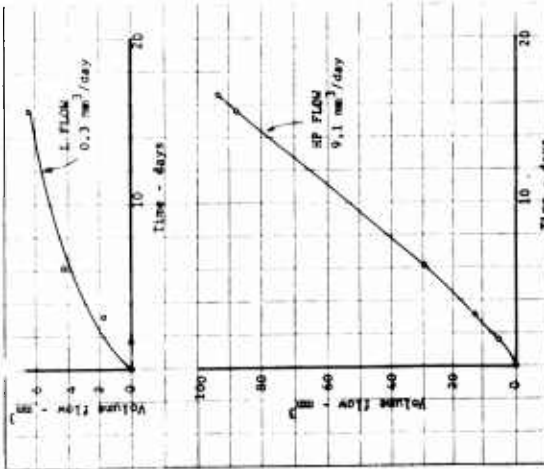


FIG. E-58

TEST V47  
 Teflon  
 L = 0.0012 cm  
 VOLUME FLOW VS TIME

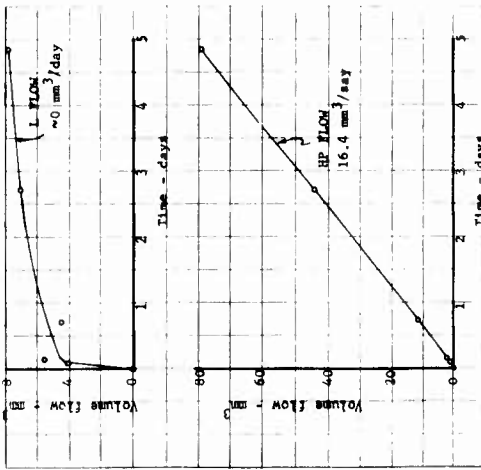


FIG. E-59

TEST V48  
 Teflon  
 L = 0.0012 cm  
 VOLUME FLOW VS TIME

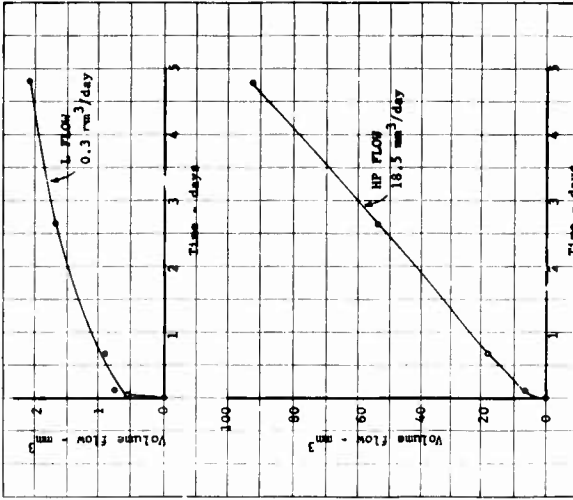


FIG. E-60

TEST V49  
 Teflon  
 L = 0.0012 cm  
 VOLUME FLOW VS TIME

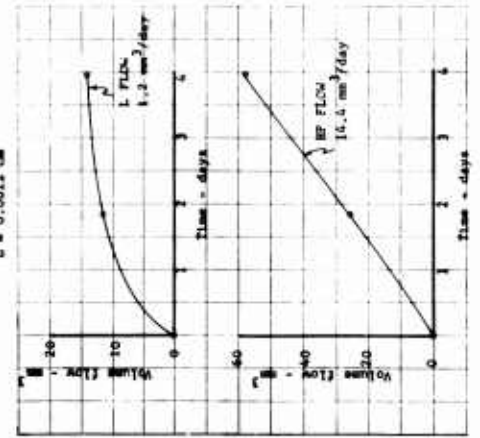


FIG. E-61

TEST V50  
 Teflon  
 L = 0.0046 cm  
 VOLUME FLOW VS TIME

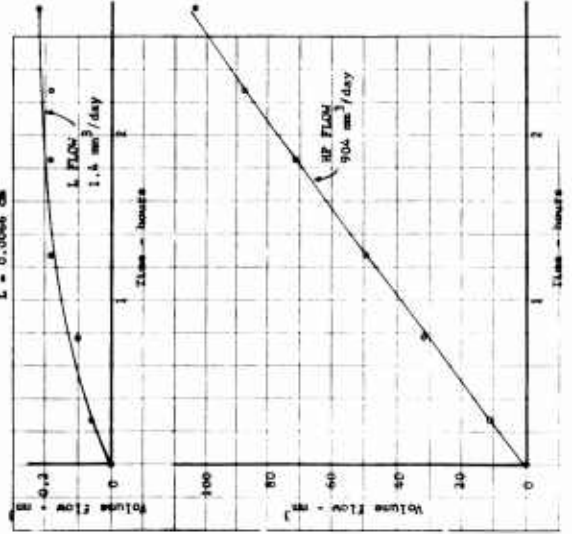


FIG. E-62

TEST V51  
 Teflon  
 L = 0.0060 cm  
 VOLUME FLOW VS TIME

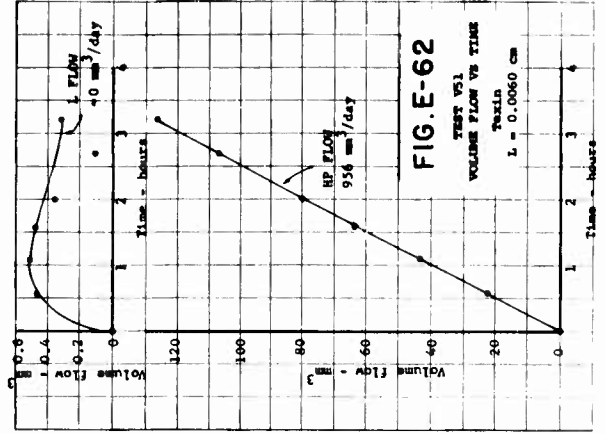


FIG. F-1

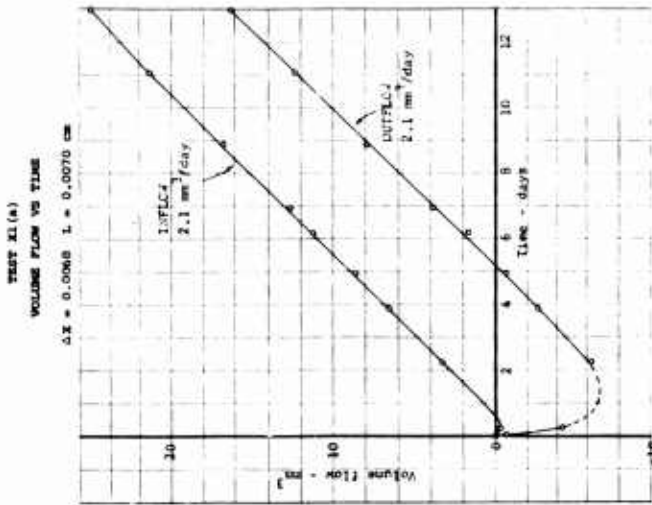


FIG. F-2

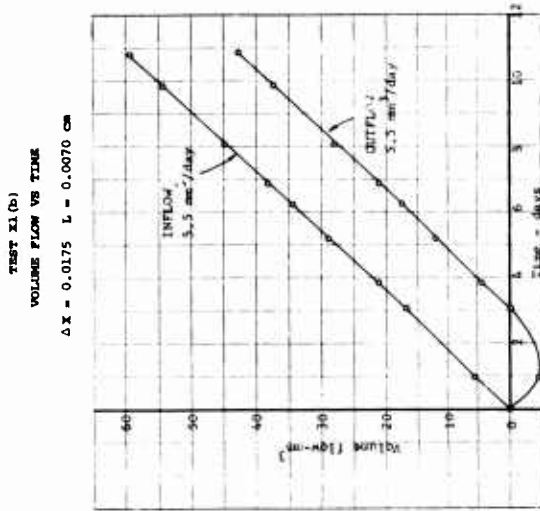


FIG. F-3

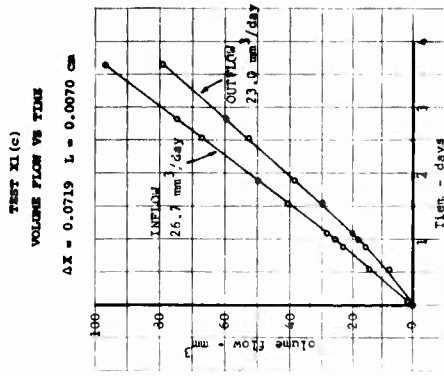


FIG. F-4

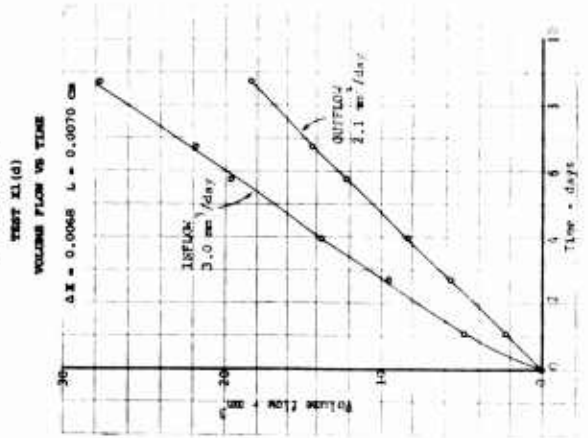


FIG. F-5

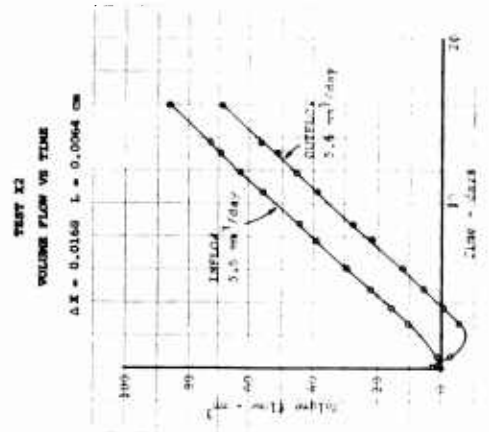


FIG. F-6

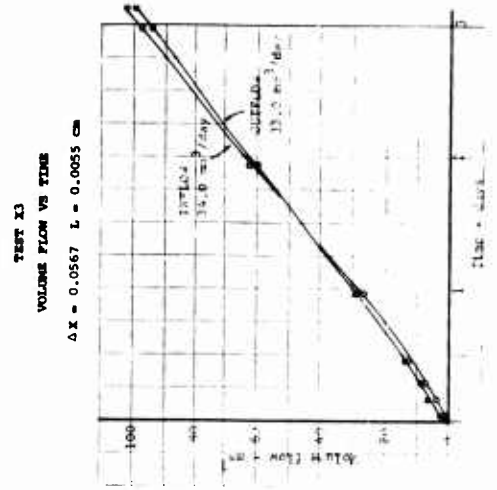


FIG. F-7

TEST X4  
 VOLUME FLOW VS TIME  
 $\Delta X = 1.0711$  L = 0.0074 cm

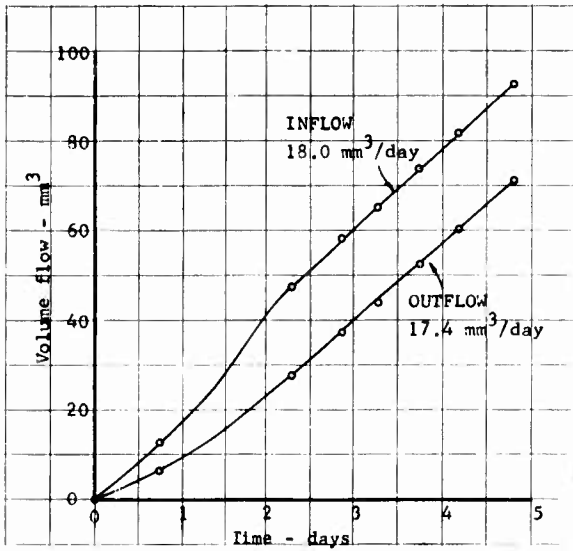


FIG. F-8

TEST X6  
 VOLUME FLOW VS TIME  
 $\Delta X = 0.0719$  L = 0.0061 cm

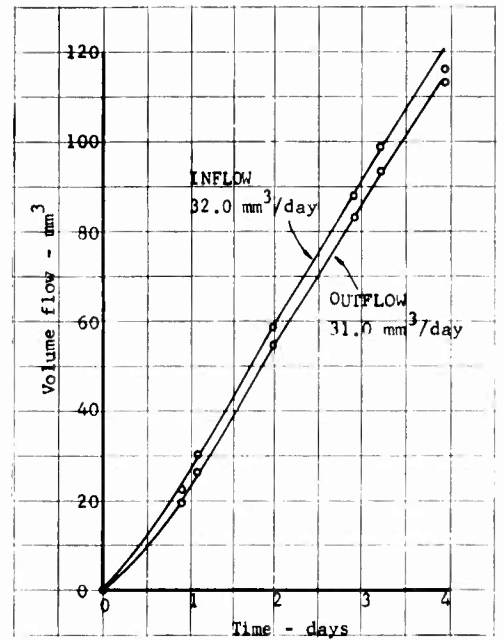


FIG. F-9

TEST X6  
 VOLUME FLOW VS TIME  
 $\Delta X = 0.0698$  L = 0.0058 cm

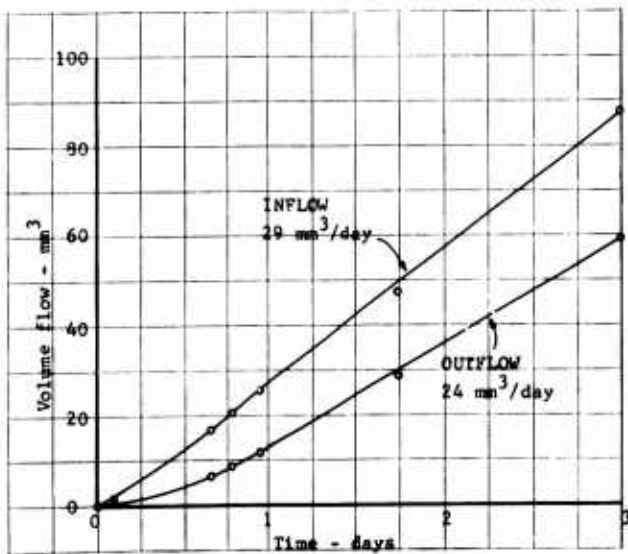
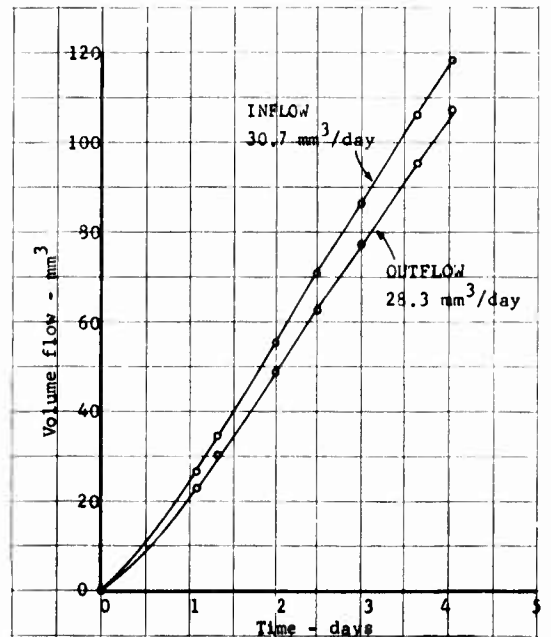


FIG. F-10

TEST X7  
 VOLUME FLOW VS TIME  
 $\Delta X = 0.0715$  L = 0.0062 cm



**FIG. G-1**

TEST B 1  
VOLUME FLOW VS TIME  
Group I

$\Delta p = 2.0 \text{ kg/cm}^2$   $L = 0.0070 \text{ cm}$

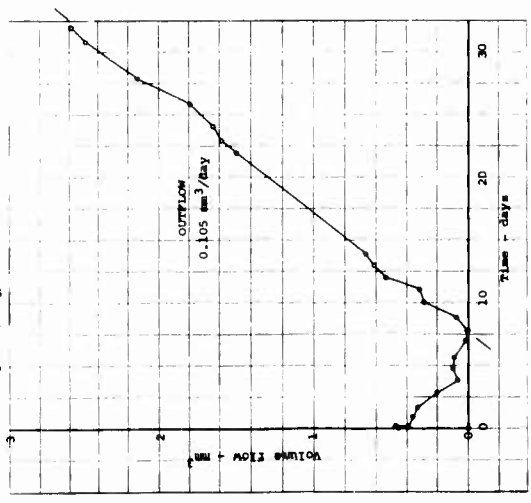


**FIG. G-2**

TEST B 2  
VOLUME FLOW VS TIME  
Group I

$\Delta p = 2.0 \text{ kg/cm}^2$   $L = 0.0072 \text{ cm}$

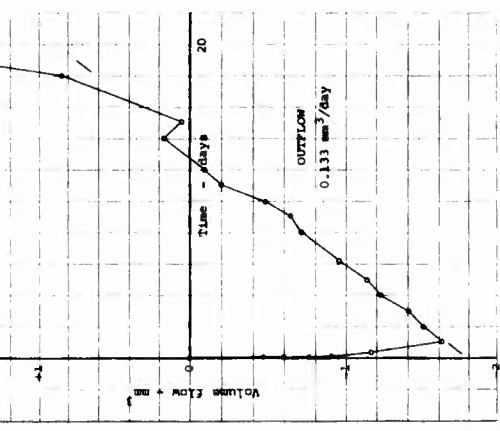


**FIG. G-3**

TEST B 3  
VOLUME FLOW VS TIME  
Group I

$\Delta p = 6.0 \text{ kg/cm}^2$   $L = 0.0061 \text{ cm}$

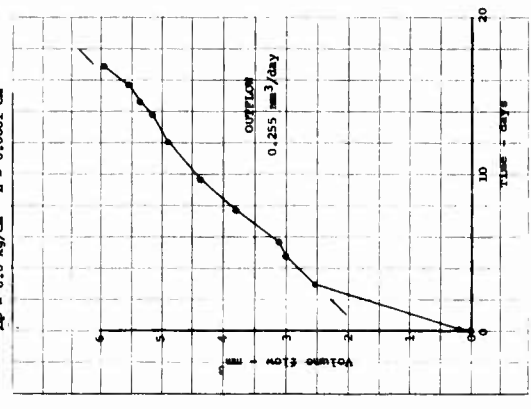


**FIG. G-4**

TEST B 4  
VOLUME FLOW VS TIME  
Group I

$\Delta p = 6.0 \text{ kg/cm}^2$   $L = 0.0069 \text{ cm}$

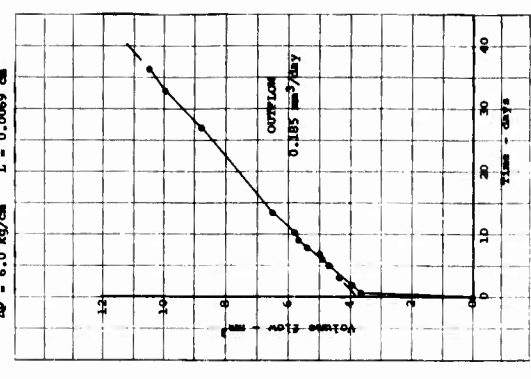


**FIG. G-5**

TEST B 5 (a) (b) (c) (d)  
VOLUME FLOW VS TIME  
Group I

$\Delta p = \text{As shown}$   $L = 0.0064 \text{ cm}$

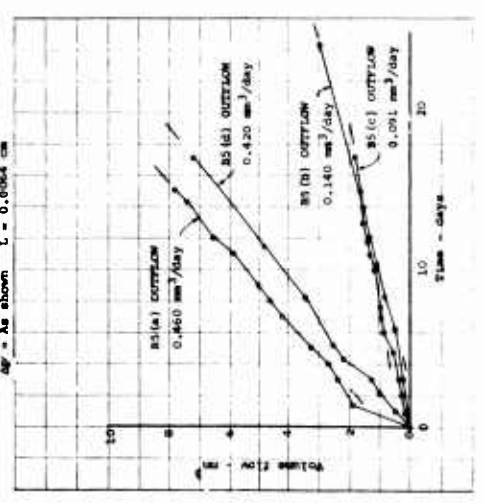


**FIG. G-6**

TEST B 6  
VOLUME FLOW VS TIME  
Group II

$\Delta p = 6.0 \text{ kg/cm}^2$   $L = 0.0131 \text{ cm}$

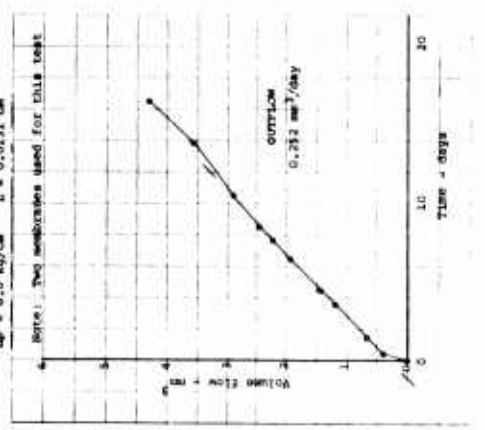


**FIG. G-7**

TEST B 7  
VOLUME FLOW VS TIME  
Group II

$\Delta p = 6.0 \text{ kg/cm}^2$   $L = 0.0123 \text{ cm}$

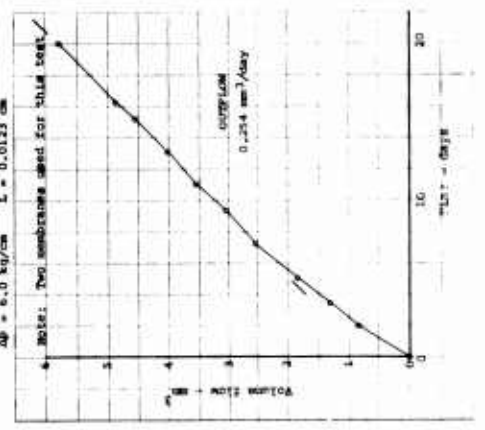


**FIG. G-8**

TEST B 8  
VOLUME FLOW VS TIME  
Group III

$\Delta p = 6.0 \text{ kg/cm}^2$   $L = 0.0062 \text{ cm}$

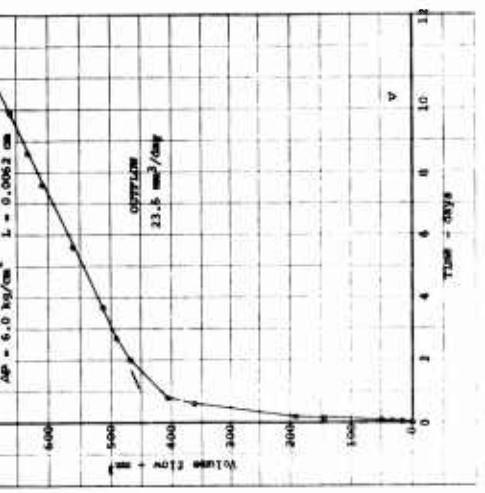
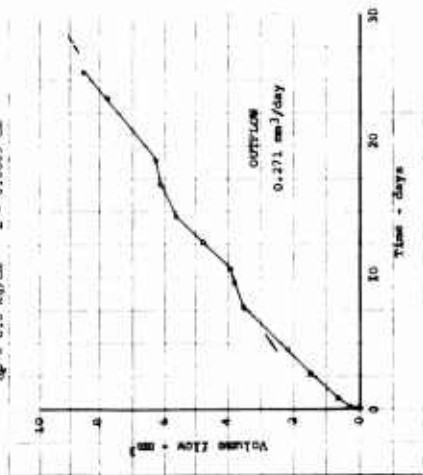


**FIG. G-9**

TEST B 9  
VOLUME FLOW VS TIME  
Group III

$\Delta p = 6.0 \text{ kg/cm}^2$   $L = 0.0069 \text{ cm}$



Plot continued on Fig. G-10 (a) with different scale for volume flow.

**FIG. G-10**

TEST B 10  
VOLUME FLOW VS TIME  
Group III

$\Delta p = 6.0 \text{ kg/cm}^2$   $L = 0.0064 \text{ cm}$

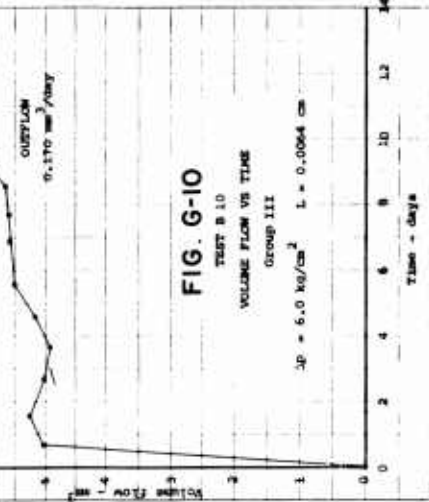


**FIG. G-10a**

TEST B 10  
VOLUME FLOW VS TIME  
Group III

$\Delta p = 6.0 \text{ kg/cm}^2$   $L = 0.0064 \text{ cm}$

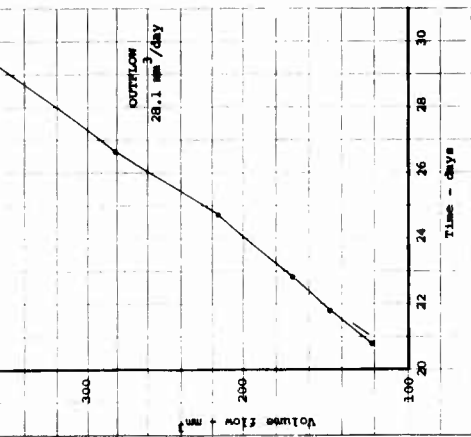


**FIG. G-11**

TEST B 11  
VOLUME FLOW VS TIME  
Group IV

$\Delta p = 2.0 \text{ kg/cm}^2$   $L = 0.0064 \text{ cm}$

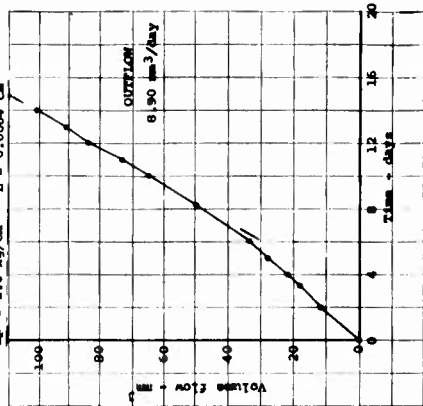


**FIG. G-12**

TEST B 12  
VOLUME FLOW VS TIME  
Group IV

$\Delta p = 6.0 \text{ kg/cm}^2$   $L = 0.0081 \text{ cm}$

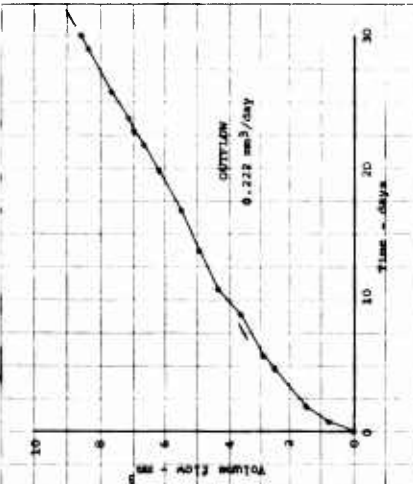


**FIG. G-13**

TEST B 13  
VOLUME FLOW VS TIME  
Group IV

$\Delta p = 6.0 \text{ kg/cm}^2$   $L = 0.0071 \text{ cm}$

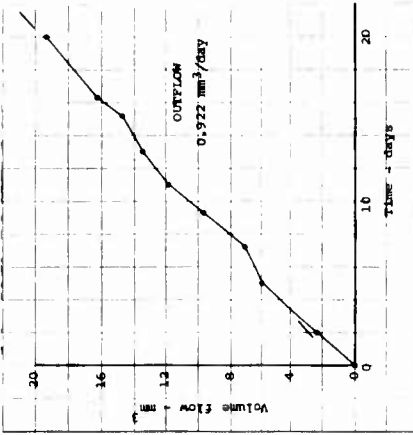


**FIG. G-14**

TEST B 14  
VOLUME FLOW VS TIME  
Group V

$\Delta p = 6.0 \text{ kg/cm}^2$   $L = 0.0057 \text{ cm}$

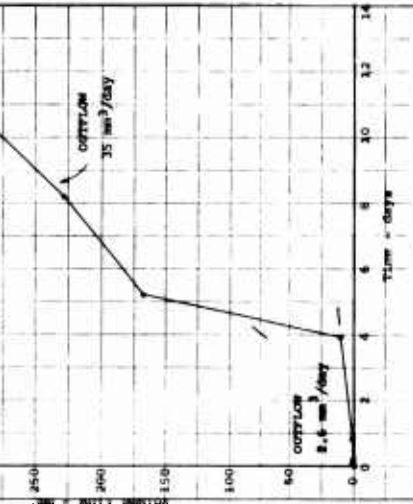


**FIG. G-15**

TEST B 15  
VOLUME FLOW VS TIME  
Group VI

$\Delta p = 6.0 \text{ kg/cm}^2$   $L = 0.0060 \text{ cm}$

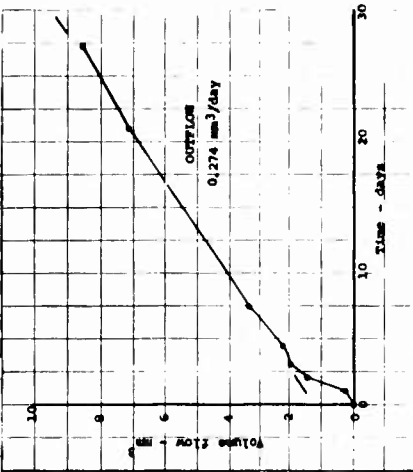


**FIG. G-16**

TEST B 16  
VOLUME FLOW VS TIME  
Group VI

$\Delta p = 6.0 \text{ kg/cm}^2$   $L = 0.0064 \text{ cm}$

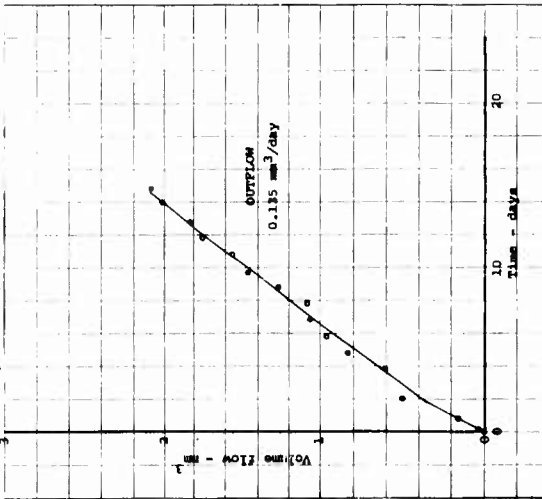


**FIG. G-17**

TEST B 17  
VOLUME FLOW VS TIME  
Group VI

$\Delta p = 6.0 \text{ kg/cm}^2$   $L = 0.0049 \text{ cm}$

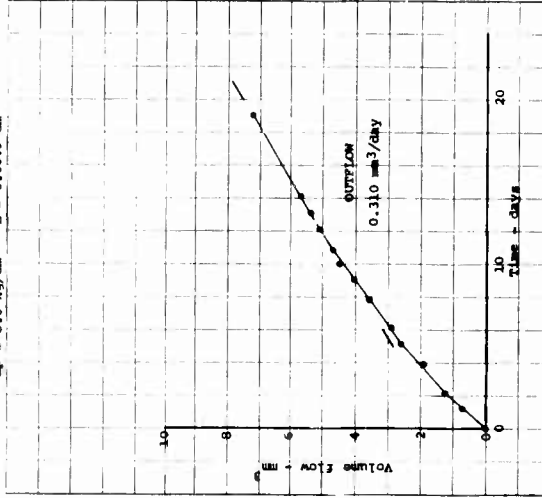


**FIG. G-18**

TEST B 18  
VOLUME FLOW VS TIME  
Group VII

$\Delta p = 6.0 \text{ kg/cm}^2$   $L = 0.0075 \text{ cm}$

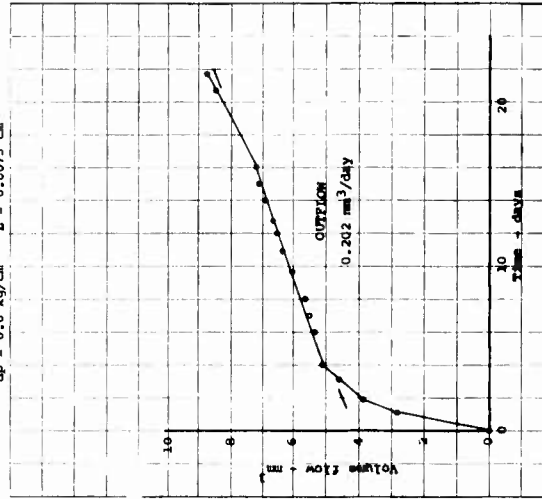


**FIG. G-19**

TEST B 19  
VOLUME FLOW VS TIME  
Group VIII

$\Delta p = 2.0 \text{ kg/cm}^2$   $L = 0.0059 \text{ cm}$

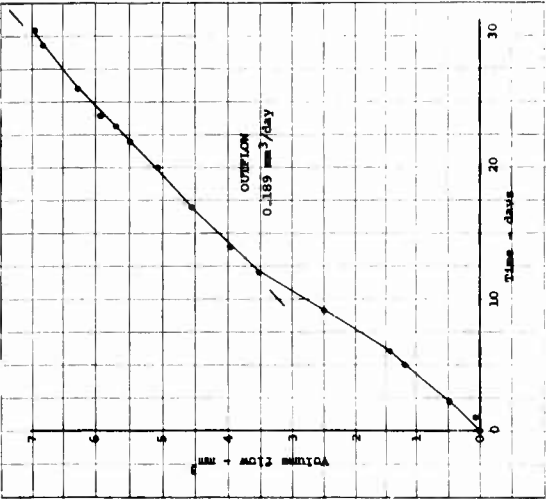


**FIG. G-20**

TEST B 20 (a)  
VOLUME FLOW VS TIME  
Group IX

$\Delta p = 2.0 \text{ kg/cm}^2$   $L = 0.0070 \text{ cm}$

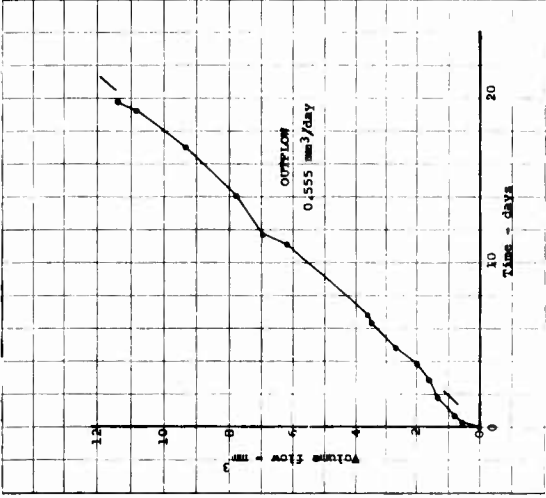


**FIG. G-21**

TEST B 20 (b)  
VOLUME FLOW VS TIME  
Group IX

$\Delta p = 4.0 \text{ kg/cm}^2$   $L = 0.0070 \text{ cm}$

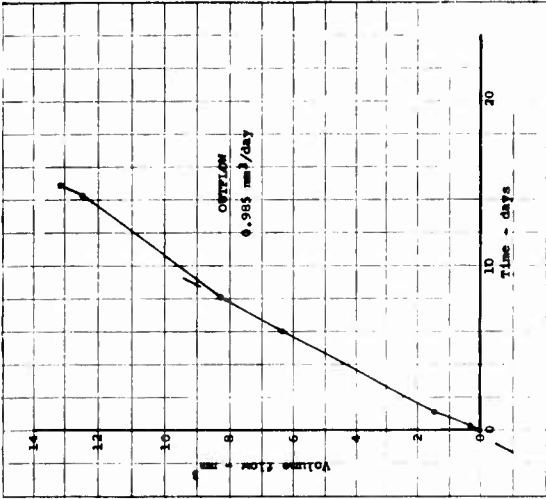


FIG. G-22

TEST B 21  
VOLUME FLOW VS TIME  
Group IX

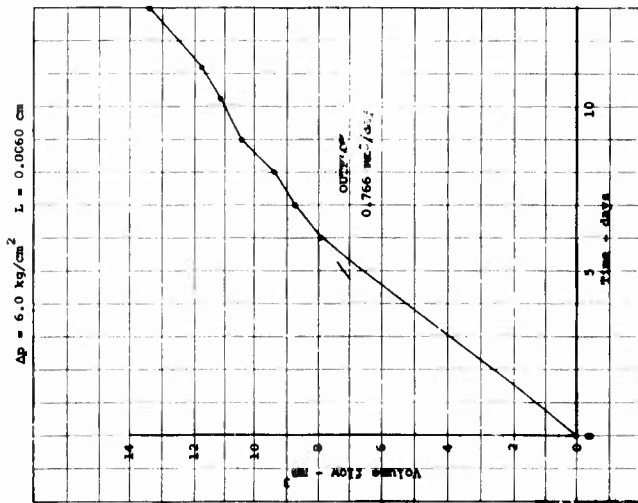


FIG. G-23

TEST B 22  
VOLUME FLOW VS TIME  
Group IX

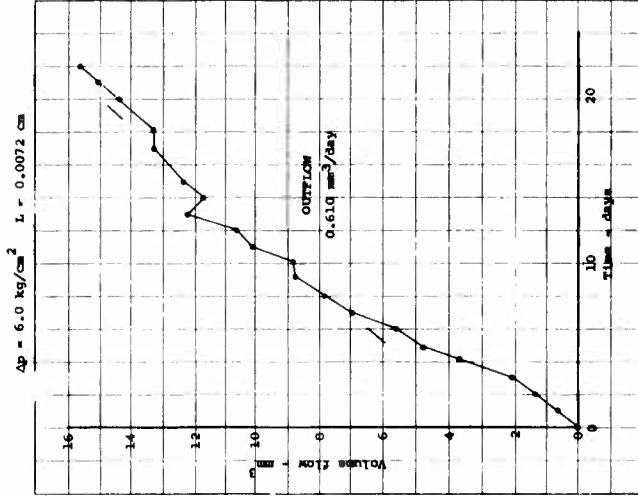


FIG. G-24

TEST B 23  
VOLUME FLOW VS TIME  
Group X

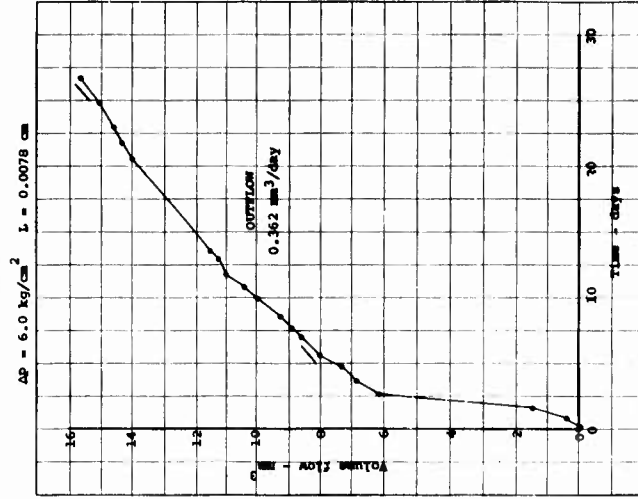


FIG. G-25

TEST B 24  
VOLUME FLOW VS TIME  
Group XI

Δp = 6.0 kg/cm² L = 0.0060 cm

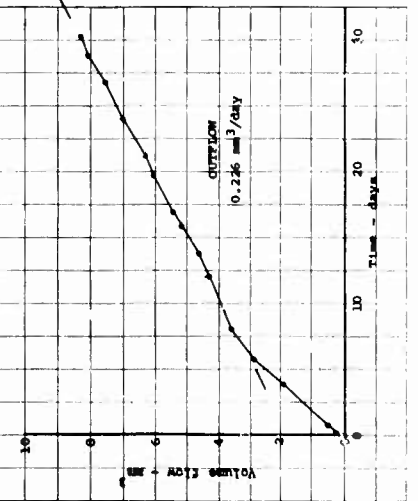
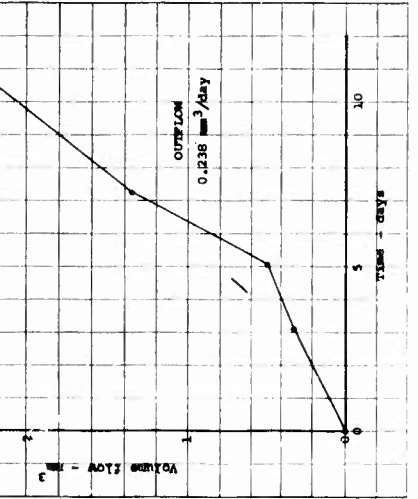
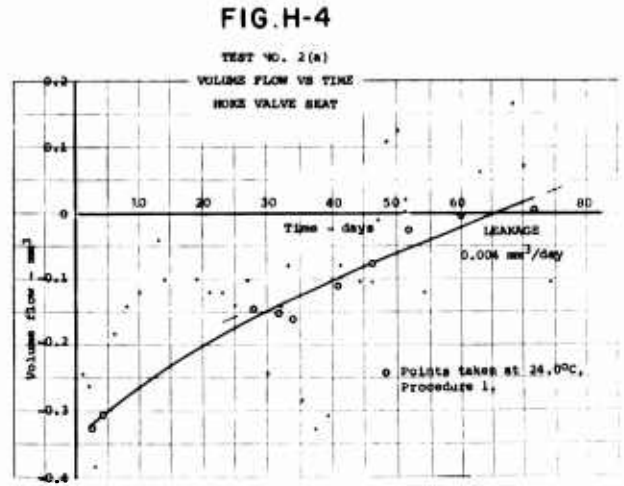
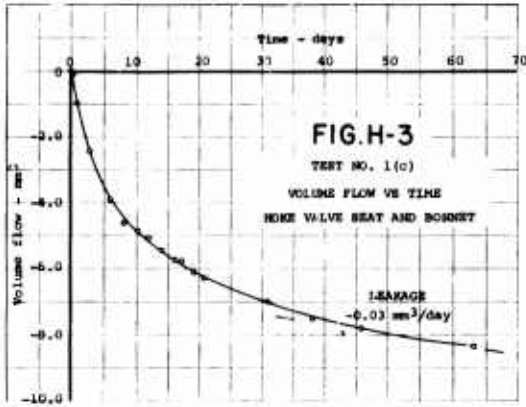
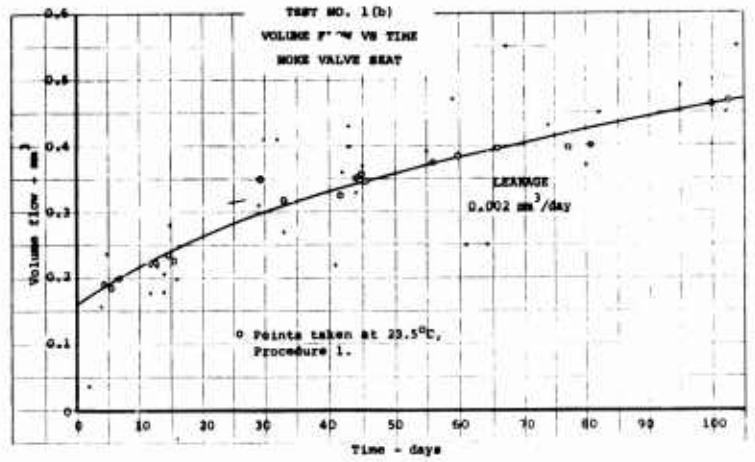
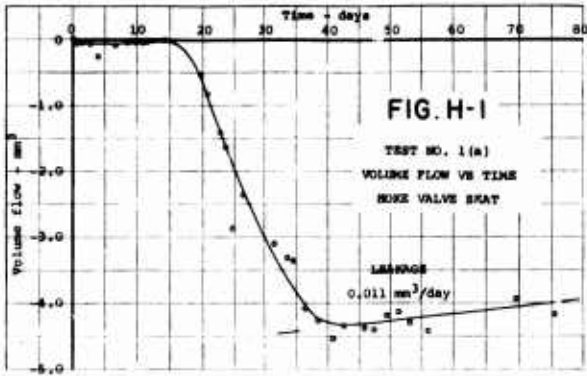


FIG. G-26

TEST B 25  
VOLUME FLOW VS TIME  
Group XI

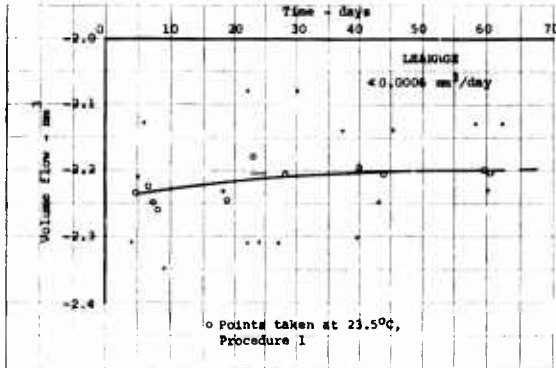
Δp = 6.0 kg/cm² L = 0.0060 cm





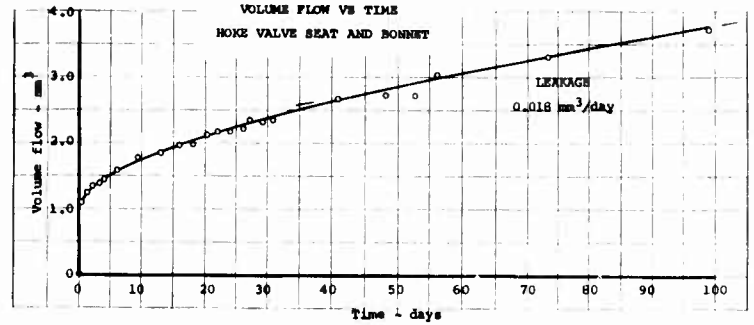
**FIG. H-5**

TEST NO. 2(b)  
VOLUME FLOW VS TIME  
HOKE VALVE SEAT



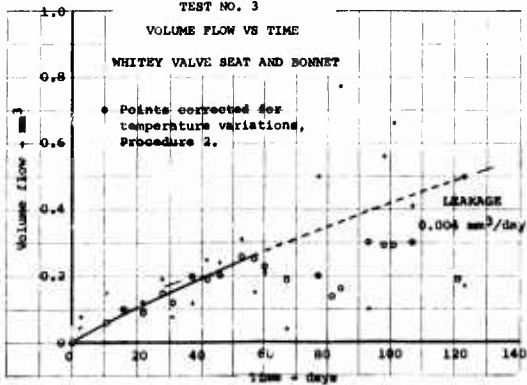
**FIG. H-6**

TEST NO. 2(c)  
VOLUME FLOW VS TIME  
HOKE VALVE SEAT AND BONNET



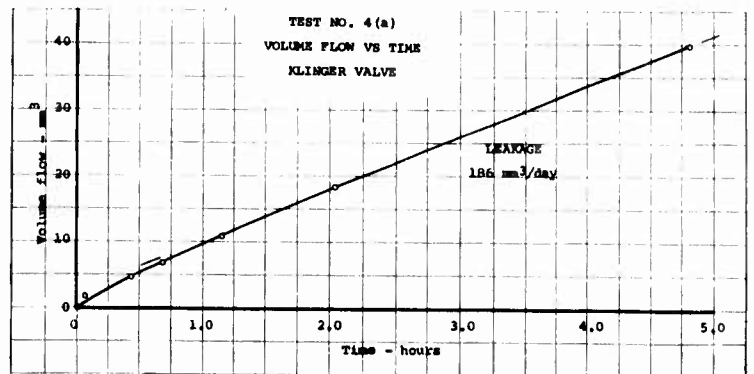
**FIG. H-7**

TEST NO. 3  
VOLUME FLOW VS TIME  
WHITEY VALVE SEAT AND BONNET



**FIG. H-8**

TEST NO. 4(a)  
VOLUME FLOW VS TIME  
KLINGER VALVE



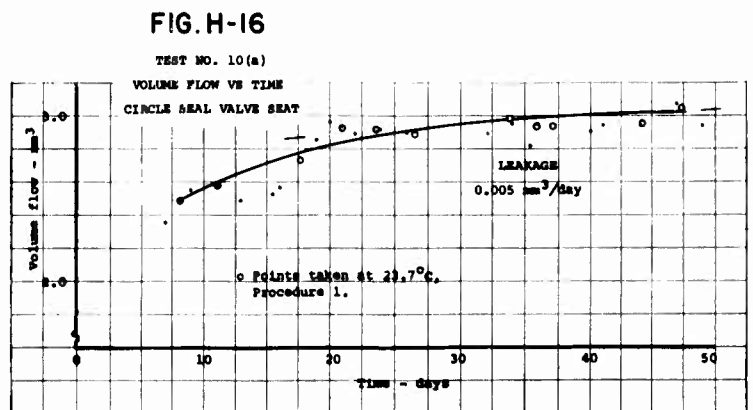
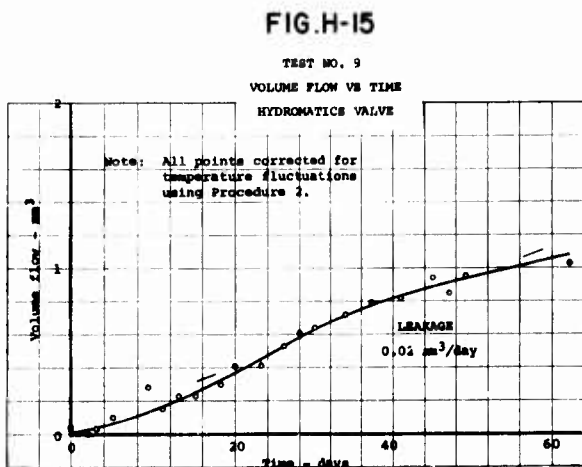
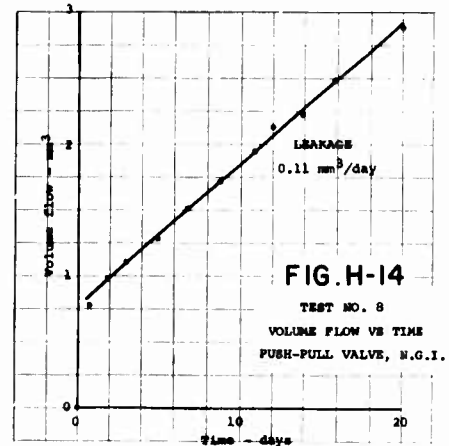
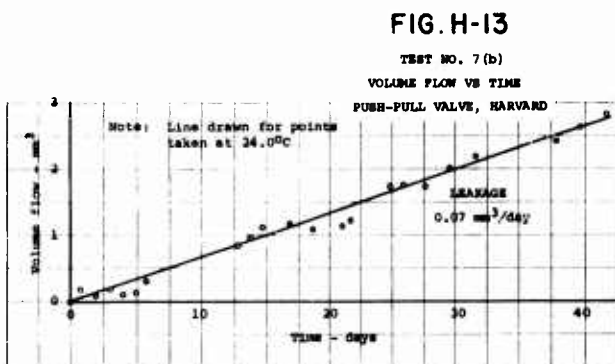
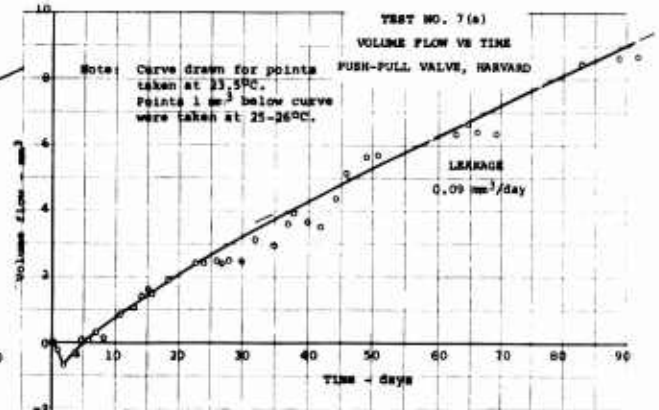
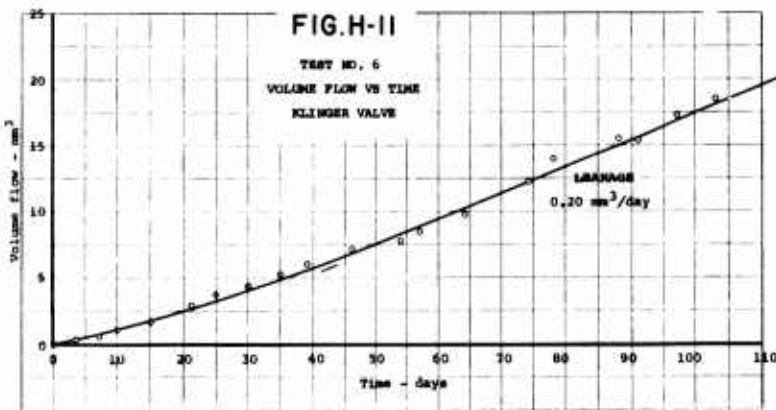
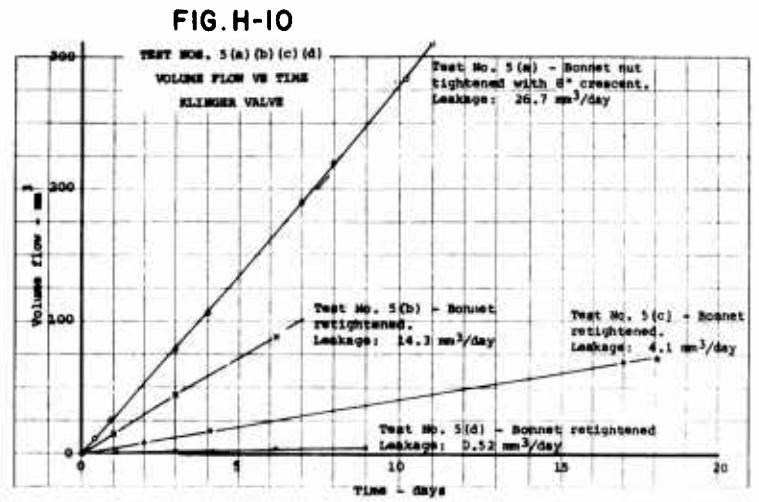
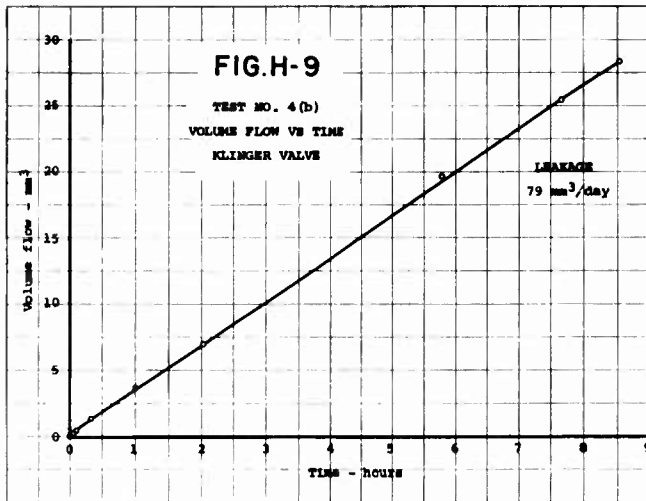


FIG.H-17

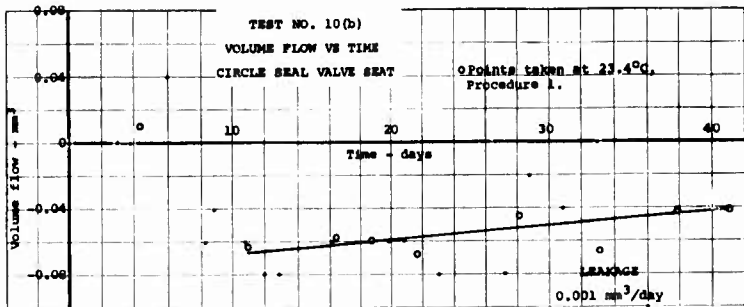


FIG.H-18

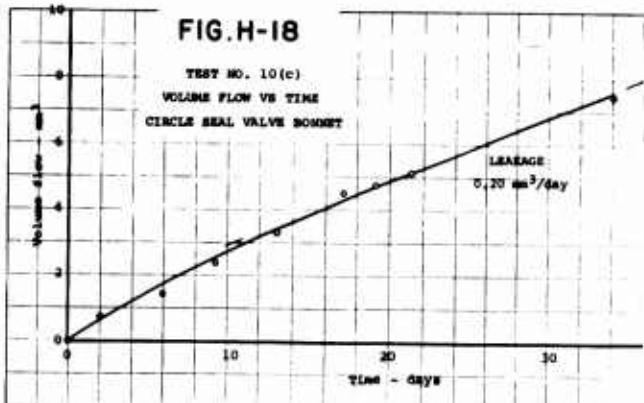


FIG.H-19

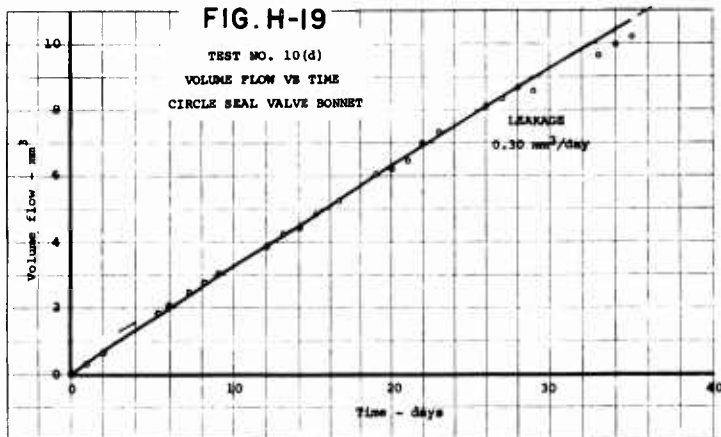


FIG.H-20

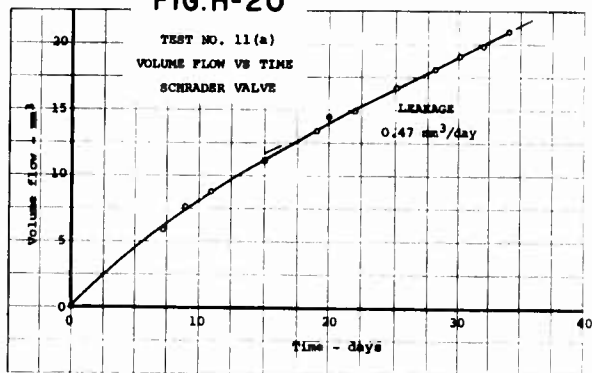


FIG.H-21

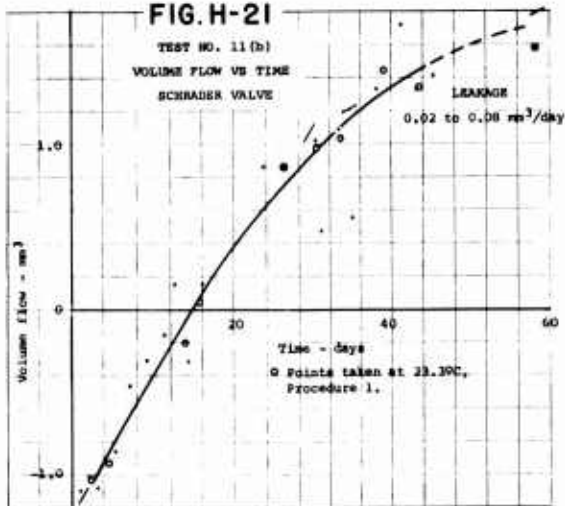


FIG.H-22

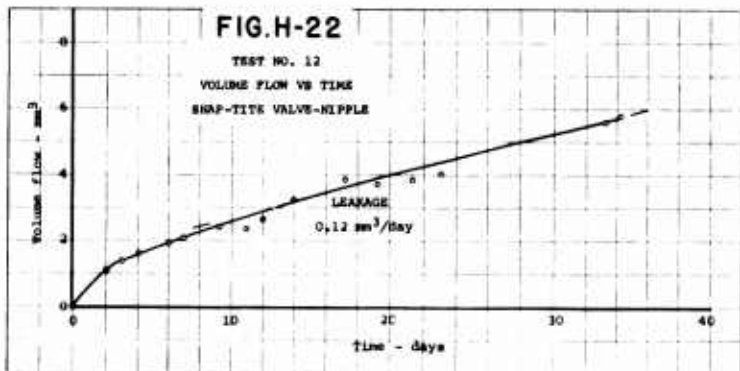


FIG.H-24

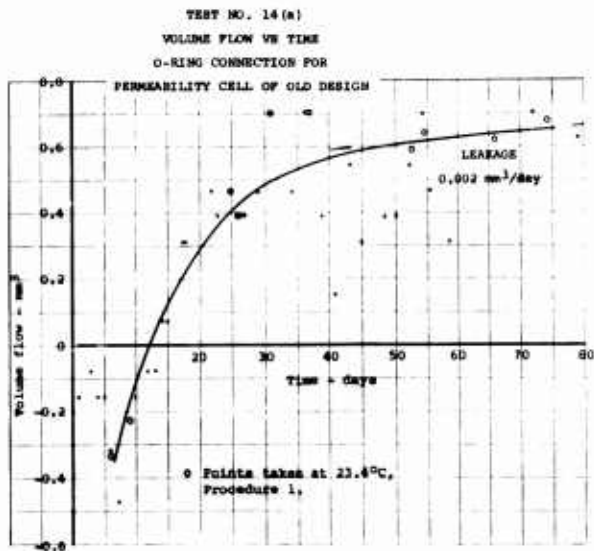


FIG.H-23

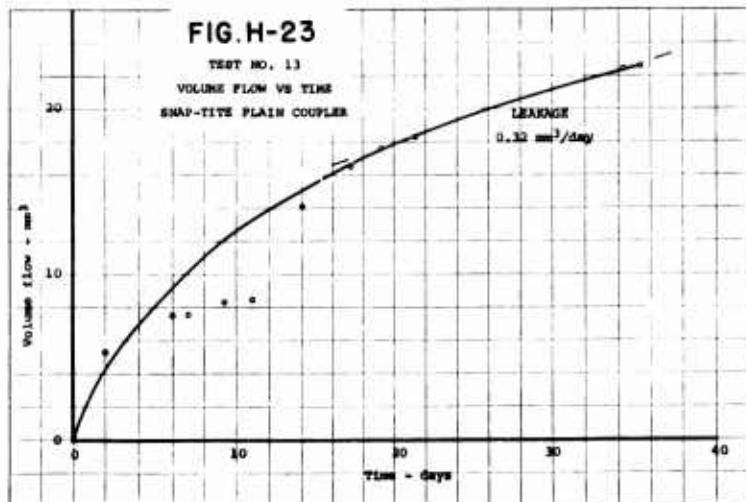


FIG.H-25

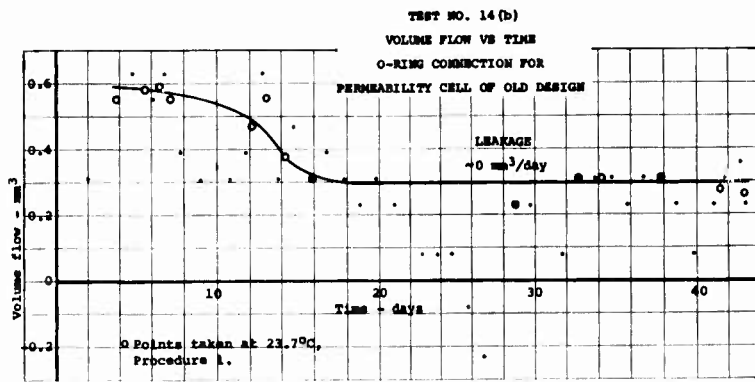


FIG.H-26

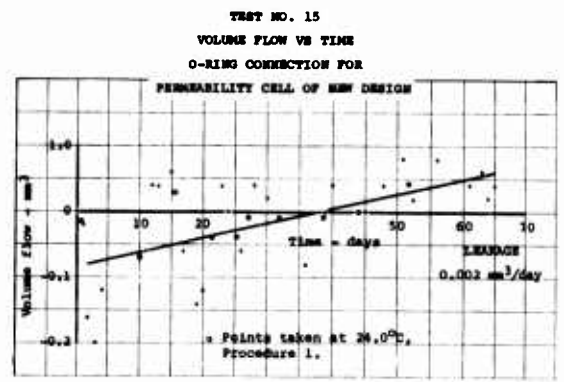


FIG.H-27

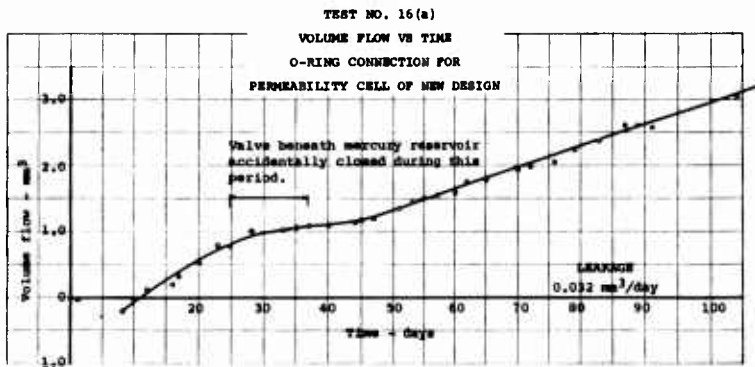


FIG.H-28

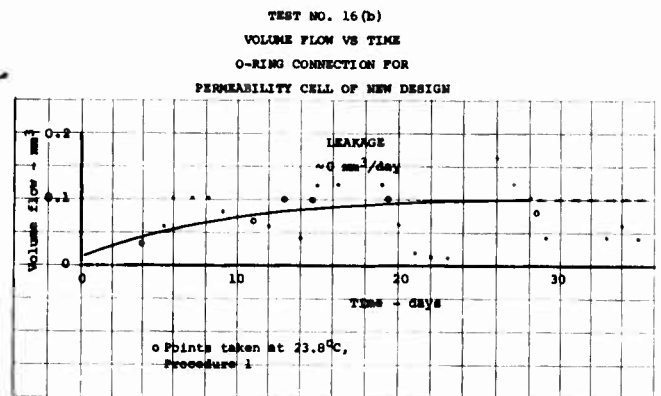


FIG.H-29

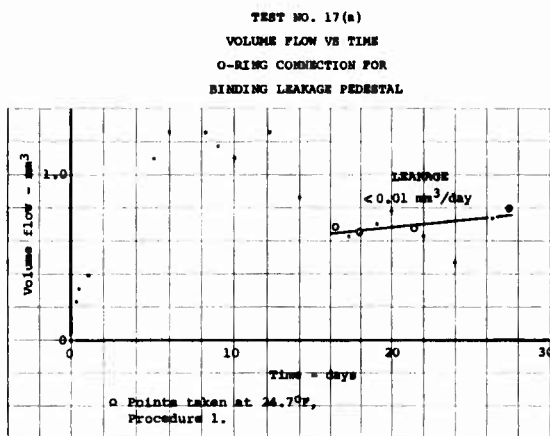


FIG.H-30

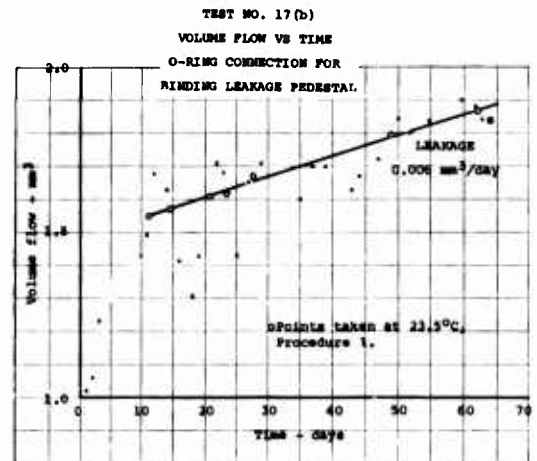


FIG.H-31

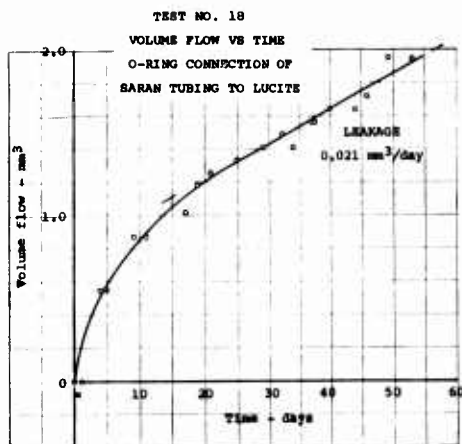


FIG.H-32

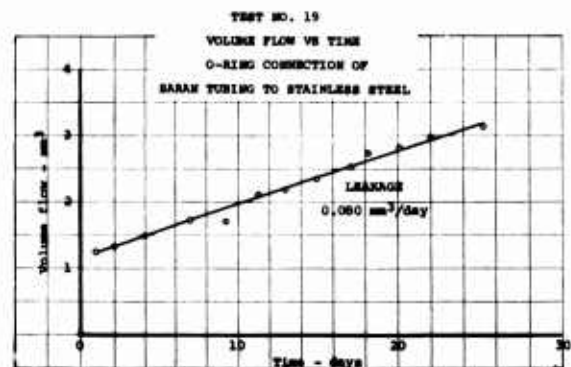


FIG. H-33

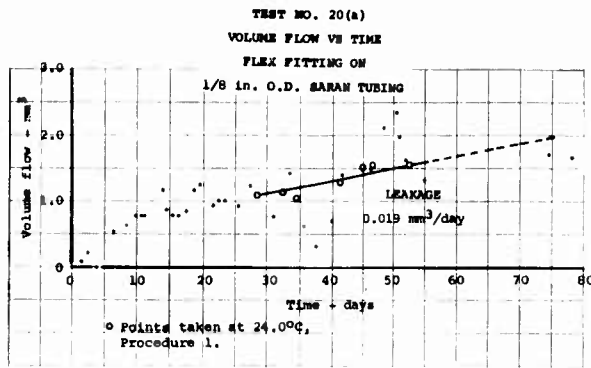


FIG. H-34

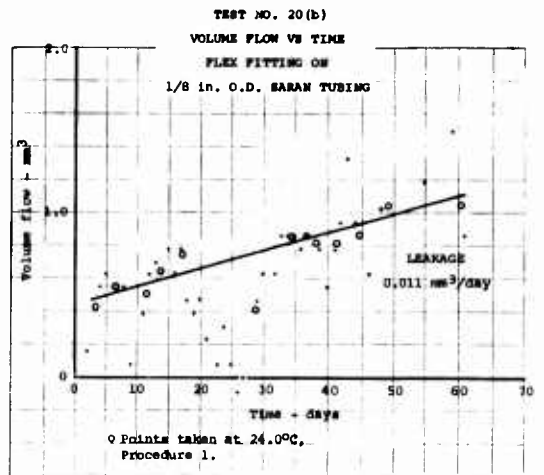


FIG. H-35(a)

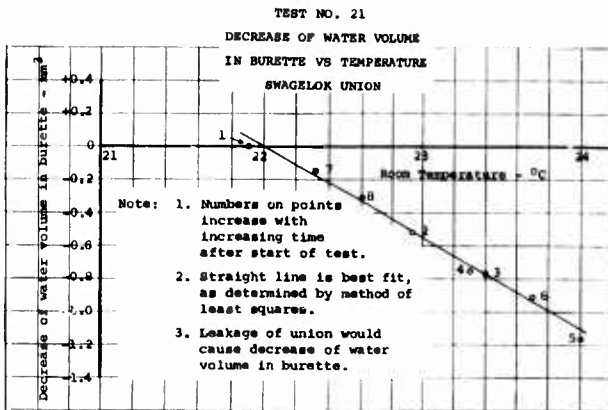


FIG. H-35(b)

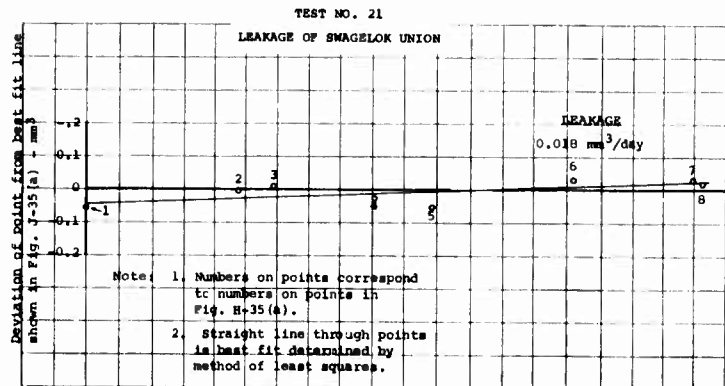


FIG. H-36

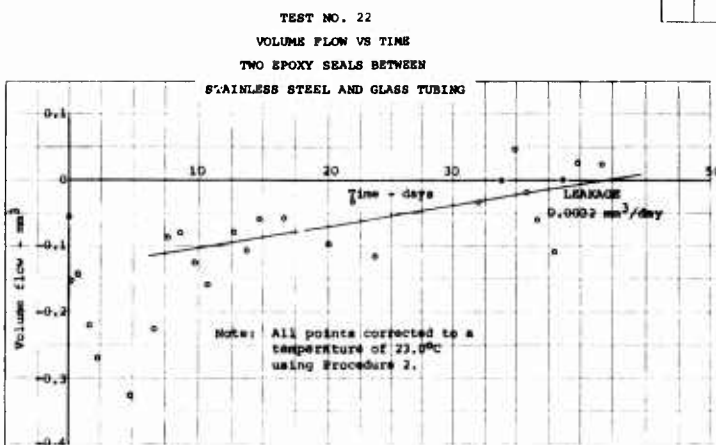


FIG. H-37

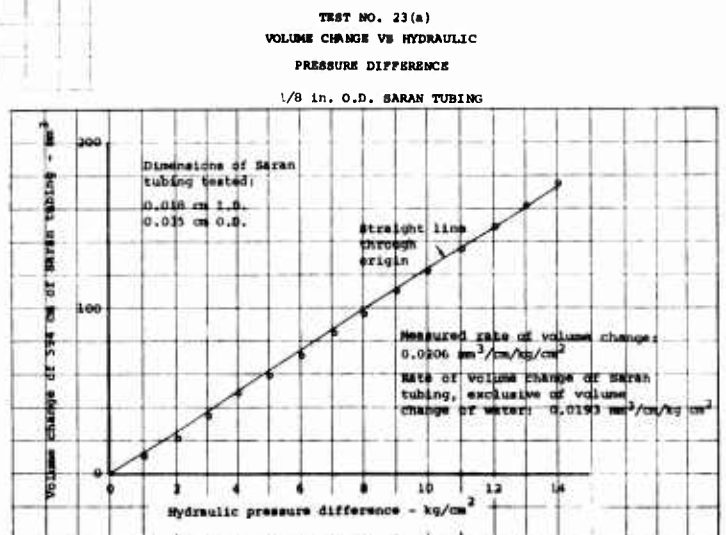


FIG. H-39(a)

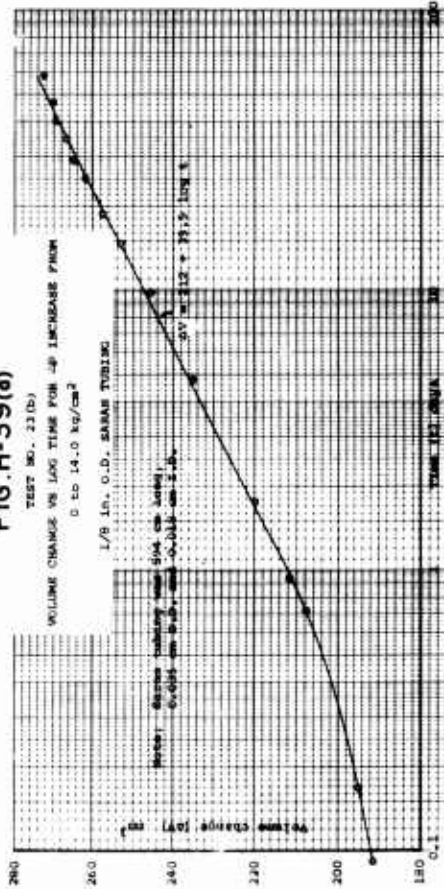


FIG. H-39(b)

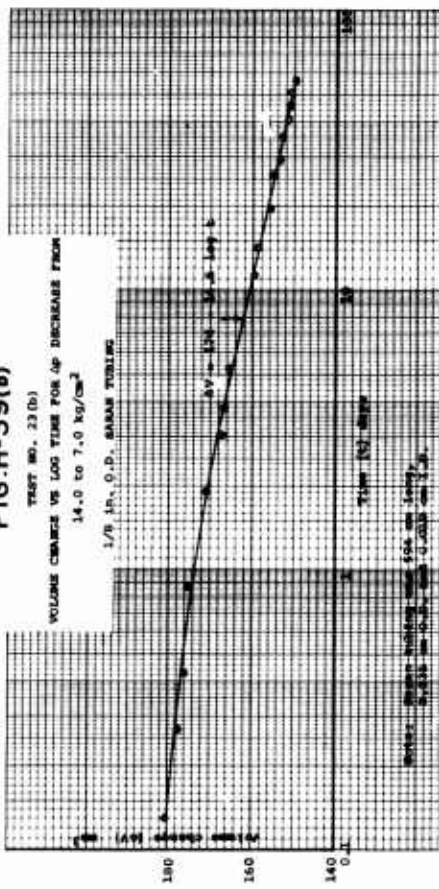


FIG. H-39(c)

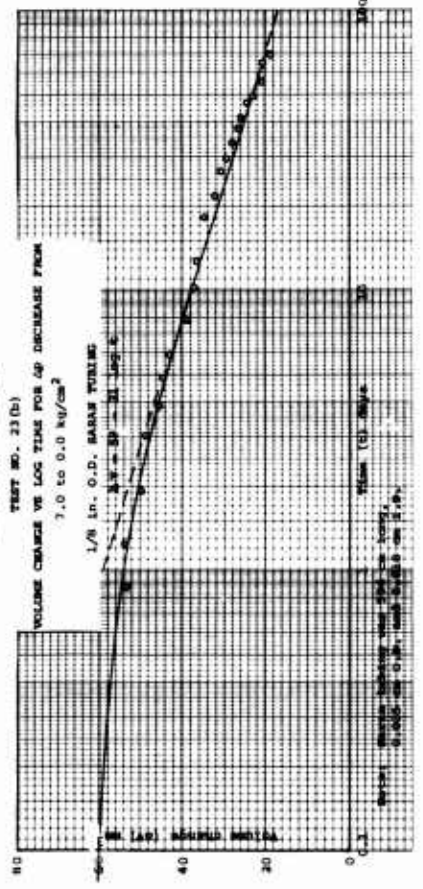


FIG. H-38

TEST NO. 23(b)  
 VOLUME CHANGE VS TIME  
 50% TO CHANGES IN  
 HYDRAULIC PRESSURE DIFFERENCE  
 1/8 in. O.D. SARAW TUBING

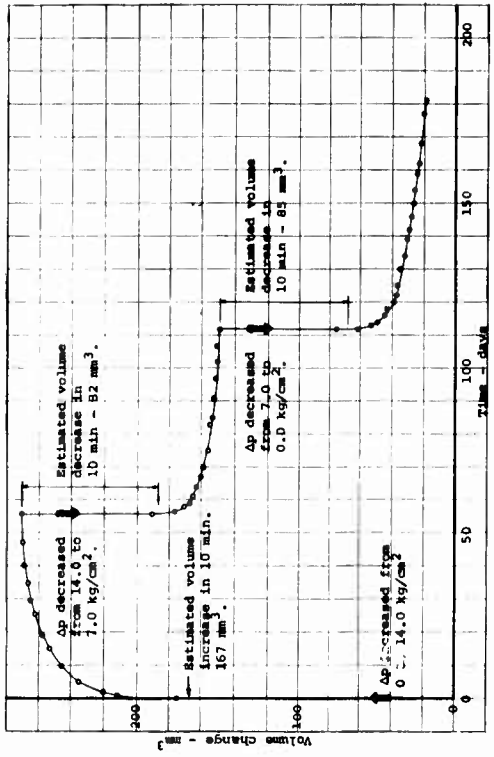


FIG. H-40

TEST NO. 23(c)  
 EVAPORATION THROUGH WALL OF  
 5/4 in. O.D. SARAW TUBING

